Synthesis, Derivatization and Characterization of Rhenium/Technetium Mono- and Bis(η^6-arene) Complexes for the Application in Medicinal Chemistry

---

Dissertation

zur

Erlangung der naturwissenschaftlichen Doktorwürde
(Dr. sc. nat.)

vorgelegt der

Mathematisch-naturwissenschaftlichen Fakultät

der

Universität Zürich

von

Giuseppe Meola

aus

Italien

Promotionskommission

Prof. Dr. Roger Alberto (Vorsitz und Leitung der Dissertation)

Prof. Dr. David Tilley

Prof. Dr. Gilles Gasser

Zürich, 2019

To my Family and Sophie

Table of Content

Summary I

1 Compounds Synthesized in this Thesis 11

1.1 $[Re(\eta^6\text{-arene})_2]^+$ Complexes 11

1.2 Complexes from the Publication: *Inorg. chem.* 2016, *55*, 11131-11139 12

1.3 Complexes related to the Publication: *Inorg. chem.* 2016, *55*, 11131-11139 13

1.4 Complexes from the Publication: *Inorg. chem.* 2017, *56*, 11, 6297-6301 14

1.5 Complexes related to the Publication: *Inorg. chem.* 2017, *56*, 11, 6297-6301 15

1.6 Complexes from the Publication: *Dalton Trans.*, 2017, *46*, 14631-14637 15

1.7 Complexes related to the Publication: *Dalton Trans.*, 2017, *46*, 14631-14637 16

2 List of Abbreviations 17

3 Published Parts of this Thesis 19

4 Introduction 20

4.1 Metal-Based Drugs 20

4.2 The Role of Rhenium in the Bioinorganic and Medicinal Chemistry 22

4.3 Mono-/Bis-Arene Metal Complexes in the Bioinorganic Chemistry 23

4.3.1 Mono-Arene Metal Complexes 23

4.3.2 Bis-Arene Metal Complexes 24

4.4 Syntheses, Stabilities, Properties and Reactivities of Bis-arene Complexes 25

4.4.1 History of Metal-Bis-Arene Complexes 25

4.4.2 Synthesis of Metal-Bis-Arene Complexes 25

4.4.3 Structure and Properties of Metal-Bis-arene Complexes 26

4.4.4 Reactivity of Metal-Bis-Arene Complexes 27

4.5 Rhenium/$^{99(m)}$Technetium Mono- and Bis(η^6-arene) Chemistry: A Small Overview 29

4.5.1 Rhenium Mono and Bis(η^6-arene) Complexes 29

4.5.2 Technetium Mono- and Bis(η^6-arene) Complexes 31

5 Motivation and Goals 33

5.1.1 Goals 33

6 Result and Discussion 35

6.1 Synthesis & Characterization of $[Re(\eta^6\text{-arene})_2]^+$ Complexes 35

6.1.1 Crystal Structures 43

6.1.2 NMR-Spectroscopy 54

6.1.3 Physico-Chemical Properties 56

6.1.4 Cytotoxicity Studies 58
6.2 Fischer Hafner Reaction with Functionalized Arene 59
6.3 Publication: Bis-arene Complexes $[Re(\eta^6\text{-arene})_2]^+$ as Highly Stable Bioorganometallic Scaffolds 60
6.4 Unpublished Results: Bis-Arene Complexes $[Re(\eta^6\text{-arene})_2]^+$ as Highly Stable Bioorganometallic Scaffolds 79
6.4.1 Carboxylic Acid Functionalized Rhenium Bis-Arene Complexes 80
6.4.2 Halogen Functionalized Rhenium Bis-Arene Complexes 82
6.4.3 Ketone Functionalized Rhenium Bis-Arene Complexes 87
6.4.4 Synthesis of Rhenium Bis-Arene Tamoxifen Derivatives via Mc-Murry Reaction 89
6.4.5 Secondary and Tertiary Alcohol Functionalized Rhenium Bis-Arene Complexes 92
6.4.6 Ester and Azide Functionalised Rhenium Bis-Arene Complexes 94
6.4.7 Phosphor Functionalized Rhenium Bis-Arene Complexes 94
6.4.8 Pyridine functionalized rhenium bis-arene complexes 96
6.5 Publication: A Mixed-Ring Sandwich Complex from Unexpected Ring Contraction in $[Re(\eta^6\text{-}C_6H_5Br)(\eta^6\text{-}C_6R_6)](PF_6)$ 97
6.6 Unpublished Results: A Mixed-Ring Sandwich Complex from Unexpected Ring Contraction in $[Re(\eta^6\text{-C6H5Br})(\eta^6\text{-}C_6R_6)](PF_6)$ 106
6.7 Publication: Structure and Reactivities of Rhenium and Technetium bis-Arene Sandwich Complexes $[M(\eta^6\text{-arene})_2]^+$ 116
6.8 Unpublished Results: Structure and Reactivities of Rhenium and Technetium bis-Arene Sandwich Complexes $[M(\eta^6\text{-arene})_2]^+$ 129
6.8.1 Light Induced Substitution Reaction of $[Re(\eta^6\text{-naphthalene})_2]^+$ ([**7p**]$^+$) 130
6.8.2 Substitution Reaction of $[Re(\eta^6\text{-naphthalene})(\eta^6\text{-benzene})]^+$ ([**6p**]$^+$) with Aromatic Ligands 133
6.8.3 Substitution Reaction of $[Re(\eta^6\text{-naphthalene})(\eta^6\text{-benzene})]^+$ ([**6p**]$^+$) and $[Re(\eta^6\text{-naphthalene})_2]^+$ ([**7p**]$^+$) with Solvent Molecules 134
7 Conclusion and Outlook 141
8 Experimental Part 145
8.1 General Information 145
8.1.1 Materials 145
8.1.2 Characterization 145
8.2 Synthetic Procedures 147
8.2.1 $[Re(\eta^6\text{-}C_6H_6)_2](OTf)$ ([**1**](OTf)) and ([**1**](PF_6)) 147
8.2.2 $[Re(\eta^6\text{-}C_6H_5CH_3)_2](OTf)$ ([**2**](OTf)) and([**2**](PF_6)) 147
8.2.3 $[Re(\eta^6\text{-}p\text{-}C_6H_4(CH_3)_2)_2](OTf)$ ([**3**](OTf)) 148

8.2.4 [Re(η^6-*o*-$C_6H_4(CH_3)_2)_2$](OTf) ([**4**](OTf)) 149

8.2.5 [Re(η^6-*m*-$C_6H_4(CH_3)_2)_2$](OTf) ([**5**](OTf)) 149

8.2.6 [Re(η^6-$C_6H_3(CH_3)_3)_2$](PF_6) ([**6**](PF_6)) 150

8.2.7 [Re(η^6-$C_6H_4(CH_2)_7CH_3)_2$)](OTf) ([**7**](OTf)) 151

8.2.8 [Re(η^6-*t*-$C_6H_4C(CH_3)_3)_2$)](OTf) ([**10**](OTf)) 152

8.2.9 [Re(η^6-$C_{10}H_{12})_2$](OTf) ([**13**](OTf)) 153

8.2.10 [Re(η^6-$C_{13}H_{10})_2$](OTf) ([**14**](OTf)) 154

8.2.11 [Re(η^6-$C_{12}H_{10})_2$](OTf) ([**15**](OTf)) 155

8.2.12 [Re(η^6-$C_{12}H_{10})_2$](OTf) ([**16**](PF_6)) 156

8.2.13 [Re(η^6-$C_6(CH_3)_6$)(η^6-C_6H_6)](OTf) ([**17**](OTf)) 156

8.2.14 [Re(η^6-$C_{10}H_8)_2$](OTf) ([**7p**](OTf)) 157

8.2.15 [Re(η^6-$C_{10}H_8$)(η^6-C_6H_6)](OTF) ([**6p**]OTf) 157

8.3 Supplementary Information: Bis-arene Complexes [Re(η^6-arene)$_2$]$^+$ as Highly Stable Bioorganometallic Scaffolds 159

8.4 Unpublished Experiment Section: Bis-arene Complexes [Re(η^6-arene)$_2$]$^+$ as Highly Stable Bioorganometallic Scaffolds 178

8.4.1 [Re(η^6-$C_6H_4COOH_2$)(η^6-C_6H_5COOH)]$^+$ ([**17**](PF_6)) 178

8.4.2 [Re(η^6-C_6H_5Cl)(η^6-C_6H_6)](PF_6) ([**18**](PF_6)) and [Re(η^6-$C_6H_5Cl)_2$](PF_6) ([**19**](PF_6)) 178

8.4.3 [Re(η^6-$C_6H_4Br_2$)(η^6-C_6H_5Br)](PF_6) ([**21**](PF_6)) 179

8.4.4 [Re(η^6-C_6H_5OMe)(η^6-C_6H_6)](PF_6) ([**22**](PF_6)) 180

8.4.5 [Re(η^6-C_6H_5-1,3-$C_3H_3N_2$)(η^6-C_6H_6)](PF_6) ([**23**](PF_6)) 180

8.4.6 [Re(η^6-$C_6H_5OMe)_2$](PF_6) ([**24**](PF_6)) 181

8.4.7 [Re(η^6-N-((naphthalen-2-yl)-2-(phenylthio)acetamide)$_2$](PF_6) ([**25**](PF_6)) 181

8.4.8 [Re(η^6-C_6H_5COEt)(η^6-C_6H_6)](PF_6) ([**26**](PF_6)) and [Re(η^6-$C_6H_5COEt)_2$](PF_6) ([**27**](PF_6)) 182

8.4.9 [Re(η^6-1,1,2-triyltribenzene-but-1-ene)(η^6-C_6H_6)](PF_6) ([**30**](PF_6)) 184

8.4.10 [Re(η^6-4,4'-(2-phenylbut-1-ene-1,1-diyl)diphenol)(η^6-C_6H_6)](PF_6) ([**32**](PF_6)) 185

8.4.11 [Re(η^6-$C_6H_5C(OH)Ph$)(η^6-C_6H_6)](PF_6) ([**33**](PF_6)) and [Re(η^6-$C_6H_5C(OH)Ph)_2$](PF_6) ([**34**](PF_6)) 186

8.4.12 [Re(η^6-$C_6H_5C(OH)(Ph)_2$)(η^6-C_6H_6)](PF_6) ([**35**](PF_6)) and [Re(η^6-$C_6H_5C(OH)(Ph)_2)_2$](PF_6) ([**36**](PF_6)) 187

8.5 Supplementary Information: A Mixed-Ring Sandwich Complex from Unexpected Ring Contraction in [M(η^6-C_6H_5Br)(η^6-C_6R_6)]$^+$. 189

8.6 Unpublished Experimental Section: A Mixed-Ring Sandwich Complex from Unexpected Ring Contraction in [M(η^6-C_6H_5Br)(η^6-C_6R_6)]$^+$ 220

8.6.1 [Re(η^6-C_6H_5OH)(η^6-C_6H_6)](PF_6) ([**2**](PF_6) 220

8.6.2 [Re(η^5-$C_5H_4CHNCH_2C_6H_5$)(η^6-C_6H_6)] (**38**) 220

8.6.3 [Re(η^5-C_5H_4COH)(η^6-C_6H_6)] (**39**) 221

8.6.4 [Re(η^5-$C_5H_4CH_2$)(η^6-C_6H_6)]$^+$ ([**40**](PF_6)) and ([**40**](OTF)) 222

8.6.5 [Re(η^6-$C_5H_4CH_3$)(η^6-C_6H_6)] (**41**) 223

8.6.6 [Re(η^6-$C_5H_4CH_2S(CH_2)_2OH$)(η^6-C_6H_6)] (**42**) 223

8.7 Supplementary Information: Structure and Reactivities of Rhenium and Technetium Bis-Arene Sandwich Complexes [M(η^6-arene)$_2$]$^+$ 225

8.8 Unpublished Experimental Section: Supplementary Information Section: Structure and Reactivities of Rhenium and Technetium Bis-Arene Sandwich Complexes [M(η^6-arene)$_2$]$^+$ 271

8.8.1 [Re(η^6-$C_6H_3(OMe_3)_3$)(η^6-C_6H_6)](PF_6) ([**43**](PF_6)) 271

8.8.2 [Re$(ACN)_6$](PF_6)$_2$ ([**44**](PF_6)$_2$) 271

8.8.3 [Re(η^6-C_6H_6)(dmso-S)$_3$] ([**45**](PF_6)) 272

8.8.4 [Re(η^6-C_6H_6)(CH_3CN)(bipy)]$^+$ ([**46**](PF_6)) 272

8.8.5 [Re(η^6-C_6H_6)(CH_3CN)(dppe)]$^+$ ([**47**](PF_6)) 273

9 References 274

10 Acknowledgement 281

11 Curriculum Vitae 283

Summary

Metal-based drugs are still an indispensable and powerful class of compounds for treatment and imaging of diseases in medicine. In particular, mono-arene complexes of ruthenium and its derivative are intensively explored and are considered as the next generation of anticancer agent. However, due to the absence of a suitable radioisotope, these complexes cannot be used for "theranostic" applications including radio imaging. In contrast to ruthenium, Re/$^{99(m)}$Tc complexes with the same molecular scaffold fulfil the requirements of the "theranostic" approach. A representative fragment for such an approach is the Re/$^{99(m)}$Tc tricarbonyl moiety which has been intensively studied in the last few years. To combine the cytotoxicity with radio imaging Re/$^{99(m)}$Tc bisarene complexes came in the focus of recent research. However, the accessibility of this core is scarily described in the literature. Hence, in thesis new synthetic pathways were development as well as novel precursors complexes evaluated for the synthesis of bis/mono-arene complexes of rhenium. The developed synthetic strategies can be adapted for technetium chemistry and thereby, generating a new platform for theranostic applications. In order to investigate the properties of this type of compounds, a various number of $[Re(\eta^6\text{-arene})_2]^+$ (arene = benzene, toluene, *o*-xylene, *m*-xylene, *p*-xylene, mesitylene, *n*-octylbenzene, tert-butylbenzene, tetralin, fluorene, biphenyl, cyclophane, hexamethylbenzene and naphthalene) compounds were synthesized, starting from $K[ReO_4]$ and in the presence of the strong Lewis acid $AlCl_3$ and zinc as a reductant. Due to trans- and dealkylation side-reaction caused by the use of $AlCl_3$, the corresponding yields of these complexes was between 60%-2%. Most of the $[Re(\eta^6\text{-arene})_2]^+$ complexes show a high stability toward oxygen and water which make them attractive building blocks for the synthesis of biologically active compounds. Exceptions are Re-complexes bearing cyclophane or naphthalene as ligands which are light and thermally sensitive. The $[Re(\eta^6\text{-arene})_2]^+$ complexes have been fully characterized, including the determination of their electrochemical potentials and structural characterization using X-ray diffraction experiments. Moreover, cytotoxicity studies were performed and the complexes $[Re(\eta^6\text{-naphthalene})_2]^+$ and $[Re(\eta^6\text{-biphenyl})_2]^+$ display IC_{50} values in the high micromolar and mid-micromolar range (Hela, A2780).

The mono- and difunctionalization of the $[Re(\eta^6\text{-benzene})_2]^+$ core was achieved by *in situ* metalations with LDA followed by the treatment with an electrophile. Reactions using *n*-BuLi as a metalation agent leads preferentially to the neutral, alkylated product $[Re(\eta^6\text{-}C_6H_6)(\eta^5\text{-}C_6H_6\text{-Bu})]$. The mono- and difunctionalized $[Re(\eta^6\text{-}C_6H_5R)(\eta^6\text{-}C_6H_{6-n}R_n)]^+$ (n = 0, 1; R = COOH, Br, Cl, COEt, C(OH)Ph, $C(OH)(Ph)_2$, $P(Ph)_2$) complexes were isolated and fully characterized. Additionally, the fundamental properties of these compounds were studied. Furthermore, UPLC-MS measurements provide some evidence that functionalization with ester and azide are possible. In order to investigate the reactivity of mono- or

difunctionalized carboxylic acid and halide derivatised rhenium bis-arene complexes, different model compounds $[Re(\eta^6\text{-}C_6H_5R)(\eta^6\text{-}C_6H_{6-n}R_n)]^+$ (n = 0, 1; R = $-SCH_2Ph$, -NHPh, $-CONHCH_2Ph$, $-C_6H_5$-COdpa, OMe) were synthesis via amide bond formation and nucleophilic aromatic substitution. Moreover, the $[Re(\eta^6\text{-benzene})_2]^+$ scaffold was successfully attached to a bioactive substance such as doxorubicin via amide bond formation. The dihydroxo tamoxifen rhenium bis-arene complex was synthesis via Mc-Murry reaction starting from $Re(\eta^6\text{-}C_6H_5COEt)(\eta^6\text{-}C_6H_6)](PF_6)$ and 4,4'-dihydroxybenzophenone. Although this complex is estrogenic no significant cytotoxicity was found in the used cell essay. These functionalized derivatives of $[Re(\eta^6\text{-benzene})_2]^+$ represent novel precursors for the synthesis of new Re bioconjugates.

The neutral complex $[Re(\eta^5\text{-}C_5H_4CHO)(\eta^6\text{-}C_6H_6)]$ was synthesized by a new synthetic pathway in almost quantitative yield with an excess of sodium hydroxide in water at 80°C, starting from $[Re(\eta^6\text{-}C_6H_5Br)(\eta^6\text{-}C_6H_6)]^+$. The ring contraction of the coordinated bromobenzene to a coordinated cyclopentadienyl-system is unprecedented and a mechanism for this reaction was proposed based on ^1H and ^2H NMR spectra and DFT calculations. Further derivatization $[Re(\eta^5\text{-}C_5H_4CHO)(\eta^6\text{-}C_6H_6)]$ were performed via imine formation with benzylamine and reduction of the aldehyde to form the corresponding primary alcohol. These compounds are all fully characterized and represent potentially class of new precursor which can be applied in biological studies.

The pentafulvene complex $[Re(\eta^5\text{:}\eta^1\text{-}C_5H_4CH_2)(\eta^6\text{-}C_6H_6)]^+$ is a new potential precursor. This complex was synthesised by treating $Re(\eta^5\text{-}C_5H_4COH)(\eta^6\text{-}C_6H_6)]$ with trimethylsilyl trifluoro-methanesulfonate or with an aqueous solution of HPF_6. The reactivity of the exo CH_2 group of the pentafulvene ligand was investigated with different nucleophiles such as hydride and thiol. In particular, the latter reaction can be quantitatively performed under physiological conditions in water. This feature shows the high potential of this precursor for the labelling of peptides or proteins.

Naphthalene ligand of the complexes $[Re(\eta^6\text{-naphthalene})_2]^+$ and $[Re(\eta^6\text{-naphthalene})(\eta^6\text{-benzene})]^+$ can be replaced thermally or photochemical. Replacement of the naphthalene ligand in $[Re(\eta^6\text{-naphthalene})(\eta^6\text{-benzene})]^+$ was achieved with triethyl-phosphite, *tert*-butyl isocyanide and 1,3,5-trimethoxybenzene. The first tri-solvato complex $[Re(\eta^6\text{-benzene})(ACN)_3]^+$ was prepared by the treatment of $[Re(\eta^6\text{-naphthalene})(\eta^6\text{-benzene})]^+$ in acetonitrile. While longer reaction times generate the paramagnetic, homoleptic $[Re(ACN)_6]^{2+}$ complex. Reaction of $[Re(\eta^6\text{-naphthalene})(\eta^6\text{-benzene})]^+$ in dmso provide the stable tri-solvato $[Re(\eta^6\text{-}C_6H_6)(dmso\text{-}S)_3]^+$. Both and $[Re(\eta^6\text{-naphthalene})(\eta^6\text{-benzene})]^+$ and $Re(\eta^6\text{-benzene})(sol)_3]^+$ (sol = ACN and dmso) might be new precursors for the synthesis of piano stool complexes in analogies to well-established ruthenium chemistry. While complex $[Re(ACN)_6]^{2+}$ might give access to novel Re(+II) complexes.

1 Compounds Synthesized in this Thesis

1.1 $[Re(\eta^6\text{-arene})_2]^+$ Complexes

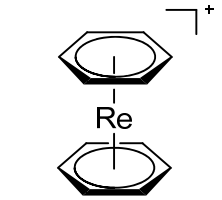

[**1**]$^+$

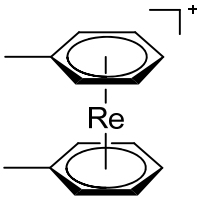

[**2**]$^+$

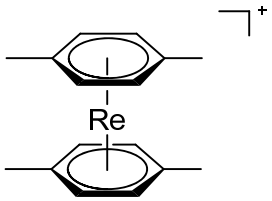

[**3**]$^+$

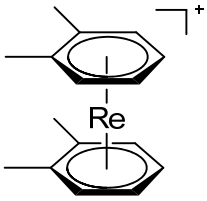

[**4**]$^+$

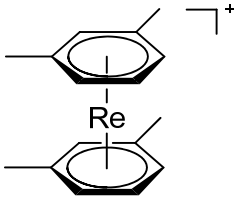

[**5**]$^+$

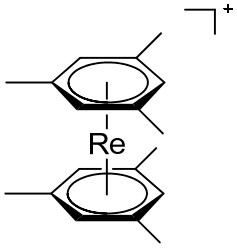

[**6**]$^+$

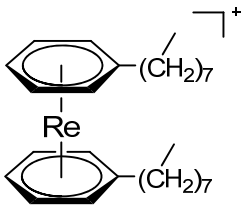

[**7**]$^+$

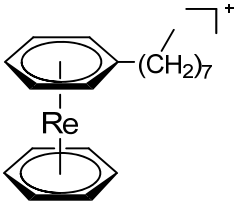

[**8**]$^+$

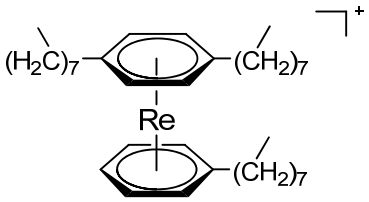

[**9**]$^+$

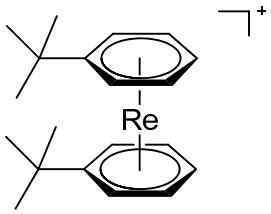

[**10**]$^+$

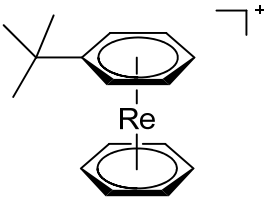

[**11**]$^+$

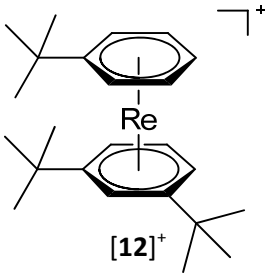

[**12**]$^+$

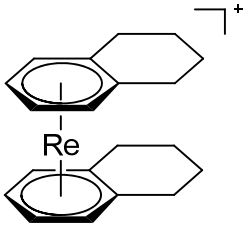

[**13**]$^+$

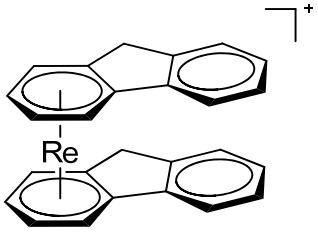

[**14**]$^+$ syn/anti

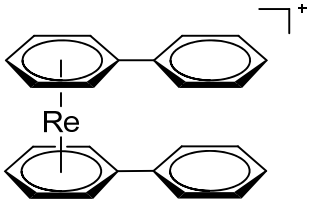

[**15**]$^+$

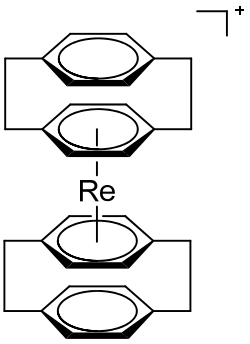

[**16**]$^+$

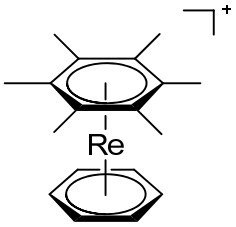

[**17**]$^+$

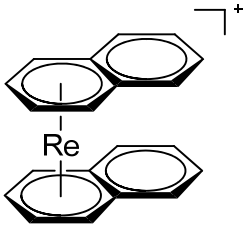

[**7p**]$^+$

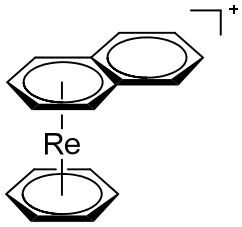

[**6p**]$^+$

1.2 Complexes from the Publication: *Inorg. chem.* 2016, *55*, 11131-11139

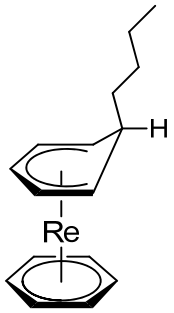

2

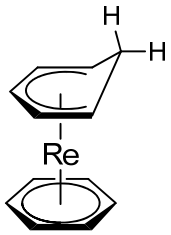

3

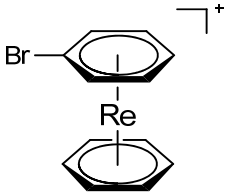

[**4**]$^+$

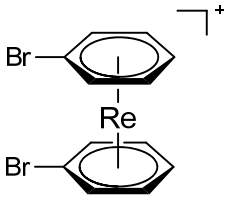

[**5**]$^+$

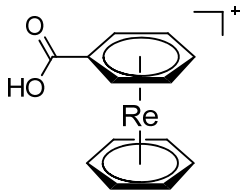

[**6**]$^+$

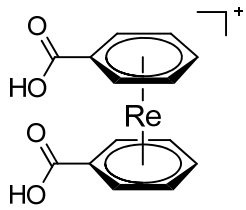

[**7**]$^+$

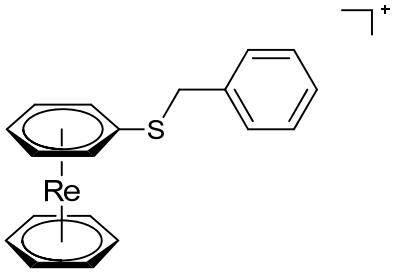

[**10**]$^+$

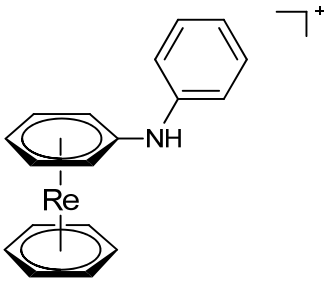

[**11**]$^+$

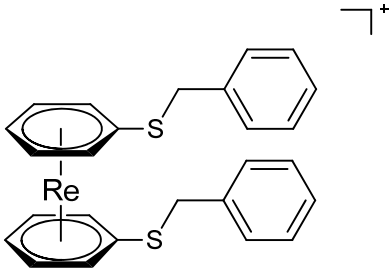

[**12**]$^+$

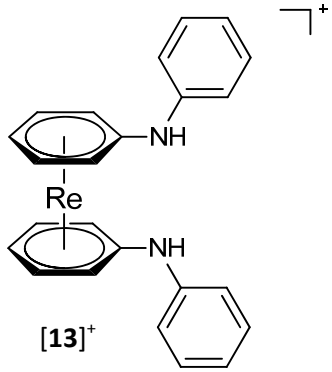

[**13**]$^+$

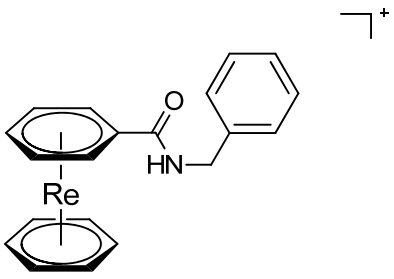

[**14**]$^+$

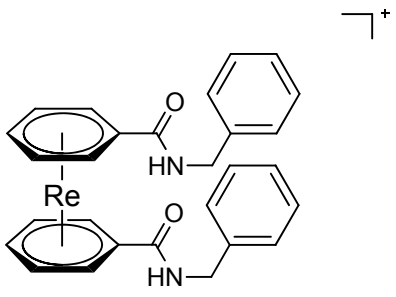

[**15**]$^+$

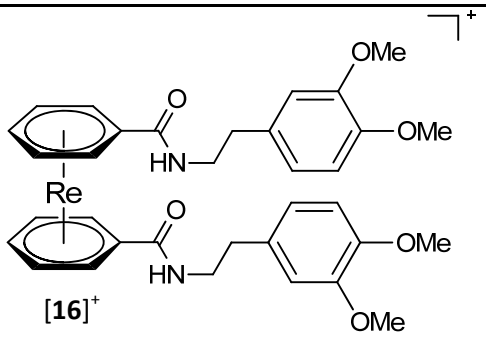

[**16**]$^{+}$

1.3 Complexes related to the Publication: *Inorg. chem.* 2016, *55*, 11131-11139

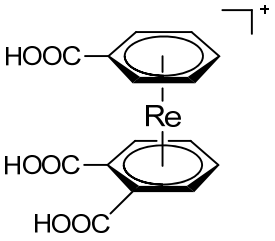

[**17**]$^{+}$

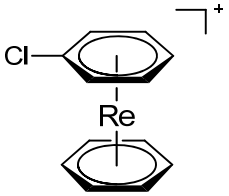

[**18**]$^{+}$

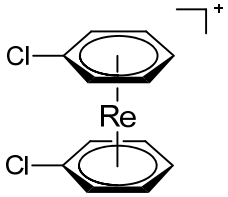

[**19**]$^{+}$

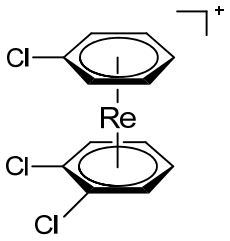

[**20**]$^{+}$

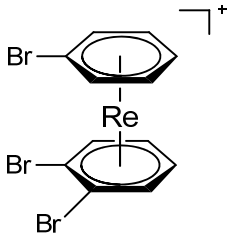

[**21**]$^{+}$

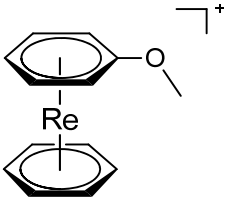

[**22**]$^{+}$

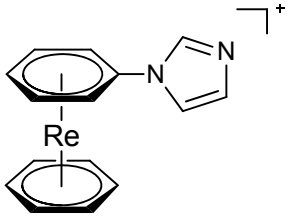

[**23**]$^{+}$

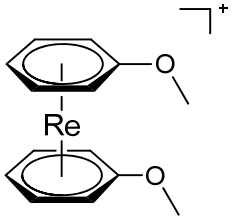

[**24**]$^{+}$

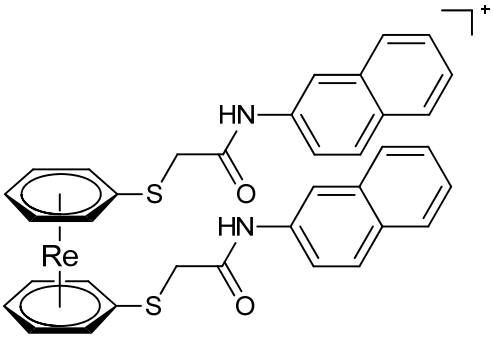

[**25**]$^{+}$

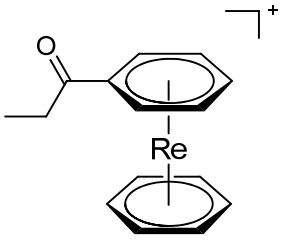

[**26**]$^{+}$

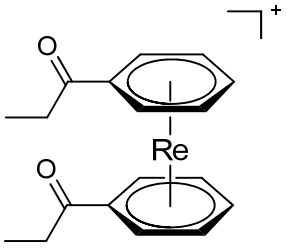

[**27**]$^{+}$

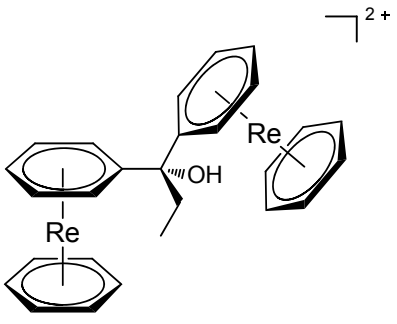

[**28**]$^{2+}$

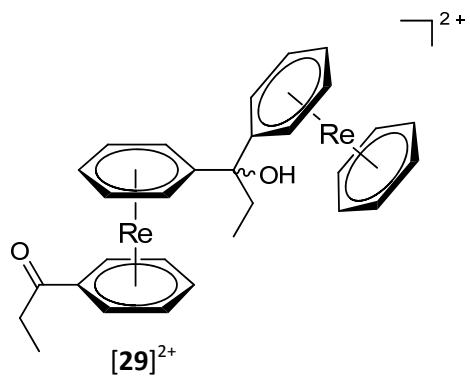

[**29**]$^{2+}$

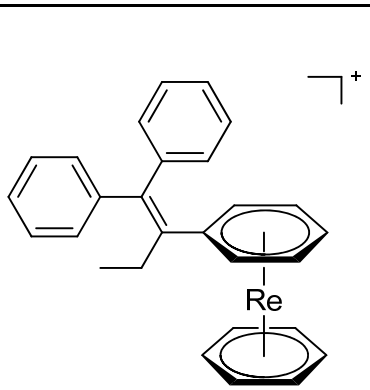

[**30**]$^+$

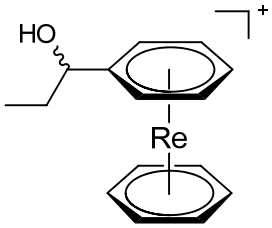

[**31**]$^+$

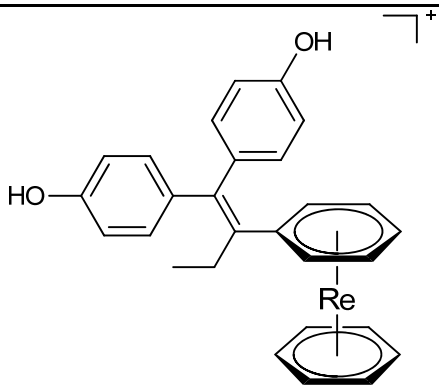

[**32**]$^+$

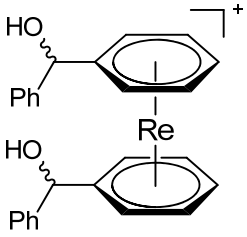

[**34**]$^+$

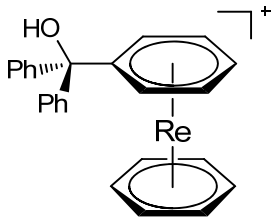

[**35**]$^+$

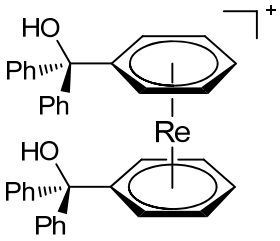

[**36**]$^+$

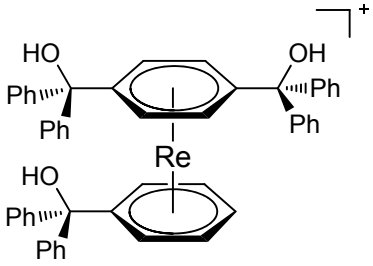

[**37**]$^+$

1.4 Complexes from the Publication: *Inorg. chem.* 2017, *56*, 11, 6297-6301

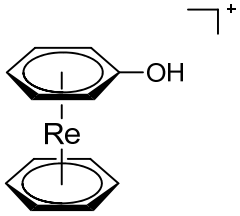

[**2**]$^+$

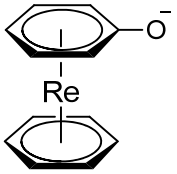

2

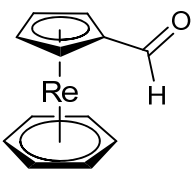

3

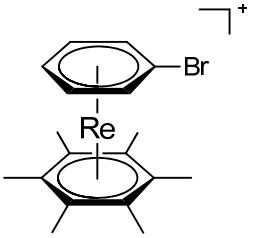

[**4**]$^+$
[**6**]$^+$ = ^{99}Tc

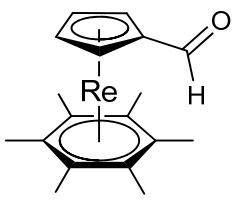

5

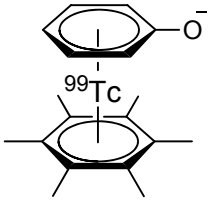

7

1.5 Complexes related to the Publication: *Inorg. chem.* 2017, *56*, 11, 6297-6301

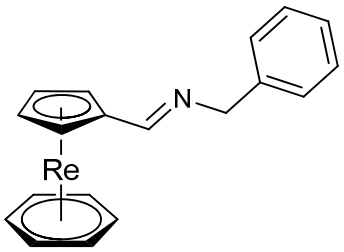

38

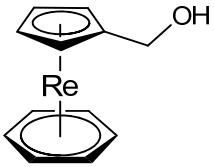

39

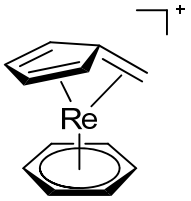

[40]$^+$

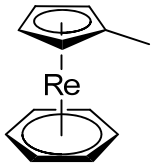

41

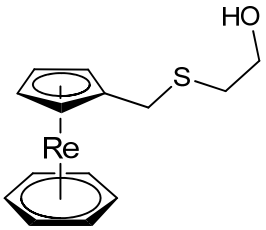

42

1.6 Complexes from the Publication: *Dalton Trans.*, 2017, *46*, 14631-14637

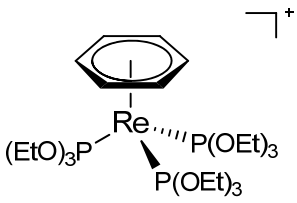

[**8**]$^+$

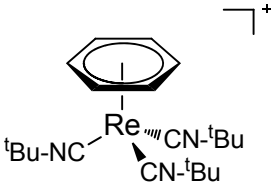

[**9**]$^+$

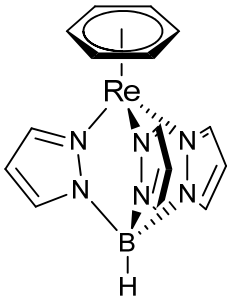

10

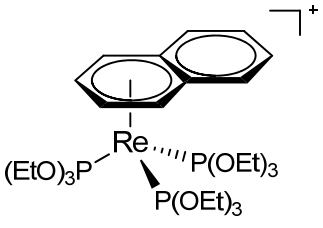

[**11**]$^+$

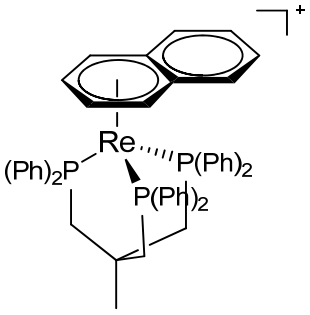

[**12**]$^+$

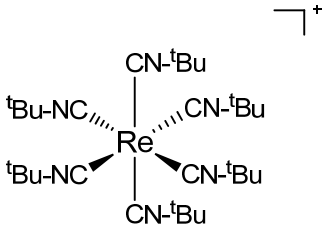

[**13**]$^+$

1.7 Complexes related to the Publication: *Dalton Trans.*, 2017, *46*, 14631-14637

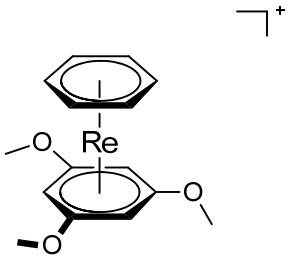

[**43**]$^{+}$

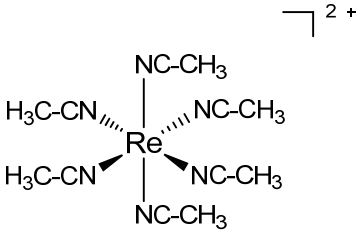

[**44**]$^{2+}$

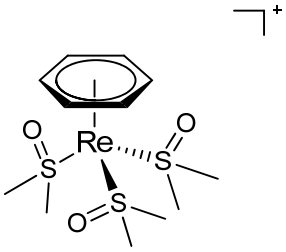

[**45**]$^{+}$

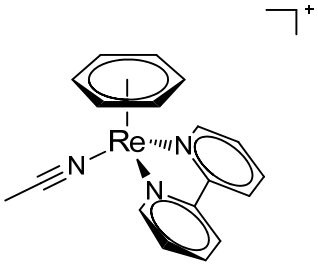

[**46**]$^{+}$

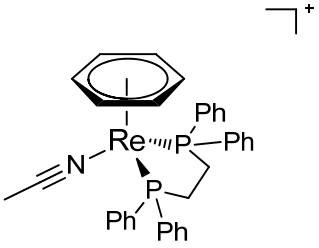

[**47**]$^{+}$

2 List of Abbreviations

ACN	acetonitrile
bipy	2,2'-bipyridine
Boc	COO^tBu
Cp	cyclopentadienyl
Cp*	pentamethylcyclopentadienyl
CV	cyclic voltammetry
COSY	correlated spectroscopy
DMF	dimethylformamide
DMSO	dimethyl sulfoxide
DNA	deoxyribonucleic acid
dppe	1,2-Bis(diphenylphosphino)ethane
DEPT	Distortionless Enhancement by Polarization Transfer
EI	electron ionization
en	ethylenediamine
E_{pc}	cathodic peak potential
equiv	equivalent
ER	estrogen receptors
ESI	electrospray ionization
FDA	Food and Drug Administration
FT	Fourier Transform
HPLC	high-performance liquid chromatography
HR	high-resolution
IL	ionic liquid
IR	infrared
LDA	lithium diisopropylamide
MCF-7	Michigan Cancer Foundation - 7
MO	molecular orbital
MS	mass spectrometry
MTBE	methyl tert-butyl ether

MRC-5	Medical Research Council cell strain 5
NMR	nuclear magnetic resonance
NOE	nuclear Overhauser effect
ORTEP	Oak Ridge thermal ellipsoid plot
OTf	trifluoromethanesulfonate
PCA	perchloroethane
PET	Positron Emission Tomography
PI	phototoxic index
py	pyridine
SHE	standard hydrogen electrode
SPECT	Single-Photon Emission Computed Tomography
S_NAr	nucleophilic aromatic substitution
TFA	trifluoroacetic acid
THF	tetrahydrofuran
TLC	thin-layer chromatography
TMSOTf	trimethylsilyl trifluoromethanesulfonate
Tp	trispyrazolylborate
UV-Vis	ultraviolet–visible
UPLC	ultra performance liquid chromatography

3 Published Parts of this Thesis

Bis-Arene Complexes [Re(η^6-arene)$_2$]$^+$ as Highly Stable Bioorganometallic Scaffolds, Meola, G.; Braband, H.; Schmutz, P.; Benz, M.; Spingler, B.; and Alberto, R. *Inorg. Chem.* **2016**, *55* (21), 11131-11139

A Mixed-Ring Sandwich Complex from Unexpected Ring Contraction in [Re(η^6-C_6H_5Br)(η^6-C_6R_6)](PF$_6$), Meola, G.; Braband, H.; Hernández-Valdés, D.; Gotzmann, C.; Fox, T.; Spingler, B.; and Alberto, R. *Inorg. Chem.* **2017**, *56* (11), 6297-6301

Structure and reactivities of rhenium and technetium bis-arene sandwich complexes [M(η^6-arene)$_2$]$^+$, Meola, G.; Braband, H.; Jord, S.; Fox, T.; Blacque, O.; Spingler, B.; and Alberto, R. *Dalton Trans.*, **2017**, *46*, 14631-14637

Alberto, R. Meola, G. Hernández-Valdés, D. (2019). Technetium and Rhenium Complexes with Aromatic Hydrocarbons as Ligands: An Entry into Biomimetic Imaging. In T. Hirao and T. Moriuchi (Eds.), *Advances in Bioorganometallic Chemistry* (pp. 215-241). Elsevier

4 Introduction

4.1 Metal-Based Drugs

Nowadays, the use of metal-based drugs has become an important alternative approach in medicine for the diagnosis and therapy of diseases. Since the discovery of its inhibition against cell division in bacteria in 1965 and the approval by the FDA in 1978, cisplatin is one of the most effective and widely applied therapeutic agents for the treatment of a number of cancers.[1, 2] Besides the great successes, cisplatin possesses different drawbacks displaying it in severer side-effects (nephrotoxicity, neurotoxicity, nepatotoxicity etc.) and belong that also the arising of drug resistance of specific cancer cells.[3] Consequently, the design and the synthesis of new high potential platinum drugs (Oxaliplatin, Carboplatin) have become important in the field of bioinorganic chemistry. Due to the limitation of derivatives the platinum core and to overcome the undesirable side-effects, the research field of anticancer drugs has been expanded to other metals. In particular, the discovery of ruthenium-containing metal complexes which exhibit similar cytotoxicity had a huge impact and are investigated with big efforts. Currently, two candidates (KP1019, NAMI-A) are in clinical phase II studies. The modes of action of the anticancer metallodrugs in biological systems have been widely investigated and can variate depending on the specific type of metal complex. In the case of cisplatin, the primary target is DNA while other metal-containing chemotherapeutic agents (e.g: RAPTA-type) show selectivity towards proteins, leading to the inhibition of their biological function.[4, 5] In several cases, the mechanism is not fully studied. Nevertheless, the list of promising anticancer therapeutics is still growing including a large variety of different metals. Additionally, metal-containing compounds are used as well as antimalarial (iron), antimicrobial (silver), antiulcer (bismuth), antidiabetic (vanadium), antiarthritic (gold) and antiprotozoal (antimony) drugs.[6-8]

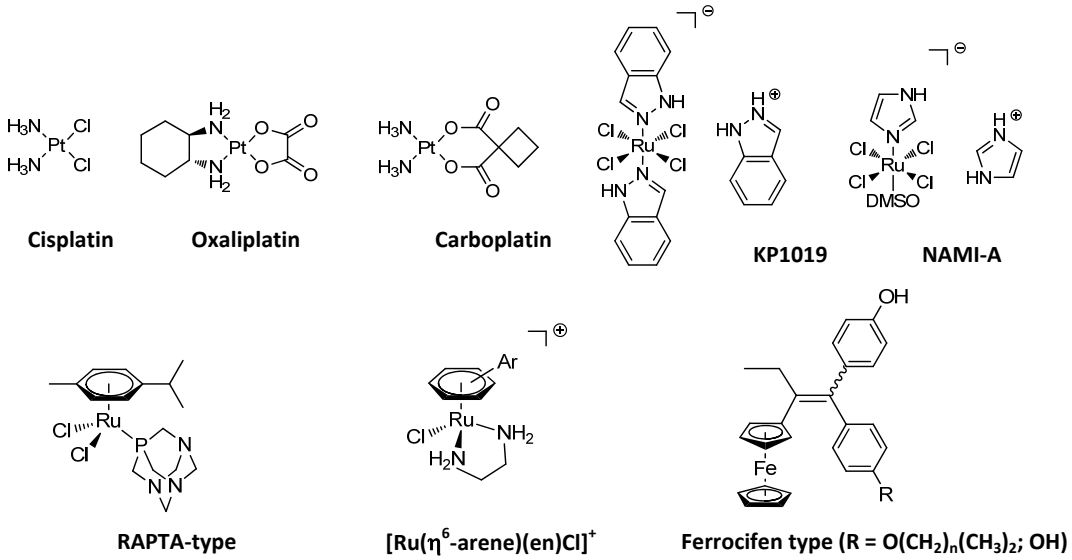

Figure 1: A selection of well-known metalodrugs for application in the medicinal chemistry[6-8]

In contrast to organic pharmaceuticals, organometallic compounds provide a wide spectrum of additional features based on the coordination geometry (3D), kinetics (ligand exchange rates), thermodynamic (stability or inertness) or redox activity of the introduced metal centre.[9] Moreover, organometallic complexes are divided into compounds with metal- or ligand-based reactivities and in complexes mimicking (sub)structures of pharmaceuticals.[10] An example for the latter approach is the successful introduction of redox active ferrocenyl fragments into the structure of tamoxifen which is a potent drug used for the treatment of hormone-dependent breast cancer introduced by Jaouen *et al.* in 1996.[11] In contrast to tamoxifen, the ferrocifen shows not only activity against breast tumours which exhibit at the estrogen receptors (ER(+)) but also towards tumours which lack this receptor (ER(-)) due to the redox properties of the metal.[12] Consequently, the introduction of the metal-fragment into organic lead structures or by binding the fragment to biologically active ligands (e.g. protein, hormone) can improve their activity profile. Thus, the gained diversity in the design of new compounds offers novel mode actions. Besides the application as therapeutic agents, metal compounds were further used in the field of radiopharmaceutical sciences/nuclear medicine as a diagnostic tool involving the synthesis, characterization and biological evaluation of target-specific metal-based radioactive complexes for nuclear imaging. More specifically, the incorporation of γ-emitting radiometals (e.g. ^{99m}Tc and ^{111}In) in complexes is applied for Single Photon Emission Computed Tomography (SPECT) whereas β^+–emitting radiometals were used (e.g. ^{68}Ga and ^{64}Cu) for Positron Emission Tomography (PET).[13-17] A famous example for a well-established SPECT - imaging agent is sestamibi which is also known under the trademark Cardiolite®. The ^{99m}Tc(I) is coordinated over isonitrile ligands $[^{99m}Tc(CNCH_2C(CH_3)_2OCH_3)_6]^+$ (Figure 2), displaying lipophilic and kinetically inert properties. This complex is originally developed as a SPECT myocardial imaging agent but currently, it is also used for both early cancer detection and non-invasive monitoring of the tumour Multidrug Resistance (MDR) transport function. [4, 18, 19]

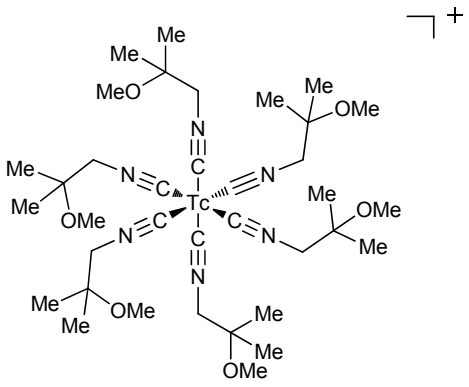

Figure 2: Chemical structures of Cardiolite®.

Moreover, it is worth to mention that radiopharmaceuticals containing β^--emitting radiometals were mainly developed for internal radiotherapy. For example, bone pain palliation is treated with ^{186}Re-HEDP (HEDP = hydroxyethylidenediphosphonate).[20] All in all, most of these examples, as shown here, display the large spectrum of application, reflecting the importance of metal-based compounds in the medical field. Hence, the design of new (organo-)metallic compounds comprising the enhancement of the effectiveness, the reducing of side effect and the exploration of new mode of actions is still an ongoing topic in bioinorganic as well as medicinal chemistry.[21]

4.2 The Role of Rhenium in the Bioinorganic and Medicinal Chemistry

Compared to ruthenium and platinum, the number of example of cytotoxic rhenium organometallic compounds found in the literature is relatively small. Promising anticancer activity has been found in Re(I) tricarbonyl bisimine complexes $[Re(CO)_3(bisimine)L]$ (L = monodentate pyridine derivative or a halide (Cl, Br) ligand). Their anti-proliferative activities against various human cancer cell lines are comparable with cisplatin or even better.[22] The coordination with *N,N,N*-tridentate ligand (dipicolylamine (Dpa) and *N,N*-bisquinoline (BQ)) to the *fac*-$[Re(CO)_3]^+$ moiety provide another type of compounds which exert cytotoxic properties. In particular, the coupling of them to target specific bioconjugated (e.g. folate, Vitamin B_{12}) which bind to overexpress receptors display in some cases an increase of their cytotoxicity from millimolar up to micromolar.[23, 24] Rhenium(I) tricarbonyl complexes with alkoxo/hydroxo, N-O bidentate, P-P or Se-Se ligand system are further compounds showing activity against suspended cancer cell line or being active only to specific cancer line.[25-28] As shown above, metal fragments are incorporated in organic pharmaceutically active lead structure that binds to enzymes or receptor for enhancing its selectivity and activity. For this purpose, the cyclopentadienyl (Cp) ligand has been introduced to incorporate the $Re(CO)_3$ core, mimicking the phenyl ring in the lead structures. The derivatisation of tamoxifen with a *fac*-$[Re(CO)_3]^+$ moiety is only one example where this approach is successfully applied. Even though the modification decreases the binding affinity to the receptor, cytotoxicity assays on MCF-7 ER(+) with Re-Tamoxifen conjugates show slightly enhancement of the activity compared to pure organic pharmaceutical.[29] Among this promising pharmaceutical property, rhenium and technetium are a so called “match pair”, meaning that the two elements in lower oxidation state shows very similar physical properties. This features allowed preparing “hot” ^{186}Re/^{188}Re and ^{99m}Tc analogues compound that can be applied for radio-imaging as well as for therapy using the same ligand system.[30, 31] In other words, rhenium has the potential to be a multimodal molecule since the hot rhenium analogues could be used for in vivo biodistribution and pharmacokinetics studies which are crucial for the development of new metallodrugs.

However, as represented in this paragraph, the rhenium tricarbonyl scaffold bearing a biologically active ligand system found large interest due to strong π-acceptor properties of CO ligands which stabilized the Re(I) centre. This thesis aims at the introduction of a novel rhenium building block for application in biological systems based on rhenium mono-/bis-arene complexes.

4.3 Mono-/Bis-Arene Metal Complexes in the Bioinorganic Chemistry

4.3.1 Mono-Arene Metal Complexes

Arene metal complexes have been found large attention in various fields of chemistry such as catalysis, organic and bioinorganic chemistry.[32] In particular, bioinorganic chemistry is dominated mainly by ruthenium (and to a smaller extent by osmium) piano stool complexes. These compounds have been handled as potent anticancer agents.[33, 34] The variation of the ligand system with monodentate, bidentate and arene allows the fine-tuning of its pharmacological and electronic properties as well as the introducing of targeting functions (Figure 3, left). For example, the activity of $[Ru(\eta^6\text{-arene})(en)(Cl)]^+$, can be increased by varying the ring size of the arene (benzene < p-cymene < biphenyl < dihydroanthracene < tetrahydroanthracen). Additionally, these compounds exhibit enhanced activity against cisplatin-resistant (A2780) human ovarian cancer cells.[35, 36]

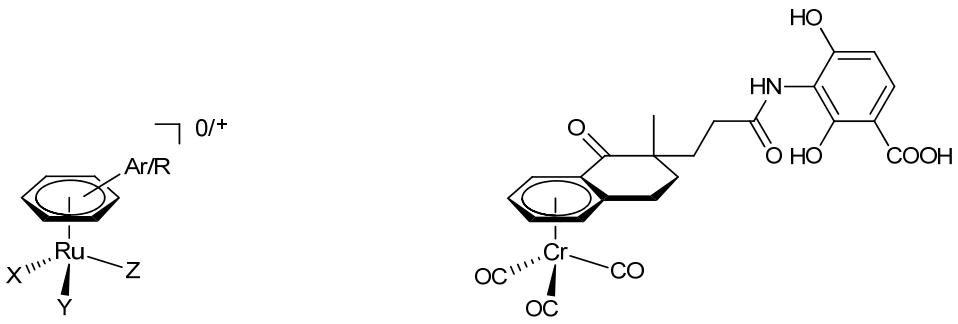

Figure 3: Typical structure of Ru(II) half-sandwich complexes and examples of chelating ligand (X= mono-dentate; Y/Z = mono- or bidentate; Ar = arene; R = biological active ligand) (left). Organometallic bioconjugates derived from platensimycin (right)

Due to their flexibility and diversity of the ligand system, the Ru(II) half-sandwich complexes provide a wider mode of action displaying not only interaction with the primary target DNA like cisplatin but also with proteins. Different studies show that these systems can interact either with nucleobase/DNA or intercalate with DNA. Moreover, these compounds can interact with amino acids or bind in the active site of proteins (enzymes) as well, thereby increasing their field of use in the medicinal chemistry.[33] Besides the chemistry of ruthenium half-sandwich complexes, $[Cr(\eta^6\text{-}$

arene)$(CO)_3$] complexes were used as integral parts of targeting structures. The {$Cr(CO)_3$} subunit has been coordinated to a variety of arene rings in organic lead structures such as steroid hormones and amino acids.[37, 38] One of the reasons for introducing this moiety in bioactive molecules is the CO ligands which provide an excellent probe for detecting the complexes in the subcellular space.[39] Furthermore, the incorporation of the lipophilic [$Cr(\eta^6$-arene$)(CO)_3$] fragment into platensimycin (a potent antibiotic) led to an unexpected cytotoxic activity against mammalian cancer cell lines which enlarge the field of use of the compound (Figure 3, right).[40]

4.3.2 Bis-Arene Metal Complexes

In contrast to mono arene metal complexes, bis-arene metal complexes are less represented for the use in biological system. The ruthenium bis(η^6-arene) complex [Ru(η^6-p-cymene)(η^6-CQDP)][BF_4]$_2$ (CQDP = chloroquine diphosphate) (Figure 4, left) is one of the few compounds which is coordinated to a biologically active molecule, showing in vitro antimalarial and antitumor activity. The complex was prepared by reacting [Ru(η^6-p-cymene)Cl_2]$_2$ with chloroquine diphosphate in water in the presence of $AgBF_4$ in 78% yield.[41] There are few examples of ruthenium bis-arene complexes coordinating to the phenyl moieties of biologically active ligands such as amino acid (e.g.: phenylalanine), dipeptide or dopamine (Figure 4, right) in perspective of protein labelling for the analysis and molecular recognition of enzyme active sites. [42-45] Furthermore, the ruthenium bis-arene frameworks have been used for N-terminal labelling of amino acids and peptides. [46]

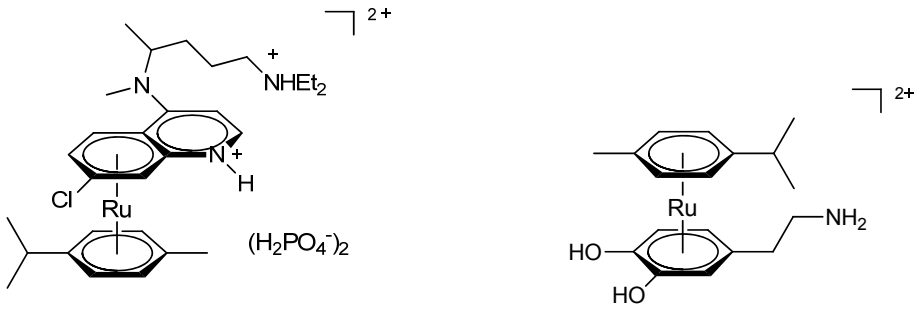

Figure 4: Structure of [Ru(η^6-p-cymene)(η^6-CQDP)] acting as antimalarial and antitumor agent (left). Structure of a dopamine coordinated ruthenium bis(η^6-arene) (right).

The coordination of [M(η^6-*p*-cymene)]$^{2+}$ (M = Ru, Os) unit to the phenyl group of the artificial sweetener aspartame showed mainly that the chemical properties of the bioactive ligand changed (acidity, electronic and redox properties), leading to no recognition of the corresponding receptor. Furthermore, these two complexes are tested against different cancer line without showing any considerable cytotoxicity.[47] Similar result has been observed by the derivatisation of tamoxifen with a

[Ru(η^6-*p*-cymene)]$^{2+}$ core to [Ru(η^6-*p*-cymene)(η^6-tamoxifen)](OTf)$_2$ which display no antiproliferative activity against human breast cancer MCF-7 cells presumably due to the bulky {Ru(η^6-p-cymene)} fragment which hindered to fit into the pocket of estrogen receptor. However, moderate anticancer activity shows [Ru(η^6-*p*-cymene)(flavanone)](PF$_6$)$_2$ bearing a flavanone as an active ligand. The mode of action of this active ruthenium bis(η^6-arene) is described as single mode of interaction with DNA.[48]

4.4 Syntheses, Stabilities, Properties and Reactivities of Bis-arene Complexes

4.4.1 History of Metal-Bis-Arene Complexes

The discovery and the correct structure interpretation of ferrocene in 1952 by Wilkinson and Fischer led to realize that apart of cyclopentadienyl ligand, aromatic hydrocarbons could also act as ligands for transition metals.[49, 50] Thus, three years later namely in 1955, the first metal-bis-arene sandwich complexes were synthesised by Fischer and Hafner by reducing anhydrous $CrCl_3$ with Al/$AlCl_3$ in benzene (Fischer-Hafner synthesis).[51] Since then a large number of metal-bis-arene complexes, containing transition metal, main group element or even lanthanides have been synthesised and characterized, respectively.[32]

4.4.2 Synthesis of Metal-Bis-Arene Complexes

In contrast to the preparation of the mono(η^6-arene) metal complexes, bearing additionally σ-donors (e.g halide, solvent molecule) or π-acid-ligands (e.g. CO, Cp), only a few approaches are described for the synthesis of metal-bis-arene complexes in the literature. As mention before the neutral dibenzenchromoium [Cr(η^6-C_6H_6)$_2$] was synthesised with the Fischer–Hafner method. This approach involved metal halide, AlX_3 (Lewis acid; halide abstractor), the presence or absence of a mild reductant (e.g Al, Zn) and the corresponding arene.[51] This reaction was also successfully applied for transition metals, lanthanides and actinides providing different results. Based on the nature of the metal it is possible to isolate not only neutral complexes but also mono- or dicationic species (e.g. [Re(η^6-arene)$_2$]$^+$, [Ru(η^6-arene)$_2$]$^{2+}$).[32, 52, 53]

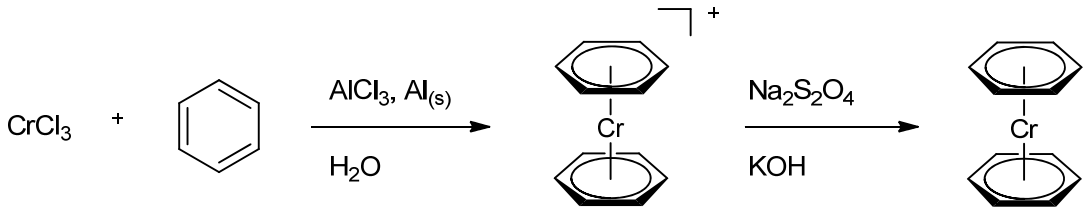

Scheme 1 Synthesis of Cr(η^6-C_6H_6)$_2$ (Fischer-Hafner)

Lanthanides (LnX_3) and halides of group metals (MX_4) generate under these conditions mainly mono-arenes of general formula $M(\eta^6\text{-arene})[(\mu\text{-}X)_2AlX_2]_2$ and $Ln(\eta^6\text{-arene})[(\mu\text{-}X)_2AlX_2]_3$ with bridging tetrahaloaluminato groups.[54, 55] Nevertheless, this synthesis method possesses some drawbacks concerning the reactivity of functionalized arenes. In fact, the reaction with oxygen- or nitrogen-containing arenes is strongly limited due to the presence of $AlCl_3$ which forms Lewis adducts. Furthermore, reactions with methyl substituted arenes undergo trans or dealkylation reactions under these conditions.[56]

To overcome these problems, the metal vapour synthesis has been developed as an alternative method which was introduced by Timms in 1969.[57] This method comprises mainly the evaporation of metal powder in an appropriate device by resistively heat or electron bombardment under high vacuum. Subsequently, the vaporized metal condensate on a nitrogen cooled surface of the reactor together with the vapour of the organic compound (arene) which leads to the formation of metal bis(η^6-arene) compounds.[58] Despite the use of a special device and the generated low yields, this technic allows to synthesis compound which cannot be obtained with other methods. For example, bis(η^6-arene) containing functional groups such as halide, esters, nitriles, or polynuclear aromatics. Furthermore, the synthesis of mixed bis(arene)(arene') system is also one of the advantages of this method.[59] Alternative approaches are cyclotrimerization of alkynes, reductive complexation, halide elimination which can be applied more in specific cases.[60] For instance, halide elimination was used for the synthesis of ruthenium bis(η^6-arene) complexes (Scheme 2).[61]

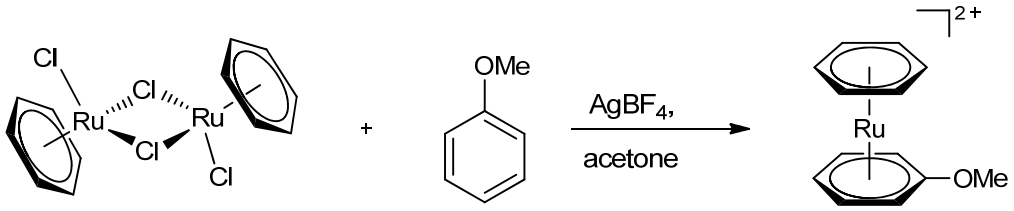

Scheme 2: The synthesis of $[Ru(\eta^6\text{-}C_6H_6)(\eta^6\text{-}C_6H_6OMe)^{2+}$ starting from the dimeric $[Ru(\eta^6\text{-}C_6H_6)Cl_2]_2$ via halide elimination.

4.4.3 Structure and Properties of Metal-Bis-arene Complexes

The coordination modes of the arenes to the metals can be varied from the more typically η^6 fashion acting as neutral 6 e^- donor ligand to the less represented η^4 and η^2 variants.[62] According to the MO scheme of the eclipsed $Cr(\eta^6\text{-}C_6H_6)_2$, the bindings situation of metal bis arene is comparable to that of

metallocenes. The main difference is based on the binding properties of e_{2g} orbitals. In the case of Cr^0/C_6H_6, the basis orbital are energetically more similar than for ferrocene and, furthermore, the overlap quality of the ligand π orbitals with the Cr($3d_{(xy),\ (x^2-y^2)}$) orbitals increase with the increase of the ring size. Thus, the δ back bonding in metal-bis-arene complexes is more prominent than in ferrocene which is reflected by a slight polarization of the Cr-C_6H_6 bonds (δ^+_{Cr} = +0.7; $\delta^-_{C_6H_6}$ = -0.35).[63] The bond energy (40 kcal/mol; 167 kJ/mol) is smaller than in ferrocene (52 kcal/mol; 217 kJ/mol), and the rotation barrier about the Cr-ring axis is very weak (< 1 kcal/mol; 4.2 kJ/mol).[64, 65] As illustrated in Table 1, most of the bis(η^6-arene) complexes tend to favour metals in low oxidation states. In particular, zero valent M(η^6-C_6H_6)^0 of the group 4, 5 and 6 are oxygen sensitive due to weak π-acceptor properties of the benzene ligand. Whereas the resulted cations for the group 6 bearing 17e$^-$ are, in general, more stable controversially to the 18e$^-$ rule.[66] Notably, motification of the benzene ligand in Cr(η^6-C_6H_6)$_2$ with a more electron-withdrawing group such as chlorobenzene leads to an air stable complex (Cr(η^6-$C_6H_5Cl_2$)$_2$).[59]

Table 1: Properties of metal-bis(η^6-arene) complexes[66]

Complexes	Electrons	Colour	Miscellaneous
Ti(η^6-C_6H_6)$_2$	16	red	air-sensitive, autocatalytic decomposition in aromatic solvents
V(η^6-C_6H_6)$_2$	17	red	very air-sensitive, paramagnetic, reducible to [V(η^6-C_6H_6)$_2$]$^-$
Cr(η^6-C_6H_6)$_2$	18	brown	air-sensitive, the cation [Cr(η^6-C_6H_6)$_2$]$^+$ is air-stable. E° = -0.69 V in DME against SCE
Mo(η^6-C_6H_6)$_2$	18	green	very air-sensitive
W(η^6-C_6H_6)$_2$	18	yellow-green	less air-sensitive than Mo(η^6-C_6H_6)$_2$
[Tc(η^6-C_6H_6)$_2$]$^+$	18	pale yellow	air-stable [67]
[Re(η^6-C_6H_6)$_2$]$^+$	18	yellow	air-stable [52]
[Fe(η^6-C_6H_6)$_2$]$^{2+}$	18	orange	decomposition in solution (CH_3CN)
[Ru(η^6-C_6H_6)$_2$]$^{2+}$	18	yellow	air-stable[68]

4.4.4 Reactivity of Metal-Bis-Arene Complexes

The reactivity of metal-bis-arene complexes is quite different compared to the metallocene chemistry due to the nature of the coordinated ligand. Reactivity can occur on the coordinated (η^6-arene) as well as on the metal centre.[69] The reactivity of the coordinated (η^6-arene) is mainly influenced by the nature of the coordinated metal. Most studies have been performed with

chromium bis(η^6-arene) compounds. In contrast to metallocene as well as uncoordinated arene molecule, metal-bis-arene complexes do not undergo electrophilic aromatic substitution due to the deactivation of the arene by coordinated metal and easily oxidising and decomplexation properties of such complexes (metal centred reactivity).[70] Even though the reactivity is strongly depended on various parameters, there are some general reactions which can be performed with metal-bis-arene complexes. So called arene exchange or arene displacement is a frequently applied reaction. In principle, the coordinated arene can be substituted by mono-, di- or trident ligand for the preparation of half sandwich complexes or by another arene (e.g functionalized arene). The latter is a useful method to synthesised functionalized bis(η^6-arene) complexes, replacing the adverse metal vapour synthesis. In the case of Cr(η^6-C_6H_6), the benzene ligand is kinetically inert, meaning the use of a catalysator (usually $AlCl_3$) is needed for the replacement which is inapplicable for functionalized arenes.[71] Alternatively, the replacement of naphthalene ligands in Cr(η^6-naphthalene)$_2$ can be performed under milder condition due to the much more labile metal-naphthalene bond.[72] This enhanced reactivity which is also called "naphthalene effect" was described by Trimmis and Kündig.[73] Due to this phenomenon, the metal can undergo facile ring slippage from e.g. $\eta^6 \rightarrow \eta^4$, thereby, opening a coordination site on the metal centre for the incoming ligand.[74] This process can be induced thermally as well as photochemically for a number of transition metals. The replacement of one or both naphthalene ligand can be controlled with the amount of the ligand or with the electronic properties of the ligand. Moreover, this method is frequently applied in the ruthenium chemistry, using a mixed ligand system like [Ru(η^6-$C_{10}H_{10}$)(L)]$^{2+}$ (L = benzene, Cp) as starting material.[32, 75, 76]

Metalation reaction with e.g. *n*-butyllithium on the coordinated arene is an alternative method for the preparation of functionalized bis(η^6-arene) complexes. Due to the coordination to the metal, protons of the arene became more acidic which facilitate proton/lithium exchange, as compared to the uncoordinated arene molecule.[77] The formation of a mixture of mono and dilitiated species is still a drawback and can be only partially controlled. In some cases, it is possible to separate these two species due to different physicochemical properties.[78] Nevertheless, this reaction allows the introduction of functionalities (e.g. halides, carboxylic acid) which can be further modified.[79] Besides the increased acidity of the arene protons, the metal centre can influence the rate of nucleophilic substitution (S_NAr) as well as solvolysis (Figure 5).[69] For example, the rate of nucleophilic substitution of chloride by $[OMe]^-$ is enhanced by up to 10^{15} times with respect to the uncoordinated arene, when chlorobenzene is coordinated to a [Cr(η^6-arene)] fragment.[80]

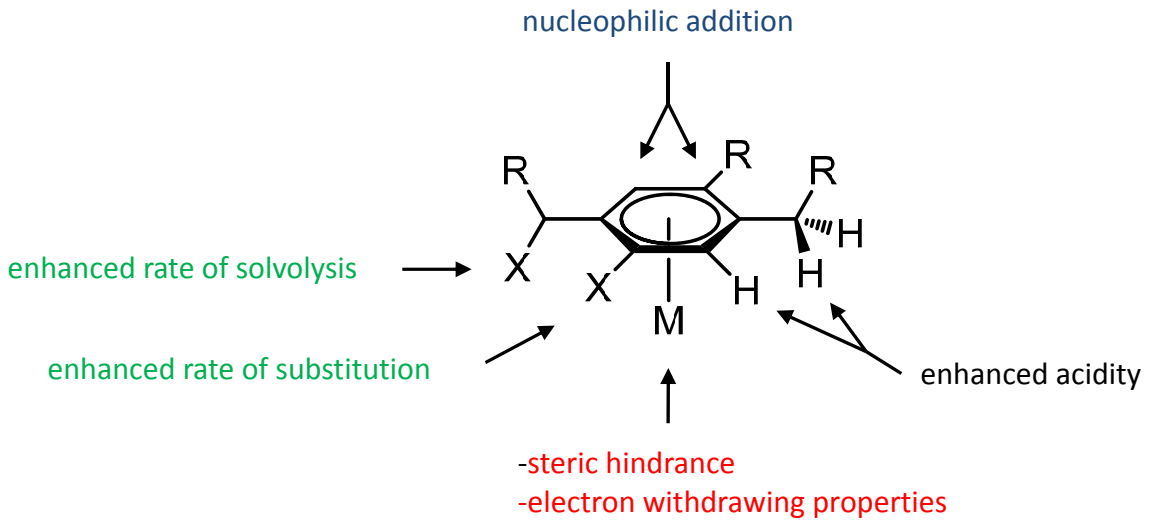

Figure 5: Reactivity and properties of the coordinated arene ring

Nucleophilic addition on the coordinated arene is more prominent to cationic bis(η^6-arene)$^{+/2+}$ species, thereby the habicity of the coordinate arene decreases (for example $\eta^6 \rightarrow \eta^5$).[81] A similar behaviour is also observed for the two-electron reduction of e.g. $[Ru(\eta^6\text{-}C_6Me_6)_2]^{2+}$, providing a 20 valence electron complex. To retain the 18 VE rule, one arene is coordinated in a η^4-mode $[Ru(\eta^6\text{-}C_6Me_6)(\eta^4\text{-}C_6Me_6)]$.[82]

4.5 Rhenium/$^{99(m)}$Technetium Mono- and Bis(η^6-arene) Chemistry: A Small Overview

4.5.1 Rhenium Mono and Bis(η^6-arene) Complexes

Mono- and bis(η^6-arene) complexes of group seven are less explored as compared to other transition metals. One reason might be the difficult accessibility or availability of suitable precursors for the preparation of such complexes. The isolation of the manganese analogues $[Mn(\eta^6\text{-arene})_2]^+$ (arene = benzene/hexamethylbenzene) proved to be very difficult due to its high instability which was described by Fischer *et al.* in 1967.[83] However, the first and more stable rhenium bis(η^6-arene) complex was synthesised in 1957 using the Fischer–Hafner process. Starting from rhenium(V)pentachloride, they were able to isolate $[Re(\eta^6\text{-benzene})_2]^+$ and $[Re(\eta^6\text{-mesitylene})_2]^+$ in low yields of 2% and 3%, respectively.[84] In 1966, the same research group published the synthesis of $[Re(\eta^6\text{-}C_6(CH_3)_6)_2]^+$ with optimised reaction condition using 12 eq. of $AlCl_3$, increasing the yields to 12-15%. Reduction experiments with $[Re(\eta^6\text{-}C_6(CH_3)_6)_2]^+$ and $[Re(\eta^6\text{-}C_6H_6)_2]^+$ under the presence of sodium and NH_3 led to the nucleophile addition of a hydride (H^-) to the arene ring instead to the

expected Re(0) species. Nevertheless, the paramagnetic and highly unstable [Re(η^6-$C_6(CH_3)_6)_2$] was detected by the reduction with lithium via EPR measurement at 77 K. Increasing the temperature leads to the oxidation of the metal centre (Re(0)→Re(I)) and consequently the formation of a dimer [(η^6-$C_6(CH_3)_6)_2$Re(I)(η^5-$C_6(CH_3)_6$)(η^5-$C_6(CH_3)_6$)Re(I)(η^6-$C_6(CH_3)_6)_2$]. In this dimer, the two hexamethyl-cyclohexadienyl moieties are bridging two rhenium centres (Figure 6). Of note, the structure was postulated according to NMR- and IR measurements.[85]

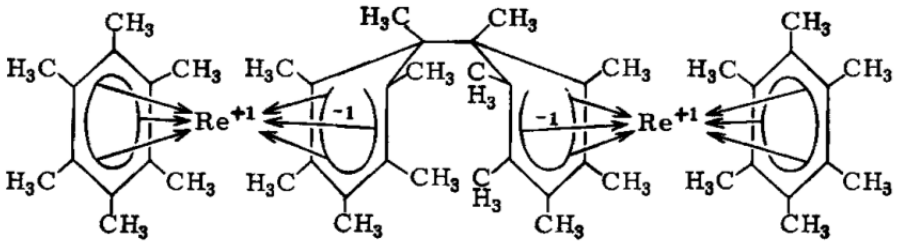

Figure 6: Original image (1966) of the postulated structure [(η^6-$C_6(CH_3)_6)_2$Re(I)(η^5-$C_6(CH_3)_6$)(η^5-$C_6(CH_3)_6$)Re(I)-(η^6-$C_6(CH_3)_6)_2$].[52]

Almost 50 years later, Kudinov *et al.* reported an improved synthesis of various cationic rhenium bis(η^6-arene) complexes [Re(η^6-arene)$_2$]$^+$ (arene = benzene, toluene, o-xylene, p-xylene, mesitylene) in 30–40% yield starting from $KReO_4$. Additionally, zinc and $AlCl_3$ were used as reducing agent and Lewis acid, respectively. Beside the structure determination of [Re(η^6-benzene)$_2$]$^+$ and [Re(η^6-mesitylene)$_2$]$^+$, they were able to isolate [Re(η^6-naphthalene)$_2$]$^+$ in low yield (5%). Furthermore, ligand exchange reactions of [Re(η^6-naphthalene)$_2$]$^+$ with ^{t}BuNC displayed the possibility to replace both naphthalene ligand, leading to the formation of [Re(^{t}BuNC)$_6$]$^+$.[52]

Rhenium half-sandwich compounds, [Re(η^6-arene)(L)$_3$]$^+$ and Re(η^6-arene)(L)$_2$X (L = CO, PMe_3, PPh_3; X = H, Hal, Me, Ph, etc.) were explored more in details compared to the bis(η^6-arene) complexes. However, the rhenium mono(η^6-arene) complexes reported in the literature are mainly dominated by methylated arene as well as by CO or dppe ligands which are directly introduced due to the use of the corresponding precursor. A common synthesis of arene rhenium tricarbonyl compound is the treatment of bromopentacarbonylrhenium $ReBr(CO)_5$ with AlX_3 (X = Cl, Br) in the corresponding arene at elevated temperature.[86] A less used method for this type of compounds is refluxing $ReBr(CO)_5$ in a mixture of the corresponding arene and CF_3COOH. The reaction was performed mainly with different methylated arene and in a lesser extent with functionalised arene (e.g. 2,4,6-$Me_3C_6H_2(CH_2)_3COOH$), which are so far the only reported functionalized mono arene rhenium compound in the literature.[87] The stability of these compounds increases with the grad of methylation of the arene. The coordinated arene display a similar reactivety in terms of nucleophilic

addition, whereas the reactivity of the {$Re(CO)_3$} fragment is limited due to strong bonding interaction.[88] However, replacements of one CO ligand by halide or alkane were already reported.[89, 90] In 1984, Green et al reported the synthesis of the dimer-[$Re(\eta^6\text{-}C_6H_6)(PMe_3)_2]_2$ (20%) and mono-arene [$Re(\eta^6\text{-}C_6H_6)(PMe_3)Ph$] (2%) by cocondensation of rhenium atoms with a benzene trimethylphosphine mixture, which are precursors for [$Re(\eta^6\text{-}C_6H_6)(PMe_3)R$] (R = H, Cl, I, Me, Et, CH = CH_2 or Ph) and [$Re(\eta^6\text{-}C_6H_6)(PMe_3)X_2](BF_4)$ complexes.[91, 92] This type of complexes were not further investigated presumably due to the inconvenient and difficult synthesis. The heptahydrido L_2ReH_7 (L = PPh_3, dppe,) compound is an additional precursor to synthesis mono(η^6-arene) compounds with the sum formula [$Re(\eta^6\text{-}C_6H_6)(L)_2H$] and [$Re(\eta^6\text{-}C_6H_6)(L)_2H_3$] by thermally or photochemically reactions.[93-95] Further rhenium arene compounds bearing specific ring systems e.g. indene, η^5-cycloheptatrienyl, η^5-cycloheptadienyl, η^5-cyclopentadienyl were mainly synthesized by cocondensation reaction in rather low yields. [96, 97] The latter compound [$Re(\eta^6\text{-}C_6H_6)(\eta^5\text{-}C_6H_5)$] was also synthesised by Fischer *et al*. in 1968, starting from $ReCl_5$ under the presence of different Grignard reagent (i-C_3H_7MgBr/C_5H_5MgBr) and additionally cyclohexadiene in diethyl ether. Despite the highly used quantities of $ReCl_5$ (5.68g), the mix Cp/benzene complex [$Re(\eta^6\text{-}C_6H_6)(\eta^5\text{-}C_6H_5)$] were isolated in 8 % yield.[98]

4.5.2 Technetium Mono- and Bis(η^6-arene) Complexes

The technetium arene chemistry is even less developed as its rhenium analogues due to the difficult handling of the metal and the need of an appropriate infrastructure. Nevertheless, the first synthesis of [$^{99(m)}Tc(\eta^6\text{-}C_6H_6)_2]^+$ was described in 1961 by Baumgärtner *et al*. The complex was prepared by element transmutation using bombardment of a [$^{98}Mo(\eta^6\text{-}C_6H_6)_2$] target with thermal neutrons.[99] In the same time, Fischer et Palm synthesised successfully [$^{99}Tc(\eta^6\text{-arene})_2]^+$ (arene = benzene, hexamethylbenzene) compounds with the Fischer-Hafner process starting from [$^{99}TcCl_4$].[100] Applying this procedure, in 1991 Wester *et al.* synthesis a variety of methylated [$^{99(m)}Tc(\eta^6\text{-arene})_2]^+$ to study the biodistribution of these complexes.[101] However, due to difficult reproducibility as well as the almost incompatible condition for the synthesis of the metastable [$^{99m}Tc(\eta^6\text{-arene})_2]^+$, these complexes were not further investigated. In 2015, Alberto *et al.* improved the synthesis of these type of complexes performing the reaction without the use of a metallic reducing agent. A various of methylated [$^{99}Tc(\eta^6\text{-arene})_2]^+$ were isolated in good yield and fully characterized, including electrochemical properties and structure determination, respectively. Moreover, the syntheses of the ^{99m}Tc analogues were optimised by applying a novel ionic liquid extraction pathway.[67] Mono arene technetium compounds are almost unexplored. One of the few syntheses was reported by Alberto *et al*. in 1990. The Na/^{99}Tc cluster compound Na[$^{99}Tc_3(CO)_9(OCH_3)_4$] was reacted in benzene

under acid condition forming the mono arene technetium tricarbonyl $[^{99}Tc(\eta^6\text{-}C_6H_6)(CO)_3]^+$ complex in 52% yield.[102]

As shown in this paragraph, mono and bis-arene bearing a rhenium or technetium core are less investigated compared to other metals due to limited synthetic pathways. In order to study these compounds, appropriate syntheses are needed.

5 Motivation and Goals

The development of multi-functional metal complexes which comprise at least one receptor binding part for target specificity and a biologically active unit for exerting cytotoxicity is of high interest. The arene ruthenium (e.g. $\{Ru(\eta^6\text{-cymene})\}^{2+}$) moieties underline the importance of the metal arene fragment in medicinal chemistry. Nevertheless, the mode of action of these compounds is only studied at the cellular level mainly with fluorescence microscopy but is in many cases still unclear.[103] For in vivo studies, optical imaging has limited applicability and only radiotracers allow for a thorough localization of time-dependent accumulation.[19, 104] It is certainly of most importance to follow concertedly cytotoxic metal complexes in vivo with imaging modalities. Ruthenium and also Platinum are element for which no suitable radionuclides exist for combining therapeutic and imaging opportunities. Therefore, an ideal pair for therapy and diagnosis is rhenium and technetium. In low valent oxidation state complexes, they form a matched-pair since their structures and physicochemical properties are essentially identical.[105, 106] Since the rhenium and technetium arene chemistry are still poorly explored, one of the goals of this thesis is to elucidate strategies to syntheses and derivatives these molecules with functional groups (or biological active molecule) that target essential biomolecules in living organisms to exert a cytotoxic action and to allow for molecular imaging. Additionally, a further goal is to study their fundamental chemistry.

5.1.1 Goals

The goals of this thesis are divided into different parts and are listed as follow:

a) Direct synthesis of $[M(\eta^6\text{-arene})_2]^+$ complexes (M = Re, $^{99(m)}$Tc) with arenes comprising one or two functional groups, targeting biomolecules or pharmacologically active functionalities.

b) Optimisation of the reaction condition of the reported synthesis of $[Re(\eta^6\text{-arene})_2]^+$ in order to improve the yields.

c) Post-functionalization of $[M(\eta^6\text{-arene})_2]^+$ scaffold via e.g metalation reaction.

d) Substitution of one arene of the $[M(\eta^6\text{-arene})_2]^+$ moiety with solvent, mono, di- or tridentate ligands, aiming at a conjugation to a targeting function, peptide or pharmaceutical lead structure.

e) Post-functionalization arene ring of stool piano stool compounds $[M(\eta^6\text{-arene})(L)]^{0/+}$.

f) Development of synthetic strategies for the preparation of $[M(\eta^6\text{-arene})(Cp\text{-}R)]$ complexes.

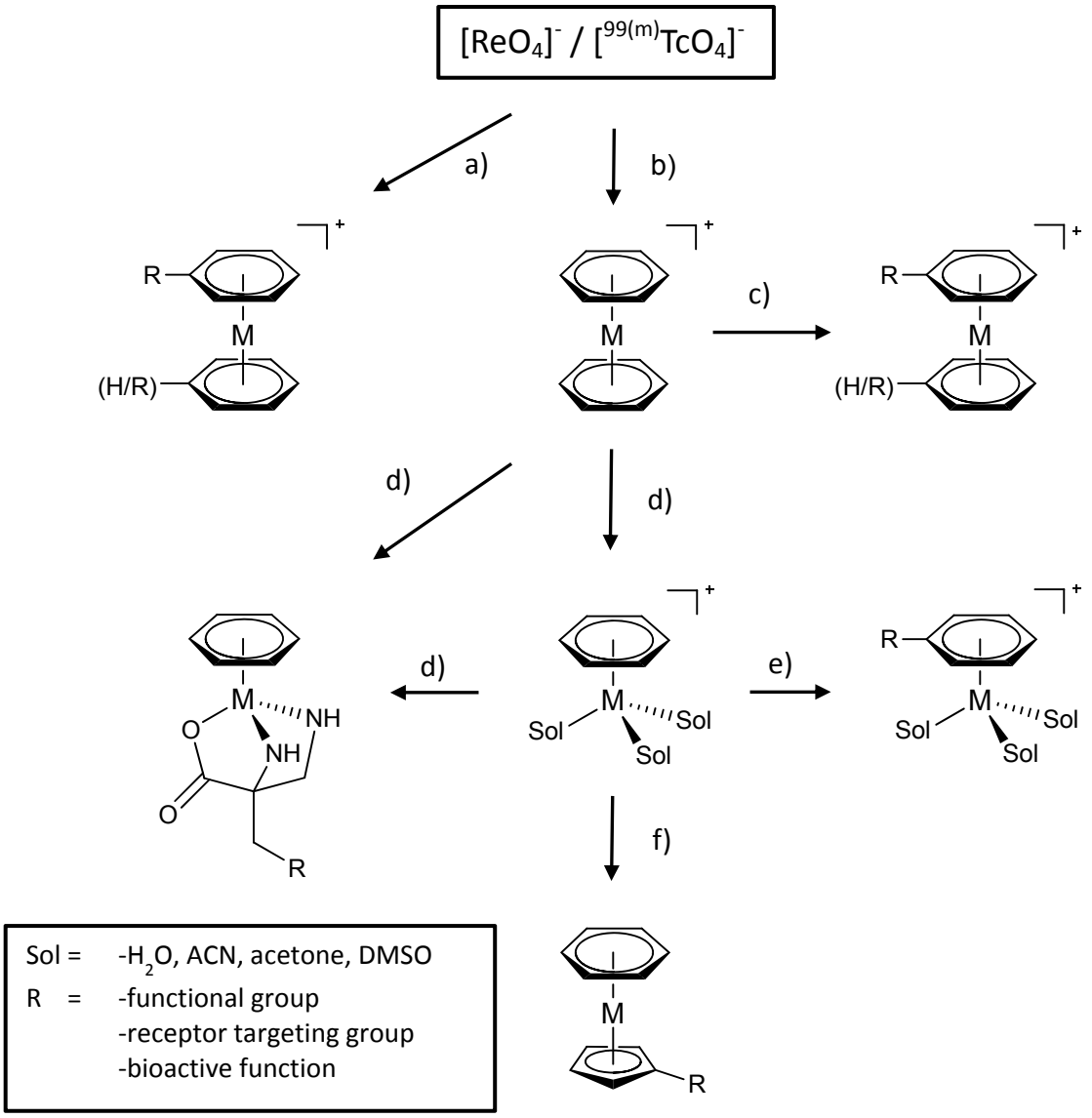

Scheme 3: Possible approaches for the synthesis of mono- and bis(η^6-arene) complexes

6 Result and Discussion

6.1 Synthesis & Characterization of $[Re(\eta^6\text{-arene})_2]^+$ Complexes

As mentioned in the previews paragraphs, the field of medicinal inorganic or bioorganometallic chemistry is dominated by bis/mono-arene complexes of ruthenium and ferrocene (derivatives).[33, 107] These compounds represent fundamental precursors for numerous reaction and show interesting biological behaviour.[32] However, due to the absence of a suitable radioisotope, these complexes cannot be used for "theranostic" applications including radio imaging. The aim of this thesis was to establish new pathways for the synthesis of bis/mono-arene complexes of rhenium, which can be adapted for technetium chemistry and thereby, generating a new platform for theranostic applications, in a second step. Recently, Kurdinov *et al.* described the synthesis of $[Re(\eta^6\text{-arene})_2]^+$ (arene = benzene, toluene, *o*-xylene, *p*-xylene and mesitylene), starting from $K[ReO_4]$ and in the presence of Lewis acid $AlCl_3$ and zinc as a reductant. The yields of these syntheses are between 30-40% due to trans- and demethylation side-reaction of the ligands. In contrast to the $[Re(\eta^6\text{-naphthalene})_2]^+$ complex which was obtained in rather low yield of about 5%.[52] Although this reaction type is well described in the literature, called Fisher-Hafner reaction, the function of $AlCl_3$ is still not fully understood. Using an adapted procedure, $K[ReO_4]$ was reacted with an excess of $AlCl_3$ and in the presence of zinc in the corresponding arenes at 85-100°C. Upon adding an excess of $AlCl_3$, the colour of the suspension changed immediately from grey to black. The reactions were monitored by UPLC-ESI-MS. The formation of the desired $[Re(\eta^6\text{-arene})_2]^+$ was observed within 1 h. In general, the reactions were stopped after 18 h, if no further reaction progress was observed in the UPLC. Purification of the compounds was achieved by evaporation of the liquid arenes or by washing with hot heptane. In a second step, the crude mixture was washed with Et_2O to remove unreacted $AlCl_3$ as well as aromatic side-products. After suspending the obtained black powder in water, unreacted zinc was filtered off. The desired products $[Re(\eta^6\text{-arene})_2](X)$ ($X = Cl^-$, ReO_4^-) (arene = benzene, toluene, xylene, mesitylene, tetralin, fluorene, biphenyl, naphthalene) were extracted into dichloromethane by the addition of NH_4PF_6 or LiOTf to the aqueous solution. In this thesis, it was possible to improve the yield of the compounds to about 60%-30% by using a continuous liquid/liquid extraction method. Finally, evaporation of the solvent leads to the desired $[Re(\eta^6\text{-arene})_2]^+$ with PF_6^- or OTf^- as counter-ion in high purity. By reaction leading to several products, separations were achieved by preparative HPLC over a C18 column.

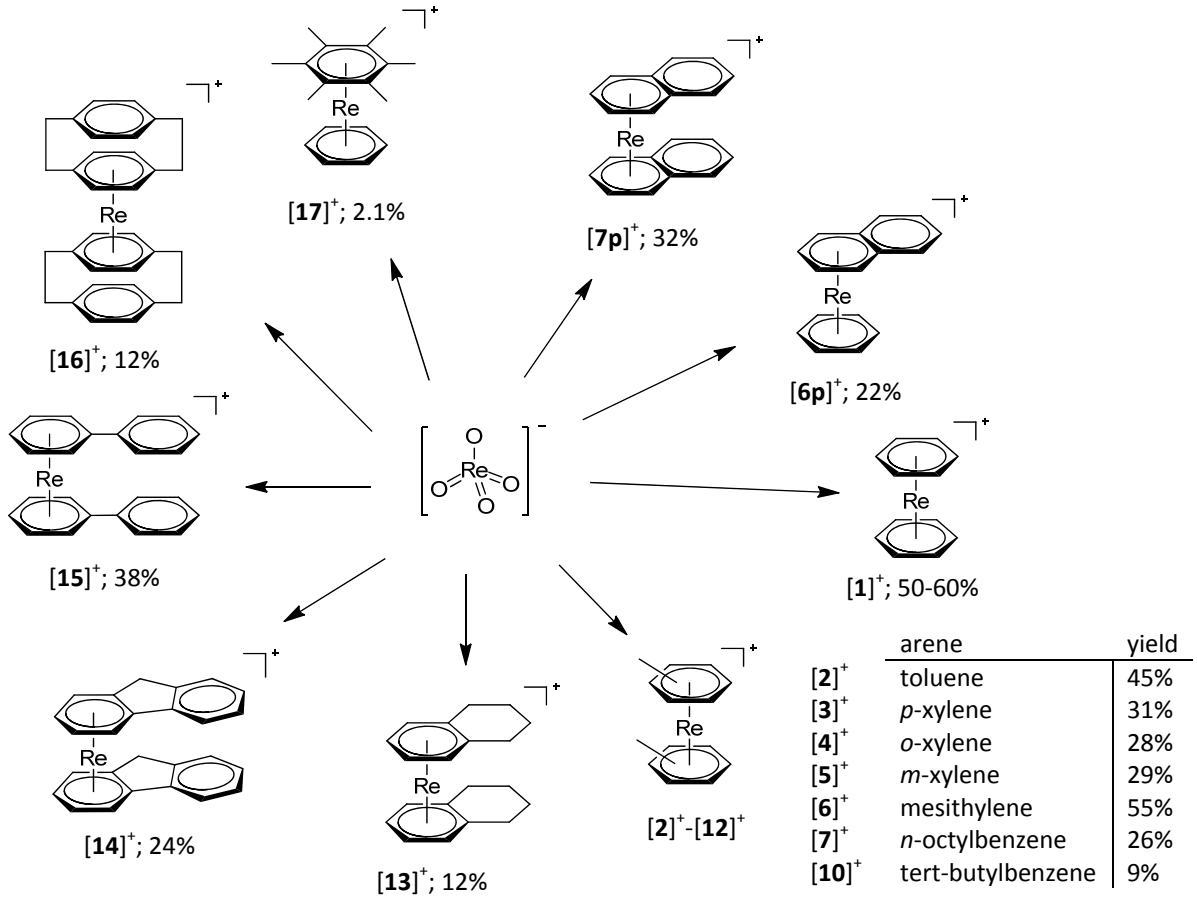

	arene	yield
[**2**]$^+$	toluene	45%
[**3**]$^+$	*p*-xylene	31%
[**4**]$^+$	*o*-xylene	28%
[**5**]$^+$	*m*-xylene	29%
[**6**]$^+$	mesithylene	55%
[**7**]$^+$	*n*-octylbenzene	26%
[**10**]$^+$	tert-butylbenzene	9%

Scheme 4: Overview of synthetized $[Re(\eta^6\text{-arene})_2]^+$ complexes, starting from $K[ReO_4]$.

An overview of synthesized $[Re(\eta^6\text{-arene})]^+$ complexes, including the corresponding reaction yields is depicted in Scheme 4. Some of the illustrated complexes were already reported in the literature and were synthesized for different purposes.[52] Especially, for the determination of the corresponding $[^{99(m)}Tc(\eta^6\text{-arene})]^+$ complexes by coinjection on a radio HPLC the rhenium analogue have been essential. The synthesis of compounds [**1**]$^+$ as BF_4 salt was well described and reported as mentioned before by Kurdinov *et al*.[52] Therefore, it was used as a model compound to modify and optimise the reaction condition due to the low yield reported in the literature of 30-40%. As starting material was used potassium or sodium perrhenate. Screening the reaction conditions, aiming at higher reaction yield, did not show any correlation between the amount of used $AlCl_3$ or zinc. In contrast, decreasing the amount of the reagents to 1-2 equiv., leads to lower yields of about 10-15%. The same reaction was performed also with different Lewis acids (BCl_3, $FeCl_3$, $InCl_3$), to gain deeper insights of the function of $AlCl_3$. However, no product formation was observed. One of the biggest drawbacks for the studied reaction was the poor solubility of $K[ReO_4]$ or $Na[ReO_4]$ in the liquid arenes. For this purpose, rhenium(VII)heptoxide $[Re_2O_7]$ and tetraethylammonium perrhenate $(NEt_4)[ReO_4]$ were chosen as starting material. The reaction with rhenium(VII)heptoxide was performed exactly under the same condition as applied for potassium perrhenate. After adding $AlCl_3$ to the reaction

suspension, no colour change to a black suspension was observed. In this experiment compounds $[\mathbf{1}]^+$ was formed only in trace amounts (yield 2%), according to UPLC-MS measurement after 18 h. Although $AlCl_3$ is a strong Lewis acid and extremely oxophilic, the absence of the colour change to a black suspension after adding the Lewis acid indicated that $AlCl_3$ not reacted or even not activated the $[Re_2O_7]$ in the same way. In the experiment using $(NEt_4)[ReO_4]$ as precursor the reaction showed the formation of $[\mathbf{1}]^+$, according to UPLC-MS measurements but purification and isolation of the pure products were not achieved due to the impurity $(NEt_4)(Cl)$. Recently, Alberto *et al*. reported a facile synthesis of bis-arene complexes $[^{99(m)}Tc(\eta^6\text{-arene})_2]^+$ from pertechnetate.[67] They performed the reaction without metallic reducing agent Zn^0. Further, they assumed that Zn^0 could over-reduce the starting material to metallic, colloidal Tc^0. Only in the case of benzene as ligand, Zn^0 was used additionally. Furthermore, they showed that under Friedel-Crafts condition, the chlorides of $AlCl_3$ could reduce Tc^{VII} or Tc^{V} to Tc^{IV} and that arenes may also act as reductants to achieve oxidation states lower than Tc^{IV}. Among the same condition, the reaction with $K[ReO_4]$ and arenes (benzene, toluene) were performed. In contrast to technetium chemistry, the products with rhenium could be isolated in rather low yields of about 5-10%. One explanation might be the higher reduction potential of $Re^{+VII/+I}$ compared to $Tc^{+VII/+I}$. Finally, the optimized conditions for the synthesis of $[\mathbf{1}]^+$ were large amounts of 10-12 equiv. of $AlCl_3$ and 3-6 equiv. of zinc dust. For a practical workup, the continuous liquid/liquid extraction is a convenient method to reach higher yields. The compounds were isolated in 50% yield as [**1**](OTf) and 60% as $[\mathbf{1}](PF_6)$, respectively. Additionally, reaction control via UPLC-ESI-MS showed the formation of a side product with the corresponding m/z = 419 $[M]^+$ in trace amounts. This mass was assigned to $[Re(\eta^6\text{-biphenyl})(\eta^6\text{-benzene})]^+$ which was formed by the addition of a phenyl group under Friedel-Crafts condition. Removing this side product could be achieved by recrystallization from dichloromethane. A further side product $[Re_2(\mu\text{-}\eta^{2:2}\text{-benzene})(\eta^6\text{-benzene})_2]^{2+}$ ($[\mathbf{1a}]^{2+}$) (Figure 7) was observed during crystallisation of the main product $[\mathbf{1}]^+$.

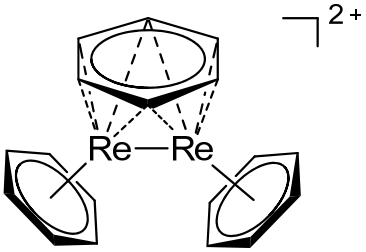

Figure 7: Structure of the dimeric rhenium arene $[Re_2(\mu\text{-}\eta^{2:2}\text{-benzene})(\eta^6\text{-benzene})_2]^{2+}$ ($[\mathbf{1a}]^{2+}$) complex

The red crystals were elucidated by X-ray diffraction analysis (crystal structure: Figure 8, top) and the composition confirmed by ESI-MS (m/z = 606.1 $[M]^+$). Due to the formation in trace amounts as well as the low reproducibility of the compound, other analytical methods like NMR and EA could not be applied. Until today, it is not known if this dimeric rhenium compound acts as an intermediate during the reaction or represents solely a side product. The dimeric rhenium(I) compound is oxygen sensitive and decomposed presumably to ReO_2. This type of compound [**17a**]$^{2+}$ could be also found by the synthesis of the [Re(η^6-$C_6(CH_3)_6$)(η^6-C_6H_6)](OTf) ([**17**]((OTf)) (which will be discussed in a later section) in low quantities. Noteworthy, instead of hexamethylbenzene as expected coordinating ligand, pentamethyl benzene was found for both terminal coordinated ligands. The crystal structure of this interesting dimers ([**1a**]$^{2+}$, [**17a**]$^{2+}$) revealed a folded benzene ring which acts as bridging ligand.

[**1a**]$^{2+}$ crystallizes as red plates in the monoclinic space group C2/c (Figure 8, ORTEP representation[108] top) with one molecule and two PF_6^- anions in the asymmetric unit. One of the counter-ions is highly disordered. While compound [**17a**]$^{2+}$ crystallizes as red plates in the orthorhombic space group Pnma (Figure 8, bottom) The dimeric Re species lies on a mirror plane which led refine only one half of the molecule in the asymmetric unit. The Re(1)-Re(2) bond lengths are 2.3888(3) Å for [**1a**]$^{2+}$ and 2.4089(4) Å for [**17a**]$^{2+}$, respectively, and lie in the typical range of Re-Re single bonds according to literature and DFT calculation.[109] A special feature of the crystal structures of [**1a**]$^{2+}$ and [**17a**]$^{2+}$ is the boat conformation of the bridged benzene ligand. Until today, this coordinated motif has not been reported in the literature for Re complexes. But also, in general, this type of syn-μ-η^2:η^2 coordinated benzene is poorly described and even crystal structures of type M_2(benzene)$_3$ or also called "Rice-Ball" geometry are not characterized.[110, 111] Only several DFT calculation of triple-decker-sandwich complexes versus "Rice-Ball" structures for tris(benzene)dimetal derivatives of the first-row transition metals (M = Ti, Cr, Mn, Fe, Co, Ni) were found in the literature.[111] The first described compounds with a crystal structure was a hybrido vanadium complex $(CpVH)_2C_6H_6$ and $(CpFe)_2C_6Me_6$ by Jonas K. *et al.* in 1983.[112, 113] Another similar structure is the tetracarbonyl(μ-$\eta^{2:2}$-2-butyne)-(μ-1,2,3,4-η:1,4,4a,8a-η-1,4-dimethylnaphthalene)-dimanganese complex which was described in 1997 by kreiter C. G. *et al.*[114] These compounds have an interesting structural feature in common, which arises the question, if the carbon atoms of the syn-bridged arene coordinated to the two metals centres? For the similar hybrido vanadium complex $(CpVH)_2C_6H_6$, only the rotation of the bridging benzene has been described by the authors.[112] In the other examples, the authors draw or assume bonds between the metal centre and the carbon atoms of the bend arene without further discussion.[113, 114] In the case of compounds [**1a**]$^{2+}$ and [**17a**]$^{2+}$ the Re-C bond lengths lie in the range of 2.438(8) Å (Re(1)-C(9)) – 2.472(7) Å (Re(2)-C(12)) and 2.428(6) Å (Re(1)-C(6)) – 2.448(6) Å (Re(2)-C(6)). The Re-carbon bonds are much longer with respect to the average of rhenium–carbons bonds and

only 5 structures were found in the CCDC database[115] within this range. However, with this fact is reasonable to assume a bond between the folded carbon and the metals even though the DFT calculation using the theory of atoms in molecules (AIM) showed no significant interaction between the metals and folded carbon. Considering the 18 electrons rule, rhenium in the oxidation state (+I), one metal-metal bond and by counting the supposed bond, the complex will contain 32 electrons meaning 16 electrons for each metal which corroborate the assumption. Without counting the supposed bond, each metal includes 14 electrons which are unlikely but not to exclude. Moreover, the analysis of the aromaticity indexes by DFT calculation shows a loss in the aromaticity for the bridged benzene compared to the side benzene which was caused by folding's effect. Concerning the C-C bond length of the folded benzene, they were found to be in a range of 1.395(12) – 1.462(10) Å [**1a**]$^{2+}$ and 1.417(15) – 1.449(9) Å [**17a**]$^{2+}$ and are slightly longer compared to the coordinated η^6-benzene of [**1a**]$^{2+}$ (1.369(9) – 1.427(9) Å) on the side. Based on this, the folded ring could be assigned more to a delocalised system rather than to a 1,4 cyclohexadiene one. The Re-C bond lengths of the side coordinated benzene of [**1a**]$^{2+}$ are in the range of 2.248(5) – 2.350(6) Å (Table 2). Especially, the Re(1)-C(1) and Re(2)-C(13) lie in the range of 2.262(5) – 2.261(6) Å compared to the opposite Re(1)-C(4) and Re(2)-C(16) which were much longer and lie between 2.3435(3) – 2.350(6) Å. The same effect was also observed for compound [**17a**]$^{2+}$.

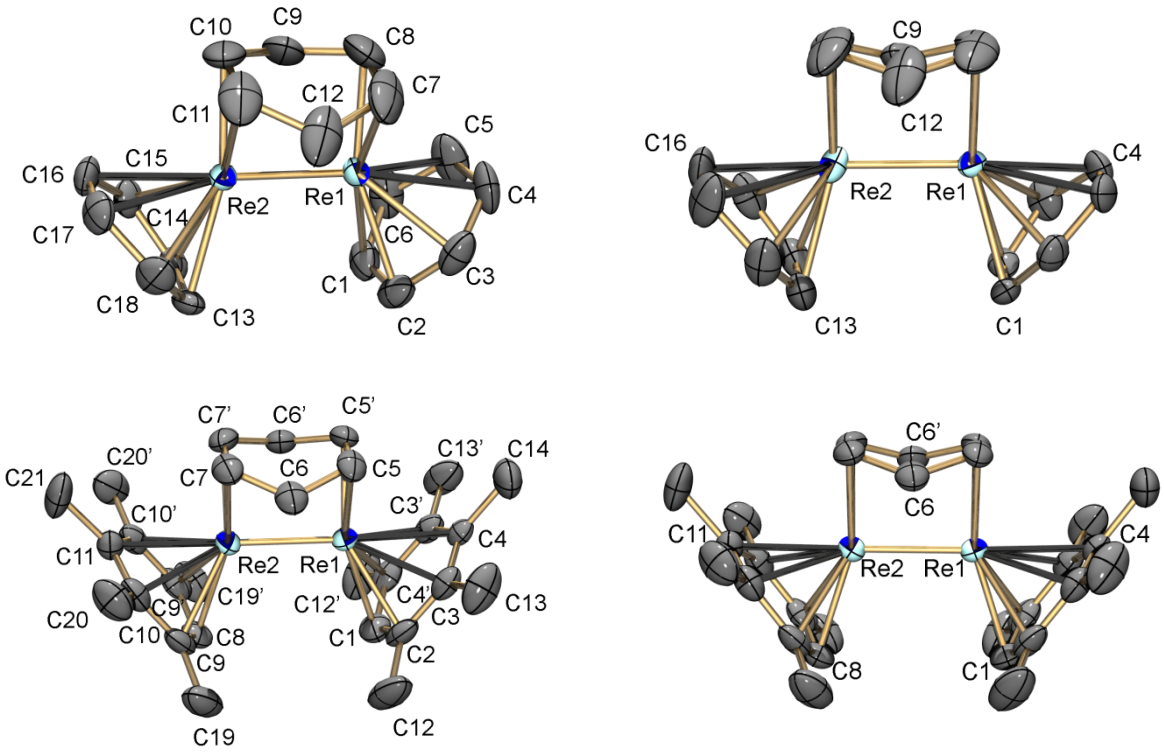

Figure 8: ORTEP representation[108] of the [Re_2(μ-$\eta^{2:2}$-benzene)(η^6-benzene)$_2$]$^{2+}$ ([**1a**]$^{2+}$) dications of the [**1a**](PF_6)$_2$ structure (above) and of [Re_2(μ-$\eta^{2:2}$-benzene)(η^6-pentamethylbenzene)$_2$]$^{2+}$ ([**17a**]$^{2+}$) dications of the [**17a**](PF_6)$_2$ structure. Thermal ellipsoids are represented at the 50% probability level. Hydrogen atoms are omitted for clarity. Bend angle: 28.3° for [**1a**]$^{2+}$ and 29.6° for [**17a**]$^{2+}$

Table 2: Selected bond lengths and angles of [**1a**]$^{2+}$ and [**17a**]$^{2+}$

Selected bond lengths [Å] of [**1a**]$^{2+}$		Selected angles [°] of [**17a**]$^{2+}$	
Re(1)-Re(2)	2.3888(3)	Re(1)-Re(2)	2.4089(4)
Re(1)-C(1)	2.262(5)	Re(1)-C(1)	2.251(8)
Re(1)-C(4)	2.234(5)	Re(1)-C(4)	2.406(8)
Re(1)-C(7)	2.142(6)	Re(1)-C(5)	2.123(6)
Re(1)-C(8)	2.132(6)	Re(1)-C(6)	2.428(6)
Re(1)-C(9)	2.438(6)	Re(2)-C(6)	2.448(6)
Re(2)-C(9)	2.457(7)	Re(2)-C(7)	2.121(5)
Re(2)-C(10)	2.139(7)	Re(2)-C(8)	2.243(9)
Re(2)-C(11)	2.152(7)	Re(2)-C(11)	2.405(7)
Re(2)-C(12)	2.472(7)		
Re(1)-C(12)	2.462(6)		
Re(2)-C(13)	2.261(6)		
Re(2)-C(14)	2.262(6)		

In the case of methylated arene complexes (toluene [**2**]$^{+}$, *p*-xylene [**3**]$^{+}$, *o*-xylene [**4**]$^{+}$, *m*-xylene [**5**]$^{+}$, mesitylene [**6**]$^{+}$), the yields are comparable with the reported value and only in a smaller extent the trans-/demethylated side-products were observed. Removing these side-products could be achieved by recrystallization from dichloromethane. Except for the complexes with the ligands *n*-octylbenzene [**7**]$^{+}$ and tert-butylbenzene [**10**]$^{+}$ where the yields are lower due to higher trans- and dealkylated side-products. As expected, compound [Re(η^6-$C_6H_5(CH_2)_7CH_3)_2$)]$^{+}$ ([**7**]$^{+}$) could be isolated as a major product with a yield of 26% after purification via preparative HPLC. The dealkylated mono-substituted species [Re(η^6-$C_6H_5(CH_2)_7CH_3$)(η^6-C_6H_6)]$^{+}$ ([**8**]$^{+}$) and the transalkylated, tri-substituted species [Re(η^6-$C_6H_5(CH_2)_7CH_3$)(η^6-$C_6H_4((CH_2)_7CH_3)_2$)]$^{+}$ ([**9**]$^{+}$) could be obtained in a lesser extent as triflate salt in yields of 4.7% and 1.3%, respectively. In contrast to the *n*-octylbenzene situation, the dominant species in the *tert*-butylbenzene case, was the dealkylated [Re(η^6-*t*-$C_6H_5C(CH_3)_3$)(η^6-C_6H_6)]$^{+}$ ([**11**]$^{+}$) with a yield of 29% and, to a smaller amount the expected [Re(η^6-*t*-$C_6H_5C(CH_3)_3)_2$)]$^{+}$ [**10**]$^{+}$ (9%) and tri-substituted [Re(η^6-*t*-$C_6H_5C(CH_3)_3$)(η^6-*t*-$C_6H_4(C(CH_3)_3)_2$)]$^{+}$ ([**12**]$^{+}$) (2.6%). It seems that the abstraction of a *tert*-butyl group is easier compared to a *n*-alkane chain. The abstraction of methyl/alkyl group is mainly caused by the presence of $AlCl_3$ and was reported by Kenndy J.D. *et al.* in 2011.[56] This phenomenon was described as the EINS mechanism (electrophile-induced nucleophilic substitution) and was elucidated by the synthesis of [Fe($ArMe_n$)$_2$]$^{2+}$ dications ($ArMe_n$ = $C_6Me_nH_{(6-n)}$, and n = 1-6). According to this approach, electrophilic $AlCl_3$ can abstract either of Me^- or H^- from the methylated arene substrate to generate either the two anionic nucleophilic particles [$HAlCl_3$]$^{-}$ and [$MeAlCl_3$]$^{-}$, together with either two carbenium cations that have the positive charge dissipated over all non-substituted positions. The anionic nucleophiles would then immediately combine with either cation to give the observed disproportionation and isomerisation products.[56] Further, if the reaction was performed at room temperature, no trans- and demethylated side-products were detected.

$Fe(II)Cl_2$ was used as starting material without any reducing agents. In the case of $K[ReO_4]$, the reaction at room temperature did not work by means of reducing Re(VII) to Re(I) required higher temperatures. In general, the use of $AlCl_3$ showed drawbacks not only by hetero atoms functionalized arenes such e.g. methyl benzoate, benzene carboxylic acid, anisole and phenols but as well as by methylated arenes.

The reaction with solid or more complex ligand such tetralin [**13**]$^+$, fluorene [**14**]$^+$, biphenyl [**15**]$^+$, cyclophane [**16**]$^+$, hexamethylbenzene [**17**]$^+$ and naphthalene [**7p**]$^+$ with $K[ReO_4]$ gave yields in a lower range of 38%-2%. In particular, the synthesis of compound $[Re(\eta^6\text{-fluorene})_2]^+$ ([**14**]$^+$) which was performed in benzene as solvent showed small quantities of the mix compound $[Re(\eta^6\text{-fluorene})(\eta^6\text{-benzene})]^+$ whereas one peak with the mass m/z = 519.1 $[M]^+$ could be assigned to the major product [**14**]$^+$ according UPLC-MS. NMR studies and crystal structure analysis of [**14**]$^+$ revealed the formation of two complexes, namely the *syn*- and *anti*-product which have the same retention time and thus the separation of these could not be obtained. Complex [**16**]$^+$ was synthesised in rather low yields of 12% after purification by preparative HPLC. However, [**16**]$^+$ is light sensitive and decomposed in solution forming a black precipitate which is presumably ReO_2 and free ligand according to ^{1}H NMR studies. As mentioned before, complex [**17**]$^+$ was synthesised in a first attempt with hexamethylbenzene in benzene and crystallized without further purification. During the crystallisation, two types of crystals with colours yellow and red were found. For the yellow one, the refinement turns out to be difficult due to the occurred high disorder and therefore an appropriate solution was not achieved. While, for the latter, crystals were analyzed by X-ray diffraction, proofing the structure of [**17a**]$^{2+}$. Additionally, according to UPLC-MS, several demethylated products were observed with the formula $[Re(\eta^6\text{-}C_6((CH_3)_{6-n})H_n)(\eta^6\text{-}C_6((CH_3)_{6-m})H_m)]^+$ (n = 1-6, m = 1-6) but the assignment on which position the demethylation occurred, were not possible. During a master thesis, the synthesis of [**17**]$^+$ was performed in a second attempt in which the mixture was additionally purified via preparative HPLC. It was possible to isolate three compounds as triflate salts in low yield, namely $[Re(\eta^6\text{-}C_6(CH_3)_6)(\eta^6\text{-}C_6H_6)]^+$ ([**17**]$^+$) (2.1%), $[Re(\eta^6\text{-}C_6H(CH_3)_5)(\eta^6\text{-}C_6H_6)]^+$ ([**17b**]$^+$) (0.7%) and $[Re(\eta^6\text{-}C_6H(CH_3)_5)(\eta^6\text{-}C_6H(CH_3)_5)]^+$ ([**17c**]$^+$) (0.3%), respectively. The crystals structures of these complexes were described in the master thesis.[116] The reactions with bigger conjugated systems like naphthalene or anthracene were also performed. As mentioned before, Kurdinov *et al.* reported the synthesis of the complex $[Re(\eta^6\text{-naphthalene})_2]^+$ ([**7p**]$^+$) in rather low yield of 5%.[52] Herein, it was possible to improve the yield of the compound [**7p**]$^+$. The crucial step was to remove the complex [**7p**]$^+$ from the undefined, black, sticky bulk which was formed during the reaction. In a first step, the bulk was washed several times with hot heptane and diethyl ether and in a second step, the residue was solved in dichloromethane. Afterwards, the complex containing a chloride as counter ions was extracted several times with water and subsequent back extracted as triflate salt with

dichloromethane. In this way, the yield of the compound [**7p**]$^+$ could be improved up to 32%.[117] However, UPLC-MS measurement showed a side-product in trace amount with a difference in mass of 4 H's. The mass of m/z = 447 [M]$^+$ could be assigned after NMR studies to the compound [Re(η^6-naphthalene)(η^6-tetralin)]$^+$. The reduction of the uncoordinated ring could be explained by the formation of hydride species like [$HAlCl_3$]$^-$ which was postulated before. Compound [**7p**]$^+$ is light and thermally sensitive and was used for substitution of one or both naphthalene ligands through several mono-, bi- and tridentate ligands.[117] Among the same way, the reaction with anthracene showed only a yellow, reduced species that might be [Re(η^6-9,10-dihydroanthracene)$_2$]$^+$ according to UPLC-MS. Moreover, reaction with indene or 1,4-diphenylbutane did not work or did not show the desirable compounds. In the latter case, the formation of [Re(η^6-tetralin)(η^6-benzene)]$^+$ was observed instead of [Re(η^6-1,4-diphenylbutane)]$^+$ due to transalkylation effects. Not only the reactivity of the [**7p**]$^+$ are of interest but also the complex [Re(η^6-naphthalene)(η^6-benzene)]$^+$ ([**6p**]$^+$) regarding substitution of one ligand. The synthesis of this compound was published in 2017 from our group in 22% yield.[117] In addition, after the purification of the mixture via preparative HPLC, numerous compounds could be isolated which were not reported in the manuscript (Table 3). These complexes were isolated in comparable low yields and fully characterised. Crystal structures were obtained for all compounds. As it is shown in Table 3, the low yield of compound [**6p**]$^+$ is caused due to the formation of large numerous side products which could not be prevented under Friedel-Crafts conditions.

Table 3: Additional formed side products by synthesis of [**6p**]$^+$

complexes	yields
[Re(η^6-benzene)$_2$]$^+$	7%
[Re(η^6-naphthalene)(η^6-benzene)]$^+$	22%
[Re(η^6-tetralin)(η^6-benzene)]$^+$	1-2%
[Re(η^6-biphenyl)(η^6-benzene)]$^+$	1%
[Re(η^6-naphthalene)$_2$]$^+$	10%
[Re(η^6-naphthalene)(η^6-tetralin)]$^+$	1-2%

Higher substitute or more complex compound were also observed by UPLC-MS measurements but only one substance was isolated in trace amount with the corresponding mass of m/z = 521 [M]$^+$ and crystallized. Single crystals were obtained by slow evaporation from an acetonitrile solution and elucidated by X-ray diffraction. The crystal structure revealed an unexpected enantiomeric pure compound [Re(η^6-dibenzobicyclo[3.2.1]octadiene)(η^6-naphthalene)]$^+$ ([**6g**]$^+$) as PF_6^- salt (Figure 9). Under Friedel-Crafts condition combined with the large excess of $AlCl_3$, might induce the addition of

benzene to the uncoordinated ring of the naphthalene ligand in order to form the dibenzobicyclo[3.2.1]octadiene framework. This is only an example of the large variety of side-products which could be formed under this harsh condition. Compound [**6g**](PF_6) crystallizes as orange needles in the orthorhombic space group $Pna2_1$. The structure contains one molecule centres in the asymmetric unit. Furthermore, the rhenium-carbon bonds lie in the range of 2.19(2) – 2.323(14) Å and are comparable with similar structures like [Re(η^6-naphthalene)$_2$]$^+$ [**7p**]$^+$ (2.213(7) – 2.289(6) Å).

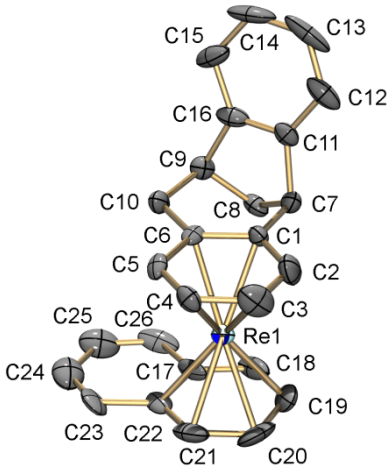

Figure 9: ORTEP representation[108] of the [Re(η^6-dibenzobicyclo[3.2.1]octadiene)(η^6-naphtalene)]$^+$ ([**6g**]$^+$) cation of the [**6g**](PF_6) structure. Thermal ellipsoids are represented at the 50% probability level. Hydrogen atoms are omitted for clarity.

6.1.1 Crystal Structures

Compound [**2**](OTf) crystallizes as yellow plates in the monoclinic space group $P2_1/c$ (Figure 10). The structure contains two independent Re centres in the asymmetric unit that are very similar. Furthermore, a disorder along C-S axis of the triflate was observed.

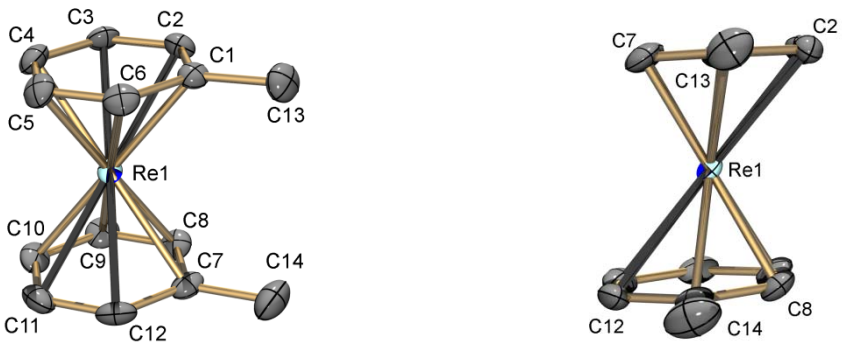

Figure 10: ORTEP representation[108] of the [Re(η^6-toluene)$_2$]$^+$ ([**2**]$^+$) cation of the [**2**](OTf) structure. Thermal ellipsoids are represented at the 50% probability level. Hydrogen atoms are omitted for clarity.

Table 4: Selected bond lengths and angles of $[\mathbf{2}]^+$

Selected bond lengths [Å]		Selected angles [°]	
Re(1)-C(1)	2.295(3)	C(1)-Re(1)-C(2)	37.32(12)
Re(1)-C(2)	2.096(3)	C(2)-Re(1)-C(3)	39.49(14)
Re(1)-C(3)	2.078(3)	C(3)-Re(1)-C(4)	38.01(14)
Re(1)-C(4)	2.252(3)	C(4)-Re(1)-C(5)	34.90(13)
Re(1)-C(5)	2.425(3)	C(5)-Re(1)-C(6)	33.83(11)
Re(1)-C(6)	2.423(3)	C(6)-Re(1)-C(1)	34.85(11)
Re(1)-C(7)	2.286(3)	C(7)-Re(1)-C(8)	34.74(11)
Re(1)-C(8)	2.422(3)	C(8)-Re(1)-C(9)	34.01(12)
Re(1)-C(9)	2.413(3)	C(9)-Re(1)-C(10)	35.12(13)
Re(1)-C(10)	2.252(3)	C(10)-Re(1)-C(11)	37.52(14)
Re(1)-C(11)	2.082(3)	C(11)-Re(1)-C(12)	39.70(13)
Re(1)-C(12)	2.085(3)	C(12)-Re(1)-C(7)	37.54(11)

The Re-C bond lengths in $[\mathbf{2}]^+$ are in the range of 2.078(3)-2.425(4) Å (Table 4). The Re(1)-C(2) and Re(1)-C(3) bonds lie in the range of 2.096(3) – 2.096(3) Å and are compared to the opposite Re(1)-C(5) and Re(1)-C(6) bonds are significantly longer (2.425(3) – 2.423(3) Å). This difference in the bond length caused a shift of 0.313 Å of the aromatic ring towards the centroid of rhenium centre (Figure 10, right). This finding can only be rationalized by packing effects. The CH_3 groups in the two toluene ligands point almost in the same directions in the solid state, while the ring atoms are eclipsed. The comparable bond length of the technetium analogues lie between 2.217(4) – 2.245(4) Å.[67]

[**3**](OTf) crystallizes as yellow needles in the orthorhombic space group Pnma but it was not possible to refine the structure because of high disorder of the molecule. [**4**](OTf) crystallizes as yellow needles in the orthorhombic space group Pnma (Figure 11). The Re molecule lies on a mirror plane which led refine only one half of the molecule in the asymmetric unit. The second half of the molecule was reproduced by symmetry operation. The triflate counter-ion lies on a mirror plane too, leading to a disorder of the F and O atoms centres.

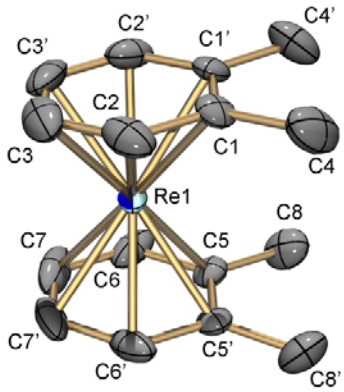

Figure 11: ORTEP representation[108] of the $[Re(\eta^6\text{-}o\text{-xylene})_2]^+$ ($[\mathbf{4}]^+$) cation of the [**4**](OTf) structure. Thermal ellipsoids are represented at the 50% probability level. Hydrogen atoms are omitted for clarity.

Table 5: Selected bond lengths and angles of $[\mathbf{4}]^+$

Selected bond lengths [Å]		Selected angles [°]	
Re(1)-C(1)	2.295(5)	C(1')-Re(1)-C(1)	36.9(3)
Re(1)-C(2)	2.230(6)	C(1)-Re(1)-C(2)	36.7(2)
Re(1)-C(3)	2.215(6)	C(2)-Re(1)-C(3)	37.0(3)
Re(1)-C(5)	2.261(5)	C(5')-Re(1)-C(5)	36.7(3)
Re(1)-C(6)	2.235(6)	C(5)-Re(1)-C(6)	36.4(2)
Re(1)-C(7)	2.206(6)	C(6)-Re(1)-C(7)	37.3(3)

The Re-C bond lengths in $[\mathbf{4}]^+$ are in the range of 2.206(6) – 2.295(5) Å (Table 5). No significant structural differences were found compared to the structure of $[\mathbf{1}]^+$ and $[\mathbf{3}]^+$, respectively. The CH_3 groups in the two *o*-xylene ligands point almost in the same directions in the solid state, while the ring atoms are eclipsed. Compound $[\mathbf{5}]^+$ was crystallized with triflate as well as with hexafluorophosphate counter-ion. In both case, due to the high symmetry and high disorders of the molecule/counter-ion, it was not possible to refine the structures below an R_1 value of 5%. Therefore $B(Ph)_4^-$ were choose as counter-ion. $[\mathbf{5}](B(Ph)_4)$ crystallizes as yellow needles in the monoclinic space group $P2_1/c$ (Figure 12). The structure contains one molecule in the asymmetric unit. The distances between the Re and the aromatic carbon atoms of the m-xylene were found to be in the range of 2.231(3) – 2.266(3) Å (Table 6) and further no significant structural differences were found compared to the structure of $[\mathbf{1}]^+$, $[\mathbf{3}]^+$ and $[\mathbf{4}]^+$. Moreover, the ring atoms are eclipsed whereas the CH_3 groups in the two *m*-xylene ligands were pointed almost in the same directions.

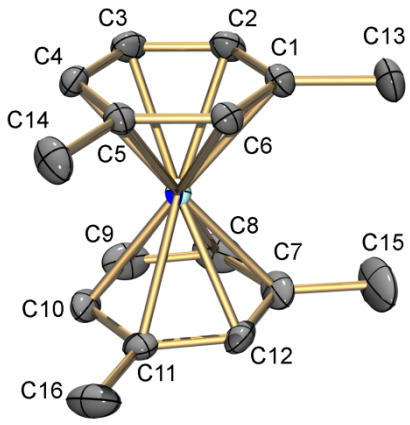

Figure 12: ORTEP representation[108] of the $[Re(\eta^6\text{-}m\text{-xylene})_2]^+$ ($[\mathbf{5}]^+$) cation of the $[\mathbf{5}](B(Ph)_4)$ structure. Thermal ellipsoids are represented at the 50% probability level. Hydrogen atoms are omitted for clarity.

Table 6: Selected bond lengths and angles of [**5**]$^+$

Selected bond lengths [Å]		Selected angles [°]	
Re(1)-C(1)	2.251(2)	C(1)-Re(1)-C(2)	36.83(8)
Re(1)-C(2)	2.243(2)	C(2)-Re(1)-C(3)	36.63(7)
Re(1)-C(3)	2.266(2)	C(3)-Re(1)-C(4)	36.68(8)
Re(1)-C(4)	2.242(2)	C(4)-Re(1)-C(5)	36.61(9)
Re(1)-C(5)	2.236(2)	C(5)-Re(1)-C(6)	37.07(9)
Re(1)-C(6)	2.233(2)	C(6)-Re(1)-C(1)	36.91(8)
Re(1)-C(7)	2.250(2)	C(7)-Re(1)-C(8)	36.76(10)
Re(1)-C(8)	2.230(2)	C(8)-Re(1)-C(9)	36.82(9)
Re(1)-C(9)	2.248(2)	C(9)-Re(1)-C(10)	36.68(9)
Re(1)-C(10)	2.243(2)	C(10)-Re(1)-C(11)	36.39(10)
Re(1)-C(11)	2.244(2)	C(11)-Re(1)-C(12)	36.57(11)
Re(1)-C(12)	2.231(3)	C(12)-Re(1)-C(7)	36.97(11)

[**6**](OTf) crystallizes as yellow plates in the triclinic space group P-1 (Figure 13), while the higher substituted compound [**7**]$^+$ and [**8**]$^+$ were oily and could not be crystallized. The structure contains one molecule in the asymmetric unit. The Re-C_{arom} bond lengths were between 2.215(3) Å and 2.253(3) Å (Table 7). The obtained values are in the same range compared to [**1**]$^+$, [**3**]$^+$-[**5**]$^+$.

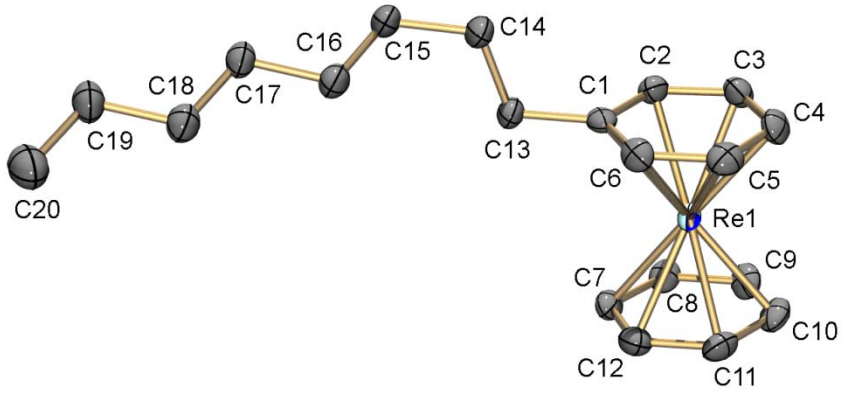

Figure 13: ORTEP representation[108] of the [Re(η^6-*n*-octylbenzene)(η^6-benzene)]$^+$ ([**6**]$^+$) cation of the [**6**](OTf) structure. Thermal ellipsoids are represented at the 50% probability level. Hydrogen atoms are omitted for clarity.

Table 7: Selected bond lengths and angles of [**6**]$^+$

Selected bond lengths [Å]		Selected angles [°]	
Re(1)-C(1)	2.253(3)	C(1)-Re(1)-C(2)	36.77(11)
Re(1)-C(2)	2.245(3)	C(2)-Re(1)-C(3)	36.84(11)
Re(1)-C(3)	2.251(3)	C(3)-Re(1)-C(4)	36.80(13)
Re(1)-C(4)	2.236(3)	C(4)-Re(1)-C(5)	37.04(12)
Re(1)-C(5)	2.222(3)	C(5)-Re(1)-C(6)	37.04(11)
Re(1)-C(6)	2.223(3)	C(6)-Re(1)-C(1)	36.77(12)
Re(1)-C(7)	2.241(3)	C(7)-Re(1)-C(8)	36.97(12)
Re(1)-C(8)	2.244(3)	C(8)-Re(1)-C(9)	36.71(11)
Re(1)-C(9)	2.241(3)	C(9)-Re(1)-C(10)	36.89(13)
Re(1)-C(10)	2.215(3)	C(10)-Re(1)-C(11)	37.14(13)
Re(1)-C(11)	2.226(3)	C(11)-Re(1)-C(12)	37.11(12)
Re(1)-C(12)	2.241(3)	C(12)-Re(1)-C(7)	36.82(13)

As mentioned before, the synthesis with *tert*-butylbenzene as ligand gave three products [**10**]$^+$-[**12**]$^+$. All of them could be isolated and crystallized. The dominant and dealkylated spices [Re(η^6-*tert*-butylbenzene)(η^6-benzene)]$^+$ ([**10**](OTf)) crystallizes as yellow plate in the monoclinic space group $P2_1/c$ (Figure 14, left) whereas the expected disubstituted compound [Re(η^6-*tert*-butylbenzene)$_2$]$^+$ ([**11**](OTf)) crystallizes as yellow plate in the triclinic space group P-1 (Figure 14, middle). Furthermore, [**12**](OTf) crystallizes as yellow blocks in the monoclinic space group $P2_1/n$ (Figure 14, right). The asymmetric unit of [**10**]$^+$ contains one molecule while compound [**11**]$^+$ consists of two very similar, independent half Re species in which the Re atoms are positioned at the inversions centre. The structure of [**12**]$^+$ includes two independent Re centres in the asymmetric unit that are enantiomeric to each other.

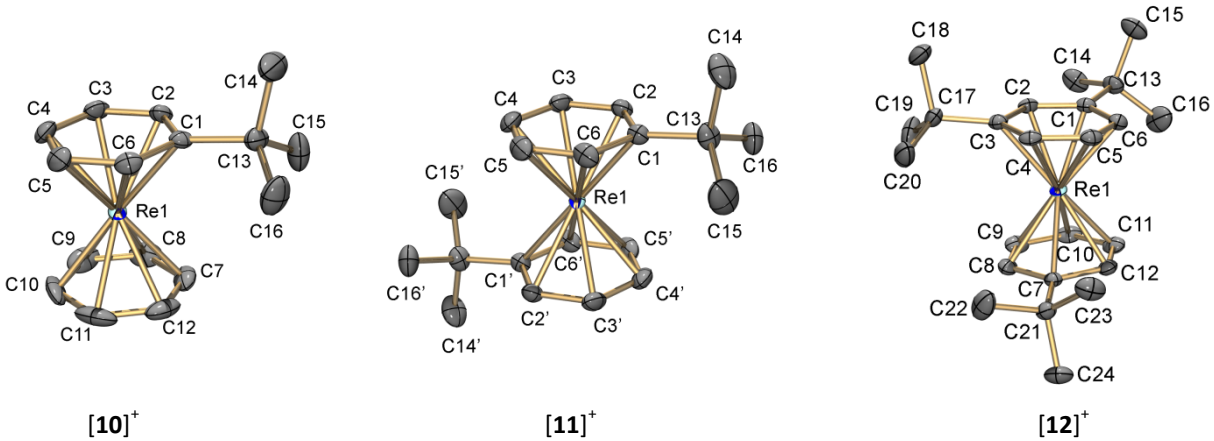

[**10**]$^+$ [**11**]$^+$ [**12**]$^+$

Figure 14: ORTEP representation[108] of the [Re(η^6-*tert*-benzene)(η^6-benzene)]$^+$ ([**10**]$^+$) (left), [Re(η^6-*tert*-benzene)$_2$]$^+$ ([**11**]$^+$) (middle) and [Re(η^6-*m*-*ditert*-benzene)(η^6-*tert*-benzene)]$^+$ ([**12**]$^+$) (right) cations. Thermal ellipsoids are represented at the 50% probability level. Hydrogen atoms and counter-ions are omitted for clarity.

Table 8: Selected bond lengths and angles of [**10**]$^+$, [**11**]$^+$ and [**12**]$^+$

	Selected bond lengths [Å]				Selected angles [°]		
	[**10**]$^+$	[**11**]$^+$	[**12**]$^+$		[**10**]$^+$	[**11**]$^+$	[**12**]$^+$
Re(1)-C(1)	2.275(2)	2.270(19)	2.279(2)	C(1)-Re(1)-C(2)	36.84(9)	36.99(7)	36.63(7)
Re(1)-C(2)	2.246(2)	2.2285(18)	2.258(2)	C(2)-Re(1)-C(3)	36.94(10)	37.08(7)	36.56(7)
Re(1)-C(3)	2.240(3)	2.2342(19)	2.293(2)	C(3)-Re(1)-C(4)	36.65(11)	36.78(8)	36.61(8)
Re(1)-C(4)	2.241(3)	2.247(2)	2.243(2)	C(4)-Re(1)-C(5)	36.78(11)	36.56(9)	36.66(9)
Re(1)-C(5)	2.230(2)	2.2321(19)	2.244(2)	C(5)-Re(1)-C(6)	36.86(10)	37.06(8)	36.55(9)
Re(1)-C(6)	2.238(2)	2.239(2)	2.258(2)	C(6)-Re(1)-C(1)	36.75(9)	37.03(7)	36.77(8)
Re(1)-C(7)	2.249(3)	-	2.259(2)	C(7)-Re(1)-C(8)	35.90(13)	-	36.89(9)
Re(1)-C(8)	2.239(3)	-	2.242(2)	C(8)-Re(1)-C(9)	36.31(14)	-	36.91(9)
Re(1)-C(9)	2.231(3)	-	2.242(2)	C(9)-Re(1)-C(10)	37.31(15)	-	36.58(9)
Re(1)-C(10)	2.231(3)	-	2.251(2)	C(10)-Re(1)-C(11)	37.13(15)	-	36.83(9)
Re(1)-C(11)	2.234(3)	-	2.230(2)	C(11)-Re(1)-C(12)	36.26(13)	-	37.08(8)
Re(1)-C(12)	2.241(3)	-	2.239(2)	C(12)-Re(1)-C(7)	35.85(13)	-	36.91(8)

The Re-C_{arom} bond lengths of all three species are between 2.2285(18) Å and 2.293(2) Å (Table 8) and lie in the range of comparable structures ([**1**]$^+$, [**3**]$^+$ and [**4**]$^+$). Especially, Re-C_{arom} bond lengths, where a *tert*-butyl group is attached are significantly longer compared to the other. This fact can be explained by the steric demand of the bulky *tert*-butyl groups. The ring atoms of [**10**]$^+$ are almost in a staggered conformation to each other whereas in [**11**]$^+$ the two ligands are eclipsed. Furthermore, the two *tert*-butyl groups are pointed in opposite directions. The structure of [**12**]$^+$ shows more a staggered conformation with a rotation angle of 79.6° between the C(3)-C(tert-butyl) and C(7)-C(tert-butyl) bonds.

[**13**](OTf) crystallizes as light yellow plates in the monoclinic space group $P2_1/n$ (Figure 15) with one molecule in the asymmetric unit. Additionally, a disorder between the triflate and chloride ion is observed with an occupancy of 93:6.

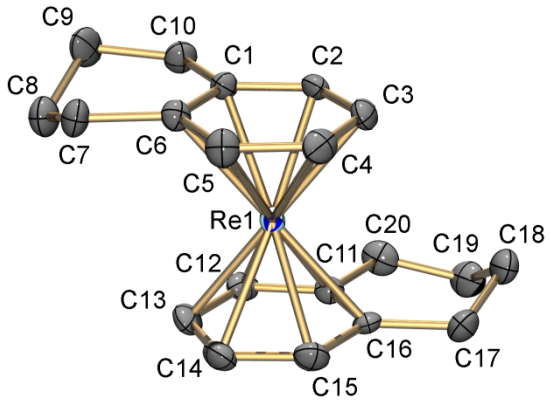

Figure 15: ORTEP representation[108] of the [Re(η^6-tetralin)$_2$]$^+$ ([**13**]$^+$) cation of the [**13**](OTf) structure. Thermal ellipsoids are represented at the 50% probability level. Hydrogen atoms are omitted for clarity.

Table 9: Selected bond lengths and angles of [**13**]$^+$

Selected bond lengths [Å]		Selected angles [°]	
Re(1)-C(1)	2.269(3)	C(1)-Re(1)-C(2)	36.78(12)
Re(1)-C(2)	2.227(3)	C(2)-Re(1)-C(3)	36.76(12)
Re(1)-C(3)	2.247(3)	C(3)-Re(1)-C(4)	36.50(12)
Re(1)-C(4)	2.245(3)	C(4)-Re(1)-C(5)	36.79(12)
Re(1)-C(5)	2.212(3)	C(5)-Re(1)-C(6)	37.35(10)
Re(1)-C(6)	2.247(3)	C(6)-Re(1)-C(1)	36.95(11)
Re(1)-C(11)	2.276(3)	C(11)-Re(1)-C(12)	36.82(11)
Re(1)-C(12)	2.226(3)	C(12)-Re(1)-C(13)	36.89(12)
Re(1)-C(13)	2.235(3)	C(13)-Re(1)-C(14)	36.67(11)
Re(1)-C(14)	2.231(3)	C(14)-Re(1)-C(15)	36.92(12)
Re(1)-C(15)	2.216(3)	C(15)-Re(1)-C(16)	37.06(11)
Re(1)-C(16)	2.263(3)	C(16)-Re(1)-C(11)	36.51(10)

The distances between the Re and the aromatic carbon atoms of the tetralin were found to be in the range of 2.212(3) – 2.276(3) Å (Table 9). No significant structural differences were found compared to the other structures. Additionally, the rings atoms are eclipsed while the two saturated rings of the ligand are rotated by about 127.6 degrees from each other. The bond length of the [^{99}Tc(η^6-tetralin)$_2$]$^+$ analogues lies between 2.217(4) – 2.245(4) Å and are comparable with [**13**]$^+$.[67]

[**14**](OTf) crystallizes as yellow needles in the monoclinic space group $P2_1/n$ (Figure 16) with one molecule in the asymmetric unit. The crystal structure of [**14**](OTf) shows strong disorders; one fluorene ligand is disordered over two sets of positions with site-occupancy factors of 0.444(14) for the syn-isomer and 0.556(14) for the anti-isomer (^{1}H NMR-ratio: 1:0.88 syn/anti). The F and O atoms of the counter-ions are disordered over two sets of positions with a site-occupancy ratio of 0.469/0.531(10) and 0.372/0.628(12), respectively.

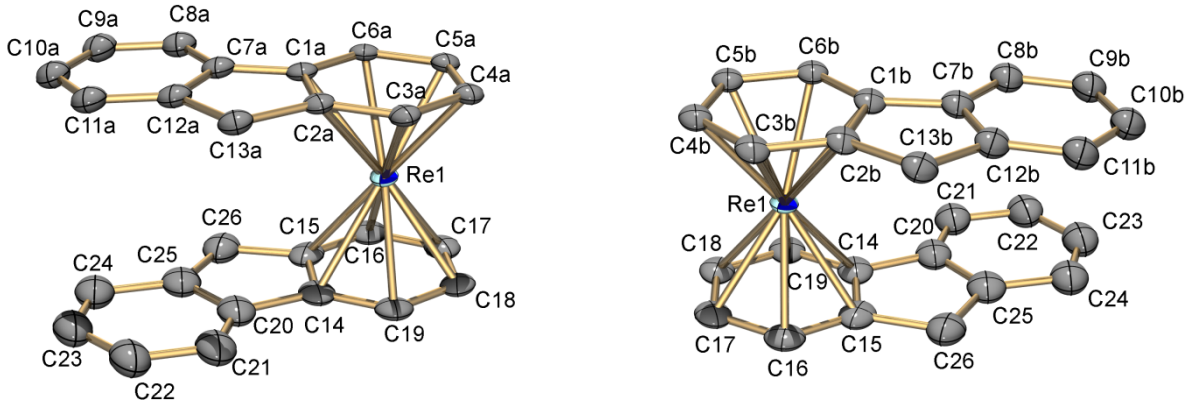

Figure 16: ORTEP representation[108] of the [Re(η^6-fluorene)$_2$]$^+$ ([**14**]$^+$) cation of the [**14**](OTf) structure. The anti- (left) and syn-isomer (right) are depicted. Thermal ellipsoids are represented at the 30% probability level. Hydrogen atoms are omitted for clarity.

Table 10: Selected bond lengths and angles of [**14**]$^+$ anti/syn

Selected bond lengths [Å]			Selected angles [°]		
	[**14**]$^+$ anti	[**14**]$^+$ syn		[**14**]$^+$ anti	[**14**]$^+$ syn
Re(1)-C(1)	2.251(11)	2.281(14)	C(1)-Re(1)-C(2)	-	-
Re(1)-C(2)	2.272(11)	2.312(14)	C(2)-Re(1)-C(3)	-	-
Re(1)-C(3)	2.247(11)	2.306(15)	C(3)-Re(1)-C(4)	37.2(2)	-
Re(1)-C(4)	2.200(12)	2.269(16)	C(4)-Re(1)-C(5)	37.8(2)	-
Re(1)-C(5)	2.177(12)	2.238(17)	C(5)-Re(1)-C(6)	37.8(2)	36.9(3)
Re(1)-C(6)	2.203(11)	2.243(16)	C(6)-Re(1)-C(1)	37.1(2)	-
Re(1)-C(14)	2.257(10)	2.257(10)	C(14)-Re(1)-C(15)	-	-
Re(1)-C(15)	2.247(10)	2.247(10)	C(15)-Re(1)-C(16)	36.2(4)	-
Re(1)-C(16)	2.229(10)	2.229(10)	C(16)-Re(1)-C(17)	36.5(4)	-
Re(1)-C(17)	2.216(10)	2.216(10)	C(17)-Re(1)-C(18)	37.1(4)	-
Re(1)-C(18)	2.223(9)	2.223(9)	C(18)-Re(1)-C(19)	36.2(4)	-
Re(1)-C(19)	2.256(10)	2.256(10)	C(19)-Re(1)-C(14)	-	-

The Re-C_{arom} bond lengths of syn-isomere (C(xb), x = 1-6) are slightly longer (2.238(17) – 2.312(18) Å) compared to the anti-isomer (2.177(12) – 2.272(11) Å). This observation can be explained by the steric demand of methylene bridged group of the syn-isomer which are pointed in the same direction. The slight distortion of the ring atoms of [**14**]$^+$ might benefit only in small extends by the elongation of the Re-C bond lengths.

[**15**](PF_6) crystallizes as light green plates in the triclinic space group P-1 (Figure 17). The structure contains one molecule in the asymmetric unit. The phenyl groups of both biphenyl moieties are pointed in opposite directions in the solid state, while the ring atoms are almost eclipsed. The Re-C_{arom} bond lengths are between 2.232(3) Å and 2.256 (3) Å (Table 11). The obtained values are in the same range compared to the other structures described in this thesis.

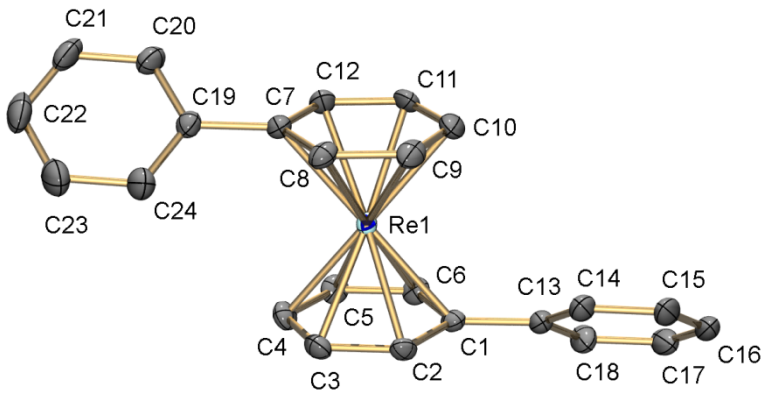

Figure 17: ORTEP representation[108] of the [Re(η^6-biphenyl)$_2$]$^+$ ([**15**]$^+$) cation of the [**15**](PF_6) structure. Thermal ellipsoids are represented at the 50% probability level. Hydrogen atoms are omitted for clarity.

Table 11: Selected bond lengths and angles of [**15**]$^{+}$

Selected bond lengths [Å]		Selected angles [°]	
Re(1)-C(1)	2.256(3)	C(1)-Re(1)-C(2)	37.13(10)
Re(1)-C(2)	2.232(3)	C(2)-Re(1)-C(3)	37.24(10)
Re(1)-C(3)	2.232(3)	C(3)-Re(1)-C(4)	36.87(12)
Re(1)-C(4)	2.243(3)	C(4)-Re(1)-C(5)	36.46(12)
Re(1)-C(5)	2.249(3)	C(5)-Re(1)-C(6)	36.81(12)
Re(1)-C(6)	2.236(3)	C(6)-Re(1)-C(1)	37.01(12)
Re(1)-C(7)	2.269(3)	C(7)-Re(1)-C(8)	36.84(11)
Re(1)-C(8)	2.233(3)	C(8)-Re(1)-C(9)	37.09(12)
Re(1)-C(9)	2.235(3)	C(9)-Re(1)-C(10)	36.93(13)
Re(1)-C(10)	2.241(3)	C(10)-Re(1)-C(11)	37.00(14)
Re(1)-C(11)	2.242(3)	C(11)-Re(1)-C(12)	36.97(12)
Re(1)-C(12)	2.241(3)	C(12)-Re(1)-C(7)	36.56(11)

The synthesis of [M(η^6-[2.2]paracyclophane)$_2$]$^{(n+)}$ (n = 0,2; M = Cr, Fe, Cr) was already reported, but to our best knowledge, none of these compounds are structurally characterised.[118-120] [**16**](PF_6) crystallizes as light green plates in the monoclinic space group P2/c (Figure 18). The structure contains one and a half-molecule with an additionally disordered solvent molecule (acetone) in the asymmetric unit. The Re(1)-C(2,3,5,6) bond lengths are between 2.198(2) Å and 2.256 (3) Å (Table 12) while the bond lengths of Re(1)-C(1,4) are significantly longer and where found to be 2.365(3) Å and 2.359 (2) Å. This elongation was caused due to the molecule strain (transannular π–π interaction) of the [2.2]paracyclophane ligand which is reflected by the boat conformation of the coordinated benzene ring with a distortion angle between 13.79-14.55° (uncoordinated [2.2]paracyclophane: 12.5°).[121] Furthermore, a twist of the ethylene bridged groups of the ligand was observed. This effect is well known and is also reflected in the ^{1}H NMR spectra in form of AA'XX' spin system.[122]

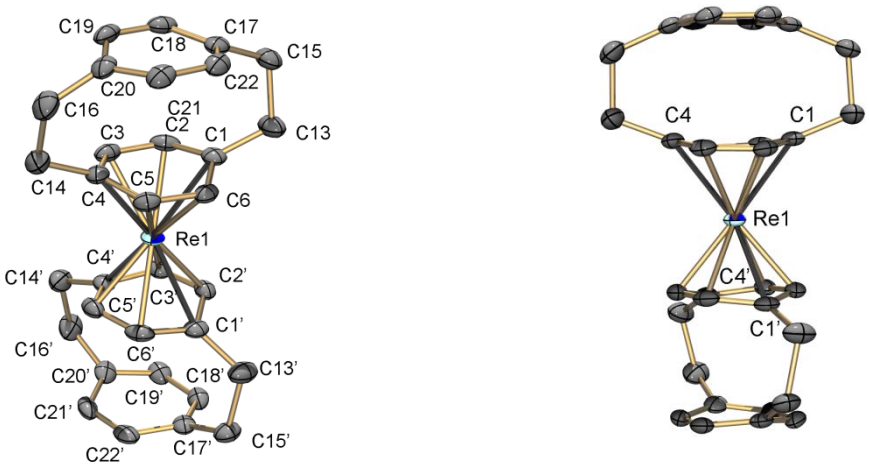

Figure 18: ORTEP representation[108] of the [Re(η^6-[2.2]paracyclophane)$_2$]$^+$ ([**16**]$^+$) cation of the [**16**](PF_6) structure. Thermal ellipsoids are represented at the 50% probability level. Hydrogen atoms are omitted for clarity.

Table 12: Selected bond lengths and angles of [**16**]$^+$

Selected bond lengths [Å]		Selected angles [°]	
Re(1)-C(1)	2.365(2)	C(1)-Re(1)-C(2)	35.41(9)
Re(1)-C(2)	2.230(2)	C(2)-Re(1)-C(3)	37.26(9)
Re(1)-C(3)	2.198(2)	C(3)-Re(1)-C(4)	35.94(9)
Re(1)-C(4)	2.359(2)	C(4)-Re(1)-C(5)	35.33(10)
Re(1)-C(5)	2.229(2)	C(5)-Re(1)-C(6)	37.4(11)
Re(1)-C(6)	2.198(2)	C(6)-Re(1)-C(1)	36.21(10)

[**7p**](OTf) crystallizes as red plates in the orthorhombic space group $P2_12_12_1$. The structure contains one molecule in the asymmetric unit. Moreover, the rhenium atoms are disordered between the two naphthalene ligands with an occupancy of 80:20. Unlike the counter-ions, a disorder of the triflate to Cl^- with occupancy of 90:10 was found. The molecular structure of [**7p**]$^+$ is shown in Figure 19 and consists of two planar and eclipsed naphthalene rings bound to the rhenium in a η^6-fashion. The Re-C_{arom} bond lengths were between 2.212(7) Å and 2.289(6) Å (Table 13). The obtained values are in the same range compared to the other rhenium arenes structures and slightly longer with comparable structures like V(η^6-$C_{10}H_8$)$_2$ (2.21(4) Å) and Cr($C_{10}H_8$)$_2$. (2.17(2) Å).[123, 124]

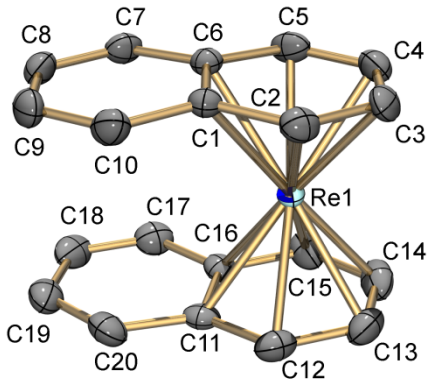

Figure 19: ORTEP representation[108] of the [Re(η^6-naphthalene)$_2$]$^+$ ([**7p**]$^+$) cation of the [**7p**](OTf) structure. Thermal ellipsoids are represented at the 50% probability level. Hydrogen atoms are omitted for clarity.

Table 13: Selected bond lengths and angles of [**7p**]$^+$

Selected bond lengths [Å]		Selected angles [°]	
Re(1)-C(1)	2.256(7)	C(1)-Re(1)-C(2)	37.4(2)
Re(1)-C(2)	2.213(7)	C(2)-Re(1)-C(3)	36.6(3)
Re(1)-C(3)	2.227(7)	C(3)-Re(1)-C(4)	37.3(3)
Re(1)-C(4)	2.231(7)	C(4)-Re(1)-C(5)	35.9(3)
Re(1)-C(5)	2.247(6)	C(5)-Re(1)-C(6)	36.6(3)
Re(1)-C(6)	2.289(6)	C(6)-Re(1)-C(1)	36.9(2)
Re(1)-C(11)	2.282(6)	C(11)-Re(1)-C(12)	36.9(3)
Re(1)-C(12)	2.241(7)	C(12)-Re(1)-C(13)	36.6(3)
Re(1)-C(13)	2.216(7)	C(13)-Re(1)-C(14)	37.2(4)
Re(1)-C(14)	2.217(8)	C(14)-Re(1)-C(15)	37.0(3)
Re(1)-C(15)	2.212(7)	C(15)-Re(1)-C(16)	37.4(3)
Re(1)-C(16)	2.227(6)	C(16)-Re(1)-C(11)	37.2(2)

The crystal structure of compound [**6p**]$^+$ is already published whereas the crystal structures of the side products [Re(η^6-tetralin)(η^6-benzene)]$^+$, [Re(η^6-biphenyl)(η^6-benzene)]$^+$ and [Re(η^6-naphthalene)-(η^6-tetralin)]$^+$ will be not discussed here. The data are listed in the section crystallographic tables.

6.1.2 NMR-Spectroscopy

The ^{1}H NMR data for the complexes were measured in $(CD_3)_2CO$, except for complexes [**7**]$^{+}$-[**14**]$^{+}$ and for the ^{99}Tc analogues which were measured in CD_3CN (Table 14). All the ^{13}C NMR data were listed in the experimental part. Albeit the measurements were performed in different solvents, several trends have been observed. For all Re and ^{99}Tc complexes, the signals of the arene protons are strongly upfield shifted as compared to the uncoordinated arenes.

Table 14: Comparison of ^{1}H NMR shifts of the CH_{arom} for Re/Tc coordinated and uncoordinated arenes.

Complex	^{1}H NMR CH_{arom} shift of uncoordinated arene (ppm)	^{1}H NMR CH_{arom} shift of coordinated arene (ppm)	^{1}H NMR CH_{arom} shift of coordinated arene (ppm) ^{99}Tc analogues
[**1**]$^{+}$	7.37[b, 125]	6.16[a]	5.65[b, 67]
[**2**]$^{+}$	7.3 – 7.1[b, 125]	6.17 – 6.00[a]	5.63 – 5.50[b, 67]
[**3**]$^{+}$	7.17[c, 126]	6.06[a]	-
[**4**]$^{+}$	7.08 – 7.01[c, 126]	6.06 – 5.92[a]	-
[**5**]$^{+}$	7.06 – 6.76 [c, 126]	6.15 – 5.93[a]	-
[**6**]$^{+}$	6.79[c, 127]	5.91[a]	5.39[b, 67]
[**7**]$^{+}$	7.28-7.14[c, 128]	5.91 – 5.79[b]	-
[**8**]$^{+}$	7.28-7.14[c, 128]	6.02 – 5.85[b]	-
[**9**]$^{+}$	7.28-7.14[c, 128]	6.00 – 5.70[b]	-
[**10**]$^{+}$	7.40 – 7.18[c, 129]	6.10 – 5.89[b]	-
[**11**]$^{+}$	7.40 – 7.18[c, 129]	6.16 – 5.89[b]	-
[**12**]$^{+}$	7.47 – 7.20[c, 130]	6.14 – 5.85[b]	-
[**13**]$^{+}$	7.09 – 7.01[c, 131]	6.09 – 5.95[a]	5.54 – 5.43[b, 67]
[**14**]$^{+}$	7.82 – 7.30[c, 132]	6.58 – 5.85[b]	-
[**15**]$^{+}$	7.60 – 7.35[c, 129]	6.68 – 6.18[a]	-
[**16**]$^{+}$	6.49[c, 133]	4.10[a]	-
[**17**]$^{+}$	7.37[b, 125]	5.66[a, 116]	5.42[b, 116]
[**7p**]$^{+}$	7.85 – 7.48[c, 129]	6.78-6.33[a, 117]	-
[**6p**]$^{+}$	7.85 – 7.48[c, 129] 7.37[b, 125]	7.32 – 6.38[a] (naphthalene) 5.83[a] (benzene)[117]	-

[a] measured in $(CD_3)_2CO$; [b] measured in CD_3CN: [c] measured in $CDCl_3$

In particular, the CH_{arom} of coordinated (alkylated)-benzene lies in the range of 6.16 – 5.79 ppm except for [**16**]$^{+}$ which was found at 4.10 ppm. While for more complex ligands such as fluorene [**14**]$^{+}$, biphenyl [**15**]$^{+}$, and naphthalene [**7p**]$^{+}$, the protons signals are shifted to slightly higher range (6.78 – 5.85 ppm). In the case of compounds with mix ligand system like [Re(η^6-$C_6(CH_3)_6$)(η^6-C_6H_6)]$^{+}$ ([**17**]$^{+}$)

and [Re(η^6-$C_{10}H_8$)(η^6-C_6H_6)]$^+$ [**6p**]$^+$, the unsubstituted coordinated benzene were shifted towards higher field (5.83 ppm, 5.66 ppm) compared to [**1**]$^+$ (6.16 ppm). Comparison between the Re and ^{99}Tc analogues displayed a shift to higher field for ^{99}Tc. Similar trends were reported for the isoelectronic group 8 ([M(benzene)$_2$]$^{2+}$; M = Fe (6.69 ppm)[56], Ru (6.90 ppm)[134]) and group 6 ([M(benzene)$_2$]; M = Cr (4.21 ppm)[135], Mo (4.60 ppm)[136], W (5.00 ppm)[136]). The latter neutral complexes are shifted towards higher field compared to [**1**]$^+$. Going from left to right in a period leads to an increase of the positive charge and electronegativity on the metal, which leads to an increased chemical shift (shift to lower field) of the CH protons. Also, going down in a group leads to an increased chemical shift of the C*H* protons. ^{13}C NMR spectroscopy of the coordinated arene shows shifts for the *C*H groups between 82.4 – 71.63 ppm and therefore considerably shifted to higher field compared to the chemical shift of e.g. benzene in CD_3CN, which is found at 129.32 ppm.[125] A clear trend is also observed by the degree of alkylation of the coordinated benzene ring. An increasing of the alkylation leads to shift the arene protons to higher field. This phenomenon is caused by the inductive effect (+I-effect) of alkyl group where the arene protons are more shielded. The assignment of the H/C NMR spectra of [**14**]$^+$ was accomplished via Nuclear Overhauser effects (NOE) experiments since the syn-/anti-isomers could not be separated. The ratio is 1:0.88 (syn/anti). For compound [**16**]$^+$ a coupling pattern AA'XX' were observed arising for the bridged ethylenic protons (2.58 ppm, 3.14 ppm). The pattern is explained due to the chemical inequivalence of the protons closer to the metal atom compared with those closer to the non-coordinated aromatic ring and the fact that the coupling constants are modified by the degree of torsion in the bridging functions.[122]

6.1.3 Physico-Chemical Properties

In order to get information about the electrochemistry and chemical stability of the complexes, cyclic voltammetry experiments were performed. CV's were measured *vs*. an Ag/AgCl reference electrode using a 0.1 M solution of TBA(PF_6) in MeCN as electrolyte. The spectra were referenced *vs*. Fc/Fc^+ at 0.45 V.

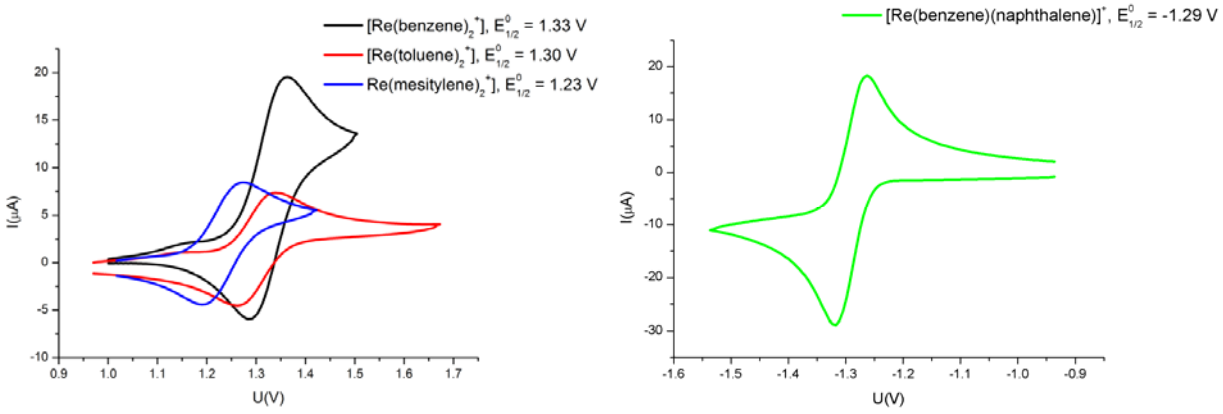

Figure 20: CV spectra of the oxidation of [**1**]$^+$ (black), [**2**]$^+$ (red) and [**6**]$^+$ (blue) with the corresponding $E^0_{1/2}$ values (left). CV spectra of the reduction of [**6p**]$^+$ (green) with the corresponding $E^0_{1/2}$ values (right).

The electrochemical analysis for $Re^{+/2+}$ as well as $^{99}Tc^{+/2+}$-arene complexes showed a fully reversible redox behaviour except for the mixed ligand systems [**7p**]$^+$ and [**6p**]$^+$ where an irreversible oxidation was observed (Table 15).[67] The $E^0_{1/2}$ values for the oxidation of the $Re^{+/2+}$ redox-couples and for the $^{99}Tc^{+/2+}$ redox-couples are in the range of 1.33 - 1.20 V and 1.52 - 1.24 V, respectively. The higher oxidation potentials of the $^{99}Tc^{+/2+}$ are in agreement with the general trends which are found in the periodic table. In contrast to the oxidation, the reduction of $M^{+/0}$ (M = Re/^{99}Tc) are for almost all complexes irreversible and were found to be more negative then <2 V. The only exception of the measured substances was compound [**6p**]$^+$ with a reversible reduction potential of -1.29 V. This $1e^-$ reduction process is presumably ligand based and is occurred due to the further stabilisation of the Re(I) centre. In the case of compound [**7p**]$^+$ the reduction is irreversible with E_{pc} value in the same range comparing [**6p**]$^+$. It seems that a stronger bound benzene ligand may stabilize the reduced species more than in the case of [**7p**]$^+$ where both naphthalenes are weaker bound. On one hand, comparisons with neighbour analogues are difficult because their electrochemistry is poorly described in the literature. However, the measurements were partially performed in different solvents (or under different conditions) and thus do not allow a direct correlation. For group 8 reduction potentials of the complex $[M(C_6Me_6)_2]^{2+/+}$ (M = Fe, Ru, Os) were found with values of -1.82 V, -1.36 V and -1.25.[137] Compared to [**1**]$^+$ the reduction potential of $[Ru(\eta^6\text{-benzene})_2]^{2+/+}$, is anodically

shifted by almost 1 V.[138] An oxidation potential of 0.82 V was reported for $[Cr(benzene)]_2$ and for Mo and W, no data are available.[139] Electrochemistry chemistry for mix (benzene/naphthalene) or for only bis-naphthalene ligand system is only reported for chromium.[140] But no correlation could be concluded due to reasons mentioned before. Another clear trend is caused by the degree of alkylation on the arenes ligand. An increasing of alkylation on the ligand effects a shift of the oxidation of $M^{+/2+}$ (M = Re, ^{99}Tc) to less positive values. This could be explained through the inductive effect (+I-effect) of alkyl group resulting in an increase of electron density on the metal and thus a lowering of the oxidation potential takes place. A lowering of the oxidation potential could be also observed by functionalized bis-arene complexes such as bromobenzene or benzoic acid.[79] In these cases, it was assumed that the ligands were oxidized rather than the metal centre which is manifested by an irreversible oxidation process. According to the same trend, reduction of Re should be harder compared to the ^{99}Tc-analogue. Since this is not the case and the reduction potentials are very similar, reduction of the ligand instead of the metal centre is assumed. This phenomenon was already observed in previous studies.[116]

Table 15: An overview of CV data of Re/^{99}Tc bis-arene complexes. All measurements were conducted in a 0.1 M TBA(PF_6) MeCN electrolyte solution and an Ag/AgCl reference electrode. The potentials were referenced *vs*. Fc/Fc+ at 0.45 V.

Re-complexes	Ox. Pot. [V]	Red. Pot. [V]	Tc-complexes[67, 116]	Ox. Pot. [V]	Ox. Pot. [V]
$[Re(benzene)_2]^+$ [**1**]$^+$	1.33[a]	-2.00[b]	$[^{99}Tc(benzene)_2]^+$	1.52[a]	-2.04
$[Re(toluene)_2]^+$ [**2**]$^+$	1.30[a]	-2.07[b]	$[^{99}Tc(toluene)_2]^+$	1.47[a]	-2.21
$[Re(tetralin)_2]^+$ [**3**]$^+$	1.24[a]	-2.1[b]	$[^{99}Tc(tetralin)_2]^+$	1.39[a]	-2.15
$[Re(mesitylen)_2]^+$ [**6**]$^+$	1.23[a]	-2.15[b]	$[^{99}Tc(mesitylen)_2]^+$	1.38[a]	-2.27
[Re(hexametylbenzene) (benzene)]$^+$ [**17**]$^+$	1.20[a]	-2.21[b]	$[^{99}$Tc(hexamety-benzene)(benzene)]$^+$	1.35[a]	-2.26
$[Re(hexametylbenzene)_2]^+$	-	-	$[^{99}$Tc(hexametyl-benzene)$_2]^+$	1.24[a]	-2.44
$[Re(naphthalene)_2]^+$ [**7p**]$^+$	1.21[b]	-1.28[b]	$[^{99}Tc(naphthalene)_2]^+$	-	-
[Re(naphthalene) (benzene)]$^+$ [**6p**]$^+$	1.16[b]	-1.29[a]	$[^{99}$Tc(naphthalene) (benzene)]$^+$	-	-

[b]reversible oxidation; [a]irreversible reduction

The higher oxidation and reduction potential of such complexes reflected their stabilities towards water, air, and also their chemical inertness concerning ligand exchange reactions. While for complex [**7p**]$^+$ and [**6p**]$^+$ the potentials are lower compared to the other compounds and thus complexes can be characterized as more reactive.

All bis-arene complexes are of yellow to red colour. UV/VIS spectra were measured for compound [**1**]$^+$ and Compound [**7p**]$^+$. The electronic spectra of these compounds are similarly structured, showing very weak bands in the visible range above 400 nm, likely to be assigned as d-d transitions due to their weak extinction coefficients. They further feature a number of shoulders below 400 nm, assigned as intra-ligand charge transfer absorptions. None of these complexes exhibits significant long-lived excited states or phosphorescence indicating triplet states resulting from intersystem crossing. No fluorescence was detected for these two compounds.

6.1.4 Cytotoxicity Studies

Cytotoxicity studies on human cervix HeLa, human ovarian carcinoma A2780 and human ovarian cisplatin resistant A2780/CP70 cancer cell lines, as well as MRC-5 non-tumorigenic cell line treated with complexes [Re(η^6-naphthalene)$_2$]$^+$ ([**7p**]$^+$), and [Re(η^6-biphenyl)$_2$]$^+$ ([**15**]$^+$) and the respective ligand 1 and 2, were performed by a fluorometric cell viability assay using Resazurin (Promocell GmbH). Briefly, one day before treatment cells were plated in triplicates in 96-well plates at a density of 4 × 10^3 cells/well in 100 µL. Upon treating cells with increasing concentrations of the rhenium complex cells were incubated at 37°C / 6% CO_2 for 4 h, the medium was removed, replaced with complete medium non-containing the complexes and irradiated at 350 nm for 10 minutes (2.58 J/cm^2) in a Rayomet Chamber Reactor. After further 44 h incubation, the medium was removed and 100 µL of complete medium containing resazurin (0.2 mg/mL final concentration) was added. After 4 h of incubation at 37 °C / 6% CO_2, the fluorescence of the highly red fluorescent resorufin product was quantified at 590 nm emission with 540 nm excitation wavelength in a SpectraMax M5 microplate Reader. The results expressed as mean ± standard deviation error bar of independent experiments (at least n = 3) is reported below (Table 16).

Table 16: Antiproliferative effects of the target rhenium complexes in different non-tumorigenic and cancer cell lines, upon irradiation at 350 nm for 10 min (2.58 J/cm2).

complex	MRC-5 IC_{50} (µM)*	HeLa			A2780			A2780 / CP70		
		IC_{50} (µM)			IC_{50} (µM)			IC_{50} (µM)		
		dark	UV-A	PI	dark	UV-A	PI	dark	UV-A	PI
[7p]$^+$	>100	>100	>100	n.a.	>100	64.8 $^{\pm 17.8}$	> 1.6	>100	64.8 $^{\pm 3.2}$	> 1.6
[15]$^+$	24.7$^{\pm 1.7}$	>100	26.4 $^{\pm 7.7}$	> 3.8	>100	40.3 $^{\pm 13.4}$	> 2.5	>100	38.9 $^{\pm 7.6}$	> 2.6

*: cell incubated in the dark for 48h

In the dark, complexes [Re(η^6-naphthalene)$_2$]$^+$ ([**7p**]$^+$) and [Re(η^6-biphenyl)$_2$]$^+$ do not show any activity while, upon light irradiation at 350 nm, they are cytotoxic. Complex [**7p**]$^+$ (higher reactivity)

displays IC_{50} values in the high micromolar range and complex ([**15**]$^+$) in the mid-micromolar range. Moreover, they are not affected by the cellular acquired resistances (CP70). As a comparison, the Ru analogues [Ru(η^6-biphenyl)$_2$]$^{2+}$ was tested in human ovarian carcinoma A2780 without showing any cytotoxicity.[48]. This preliminary experiment shows mainly their potential but further investigations are needed.

6.2 Fischer Hafner Reaction with Functionalized Arene

Reactions with functionalized arene ligands such methyl benzoate, methyl phenyl benzoate, methoxybenzene, benzyl alcohol, phenols, dibenzyl ether, benzaldehyde and Indoles and in the presence of $AlCl_3$ did not work due to its high oxophility or reactivity toward lone pairs. By using halogenated arenes and/or in combination with hexamethylbenzene as ligands, reactions were carried out and desired products were isolated in low yields.[141] Recently, some preliminary studies showed that substituted aniline derivatives are an alternative to alkylbenzene and can be applied under this harsh condition. However, the yields are below 10% except for complex [Re(η^6-$C_6H_5N(CH_3)_2)_2$]$^+$ which could be isolated in yields about 30%.[142] Nevertheless, $AlCl_3$ is still used for ligand exchange reaction for example in the synthesis of arene cyclopentadienyl iron complexes form ferrocene (arene = benzene, alkylbenzenes, arylbenzenes, halobenzenes, benzyl ethers, benzylamides, polycyclic compounds and heterocycles). Furthermore, by using microwave dielectric heating, the reaction time of ligand exchange can be even reduced within a few minutes. This fact allowed reaction with more bulky alkyl arenes, phenols, benzyl alcohol and benzaldehyde in high yield and even in the presence of $AlCl_3$.[143] Since compound [**1**]$^+$ is more stable compared ferrocene, ligand exchange reaction did not work. Also, under UV/light irradiation or thermally treatment no reaction was observed. Besides, ligand substitution could be achieved by using [**7p**]$^+$ and [**6p**]$^+$ as starting compounds. The reactions were light and thermally induced. Since Friedel–Crafts acylation on [**1**]$^+$ with acyl halide did not work by using $FeCl_3$ or $AlCl_3$ due to its deactivated benzene. A requirement of mono- and di-functionalized [Re(η^6-C_6H_5R)(η^6-$C_6H_{6-n}R_n$)]$^+$ (n = 0, 1) is still needed and therefore other pathways were elucidated and published in the following paper. Furthermore, some unpublished results related to the manuscript are described afterwards.

6.3 Publication: Bis-arene Complexes $[Re(\eta^6\text{-arene})_2]^+$ as Highly Stable Bioorganometallic Scaffolds

Bis-arene Complexes $[Re(\eta^6\text{-arene})_2]^+$ as Highly Stable Bioorganometallic Scaffolds

*Giuseppe Meola, Henrik Braband, Paul Schmutz, Michael Benz, Bernhard Spingler and Roger Alberto**

Department of Chemistry, University of Zürich, Winterthurerstrasse 190, CH-8057 Zürich Switzerland

Abstract: The syntheses of mono- and di-functionalized $[Re(\eta^6\text{-}C_6H_5R)(\eta^6\text{-}C_6H_{6\text{-}n}R_n)]^+$ (n = 0, 1; R = COOH, Br complexes starting from $[Re(\eta^6\text{-benzene})_2]^+$ is described. The lithiation of $[Re(\eta^6\text{-benzene})_2]^+$ with *n*-BuLi leads preferentially to the neutral, alkylated product $[Re(\eta^6\text{-}C_6H_6)(\eta^5\text{-}C_6H_6\text{-Bu})]$ but not to the expected deprotonation of the arene ring. Deprotonation/lithiation with LDA gave the mono- and the di-lithiated products *in situ*. Their reactions with of 1,1,2,2-tetra-bromoethane (TBE) or with CO_2 respectively gave the $[Re(\eta^6\text{-}C_6H_5Br)(\eta^6\text{-}C_6H_6)]^+$, $[Re(\eta^6\text{-}C_6H_5Br)_2]^+$ or $[Re(\eta^6\text{-}C_6H_5COOH)(\eta^6\text{-}C_6H_6)]$(TFA), $[Re(\eta^6\text{-}C_6H_5COOH)_2]$(TFA). These functionalized derivatives of $[Re(\eta^6\text{-benzene})_2]^+$ represent novel precursors for the synthesis of bioconjugates to bioactive structures, comparable to $[Co(Cp)_2]^+$ or $[Fe(Cp)_2]$. Different model compounds $[Re(\eta^6\text{-}C_6H_5R)(\eta^6\text{-}C_6H_{6\text{-}n}R_n)]^+$ (n = 0, 1; R = $-SCH_2Ph$, -NHPh, $-CONHCH_2Ph$, $-C_6H_5$-COdpa) were synthesis via amide bond formation and nucleophilic aromatic substitution. These conjugates were fully characterized including X-ray structure analyses of most products. For all complexes, the ^1H NMR arene proton signals are strongly upfield shifted as compared to the non-coordinated arenes. The electrochemical analyses show an irreversible, probably substituent-centered oxidation, which contrasts the cyclic voltammetry of the underivatized complexes where oxidation is fully reversible. The stability of the core and the reactivity of the substituents make these bis-arene complexes useful precursors in medicinal inorganic chemistry, comparable to cobaltocenium or ferrocene.

Introduction

Over the recent decades, organometallic complexes emerged as convenient modalities in multiple fields of life sciences. Albeit being considered as air - and water sensitive, a number of very stable organometallic complexes and building blocks are key for bioorganometallic chemistry.[1] They complement with their distinct metal-or ligand-based reactivities current inorganic medicinal drugs. Coordination compounds such as cisplatin and successors are pivotal in cancer therapy and dominate widely the field of cancer therapy. Bioorganometallic chemistry has become a well-established research direction, complementing bioinorganic chemistry.[2] Complexes with ligands such as

cyclopentadienyl (Cp, mainly with iron or cobalt) and derivatives or arenes (with ruthenium) tune the properties and, thus, the reactivities of given metal centres. They are conjugated to vectors to obtain target-specific inorganic compounds, which exert authentic actions.[3, 4] Currently, two major building blocks are at the core of bioorganometallic chemistry, namely the $\{Ru(arene)\}^{2+}$ fragments[4] and ferrocene (Fc) derivatives.[2, 5-7]

Conceptually, organometallic complexes are divided in compounds with metal- or ligand-based reactivities and in complexes mimicking (sub)structures of pharmaceuticals, the latter ones prototypically being based on organometallic ruthenium, Fc or cobaltocenium $[Co(Cp)_2]^+$ moieties.[8-10] A further field of application for organometallic complexes is imaging. Technetium complexes with the $\{^{99m}Tc(CO)_3\}^+$ core have been studied intensely in this respect and one compound designed for targeting the prostate specific membrane antigen recently finished phase II clinical trials.[11] In combination with the Cp ligand, complexes of the form $[(\eta^5\text{-}C_5H_4\text{-}R)^{99m}Tc(CO)_3]^+$ and their rhenium homologues show great potential for a molecule-based theranostic approach.[12, 13]

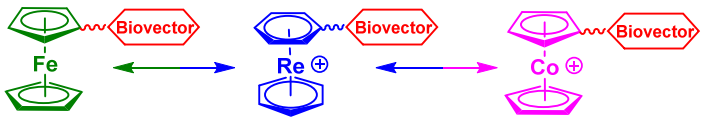

Scheme 1: Concept of Ferrocene, Cobaltocenium and "Rhenocene"; structurally related organometallics conjugated to targeting vectors

Ferrocene (Fc) is probably the most widely studied building block in bioorganometallic chemistry, as an analytical in vivo and in vitro probe or as a structural mimic of pharmaceutical lead structures.[14, 15] Its isoelectronic congener cobaltocenium $[Co(Cp)_2]^+$ is equally important for this report, but substantially less studied.[16-19] Arene-based sandwich complexes found almost no attention in this context despite their structural similarity to Fc or $[Co(Cp)_2]^+$. Their preparations are distinctly more difficult than cyclopentadienyl analogues and the arene ligand is generally less stably bound due to its uncharged nature. In addition, arene-sandwich complexes of the type $[M(\eta^6\text{-arene})_2]^{0/n+}$ are prone to oxidation and/or ligand loss.[20] Introduction of functionalities into $[M(\eta^6\text{-arene})_2]^{0/n+}$ as a next step was described for Cr or Mo[21-25] but studies with $[M(\eta^6\text{-arene})_2]^{n+}$ in bioorganometallic chemistry are generally rare. Only ruthenium and osmium are exceptions.[4, 26-30] Whereas $[M(\eta^6\text{-arene})_2]$ for M = Cr, Mo are stable but air sensitive, the group 7 homologous $[M(\eta^6\text{-arene})_2]^+$ compounds remain essentially unstudied in any respect. The $[Mn(\eta^6\text{-arene})_2]^+$ complex is highly unstable and was obtained via metal vapour synthesis and in situ oxidation in low yields.[31] The syntheses of the technetium and rhenium homologous were described in the early sixties, but focused approaches to

the exploration of their chemistry neglected. To our knowledge, no exploration of their biological activities exist, likely due to the difficult preparation. Only recently, Kudinov et al. reported a more convenient approach to $[Re(\eta^6\text{-arene})_2]^+$ type complexes, albeit in moderate yields, and studied the photolytic substitution of e.g. naphthalene rings.[32] Being convinced about their suitability for bioorganometallic chemistry, we presented a high yield approach to $[M(\eta^6\text{-arene})_2]^+$ (M = $^{99(m)}$Tc, Re) type complexes directly from $[MO_4]^-$, overcoming the original tedious and lengthy synthetic procedures.[33] These bis-arene complexes for Re and Tc turned out to be remarkably stable and insensitive towards oxidation or hydrolysis, ideal prerequisites for application as building blocks or structural elements in combination with pharmaceutical lead structures or biological vectors. $[Re(\eta^6\text{-arene})_2]^+$ resembles structurally ferrocene or cobaltocenium (Scheme 1). The "+1" charge renders them more water soluble but introduces a charge, which must not be an immediate disadvantage in combination with biomolecules.[17, 18]

To further extend the basic sandwich structures with biologically active functions, we present in this study arene functionalization of $[Re(\eta^6\text{-benzene})_2]^+$ followed by conjugation to model biomolecules. Their integration into pharmaceutical lead structures follows principally the same approaches. The key compounds are sketched in Scheme 2. Biological investigations and comparison to ferrocene analogues will prove or disprove their equivalence to Fc or $[Co(Cp)_2]^+$ as building blocks.

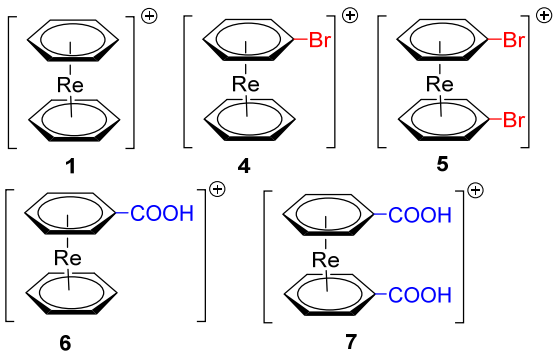

Scheme 2. Basic $[Re(\eta^6\text{-}C_6H_6)_2]^+$ (1) "rhenocenes" and derivatives thereof [**4**-**5**]PF_6 and [**6**-**7**]TFA for conjugation to functional molecules.

Results and discussion

Syntheses: The starting complex $[Re(\eta^6\text{-benzene})_2]^+$ was synthesized as the triflate salt ([**1**$^+$]OTf) according to a modified procedure of Kudinov et al.[32] as published by our group (electronic supplementary information, ESI).[33] The cationic, closed shell 18e$^-$ complex **1**$^+$ is water soluble as the Cl^- salt, very air - and water stable at temperatures well above 100°C and not prone for oxidation or reduction due to their electrochemical properties as discussed below. Arene release in water or organic solvents with concomitant decomposition to undefined products was only observed upon

irradiation with UV light. Thus, the physico-chemical properties of [Re(η^6-benzene)$_2$]$^+$ and derivatives resemble those of ferrocene. From this perspective, they may represent suitable markers for biomolecules since stable under physiological conditions. The ^{99}Tc homologous exhibit a similar electrochemistry but their $E°_{1/2}$ ($Tc^{I/II}$) oxidation potentials are even more cathodically shifted than those of rhenium are. It is safe to state that the bis-arene complexes of rhenium and technetium are the most stable ones as compared to the congeners of the neighbouring elements. For later conjugations to functionalities, derivatization of one, or both, of the coordinated arene rings is required. Typically, introduction of halides as good leaving groups for nucleophilic aromatic substitution or carboxylic acids for amide bond formation are common strategies for coupling such moieties to targeting vectors.

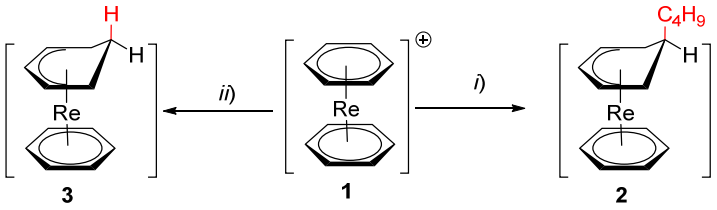

Scheme 3: Reaction scheme for direct nucleophilic attack to one coordinated arene in [Re(η^6-benzene)$_2$]$^+$: *i*) *n*-BuLi, -78°C, THF, H_2O. *ii*) $NaBH_4$ 6h, THF.

Functionalization: Lithiation of the benzene ring and subsequent bromination with tetra-bromo-ethane, $C_2H_2Br_4$ (TBE), or reaction with CO_2 respectively, represents the first step of arene functionalization as reported for neutral [M(η^6-benzene)$_2$] type complexes of V,[24, 34], Cr[34-36] or Mo[35, 37, 38]. Since the acidity of the neutral bis-arene complexes of group 5 and 6 transition elements is very low, *n*-butyl-lithium (*n*-BuLi) as a very strong base was required for deprotonation/lithiation. For cationic **1**$^+$, however, attempted lithiation with *n*-BuLi at -78°C, with or without the addition of tetra-methyl-ethylene-diamine (TMEDA), lead preferentially to a direct nucleophilic attack of the butyl anion to the coordinated arene, and not to the expected ring deprotonation (Scheme 3). The very strong binding of the arene to "Re$^+$" (electron withdrawing group) renders the aromatic system more acidic, but also prone to direct nucleophilic attack. In the competition lithiation *vs.* alkylation, the latter prevails and the neutral complex [Re(η^6-C_6H_6)(η^5-C_6H_6-Bu)] (**2**) (Scheme 3) was isolated as orange crystals from dry hexane in excellent yield (92%). Complex **2** is soluble in most organic solvents, is air and moisture sensitive as solid and in solution, but stable for weeks under an inert atmosphere. The ESI-MS of compound **2** showed the molecule peak at m/z = 401.1 [MH]$^+$. In the ^{1}H NMR spectra, the signals of the arene protons are strongly high-field shifted (5.84, 4.81 and 3.54 ppm) as compared to [**1**$^+$]OTf (6.16 ppm). Rhenium complexes containing a single η^5-coordinated cyclohexadienyl ligand in combination with other ligands are known since some time,[39, 40] crystal

structures of this class of compounds with other elements are rare, however.[41-43] X-ray quality crystals of **2** were obtained from slow evaporation of hexane solution. Figure 1 shows an ORTEP representation[44] of compound **2**.

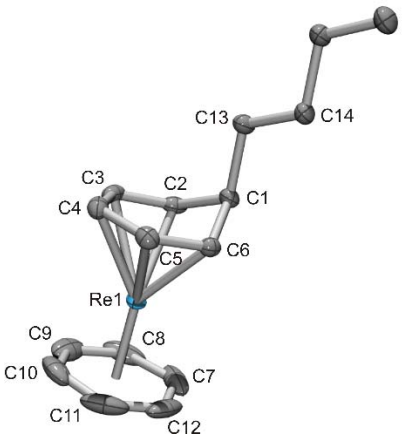

Figure 1: ORTEP[186] of complex **2**. Thermal ellipsoids are drawn on the 50% probability level. Hydrogen atoms are omitted for clarity. Selected bond lengths [Å] and angles [°]: Re1-C2 2.240(3), Re1-C3 2.219(3), Re1-C4 2.253(3), Re1-C5 2.233(3), Re1-C6 2.253(3), Re1-C7 2.192(4), Re1-C8 2.217(3), Re1-C9 2.237(4), Re1-C10 2.186(4), Re1-C11 2.239(4),Re1-C12 2.225(4), C1-C2-C3 117.5(3), C1-C6-C5 117.9(3).

The rhenium carbon bond lengths are in a similar range (2.186(4) - 2.253(3) Å) as in [**1**]BF_4 (2.212(9) - 2.301(9) Å).[187] The C1-C2-C3 and C1-C6-C5 angles of 117.5(3)° and 117.9(3)° respectively, lead to an envelop like conformation of coordinated cyclohexadienyl. C1 is in average twisted by 62.3° out of the arene plain. This expected conformational change by reduction/alkylation of the arene ligand have been observed in mono-arene complexes of group 6 (Cr,[46] Mo[47]), group 7 (Mn,[48-57] Re[41-43]) and group 8 (Fe,[58-60] Ru[61-67]) elements, but rarely for bis-arene complexes.[68] Crystallographic details for this and all subsequent structures are found in the electronic supplementary information Table S1-S3. Similarly, reaction of $\mathbf{1}^+$ with $Na[AlH_4]$ or $Na[BH_4]$ gave the neutral complex [Re(η^6-C_6H_6)(η^5-C_6H_7)] (**3**) in moderate yields (53%). Wilkinson and co-workers reported the ^{1}H NMR spectrum of this air and moisture sensitive complex.[39] Isolation, characterization and crystallisation of **3** was achieved by slow evaporation of a dry hexane solution and its structure has been confirmed by X-ray structure analysis (see ESI Table S1).

The coordinated benzene rings are thus prone to direct, nucleophilic attack, a reactivity pattern not found for coordinated arenes in neutral complexes. The overall mono-positive charge together with the strong electron donation of coordinated arene into the rhenium orbitals, lead to polarization and facile nucleophilic attack. In parallel, the {Re(η^6-benzene)}$^+$ moiety leads to mutual electron depletion and imposes a partial, positive charge to the rings. This push-pull situation allows good nucleophiles

to attack directly. The high-field shifted ^{1}H NMR signals in **2** indicate a reduced shielding by the ring current, in agreement with charge delocalization towards the rhenium centre. Similar observations were made for $[Mo(\eta^6\text{-}C_6H_6)_2]$[69] and $[Ru(\eta^6\text{-}C_6H_6)_2]^{2+}$.[70] Consequently and to avoid direct nucleophilic attack in favour of deprotonation of "strongly" acidic $\mathbf{1}^+$, a milder and less nucleophilic base was employed.

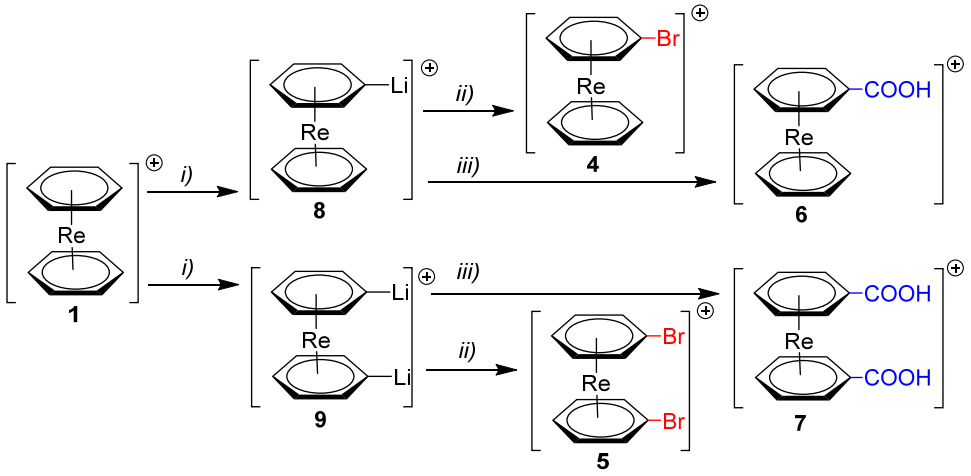

Scheme 4: Mono- and di-lithiation of $[Re(\eta^6\text{-}C_6H_6)_2]^+$ with LDA to yield complexes 8 and 9 as in situ intermediates and subsequent reactions to yield complexes 4-7: *i*) 2.5 eq. LDA, THF -78°C, 1.5h. *ii*) $C_2H_2Br_4$ (TBE), -78°C, 5h, H^+/H_2O and *iii*) CO_2 -78°C, 5h, H^+/H_2O.

With $Li(N(^{i}prop)_2)$ (LDA), deprotonation/lithiation occurred without a nucleophilic attack of the benzene ring (Scheme 4). Due to the high reactivity of the lithiated intermediates, the mixtures were directly reacted further without isolation and purification. Despite careful control of experimental conditions, the mono-lithiated product $\mathbf{8}^+$ together with di-lithiated $\mathbf{9}^+$ was consistently obtained *in situ* as evident from the subsequent reactions, always yielding mixtures of mono- and di-functionalized products. By altering the LDA concentration, the product ratio can slightly be influenced but exclusive formation of one product was not achieved. Of note, excess amounts of LDA lead to the formation of even higher substituted derivatives such as tri- tetra and penta-lithiated complexes. Subsequent bromination evidenced the m/z signals for all corresponding multi-brominated species, which could clearly be identified by UPLC MS but were not isolated. The mono- and di-substituted arene complexes could only be separated by preparative HPLC.

The reaction of $\mathbf{8}^+$ and $\mathbf{9}^+$ with of 1,1,1,2-tetra-bromoethane (TBE) gave air and water stable $[Re(\eta^6\text{-}C_6H_5Br)(\eta^6\text{-}C_6H_6)](PF_6)$ ($[\mathbf{4}^+]PF_6$) and $[Re(\eta^6\text{-}C_6H_5Br)_2]^+$ ($[\mathbf{5}^+]PF_6$) in 43% and 18% isolated yield. Under strongly alkaline conditions and extended reaction times, one Br^- was slowly substituted by hydroxide to yield the corresponding phenolato complex. The $[F_3CCO_2]^-$ salts (TFA) of $\mathbf{4}^+$ and $\mathbf{5}^+$ are water soluble but the cations can be precipitated with PF_6^- from aqueous solutions. Due to reduced

symmetry, the ^{1}H NMR spectra showed an extended set of signals. Single crystal X-ray diffraction analysis confirmed the structures of [**4**$^{+}$]PF_6 and [**5**$^{+}$]PF_6 and an ORTEP representation of **5**$^{+}$ is shown in Figure 2. The Re-C bond lengths in [**4**$^{+}$]PF_6 (2.219(6) - 2.236(6) Å) are in the same range as in [**1**$^{+}$]BF_4 (2.212(9) - 2.301(9) Å) and only slightly shorter than in [Re(η^6-1,3,5-$C_6H_3Me_3$)$_2$](BF_4) (2.233(4) - 2.268(4) Å).[45] The Re1-C1 bond length (2.234(5) Å) is not influenced by the Br^- and compares well with the other Re-C bond lengths. The eclipsed conformation of the two bromo-benzene rings may indicate a Br-Br interaction or just be a consequence of crystal packing.

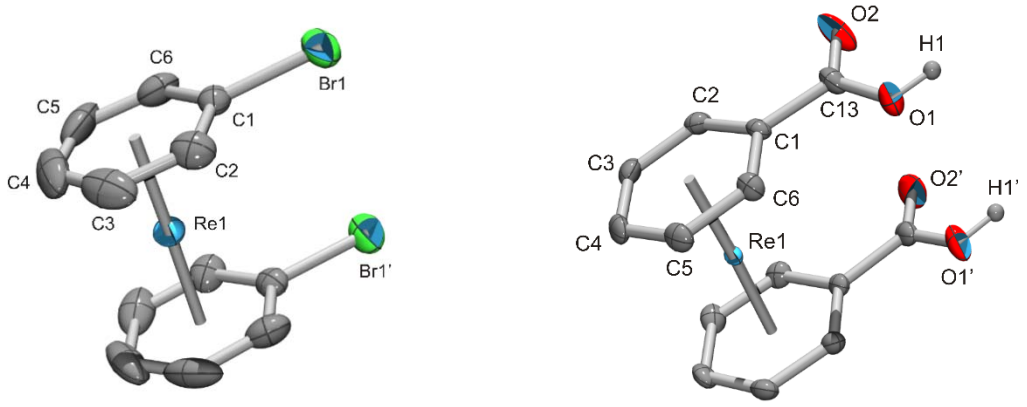

Figure 2. ORTEP representation of [Re(η^6-C_6H_5Br)$_2$](PF_6) [**5**$^{+}$]PF_6 (left) and [Re(η^6-C_6H_5COOH)$_2$](TFA) [**7**$^{+}$]TFA (right). Hydrogen atoms (except H1 in **7**$^{+}$) and anions are omitted for clarity, thermal ellipsoids represent 50% probability. Selected bond lengths [Å] for [**5**$^{+}$]: Re1-C1 2.234(5), Re1-C2 2.233(5), Re1-C3 2.220(6), Re1-C4 2.236(6), Re1-C5 2.219(6), Re1-C6 2.230(6), C1-Br1 1.888(5)and for [**7**$^{+}$]: Re1-C1 2.244(2), Re1-C2 2.245(2), Re1-C3 2.243(2), Re1-C4 2.239(2), Re1-C5 2.247(2), Re1-C6 2.243(2), C1-C13 1.499(3), C13-O1 1.319(3), C13-O2 1.207(3).

In analogy to the procedure for [**4**$^{+}$]PF_6 and [**5**$^{+}$]PF_6, the reaction of **8**$^{+}$ and **9**$^{+}$ with CO_2 at -78°C for 5h and purification by preparative HPLC gave the water soluble complexes [Re(η^6-C_6H_5COOH)(η^6-C_6H_6)](TFA) ([**6**$^{+}$]TFA) and [Re(η^6-C_6H_5COOH)$_2$]$^{+}$ ([**7**$^{+}$]TFA) in 48% and 27% yield after separation, respectively. Both are water stable and no decomposition under any conditions was observed An ORTEP representation of **7**$^{+}$ is given in Figure 2. Physico-chemical properties for salts of **4**$^{+}$ - **7**$^{+}$ are discussed below.

Conjugation to model substrates

The convenient syntheses of functionalized bis-arene complexes [**4**$^{+}$]PF_6, [**5**$^{+}$]PF_6, [**6**$^{+}$]TFA and [**7**$^{+}$]TFA, together with their hydrolytic stability and redox-inert behavior makes them well suited as probes and markers for biological vectors, in analogy to ferrocene or cobaltocenium. Depending on the nature of the anchoring group on the biomolecule side, coupling can be effectuated by bromide

substitution in **4**$^+$ and **5**$^+$ or by classical amide bond formation in **6**$^+$ and **7**$^+$. Since thiol – or amine groups are frequent functionalities in biomolecules, we exemplify coupling strategies to **4**$^+$ and **5**$^+$ with benzyl-thiolate and aniline, and to **6**$^+$ and **7**$^+$ with benzyl-amine and dimethoxy-phenethylamine (dpa), a dopamine precursor. These reactions are depicted in Scheme 5.

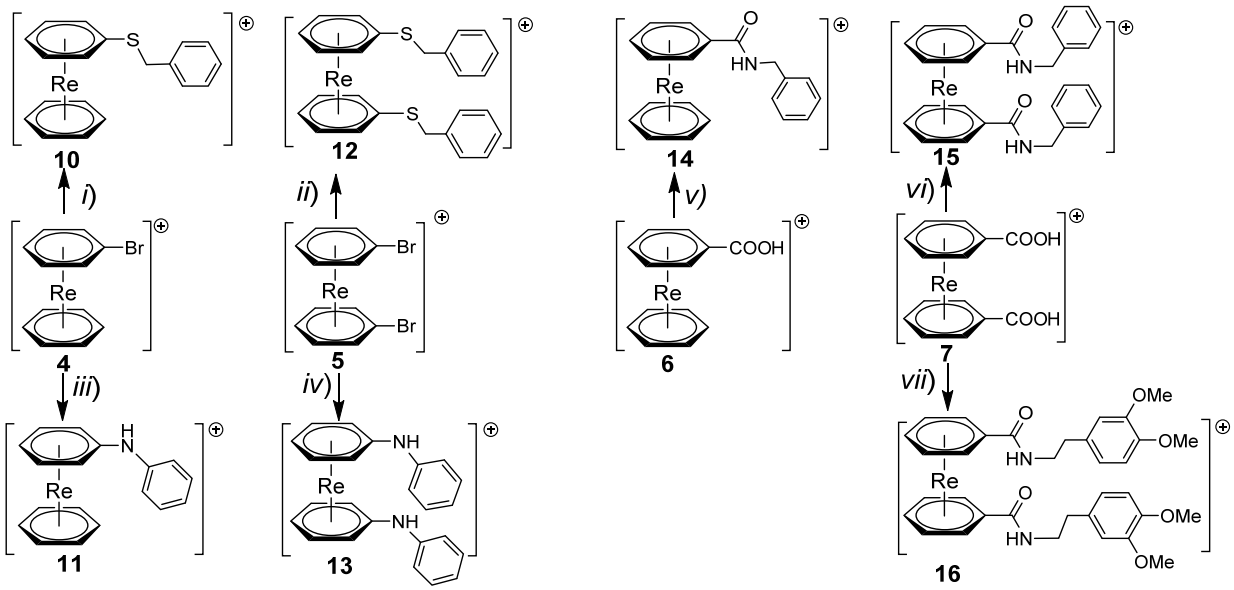

Scheme 5: Conjugation of substrate models to the bis-arene precursors **4**$^+$-**7**$^+$; reaction conditions: i) and (ii) benzyl mercaptan, DIPEA, acetonitrile, 70 °C 15 h, 90% and 88%; iii) and iv) NaH, aniline, 70 °C, 2 h, THF, 70 °C, 3 h, 72 % and 67.5 %; v) and vi) DIPEA, 3-[bis(dimethylamino)methyliumyl]-3H-benzotriazol-1-oxide hexafluorophosphate (HBTU), benzylamine, DMF, rt, 30 min, 73% and 79%; vii) DIPEA, 3-[bis(dimethylamino)methyliumyl]-3H-benzotriazole-1-oxide hexafluorophosphate (HBTU), 3,4-dimethoxyphenethylamine, DMF, rt, 30 min, 72%.

For both substrates, the reactions with benzyl-thiolate and aniline after deprotonation gave the corresponding conjugates $[Re(\eta^6\text{-}C_6H_5\text{-}SCH_2Ph)(\eta^6\text{-}C_6H_6)]PF_6$ ([**10**$^+$]PF_6), $[Re(\eta^6\text{-}C_6H_5\text{-}NHPh)(\eta^6\text{-}C_6H_6)]PF_6$ ([**11**$^+$]PF_6), $[Re(\eta^6\text{-}C_6H_5\text{-}SCH_2Ph)_2]PF_6$ ([**12**$^+$]PF_6) and $[Re(\eta^6\text{-}C_6H_5\text{-}NHPh)_2]PF_6$ ([**13**$^+$]PF_6) in very good yields (ESI). Following classical peptide conjugation with 3-[Bis(dimethylamino)methyliumyl]-3*H*-benzotriazol-1-oxide hexafluorophosphate (HBTU) as activating agent, complexes $[Re(\eta^6\text{-}C_6H_5\text{-}CONHCH_2Ph)(\eta^6\text{-}C_6H_6)]PF_6$ ([**14**$^+$]PF_6), $[Re(\eta^6\text{-}C_6H_5\text{-}CONHCH_2Ph)_2]PF_6$ ([**15**$^+$]PF_6), and $[Re(\eta^6\text{-}C_6H_5\text{-}COdpa)_2]PF_6$ ([**16**$^+$]PF_6) could be obtained. All complexes are fully characterized (ESI) and X-ray structure analyses confirmed the authenticity of ([**12**$^+$]PF_6), ([**13**$^+$]PF_6) and ([**15**$^+$]PF_6). ORTEP drawings of [**12**$^+$] and [**13**$^+$] are given in Figure 3. All compounds are air – and water stable.

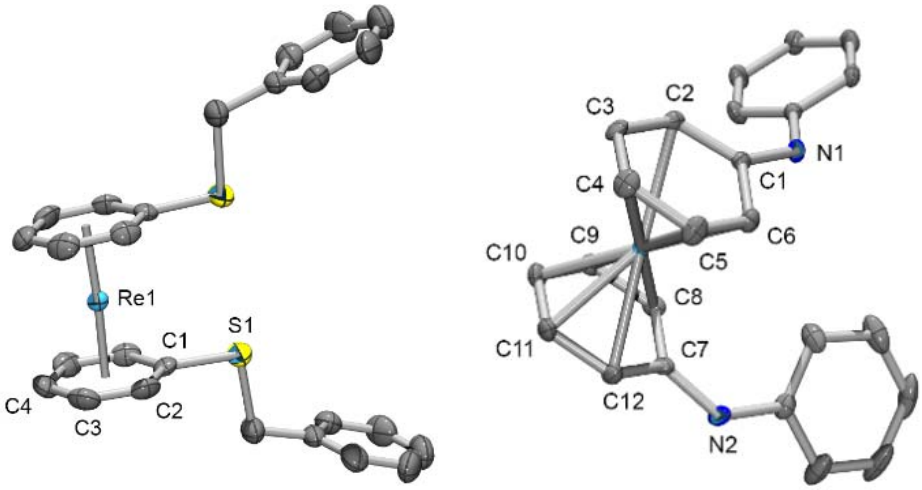

Figure 3. ORTEP representations of complexes [**12**$^+$] (left) and [**13**$^+$] (right). Hydrogen atoms and anions are omitted for clarity, thermal ellipsoids represent 50% probability. Selected bond lengths [Å] for **12**$^+$: Re1-C1 2.232(3), Re1-C2 2.233(3), Re1-C3 2.232(3), Re1-C4 2.230(4), C1-S1 1.781(3) and for **13**$^+$: Re1-C1 2.359(3), Re1-C2 2.263(3), Re1-C3 2.206(3), Re1-C4 2.236(3), Re1-C5 2.230(3), Re1-C6 2.231(3), Re1-C7 2.351(3), Re1-C8 2.245(3), Re1-C9 2.237(3), Re1-C10 2.251(3), Re1-C11 2.213(3), Re1-C12 2.230(3), C1-N1 1.382(4), C7-N2 1.369(5)

These examples corroborate the potential of [**4**$^+$]-[**7**$^+$] as building blocks or markers in conjunction with the labeling of small to large biomolecules. Either coupling strategy is feasible in aqueous environment due to the stabilities of the precursor complexes and the products. In contrast to ferrocene analogous, the products are often slightly water soluble due to the remaining, positive overall charge. The nucleophilic substitution of the bromide(s) in [**4**$^+$] and [**5**$^+$] can be applied to other nucleophilic, attacking groups as well, following in essence synthetic strategies from organic chemistry. Bis-arene "rhenocenes" are therefore "functionalities" which can be introduced in any kind of biomolecule or pharmaceutical lead structure as phenyl mimic as is done with ferrocene, but likely to result in different pharmaceutical and pharmacological properties.

A number of ferrocene amide conjugates, coupled to amino acids (his[71]), peptides (di or tri[72]) or with carbohydrates[73] have been reported. These conjugates were investigated e.g. on the inhibition of $A\beta_{1-42}$ fibrillogenesis (Alzheimer disease) as well as anticancer and antimalarial agents.[71-73] In contrast to **4** and **5**, the conjugation of biomolecules to bromo-ferrocene is more difficult due to its different reactivity towards nucleophiles. The bromo-ferrocene does not undergo nucleophilic aromatic substitution (S_nAr) but can be easily lithiated with *n*-BuLi[74] or further activated with $ZnCl_2$ for Negishi type cross-coupling reactions.[75]

Table 1: ^{1}H chemical shifts in complex cations [**4**$^{+}$]-[**7**$^{+}$], [**10**$^{+}$]-[**16**$^{+}$] and in non-coordinated ligands. Redox potentials E_{pa} of [**4**$^{+}$], [**6**$^{+}$], [**10**$^{+}$], [**11**$^{+}$] vs. Ag/AgCl in acetonitrile and TBA(PF_6) 0.1M as inert electrolyte (Fc/Fc^{+} = 0.45V).

complex	^{1}H NMR shifts (ppm)			^{1}H NMR shifts (ppm) pure arenes			E_{pa} (I/II) [V]
	δ_{ortho}	δ_{meta}	δ_{para}	δ_{ortho}	δ_{meta}	δ_{para}	
4^{+}	6.51	6.01	5.87	8.15	7.49	7.63	1.56
5^{+}	6.55	6.11	5.99				n/a
6^{+}	6.70	6.26	6.20	7.48	7.30-7.20		1.41
7^{+}	6.70	6.30	6.24				n/a
10^{+}	6.13	5.94	5.86	7.31-7.21			1.40
11^{+}	6.16	5.95	5.71	7.28-7.24	7.08-7.06	6.92	1.13
12^{+}	6.04	5.88	5.78	7.31-7.21			n/a
13^{+}	5.93	5.72	5.50	7.28-7.24	7.08-7.06	6.92	n/a
14^{+}	6.50	6.09	6.02	7.73-7.71	7.45-7.22		n/a
15^{+}	6.36	6.10	6.02				n/a
16^{+}	6.10	5.98	5.94	7.69	7.41	7.48	n/a

Chemical shifts are in ppm relative to solvent residue.

Physico-chemical properties: Electrochemical analyses of the bis-arene complexes allow insights into the electronics at the rhenium centre. The starting complex [**1**$^{+}$] displays a fully reversible redox behaviour with $E°_{1/2}$ for **1**$^{+/2+}$ at +1.3V vs Ag/AgCl in acetonitrile. Irreversible reduction is found more negative than -2V.[33] To our knowledge, data for the molybdenum analogues are not available and only the potential for chromium $E°_{1/2}$ for $[Cr(\eta^6\text{-}C_6H_6)_2]^{0/+}$ was reported to be about +0.82V.[76] According to general trends in the periodic table, we therefore estimate the corresponding oxidation potential of the ^{99}Tc homologue to be anodically shifted by about 0.2V.[33] We note that [**1**$^{+}$] is essentially redox inert, consistent with its behaviour towards air and water. The systematic influence of the different substituents on these potentials is of interest to state if redox stability limitations could arise from electron donating or - withdrawing groups, respectively. In contrast to all complexes $[Re(\eta^6\text{-}C_6H_{6\text{-}n}R_n)_2]^{+}$ (R = alkyl groups), E_{pa} for **X**$^{+/2+}$ (X = [**4**$^{+}$], [**6**$^{+}$], [**10**$^{+}$], [**11**$^{+}$]) were irreversible in cyclic voltammetry. Even rapid scanning did not lead to a partial reversibility. Corresponding CVs are shown in figure 4.

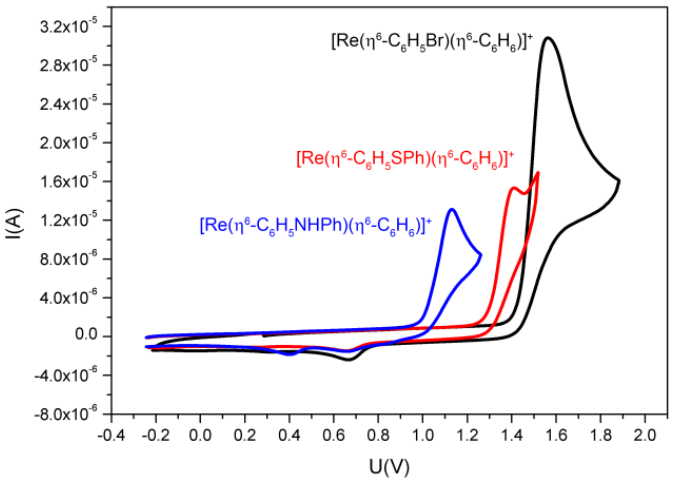

Figure 4: Cyclic voltammograms of [Re(η^6-C_6H_5Br)(η^6-C_6H_6)](PF_6) ([**4**$^+$]PF_6) (black line, E_{pa} = 1.56 V), [Re(η^6-C_6H_5-SCH_2Ph)(η^6-C_6H_6)](PF_6) ([**10**$^+$]PF_6) (red line, E_{pa} = 1.40 V), and [Re(η^6-C_6H_5-$CONHCH_2Ph$)(η^6-C_6H_6)](PF_6) ([**11**$^+$]PF_6) (blue line, E_{pa} = 1.13 V) in acetonitrile *vs.* Ag/AgCl (Fc/Fc^+ = 0.45V). 0.1 M [TBA][PF_6] (electrolyte), glassy carbon working electrode (i.d.= 3 mm), Pt auxiliary electrode and Ag/AgCl reference electrode, analyte concentrations 0.001 M, voltage step: 0.006 V, sweep rate: 0.1 V/s.

The first oxidation peaks/waves appear still at highly positive potentials. The observed irreversibility does not indicate oxidation at the rhenium center, which is well behaved in the corresponding complexes [Re(η^6-$C_6H_{6-n}R_n$)$_2$]$^+$. Rather, oxidation takes place at the substituents, followed by rapid, structural rearrangements leading to new products or to decomposition. Comparing $E°_{pa}$ for **1**$^{+/2+}$ with the one of [**4**]$^{+/2+}$, the latter one is increased by about 0.18 V.

The ^{1}H NMR data for [**4**$^+$]-[**7**$^+$] and [**10**$^+$]-[**16**$^+$] in D_3CCN are given in Table 1, the ^{13}C NMR data in the supplementary information. For all complexes, the signals of the arene protons are strongly upfield shifted as compared to the non-coordinated arenes. Such shifts to higher field are also observed for [Mo(η^6-C_6H_6)$_2$] (4.53 ppm),[69] [Cr(η^6-C_6H_6)] (4.23 ppm)[77] and [Ru(η^6-C_6H_6)]$^{2+}$ (6.82 ppm)[70] the latter one being closest to [Re(η^6-C_6H_6)]$^+$ at 6.16ppm. The peripheral protons are thus less deshielded, indicating a reduced ring current due to electron delocalization from the arene to the positively charged rhenium centre. The opposite influence of the shielding cone of the non-functionalized ring seems to be minimal, if ever, since the chemical shifts in the mono- and the bis-functionalized arene complexes, e.g. [**4**$^+$] and [**5**$^+$] or [**6**$^+$] and [**7**$^+$], are essentially identical for the doublets and the two triplets. Thus, the high field shift might be a result of a changed ring current through donor-acceptor interactions between the coordinated arene and the rhenium centre. The chemical shifts in the derivatized compounds [**10**$^+$]-[**16**$^+$] show similar trends, all are shifted upfield with respect to the free

ligands. A correlation with the Hammett parameters is not obvious, corroborating the multiple electronic influence of the metal centre onto the overall electronic system.

All bis-arene complexes are of yellow to orange colour. Corresponding UV/VIS spectra are shown in figure 5. The electronic spectra of the compounds are similarly structured, showing very weak bands in the visible range above 400 nm, likely to be assigned as d-d transitions due to their weak extinction coefficients. They further feature a number of shoulders below 400 nm, assigned as intra-ligand charge transfer absorptions. None of the complexes exhibits long-lived excited states or phosphorescence indicating triplet states resulting from intersystem crossing. No fluorescence was detected for all these compounds.

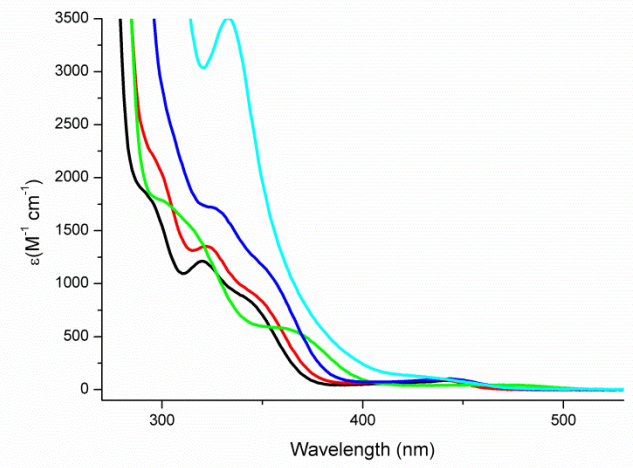

Figure 5. UV-Vis spectra of compounds [**1**$^+$] (black), [**4**$^+$] (red), [**6**$^+$] (green), [**10**$^+$] (blue) and [**11**$^+$] (light blue)

Conclusion

Ferrocene mimics phenyl rings or related structural features in pharmacophores. The arene-based rhenium (and technetium) sandwich complexes $[Re(\eta^6\text{-arene})_2]^+$ presented in here amplify this pattern and complement the armoury of building blocks in medicinal inorganic chemistry. These cationic "rhenocenes" are of high chemical stability, do not suffer from water or oxygen sensitivity and can be functionalized in a multitude of ways for subsequent biomolecule conjugation. Generally, $[Re(\eta^6\text{-arene})_2]^+$ type complexes are water soluble and slightly coloured. The cationic charge is not necessarily a disadvantage since it has been shown that the replacement of ferrocene by e.g. cobaltocenium did not result in metallo-bioconjugates with inferior properties.[17, 18] We conclude that the present work paves the way towards new bioorganometallic, targeting conjugates, exposing six-

instead of five-membered rings to potential receptors, thereby complementing the opportunities offered by metallocenes. We emphasize, that the preparation of the corresponding ^{99m}Tc homologues represent a perfect matched-pair for combining therapy (Re) with imaging (^{99m}Tc).

Experimental Part

Experimental methods, synthetic procedures and analytical data for all compounds are described in detail in the electronic supplementary information. We give here only the procedures for the key compounds [**4**$^+$]PF_6, [**5**$^+$]PF_6, [**6**$^+$]PF_6 and [**7**$^+$]PF_6.

[Re(η^6-C_6H_5Br)(η^6-C_6H_6)](PF_6) ([**4**$^+$]PF_6) and [Re(η^6-$C_6H_5Br)_2$](PF_6) ([**5**$^+$]PF_6):

300 mg (0.61 mmol) of [**1**$^+$]OTf were dissolved in 30 mL dry THF and cooled to -78°C. 1.5 mL (1.53 mmol, 2.5 eq.) of a 1 M LDA solution (THF/hexane) was added slowly to the yellow suspension. The reaction was stirred for 1.5 h at -78°C and 0.7 mL (6.1 mmol, 10 eq.) 1,1,2,2-tetrabromoethane (TBE) was added to the clear orange solution. Stirring continued for 5 h at -78 °C. The colour changed from orange to yellow. The reaction was quenched with acidified MeOH (MeOH/HCl 2:1) and the volume of the mixture reduced to 5 mL. The orange solution was extracted with hexane (3 x 2.5 mL), the remaining solvent evaporated in *vacuo* and purified by preparative HPLC (Reprosil 100 C18, 250x40 mm, 0.1% TFA/CH_3CN, Gradient: G2). Analytically pure yellow [**4**$^+$]PF_6 and [**5**$^+$]PF_6 respectively precipitated from the fractions upon addition of NH_4PF_6. Single crystals, suitable for X-ray diffraction analysis were obtained by slow evaporation of a CH_3CN/H_2O (1:1) solution of [**4**$^+$]PF_6 and [**5**$^+$]PF_6. Yields: 167.4 mg (0.26 mmol, 43%) for [**5**$^+$]PF_6 and 62.3 mg (0.11 mmol, 20%) for [**4**$^+$]PF_6.

Analysis [**4**$^+$]PF_6: ^{1}H NMR (500 MHz, CD_3CN) δ [ppm]: 6.51 (d, 2H, *o*-CH_{arom}), 6.02 (s, 6H, CH_{arom}), 6.01 (t, 2H, *m*-CH_{arom}), 5.87 (t, 1H, *p*-CH_{arom}). ^{13}C NMR (125 MHz, CD_3CN) δ [ppm]: 84.69 (*C*Br), 81.72 (*o*-*C*H$_{arom}$), 80.98 (*C*H$_{arom}$), 76.94 (*p*-*C*H$_{arom}$), 76.43 (*m*-*C*H$_{arom}$). ESI-MS: m/z = 421.0 [M]$^+$. IR ν: 3097 (m), 1435 (m), 1425 (m), 1426 (m), 1393 (m), 1134 (w), 1050 (m), 930 (w), 811 (s) cm^{-1}. Anal. calcd. for $C_{12}H_{11}Br_1F_6PRe$: C 25.45, H 1.96; found: C 25.12, H 1.98.

[**5**$^+$]PF_6: ^{1}H NMR (500 MHz, CD_3CN) δ [ppm]: 6.55 (d, 4H, *o*-CH_{arom}), 6.11 (t, 4H, *m*-CH_{arom}), 5.99 (t, 2H, *p*-CH_{arom}). ^{13}C NMR (125 MHz, CD_3CN) δ [ppm]: 87.25 (*C*Br), 84.61 (*o*-*C*H$_{arom}$), 79.70 (*p*-*C*H$_{arom}$), 79.49 (*m*-*C*H$_{arom}$). ESI-MS: m/z = 500.9 [M]$^+$. IR ν: 3094 (m), 1468 (w), 1427 (m), 1392 (m), 1278 (w), 1060 (m), 1008 (w), 930 (m), 906 (w), 818 (s) cm^{-1}. Anal. calcd. for $C_{12}H_{1o}Br_2F_6PRe$: C 22.34, H 1.56; found: C 22.30, H 1.68.

[Re(η^6-C_6H_5COOH)(η^6-C_6H_6)](TFA) ([**6**$^+$]TFA) and [Re(η^6-$C_6H_5COOH)_2$](TFA) ([**7**$^+$]TFA):

300 mg (0.61 mmol) of [**1**$^+$]OTf were dissolved in 30 mL dry THF and cooled to -78°C. 1.5 mL (1.53 mmol, 2.5 eq.) 1 M LDA solution (THF/hexane) was added to the yellow suspension. The reaction was stirred for 1.5 h at -78 °C. Subsequently, CO_2 gas was passed through the clear orange solution for 5h at -78°C (monitored by UPLC-MS). The colour of the solution changed from orange to yellow and a yellow precipitate formed. The reaction was quenched with MeOH/HCl and the solvents evaporated *in vacuo.* The residue was purified by preparative HPLC (Reprosil 100 C18, 250x40 mm, 0.1% TFA/CH_3CN, Gradient: G3). Yield: 157.7 mg (0.29 mmol, 48%) of analytically pure orange [**7**$^+$]TFA and 85.2 mg (0.27 mmol, 27%) of analytically pure yellow [**6**$^+$]TFA. Crystals suitable for X-ray diffraction analysis were obtained by slow evaporation of a CH_3CN/H_2O (1:1) solution of [**6**$^+$]TFA and [**7**$^+$]TFA.

Analysis [**6**$^+$]TFA**:** ^{1}H NMR (500 MHz, CD_3OD) δ [ppm]: 6.70 (d, 2H, *o*-CH_{arom}), 6.26 (t, 2H, *m*-CH_{arom}), 6.20 (t, 1H, *p*-CH_{arom}), 6.13 (s, 6H, CH_{arom}). ^{13}C NMR (125 MHz, CD_3OD) δ [ppm]: 170.54 (*C*OOH), 162.91 (q, *C*OOH, TFA), 118.31 (q, *C*F, TFA), 82.02 (C_{arom}-COOH), 80.06 (C_{arom}), 78.33 (*o*-*C*H$_{arom}$), 77.91 (*m*-*C*H$_{arom}$), 77.21 (*p*-*C*H$_{arom}$). ESI-MS: m/z = 387.1 [M]$^+$. IR ν: 3079 (w), 1705 (s), 1518 (w), 1434 (w), 1395 (m), 1286 (m), 1264 (m), 1169 (s), 1121 (s), 1041 (s), 999 (m), 863 (w), 815 (m),787 (s), 713 (s) cm^{-1}. Anal. calcd. for $C_{15}H_{12}F_3O_4Re$: C 36.07, H 2.42; found: C 35.74, H 2.28.

[**7**$^+$]TFA: ^{1}H NMR (500 MHz, CD_3OD) δ [ppm]: 6.70 (d, 4H, *o*-CH_{arom}), 6.30 (t, 4H, *m*-CH_{arom}), 6.24 (t, 2H, *p*-CH_{arom}). ^{13}C NMR (125 MHz, CD_3OD) δ [ppm]: 169.14 (*C*OOH), 162.65 (q, *C*OOH, TFA), 118.24 (q, *C*F, TFA), 81.79 (C_{arom}-COOH), 80.61 (*o*-*C*H$_{arom}$), 80.28 (*m*-*C*H$_{arom}$), 79.47 (*p*-*C*H$_{arom}$). ESI-MS: m/z = 431.1 [M]$^+$. IR ν: 3078 (w), 1732 (s), 1614 (s,) 1527 (w) , 1501 (w), 1401 (m), 1332 (m), 1283 (m), 1263 (m), 1155 (s), 1134 (s), 1114 (s), 1038 (m), 1010 (w), 989 (w), 869 (m), 796 (m), 775 (m), 717 (m) cm^{-1}. Anal. calcd. for $C_{16}H_{12}F_3O_6Re$: C 35.36, H 2.32; found: C 35.00, H 2.26.

References

(1) Gasser, G.; Metzler-Nolte, N. The potential of organometallic complexes in medicinal chemistry. *Curr. Opin. Chem. Biol.* **2012,** *16*, 84-91.

(2) Hartinger, C. G.; Metzler-Nolte, N.; Dyson, P. J. Challenges and Opportunities in the Development of Organometallic Anticancer Drugs. *Organometallics* **2012,** *31*, 5677-5685.

(3) Monney, A.; Albrecht, M. Transition metal bioconjugates with an organometallic link between the metal and the biomolecular scaffold. *Coord. Chem. Rev.* **2013,** *257*, 2420-2433.

(4) Perekalin, D. S.; Karslyan, E. E.; Petrovskii, P. V.; Nelyubina, Y. V.; Lyssenko, K. A.; Kononikhin, A. S.; Nikolaev, E. N.; Kudinov, A. R. Simple Synthesis of Ruthenium pi Complexes of Aromatic Amino Acids and Small Peptides. *Chem. Eur. J.* **2010,** *16*, 8466-8470.

(5) Jaouen, G.; Vessieres, A.; Top, S. Ferrocifen type anti cancer drugs. *Chem. Soc. Rev.* **2015,** *44*, 8802-8817.

(6) Patra, M.; Gasser, G. Organometallic Compounds: An Opportunity for Chemical Biology? *Chembiochem* **2012,** *13*, 1232-1252.

(7) Hillard, E. A.; Jaouen, G. Bioorganometallics: Future Trends in Drug Discovery, Analytical Chemistry, and Catalysis. *Organometallics* **2011,** *30*, 20-27.

(8) Bregman, H.; Williams, D. S.; Atilla, G. E.; Carroll, P. J.; Meggers, E. An organometallic inhibitor for glycogen synthase kinase 3. *J. Am. Chem. Soc.* **2004,** *126*, 13594-13595.

(9) Blanck, S.; Maksimoska, J.; Baumeister, J.; Harms, K.; Marmorstein, R.; Meggers, E. The Art of Filling Protein Pockets Efficiently with Octahedral Metal Complexes. *Angew. Chem. Int. Ed.* **2012,** *51*, 5244-5246.

(10) Streib, M.; Kraling, K.; Richter, K.; Xie, X. L.; Steuber, H.; Meggers, E. An Organometallic Inhibitor for the Human Repair Enzyme 7,8-Dihydro-8-oxoguanosine Triphosphatase. *Angew. Chem. Int. Ed.* **2014,** *53*, 305-309.

(11) Vallabhajosula, S.; Polack, B.; Jhanwar, Y. S.; Nikolopoulou, A.; Armor, T.; Tagawa, S. T.; Scherr, D.; Robinson, B.; Goldsmith, S. J.; Babich, J. W. PSMA SPECT imaging with Tc-99m-MIP-1404 in patients with prostate cancer (PCa): Comparison with Bone scan, CT or MRI. *Eur. J. Nucl. Med. Mol I.* **2014,** *41*, S236-S236.

(12) Can, D.; Spingler, B.; Schmutz, P.; Mendes, F.; Raposinho, P.; Fernandes, C.; Carta, F.; Innocenti, A.; Santos, I.; Supuran, C. T.; Alberto, R. [(Cp-R)M(CO)$_3$] (M=Re or ^{99m}Tc) Arylsulfonamide, Arylsulfamide, and Arylsulfamate Conjugates for Selective Targeting of Human Carbonic Anhydrase IX. *Angew. Chem. Int. Ed.* **2012,** *51*, 3354-3357.

(13) Ursillo, S.; Can, D.; N'Dongo, H. W. P.; Schmutz, P.; Spingler, B.; Alberto, R. Cyclopentadienyl Chemistry in Water: Synthesis and Properties of Bifunctionalized [(η^5-C$_5$H$_3${COOR}$_2$)M(CO)$_3$] (M = Re and Tc-99m) Complexes. *Organometallics* **2014,** *33*, 6945-6952.

(14) van Staveren, D. R.; Metzler-Nolte, N. Bioorganometallic Chemistry of Ferrocene. *Chem. Rev.* **2004,** *104*, 5931-5985.

(15) Albada, H. B.; Prochnow, P.; Bobersky, S.; Bandow, J. E.; Metzler-Nolte, N. Highly active antibacterial ferrocenoylated or ruthenocenoylated Arg-Trp peptides can be discovered by an L-to-D substitution scan. *Chem. Sci.* **2014,** *5*, 4453-4459.

(16) van Staveren, D. R.; Weyhermuller, T.; Metzler-Nolte, N. Organometallic beta-turn mimetics. A structural and spectroscopic study of inter-strand hydrogen bonding in ferrocene and cobaltocenium conjugates of amino acids and dipeptides. *Dalton T.* **2003**, 210-220.

(17) Noor, F.; Wustholz, A.; Kinscherf, R.; Metzler-Nolte, N. A cobaltocenium-peptide bioconjugate shows enhanced cellular uptake and directed nuclear delivery. *Angew. Chem. Int. Ed.* **2005,** *44*, 2429-2432.

(18) Noor, F.; Kinscherf, R.; Bonaterra, G. A.; Walczak, S.; Wolfl, S.; Metzler-Nolte, N. Enhanced Cellular Uptake and Cytotoxicity Studies of Organometallic Bioconjugates of the NLS Peptide in Hep G2 Cells. *Chembiochem* **2009,** *10*, 493-502.

(19) Chantson, J. T.; Falzacappa, M. V. V.; Crovella, S.; Metzler-Nolte, N. Antibacterial activities of ferrocenoyl- and cobaltocenium-peptide bioconjugates. *J. Organomet. Chem.* **2005,** *690*, 4564-4572.

(20) Pampaloni, G. Aromatic hydrocarbons as ligands. Recent advances in the synthesis, the reactivity and the applications of bis(η^6-arene) complexes. *Coord. Chem. Rev.* **2010,** *254*, 402-419.

(21) Elschenbroich, C.; Heikenfeld, G.; Wünsch, M.; Massa, W.; Baum, G. Elektron-Elektron/Spin-Spin-Wechselwirkung über große Distanz, studiert am Diradikaldikation [Di{bis(dimethylphosphino-η^6-benzol)chrom(I)}-nickel(0)]. *Angew. Chem.* **1988,** *100*, 397-399.

(22) Braunschweig, H.; Homberger, M.; Hu, C.; Zheng, X.; Gullo, E.; Clentsmith, G.; Lutz, M. Synthesis and Structure of [Cr{(η^6-C_6H_5)$_2$B{NtBu($SiMe_3$)}}] and [Cr{(η^6-C_6H_5)$_2$($BNMe_2$)$_2$}], the First Boron-Bridged Metalloarenophanes. *Organometallics* **2004,** *23*, 1968-1970.

(23) Hultzsch, K. C.; Nelson, J. M.; Lough, A. J.; Manners, I. Synthesis, Characterization, and Homopolymerization and Copolymerization Behavior of the Silicon-Bridged [1]Chromarenophane Cr(η^6-C_6H_5)$_2$SiMe. *Organometallics* **1995,** *14*, 5496-5502.

(24) Braunschweig, H.; Kaupp, M.; Adams, C. J.; Kupfer, T.; Radacki, K.; Schinzel, S. Synthesis, Reactivity, and Electronic Structure of [n]Vanadoarenophanes: An Experimental and Theoretical Study. *J. Am. Chem. Soc.* **2008,** *130*, 11376-11393.

(25) Braunschweig, H.; Damme, A.; Demeshko, S.; Dück, K.; Kramer, T.; Krummenacher, I.; Meyer, F.; Radacki, K.; Stellwag-Konertz, S.; Whittell, G. R. A Paramagnetic Heterobimetallic Polymer: Synthesis, Reactivity, and Ring-Opening Polymerization of Tin-Bridged Homo- and Heteroleptic Vanadoarenophanes. *J. Am. Chem. Soc.* **2015,** *137*, 1492-1500.

(26) Perekalin, D. S.; Novikov, V. V.; Pavlov, A. A.; Ivanov, I. A.; Anisimova, N. Y.; Kopylov, A. N.; Volkov, D. S.; Seregina, I. F.; Bolshov, M. A.; Kudinov, A. R. Selective Ruthenium Labeling of the Tryptophan Residue in the Bee Venom Peptide Melittin. *Chem. Eur. J.* **2015,** *21*, 4923-4925.

(27) Perekalin, D. S.; Molotkov, A. P.; Nelyubina, Y. V.; Anisimova, N. Y.; Kudinov, A. R. Synthesis of amino acid esters of the ruthenium naphthalene complex [($C_5Me_4CH_2OH$)Ru($C_{10}H_8$)]$^+$. *Inorg. Chim. Acta* **2014,** *409*, 390-393.

(28) Perekalin, D. S.; Karslyan, E. E.; Petrovskii, P. V.; Borissova, A. O.; Lyssenko, K. A.; Kudinov, A. R. Arene Exchange in the Ruthenium-Naphthalene Complex [CpRu($C_{10}H_8$)]$^+$. *Eur. J. Inorg. Chem.* **2012**, 1485-1492.

(29) Perekalin, D. S.; Babak, M. V.; Novikov, V. V.; Lyssenko, K. A.; Corsini, M.; Zanello, P.; Kudinov, A. R. (Mesitylene)ruthenium π-complexes with benzo-15-crown-5 and dibenzo-18-crown-6. *J. Organomet. Chem.* **2010,** *695*, 1200-1204.

(30) Gray, J. C.; Habtemariam, A.; Winnig, M.; Meyerhof, W.; Sadler, P. J. Sweetening ruthenium and osmium: organometallic arene complexes containing aspartame. *J. Biol. Inorg. Chem.* **2008,** *13*, 1111-1120.

(31) Billups, W. E.; Moorehead, A. W.; Ko, P. J.; Margrave, J. L.; Bell, J. P.; McCormick, F. B. Metal vapor synthesis of bis(arene)manganese cations utilizing in situ oxidation. *Organometallics* **1988,** *7*, 2230-2231.

(32) Trifonova, E. A.; Perekalin, D. S.; Lyssenko, K. A.; Kudinov, A. R. Synthesis and structures of cationic bis(arene) rhenium complexes. *J. Organomet. Chem.* **2013,** *727*, 60-63.

(33) Benz, M.; Braband, H.; Schmutz, P.; Halter, J.; Alberto, R. From Tc-VII to Tc-I; facile syntheses of bis-arene complexes [Tc-99(m)($arene)_2$]$^+$ from pertechnetate. *Chem. Sci.* **2015,** *6*, 165-169.

(34) Elschenbroich, C.; Hurley, J.; Metz, B.; Massa, W.; Baum, G. Metal π-complexes of benzene derivatives. 34. Tetraphenylsilane as a chelating ligand: synthesis, structural characterization, and reactivity of the tilted bis(arene) metal complexes [(C_6H_5)$_2$Si(η^6-C_6H_5)$_2$]M (M = vanadium, chromium). *Organometallics* **1990,** *9*, 889-897.

(35) Braunschweig, H.; Kupfer, T. Transition-Metal-Catalyzed Bis-Silylation of Propyne by [2]Chromoarenophanes. *Organometallics* **2007,** *26*, 4634-4638.

(36) Elschenbroich, C. Metalation of dibenzenechromium by N,N,N´,N´-tetramethylethylenediamine complexes of n-butyllithium and phenyllithium. *J. Organomet. Chem.* **1968,** *14*, 157-163.

(37) Lund, C. L.; Schachner, J. A.; Quail, J. W.; Müller, J. [1]Molybdarenophanes: Strained Metallarenophanes with Aluminum, Gallium, and Silicon in Bridging Positions. *J. Am. Chem. Soc.* **2007,** *129*, 9313-9320.

(38) Green, M. L. H.; Treurnicht, I.; Bandy, J. A.; Gourdon, A.; Prout, K. Synthesis and polymerisation of bis(η^6-styrene)molybdenum and related studies: crystal structures of Mo(η^6-$C_6H_5CH_2CH{=}CH_2)_2$ and [Mo(η^6-$C_6H_5SiMe_2H)_2$]BF_4. *J. Organomet. Chem.* **1986,** *306*, 145-165.

(39) Jones, D.; Pratt, L.; Wilkinson, G. 863. pi-Cyclohexadienyl compounds of manganese, rhenium, iron, and ruthenium. *J. Chem. Soc.* **1962**, 4458-4463.

(40) Fischer, E. O.; Schmidt, M. W. Über Aromatenkomplexe von Metallen, XCI. Über monomeres und dimeres Bis-hexamethylbenzol-rhenium. *Chem. Ber.* **1966,** *99*, 2206-2212.

(41) Löwe, C.; Shklover, V.; William Bosch, H.; Berke, H. Chemie des η1-Rhenium-koordinierten Triphenylcyclopropenyl-Liganden. *Chem. Ber.* **1993,** *126*, 1769-1779.

(42) Gutierrez, A.; Wilkinson, G.; Hussain-Bates, B.; Hursthouse, M. B. t-Butylimido and t-butylimido oxo aryls of rhenium. X-ray crystal structures of Re(NBut)$_2$(2,6-$Me_2C_6H_3)_2$, Re(NBut)(2,4,6-$Me_3C_6H_2$)($C_{27}H_{32}$), Re(NBut)$_3$(2,4,6-$Me_3C_6H_2$), [(ButN)Br(2,4,6-$Me_3C_6H_2$)Re(μ-NBut)(μ-O)Re($OC_6H_2Me_2CH_2$)(NBut)], [Re(NBut)(O)Ar(μ-O)]$_2$, Ar = 2,6-C_6H_3 and 2,4,6-C_6H_2. *Polyhedron* **1990,** *9*, 2081-2096.

(43) Rosini, G. P.; Jones, W. D. An unorthodox reaction of indene with $ReH_7(PPh_3)_2$: the competitive formation of an .eta.5-indanyl ligand versus an .eta.5-indenyl ligand. *J. Am. Chem. Soc.* **1993,** *115*, 965-974.

(44) Farrugia, L. J. *ORTEP-3 for Windows - a version of ORTEP-III with a Graphical User Interface (GUI)*, 1997.

(45) Trifonova, E. A.; Perekalin, D. S.; Lyssenko, K. A.; Kudinov, A. R. Synthesis and structures of cationic bis(arene)rhenium complexes. *J.Organomet. Chem.* **2013,** *727*, 60-63.

(46) Semmelhack, M. F.; Hall, H. T.; Farina, R.; Yoshifuji, M.; Clark, G.; Bargar, T.; Hirotsu, K.; Clardy, J. .eta.5-Cyclohexadienyltricarbonylchromium(0) complexes from addition of carbon nucleophiles to .eta.6-benzenetricarbonylchromium(0). Formation, chemical and spectroscopic features, and x-ray diffraction analysis. *J. Am. Chem. Soc.* **1979,** *101*, 3535-3544.

(47) Kündig, E. P.; Fabritius, C.-H.; Grossheimann, G.; Robvieux, F.; Romanens, P.; Bernardinelli, G. trans-Addition of Two Carbon Substituents across a Benzene Double Bond in [(η^6-Benzene)Mo$(CO)_3$]. *Angew. Chem. Int. Ed.* **2002,** *41*, 4577-4579.

(48) Bao, J.; Park, S.-H. K.; Geib, S. J.; Cooper, N. J. Addition of the Iminium Salt [Me_2NCMe_2][BF_4] to the Reductively Activated Benzene in [Cr(η^6-C_6H_6)$(CO)_3]_2$. *Organometallics* **2003,** *22*, 3309-3312.

(49) Yeh, M.-C. P.; Hwu, C.-C.; Lee, A.-T.; Tsai, M.-S. Alkylation of (η^6-Arene)Mn$(CO)_3$ Cations with Organozinc Reagents. *Organometallics* **2001,** *20*, 4965-4968.

(50) Connelly, N. G.; Freeman, M. J.; Orpen, A. G.; Sheehan, A. R.; Sheridan, J. B.; Sweigart, D. A. Reduction-oxidation properties of organotransition-metal complexes. Part 21. Synthesis and X-ray structural characterisation of the redox-related pair of cyclohexadienyl complexes

[Mn(CO)(dppe)(η^5-C_6H_6Ph)] and [Mn(CO)(dppe)(η^5-C_6H_6Ph)][PF_6]0.5CH_2Cl_2. *J. Chem. Soc., Dalton Trans.* **1985**, 1019-1026.

(51) Ittel, S. D.; Whitney, J. F.; Chung, Y. K.; Williard, P. G.; Sweigart, D. A. X-ray structural studies of tricarbonyl(cyclohexadienyl)manganese, dicarbonylnitrosyl(cyclohexadienyl)manganese, and dicarbonylnitrosyl(cyclohexadiene)manganese complexes. *Organometallics* **1988,** *7*, 1323-1328.

(52) Shao, L.; Badger, P. D.; Geib, S. J.; Cooper, N. J. Vilsmeier-Haack-Arnold Acylation of the Reductively Activated Benzene Ligand in [$Mn(CO)_3(\eta^6$-$C_6H_6)$]. *Organometallics* **2004,** *23*, 5939-5943.

(53) Churchill, M. R.; Scholer, F. R. Crystal and molecular structure of π-cyclohexadienylmanganese tricarbonyl. *Inorg. Chem.* **1969,** *8*, 1950-1955.

(54) Sheridan, J. B.; Padda, R. S.; Chaffee, K.; Wang, C.; Huang, Y.; Lalancette, R. Synthesis and reactions of acyl(cyclohexadienyl)manganates. *J. Chem. Soc., Dalton T.* **1992**, 1539-1549.

(55) Pike, R. D.; Alavosus, T. J.; Hallows, W. H.; Lennhoff, N. S.; Ryan, W. J.; Sweigart, D. A.; Bushweller, C. H.; DiMeglio, C. M.; Brown, J. H. Stereodynamics of 6-exo-phenylcyclohexadienyl complexes of manganese and rhenium. *Organometallics* **1992,** *11*, 2841-2854.

(56) Shao, L.; Geib, S. J.; Badger, P. D.; Cooper, N. J. 1,3-Dipolar [3 + 2] Cycloaddition of N-α Diphenyl Nitrone to the Benzene Ligand in Reductively Activated [$Mn(CO)_3(\eta^4$-$C_6H_6)]^-$. *Organometallics* **2003,** *22*, 2811-2813.

(57) Park, S.-H. K.; Geib, S. J.; Cooper, N. J. Addition of Iminium Salts to the Reductively Activated Benzene in [$Mn(\eta^6$-$C_6H_6)(CO)_3$]. *J. Am. Chem. Soc.* **1997,** *119*, 8365-8366.

(58) Brown, S. D.; Peters, J. C. Hydrogenolysis of [$PhBP_3$]FeN-p-tolyl: Probing the Reactivity of an Iron Imide with H_2. *J. Am. Chem. Soc.* **2004,** *126*, 4538-4539.

(59) Kudinov, A. R.; Zanello, P.; Herber, R. H.; Loginov, D. A.; Vinogradov, M. M.; Vologzhanina, A. V.; Starikova, Z. A.; Corsini, M.; Giorgi, G.; Nowik, I. Ferracarborane Benzene Complexes [η-9-L-7,8-$C_2B_9H_{10}$)Fe(η-C_6H_6)]$^+$ (L = SMe_2, NMe_3): Synthesis, Reactivity, Electrochemistry, Mössbauer Effect Studies, and Bonding. *Organometallics* **2010,** *29*, 2260-2271.

(60) Zanello, P.; Herber, R. H.; Kudinov, A. R.; Corsini, M.; de Biani, F. F.; Nowik, I.; Loginov, D. A.; Vinogradov, M. M.; Shul'pina, L. S.; Ivanov, I. A.; Vologzhanina, A. V. Synthesis, structure, electrochemistry, and Mössbauer effect studies of (ring)Fe complexes (ring = Cp, Cp*, and C_6H_7). Photochemical replacement of benzene in the cyclohexadienyl complex [(η^5-C_6H_7)Fe(η-C_6H_6)]$^+$. *J. Organomet. Chem.* **2009,** *694*, 1161-1171.

(61) Trifonova, E. A.; Loskutova, N. L.; Perekalin, D. S.; Nelyubina, Y. V.; Kudinov, A. R. Synthesis and reactivity of the cyclohexadienyl ruthenium complex [η^5-C_6H_7)$Ru(MeCN)_3$]$^+$ with labile acetonitrile ligands. *Mendeleev Commun.* **2013,** *23*, 133-134.

(62) Mishra, H.; Patra, A. K.; Mukherjee, R. Relative stability of half-sandwich η^6-benzene Ru(II) complexes of tridentate (2-pyridyl)alkylamine ligands of varying chelate ring-size: Nucleophilic addition of hydride ion onto the benzene ring. *Inorg. Chim. Acta* **2009,** *362*, 483-490.

(63) Bhambri, S.; Bishop, A.; Kaltsoyannis, N.; A. Tocher, D. Synthesis, NMR studies, and molecular orbital calculations on cyclohexadienyl derivatives of (η^6-arene)tris(pyrazolyl)ruthenium(II) compounds. *J. Chem. Soc., Dalton Trans.* **1998**, 3379-3390.

(64) Perekalin, D. S.; Trifonova, E. A.; Nelyubina, Y. V.; Kudinov, A. R. Synthesis of cyclohexadienyl ruthenium arene complexes by replacement of acetonitrile ligands in $[\eta^5\text{-}C_6H_7)Ru(MeCN)_3]^+$. *J. Organomet. Chem.* **2014,** *754*, 1-4.

(65) Yang, S.-M.; Chan, M. C.-W.; Peng, S.-M.; Che, C.-M. Synthesis and Structural Characterization of Ruthenium π-Arene and π-Cyclodienyl Complexes Containing 1,4,7-Trimethyl-1,4,7-triazacyclononane. *Organometallics* **1998,** *17*, 151-155.

(66) Shirin, Z.; Pramanik, A.; Ghosh, P.; Mukherjee, R. Stable Cyclohexadienyl Complexes of Ruthenium in a Piano Stool Geometry Containing a Tridentate Nitrogen Donor Ligand. First Structural Characterization of the (η^5-Cyanocyclohexadienyl)ruthenium(II) Complex and Spectroelectrochemical Correlation. *Inorg. Chem.* **1996,** *35*, 3431-3433.

(67) Bhambri, S.; Tocher, D. A. Cyclohexadienyl derivatives of (η^6-arene)(hydrido tris(pyrazolyl)borato)ruthenium(II) compounds. *J. Organomet. Chem.* **1996,** *507*, 291-293.

(68) Sturge, K. C.; Zaworotko, M. J. Pseudoferrocenes. *J. Chem. Soc., Chem. Commun.* **1990**, 1244-1246.

(69) Lund, C. L.; Schachner, J. A.; Quail, J. W.; Muller, J. [1]Molybdarenophanes: Strained metallarenophanes with aluminum, gallium, and silicon in bridging positions. *J. Am. Chem. Soc.* **2007,** *129*, 9313-9320.

(70) Lavallee, R. J.; Kutal, C. Substitutional photochemistry of sandwich and half-sandwich complexes of ruthenium(II)1. *J. Organomet. Chem.* **1998,** *562*, 97-104.

(71) Mandal, H. S.; Kraatz, H.-B. Ferrocene-histidine conjugates: N-ferrocenoyl-histidyl(imN-ferrocenoyl)methylester: synthesis and structure. *J. Organomet. Chem.* **2003,** *674*, 32-37.

(72) Zhou, B.; Li, C.-L.; Hao, Y.-Q.; Johnny, M. C.; Liu, Y.-N.; Li, J. Ferrocene tripeptide Gly-Pro-Arg conjugates: Synthesis and inhibitory effects on Alzheimer's Aβ1–42 fibrillogenesis and Aβ-induced cytotoxicity in vitro. *Bioorg. Med. Chem.* **2013,** *21*, 395-402.

(73) Ferreira, C. L.; Ewart, C. B.; Barta, C. A.; Little, S.; Yardley, V.; Martins, C.; Polishchuk, E.; Smith, P. J.; Moss, J. R.; Merkel, M.; Adam, M. J.; Orvig, C. Synthesis, Structure, and Biological Activity of Ferrocenyl Carbohydrate Conjugates. *Inorg. Chem.* **2006,** *45*, 8414-8422.

(74) Dong, T.-Y.; Lai, L.-L. A novel method to synthesize asymmetrical disubstituted ferrocenes. *J. Organomet. Chem.* **1996,** *509*, 131-134.

(75) Neumann, P.; Dib, H.; Caminade, A.-M.; Hey-Hawkins, E. Redox Control of a Dendritic Ferrocenyl-Based Homogeneous Catalyst. *Angew. Chem. Int. Ed.* **2015,** *54*, 311-314.

(76) Yur'eva, L. P.; Lev, N. N.; Svetlana, M. P. Electrochemistry of diarenechromium complexes. *Russ. Chem. Rev.* **1993,** *62*, 121.

(77) Phillips, L.; Separovic, F.; Aroney, M. J. The aromaticity of ferrocene and some derivatives, ruthenocene and dibenzenechromium as determined via ring current assessment and C-13 anisotropic contributions to the H-1 NMR shielding. *New J. Chem.* **2003,** *27*, 381-386.

6.4 Unpublished Results: Bis-Arene Complexes [Re(η^6-arene)$_2$]$^+$ as Highly Stable Bioorganometallic Scaffolds

As a proof of concept further compounds have been synthesised, leading to preliminary insights into this new field of bioorganometallic chemistry. It is to note that, for the lithiation reaction of [**1**]$^+$ solubility in dry THF is an important requirement. Thus [**1**](OTf) was used instead of [**1**](PF_6). Since the lithiation reaction is a crucial step for the formation of functionalized bis-arene complexes it was investigated more in detail. By adding ≤1 equivalent of base (LDA) during the reaction and even in the presence of tetramethylethylenediamine (tmeda), formation of polynuclear complexes (Figure 21) could be observed according to MS and NMR-studies in deuterated THF. Purification and isolation of these compounds were not achieved due to their high sensitivity toward oxygen and water. Also, hydrid abstraction in the presence of triphenylcarbenium hexafluorophosphate leads not to the formation of bi-/trinuclear complexes as e.g. μ(η^6:η^6-biphenyl)-bis[η^6-benzol)rhenium]$^{2+}$ but decomposition. Furthermore, by increasing the amount of base to ≥2.5 eq., formation of even higher substituted derivatives such as tri-, tetra- and pentasubstituted complexes were found according to UPLC-MS measurement.

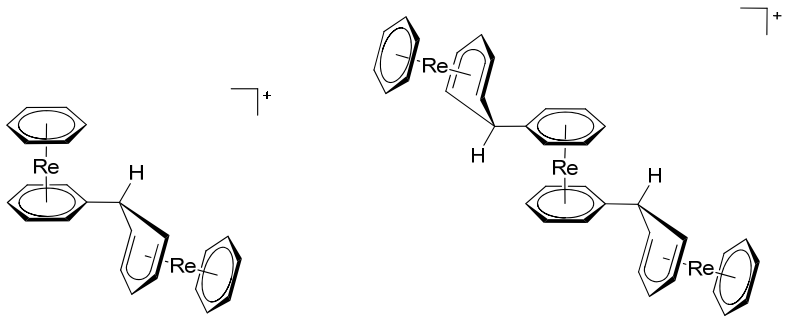

Figure 21: Binuclear (left) and trinuclear (right) rhenium complexes.

After *in situ* lithiation, compound [**8**]$^+$ and [**9**]$^+$ were further treated with different electrophile such e.g. aldehyde, ketone or with halogenation reagent such (N-fluorobenzene sulfonimide (NFSI), hexachloroethane (PCA), and iodine) in order to investigate their reactivity. Mono-/difunctionalized bromide, as well as carboxylic acid rhenium bis-arene complexes, were already described in the previous manuscript while the other complexes depicted also in Scheme 5 will be discussed in this section. Furthermore, tri-substituted compounds which were isolated in later attempts are reported herein.

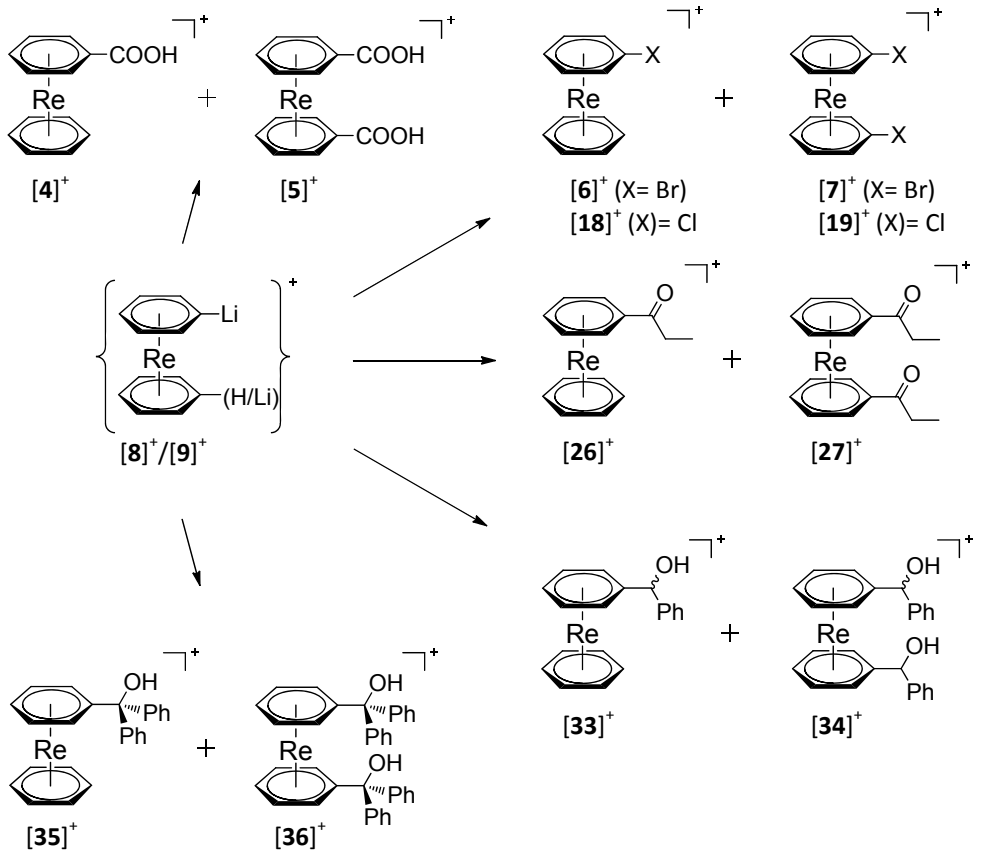

Scheme 5: An overview of the derivative $[Re(\eta^6\text{-arene})_2]^+$ moiety via *in situ* lithiation.

6.4.1 Carboxylic Acid Functionalized Rhenium Bis-Arene Complexes

In addition to the mono- and di-functionalized rhenium bis-arene complexes, tri-substituted could be isolated in lower amounts. Separation was performed via preparative HPLC in which [**17**]$^+$ was collected as first fraction due to its highly hydrophilic nature. Single crystals were obtained by slow evaporation from an acetonitrile/water solution and characterized by X-ray diffraction. **17** crystallizes as light red plates in the monoclinic space group $P2_1/c$ with two molecules in the asymmetric unit. Furthermore, the asymmetric unit consists of one PF_6^-, one hydronium ion H_3O^+ and two water molecules. The molecule itself is neutral due to one deprotonated carboxyl group in the phthalate moiety. It is reasonable that the third carboxyl group is directed in ortho position because of the more acidic protons adjacent in ortho position to the first carboxyl group and thus easier to deprotonate with an excess of base. The two molecules are connected over hydrogen bonds from the deprotonated carboxylic group (phthalate moiety) to the mono functionalized one (Figure 22).

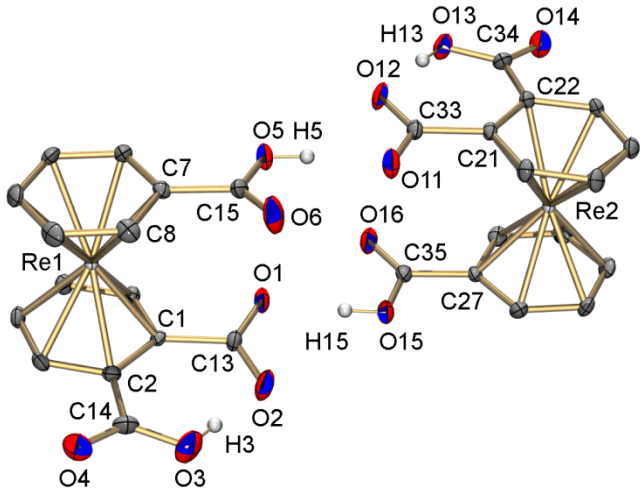

Figure 22: ORTEP representation[108] of the [Re(η^6-hydrogenphthalat)(η^6-carboxybenzene)] (**17**). Thermal ellipsoids are represented at the 50% probability level. Arene-hydrogen atoms and counter ions are omitted for clarity.

Molecules with tri-substituted carboxylic groups like **17** have been not described so far. The Re-C bond lengths in **17** are in the range of 2.224(3) – 2.253(3) Å (Table 2). No significant structural differences were found compared to the structure with the mono- and bis-functionalized carboxylic group.

Functionalizing of compound [**6**]$^+$ with different substrates like benzylamine and dimethoxy-phenethylamine (dpa) via amide bond formation were already described before. Nevertheless, this approach was also used for biological active molecule such as doxorubicin which is a potent chemotherapeutic agent. Recently, it was demonstrated that bioconjugate with rhenium Cp-complex and doxorubicin showed selectively accumulation in mitochondria. Moreover, this conjugate displays excellent toxicity towards HeLa cells.[144] Following the same procedure, the analogue positively charged conjugate with [**6**]$^+$ as scaffold has been synthesized. The reaction showed a quantitative conversion after 30 min in dry DMF at room temperature according to UPLC-MS measurement with the corresponding molecule peak of m/z = 912 [M]$^+$. No further studies have been performed so far.

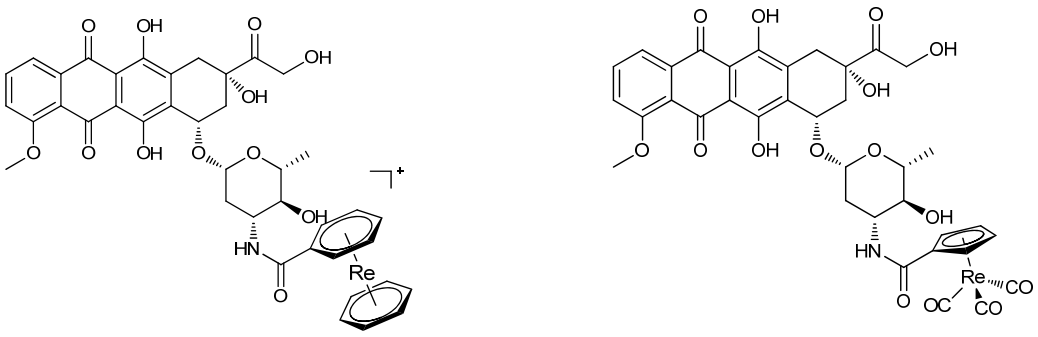

Figure 23: Bioconjugated [**6**]$^+$-doxorubicin (left) and rhenium Cp-doxorubicin complex (right).

6.4.2 Halogen Functionalized Rhenium Bis-Arene Complexes

It is well known that halogen benzene with para substituted electron withdrawing groups like e.g. nitro group undergoes nucleophile aromatic substitution (S_NAr).[145] Rhenium (+I) centre as well can act in a similar way like an electron withdrawing group due to its oxidation state, coordination and Lewis acidity. Thus, the carbon bound to a halogen atom is more electrophilic and prone to nucleophilic attack. The reaction rate can be controlled either by the amount or strength of the nucleophiles or by the variation of the halogen. Going from fluorine to iodine in the periodic system, the reaction rate of S_NAr reactions decrease or even no reaction occurs. This phenomenon is explained by the decreasing electronegativity in the halogen group as well as by the ability to polarize bond.[146] For this purpose, reactions were performed following the same procedure described in the manuscript and with mild electrophilic fluorinating reagent as N-Fluorobenzenesulfonimide (NFSI). Unexpectedly, the reaction did not form the mono-/difluoride derivatives, even when the reagent was applied in an excess of 10 – 20 eq.. Nevertheless, the major product could be assigned to [Re(η^6-biphenyl)(η^6-benzene)]$^+$ according to UPLC-MS measurements. Although the mechanism is not fully understood, it could be assumed that the *in situ* formed rhenium-fluorobenzene derivative reacts instantaneously with another lithiated [Re(η^6-C_6H_5Li)(η^6-C_6H_6)]$^+$ ([**8**]$^+$) species, considering its high reactivity toward strong nucleophiles. However, no evidence was found for the following decomplexation of the second rhenium centre and therefore it is still unclear. The mono-/dichloride derivatives have been synthesized with hexachloroethane as reagent. After purification via preparative HPLC, the mono-/di- and trisubstituted chloro derivatives have been isolated in yields of 47.6% for [**19**](PF_6), 15% for [**18**](PF_6) and 2.5% [**20**](PF_6), respectively. All compounds were fully characterized and crystal structures were elucidated by X-ray diffraction. Suitable crystals for X-ray diffraction were obtained for all compounds by slow evaporation of CH_3CN/H_2O (1:1) solutions. The dominant, disubstituted spices [Re(η^6-$C_6H_5Cl)_2$](PF_6) ([**19**](PF_6)) crystallizes as yellow plates in the monoclinic space group C2/c and it is isostructural to the dibromide substituted rhenium analogue [**5**]$^+$ whereas the monosubstituted [**18**](PF_6) crystallizes as yellow needles in the triclinic space group P-1. Furthermore, [**20**](PF_6) crystallizes as yellow plates in the monoclinic space group $P2_1/c$ (Figure 24, left). The asymmetric unit of [**18**](PF_6) contains one molecule with a counter-ion while compound [**19**]$^+$ consists of half-molecules. In this structure, the Re atom is located at the mirror plane of this space group. The structure of [**20**]$^+$ includes one molecule with a PF_6^- as counter-ion in the asymmetric unit. The distances between the Re and the aromatic carbon atoms of [**18**]$^+$ were found to be in the range of 2.2187(19) – 2.247(2) Å and lie in the same region as compared to compound [**19**]$^+$ (2.230(2) – 2.241(3) Å) (see crystallographic tables). The Re-C_{arom} bond lengths of [**20**]$^+$ were between 2.210(5) and 2.252(4) Å. and were comparable with the analogue bromide compound [**21**]$^+$ (2.212(4) – 2.244(4) Å).

Figure 24: ORTEP representation[108] of Re(η^6-$C_6H_4Cl_2$)(η^6-C_6H_5Cl)](PF_6) ([**20**](PF_6)) (left) and [Re(η^6-$C_6H_4Br_2$)(η^6-C_6H_5Br)](PF_6) ([**21**](PF_6)) (right). Hydrogen atoms and anions are omitted for clarity, thermal ellipsoids represent 50% probability. Selected bond lengths [Å] for [**20**]$^+$: Re1-clorobenzene (centroid) 1.732(2), Re1-1,2-diclorobenzene (centroid) 1.7265(18), C1-Cl1 1.728(4), C7-Cl2 1.733(5), C2-Cl3 1.737(4) and for [**21**]$^+$: Re1-bromobenzene (centroid) 1.728(2), Re1-1,2-dibromobenzene (centroid) 1.724(2), C1-Br1 1.875(5), C7-Br2 1.876(4), C2-Br3 1.897(5).

Direct bromination of [Re(benzene)$_2$]$^+$ with Br_2 gave not the desired complex but [Re(benzene)$_2$](Br_3) according to UPLC-MS data and X-ray crystal structure. The successful syntheses of mono-/ disubstituted bromide rhenium bis-arene complexes have been already described in the manuscript. In later attempts, it was also possible to isolate the tribromide substituted side-product [Re(η^6-$C_6H_4Br_2$)(η^6-C_6H_5Br)](PF_6) ([**21**](PF_6)) from the reaction of [**4**](PF_6) and [**5**](PF_6) in low yields of about 3%. The yield of [**21**]$^+$ might be improved by the addition of 3-4 equivalents of base but was not one of the main scopes of this thesis. [**21**]$^+$ has been fully characterised and X-ray diffraction analysis confirmed its authenticity (Figure 24, right). Moreover, reaction with iodine as reagent gave a mixture of multi-substituted iodide derivatives which were not isolated.

In order to analyze the reactivity in relation to the nucleophilic aromatic substitution of [**4**](PF_6) and [**5**](PF_6), reactions were performed in small scale batches of 3-10 mg with different nucleophiles and analysed via UPLC-MS. In few cases, the formed products could be purified and partially characterised. Herein, some further examples are described as an addition to the manuscript. Prolonged reaction time was mainly observed for weaker nucleophiles such as amine and imidazole whereas, for stronger nucleophiles like methoxide or thiolates, the reaction is straightforward and showed high conversions up to 95% The substitution reactions with the monobromide derivative [**4**]$^+$ are listed in Table 17.

Table 17: Substitution reactions with the monobromide derivative [**4**]$^+$

nucleophiles	conversion (UPLC)	conditions
MeO^-	95%	excess, 60°C, 4 h, in MeOH
cysteine	95%	2 eq, K_2CO_3, 60°C, 7 h, in H_2O/MeOH (1:1)
$PhCH_2NH_2$	90%	10 eq, DIPEA, 70°C, 18 h, in ACN
imidazole	90%	10 eq, DIPEA, 70°C, 48 h, in ACN
2-naphthylamine	50%	2 eq, NaH, 50°C, 5 h in THF

Besides, substitution reaction of deprotonated 2-naphthylamine and [**4**](PF_6) was possible with a lower conversion of 50%. Also, prolongation of the reaction time did not increase the conversion of this reaction. Furthermore, only Re(η^6-C_6H_5OMe)(η^6-C_6H_6)](PF_6) ([**22**](PF_6)) and [Re(η^6-C_6H_5-1,3-$C_3H_4N_2$)(η^6-C_6H_6)](PF_6) ([**23**](PF_6)) were isolated in yields of 88% ([**22**]$^+$) and 87% ([**23**]$^+$). Moreover, complex [**22**]$^+$ was fully characterized while compound [**23**]$^+$ was analyzed by UPLC-MS and X-ray diffraction. [**22**](PF_6) crystallizes as yellow plates in the triclinic space group P-1 (Figure 25, left). The crystal structure contains one molecule in the asymmetric unit. The distances between the Re and the aromatic carbon atoms of [**22**]$^+$ were found to be in the range of 2.215(3) – 2.235(3) Å except for the Re1-C1 bond length where the methoxy group is attached, is significantly longer with 2.272(3) Å. Single crystals of [**23**](PF_6) were obtained by slow evaporation from a water solution of this compound. The crystals were characterized by X-ray diffraction analysis. [**23**](PF_6) crystallizes as colourless needles in the monoclinic space group $P2_1/c$ (Figure 25, right). The asymmetric unit includes two independent Re centres and three PF_6^- that are very similar. This suggests that one of the imidazoles is protonated. Indeed, the proton lies between the two independent imidazole moieties and therefore it was refined as half occupied proton for each imidazole. Considering that free imidazole has a pks of 7, it is not unexpected that both species could be crystallized from water. The Re-C bond lengths in [**23**]$^+$ are in the range of 2.221(3) – 2.247(3) Å.

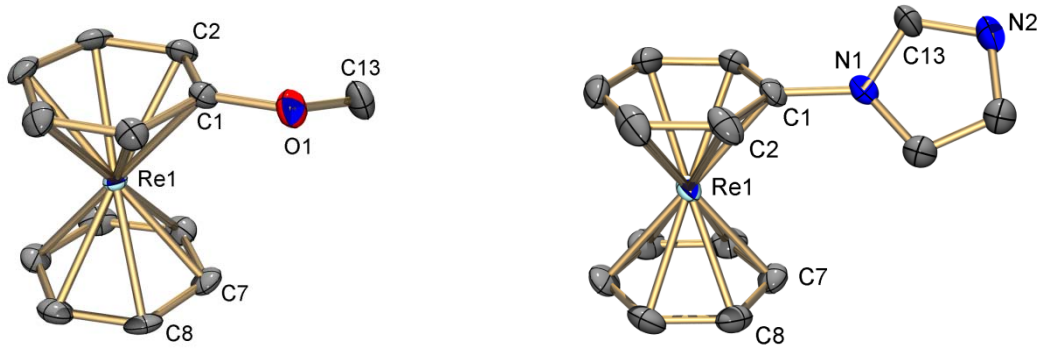

Figure 25: ORTEP representation[108] of Re(η^6-C_6H_5OMe)(η^6-C_6H_6)](PF_6) ([**22**](PF_6)) (left) and [Re(η^6-C_6H_5-1,3-$C_3H_3N_2$)(η^6-C_6H_6)](PF_6) ([**23**](PF_6)) (right). Hydrogen atoms and anions are omitted for clarity, thermal ellipsoids represent 50% probability. Selected bond lengths [Å] for [**22**]$^+$: Re1-methoxybenzene (centroid) 1.7336(13), Re1-benzene (centroid) 1.7301(15), C1-O1 1.344(4) and for [**23**]$^+$: Re1-phenylimidazol (centroid) 1.7269(16), Re1-benzene (centroid) 1.7354(15), C1-N1 1.434(4).

In general, the substitution of both bromide atoms in compound [**5**]$^+$ requires longer reaction times due to the change of the electronic property after the first substitution. Exceptions are strong nucleophiles. To speed up the reaction with moderate nucleophile an excess has to be used. This difference in substitution rates could be an advantage by the difunctionalization of the rhenium bis-arene moiety with two different types of nucleophiles. Reaction with 2.5 equivalents of cysteine showed substitution of the first bromide with conversions of 90% after 40 min at 60°C (Scheme 6).

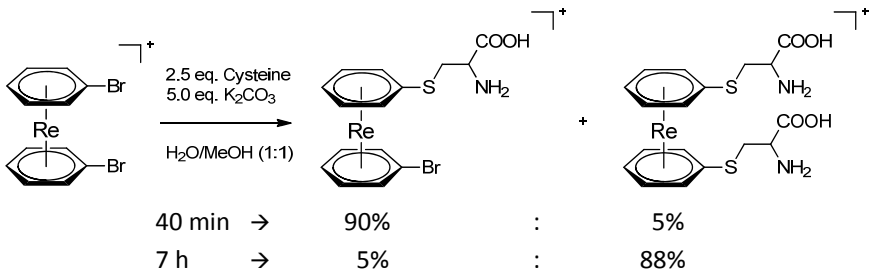

Scheme 6: Formation of mono-/di substituted cysteine rhenium-arene derivatives

The second substitution was achieved after 7 h at 60°C with conversions of 88% according to UPLC-MS. This reactivity allows substitution with different nucleophiles. By first substitution reaction with a weaker nucleophile and in a second step substitution with the stronger nucleophile a straight forward synthesis of mixed rhenium bis-arene complexes will be realized. Moreover, reactions with strong nucleophiles such as methoxide (1.5-2 equivalents) lead to quantitative transformation into the monosubstituted [Re(η^6-C_6H_5OMe)(η^6-C_6H_5Br)]$^+$ after 5 h under reflux condition. Single crystals of Re(η^6-C_6H_5OMe)(η^6-C_6H_5Br)]$^+$ were obtained by slow evaporation of an acetonitrile solution and were

characterized by X-ray diffraction analysis (see crystallographic tables). Further examples of disubstitution of [**5**]$^+$ were listed in Table 18.

Table 18: Substitution reactions with the dibromo derivative [**5**]$^+$

nucleophiles	conversion (UPLC)	conditions
MeO^-	95%	excess, 60°C, 4 h, in MeOH
Naphthyl-$NHCOCH_2S^-$	79% (yield)	5 eq, DIPEA, 70°C, 15 h, in ACN
$PhCH_2NH_2$	60%	10 eq, DIPEA, 70°C, 36 h, in ACN

Compounds [Re(η^6-$C_6H_5OMe)_2$](PF_6) ([**24**](PF_6)) and [Re(η^6-N-(naphthalene-2-yl)-2-(phenylthio)-acetamide)$_2$](PF_6) ([**25**](PF_6)) were isolated in yields of 91% [**24**]$^+$ and 79% [**25**]$^+$, respectively. Both compounds were fully characterized and single crystals were obtained for both complexes by slow evaporation of an acetonitrile solution. [**24**](PF_6) crystallizes as light yellow plates in the triclinic space group P-1 (Figure 26, left). The asymmetric unit of [**24**]$^+$ contains a half-molecule with a disordered PF_6^- counter ion in which the inversions centre lies on Re atoms. This implies that the two methoxys were pointed in opposite directions. The Re-C bond lengths in [**24**]$^+$ are in the range of 2.225(4) – 2.254(3) Å. Also, in this case, the Re1-C1 bond length with the bound methoxy group is significantly longer (2.279(3) Å) and lies in the same range compared to [**22**]$^+$. Complex [**25**]$^+$ crystallizes as light yellow plates in the monoclinic space group $P2_1/c$ with an additional acetonitrile solvent molecule in the asymmetric unit (Figure 26, right). Moreover, one of the naphthyl rests has a disorder. The distances between the Re and the aromatic carbon atoms of [**25**]$^+$ were found to be in the range of 2.228(6) – 2.269(5) Å. Furthermore, the proton of the nitrogen atom (N1) built a hydrogen bond to the oxygen atom (O2) with a length of 2.20 Å whereas the distance between the donor and acceptor lies by 2.977(7) Å.

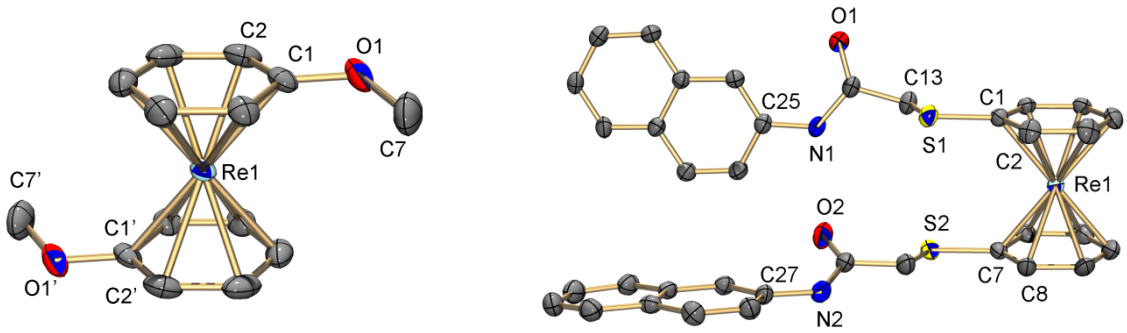

Figure 26: ORTEP representation[108] of [Re(η^6-$C_6H_5OMe)_2$](PF_6) ([**24**](PF_6)) (left) and [Re(η^6-N-(naphthalen-2-yl)-2-(phenylthio)-acetamide)$_2$](PF_6) ([**25**](PF_6)) (right). Hydrogen atoms and anions are omitted for clarity, thermal ellipsoids represent 50% probability. Selected bond lengths [Å] for [**24**]$^+$: Re1-methoxybenzene (centroid) 1.7452(17), C1-O1 1.356(5) and for [**25**]$^+$: Re1-phenyl-S-R (centroid) 1.738(2)-1.744(2), C-S 1.763(5)-1.769(5).

Kinetics studies of chloride/bromide substituted rhenium bis(η^6-arene) complexes were not performed so far. Nevertheless, it is well known that the chloride derivatives react faster compared to the bromide substituted.[146] The rate determining step is the nucleophilic attack of the incoming substituent to the corresponding carbon atom (C-X, X = Cl, Br). According to ^{13}C NMR studies of the monohalogen substituted derivatives, the signal of the carbon atom bound to the chloride atom is shifted by 15 ppm to lower field in respect to the carbon atom of the monobromide species. Consequently, the carbon (*C*-Cl) atom is more deshilded and therefore, more electrophilic. This interpretation of the ^{13}C NMR data is consistent with their higher reactivity. Furthermore, this implies that complexes, containing chloride substituted arenes are more suitable for substitution reaction with weaker nucleophiles.

6.4.3 Ketone Functionalized Rhenium Bis-Arene Complexes

Following the general procedure, the *in situ* formed lithiated species were treated with 10 eq. of propionyl chloride to generate the mono- and disubstituted ethyl ketone derivatives [Re(η^6-C_6H_5COEt)(η^6-C_6H_6)](PF_6) ([**26**](PF_6)) and [Re(η^6-$C_6H_5COEt)_2$](PF_6) ([**27**](PF_6)). After purification via preparative HPLC, the compounds were isolated in yields of 41% for [**26**](PF_6) and 17% for [**27**](PF_6), respectively. In the IR spectra of [**26**]$^+$ and [**27**]$^+$, the absorption of the distinctive carbonyl vibrations can be observed at 1694 cm^{-1} ([**26**]$^+$) and 1699 cm^{-1} ([**27**]$^+$), respectively. Furthermore, these complexes were fully characterized. In both cases, single crystals, suitable for X-ray diffraction analysis, were obtained by slow evaporation of a CH_3CN/H_2O (1:1) solution.

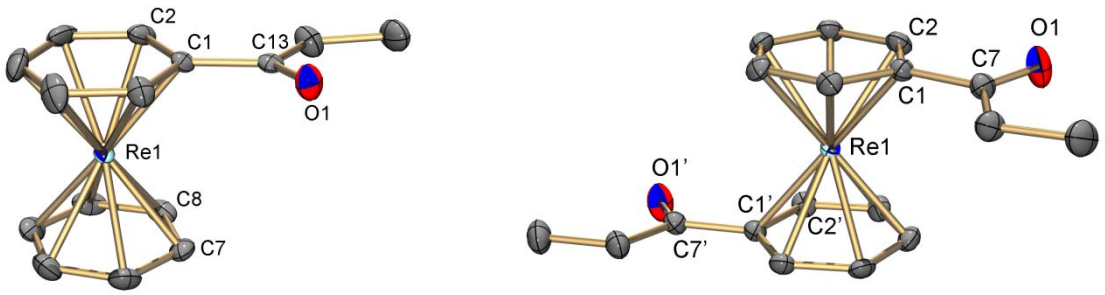

Figure 27: ORTEP representation[108] of [Re(η^6-C_6H_5COEt)(η^6-C_6H_6)](PF_6) ([**26**](PF_6)) (left) and [Re(η^6-$C_6H_5COEt)_2$](PF_6) ([**27**](PF_6)) (right). Hydrogen atoms and anions are omitted for clarity, thermal ellipsoids represent 50% probability. Selected bond lengths [Å] for [**26**]$^+$: Re1-$C_6H_5COCH_2CH_3$ (centroid) 1.7389(18), Re1-C_6H_6 (centroid) 1.7393(17), C13-O1 1.216(5) and for [**27**]$^+$: Re1-$C_6H_5COCH_2CH_3$ (centroid) 1.7388(10), C7-O1 1.207(4).

[**26**](PF_6) crystallizes as yellow prisms in the monoclinic space group $P2_1/c$ with one molecule per asymmetric unit. The Re-C bond lengths in [**26**]$^+$ are in the range of 2.228(3) – 2.250(4) Å. Complex [**27**]$^+$ crystallizes as light brown prisms in the monoclinic space group P2/n. The molecule is located at the 2 fold axis perpendicular to a mirror plane of this space group. Therefore, only one half of the molecule is in the asymmetric unit. The distances between the Re and the aromatic carbon atoms of [**27**]$^+$ were found to be in the range of 2.236(3) – 2.250(2) Å. The synthesis of similar structures was reported for chromium, molybdenum and ruthenium but only one crystal structures containing metal bis-arene moiety with ketones groups are described.[61, 147, 148] In contrast, examples of crystal structures with $Cr(CO)_3$ or Ru(Cp) bearing phenyl ketones as ligands are well represented in the literature.[149, 150]

During the reaction of [**27**]$^+$, two further dimeric species were found in low quantities with corresponding masses of m/z = 377.1 $[M]^{2+}$ and m/z = 399.1 $[M]^{2+}$. After isolation, NMR studies revealed structure [**28**]$(PF_6)_2$ and [**29**]$(PF_6)_2$ (Figure 28). The formation of [**28**]$(PF_6)_2$ and [**29**]$(PF_6)_2$ might be induced by the nucleophilic attack of the lithiated species $[Re(\eta^6\text{-}C_6H_5Li)(\eta^6\text{-}C_6H_6)]^+$ to [**26**]PF_6 or [**27**]PF_6. The formation of these dimeric compounds could not be prevented even at 10 eq. of reagent by -78°C. This type of structures was also reported as product by the reaction of a lithiated benzene tricarbonyl chromium complex with benzoyl chloride. By this reaction, the discussed type of complex was formed as the minor product with a yield of 20%.[151] For [**28**]$(PF_6)_2$, single crystals were obtained by slow evaporation of an acetonitrile solution and studied by X-ray diffraction analysis.

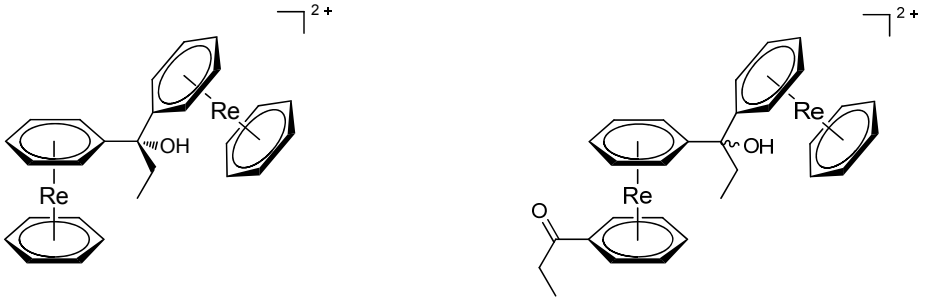

[**28**]$(PF_6)_2$ [**29**]$(PF_6)_2$

Figure 28: Chemical structure of $[(\eta^6\text{-}C_6H_6)Re(\eta^6\text{-}C_6H_5C(OH)Et)Re(\eta^6\text{-}C_6H_6)](PF_6)_2$ ([**28**]$(PF_6)_2$) (left) and $[(\eta^6\text{-}C_6H_6)Re(\eta^6\text{-}C_6H_5C(OH)Et)Re(\eta^6\text{-}C_6H_5COEt)](PF_6)_2$ ([**29**]$(PF_6)_2$) (right)

[**28**]$(PF_6)_2$ crystallizes as light green plates in the orthorhombic space group $P2_12_12_1$, showing one molecule per asymmetric unit. The Re1-C bond lengths in [**28**]$^{2+}$ are in the range of 2.219(7) – 2.274(7) Å. The distances between the second rhenium centre (Re2) and the aromatic carbon atoms were found to be in the range of 2.219(9) – 2.269(7) Å. Besides, the dimeric chromium structure mentioned above, only one similar crystal structures were found in the CCD database.[115]

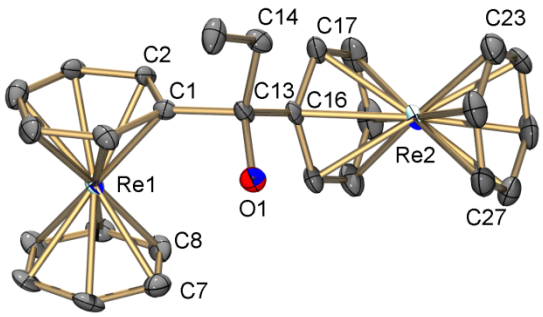

Figure 29: ORTEP representation[108] of [Re(η^6-C_6H_5COEt)(η^6-C_6H_6)](PF_6) ([**28**](PF_6)$_2$). Hydrogen atoms and anions are omitted for clarity, thermal ellipsoids represent 50% probability. Selected bond lengths [Å] for [**28**]$^{2+}$: Re1-$C_6H_5COCH_2CH_3$ (centroid) 1.738(3), Re1-C_6H_6 (centroid), 1.732(3), Re2-$C_6H_5COCH_2CH_3$ (centroid) 1.738(3), Re2-C_6H_6 (centroid) 1.742(4), C13-O1 1.414(8).

6.4.4 Synthesis of Rhenium Bis-Arene Tamoxifen Derivatives via Mc-Murry Reaction

Although tamoxifen is a well-known and highly potent pharmaceutical against breast cancer, long-term tamoxifen therapy (over five years) frequently leads to drug resistance. Hence, metal complex SERMs (selective estrogen receptor modulators) were discovered and studied in details. For tamoxifen analogues with ((R,R)-trans1,2-diaminocyclohexane)platinum(II), cyclopentadienyl rhenium tricarbonyl, and ruthenocene, no enhancement of the antiproliferative effect was observed on estrogen receptor-positive cells.[152] However, tamoxifen derivatives which contain a ferrocene moiety instead of a phenyl ring showed strongly cytotoxicity.[12] For this purpose, tamoxifen derivatives with a rhenium bis-arene moiety have been synthesized via Mc-Murry reaction. In a first attempt, the reductive coupling to the olefin was performed in small batches with benzophenone as model compound and [**26**]$^+$. Under reflux and after 24 hours reaction time, no olefin [Re(η^6-1,1,2-triyltribenzene-but-1-ene)(η^6-C_6H_6)](PF_6) ([**30**](PF_6)) formation was observed. Only the reduction to the secondary alcohol [Re(η^6-$C_6H_5C(OH)Et$)(η^6-C_6H_6)](PF_6) ([**31**](PF_6)) was found with a conversion of 40%. Furthermore, the formation of the pinacol side-product was detected in small quantities according to UPLC ESI-MS measurement. In particular, the competing reduction to the secondary alcohol by using bulky alkyl or aryl ketones under Mc-Murry condition is not unexpected and was already described in 1977 by Lenoir and verified by Weyerstahl *et al.* in 1982.[153, 154] This fact is one of the drawbacks and leads to lower yields of the desired olefin. Performing the reaction by elevated temperature (100°C), for 2 h in a microwave reactor, product [**30**]$^+$ could be detected with the corresponding m/z = 549.1 [M]$^+$ according to ESI MS data. After purification, [**30**]$^+$ could be isolated in 18 % yield, which is slightly lower than the reported yield of Ferrocifen derivatives synthesize by Zhao *et al.*[155] The secondary alcohol [**31**]$^+$ was isolated in 56 % yield. Both compounds were fully characterized. Single crystals of [**30**](PF_6), suitable for X-ray diffraction analysis, were obtained by slow evaporation of a CH_2Cl_2 solution. Single crystals of [**31**](PF_6) were obtained by slow evaporation

of an acetonitrile solution. Following the same procedure, the reaction was carried out with 4,4'-dihydroxybenzophenone instead of benzophenone. In this reaction, yields were obtained in moderate quantities of 46% for the olefin product [Re(η^6-4,4'-(2-phenylbut-1-ene-1,1-diyl)diphenol)(η^6-C_6H_6)](PF_6) ([**32**](PF_6)) and 32% for the secondary alcohol [**31**](PF_6). Further analytical methods like $^1H/^{13}C$ NMR and X-ray-diffraction analysis confirmed the structure [**32**]$^+$. Furthermore, in cooperation with the Institut Parisien de Chimie Moléculaire (Anne Vessiers), compound [**32**]$^+$ was testes in MCF-7 cells regarding its cytotoxicity. The complex is estrogenic and recognized by the receptors but does not show significant cytotoxicity. It might be possible that modification at the benzophenone with aminoalkyl moieties could induce cytotoxicity toward breast cancer cells as shown in the case of bis-(diaminoethoxy)cobaltifens.[156] Further studies are needed to evaluate the full potential of these compounds, in the near future.

[**30**](PF_6) crystallizes as yellow prisms in the monoclinic space group $P2_1/c$, containing one molecule per asymmetric unit (Figure 30, left). While [**32**](PF_6) crystallizes as yellow plates in the monoclinic space group $P2_1/c$. The structure contains three independent Re centres in the asymmetric unit that are very similar (Figure 30, right). The Re1-C bond lengths for both complexes lies in the same ranges and were found between of 2.2299(13) – 2.2877(12) Å for [**30**]$^+$ and 2.212(3) – 2.298(3) Å for [**32**]$^+$, respectively. The geometric parameters are very similar to those of the already reported hydroxyferrocifens; in [**30**]$^+$ the central double bond length is 1.3511(17) Å and in [**32**]$^+$, these bonds lie between 1.353(4) – 1.356(4) Å (1.36 Å, hydroxyferrocifens).[156] Furthermore, the substituents of the central double bond are not coplanar. The twist angle between the planes defined by C(1)–C(13)–C(15) and by C(20)–C(14)–C(26) is 13.42° for [**30**]$^+$ whereas for [**32**]$^+$, the angles are between 10.14 – 10.29° (12.8° in hydroxyferrocifens).[156]

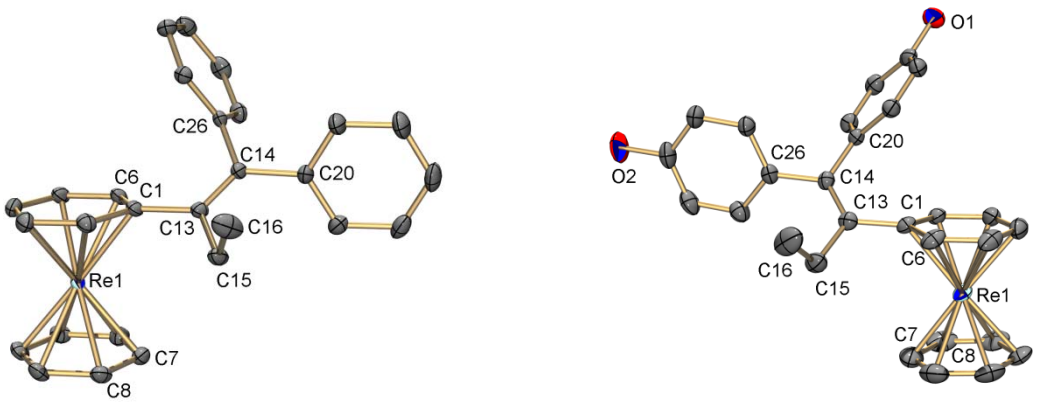

Figure 30: ORTEP representation[108] of [Re(η^6-1,1,2-triyltribenzene-but-1-ene)(η^6-C_6H_6)](PF_6) ([**30**](PF_6)) (left) and [Re(η^6-4,4'-(2-phenylbut-1-ene-1,1-diyl)diphenol)(η^6-C_6H_6)](PF_6) ([**32**](PF_6)) (right). Hydrogen atoms and anions are omitted for clarity, thermal ellipsoids represent 50% probability. Selected bond lengths [Å] for [**30**]$^+$: Re1-$C_6H_5C(Et)C(Ph)_2$ (centroid) 1.7389(6), Re1-C_6H_6 (centroid) 1.7381(6) and for [**32**]$^+$: Re-$C_6H_5C(Et)C(PhOH)_2$ (centroid) 1.7371(13)-1.7409(13), Re-C_6H_6 (centroid) 1.7273(15)-1.7341(15).

Yellow plates of [**31**](PF_6) can be isolated as racemic mixture. The enantiomers crystallize in the triclinic space group P-1 (Figure 31). The structure includes two independent Re centres together with two PF_6^- counter-ions per asymmetric unit. Due to the racemic mixtures, the *(S)* enantiomer crystallize without any disorder while the correspond *(R)* enantiomer contain a disorder with an occupancy of 89:11 (*(R)*:*(S)*) leading to an overall ratio of 1:0.8 *(R)*:*(S)* in the solid state. The rhenium carbon bond lengths were found to be in the range of 2.221(2) – 2.255(2) Å (*(S)*-enantiomer) and 2.225(2) – 2.245(2) Å (*(R)*-enantiomer), respectively, and are comparable with related structures such as [**26**]$^+$.

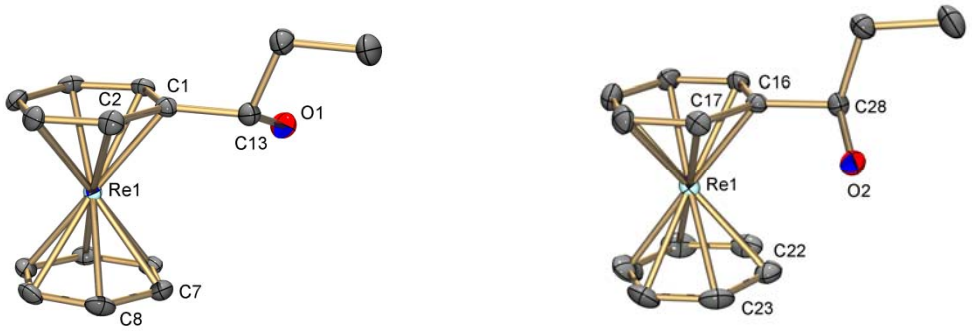

Figure 31: ORTEP representation[108] of *(S)*-Re(η^6-$C_6H_5C(OH)Et$)(η^6-C_6H_6)](PF_6) (*(S)*-[**31**](PF_6)) (left) and *(R)*-Re(η^6-$C_6H_5C(OH)Et$)(η^6-C_6H_6)](PF_6) (*(R)*-[**31**](PF_6)) (right). Hydrogen atoms and anions are omitted for clarity, thermal ellipsoids represent 50% probability. Selected bond lengths [Å] for *(S)*-[**31**]$^+$: Re1-$C_6H_5C(OH)Et$ (centroid) 1.7302(10), Re1-C_6H_6 (centroid) 1.7418(11) and for *(R)*-[**31**]$^+$: Re1-$C_6H_5C(OH)Et$ (centroid) 1.7359(11), Re1-C_6H_6 (centroid) 1.7314(13).

Wittig reactions are an alternative pathway for the formation of olefins and for this reason complex Re(η^6-$C_6H_5C(CH_2)Et$)(η^6-C_6H_6)] was synthesised from [**26**]$^+$ in small scales, leading to preliminary results. After protonation of methyltriphenylphosphonium bromide (MTPPB) with *n*-Buli in dry THF at 0°C, a solution of [**26**]$^+$ in THF was added and the reaction was further stirred for 24 h under reflux. Upon reaction control by UPLC-ESI-MS after 24 h, product Re(η^6-$C_6H_5C(CH_2)Et$)(η^6-C_6H_6)]$^+$ could be detected with a conversion of 45% with the corresponding m/z = 397.2 [M]$^+$. The retention time of Re(η^6-$C_6H_5C(CH_2)Et$)(η^6-C_6H_6)]$^+$ is shifted almost by 1 min compared to [**26**]$^+$ to higher values (Figure 32) due to the loss of the polarity induced by CH_2 group. Prolonged reaction time did not increase the conversion and further studies are needed to optimize this reaction to finally isolate the desired compound. Nevertheless, it was shown that Wittig reaction with (MTPPB) could be an accessible alternative to the Mc-Murry reaction.

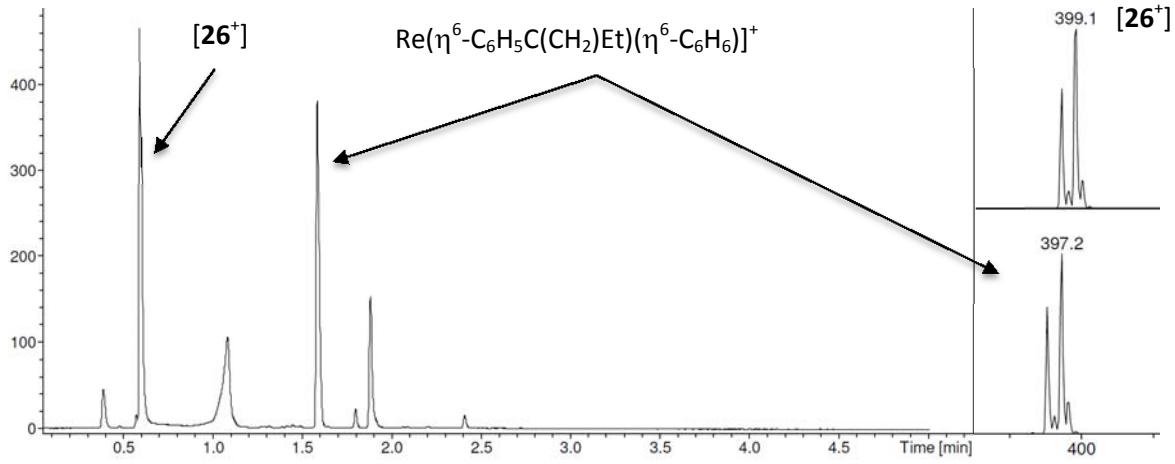

Figure 32: UV spectrum (left) and ESI-MS patterns (right) from the Wittig reaction mixture.

6.4.5 Secondary and Tertiary Alcohol Functionalized Rhenium Bis-Arene Complexes

Treatment of [**8**]$^+$ and [**9**]$^+$ with aldehydes or ketones under dry conditions lead to the formation of secondary or tertiary alcohol bis-arene complexes. The reactions were performed with benzaldehyde and benzophenone as an electrophile source. After quenching and purification of crudes mixtures, compound [Re(η^6-$C_6H_5C(OH)Ph)_2$](PF_6) ([**34**](PF_6)) was isolated in 55%, compound [Re(η^6-$C_6H_5C(OH)(Ph)_2$)(η^6-C_6H_6)](PF_6) ([**35**](PF_6)) in 5%, compound [Re(η^6-$C_6H_5C(OH)(Ph)_2)_2$](PF_6) ([**36**](PF_6)) in 39% and compound [Re(η^6-$C_6H_5(C(OH)(Ph)_2)_2$)(η^6-$C_6H_5C(OH)(Ph)_2$](PF_6) ([**37**](PF_6)) in 24%, respectively. In particular, [**34**](PF_6) was formed without significant amounts of the monosubstituted derivatives. Also, in the case of the tertiary alcohol functionalized complexes, the product distribution shifts more to the higher substituted derivatives (di/tri). The presence of a chiral centre in the side-chain of complexes [**34**](PF_6) renders the two ortho and meta positions diastereotopic which is manifested in ^{1}H NMR spectrum of [**34**]$^+$ in form of 2 triplets at δ = 6.44 ppm and 6.08 ppm (ortho-position) and 2 triplets at δ = 5.96 ppm and 5.88 ppm with integral ratios of 2:2:2:2 for both ligands. Moreover, in [**37**]$^+$ the third tertiary alcohol group is not bound at the ortho position as found for trisubstituted complexes but at the para position according to ^{1}H NMR measurement (one singlet at 5.87 ppm) and X-ray diffraction analysis. This can be explained by the steric hindrance of the bulky group.

[**34**]Cl crystallizes as colourless needles in the trigonal space group R-3. The Re atom is situated at the inversion centre, leading to refine only one half of the molecule in the asymmetric unit. Due to symmetry reason, the chloride counter-ion is half occupied. The crystal structure shows a disorder at the O1 atom with an occupancy of 87:13 which suggest that the major product is the (*S*,*R*)-

enantiomer (counting from O1) in the solid state (Figure 33, right). The rhenium carbon bond lengths were found to be in the range of 2.221(5) – 2.245(5) Å which are comparable with [**31**]$^+$.

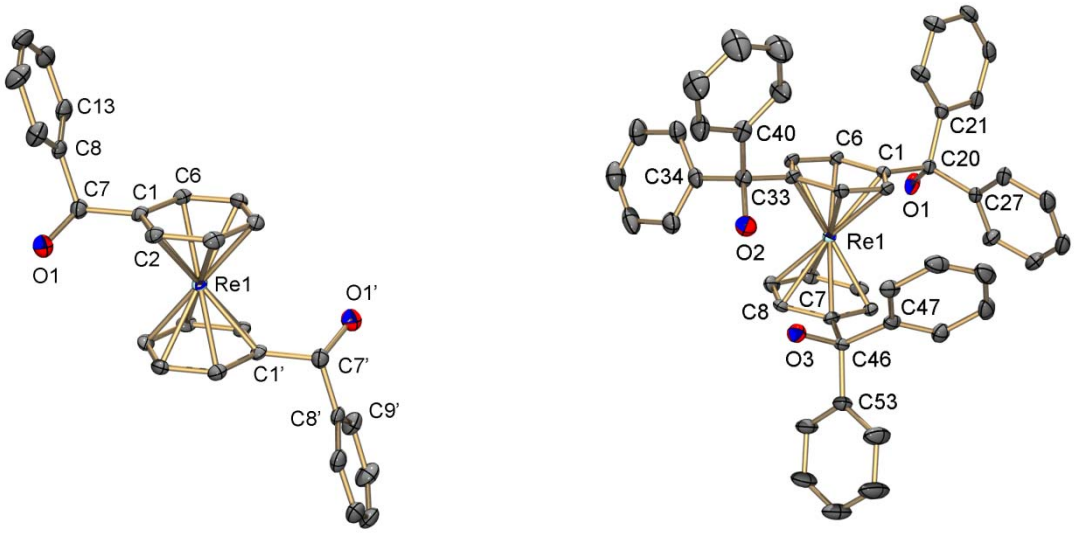

Figure 33: ORTEP representation[108] of [Re(η^6-$C_6H_5C(OH)Ph)_2$](PF_6) ([**34**]Cl) (left) and [Re(η^6-$C_6H_5(C(OH)(Ph)_2)_2$)(η^6-$C_6H_5C(OH)(Ph)_2$](PF_6) ([**37**](PF_6)). Hydrogen atoms and anions are omitted for clarity, thermal ellipsoids represent 50% probability. Selected bond lengths [Å] for [**34**]$^+$: Re1-$C_6H_5C(OH)Ph$ (centroid) 1.730(2) and for [**37**]$^+$: Re1-$C_6H_5(C(OH)(Ph)_2)_2$ (centroid) 1.7384(18), Re1-$C_6H_5C(OH)(Ph)_2$ (centroid) 1.743.

Single crystals of [**35**]$^+$-[**37**]$^+$, suitable for X-ray diffraction analysis, were obtained by vapour diffusion of cyclohexane into THF solution. [**35**](PF_6) crystallizes as light green plates in the monoclinic space group $P2_1/c$. The asymmetric unit includes one molecule with one PF_6^- as counter-ion and two THF solvent molecules. One of the THF molecules is connected via a hydrogen bond to the protons of the alcohol groups. The distances between the Re and the aromatic carbon atoms of [**35**]$^+$ were found to be in the range of 2.228(2) – 2.253(2) Å (see crystallographic table). No significant structural differences were found compared to the other structures such as [**34**]$^+$. The major species [**36**](PF_6) crystallizes as colourless plates in the triclinic space group P-1, including one molecule, one PF_6^- and two solvent molecules which correspond to THF and cyclohexane in the asymmetric unit. Furthermore, hydrogen bonds were found between the proton of the hydroxyl group (O2) and the oxygen of the second hydroxyl group O1. Another hydrogen bond was found between the hydroxyl group of O1 and THF molecule (see crystallographic table). The Re1-C bond lengths (2.221(4) – 2.268(4) Å) are in the same ranges as found for the monosubstituted [**35**]$^+$ (2.228(2) – 2.253(2) Å). The minor trisubstituted product [**37**]$^+$ (Figure 33, right) crystallizes as light yellow plates in the monoclinic space group $P2_1/c$. The asymmetric unit contains one molecule with one PF_6^- as counter-ion and two THF solvent molecules. Also, in this case, hydrogen bond formation is observed with the

same connectivity as found in [**35**]$^+$. Moreover, both THF solvent molecules are disordered. The Re1-C bond lengths are in the range of 2.231(5) – 2.261(5) Å and are comparable with the related structures [**35**]$^+$ and [**36**]$^+$.

6.4.6 Ester and Azide Functionalised Rhenium Bis-Arene Complexes

Of note, reactions were carried out only in small scales and as proof of concept without isolating the products. Reacting the *in situ* formed lithiated species [**8**]$^+$ and [**9**]$^+$ with ethyl chloroformate, gave the monosubstituted complex [Re(η^6-C_6H_5COOEt)(η^6-C_6H_6)]$^+$ and the disubstituted complex [Re(η^6-$C_6H_5COOEt)_2$]$^+$ with a conversion of 15% and 45% after 6h at -78°C. Also in this reaction, the formations of dimeric species were observed. During the reaction, a nucleophilic attack at the ester group with [**8**]$^+$ take place which leads to the formation of dimeric compounds bound via a keton group according to UPLC-ESI-MS data. Ester functionalized rhenium bis-arene complexes such as [Re(η^6-C_6H_5COOMe)(η^6-C_6H_6)]$^+$ can also be prepared by reacting Re(η^6-C_6H_5COOH)(η^6-C_6H_6)](TFA) ([**6**](TFA)) with a powerful methylating reagent like methyl trifluoromethanesulfonate under mild alkaline conditions in methanol. The reaction proceeds almost quantitative. Besides, ester group which are a potent group for further functionalisation, azides are an attractive alternative. They can be used for functionalization via click chemistry. In this context, [**8**]$^+$ and [**9**]$^+$ were treated with tosyl azide under dry condition for 5h at -78°C in THF. Reaction control was monitored by UPLC-ESI-MS and showed the formation of monosubstituted [Re(η^6-$C_6H_5N_3$)(η^6-C_6H_6)]$^+$ and disubstituted [Re(η^6-$C_6H_5N_3)_2$]$^+$ with a conversion of 13% and 57%, respectively. In summary, the introduction of these two functional groups into rhenium bis-arene scaffold enlarged the library of potential reaction with these compounds and will be extremely useful for the synthesis of further versatile complexes for application in bioinorganic chemistry, in the futures.

6.4.7 Phosphor Functionalized Rhenium Bis-Arene Complexes

As electrochemical studies in this thesis showed, is the rhenium bis-arene scaffold one of the most stables bis-arene motifs, and it is even more stable then ferrocene. Therefore, it is very attractive to widen the scope of potential applications for this class of compounds from bioinorganic to catalysis. For examples, 1,1'-bis(diphenylphosphino)ferrocene (dppf) is a well-known and promising candidate for such an application. Incorporating a catalytic active metal centre (usually from the platinum group) between the phosphines, leads to a series of different high-efficiency catalysts, especially for cross-coupling reactions.[157, 158] Another example for catalysis is the carbonyl-chloro-(dppf)-rhodium(I) which is an efficient catalyst for hydroformylation reactions.[159] To verified this concept on the

rhenium bis-arene scaffold, a master thesis with the goal to synthesise 1,1'-bis(η^6-phenyl-diphenylphosphino)rhenium(I) analogues was started.[160] Furthermore, the catalytical activity of 1,1'-bis(η^6-phenyl-diphenylphosphino)rhenium(I) complexes with different incorporated active metal centres was performed. Following the general procedure, chlorodiphenylphosphine ($P(Ph)_2Cl$) was added to the lithiated species [**8**]$^+$ and [**9**]$^+$ and stirred for 60 min at -78°C. Reaction control via UPLC–MS shows the product distribution of the obtained substituted species (Figure 34)

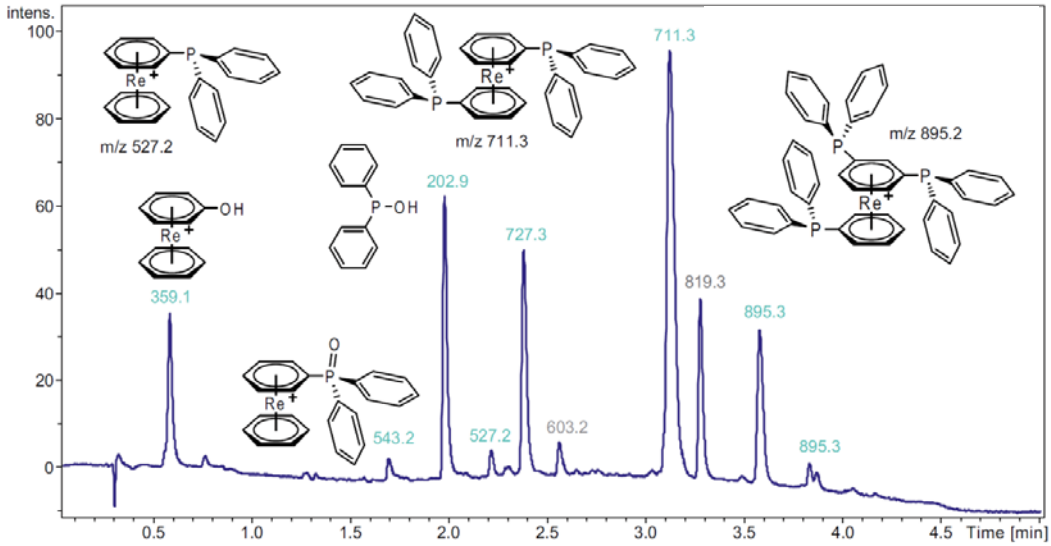

Figure 34: UPLC-ESI-MS analysis (positive mode) of the crude of 1,1'-Bis(η^6-phenyldiphenyl-phosphino)-rhenium(I) analogues.

After quenching and purification by preparative HPLC, the (1,1'-bis(η^6-phenyl-diphenyl-phosphine)rhenium(I) triflate complex was isolated with minor impurities of the monosubstituted Re complex (13% yield). Due to oxygen and moisture sensitivity of these the compounds, the purification of this mixture was rather difficult, which led to the low yield. Nevertheless, the compound could be fully characterized including crystal structure analysis. Unfortunately, the complexation experiment with palladium, nickel or rhodium was not successful. It seems that the chemistry with the positively charged rhenium is quite different compared to ferrocene and therefore more investigations are needed.

6.4.8 Pyridine functionalized rhenium bis-arene complexes

As an addition to the phosphor chemistry, pyridine moieties could be an alternative. Therefore, 1,1'-bis(2-(η^6-benzoyl)-pyridine)rhenium(I) and 1,1'-Bis(η^6-phenyl(2-pyridinyl)methanol)-rhenium(I) was synthesised and characterized.[160] However, coordination with palladium(II) or platinum(II) was not successful and need more investigations.

In summery and in addition to the published manuscript, a large variety of different functionalized complexes has been synthesised and characterized. Most of them showed quite high stability and can be used for further experiments such as cytotoxicity studies. In particular, one example showed an unknown and unexpected reactivity. The substitution of [Re(η^6-C_6H_5Br)(η^6-C_6H_6)](PF_6) ([**4**](PF_6)) with hydroxide in water turned out to be concentration dependent and led to an unexpected complex. Detailed insights for this type of reaction will be discussed in the following manuscript which was published in 2017 in Inorganic Chemistry.[141] Furthermore unpublished and related results will be described in chapter 6.6.

6.5 Publication: A Mixed-Ring Sandwich Complex from Unexpected Ring Contraction in [Re(η^6-C_6H_5Br)(η^6-C_6R_6)](PF_6)

A Mixed-Ring Sandwich Complex from Unexpected Ring Contraction in [Re(η^6-C_6H_5Br)(η^6-C_6R_6)](PF_6)

Giuseppe Meola, Henrik Braband, Daniel Hernández-Valdés, Carla Gotzmann, Thomas Fox, Bernhard Spingler, Roger Alberto*

Department of Chemistry, University of Zurich, Winterthurerstr. 190, CH-8057 Zurich Switzerland.

ABSTRACT: The contraction of coordinated aromatic hydrocarbons is a rare reactivity pattern in organometallic chemistry. We describe the conversion of a bromo-benzene coordinated to a Re^{I} center into a cyclopentadienyl-aldehyde. Under mildly alkaline conditions, the expected phenol complex is formed with Re and ^{99}Tc but under strong basic conditions, ring contraction occurs in close to quantitative yields for Re only. A mechanism for this unprecedented reaction is proposed based on ^{1}H and ^{2}H NMR spectra and DFT calculations.

Sandwich complexes of d- and f-elements are core elements in many fields of contemporary science and are key players namely in homogeneous catalysis, material sciences and in biological or medicinal oriented research topics.[1, 2] These organometallics complemented coordination compounds over the recent years in life sciences in particular. Many examples corroborate their superiority to coordination compounds, mainly due to additional options such as metal- or ligand centered reactivities and optical imaging through fluorescence.[3, 4] The selection of organometallic building blocks comprising aromatic ligands is however relatively limited. Ferrocene (Fc) is an exceptional multi-modal key player as a diagnostic and a therapeutic label the same time due to its induction of ROS formation.[5, 6] Furthermore, the $\{Ru^{II}(arene)\}^{2+}$ fragment coordinates directly to phenyl groups in biomolecules, a convenient way of labeling for proteomic purposes, for instance.[7, 8] In the bioorganometallic field, sandwich complexes with mixed aromatic ligands of various hapticities are essentially absent. Although known since the advent of organometallic chemistry, little is known about such compounds and few have found interest beyond structures and properties. Mixed-aromatic sandwich complexes often obey the 18 electron rule which limits the combinatorial chemistry of two different aromatic ligands. For group 4 and 5 elements, combinations between [η^7-C_7H_7]$^+$ and [η^5-C_5H_5]$^-$ were reported,[9] for group 6 and 8, combinations between [η^6-C_6H_6] and [η^5-C_5H_5]$^-$ and for group 9 [η^5-C_5H_5]$^-$ and [η^4-C_4H_4] π-complexes are prototypical.[10, 11] Probably best investigated are mixed-ring sandwich complexes of iron [Fe(η^5-C_5H_5)(η^6-C_6H_6)]$^+$ for which all kind of organic reactions at the arene ring are described but leaving the cyclopentadienyl untouched.[12] For group 7, there is a gap in the systematics of mixed-aromatic sandwiches and only[M(η^5-C_5H_5)(η^6-

C_6H_6)] (M = Mn, Re) are experimentally set.[13-16] To obtain these mixed-aromatic sandwich complexes, the ligands are introduced directly as neutral arenes, tropylium or cyclopentadienyl salts by various substitution reactions. Along their studies on substitution reactions on coordinated aromatic ligands, Pauson et al. reported in the sixties a ring contraction of tropylium, coordinated to the $\{Cr(CO)_3\}$ moiety, to benzene upon attack of strong nucleophiles.[17, 18] This uncommon reaction found only punctual interest. Easy nucleophilic attack to the positively charged tropylium ligand and concomitant formation of highly stabilized benzene was interpreted as the underlying driving force.[18]

In our search for new organometallic building blocks for life sciences, we have recently introduced sandwich complexes of the type $[M(arene)_2]^+$ (M = $^{99(m)}$Tc, Re) along a convenient route and directly from $[MO_4]^-$.[19] The arene rings can be functionalized for conjugation to targeting molecules, e.g. with bromide for nucleophilic substitution.[20] Since phenols are frequent modalities in biomolecules, we attempted to replace the bromide group in $[Re(\eta^6\text{-}C_6H_5Br)(\eta^6\text{-}C_6H_6)]^+$ (**1**$^+$) by hydroxide to obtain $[Re(\eta^6\text{-}C_6H_5OH)(\eta^6\text{-}C_6H_6)]^+$ (**2**$^+$) (Scheme 1). This reaction proceeded as expected and the structure of compound [**2**](OTf) was confirmed by X-ray structure analysis (see ESI).

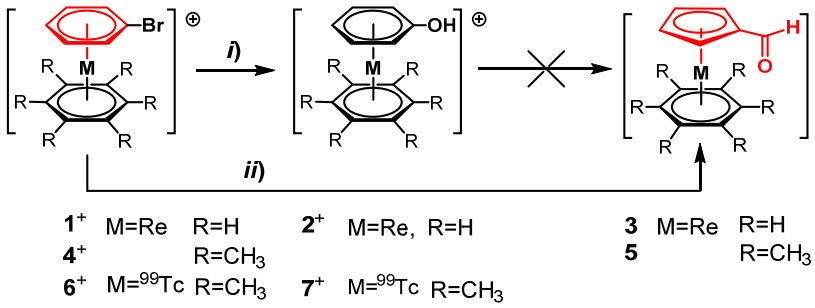

Scheme 1: Reaction pathways of $[Re(\eta^6\text{-}C_6H_5Br)(\eta^6\text{-}C_6R_6)]^+$ with small (*i*) and large excess of NaOH (*ii*). Under the shown conditions, the –OH group is deprotonated in the reaction.

In agreement with the electrophilic reactivity of coordinated hydrocarbons,[21] complex **2**$^+$ was formed in almost quantitative yield in water under mildly alkaline conditions and elevated temperature of 60° - 80°C. However, at temperatures of 80° C or higher (microwave), and with hydroxide being in large excess over **1**$^+$ (>100:1), complex **2**$^+$ (in solution as its conjugate base **2**) formed only as a minor side product. The main product precipitated from solution. Upon isolation, we identified this compound as the mixed-aromatic sandwich complex $[Re(\eta^5\text{-}C_5H_4CHO)(\eta^6\text{-}C_6H_6)]$ (**3**). Along the reaction pathway, the coordinated bromo-benzene ligand obviously contracted into a cyclopentadienyl system and the "excess" carbon from the former benzene ring was transformed into the pendent aldehyde group. Besides common analytical characterization (see ESI), we confirmed the authenticity of **3** by X-ray structure analysis (Figure 1).

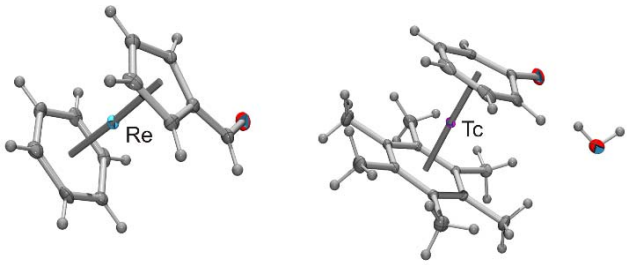

Figure 1: ORTEP of [Re(η^5-C_5H_4CHO)(η^6-C_6H_6)] (**3**, left) and [^{99}Tc(η^6-C_6H_5O)(η^6-C_6Me_6)] (**7**, deprotonated form, right). Relevant bond lengths (Å) are for **3**: Re1-Cp 1.888(8), Re1-benzene (centroid) 1.705(7) and for **7**: Tc1-C_6Me_6 1.7137(6), Tc1-C_6H_5O 1.7321(7).

To our knowledge, the formation of **3** by ring contraction of an arene to a cyclopentadienyl is unprecedented. Although aromatic systems coordinated to metals cannot directly be compared to free aromatic molecules, it is unexpected that the prototypical and highly resonance stabilized aromatic bromo-benzene is converted to cyclopentadienyl. We assume, however, that its interaction with the formally positive charge of the rhenium center in conjunction with resonance stabilization by the formyl group still favors this ring-contraction. Since the Re^{I} center partially polarizes the coordinated bromo-benzene, it becomes more prone to nucleophilic attack or, in other words, the coordinated hydrocarbon becomes more electrophilic. Hypothesizing that the phenol complex **2**$^+$ or its conjugated base would be a preceding intermediate in the ring contraction reaction, we first determined its pK_a value in aqueous solution. Potentiometric titration gave an acidity constant of pK_a=5.34(1) which is almost 5 orders of magnitude lower than phenol itself. This distinct acidification is consistent with strong π-bonding from the arene into the rhenium center as well as with the ^{1}H NMR data, evidencing substantial deshielding of the aromatic protons (see ESI).

Ring contraction is not limited to compound **1**$^+$ but tolerates alterations in the 2nd arene ring. We chose [Re(η^6-C_6H_5Br)(η^6-C_6Me_6)]$^+$ (**4**$^+$) as an another “extreme”. Applying similar conditions as for **1**$^+$ lead directly to the corresponding Cp-aldehyde complex [Re(η^5-C_5H_4CHO)(η^6-C_6Me_6)] (**5**) albeit in lower yields due to decreased water solubility of [**4**]Br. Common chemical analyses and an X-ray structure determination confirmed the structure of **5** (see ESI).

No mixed sandwich complexes are known so far for ^{99}Tc. To elucidate if this ring contraction is of more general nature, and would also apply for ^{99}Tc, we prepared [^{99}Tc(η^6-C_6H_5Br)(η^6-C_6Me_6)]$^+$ (**6**$^+$) and subjected it to the same conditions as **4**$^+$. However, in contrast to **4**$^+$, no ring contraction was observed and only the phenol complex [^{99}Tc(η^6-C_6H_5OH)(η^6-C_6Me_6)] (**7**$^+$) was formed. Thus, the observed ring contraction tolerates different opposite arene ligands but (so far) not another element of the group 7 triad. The fact that this ring contraction has not been observed previously in other d-element bis-arene complexes may be related to their respective instabilities under strongly alkaline

conditions. Still, it is worthwhile to extend the study also to the neighboring elements and to iron or ruthenium in particular.[12]

The reported reactivity of the ^{99}Tc complex entails the question about the availability of the ^{99m}Tc homologues. At very high dilution with ^{99m}Tc, kinetics often governs product formation, which might be different from thermodynamically driven ^{99}Tc chemistry. We emphasize that the successful reaction with ^{99}Tc does not necessarily stand for an identical behavior with ^{99m}Tc. We prepared $[^{99m}Tc(\eta^6\text{-}C_6H_5Br)(\eta^6\text{-}C_6Me_6)]^+$ as described before[19] and transferred it into a strongly alkaline solution of pH ≈ 12. Heating to 100°C lead to a slow but close to quantitative formation of the ^{99m}Tc analogue of **7**$^+$ (deprotonated in this solution) indeed. Comparison of HPLC retention time confirmed its nature (see ESI).

The mixed-ring sandwich complexes **3** and **7** are neutral 18 electron species, comparable to e.g. ferrocene (Fc) or $[Cr(\eta^6\text{-}C_6H_6)_2]$. Since Fc in particular is frequently applied in bioorganometallic chemistry and other fields, a comparison of the respective electrochemical data is of interest. A cyclic voltammogram of **3** is shown in Figure 2 as an overlay with the ones of Fc and $[Re(\eta^6\text{-}C_6H_6)_2]^+$.

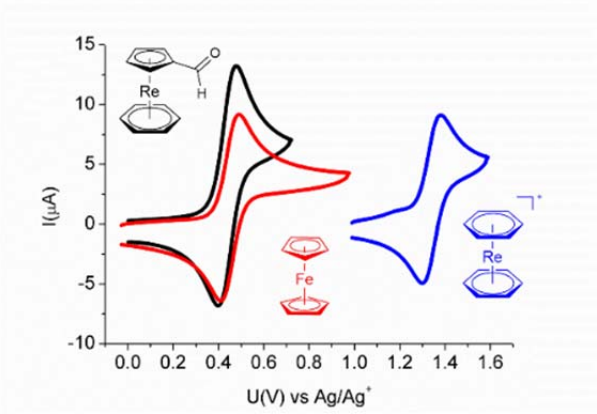

Figure 2: Cyclic voltammograms of ferrocene (red), $[Re(\eta^6\text{-}C_6H_6)_2]^+$ (blue) and the mixed-ligand sandwich complex **3** (black). Acetonitrile, 0.1 M [TBA][PF_6] (electrolyte), glassy carbon working electrode (i.d. = 3 mm), Pt auxiliary electrode and Ag/AgCl reference electrode, analyte concentrations 1 mM, voltage step: 6 mV, sweep rate: 0.1 V/s.

Figure 2 shows that the two compounds Fc and **3** display under identical conditions about the same $E°_{1/2}$, namely 0.45 V for Fc/Fc^+ and 0.44 V for **3°/3**$^+$ vs. Ag/AgCl in acetonitrile. We note that this potential is substantially shifted as compared to the isoelectronic complex $[Re(\eta^6\text{-}C_6H_6)_2]^+$ for which $E°_{1/2}$ is +1.34V vs Ag/AgCl.[19] Identifying trends for comparable isoelectronic mixed-ring sandwich complexes along triads or within the same period but with neighboring elements is difficult since most of these electrochemical data are missing or were acquired under different conditions. Based on electrochemical data from Figure 2, the chemical reactivity of **3** parallels the one of Fc, which might have implications for application in life sciences. Whereas **3** is stable in solution over an

extended period in the absence of oxygen, it starts to decompose slowly when exposed to air, comparable to Fc and in agreement with electrochemical data. Whether reactive oxygen species are formed as in case of Fc remains to be clarified.

The mechanism of this ring contraction is a key question. We assumed that the phenol complex $\mathbf{2}^+$ or its conjugate base **2** might be an intermediate along the reaction pathway (vide infra and Scheme 1). To (dis)confirm this hypothesis, we exposed the separately synthesized and isolated complex $\mathbf{2}^+$ to the same reaction conditions as in the direct synthesis of $\mathbf{1}^+$ to **3**. Even at T > 100° C in water and at pH=14, $\mathbf{2}^+$ (present in its deprotonated form) did not react to **3** but remained completely stable. Although DFT calculations show that **3** is by 151 kJ/mol more stable than $\mathbf{2}^+$, the formation of intermediate D seems to be a key step to cross the high energetic barrier to obtain product **3** (see ESI). The intermediate D is only accessible from $\mathbf{1}^+$ as the formation of **3** from $\mathbf{2}^+$ is not possible even in the presence of excess NaBr and NaOH and at 80°C.

Pauson proposed a mechanism for the tropylium→benzene rearrangement in $[Cr(\eta^7\text{-}C_7H_7)(CO)_3]^+$ with strong nucleophiles.[17] In a first step, they hypothesized a nucleophilic attack (of e.g. cyclopentadienyl) to the tropylium under formation of a cycloheptadienyl complex as a first intermediate. In a second step, "electronic shifts" lead to ring contraction.[20] In a similar approach as the one of Pauson et al., we showed previously that the nucleophilic attack of n-butyl lithium (^{n}BuLi) to $[Re(\eta^6\text{-}C_6H_6)_2]^+$ gave the cyclohexadienyl complex $[Re(\eta^5\text{-}C_6H_6\text{-}^n\text{Bu})(\eta^6\text{-}C_6H_6)]$ but did not lead to any ring contractions.[254] Reaction of ^{n}BuLi with $\mathbf{1}^+$ resulted expectedly in a nucleophilic aromatic substitution of the bromide. The same reactivity pattern was observed with low concentrations of $[OH]^-$ and at temperatures up to 80°C, only the phenol complex $\mathbf{2}^+$ was obtained as mentioned before. To gain a closer insight into a potential mechanism for the ring contraction, we performed the reaction $\mathbf{1}^+ \rightarrow \mathbf{3}$ in $D_2O/[OD]^-$ to assess by deuterium ^{2}H NMR spectroscopy which of the positions in the final product would carry a "D" instead of an "H". The D(^{2}H) together with a ^{1}H NMR spectra of the product **3** at the end of this reaction are shown in Figure 3. Since both spectra were recorded from the very same sample tube, the integrals give the correct respective ratios of H/D distributions (see ESI for NMR details).

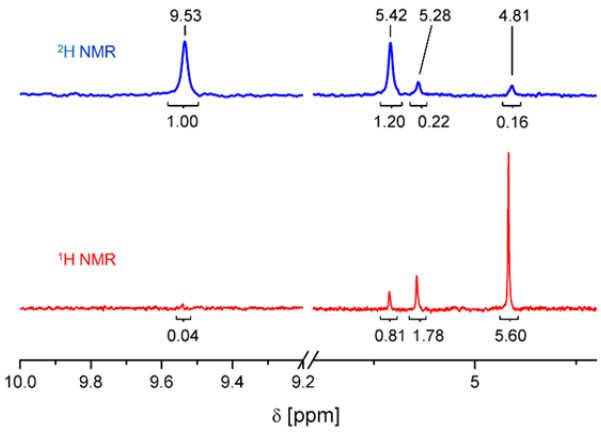

Figure 3: D(^{2}H) (blue) and ^{1}H NMR spectra (red) of **3** after reaction in D_2O/NaOD (recorded on a 500 MHz (^{2}H, 76.79 MHz) device in acetonitrile as solvent)

The ^{1}H NMR spectrum of the product displays no ^{1}H on the aldehyde (9.53 ppm) (Figure 3). Therefore, the ^{2}H integral of -CD=O was set to 1. The ^{2}H strength of the α-CD is 1.2 relative to -CD=O and the α-CH signal accounts for 0.8. The ratio between –CD=O and α-CD is thus about 1:1 taking some self-exchange into consideration. The β-CD amount is small (0.2) and sums up with the corresponding β-CH (1.8) to the required integral of 2. Since the product precipitates from solution, further self-exchange H→D occurs to a minor amount only, if at all. In a separate experiment, we noted that heating of non-deuterated, essentially insoluble **3** in D_2O lead to a small exchange of the α-CH to α-CD, corroborating the previous statements. The observed isotope distribution pattern (Scheme 2) after the reaction implies that one α-CD and the aldehyde proton (^{2}H) originate from a D_2O protonation step in one of the intermediates or to an intramolecular D-shift during the reaction.

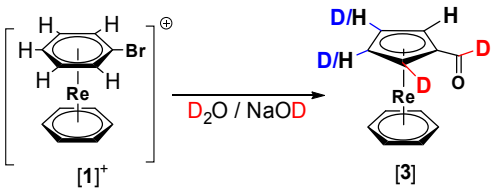

Scheme 2: Observed isotope exchange pattern in the ring contraction reaction

To account for this isotope pattern, we propose the reaction mechanism depicted in Scheme 3. Reversible, nucleophilic attack of a hydroxide to coordinated bromo-benzene leads to the relatively stable cyclohexadienyl complex **A** (reaction *i*). Its mesomeric form **B** can reversibly be protonated (D^+) to **C**. If fast enough, these steps can happen twice to finally reach **D**. All forms **A**-**D** are in a dynamic acid-base equilibrium, including a further but less stable intermediate with a D in the para-position (not shown in Scheme 3) and giving rise to the small ^{2}H signal of β-CD in the ^{2}H NMR spectrum of **3**

(vide supra). Since the reaction was run in D_2O, all intermediates must ultimately be present in the doubly deuterated mesomere **D** or its conjugate acid **C**. From **C** or **D**, slow reactions may branch into *ii*) which leads to bromide dissociation and the side product $\mathbf{2}^+$ or into the ring-contraction mechanism *iii*). The main direction the reaction takes, depends on the excess hydroxide since **C** and **B** are in a protolysis equilibrium; large excess favors *iii*) and small excess *ii*).

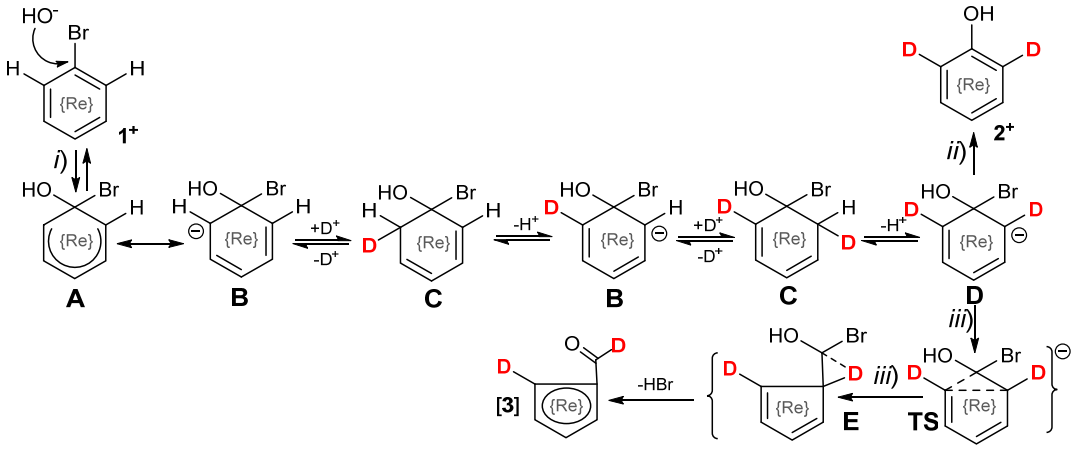

Scheme 3: Proposed ring contraction mechanism to 3 based on the observed isotope pattern. {Re} represents the $\{Re(\eta^6\text{-}C_6R_6)\}^+$ (R=-H, $-CH_3$) fragment, the middle scheme the underlying isotope exchange reactions.

To assess that the relative rates for establishing the equilibria in processes leading from **A** to **D** are much faster than dissociation of bromide (*ii*) or hydroxide, we run the reaction in D_2O/NaOD under conditions leading to exclusive formation of soluble $\mathbf{2}^+$. After 12h at 70°C, UPLC-MS analysis revealed m/z = 361.1 which accounted for the molecular mass of $\mathbf{2}^+$+2 of the final main product, evidencing the replacement of two hydrogens by two deuterons. In addition, we detected in the UPLC peak of $\mathbf{1}^+$ m/z values of 423.0 and 424.1 These masses are assigned to $\mathbf{1}^+$+1 and $\mathbf{1}^+$+2 respectively, with one or two protons exchanged for deuterons, confirming the reversibility of reaction *i*) and the rapid equilibria **A**-**D** (see ESI).

In an attempt to support reaction *iii*), DFT calculations were performed. The intermediate structures **D** and **E** as well as the product **3** and the transition state **TS** were optimized. For the step **D** → **E**, the resulting Gibbs free energy of activation was found as $\Delta G^{\neq}$ = 150kJ/mol. (ESI shows the structure of the transition state). The high value of the activation barrier explains the importance of heating over 80°C to obtain product **3**. Natural population analysis shows a negative partial charge on the *ortho*-carbons in complex **D** (see ESI). This and the transition state found, support the hypothesis of a ring contraction with a concomitant, intramolecular proton (deuteron) transfer as a key step in the

formation of the Cp-aldehyde complex. Thermodynamic seems to be the driving force for the last step (**E** → **3**) since the final product is by 274.3 kJ/mol more stable than the intermediate **E**.

Reactivities of metal-coordinated molecules or ions are key in organometallic chemistry. Many basic reactivity patterns have been described since its advent, including ring contractions from coordinated tropylium to benzene. These reactions are of fundamental relevance and the base for their utility in directed organic syntheses and chemical transformations. We elucidated in this report an unprecedented ring contraction of a coordinated bromo-benzene to a cyclopentadienyl ligand. This conversion applies for rhenium but not for technetium but still implies a more general scheme, likely to be observed for other d-element arene complexes as well. This reaction belongs therefore to a basic series, supporting metal-mediated activation of arenes towards the syntheses of organic compounds.

On the more applied side, the physico-chemical similarity of key compound **3** to ferrocene might induce bioorganometallic studies with a building block appropriate for imaging (^{99m}Tc) and therapy (Re) in the field of theranostics in future.

REFERENCES

(1) Pampaloni, G. Aromatic hydrocarbons as ligands. Recent advances in the synthesis, the reactivity and the applications of bis(h^6-arene) complexes. *Coord. Chem. Rev.* **2010**, *254*, 402-419.

(2) Calderazzo, F.; Pampaloni, G. Aromatic-Hydrocarbons, Carbocyclic Ligands Spanning Several Oxidation-States in Both Main-Group and Transition-Elements-Recent Advances with Early Transition-D Elements. *J. Organomet. Chem.* **1995**, *500*, 47-60.

(3) Stephenson, K. A.; Banerjee, S. R.; Besanger, T.; Sogbein, O. O.; Levadala, M. K.; McFarlane, N .; Lemon, J. A.; Boreham, D. R.; Maresca, K. P.; Brennan, J. D.; Babich, J. W.; Zubieta, J.; Valliant, J. F. Bridging the Gap between In Vitro and In Vivo Imaging: Isostructural Re and Tc-99m Complexes for Correlating Fluorescence and Radioimaging Studies. *J. Am. Chem. Soc.* **2004**, *126*, 8598-8599.

(4) Romanski, S.; Rucker, H.; Stamellou, E.; Guttentag, M.; Neudorfl, J. M.; Alberto, R.; Amslinger, S.; Yard, B.; Schmalz, H. G. Iron Dienylphosphate Tricarbonyl Complexes as Water-Soluble Enzyme-Triggered CO-Releasing Molecules (ET-CORMs). *Organometallics* **2012**, *31*, 5800-5809.

(5) Hartinger, C. G.; Metzler-Nolte, N.; Dyson, P. J. Challenges and Opportunities in the Development of Organometallic Anticancer Drugs. *Organometallics* **2012**, *31*, 5677-5685.

(6) Hillard, E.; Vessieres, A.; Thouin, L.; Jaouen, G.; Amatore, C. Ferrocene-mediated proton-coupled electron transfer in a series of ferrocifen-type breast-cancer drug candidates. *Angew. Chem. Int. Ed.* **2006**, *45*, 285-290.

(7) Novakova, O.; Chen, H. M.; Vrana, O.; Rodger, A.; Sadler, P. J.; Brabec, V. DNA interactions of monofunctional organometallic ruthenium(II) antitumor complexes in cell-free media. *Biochemistry* **2003**, *42*, 11544-11554.

(8) Perekalin, D. S.; Novikov, V. V.; Pavlov, A. A.; Ivanov, I. A.; Anisimova, N. Y.; Kopylov, A. N.; Volkov, D. S.; Seregina, I. F.; Bolshov, M. A.; Kudinov, A. R. Selective Ruthenium Labeling of the Tryptophan Residue in the Bee Venom Peptide Melittin. *Chem. Eur. J.* **2015**, *21*, 4923-4925.

(9) Green, M. L. H.; Ng, D. K. P. Cycloheptatriene and Cycloheptatrienyl Complexes of the Early Transition-Metals. *Chem. Rev.* **1995**, *95*, 439-473.

(10) O'Donohue, P.; McAdam, C. J.; Courtney, D.; Ortin, Y.; Muller-Bunz, H.; Manning, A. R.; McGlinchey, M. J.; Simpson, J. The preparation, spectroscopy, structure and electrochemistry of some [Co(h^4-C_4Ph_4)(h^5-C_5H_4R)] complexes. *J. Organomet. Chem.* **2011**, *696*, 1496-1509.

(11) Tamm, M. Synthesis and reactivity of functionalized cycloheptatrienyl-cyclopentadienyl sandwich complexes. *Chem. Commum.* **2008**, 3089-3100.

(12) Abd-El-Aziz, A. S.; Bernardin, S. Synthesis and reactivity of arenes coordinated to cyclopentadienyliron cations. *Coord. Chem. Rev.* **2000**, *203*, 219-267.

(13) Fischer, E. O.; Wehner, H. W. Aromatic Complexes from Metals. 104. Cyclopentadienyl-Rhenium(I)-Benzene a New Metallorganic Base and Its Behavior in Acetylation According to Friedel-Crafts. *Chem. Ber.* **1968**, *101*, 454-462.

(14) Herberhold, M.; Hofmann, T.; Milius, W.; Wrackmeyer, B. New Studies on 2 Old Sandwich Compounds - Cyclopentadienyl-manganese Benzene and Cyclopentadienyl-manganese Biphenyl. *J. Organomet. Chem.* **1994**, *472*, 175-183.

(15) Green, M. L. H.; Ohare, D. Synthesis of Eta-Arene Rhenium Compounds Using Rhenium Atoms - Crystal-Structures of [Re_2(h-C_6H_6)(h-C_6H_8)$_2$(m-H)$_2$] and [Re(h^6-C_6H_6)(h-C_6H_8)H]. *J. Chem. Soc., Dalton Trans.* **1987**, 403-410.

(16) Green, M. L. H.; Lowe, N. D.; Ohare, D. Synthesis, Characterization, and Reactivity of (h^6-Indene)(h^5-Indenyl)Rhenium - a Precursor to Heterobimetallic (m-h^3-h^6-Indenyl) Derivatives. *J. Chem. Soc., Chem. Commum.* **1986**, 1547-1548.

(17) Munro, J. D.; Pauson, P. L. Cycloheptatriene- and Tropylium-Metal Complexes. 2. Rearrangement to Benzene Complexes. *J. Chem. Soc.* **1961**, 3479-3483.

(18) Pauson, P. L. Nucleophilic-Addition to Transition-Metal Complexes. *J. Organomet. Chem.* **1980**, *200*, 207-221.

(19) Benz, M.; Braband, H.; Schmutz, P.; Halter, J.; Alberto, R. From Tc-VII to Tc-I; facile syntheses of bis-arene complexes [Tc-99(m)(arene)$_2$]$^+$ from pertechnetate. *Chem. Sci.* **2015**, *6*, 165-169.

(20) Meola, G.; Braband, H.; Schmutz, P.; Benz, M.; Spingler, B.; Alberto, R. Bis-Arene Complexes [Re(η^6-arene)$_2$]$^+$ as Highly Stable Bioorganometallic Scaffolds. *Inorg. Chem.* **2016**, *55*, 11131-11139.

(21) Pike, R. D.; Sweigart, D. A. Electrophilic reactivity of coordinated cyclic pi-hydrocarbons. *Coord. Chem. Rev.* **1999**, *187*, 183-222.

6.6 Unpublished Results: A Mixed-Ring Sandwich Complex from Unexpected Ring Contraction in [Re(η^6-C6H5Br)(η^6-C_6R_6)](PF_6)

As mention in the manuscript, the ring contraction of a bromo-benzene coordinated to a Re^I centre into a cyclopentadienyl-aldehyde is an uncommon reaction. In order to investigate the ring contraction with further weak nucleophiles, reactions were carried out following the same procedure with NaSH, NaCN and NaN_3. The reaction between sulfanide and [Re(η^6-C_6H_5Br)(η^6-C_6H_6)]$^+$ ([**1**]$^+$) gave only the substituted product [Re(η^6-C_6H_5SH)(η^6-C_6H_6)]$^+$ in quantitative conversion according to UPLC-MS measurements. Furthermore, reactions with cyanides and azides showed only negligible amount of the substitution products. The conversion of those might be improved by prolongation of the reaction time but further investigations were not performed so far. Despite the screening with different nucleophiles, a ring contraction was only found in the presence of an excess of hydroxide. Concerning the substitution of the dibromide derivative Re(η^6-$C_6H_5Br)_2$]$^+$ ([**5**](PF_6)), it was already shown in section (6.4.2), that the replacement of the second bromine is slower compared to the first one. Taking this into account, reaction with [**5**](PF_6) and hydroxide were performed under the same conditions used for the ring contraction in [**1**]$^+$. According to UPLC-MS data, no ring contraction was observed. The only detected product in this reaction was the monosubstituted hydroxy [Re(η^6-C_6H_5OH)(η^6-C_6H_5Br)]$^+$ (quantitative conversion). The replacement of the second bromine was not achieved even by increasing the temperature (100-120°C) combined with longer reaction time (12 h). Presumably, the nucleophilicity of hydroxides is too low to replace the second bromide under this condition. As an alternative complex Re(η^6-$C_6H_5Cl)_2$]$^+$ ([**19**]$^+$) bearing two chlorines could be used, because this complex shows higher reactivity towards substitution reaction. Furthermore, the authenticity of [Re(η^6-C_6H_5OH)(η^6-C_6H_5Br)]$^+$ was elucidated by X-ray diffraction analysis (see crystallographic tables). Nevertheless, a ring contraction of [**5**](PF_6) was obtained by reacting [**5**]$^+$ in THF in the presence of small amount of water and an additional strong base (NaH or $NaNH_2$). The reaction was performed in a microwave reactor for 2 h at 80°C. UPLC-MS analysis showed the formation of two products with different retention time but the same mass. The first peak with a retention time of 1.1 min could be assigned to the monosubstituted [Re(η^6-C_6H_5OH)(η^6-C_6H_5Br)]$^+$ (m/z = 437.1 [M]$^+$) whereas the second has a retention time of 2.6 min and corresponds presumably to the desired [Re(η^5-C_5H_4CHO)(η^6-C_6H_5Br)] (m/z = 437.1 [M-H]$^+$). Due to the ring contraction, the molecule is neutral, which is consistent with the longer retention time found in the chromatogram. [Re(η^5-C_5H_4CHO)(η^6-C_6H_5Br)] was not isolated or investigated but it might be an interesting molecule for further functionalization reaction at the arene ring.

The synthesis of the mixed Re(η^5-C_5H_5)(η^6-C_6H_6)] is rarely reported and functionalization of this complex type are even less represented in the literature. Fischer *et al.* described the only [Re(η^5-$C_5H_{(5-n)}R_n$)(η^6-$C_6H_{(6-m)}R_m$)] (n,m = 0-1; n≠m; R =-$COCH_3$) derivative in 1968. They were able to isolate Re(η^6-C_5H_5)(η^6-$C_6H_5COCH_3$)] (16%) and Re(η^6-$C_5H_4COCH_3$)(η^6-C_6H_5)] (18%), respectively, by reacting Re(η^6-C_5H_5)(η^6-C_6H_6)] with CH_3COCl and $AlBr_3$ under Friedel-Crafts acetylation condition.[98] However, the direct introduction of the aldehyde group by ring contraction developed in this thesis allows facile access to further derivatisation. As an addition to the previous manuscript, functionalization on the Cp-aldehyde moiety of **3** will be described in the following paragraph.

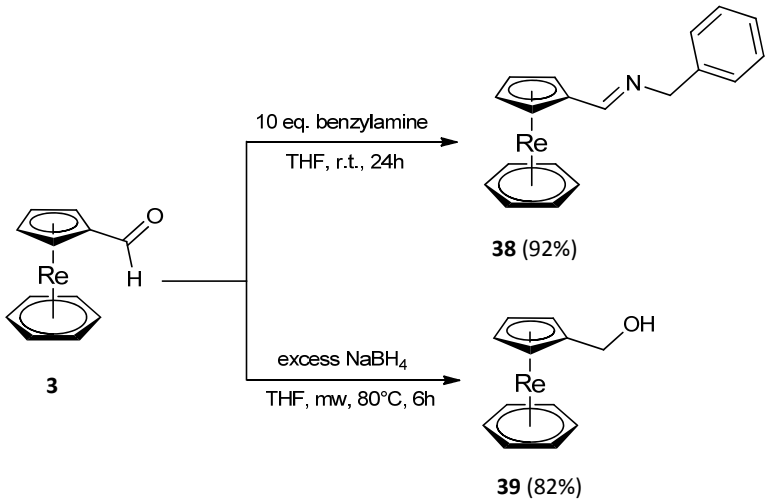

Scheme 7: Synthesis of (**38**) and (**39**) starting from Re(η^5-C_5H_4CHO)(η^6-C_6H_6)] (**3**)

As shown in Scheme 7, [Re(η^5-C_5H_4CHO)(η^6-C_6H_6)] (**3**) was reacted with benzylamine to the corresponding imine [Re(η^5-$C_5H_4CHNCH_2C_6H_5$)(η^6-C_6H_6)] (**38**) (92% yield). Further, reducing the aldehyde group with an excess of $NaBH_4$ leads to the formation of the corresponding primary alcohol [Re(η^5-$C_5H_4CH_2OH$)(η^6-C_6H_6)] (**39**). The latter complex has been obtained in good yield of 82%. The reaction of **38** was performed in THF and in the presence of 10 equivalent of benzylamine. After stirring the reaction for 24 hours, a colour change of the reaction mixtures from orange to yellow was observed. Furthermore, UPLC-MS measurements revealed almost quantitative conversion from the educt to the desired product with the corresponding m/z = 448.4 $[M-H]^+$. **38** is soluble in methanol, acetonitrile and diethyl ether but insoluble in water. The crude product was washed several times with degassed water and cold pentane to separate the unreacted benzylamine. Finally, it was recrystallized from a THF solution. In the ^1H NMR spectrum of **38**, the characteristic signals of the α-*H* as well as the β-*H* of the Cp-ring were found at 5.49 ppm and 5.15 ppm, which are comparable chemical shifts as in compound **3**. In contrast to compound **3**, the protons of the coordinated benzene are shifted more to higher field and are at 4.69 ppm. Compound **38** is oxygen sensitive and therefore crystallisation was performed under an inert atmosphere. By slow

evaporation of a THF solution of **38**, single crystals suitable for X-ray diffraction analysis were obtained. The crystal structure is shown in Figure 35. The compound crystallises as yellow plates in the triclinic space group P-1, including one molecule in the asymmetric unit.

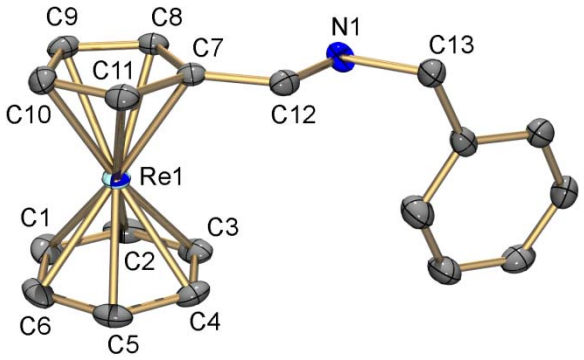

Figure 35: ORTEP representation[108] of [Re(η^5-$C_5H_4CHNCH_2C_6H_5$)(η^6-C_6H_6)] (**38**). Hydrogen atoms are omitted for clarity, thermal ellipsoids represent 50% probability. Selected bond lengths [Å] for **38**: Re1-Cp-$CHNCH_2C_6H_5$ (centroid) 1.886(2), Re1-C_6H_6 (centroid) 1.699(2), C12-N1 1.292(7).

The Re1-Cp-carbon bond lengths in **38** are in the range of 2.231(5) – 2.264(5) Å whereas the distance between rhenium and the aromatic carbon are shorter and were to be found in the range of 2.195(6) – 2.219(6) Å. These bond lengths are comparable with compound **3**.

[Re(η^5-$C_5H_4CH_2OH$)(η^6-C_6H_6)] (**39**) has been synthesised by reduction of **3** with $NaBH_4$. The synthesis was performed in a microwave reactor at 60°C for 6 h. During the reaction, the colour of the solution turned from orange to almost colourless. After quenching with degassed water and extraction with Et_2O, the product was obtained in high purity and in good yield (82%). The ^{1}H NMR spectrum shows the shifts of the α-*H* (5.15 ppm)/β-*H* (4.97 ppm) protons of the Cp-ring to higher field compared to the imine derivative **38**. This reflects the weaker deshielding effect of the OH-group. In contrast, the chemical shift of the protons of the coordinated benzene is within the same range as in **38** (4.66 ppm). Due to the oxygen sensitivity of the compound, single crystals suitable for X-ray diffraction analysis were obtained in an inert atmosphere by slow evaporation of an Et_2O solution of **39**. The complex **39** crystallizes as light yellow needles in the monoclinic space group I2/a (Figure 36). The asymmetric unit of **39** contains 3 molecules which are connected over hydrogen bonds. The bond lengths of the Re1 atom to the carbon atoms of the Cp ligand are between 2.2356 (7) – 2.251(7) Å which are comparable bond lengths as in complexes **3** and **38**. Also here, the distances between rhenium atom and the aromatic carbon atoms are shorter and were found in the same range (2.196(7) – 2.214(7) Å) and in a comparable length to similar complexes **3** and **38**.

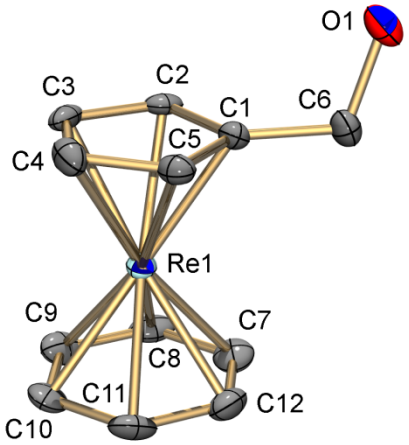

Figure 36: ORTEP representation[108] of [Re(η^5-$C_5H_4CH_2OH$)(η^6-C_6H_6)] (**39**). Hydrogen atoms are omitted for clarity, thermal ellipsoids represent 50% probability. Selected bond lengths [Å] for **39**: Re1-Cp-CH_2OH (centroid) 1.885(3)-1.892(2), Re1-C_6H_6 (centroid) 1.694(3)-1.702(2), C6-O1 1.439(8).

UPLC-MS measurement of **39** revealed an unexpected peak with the corresponding mass of m/z = 343.1 $[M]^+$ instead of the expected mass of m/z = 361.1 $[M\text{-}H]^+$. The different correspond presumably to a water molecule. Since the conditions of the UPLC-measurement are acidic, protonation of the OH-group followed by elimination of water could be reasonable. Such reactions were described with the ruthenocene analogue [Ru(η^5-$C_5H_4CH_2OH$)(η^5-C_5H_5)] in which after protonation and elimination of a water molecule, a fulvene-type complex was formed.[161] The elimination of water implies a positive charge on the complex. This fact is consistent with the observed retention time (0.6 min) which is more in the range of cationic species [Re(η^6-C_6H_6)$_2$]$^+$ = 0.5 min as in the range of neutral derivative [Re(η^5-C_5H_4CHO)(η^6-C_6H_6)] = 2.2 min. This observation could be an indication for a new synthetic pathway for the synthesis of new rhenium compounds.

Rhenium complexes bearing a pentafulvene moiety as ligands are poorly described in the literature. In contrast to iron or ruthenium, which are easily accessible and widely used.[161] Most of the reported rhenium complexes are coordinated to a fully methylated fulvene which can be synthesised either by photolysis of [(Cp*)Re(CO)$_3$] or by co-condensation reactions.[162, 163] Besides DFT calculations which are published in 2009, complexes with the compositions [Re(η^5:η^1-$C_5H_4CH_2$)(η^6-C_6H_6)]$^+$ or [Re(η^5:η^1-$C_5H_4CH_2$)(η^5-C_5H_5)] are not reported so far.[164] Using an adapted procedure which was applied for a ruthenium analogue, **39** were treated with trimethylsilyl trifluoro-methanesulfonate or with an aqueous solution of HPF_6 to generate [Re(η^5:η^1-$C_5H_4CH_2$)(η^6-C_6H_6)]$^+$ [**40**]$^+$ (Scheme 8).

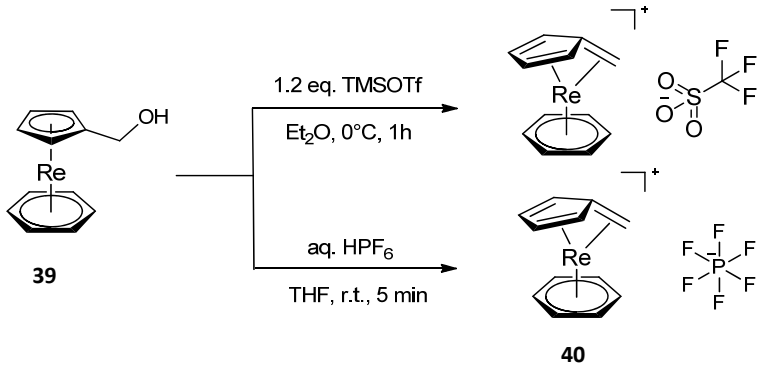

Scheme 8: Synthesis of [**40**](OTf) and [**40**](PF_6) starting from Re(η^5-C_5H_4CHO)(η^6-C_6H_6)] (**39**)

[**40**](OTF) was precipitated as a yellow powder by the addition of trimethylsilyl trifluoromethanesulfonate to an ether solution of **39**. After separation, [**40**](OTF) was obtained in high purity and in good yields of 86%. The hexafluorophosphate analogue [**40**](PF_6) was synthesised by adding an aqueous HPF_6 (65%) solution to a THF solution of **39**. By further addition of water, [**40**](PF_6) precipitated in high purity with a yield of 81%. The complex is stable towards water and oxygen which is a desired property for application in bioinorganic chemistry. The observed stability of [**40**]$^+$ is in contrast to the stability related complexes such as [Mo(η^5:η^1-$C_5C_4(CH_3)_2$)(η^6-C_6H_5)] or [M(η^5:η^1-$C_5H_4CH_2$)(η^6-C_5H_5)]$^+$ (M = Ru, Fe) which are oxygen sensitive and decompose or dimerise.[161, 165-167] The binding mode of the fulvene ligand to a metal can vary between a (η^2:η^2:η^2) coordination as found in tricarbonyl-6,6'-dimethylfulvene chromium(0) complex or a (η^5:η^1) coordination which have been observed for early transition metals complexes.[168] In the ^{1}H NMR spectrum of [**40**]$^+$ measured in CD_3CN, the protons of the cyclopentadienyl ligand (fulvene) were found at 6.01 ppm and 5.41 ppm and lie in the same range compared to similar complexes such as [Ru(η^5:η^1-$C_5H_4CH_2$)(η^5-C_5H_5)]$^+$ (6.11 ppm, 5.14 ppm; CD_2Cl_2).[161] In contrast to the aromatic protons of the coordinate benzene, which were observed at 5.47 ppm and lie between the isomeric cationic species [Re(η^6-C_6H_6)$_2$]$^+$ (6.16 ppm; $(CD_3)_2CO$) and the neutral complex Re(η^5-C_5H_4CHO)(η^6-C_6H_6)] (**3**) (4.88 ppm; CD_3CN), respectively. This suggests that the fulvene ligand is a stronger π-donor compared to the arene but weaker with respect to a coordinated Cp ligand. Unexpectedly, the protons of the exocyclic methylene group showed a significantly strong shift towards high field (3.95 ppm). The only comparable complex with a similar shift is [Cr(fulvene)$(CO)_3$] (3.97 ppm; $CDCl_3$), whereas all other unsubstituted coordinated pentafulvene ligand reported in the literature, as well as the free pentafulvene, were found at lower field (Table 19).[169]

Previous DFT calculations predict an increase of the metal-fulvene interaction going from the lighter to the heavier metals. Due to the bending effect of the pentafulvene ligand, the HOMO orbital can be

more stabilised.[170] Since [**40**]$^+$ is the only known heavy metal compound so far, the strong interaction between the electropositive polarized exo-CH_2 and the metal centre (due to back donation) might be the reason for the strong shift of exocyclic protons as well as the high stability of the compound toward decomposition or dimerisation.

Table 19: Comparison of the ^{1}H NMR shifts (exocyclic-CH_2 protons) and stabilities properties between the corresponding free and coordinated pentafulvene ligand at different metal centres.

Compounds	^{1}H NMR exocyclic -CH_2 protons	stability
Pentafulvene (free ligand)	5.89 ppm ($CDCl_3$)[171]	- polymerized
[Fe(fulvene)(Cp)]$^+$	6.00 ppm ($CDCl_3$; -30°C)[172]	- sensitive to moisture - slowly dimerization
[Ru(fulvene)(Cp)]$^+$	5.07 ppm (CD_2Cl_2)[161]	- stable under nitrogen - decompose under oxygen
[Cr(fulvene)($CO)_3$]	3.97 ppm ($CDCl_3$)[169]	- pyrophore crystals - slow decomposition at r.t. over days
[Re(fulvene)(benzene)]$^+$	3.95 ppm (CD_3CN)	- highly stable

To get insights into the electrochemistry and chemical stability of the complex, cyclic voltammetry (CV) measurements were performed. CV's were measured *vs*. an Ag/AgCl reference electrode using a 0.1 M solution of TBA(PF_6) in MeCN as electrolyte. The spectra were referenced *vs*. Fc/Fc$^+$ at 0.45 V. The cyclo voltammogram revealed irreversible oxidation at 1.44 V which is shifted around 0.11 V anodically compared to the rhenium bis-benzene isomer [Re(η^6-$C_6H_6)_2$]$^+$. This fact suggests that the pentfulvene ligand is a weaker π-donor compared to the benzene ligand. The oxidation itself could not be assigned, with the available date, to a ligand or metal-based process. However, it reflects the high stability of the compound. On the other side, the reduction potential of [**40**]$^+$ was found at -1.41 V which display an irreversible process and lies in the same range compared to the ruthenium species [Ru(η^5:η^1-$C_5H_4CH_2$)(η^5-C_5H_5)]$^+$ (1.45V). Chemically reduction of [Ru(η^5:η^1-$C_5H_4CH_2$)(η^5-C_5H_5)]$^+$ with sodium amalgam in THF afforded a dimeric species [(η^5-C_5H_5)]$^+$Ru(η^5-$C_5H_4CH_2CH_2C_5H_4$-η^5)Ru(η^5-C_5H_5)]$^+$ which it is attributed to ligand-based reduction.[161] This fact could be also assumed for the reduction of [**40**]$^+$ since the reduction potential of both species were almost equal.

Single crystals of [**40**](PF_6) were obtained by slow evaporation from an acetonitrile solution and characterized by X-ray diffraction analysis. [**40**](PF_6) crystallizes as yellow needles in the orthorhombic space group Pnma. The asymmetric unit includes two independent half Re molecules and one PF_6^- counterion. Additionally, one of the half Re molecules is highly disordered. The following discussion focuses only on the non-disordered molecule in the asymmetric unit. However, the described structural features are in both molecules similar. The coordinated fulvene ligand itself

is bent with the corresponding angle of 40.3° which is smaller compared to the ruthenium-Cp species (42.6°).[161] The Re-$CH_{2(exo)}$ and C7-C8 bond lengths were found to be 2.267(9) Å and 1.351(11) Å, respectively, and are slightly shorter with respect to DFT calculations (2.32 Å and 1.42 Å).[170] The bent fulvene ligand entailed that the two rings are nonparallel and this effected a tilt angle of 9.1°. Furthermore, the Re-C_{arom} bond lengths lie in the range of 2.217(5) – 2.267(8) Å while the Re-$C_{fulvene}$ bond lengths lie between 2.105(7) – 2.281(6) Å, respectively.

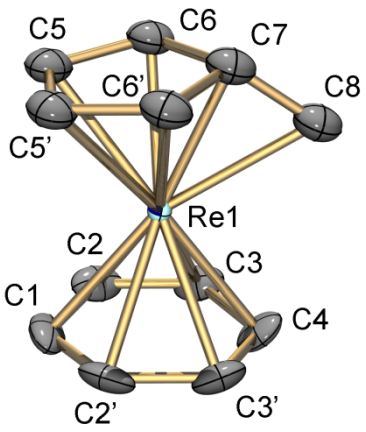

Figure 37: ORTEP representation[108] of [Re(η^5:η^1-$C_5H_4CH_2$)(η^6-C_6H_6)](PF_6) ([**40**](PF_6)). Hydrogen atoms and anions are omitted for clarity, thermal ellipsoids represent 50% probability. Selected bond lengths [Å] for [**40**]$^+$: Re1-C8 2.267(9) and Re1-C_6H_6 (centroid) 1.740(3).

Until today, biological studies with the neutral [Re(η^5-Cp)(η^6-benzene)] scaffold in biologically active molecule such peptides or proteins were not possible due to the lack of practical or accessible synthetic pathways. One of the goals of this thesis is to synthesise and studies the properties of functionalized [Re(η^5-Cp)(η^6-benzene)] moieties. For this project, the fulvene ligand was an interesting precursor. The reactivity of coordinated methylated fulvene to rhenium (or ruthenium) towards nucleophilic attack of the exo CH_2 group with e.g. amine, methoxide, hydroxide, phosphines or Grignard reagent is already reported.[173, 174] After the addition of a nucleophile to the fulvene moieties, a functionalized coordinated Cp-ligand can be formed. Another outstanding feature of [**40**](OTf) is its solubility and stability in water, which allows coupling to peptides or proteins. In a first attempt, the reactivity of [**40**](OTf) was investigated in acetonitrile by the addition of $NaBH_4$. The nucleophilic attack of the hydride afforded the methylated derivative [Re(η^5-CpMe)(η^6-benzene)] (**41**) in a quantitative amount after stirring for 20 min at room temperature. **41** was isolated from the crude by washing several times with Et_2O in 71% yields. Compound **41** was fully characterised including the determination of the crystal structure by X-ray diffraction. The ^{1}H NMR spectra show the characteristic Cp protons at 5.07 ppm (α-*H*) and 4.91 (β-*H*) which are shifted more to high field

compared to compound **39** due to the electron donating properties of the methyl group. While the methyl protons and aromatic protons were found at 4.58 ppm and 2.02 ppm, respectively. Due to the oxygen sensitivity of **41**, single crystals suitable for X-ray analysis were obtained by slow evaporation from a diethyl ether solution of **41** stored in a glove box. **41** crystallize as yellow needles in the monoclinic space group $P2_1/c$ (Figure 38). The structure contains one molecule in the asymmetric unit. The Re-benzene bond lengths are between 2.195(4) Å and 2.206(4) Å while the Re-Cp bond lengths are significantly longer and are found between 2.234(4) Å and 2.253(3) Å. The obtained values are in the same range compared to similar structures (**3**, **38** and **39**).

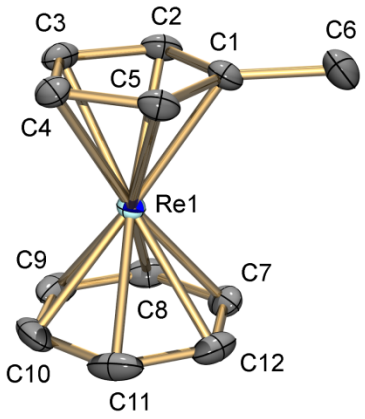

Figure 38: ORTEP representation[108] of [Re(η^5-$C_5H_4CH_3$)(η^6-C_6H_6)] (**41**). Hydrogen atoms are omitted for clarity, thermal ellipsoids represent 50% probability. Selected bond lengths [Å] for **41**: Re1-CpMe (centroid) 1.8855(18), Re1-C_6H_6 (centroid) 1.689(2), C1-C6 1.500(6)

In a second attempt, the reactivity of [**40**](OTf) was explored in water and therefore two water-soluble nucleophiles such as tris(2-carboxyethyl)phosphine (TCEP) and 2-mercaptoethanol were used. The reaction with (tris(2-carboxyethyl)phosphine) was performed only in a preliminary extent in degassed water at pH 8. After the addition of TCEP to a solution of [**40**](OTf), the positively charged product (acidification during UPLC measurement) [Re(η^5-Cp-CH_2-P(CH_2CH_2COOH)$_3$)(η^6-benzene)]$^+$ was formed after stirring the reaction for 10 min at room temperature. UPLC-MS measurement confirmed the product formation in quantitative amount with the corresponding m/z = 593.1 $[M]^+$. The second reaction with 2-mercaptoethanol was conducted in a degassed water solution of [**40**](OTf) at room temperature (at pH 7.5). The corresponding thioether product [Re(η^6-$C_5H_4CH_2S(CH_2)_2OH$)(η^6-C_6H_6)] (**42**) was precipitated after the addition of 2-mercaptoethanol in quantitative amount. Purification of **42** was carried out by washing several times with degassed water which gave **42** in high purity and 90% yield. Furthermore, it reacts selectively and very rapidly with thiols. However, other nucleophilic groups do not react with this group at neutral pH. This means that the complex can be introduced to essentially any biomolecule without the need of the previous derivatization. The ^{1}H NMR spectra of **42** revealed two singlets at 5.17 ppm and 4.97 ppm

which correspond to the Cp protons while the arene protons were found at higher field at 4.64 ppm. The triplet at 3.68 ppm was assigned to the proton of the hydroxide group and confirmed that the deprotonated thiol is in involved as expected in the reaction. Single crystals of **42** suitable for X-ray diffraction were grown by slow evaporation from a diethyl ether solution. **42** crystallizes as light yellow needles in the tetragonal space group $P4_2$ (Figure 39). The structure contains two molecules in the asymmetric unit. The Re-benzene bond lengths are between 2.197(9) Å and 2.220(8) Å while the Re-Cp bond lengths are significantly longer and are found between 2.241(9) Å and 2.253(8) Å. The obtained values are in the same range compared to similar structures.

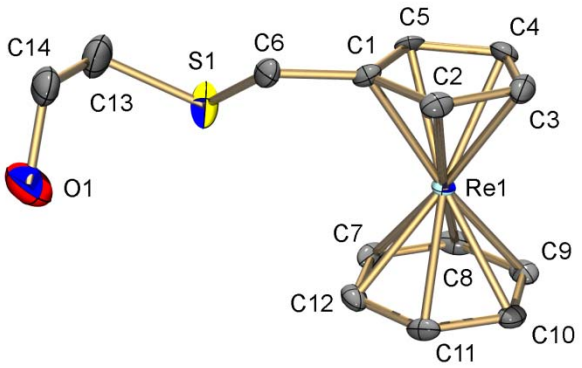

Figure 39: ORTEP representation[108] of [Re(η^6-$C_5H_4CH_2S(CH_2)_2OH$)(η^6-C_6H_6)] [**42**]. Hydrogen atoms are omitted for clarity, thermal ellipsoids represent 50% probability. Selected bond lengths [Å] for **42**: Re1-Cp-$S(CH_2)_2OH$ (centroid) 1.890(4), Re1-C_6H_6 (centroid) 1.702(4).

It is to emphasize that the fulvene complex is also an excellent opportunity for proteomics since the cysteines in proteins are the exclusive target. The resulting thioether complex might, in addition, exert some metal-centred reactivity, due to the high electron density at the metal centre. This can induce some subsequent biological reactions and will be studied in detail, in the near future.

Besides the fulvene complex, which has remarkable potential in the field of biochemistry, rhenium and technetium mono-arene complexes are in the scope of the described research as new building blocks for bioinorganic applications. Analogues compounds containing ruthenium are well known and well-studied in different cancer cell lines and some of them showed excellent cytotoxicity values.[175] In contrast to the ruthenium chemistry, the accessibility of such compounds with rhenium or technetium is more difficult. Therefore, a synthetic strategy was developed, starting from [Re(η^6-naphthalene)$_2$]$^+$ [**7p**]$^+$ or [Re(η^6-naphthalene)(η^6-benzene)]$^+$ [**6p**]$^+$. Upon light irradiation or thermally treatment, one or both of the naphthalene ligands were susceptible for substitution by mono- or multidentate ligands due to their weaker donors and acceptors properties. This is in analogy to the

reactivity found for the $[M(OH_2)_3(CO)_3]^+$ (M = Re, $^{99(m)}$Tc) complexes, where the three H_2O ligands are fast substituted, whereas the three CO's remain untouched. Conceptually advancing the field of carbonyl chemistry, the $[Tc/Re(\eta^6\text{-}C_6H_6]^+$ moiety can be considered as an isoelectronic $[Tc/Re(CO)_3]^+$ analogue. The synthesis procedures, as well as the reactivity of these complexes, are discussed in the following manuscript. Some further investigation and findings were described in the section unpublished results after the manuscript.

6.7 Publication: Structure and Reactivities of Rhenium and Technetium Bis-Arene Sandwich Complexes $[M(\eta^6\text{-arene})_2]^+$

Structure and Reactivities of Rhenium and Technetium bis-Arene Sandwich Complexes $[M(\eta^6\text{-arene})_2]^+$

Giuseppe Meola, Henrik Braband, Sara Jordi, Thomas Fox, Olivier Blacque, Bernhard Spingler and Roger Alberto*

University of Zurich, Department of Chemistry, Winterthurerstr. 190, CH-8057 Zurich Switzerland

Abstract: Sandwich complexes are important building blocks in medicinal inorganic chemistry for group 6 and 8 elements but are almost unknown for the manganese triad. We present the syntheses and full characterizations of the mixed-arene ^{99}Tc sandwich complexes $[^{99}Tc(\eta^6\text{-hmbz})(\eta^6\text{-}C_6H_5\text{-}NH_3)](PF_6)_2$ and $[^{99}Tc(\eta^6\text{-hmbz})(\eta^6\text{-}C_6H_5\text{-Br})](PF_6)$. Both comprise functionalities for conjugation to targeting molecules or for being included as substructures in pharmaceutically active lead compounds. Since η^6-benzene ligands are too stably bound to be replaced by incoming ligands, we prepared the naphthalene complexes $[Re(\eta^6\text{-}C_6H_6)(\eta^6\text{-napht})]^+$ and $[Re(\eta^6\text{-napht})_2]^+$. Their reactivities towards substitution are increased and one or both naphthalene ligands can be replaced by mono- or multi-dentate ligands. Combining the features of ^{99}Tc and Re may lead to a molecule-based theranostic approach.

Introduction: Novel metal complexes for routine therapy, impacting health care to a "cisplatin-like" level, did not yet complement this pioneering inorganic medicinal drug to a comparable extent.[1-3] A number of metallodrugs for cancer therapy were subjected to preclinical trials or entered clinical trial phases but a breakthrough has not yet been accomplished, despite intense research efforts going on worldwide.[4-11] The lack of acceptance of metallodrugs by the pharmaceutical industry may be one of the reasons, another one the relatively small number of (core) structures with known reactivities such as the aforementioned cisplatin complex and its successors oxaliplatin, carboplatin or satraplatin. Meggers *et al.* pointed out, that the three-dimensionality of octahedral complexes together with their space-filling ability would lead to an enormous structural diversity, greatly boosting the field of medicinal inorganic drugs.[12-15] However, just the synthetic approach to such a structural realm would be truly challenging. The validity of the concept has been shown impressively by the same group. One of the particularities of medicinal inorganic compounds is metal-centred reactivities. These may lead to a specific biological action such as DNA cross-linking. Unpredictable decomposition and side reactions in the system affect acceptance by the authorities and pharmaceutical companies though. These "side reactions" are much better under control for organic drugs. In addition, whereas organic compounds have an essentially unlimited structural diversity, inorganic or organometallic compounds are concentrated on a few essential core structures for

reactivity (or inertness) reasons. The advantage of metal-centred reactivity may turn into a disadvantage if it is not exclusively exerted at the targeted site. The 3D space occupation concept in which the metal complex serves as an integral, structure determining portion, directing selectivity as well as activity leads e.g. to inhibitors with structure rather than metal-based reactivities.[13, 16-18] There are many very promising examples in literature, ferrocifen and ferroquine being probably the most prominent ones.[19-23] Ferrocene (Fc) has been successfully integrated in many more pharmaceutically active structures.[24-26] Its mode of action may be structure related or combined with redox chemistry in the presence of oxygen.[27] Beside Fc, group 4 metallocenes played an essential role in bioorganometallic chemistry although their unpredictable *in vivo* behaviour affected a practical therapeutic role. Beside the cyclopentadienyl ligand as a structure determining feature, arene rings are key motifs in numerous complexes of the $\{(\eta^6\text{-arene})Ru^{II}\}^{2+}$ type as reported by the groups of Sadler and Dyson with great success.[28-32] In addition, Ag^+ and Au^+ carbene complexes are currently studied due to their anti-cancer activities.[33]

Contrasting medicinal inorganic drugs for therapy, molecular imaging with radionuclides requires innocent complexes; metal-based reactivity is not desired.[34-36] Targeting compounds labelled with e.g. ^{99m}Tc must behave exactly as if labelled with innocent main group radionuclides such as ^{18}F or ^{11}C. Complexes based on the $\{^{99m}Tc(CO)_3\}^+$ are innocent due to their kinetic stability but are much larger than ^{18}F or ^{11}C.[37-39] The remaining coordination sites are occupied by e.g. a targeting molecule conjugated to tridentate ligands.[40-45] The Santos group reported numerous representative examples e.g. with tridentate borohydride complexes exhibiting agostic $^{99(m)}$Tc-H interactions, stable under physiological conditions.[40] In contrast to most therapeutically active elements, the pure diagnostic features of ^{99m}Tc bioconjugates can principally be combined with the radiotherapeutic properties of their $^{186/188}$Re homologues. Complexes in the oxidation state "+I" of the two elements are isostructural and physiologically robust. This so-called "matched-pair" paradigm is a unique feature, leading to a molecule-based, theranostic platform with $^{186/188}$Re alone (γ-emission for diagnosis, hard β^- emission for therapy) or in combination with ^{99m}Tc homologues (Scheme 1a).[46] As we showed in collaboration with the Santos group, the emission of Auger electrons by ^{99m}Tc can induce radiotoxicity if the compound is delivered into the cell nucleus (Scheme 1b).[47-52] A further and so far little explored theranostic approach consists in the combination of a ^{99m}Tc-based biomimetic with its organometallic but non-radioactive rhenium homologue (Scheme 1c). In its essence, the rhenium complex should be therapeutically active through its structure while the ^{99m}Tc homologue allows for visualizing the pharmacology. The cytotoxicity of rhenium-based medicinal inorganic drugs has not sufficiently been exploited as recently pointed out by Gasser et al. but there are many promising options.[3, 53] Structure-based toxicity by receptor inhibition of cold rhenium complexes matches perfectly the imaging concept with ^{99m}Tc. This metal complex-based theranostic option is probably

unique amongst transition elements but provides metallodrugs a clear asset over purely organic pharmaceuticals. The different concepts are shown in Scheme 1.

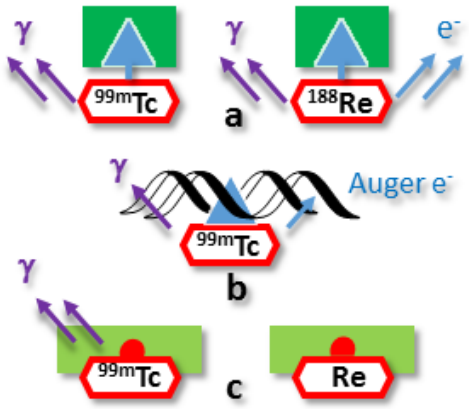

Scheme 1: Concepts of molecule-based theranostics: *a)* receptor targeting homologous ^{99m}Tc (imaging) and $^{186/188}$Re complexes (radiotherapy and optionally imaging), *b)* ^{99m}Tc γ-emission for imaging and Auger electrons for therapy, DNA intercalation required and *c)* ^{99m}Tc inhibitor for imaging and macroscopic amounts of cold, homologue rhenium complex for therapy.

The combination of a diagnostic ^{99m}Tc with a therapeutic Re compound has though its constraints. Whereas the preparation of the rhenium compound has no experimental limits, the homologous ^{99m}Tc complex must be synthesized from water and on site. We exemplified this strategy with carbonic anhydrase inhibitors based on cyclopentadienyl complexes of ^{99m}Tc and for doxorubicin with various chelators.[54, 55] For these examples, all constraints were fulfilled and a matched-pair pharmaceutical was developed.

In order to extend convenient building blocks for theranostic concepts for group 7 elements, we recently introduced $[(\eta^6\text{-}C_6H_5R)_2M]^+$ bis-arene type complexes of Re^I and $^{99(m)}Tc^I$.[56] Arene complexes, as structural subunits of organic lead structures, showed their versatility already for $[(\eta^6\text{-}C_6H_5R)Cr(CO)_3]$.[57] The mono-cationic sandwich complexes of group 7 elements are of high thermodynamic stabilities. Therefore, they are perfectly suited for incorporation into organic lead structures. They can be combined with targeting functions by direct conjugation at the arene rings or by direct reaction with corresponding arene ligand systems.[58] Although intriguing by its principal structural flexibility, replacing one or both of the arene systems by further incoming ligands would substantially extend the potential of this core. We report here a fundamental, synthetic study of the preparation of functionalized bis-arene complexes with ^{99}Tc and ligand substitution reactions with mixed benzene-naphthalene sandwiches of Re. This study enables the preparation of homologues complexes of the two elements, ultimately for theranostic strategy c) outlined in scheme 1.

Results and Discussion

$[^{99}Tc(arene)_2]^+$ complexes were originally prepared by Fischer *et al.*[321] Kudinov et al. reported recently an improved preparation of the rhenium homologues.[60] Whereas bis-arene chemistry of all neighbouring elements is very well developed, only few examples of group 7 elements are known.[61] Direct reactions with functionalized arenes are, to our knowledge, essentially inexistent. For the purpose of diversity, approaches to mixed-ligand arene complexes $[M(\eta^6\text{-}C_6R_6)(L^3)]$ with L^3 being one or more ligand(s) of appropriate denticities is important. Ligand(s) L^3 can serve as potential anchoring groups or for tuning the pharmacological properties. With the scope of transformation to ^{99m}Tc chemistry, an aqueous reaction was desirable. As reported by us, the basic complexes $[M(\eta^6\text{-}C_6R_6)_2]^+$ are extremely stable and the substitution of a benzene ring by any incoming ligand was not possible so far.[56] The coordinated aromatic rings can, however, be functionalized with halides or carboxylato groups.[58] Post-synthetic modifications of a ^{99m}Tc complex are though less favoured for routine applications in nuclear medicine. Therefore, we focused at the development of procedures for the direct synthesis of functionalized $^{99(m)}Tc$ bis-arene complexes (scheme 2).

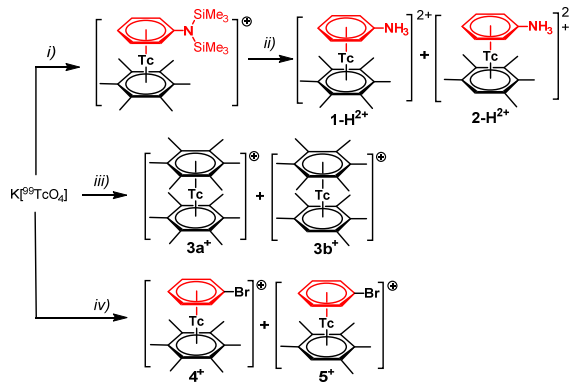

Scheme 2: Reaction conditions to bis-hexamethyl-benzene and mixed-arene sandwich complexes of $^{99}Tc^{I}$: *i*) 50 eq $C_6(CH_3)_6$ (hmbz), 30 eq $AlCl_3$, 3 eq Zn, 20 eq. $C_6H_5N(SiMe_3)_2$, cyclohexane, 80°C, 4 h; *ii*) H_2O, conc. HCl, 23 h room temperature, NH_4PF_6; *iii*) +20 eq hmbz, 30 eq $AlCl_3$, cyclohexane, 80°C, 4 h, H_2O, NH_4PF_6; *iv*) 10 eq hmbz, 30 eq $AlCl_3$, bromo-benzene, 80°C, 4 h, H_2O, NH_4PF_6.

The direct introduction of C_6H_5-R type ligands in the reaction from $[MO_4]^-$ (M = $^{99(m)}Tc$, Re) is limited by cross-reactivities with $AlCl_3$, present in the synthesis. Groups such as $-OCH_3$ and other oxygen containing functionalities are incompatible and lead in general to undefined products. Amino groups, frequent functionalities in pharmaceuticals, cross react depending on the number and nature of substituents on the amino group. Since amino-benzenes (aniline) are interesting subunits, $[^{99}TcO_4]^-$ was reacted with silyl-protected aniline $C_6H_5N(SiMe_3)_2$ in the presence of $AlCl_3$. For this synthesis

hexamethyl-benzene (hmbz) had to be used as "auxiliary" ligand, because the reaction of C_6H_5-$N(SiMe_3)_2$ alone with $[^{99}TcO_4]^-$ and $AlCl_3$ did not lead to the desired bis-functionalized ^{99}Tc complex. By the addition of 1.5 *eq*. hmbz, relative to C_6H_5-$N(SiMe_3)_2$, to the reaction mixture, the mixed ^{99}Tc bis-arene complex $[^{99}Tc(\eta^6\text{-hmbz})(\eta^6\text{-}C_6H_5\text{-}N(SiMe_3)_2)](PF_6)_2$ was synthesized. The raw product (60%) was separated and the silyl protecting groups removed by $HCl_{(aq)}$ to obtain $[^{99}Tc(\eta^6\text{-hmbz})(\eta^6\text{-}C_6H_5\text{-}NH_3)](PF_6)_2$ ([**1-H**]$(PF_6)_2$) in moderate yields after purification. Single crystals of the deprotonated complex [**1**](PF_6) were obtained by slow vapour diffusion of Et_2O into a solution of [**1**-H]$(PF_6)_2$ in acetone. The structure of [**1**](PF_6) has been elucidated by X-ray diffraction analysis and its ORTEP representation is given in figure 1.

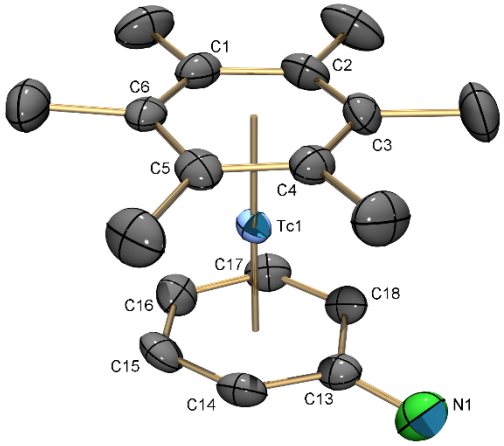

Figure 1: ORTEP representation of the $\mathbf{1}^+$ cation of [**1**](PF_6). Hydrogen atoms and the anion are omitted for clarity. Important bond lengths [Å] are: Tc1-hmbz (centroid) 1.753(6), Tc1-C_6H_5-NH_3 (centroid) 1.739(6). Ellipsoids are drawn on the 50% level.

For this and the subsequent reactions with hmbz, we observed minor side products with consistent shifts in the ^{99}Tc NMR by 40 - 50 ppm relative to the main product (Figure 2). Due to their similar physical properties, they could not be separated. ^{1}H NMR investigations evidenced a similar complex as $[\mathbf{1}\text{-H}]^{2+}$, but with only five methyl groups on the "η^6-hmbz". Thus, the hexamethyl-benzene was demethylated to pentamethyl-benzene (η^6-pmbz) during the reaction and the complex $[^{99}Tc(\eta^6\text{-pmbz})(\eta^6\text{-}C_6H_5\text{-}NH_3)](PF_6)_2$ ([**2**-H]$(PF_6)_2$) formed. Such trans- and demethylation reactions are not uncommon under Fischer-Hafner conditions.[62, 63]

This approach towards mixed-arene ligand sandwich complexes applies to other complexes. Along the same route, $[^{99}Tc(\eta^6\text{-hmbz})_2](PF_6)$ ([**3a**](PF_6)), mono-demethylated $[^{99}Tc(\eta^6\text{-hmbz})(\eta^6\text{-pmbz})](PF_6)$ ([**3b**](PF_6)) as well as the mixed arene complexes complex $[^{99}Tc(\eta^6\text{-hmbz})(\eta^6\text{-}C_6H_6)](PF_6)$ and $[^{99}Tc(\eta^6\text{-}$

pmbz)(η^6-C_6H_6)](PF_6) have been synthesized in yields of 77 and 79% (for the product mixture), respectively. Furthermore, the procedure is suited for the direct synthesis of [^{99}Tc(η^6-hmbz)(η^6-C_6H_5-Br)](PF_6) ([**4**](PF_6)) by using bromo-benzene as solvent. This reaction yielded the desired [^{99}Tc(η^6-hmbz)(η^6-C_6H_5-Br)](PF_6) ([**4**](PF_6)) in yields as high as 80% but gave also [^{99}Tc(η^6-pmbz)(η^6-C_6H_5-Br)](PF_6) ([**5**](PF_6)) as a side product. In contrast to all other presented complexes, $\mathbf{4}^+$ (hmbz) and $\mathbf{5}^+$ (pmbz) could be separated, isolated and characterized. This confirmed the results of NMR studies concerning the nature of the side product. Whereas [**1**-H]$^{2+}$ enables further modifications by peptide bond formation, $\mathbf{4}^+$ allows for nucleophilic aromatic substitutions reactions. The developed synthetic procedure paves therefore the way towards a library of complementary compounds for further systematic studies.

Although the symmetry of the complexes bearing functionalized arenes is broken, the ^{99}Tc NMR spectra of all complexes exhibit sharp lines with small half line widths ($\nu_{1/2}$). The chemical shifts of complexes [**1**-H]$^{2+}$ to $\mathbf{5}^+$ follow the expected trend, the better the donors on the ring, the higher the field at which the ^{99}Tc NMR signals appear, e.g. -1415ppm (40 Hz) for [**1**-H]$^{2+}$, -1461ppm (30 Hz) for [**2**-H]$^{2+}$, -1308ppm (103 Hz) for $\mathbf{3a}^+$, -1346 ppm (83 Hz) for $\mathbf{3b}^+$, -1563ppm (54 Hz) for $\mathbf{4}^+$ and -1603ppm (41 Hz) for $\mathbf{5}^+$ respectively (see ESI for details). A representative ^{99}Tc NMR spectrum of [^{99}Tc(η^6-hmbz)(η^6-C_6H_6)](PF_6) and its demethylated form [^{99}Tc(η^6-pmbz)(η^6-C_6H_6)](PF_6) is shown in Figure 2, displaying the typical $\Delta\delta$ of about 50ppm.

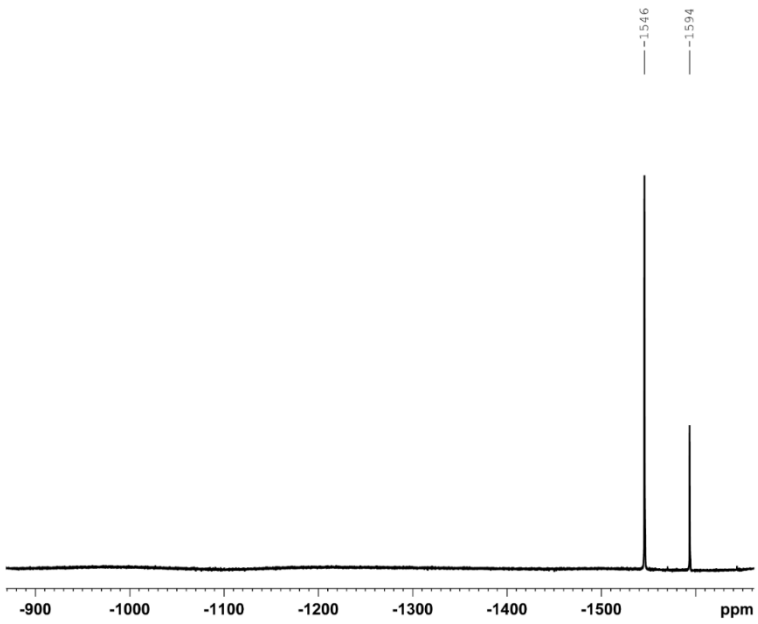

Figure 2: ^{99}Tc NMR of [^{99}Tc(η^6-hmbz)(η^6-C_6H_6)](PF_6) at -1546 ppm and [^{99}Tc(η^6-pmbz)(η^6-C_6H_6)](PF_6) at – 1594 ppm.

All ^{99}Tc complexes are perfectly water - and air stable and do not decompose even at elevated temperature or if exposed to air. These properties are basic for the development of new building

blocks for life science applications. The bromide group on the arene ring is rapidly substituted by a variety of incoming, nucleophilic functions.[58] The resistance of complexes [**1**-H]$^{2+}$ - **5**$^{+}$ against light induced or thermal substitution of one or both arene ligands is remarkable and contrasts the behaviour of the isoelectronic [Ru(η^6-arene)$_2$]$^{2+}$, [Fe(η^6-arene)$_2$]$^{2+}$ or [Ru(η^5-C_5H_5)(η^6-arene)]$^{+}$ congeners.[61, 64-69] In these precursors, benzene, naphthalene or higher aromatic hydrocarbons are replaced by incoming ligands, occasionally bearing a biologically active function.[68,70,71] To enable the concept of structural diversity also with the {Re(η^6-arene)}$^{+}$ fragment, it is thus desirable to replace one or both rings by different C- or heteroatom-type ligands. The chemistry with rhenium presented here also serves as a model for analogous $^{99(m)}$Tc chemistry, which has to follow inevitably. For [Re(η^6-arene)$_2$]$^{+}$ (arene = benzene derived ligands), no substitution occurred even with large amounts of appropriate ligands such as isocyanides and under prolonged heating or microwave conditions. For more extended aromatic hydrocarbons such as naphthalene (napht), the larger π-system leads to a stabilized HOMO and a destabilized LUMO. Consequently, these systems are substantially more weakly bound to a metal centre than benzene (derivatives) and more easily substituted as shown for iron or ruthenium in particular.

To assess the possibility of substituting η^6-hydrocarbons for rhenium and to attain complexes of the type [M(η^6-C_6R_6)(L^3)], starting compounds with one or two naphthalene ligands are required. Kudinov reported the synthesis of [Re(η^6-napht)$_2$]$^{+}$.[56, 60] If standard reaction conditions were applied in the presence of e.g. benzene and naphthalene, the mixed-ligand complex [Re(η^6-C_6H_6)(η^6-napht)]$^{+}$ (**6**$^{+}$) was obtained in moderate yields (22%) together with small amounts of [Re(η^6-napht)$_2$]$^{+}$ (**7**$^{+}$) and [Re(η^6-C_6H_6)$_2$]$^{+}$ (scheme 3). Complex **7**$^{+}$ was obtained when the reaction was performed in the sole presence of naphthalene (see ESI for details).

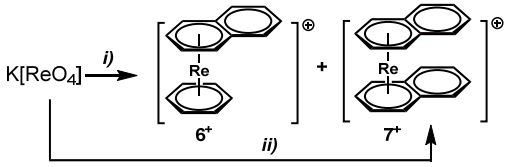

Scheme 3: Synthesis of the naphthalene complexes [Re(η^6-C_6H_6)(η^6-napht)]$^{+}$ (**6**$^{+}$) and [Re(η^6-napht)$_2$]$^{+}$ (**7**$^{+}$); conditions *i*) + 3 eq. Zn, 10 eq., 15 eq. naphthalene, 3.5 ml benzene, 90°C, 18 h; and *ii*) + 3 eq. Zn, 5 eq., 16 eq. naphthalene, 100°C, 18 h.

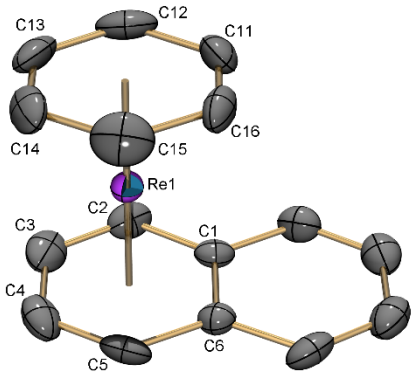

Figure 3: ORTEP representation of the cation of [Re(η^6-C_6H_6)(η^6-napht)](Tf)·Li(Tf) ([**6**]Tf·Li(Tf)). Hydrogen atoms, triflate anions and the lithium cation are omitted for clarity. Important bond lengths [Å] are: Re1-napht (centroid) 1.758(2), Re1- C_6H_6 (centroid) 1.716(2). Ellipsoids are drawn on the 50% level.

The structure of **6**$^+$ could be confirmed by X-ray structure analysis and an ORTEP representation is given in figure 3. In both complexes **6**$^+$ and **7**$^+$, the naphthalene ligands are substantially more weakly bound and prone to light and thermal induced cleavage. After arene loss, they decompose in the absence of potential ligands which could stabilize the Re^I centre. Both complexes are, however, water and air stable in the absence of light. Based on the lability of naphthalene, we reacted both complexes with the tridentate ligands triphos and [HB(pyz)$_3$]$^-$ (Trofimenko ligand) as well as with mono-dentate triethyl-phosphite (tep) and the isocyanide ^{t}BuN≡C (Scheme 4). Although not biological by nature, these ligands should provide a proof of principle for the replacement of η^6-ligands in Re^I complexes. The reaction of **6**$^+$ with the mono-dentate ligands is straightforward, the naphthalene is easily replaced to yield [Re(η^6-C_6H_6)(tep)$_3$]$^+$ (**8**$^+$) and [Re(η^6-C_6H_6)(CN-^{t}Bu)$_3$]$^+$ (**9**$^+$) (Scheme 4).

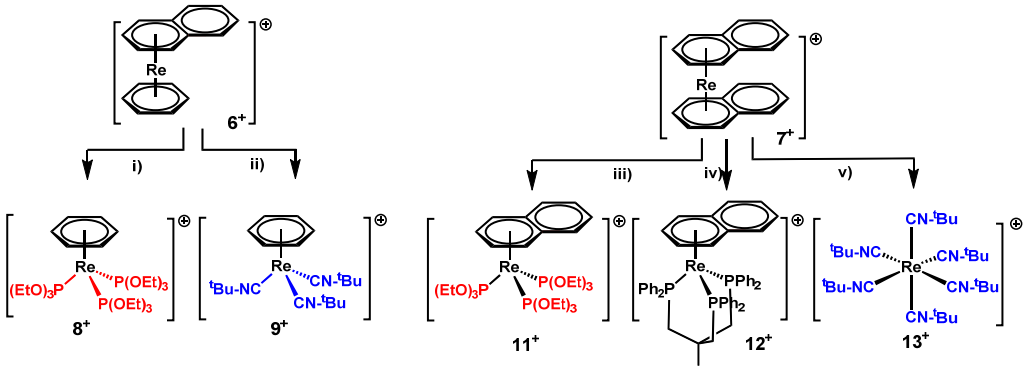

Scheme 4: Replacing naphthalene ligands in [Re(η^6-C_6H_6)(η^6-napht)]$^+$ (**6**$^+$) and [Re(η^6-napht)$_2$]$^+$ (**7**$^+$); conditions i) +20 eq. triethyl-phosphite, acetone, 80°C (microwave), 6h; ii) +10 eq. *tert*-butyl isocyanide, acetone, 80°C (microwave), 9h; iii) +10 eq. triethyl-phosphite, acetone, 100°C

(microwave), 9h; iv) +5 eq. 1,1,1-tris(diphenylphosphinomethyl)ethane, acetone, 100°C (microwave), 9h; and v) + 5 eq. *tert*-butyl isocyanide, acetone; 100°C (microwave), 4h.

The complexes $\mathbf{8}^+$ and $\mathbf{9}^+$ were fully characterized (see ESI), including X-ray diffraction analysis. An ORTEP representation of $\mathbf{9}^+$ is given in figure 4. The i.r. spectra of [**9**](PF_6) exhibits ν_{st} of the isocyanide ligands at 2147, 2107 and 2059cm^{-1}. The single naphthalene ligand in $\mathbf{6}^+$ can thus conveniently be replaced by mono-dentate and, according to thermodynamic principle, also by multi-dentate chelators. This is shown by the substitution of the naphthalene ligand by $[HB(pyz)_3]^-$, yielding [Re(η^6-C_6H_6)($HB(pyz)_3$)] (**10**). In contrast to the other substitution reactions, it was not possible to separate **10** from the excess ligand which was necessary for a complete conversion of the educt. However, X-ray structure analysis of single crystals, obtained by crystallizing a product/ligand mixture, confirmed the formation of **10**.

Reacting $\mathbf{7}^+$ with tep, in analogy to the reaction with $\mathbf{6}^+$, leads straightforward to the naphthalene analogue of $\mathbf{8}^+$, namely to [Re(η^6-napht)$(tep)_3$]$^+$ ($\mathbf{11}^+$). Prolonged heating did not replace the second naphthalene to obtain the homoleptic complex $[Re(tep)_6]^+$. Possibly, harsher conditions are needed for a complete substitution since homoleptic phosphine complexes $[M(PR_3)_6]^+$ are known for both, ^{99}Tc and Re.[72]

The reaction with triphos gave the corresponding complexes [Re(η^6-napht)(triphos)]$^+$ ($\mathbf{12}^+$) in good isolated yield of 56%. The reaction of $\mathbf{6}^+$ with isocyanide ligands stopped after the replacement of the single naphthalene. It was not possible to substitute the benzene ring as well. The situation is different for $\mathbf{7}^+$ as already shown by Kudinov et al.[60] With complex [Re(η^6-napht)(CN-^{t}Bu)$_3$]$^+$ being an intermediate, the reaction goes through to the homoleptic isocyanide complex [Re(CN-^{t}Bu)$_6$]$^+$ ($\mathbf{13}^+$), both naphthalene rings being easily substituted (scheme 4).

The class of homoleptic Re^I and especially $^{99m}Tc^I$ isocyanide complexes are very prominent since the complex [^{99m}Tc(CN-R)$_6$]$^+$ (R = methoxy-isobutyl) is the most important ^{99m}Tc-based myocardial imaging agent, known under the trade name Cardiolite®.[73, 74] Although already reported in the early nineties, structures of $[M(CN\text{-}R)_6]^+$ (M = ^{99}Tc, Re) type complexes have not been elucidated to date. Compound $\mathbf{13}^+$ was crystallized as OTf^- salt from a MeCN solution. An ORTEP representation together with the structures of [**12**](PF_6) and [**9**](PF_6) is shown in Figure 4.

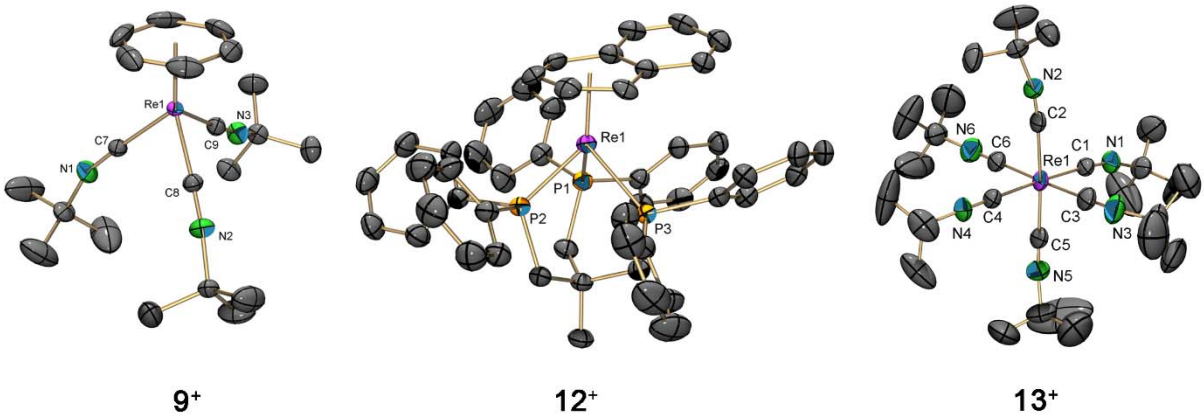

9^{+} **12**$^{+}$ **13**$^{+}$

Figure 4: ORTEP representation of the cations $[Re(\eta^6\text{-}C_6H_6)(CN\text{-}^tBu)_3]^+$ (**9**$^{+}$), $[Re(\eta^6\text{-napht})(triphos)]^+$ (**12**$^{+}$) and $[Re(CN\text{-}^tBu)_6]^+$ (**13**$^{+}$). Hydrogen atoms and anions are omitted for clarity. Important bond lengths [Å] are: **9**$^{+}$) Re1-C_6H_6 (centroid) 1.775(1), Re1-C7 1.979(2), Re1-C8 1.992(2), Re1-C9 1.995(2), C7-N1 1.166(3), C8-N2 1.166(3), C9-N3 1.156(3); **12**$^{+}$) Re1-napth (centroid) 1.830(2), Re1-P1 2.384(2), Re1-P2 2.326(1), Re1-P3 2.357(1); **13**$^{+}$) Re1-C1 2.036(4), Re1-C2 2.046(3), Re1-C3 2.037(4), Re1-C4 2.044(4), Re1-C5 2.018(4), Re1-C6 2.040(4), C1-N1 1.147(5), C2-N2 1.155(4), C3-N3 1.153(5), C4-N4 1.144(4), C5-N5 1.161(5), C6-N6 1.151(5). Ellipsoids are drawn on the 50% level.

Conclusion

Whereas the bioorganometallic chemistry of the $\{Ru(\eta^6\text{-cymene})\}^{2+}$ moiety was and is exploited in great detail, the one of its isoelectronic congener $\{Re(\eta^6\text{-arene})\}^+$ has found little attention. The exploration of its chemistry is lagging behind, likely due to the (in)accessibility to rhenium precursors, paralleling the convenience of $[Ru(\eta^6\text{-arene})_2]^{2+}$ and other arene containing complexes. We have shown in this report that a similar chemistry can be developed, starting from arene sandwich complexes of the type $[Re(\eta^6\text{-napht})_2]^+$ or $[Re(\eta^6\text{-}C_6H_6)(\eta^6\text{-napht})]^+$. Despite the difference to ruthenium in the overall charge, substitution reactions can be performed, thereby replacing one naphthalene ring in the rhenium complexes, comparable to replacing one benzene ring in the ruthenium precursors. If the resulting complexes will exert similar and as favourable cytotoxic properties as the ruthenium counter-parts, remains to be shown. This report contributes to the underlying fundamental chemistry and, conceptually, to the theranostic approach as shown in scheme 1 with ^{99m}Tc for diagnosis and cold Re for therapy. This novel extension of the well-known "matched pair" approach requires innovative synthetic strategies towards the preparation of the corresponding homologues. In this sense, we developed procedures for the direct syntheses of functionalized mixed bis-arene ^{99}Tc complexes. The authors believe that the current state of research in the development of the bis-arene chemistry of rhenium and technetium is comparable with the one for $[^{99m}Tc(OH_2)_3(CO)_3]^+$ chemistry years ago. For the understanding of fundamental aspects with

this complex, Isabel Santos and her group contributed substantially. In this spirit, the synthesis of ^{99m}Tc arene complexes is an incentive to be solved in the forthcoming years.

Acknowledgments

The group of the corresponding author has a long standing, fruitful and synergistic collaboration with Isabel Santos and her group. Many results would not have been possible without. Roger Alberto expresses his gratitude and hopes that the collaboration will continue. Financial support from COST/SBFI project C13.0080 / SNF IZCSZ0-174553 and the University of Zurich is acknowledged.

The first two authors contributed equally to this paper.

References

1. K. D. Mjos and C. Orvig, *Chem. Rev.,* 2014**, 114**, 4540-4563.
2. E. A. Hillard and G. Jaouen, *Organometallics,* 2011**, 30**, 20-27.
3. G. Gasser and N. Metzler-Nolte, *Curr. Opin. Chem. Biol.,* 2012**, 16**, 84-91.
4. A. Bergamo and G. Sava, *Dalton Trans.,* 2011**, 40**, 7817-7823.
5. C. G. Hartinger, M. A. Jakupec, S. Zorbas-Seifried, M. Groessl, A. Egger, W. Berger, H. Zorbas, P. J. Dyson and B. K. Keppler, *Chem. Biodivers.,* 2008**, 5**, 2140-2155.
6. C. G. Hartinger, S. Zorbas-Seifried, M. A. Jakupec, B. Kynast, H. Zorbas and B. K. Keppler, *J. Inorg. Biochem.,* 2006**, 100**, 891-904.
7. C. G. Hartinger and P. J. Dyson, *Chem. Soc. Rev.,* 2009**, 38**, 391-401.
8. W. H. Ang, A. Casini, G. Sava and P. J. Dyson, *J. Organomet. Chem.,* 2011**, 696**, 989-998.
9. K. J. Kilpin and P. J. Dyson, *Chem. Sci.,* 2013**, 4**, 1410-1419.
10. Z. Liu, I. Romero-Canelon, B. Qamar, J. M. Hearn, A. Habtemariam, N. P. E. Barry, A. M. Pizarro, G. J. Clarkson and P. J. Sadler, *Angew. Chem. Int. Ed.,* 2014**, 53**, 3941-3946.
11. Y. K. Yan, M. Melchart, A. Habtemariam and P. J. Sadler, *Chem. Commun.,* 2005, 4764-4776.
12. E. Meggers, *Curr. Opin. Chem. Biol.,* 2007**, 11**, 287-292.
13. L. Feng, Y. Geisselbrecht, S. Blanck, A. Wilbuer, G. E. Atilla-Gokcumen, P. Filippakopoulos, K. Kraling, M. A. Celik, K. Harms, J. Maksimoska, R. Marmorstein, G. Frenking, S. Knapp, L. O. Essen and E. Meggers, *J. Am. Chem. Soc.,* 2011**, 133**, 5976-5986.
14. E. Meggers, G. E. Atilla-Gokcumen, K. Grundler, C. Frias and A. Prokop, *Dalton Trans.,* 2009, 10882-10888.
15. E. Meggers, *Chem. Commun.,* 2009, 1001-1010.
16. K. H. Thompson and C. Orvig, *Dalton Trans.,* 2006, 761-764.
17. N. Pagano, J. Maksimoska, H. Bregman, D. S. Williams, R. D. Webster, F. Xue and E. Meggers, *Org. Biomol. Chem.,* 2007**, 5**, 1218-1227.
18. L. Raszeja, A. Maghnouj, S. Hahn and N. Metzler-Nolte, *ChemBioChem,* 2011**, 12**, 371-376.
19. G. Jaouen, A. Vessieres and S. Top, *Chem. Soc. Rev.,* 2015**, 44**, 8802-8817.
20. W. A. Wani, E. Jameel, U. Baig, S. Mumtazuddin and L. T. Hun, *Eur. J. Med. Chem.,* 2015**, 101**, 534-551.
21. G. Jaouen, S. Top, A. Vessieres and R. Alberto, *J. Organomet. Chem.,* 2000**, 600**, 23-36.
22. M. Navarro, W. Castro and C. Biot, *Organometallics,* 2012**, 31**, 5715-5727.

23. D. Dive and C. Biot, *ChemMedChem,* 2008**, 3**, 383-391.
24. N. Husken, G. Gasser, S. D. Koster and N. Metzler-Nolte, *Bioconjugate Chemistry,* 2009**, 20**, 1578-1586.
25. M. Patra and G. Gasser, *ChemBioChem,* 2012**, 13**, 1232-1252.
26. D. R. van Staveren and N. Metzler-Nolte, *Chem. Rev.,* 2004**, 104**, 5931-5985.
27. E. Hillard, A. Vessieres, L. Thouin, G. Jaouen and C. Amatore, *Angew. Chem. Int. Ed.,* 2006**, 45**, 285-290.
28. K. A. Stephenson, S. R. Banerjee, T. Besanger, O. O. Sogbein, M. K. Levadala, N. McFarlane, J. A. Lemon, D. R. Boreham, K. P. Maresca, J. D. Brennan, J. W. Babich, J. Zubieta and J. F. Valliant, *J. Am. Chem. Soc.,* 2004**, 126**, 8598-8599.
29. I. Romero-Canelon and P. J. Sadler, *Proc. Natl. Acad. Sci. USA,* 2015**, 112**, 4187-4188.
30. H. K. Liu, H. Kostrhunova, A. Habtemariam, Y. Q. Kong, R. J. Deeth, V. Brabec and P. J. Sadler, *Dalton Trans.,* 2016**, 45**, 18676-18688.
31. A. A. Nazarov, S. M. Meier, O. Zava, Y. N. Nosova, E. R. Milaeva, C. G. Hartinger and P. J. Dyson, *Dalton Trans.,* 2015**, 44**, 3614-3623.
32. G. Agonigi, T. Riedel, S. Zacchini, E. Paunescu, G. Pampaloni, N. Bartalucci, P. J. Dyson and F. Marchetti, *Inorg. Chem.,* 2015**, 54**, 6504-6512.
33. S. J. Berners-Price and A. Filipovska, *Metallomics,* 2011**, 3**, 863-873.
34. M. D. Bartholoma, A. S. Louie, J. F. Valliant and J. Zubieta, *Chem. Rev.,* 2010**, 110**, 2903-2920.
35. S. Liu, *Chem. Soc. Rev.,* 2004**, 33**, 445-461.
36. W. Eckelman, *Nucl. Med. Biol.,* 2011**, 38**, 613-616.
37. R. Alberto, K. Ortner, N. Wheatley, R. Schibli and A. P. Schubiger, *J. Am. Chem. Soc.,* 2001**, 123**, 3135-3136.
38. M. Morais, A. Paulo, L. Gano, I. Santos and J. D. G. Correia, *J. Organomet. Chem.,* 2013**, 744**, 125-139.
39. R. Alberto, J. K. Pak, D. van Staveren, S. Mundwiler and P. Benny, *Biopolymers,* 2004**, 76**, 324-333.
40. L. Maria, A. Paulo, I. C. Santos, I. Santos, P. Kurz, B. Spingler and R. Alberto, *J. Am. Chem. Soc.,* 2006**, 128**, 14590-14598.
41. Y. Liu, J.-K. Pak, P. Schmutz, M. Bauwens, J. Mertens, H. Knight and R. Alberto, *J. Am. Chem. Soc.,* 2006**, 128**, 15996-15997.
42. S. Alves, J. D. G. Correia, L. Gano, T. L. Rold, A. Prasanphanich, R. Haubner, M. Rupprich, R. Alberto, C. Decristoforo, I. Santos and C. J. Smith, *Bioconjugate Chem.,* 2007**, 18**, 530-537.
43. S. James, K. P. Maresca, D. G. Allis, J. F. Valliant, W. Eckelman, J. W. Babich and J. Zubieta, *Bioconjugate Chem.,* 2006**, 17**, 579-589.
44. R. Garcia, A. Paulo, A. Domingos, I. Santos, K. Ortner and R. Alberto, *J. Am. Chem. Soc.,* 2000**, 122**, 11240-11241.
45. M. Bartholoma, J. Valliant, K. P. Maresca, J. Babich and J. Zubieta, *Chem. Commun.,* 2009, 493-512.
46. S. S. Kelkar and T. M. Reineke, *Bioconjugate Chem.,* 2011**, 22**, 1879-1903.
47. S. Imstepf, V. Pierroz, P. Raposinho, M. Bauwens, M. Felber, T. Fox, A. B. Shapiro, R. Freudenberg, C. Fernandes, S. Gama, G. Gasser, F. Motthagy, I. R. Santos and R. Alberto, *Bioconjugate Chem.,* 2015**, 26**, 2397-2407.

48. T. Esteves, F. Marques, A. Paulo, J. Rino, P. Nanda, C. J. Smith and I. Santos, *J. Biol. Inorg. Chem.,* 2011**, 16**, 1141-1153.
49. R. F. Vitor, I. Correia, M. Videira, F. Marques, A. Paulo, J. C. Pessoa, G. Viola, G. G. Martins and I. Santos, *ChemBioChem,* 2008**, 9**, 131-142.
50. R. F. Vitor, T. Esteves, F. Marques, P. Raposinho, A. Paulo, S. Rodrigues, J. Rueff, S. Casimiro, L. Costa and I. Santos, *Cancer Biother. Radio.,* 2009**, 24**, 551-563.
51. N. Agorastos, L. Borsig, A. Renard, P. Antoni, G. Viola, B. Spingler, P. Kurz and R. Alberto, *Chem. Eur. J.,* 2007**, 13**, 3842-3852.
52. P. Haefliger, N. Agorastos, A. Renard, G. Giambonini-Brugnoli, C. Marty and R. Alberto, *Bioconjugate Chem.,* 2005**, 16**, 582-587.
53. A. Leonidova and G. Gasser, *ACS Chem. Biol.,* 2014**, 9**, 2180-2193.
54. D. Can, B. Spingler, P. Schmutz, F. Mendes, P. Raposinho, C. Fernandes, F. Carta, A. Innocenti, I. Santos, C. T. Supuran and R. Alberto, *Angew. Chem. Int. Ed.,* 2012**, 51**, 3354-3357.
55. S. Imstepf, V. Pierroz, R. Rubbiani, M. Felber, T. Fox, G. Gasser and R. Alberto, *Angew. Chem. Int. Ed.,* 2016**, 55**, 2792-2795.
56. M. Benz, H. Braband, P. Schmutz, J. Halter and R. Alberto, *Chem. Sci.,* 2015**, 6**, 165-169.
57. M. Patra, G. Gasser, A. Pinto, K. Merz, I. Ott, J. E. Bandow and N. Metzler-Nolte, *ChemMedChem,* 2009**, 4**, 1930-1938.
58. G. Meola, H. Braband, P. Schmutz, M. Benz, B. Spingler and R. Alberto, *Inorg. Chem.,* 2016**, 55**, 11131-11139.
59. C. Palm and E. O. Fischer, *Tetrahedron Lett.,* 1962**, 6**, 253-254.
60. E. A. Trifonova, D. S. Perekalin, K. A. Lyssenko and A. R. Kudinov, *J. Organomet. Chem.,* 2013**, 727**, 60-63.
61. G. Pampaloni, *Coord. Chem. Rev.,* 2010**, 254**, 402-419.
62. B. Stibr, M. Bakardjiev, Z. Hajkova, J. Holub, Z. Padelkova, A. Ruzicka and J. D. Kennedy, *Dalton T.,* 2011**, 40**, 5916-5920.
63. B. Stibr, M. Bakardjiev, J. Holub, A. Ruzicka and M. Kvicalova, *Inorg. Chem.,* 2009**, 48**, 10904-10906.
64. E. P. Kundig, P. Jeger and G. Bernardinelli, *Inorg. Chim. Acta,* 2004**, 357**, 1909-1919.
65. B. Therrien, *Coord. Chem. Rev.,* 2009**, 253**, 493-519.
66. J. A. K. Will, William S. Sheldrick and Dirk Wolters *J. Biol. Inorg. Chem.,* 2007**, 12**, 883-894.
67. K. Severin, R. Bergs and W. Beck, *Angew. Chem. Int. Edit.,* 1998**, 37**, 1635-1654.
68. D. S. Perekalin and A. R. Kudinov, *Coord. Chem. Rev.,* 2014**, 276**, 153-173.
69. R. D. Pike and D. A. Sweigart, *Coord. Chem. Rev.,* 1999**, 187**, 183-222.
70. E. A. Trifonova, D. S. Perekalin, N. L. Loskutova, Y. V. Nelyubina and A. R. Kudinov, *J. Organomet. Chem.,* 2015**, 785**, 106-111.
71. D. S. Perekalin, E. E. Karslyan, E. A. Trifonova, A. I. Konovalov, N. L. Loskutova, Y. V. Nelyubina and A. R. Kudinov, *Eur. J. Inorg. Chem.,* 2013, 481-493.
72. D. W. Wester, D. H. White, F. W. Miller and R. T. Dean, *Inorg. Chem.,* 1984**, 23**, 1501-1502.
73. A. G. Jones, M. J. Abrams, A. Davison, J. W. Brodack, A. K. Toothaker, S. J. Adelstein and A. I. Kassis, *Int. J. Nucl. Med. Biol.,* 1984**, 11**, 225-234.
74. M. J. Abrams, A. Davison, A. G. Jones, C. E. Costello and H. Pang, *Inorg. Chem.,* 1983**, 22**, 2798-2800.

6.8 Unpublished Results: Structure and Reactivities of Rhenium and Technetium bis-Arene Sandwich Complexes $[M(\eta^6\text{-arene})_2]^+$

The previous manuscript describes the access to a class of rhenium compounds of the type $[Re(\eta^6\text{-}C_6R_6)(L^3)]$. But still, these compounds are rarely reported in the literature and only few information about stability, reactivity and cytotoxicity are available. In contrast, the ruthenium chemistry of this complex type is well established. For example, the discovery of the antitumoral activity of ruthenium-arene-PTA complexes (RAPTA) has boosted significant synthetic efforts towards this class of compounds.[176] In particular, the introduction of one 1,3,5-Triaza-7-phosphaadamantane (PTA) ligand into the scaffold of the mono-arene complex seems to have a huge impact in terms of antitumoral activity.[177] The reactivity of the corresponding Re complexes was studied by Prof. Dr Enzo Alessio at his time as visitor at the Department of chemistry. In particular, the reactivity of $[Re(\eta^6\text{-naphthalene})_2]^+$ ([**7p**]$^+$) in the presence of PTA ligands was investigated. It is important to note, the reported experiments lead only to preliminary results. Furthermore, detailed studies are necessary to gain deeper insights into this field in the future. In a first attempt, [**7p**]$^+$ were treated with 6 eq. of PTA in a microwave reactor. Reactions were conducted overnight at 80°C in acetone and methanol. Both reaction shows almost quantitative conversion to $[Re(\eta^6\text{-naphthalene})(PTA)_3]^+$ with the corresponding m/z = 786.3 $[M]^+$ according to UPLC-MS analysis. During the reaction with methanol as solvent, $[Re(\eta^6\text{-naphthalene})(PTA)_3]^+$ partially precipitate as an orange powder in high purity with 42 % yield. The complex is soluble in water, nitromethane, and acetone and is stable in solution at room temperature. Furthermore, $[Re(\eta^6\text{-naphthalene})(PTA)_3]^+$ were characterized by X-ray diffraction analysis. Single crystals of $[Re(\eta^6\text{-naphthalene})(PTA)_3]^+$ were grown by slow evaporation of a water solution. The complex crystallizes as pink plates in the monoclinic space group $P2_1/c$ (Figure 40). The asymmetric unit includes two independent Re centres, two PF_6^- and seven water molecules. The protons of the water molecules could not be found due to the moderate quality of the measured crystal (R1 = 4.6%). The Re-naphthalene bond lengths are between 2.242(4) Å and 2.415(4) Å and are in a similar range as for the comparable two structures $[Re(\eta^6\text{-naphthalene})(tep)_3]^+$ and $[Re(\eta^6\text{-naphthalene})(triphos)]^+$ described in the manuscript. The bond lengths between the rhenium centre and phosphorous are found in the range of 2.3230(10) Å and 2.3432(10) Å and are comparable with the bond lengths in the structure of $[Re(\eta^6\text{-naphthalene})(triphos)]^+$ which contains a tridentate 1,1,1-tris(diphenylphosphinomethyl)ethane as ligand system. The same reaction in acetonitrile led to the formation of [*trans*-$Re(PTA)_4(ACN)_2](PF_6)$, proven by UPLC-MS data and NMR spectra (^1H and ^{31}P, in nitromethane). This small section of experiments shows the diversity in the reactivity of $[Re(\eta^6\text{-naphthalene})_2]^+$ which could be further used for the synthesis of novel rhenium compounds for e.g. biological applications. However, more investigations are required to get insights regarding the reactivity with other ligand system such chlorides, amines and/or in combination with PTA to

synthesis similar complexes like the ruthenium analogues and further to analyse their biological activity against cancer cell line.

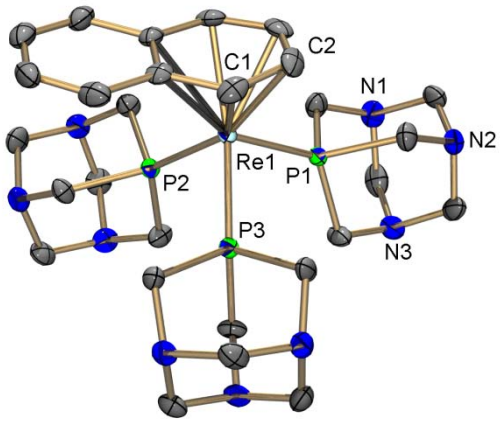

Figure 40: ORTEP representation[108] of [Re(η^6-naphthalene)$(PTA)_3]^+$. Hydrogen atoms and anions are omitted for clarity, thermal ellipsoids represent 50% probability. Selected bond lengths [Å] for [Re(η^6-naphthalene)$(PTA)_3]^+$: Re1-P 2.3230(10)-2.3432(10) and Re1-$C_{10}H_8$ (centroid) 1.8302(16)-1.8306(16).

Most of the substitutions reactions described in the manuscript where mainly performed thermally and under the presence of mono and tridentate ligands. However, light induced substitution reaction on [Re(η^6-naphthalene$)_2]^+$ as well as the reactivity of [Re(η^6-naphthalene$)_2]^+$ and [Re(η^6-naphthalene)(η^6-benzene)]$^+$ concerning solvents or bidentate ligands are discussed in the following section.

6.8.1 Light Induced Substitution Reaction of [Re(η^6-naphthalene$)_2]^+$ ([**7p**]$^+$)

It is well-known that coordinative metal naphthalene bonds can be cleaved under light irradiation.[178] In this scope, some additionally and preliminary substitution experiment with a numerous of different ligand such as dimethoxycarbonylcyclopentadienyl sodium (1,2-Cp-dimethylester), 1,2-bis(diphenylphophino)-ethane (dppe), chlorides and thiocyanate on [**7p**]$^+$ were performed. The reaction with 1,2-Cp-dimethylester was carried out with an excess of 5 equivalent in acetone at room temperature. The reaction mixture was irradiated for 12 h which led to the substitution of one naphthalene ligand by a 1,2-Cp-dimethylester with conversion up to 30 %, according to UPLC-MS measurement. Even the addition of more ligand combined with prolonged reaction time did not increase the conversion of the reaction. In contrast to the other substitution reactions, purification of the product was not possible. However, an X-ray structure of [Re(η^5-1,2-Cp-dimethylester)(η^6-

naphthalene)] was obtained by analysing single crystals, isolated by crystallizing a product/ligand mixture form a THF solution.

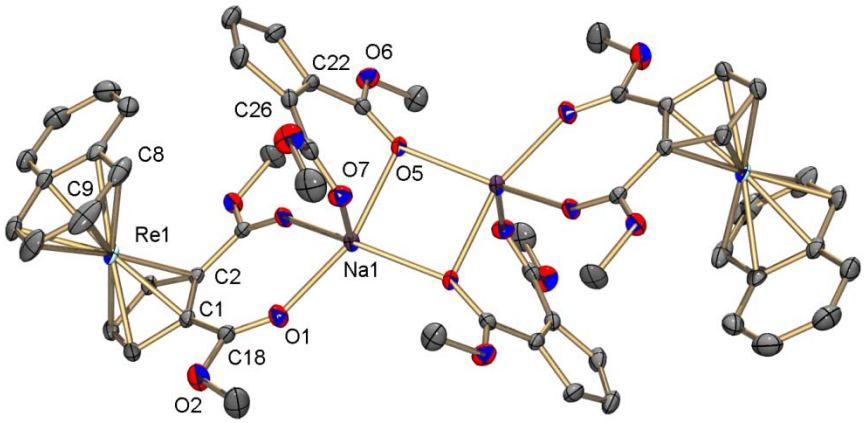

Figure 41: ORTEP representation[108] of [Re(η^5-1,2-Cp-dimethylester)(η^6-naphthalene)]. Hydrogen atoms omitted for clarity, thermal ellipsoids represent 50% probability. Selected bond lengths [Å] for [Re(η^5-1,2-Cp-dimethylester)(η^6-naphthalene)]: Re1-Cp--dimethylester (centroid) 1.852(3) and Re1-$C_{10}H_8$ (centroid) 1.727(3).

[Re(η^5-1,2-Cp-dimethylester)(η^6-naphthalene)] crystallizes as pink plates in the triclinic space group P-1. The asymmetric unit consists of one molecule and one ligand which are both coordinating the sodium atom over the oxygens of the carbonyl group. Furthermore, by extending the asymmetric unit it is evident that the oxygen O5 acts as a bridged ligand whereby both sodium atoms are coordinated over five oxygen (Figure 41). The Re-arene bond lengths are between 2.195(7) Å and 2.290(7) Å and show a broader range compared to the [Re(Cp-R)(benzene)] systems due to weaker coordination of the naphthalene ligand. The Re-Cp bond lengths are significantly shorter to related complexes and are between 2.185(6) Å and 2.220(7) Å. Further investigation in terms of reactivity, physical properties and cytotoxicity were not performed so far. Nevertheless, this is an alternative synthetic to get access to arene/Cp(functionalised) Re complexes.

Furthermore, light induced reactions on [**7p**]$^+$ were performed with a mixture of 1,2-bis(diphenylphosphino)ethane and chloride in a ratio of 1:1. Since most of this reaction were conducted in acetone, the addition of chlorides leads to an anion exchange in which [**7p**]$^+$ precipitated as chloride salt. Therefore, the addition of small quantities of methanol was used to redissolved the educt. The reaction mixture was irradiated overnight at room temperature. UPLC - MS measurement revealed the formation of different products in which some of them could be assigned to [$ReCl_2(dppe)_2$] and [$ReCl(MeOH)(dppe)_2$] but the oxidation state of the rhenium centre could not be determined assuredly. Purification and separation of the products were not achieved. In

order to investigate the oxidation state of the rhenium, potassium thiocyanate was used since it is soluble in acetone. The reaction was performed under the same condition described above. During the reaction, a colour change from red to light pink was observed. UPLC-MS analysis indicated the formation of a new product in quantitative amount with the corresponding m/z = 1099.17 $[M-H]^+$. After purification, single crystals were obtained by slow evaporation from a THF solution and elucidated by X-ray diffraction analysis. The crystallographic data disclose the *trans*-$[Re(SCN)_2(dppe)_2]$ product. In this structure, the rhenium atom is at the formal oxidation state (+II) whereby the two trans-thiocyanate ligands are bound via the nitrogen. This coordination motive can be explained by the HASB model since rhenium in the oxidation state +II can be described as "harder" compared to rhenium at the oxidation +I which favours coordination via the nitrogen atom.

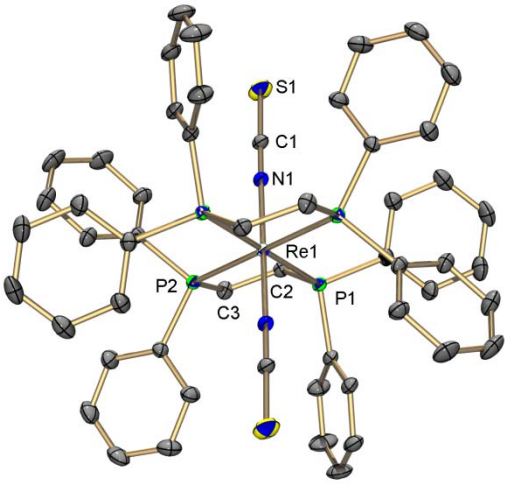

Figure 42: ORTEP representation[108] of *trans*-$[Re(SCN)_2(dppe)_2]$. Hydrogen atoms are omitted for clarity, thermal ellipsoids represent 50% probability. Selected bond lengths [Å] for trans-$[Re(SCN)_2(dppe)_2]$: Re1-P 2.267(9) and Re1-N 2.048(2).

trans-$[Re(SCN)_2(dppe)_2]$ crystallizes as pink plates in the triclinic space group P-1 (Figure 42). The asymmetric unit contains half of a molecule. The rhenium atom is located at the inversion centre of this space group. The Re-N bond lengths are found at 2.048(2) Å while the Re-P bond lengths are significantly longer and are found between 2.4164(6) Å and 2.4194(6) Å. The bond lengths are in the same range compared to similar structures.[179, 180] The oxidation from $Re^{(+I)}$ to $Re^{(+II)}$ is rather surprising and not fully understood until today. One explanation might be the excitation of an electron by light irradiation which could reduce one of naphthalene ligand to a naphthalide. This explanation is supported by the formation of bisnaphthalene and higher substitute aromatic compounds which have been detected by UPLC-MS in the reaction mixture. Further experiments are needed to investigate this reaction more in details. However, this reactivity paves the way for

another synthetic strategy to access Re(II) compounds and will lead to more detailed studies of the properties of these rare rhenium compounds.

6.8.2 Substitution Reaction of [Re(η^6-naphthalene)(η^6-benzene)]$^+$ ([**6p**]$^+$) with Aromatic Ligands

One aim of this thesis was the synthesis of rhenium bis-arene complexes with higher substituted or bioactive arene ligands like tyrosine. Since the direct synthesis with functionalized arene containing hetero atoms is only possible in a limited extent due to their reactivity towards $AlCl_3$, the synthesis of such complexes had to be started from [Re(η^6-naphthalene)(η^6-benzene)]$^+$. A similar approach was already described and applied in ruthenium chemistry. In this approach [CpRu(η^6-$C_{10}H_8$)]$^+$ was used because the labile bound naphthalene ligand can be replaced by other strong ligands.[181] Following a similar procedure, reaction with [**6p**]$^+$ were performed in the corresponding arene with additional acetone as solvent due to solubility reason. In a first attempt, [**6p**]$^+$ was dissolved in a mixture of toluene/acetone (8:1) and heated in a microwave reactor for 6 h at 100°C. UPLC-MS measurement revealed the formation of [Re(η^6-toluene)(η^6-benzene)]$^+$ with the corresponding m/z = 357.1 [M]$^+$ with quantitative conversion. The second reaction was performed with 1,3,5-trimethoxybenzene (100 eq. excess) under the same conditions. The product [Re(η^6-1,3,5-trimethoxybenzene)(η^6-benzene)]$^+$ ([**43**](PF_6)) was isolated in 52% yield and fully characterized. In the NMR spectra, the protons of the coordinated benzene are shifted to higher field (5.66 ppm) compared to the [Re(η^6-benzene)$_2$]$^+$ (6.16 ppm) due to the stronger π-donor properties of the 1,3,5-trimethoxybenzene ligand. Furthermore, single crystals of [**43**](ClO_4) were obtained by slow evaporation of an acetonitrile solution and the structure was elucidated via by X-ray diffraction analysis. [**43**](ClO_4) crystallizes as light yellow plates in the monoclinic space group Cc (Figure 43). The structure contains one molecule in the asymmetric unit. The Re-$C_{1,3,5\text{-trimethoxybenzene}}$ bond lengths are between 2.247(9) Å and 2.304(11) Å. The Re-$C_{benzene}$ bond lengths are shorter and can be found between 2.216(9) Å and 2.231(18) Å.

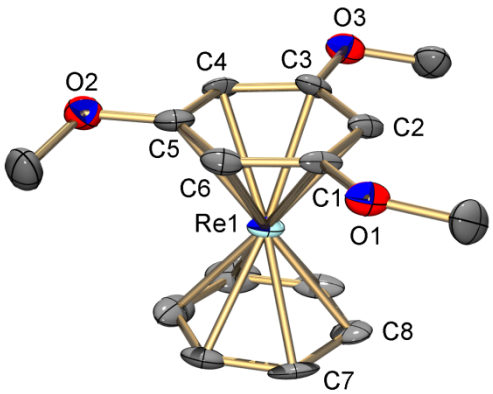

Figure 43: ORTEP representation[108] of [Re(η^6-1,3,5-trimethoxybenzene)(η^6-benzene)](ClO_4) ([**43**](ClO_4)). Hydrogen atoms and anions are omitted for clarity, thermal ellipsoids represent 50% probability. Selected bond lengths [Å] for [**43**]$^+$: Re1-$C_6H_3(OCH_3)_3$ (centroid) 1.779(5) and Re1-C_6H_6 (centroid) 1.720(6).

Additional reactions were performed with Boc-L-tyrosine methyl ester which is a protected tyrosine derivative. In this reaction, the conversion to the product was about 45% after 6 h at 100°C which was determined by UPLC-MS measurements. In order to increase the product formation, substitution reactions were also performed in acetonitrile instead of acetone. Surprisingly, no product formation was observed, however, a new Re species ($[Re(\eta^6\text{-benzene})(ACN)_3]^+$, $[Re(ACN)_6]^{2+}$) were found which will be discussed in detail in the next section. It was shown that this synthetic pathway can lead to the synthesis of new rhenium bis-arene complexes with more complex and biological active ligands

6.8.3 Substitution Reaction of $[Re(\eta^6\text{-naphthalene})(\eta^6\text{-benzene})]^+$ ($[\mathbf{6p}]^+$) and $[Re(\eta^6\text{-naphthalene})_2]^+$ ($[\mathbf{7p}]^+$) with Solvent Molecules

The syntheses of complexes of the type $[M(\eta^6\text{-arene})(sol)_3]^{2+}$ (M = Ru, Os; sol = acetone, acetonitrile), were already reported in the literature.[182-185] These partially stable complexes are used as precursors for further substitution reaction.[182-185] However, this class of compounds are not described for group 7. One of the reasons for this gap of knowledge might be the hard accessibility through conventional synthetic routes with known precursors or simply a lack of interest. A facile synthesis of this type of complexes for rhenium can be fundamental for further investigation in terms of reactivity and biological activity in comparison to the analogues of ruthenium and osmium. As a note, Mann R. et al. described that $[Os(\eta^6\text{-naphthalene})(\eta^6\text{-benzene})]^{2+}$ decompose in acetonitrile to form $[Os(\eta^6\text{-benzene})(ACN)_3]^{2+}$ but did not give any further information.[185] The rhenium analogue $[Re(\eta^6\text{-benzene})(ACN)_3]^+$ has been synthesised quantitatively from $[Re(naphthalene)(benzene)]^+$ in acetonitrile at 80°C for 2 h (microwave reactor). UPLC-MS-releveled one peak at 1.5 min with the corresponding m/z = 306.0 $[M]^+$ $[Re(\eta^6\text{-benzene})(ACN)]^+$) and 347.1 $[M]^+$ ($[Re(\eta^6\text{-benzene})(ACN)_2]^+$), respectively. The complex can be precipitated by the addition of dry toluene as yellow crystalline powder. Due to its high instability and sensitivity towards oxygen, moistures and light, it is difficult to isolate this compound as pure powder. However, single crystals were obtained by fast evaporating (within 1 h) of a mixture of acetonitrile/toluene by use of N_2 stream. Longer crystallisation times, even in the dark, led to decomposition of the complex and the formation of free benzene (UPLC) while the colour of the solution changed from yellow to black. Although the quality of the crystal is moderate, X-ray measurement provided the authenticity of the structure (Figure 44). In contrast to the rhenium complex, the analogues ruthenium and osmium are quite stables and replacement of the acetonitrile ligands can be induced thermally or by photolysis.[185, 186]

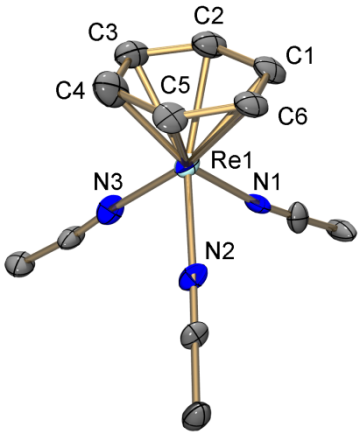

Figure 44: ORTEP representation[108] of [Re(η^6-benzene)(ACN)$_3$]$^+$.

Prolongation of the reaction time to 6 h at the same temperature leads to the substitution of the coordinated benzene ligand with additional acetonitrile ligands. The formation of the paramagnetic, homoleptic species [Re(ACN)$_6$]$^{2+}$ ([**44**](PF$_6$)$_2$) has been detected with UPLC-MS with the corresponding retention time of 0.2 min and m/z = 432.1 [M]$^+$ (fragmentation: m/z = 391.1 [M]$^+$ ([Re(ACN)$_5$]$^{2+}$); m/z = 350.1 [M]$^+$ ([Re(ACN)$_4$]$^{2+}$); m/z = 309.1 [M]$^+$ ([Re(ACN)$_3$]$^{2+}$). After precipitation with dry toluene, [**44**]$^{2+}$ was isolated in moderate yields of 45%. Until today, the oxidation from Re(+I) to Re(+II) is not fully understood. Alternatively, the reaction can be performed with [Re(η^6-naphthalene)$_2$]$^+$ ([**7p**]$^+$) as starting material with similar yields. The IR spectrum shows the distinctive ν(CN) at 2264 cm^{-1} and is lower compared to the manganese (2309 and 2280 cm^{-1}) and technetium (2319 and 2280 cm^{-1}) analogues as expected.[187, 188] Furthermore, it is stable in MeCN and degassed water while in oxygenated water solution, the compound decomposed slowly to perrhenate. Single crystals suitable for X-ray diffraction analysis were obtained by slow evaporation of an acetonitrile solution of [**44**](PF$_6$)$_2$ in a glove box. [**44**](PF$_6$)$_2$ crystallizes as red plates in the trigonal space group R-3 and is isostructural to [M(ACN)$_6$]$^{2+}$ (M = Ru and Fe) (Figure 45).[189] The asymmetric unit contains one-sixth of the molecule. Furthermore, the counter-ions (PF$_6^-$/ReO$_4^-$) have a disorder with occupancy of 64:36. The Re-N1 (ACN) bound length is 2.061(4) Å while the N1'-Re1-N1 angles are in the range 88.16(18) – 91.84(18)°. The values are comparable with the technetium analogue [^{99}Tc(ACN)$_6$]$^{2+}$ (Tc-N = 2.062(4); N-Tc-N = 88.8 – 91.2°)[188]. [M(ACN)$_6$]$^{2+}$ (e.g. M = Mn, Ru and Fe) complexes were used as a precursor for a large number of substation reaction.[187, 190, 191] The synthesis of rhenium complexes containing only solvents ligand is not reported in the literature. This complex may provide access to a new class of rhenium(I/II) compounds. Due to the high potential of these compounds as precursor complexes studies are ongoing to investigate the electrochemistry as well as the kinetics of ligand exchange

reaction. A highly interesting target compound for this future studies is the synthesis of the *aquo* complex $[Re(H_2O)_6]^{+/2+}$.

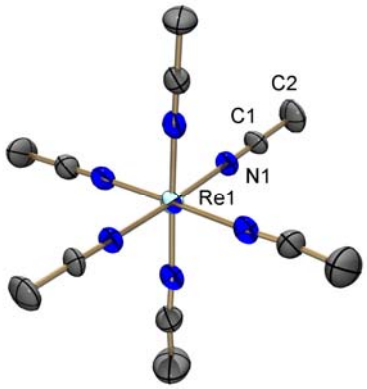

Figure 45: ORTEP representation[108] of $[Re(ACN)_6]^{2+}$ ([**44**]$(PF_6)_2$). Hydrogen atoms and anions are omitted for clarity, thermal ellipsoids represent 50% probability. Selected bond lengths [Å] for [**44**]$^{2+}$: Re1-N1 2.061(4).

$[Re(\eta^6\text{-}C_6H_6)(dmso\text{-}S)_3]^+$ ([**45**](PF_6)) was synthesised by thermally substitution of the naphthalene ligand of [**6p**]$^+$ in dmso. The synthesis was performed in a microwave reactor at 60°C for 1 h. After evaporation of the solvent, [**45**](PF_6) was purified by washing the solid few times with Et_2O. The product was isolated in high purity with a yield of 86%. The ^{1}H NMR spectra of [**45**]$^+$ reveal two singlets at 5.36 ppm and 3.35 ppm which correspond to the benzene protons and CH_3 group, respectively. As a result of the stronger σ-donation properties of monodentate dmso ligand compared to the benzene in $[Re(\eta^6\text{-}C_6H_6)_2]^+$, the aromatic protons are found at higher field. Furthermore, the binding mode of the dmso ligands was confirmed by X-ray diffraction analysis. Suitable single crystals for X-ray studies were obtained by slow evaporation of a dmso solution. [**45**](PF_6) crystallizes as light yellow plates in the monoclinic space group $P2_1/c$. The structure contains two independent Re molecules in the asymmetric unit which are very similar. One of the PF_6^- counter-ion is highly disordered. All three dmso ligands are coordinated to Re over the sulfur atoms as represented in Figure 46. The Re-S bond lengths are between 2.3307(10) Å and 2.3626(9) Å while Re-benzene bond lengths are found between 2.235(3) Å and 2.271(4) Å and are in same range compared to similar structures e.g. $[Re(\eta^6\text{-naphthalene})(PTA)_3]^+$.

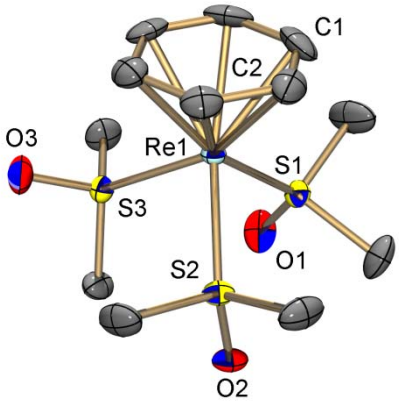

Figure 46: ORTEP representation[108] of $[Re(\eta^6\text{-}C_6H_6)(dmso\text{-}S)_3]^+$ ([**45**](PF_6)). Hydrogen atoms and anions are omitted for clarity, thermal ellipsoids represent 50% probability. Selected bond lengths [Å] for [**45**]$^+$: Re1-S 2.3230(10) - 2.3432(10) and Re1-C_6H_6 (centroid) 1.7570(18)-1.7618(17).

In agreement with the HASB concept, the "softer" sulphur atom of the dmso ligand is acting as weak σ-donors as well as π-acceptors to the softer Re(I) centre. This is the first structurally characterized compound containing three sulphur coordinated dmso molecules. In most of the known Re-dmso complexes, the dmso ligands are coordinated via oxygen atoms. Until today, the only isolated and characterized Re complex, containing a sulphur coordinated dmso molecule is $[(\eta^5\text{-}C_5H_5)Re(NO)(PPh_3)(dmso\text{-}S)](BF_4)$.[192] An explanation for this finding can be that in most of the reported Re-dmso complexes the metal centre is in a higher oxidation state (+III, +V). Therefore, the coordination with harder ligands such as oxygen is favoured.[193, 194] Re-dmso complexes containing the metal in a lower oxidation state (+I) and bearing additionally strong π-acceptor ligands (e.g. CO, NO) also prefer the coordination of an oxygen as it has been described in the rhenium(I)tricarbonyl *fac*-$[Re(CO)_3(dmso\text{-}O)_3]^+$.[195] In the synthesized complex [**45**]$^+$, the coordinated benzene ligand is a weak π-acceptor which renders the metal centre rather electron rich and leads to the observed coordination via the sulfur atom. Unlike the ruthenium analogue complexe $[Ru(\eta^6\text{-}C_6H_6)(dmso\text{-}O)_3]^{2+}$ where the dmso ligands are coordinated via the oxygen atom according to NMR studies.[196] Complex [**45**]$^+$ is stable in acetonitrile and dmso under further under ambient conditions for few days. As mention above, the coordination of the three dmso molecules via the sulphur atoms in [**45**]$^+$ is unprecedently and might be an interesting precursor for further developments. However, further investigations are required to gain deeper insights into the reactivity towards other ligands (e.g. water, phosphine), kinetics (ligand exchange), and biological studies (cytotoxicity).

As shown before, the replacement of the naphthalene ligand in [**6p**]$^+$ trough functionalized arenes did not work in acetonitrile even at high temperatures, however, the formation of $[Re(\eta^6\text{-}benzene)(ACN)_3]^+$ was observed. Since arene ligands have weak π-acceptor/donors properties compared to ACN ligands reactions were carried out with stronger bidentate σ-donor ligands such as

1,2-bis(diphenylphosphino)ethane (dppe) and 2,2'-bipyridine (bipy), respectively, in order to investigate their reactivity.

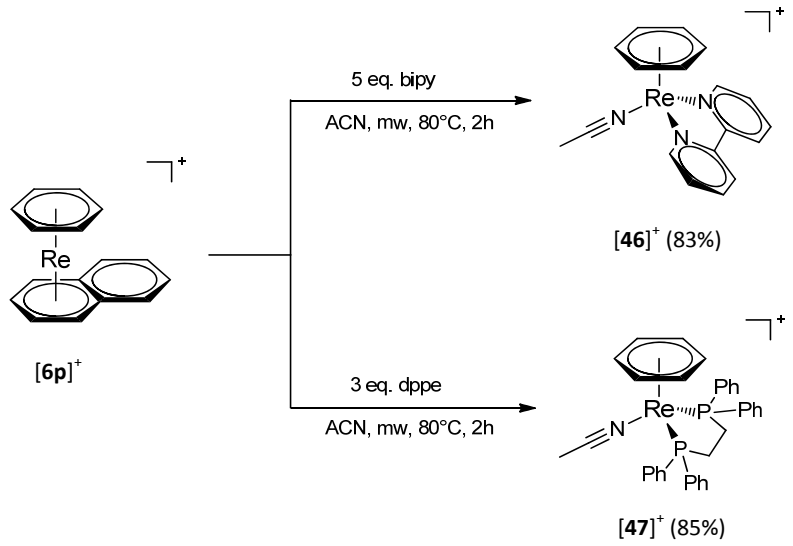

Scheme 9: Synthesis of $[Re(\eta^6\text{-}C_6H_6)(ACN)(bipy)](PF_6)$ ([**46**](PF_6)) and $[Re(\eta^6\text{-}C_6H_6)(ACN)(dppe)](PF_6)$ ([**47**](PF_6)) starting from [**6p**]$^+$

Treating $[Re(\eta^6\text{-naphthalene})(\eta^6\text{-benzene})]^+$ ([**6p**]$^+$) with bipy and dppe in a microwave reactor for 2 h at 80°C afforded the corresponding complexes $[Re(\eta^6\text{-}C_6H_6)(ACN)(bipy)]^+$ ([**46**]$^+$) and $[Re(\eta^6\text{-}C_6H_6)(ACN)(dppe)]^+$ ([**47**]$^+$), respectively. Upon washing the residues with Et_2O and recrystallization, complex [**46**]$^+$ was isolated as dark violet crystals in good yield of 83% whereas [**47**]$^+$ was obtained as yellow crystals in 86% (Scheme 9). Performing the same reaction with 0.5 eq. dppe, showed the formation of two products, the expected product [**47**]$^+$ and $[Re(\eta^6\text{-benzene})(ACN)_3]^+$ in a ratio of 1:1 according to UPLC-MS measurement. The further addition of dppe during the reaction led to a full conversion of $[Re(\eta^6\text{-benzene})(ACN)_3]^+$ into [**47**]$^+$. This experiment proved the lability of the acetonitrile ligands in $[Re(\eta^6\text{-benzene})(ACN)_3]^+$ and showed that they can be replaced by potential σ-donors. [**46**]$^+$ is highly sensitive towards water and oxygen. The decomposition can be observed by a colour change of the solution from dark violet to colourless. Complex [**47**]$^+$ shows similar sensitivity towards water but contrarily it is more stable under ambient condition. Both compounds were fully characterized including crystal structure determination by X-ray diffraction analysis. For both compounds, the signals for the $\eta^6\text{-}C_6H_6$ protons in the ^{1}H NMR spectra are shifted similarly to high field due to the σ-donor properties of the ligands (bipy and dppe) and can be found at 4.70 ppm ([**46**]$^+$) and 4.73 ppm ([**47**]$^+$), respectively. The chemical shift of the signals of CH_3- protons of the coordinated acetonitrile molecules differ significantly. They can be found at 2.40 ppm ([**46**]$^+$) and 1.66 ppm ([**47**]$^+$), respectively. This can be explained by the different electron properties of the bidentate ligands. The dppe ligand is a pure σ-donor while the bipy act as both σ-donor and π-

acceptor and cause the deshielding of the CH_3 group. Single crystals were obtained for both compounds by slow evaporation of acetonitrile from acetonitrile/toluene (1:1) solution. [**46**]PF_6 crystallizes as violet blocks in the orthorhombic space group $Pna2_1$ (Figure 47). The structure contains one molecule in the asymmetric unit. The Re-benzene bond lengths are between 2.160(5) Å and 2.209(6) Å. The Re-N (ACN) bound length is 2.082(4) Å while the Re-N (bipy) are longer (2.106(3) Å and 2.110(4) Å.)

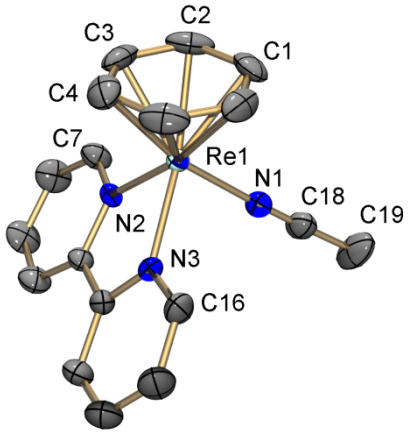

Figure 47: ORTEP representation[108] of [Re(η^6-C_6H_6)(ACN)(bipy)](PF_6) ([**46**](PF_6)). Hydrogen atoms and anions are omitted for clarity, thermal ellipsoids represent 50% probability. Selected bond lengths [Å] for [**46**]$^+$: Re1-C_6H_6 (centroid) 1.681(3).

[**47**]PF_6 crystallizes as brown plates in the monoclinic space group $P2_1/n$ (Figure 48). The structure contains one molecule in the asymmetric unit. The Re-benzene bond lengths are between 2.189(4) Å and 2.234(4) Å. The Re-ACN bound length is 2.068(3) Å while the Re-P (dppe) are longer (2.3470(9) Å and 2.3622(9) Å).

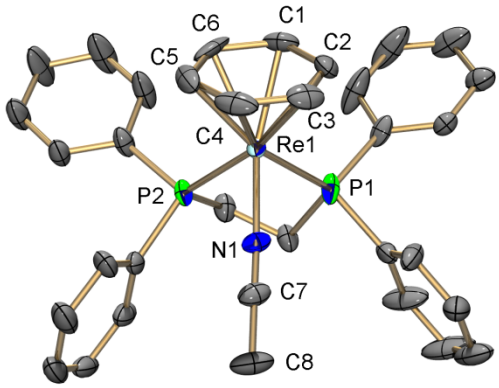

Figure 48: : ORTEP representation[108] of [Re(η^6-C_6H_6)(ACN)(dppe)](PF_6) ([**47**](PF_6)). Hydrogen atoms and anions are omitted for clarity, thermal ellipsoids represent 50% probability. Selected bond lengths [Å] for [**47**]$^+$: Re1-C_6H_6 (centroid) 1.731(2).

This approach is a possible synthetic route for the synthesis of new rhenium piano stool complexes for biological studies. However, further investigations are necessary. The ruthenium analogue was synthesis from $[Ru(\eta^6\text{-benzene})(ACN)_3]^{2+}$ at room temperature. Moreover, the coordinated benzene of these complexes $[Ru(\eta^6\text{-}C_6H_6)(ACN)(L)]^{2+}$ (L = bipy, dppe) can be displaced photochemically in acetonitrile to generate $[Ru(ACN)_4(L)]^{2+}$.[186] This method could be an alternative synthetic route for the synthesis of rhenium analogue of the type $[Re(ACN)_4(L)]^{+}$ which are not accessible until now. This type of complexes can be valuable precursors for further reactions.

7 Conclusion and Outlook

The bioorganometallic chemistry of the $\{Ru(\eta^6\text{-arene})\}^{2+}$ moiety was and still is exploited in great detail due to its high potential for the medical applications (e.g. as anticancer agent). In contrast, the isoelectronic congener $\{Re(\eta^6\text{-arene})\}^{+}$ has found only little attention. The exploration of its chemistry is lagging behind, due to missing rhenium precursor complexes. In this thesis, new synthetic pathways for the synthesis of mono/bis(η^6-arene) rhenium (and technetium) complexes were developed, making this type of compounds easier accessible. In the curse of this thesis Re arene complexes have been developed from a rather rare and exotic type of complexes into a new building block (or scaffold) for biological and medical applications with a strong focus on a theranostic approach. Moreover, these compounds have been derivatised, fully characterized and fundamentally studied in terms of properties, reactivates and, to a smaller extent, biological activity. In the first part, the synthesis of compound $[Re(\eta^6\text{-benzene})]^{+}$ was optimised, improving the yield up to 60%. Besides the optimisation novel dimeric species $[Re_2(\mu\text{-}\eta^{2:2}\text{-benzene})(\eta^6\text{-benzene})_2]^{2+}$ ($[\mathbf{1a}]^{2+}$) was identified. For the methylated arene complexes (toluene $[\mathbf{2}]^{+}$, *p*-xylene $[\mathbf{3}]^{+}$, *o*-xylene $[\mathbf{4}]^{+}$, *m*-xylene $[\mathbf{5}]^{+}$, mesitylene $[\mathbf{6}]^{+}$ *n*-octylbenzene $[\mathbf{7}]^{+}$ and tert-butylbenzene $[\mathbf{10}]^{+}$), the yields are comparable with the reported values. The formation of trans-/ dealkylated side products during the synthesis of $[Re(\eta^6\text{-arene})]^{+}$ is still a common problem by using $AlCl_3$ as activating reagent. Purification of these compounds was achieved by recrystallization or by preparative HPLC. The reaction with solid or more complex ligand such tetralin $[\mathbf{13}]^{+}$, fluorene $[\mathbf{14}]^{+}$, biphenyl $[\mathbf{15}]^{+}$, cyclophane $[\mathbf{16}]^{+}$, hexamethylbenzene $[\mathbf{17}]^{+}$ and naphthalene $[\mathbf{7p}]^{+}$ with $K[ReO_4]$ gave yields in a lower range of 38%-2%. Most of these complexes are of high chemical stability except $[\mathbf{16}]^{+}$, $[\mathbf{7p}]^{+}$ and $[\mathbf{6p}]^{+}$ which are light or thermally sensitive. The $E^0_{1/2}$ values for the oxidation of the couples for $Re^{+/2+}$ and $^{99}Tc^{+/2+}$ are in the range of 1.33 - 1.20 V and 1.52 - 1.24 V, respectively. The higher oxidation potentials for the $^{99}Tc^{+/2+}$ couples are in agreement with the general trends in the periodic table. The reductions of $M^{+/0}$ (M = Re/^{99}Tc) are for almost all complexes described in this thesis irreversible and were found to be more negative then <2 V. The only exception was $[Re(naphthalene)(benzene)]^{+}$ ($[\mathbf{6p}]^{+}$) with a reversible reduction at a potential of -1.29 V. Furthermore, rhenium-(η^6-arene) complex bearing one or two naphthalene ligands have been used as precursors for arene displacement reactions. Complex $[Re(\eta^6\text{-naphthalene})_2$ $[\mathbf{7p}]^{+}$ (the more reactive complex) displays IC_{50} values in the high micromolar range while complex $[\mathbf{15}]^{+}$ in the mid-micromolar range (Hela, A2780). The synthesis of $[Re(\eta^6\text{-arene})_2]^{+}$ complexes is currently limited to alkylated arenes. Future research should aim at the development of functional group tolerant reaction conditions, to widen the scope of this chemistry. In the second part of this thesis, the $[Re(\eta^6\text{-benzene})]^{+}$ framework was derivatised with several functionalities by metalation of the coordinated

benzene. The lithiation of $[Re(\eta^6\text{-benzene})_2]^+$ with *n*-BuLi leads preferentially to the neutral, alkylated product $[Re(\eta^6\text{-}C_6H_6)(\eta^5\text{-}C_6H_6\text{-Bu})]$ but not to the expected deprotonation of the arene ring. Deprotonation/lithiation with LDA gave the mono- and the di-lithiated products *in situ*. The lithiated species were treated with various electrophiles to generate a large library of functionalized $[Re(\eta^6\text{-}C_6H_5R)(\eta^6\text{-}C_6H_{6-n}R_n)]^+$ (n = 0, 1) complexes. In particular, reactions with of 1,1,2,2-tetra-bromoethane (TBE) or CO_2 led to the formation of $[Re(\eta^6\text{-}C_6H_5Br)(\eta^6\text{-}C_6H_6)]^+$ ([**4**]$^+$), $[Re(\eta^6\text{-}C_6H_5Br)_2]^+$ ([**5**]$^+$) or $[Re(\eta^6\text{-}C_6H_5COOH)(\eta^6\text{-}C_6H_6)]$(TFA) ([**6**](TFA)) and $[Re(\eta^6\text{-}C_6H_5COOH)_2]$(TFA) ([**7**](TFA)). These functionalized derivatives of $[Re(\eta^6\text{-benzene})_2]^+$ represent a novel class of precursors for the synthesis of bioconjugates which are comparable to the important buildings blogs of chemical biology $[Co(Cp)_2]^+$ and $[Fe(Cp)_2]$. Different model compounds $[Re(\eta^6\text{-}C_6H_5R)(\eta^6\text{-}C_6H_{6-n}R_n)]^+$ (n = 0, 1; R = -SCH_2Ph, -NHPh, -$CONHCH_2$Ph, -C_6H_5-COdpa) were synthesised via amide bond formation and nucleophilic aromatic substitution. Based on these studies, ongoing projects will use this scaffold for the development of water or CO_2 reduce catalyst. Another project dealt with the incorporation of the $[Re(\eta^6\text{-arene})_2]^+$ moiety in lead structures such as doxorubicin or Hoechst dye. Additionally, procedures were developed to bind this Re complexes to amino acids and peptides for DNA-or enzyme targeting.

The neutral $[Re(\eta^5\text{-Cp})(\eta^6\text{-benzene})]$ framework is very difficult to access, therefore the development of a novel synthetic pathway for this target moiety is described in the third part of this thesis. Furthermore, this part gives deeper insights into the reaction mechanism of the complex formation via ring contraction. Complex $[Re(\eta^5\text{-}C_5H_4CHO)(\eta^6\text{-}C_6H_6)]$ (**3**) was synthesized in almost quantitative yield with an excess of sodium hydroxide in water at 80°C, starting from $[Re(\eta^6\text{-}C_6H_5Br)(\eta^6\text{-}C_6H_6)]^+$. The compound $[Re(\eta^6\text{-}C_6H_5OH)(\eta^6\text{-}C_6H_6)]^+$ ([**2**]$^+$) was synthesized under mildly alkaline conditions at 60°C. Furthermore, reactions with other nucleophiles (e.g. SH^-, CN^- and N_3^-) did not lead to any ring contraction. The formation of **3** by ring contraction of bromobenzene to a cyclopentadienyl-system is unprecedented, even without the coordination of a metal. The ring contraction is not limited to $[Re(\eta^6\text{-}C_6H_5Br)(\eta^6\text{-}C_6H_6)]^+$ but it tolerates also other systems such as $[Re(\eta^5\text{-}C_5H_4CHO)(\eta^6\text{-}C_6Me_6)]$ (**5**). In contrast to rhenium, reactions with the technetium analogue $[^{99}Tc(\eta^6\text{-}C_6H_5Br)(\eta^6\text{-}C_6Me_6)]^+$ (**6**)$^+$ led under the same reaction conditions to the formation of the phenol complex $[^{99}Tc(\eta^6\text{-}C_6H_5OH)(\eta^6\text{-}C_6Me_6)]$ (**7**$^+$). The complex $[^{99}Tc(\eta^6\text{-}C_6H_5Br)(\eta^6\text{-}C_6H_6)]^+$ cannot be synthesised until today, but it might be an interesting alternative for the ring contraction reaction since it is better water soluble as compared to compound (**6**)$^+$. The reaction of $[Re(\eta^6\text{-}C_6H_5Cl)(\eta^6\text{-}C_6H_6)]^+$ under ring contraction conditions showed mainly the formation of $[Re(\eta^6\text{-}C_6H_5OH)(\eta^6\text{-}C_6H_6)]^+$ [**2**]$^+$ and only negligible quantities of **3**. To gain deeper insights into the reaction mechanism complexes containing iodine $[M(\eta^6\text{-}C_6H_5I)(\eta^6\text{-}C_6H_6)]^+$ (M = Re/^{99}Tc) might be alternative precursors because iodine is not such a good leaving group as compared to chloride/bromide, which could stabilize the important transition

state of the ring contraction reaction. The [Re(η^5-Cp)(η^6-benzene)] system are in general easier to oxidize as compared to the [Re(η^6-arene)$_2$]$^+$ complexes due to the stronger π-donor properties of the Cp-ring. The formation of a formyl group on the generated Cp-system allowed further derivatization of the [Re(η^5-Cp)(η^6-benzene)] moiety. [Re(η^5-C_5H_4CHO)(η^6-C_6H_6)] (**3**) was reacted with benzylamine to the corresponding imine [Re(η^5-$C_5H_4CHNCH_2C_6H_5$)(η^6-C_6H_6)] (**38**) in 92% yield. Reducing the aldehyde group with an excess of $NaBH_4$ leads to the formation of the corresponding primary alcohol derivative [Re(η^5-C_5H_4COH)(η^6-C_6H_6)] (**39**). The latter complex has been obtained in a good yield of 82%. In the future, this new building blogs will be linked to biological active substance and the physico-(bio)chemical properties will be studied.

Until today, the pentafulvene complex [Re(η^5:η^1-$C_5H_4CH_2$)(η^6-C_6H_6)]$^+$ [**40**]$^+$ was not synthesised and isolated. Only DFT calculations confirmed the possibility of the existents. In the fourth part of this thesis, the synthesis of this novel rhenium precursor is reported. [**40**]$^+$ was synthesised from Re(η^5-C_5H_4COH)(η^6-C_6H_6)] (**39**), by treating it with trimethylsilyl trifluoro-methanesulfonate or with an aqueous solution of HPF_6. The water-soluble and highly stable [**40**]$^+$ could be an alternative for the synthesis of functionalized [Re(η^5-Cp)(η^6-benzene)] systems since the exo CH_2 group of the pentafulvene ligand is prone for nucleophilic attack. In particular, the reaction [**40**]$^+$ in water under physiological conditions with mercaptoethanol shows almost quantitative conversion to [Re(η^6-$C_5H_4CH_2S(CH_2)_2OH$)(η^6-C_6H_6)] (**42**) within few minutes. These promising features enable an efficient new way of labelling cysteine residues of proteins with [**40**]$^+$ and make this compound very interesting for applications in a theranostic context.

The last part of this thesis describes the thermally or photochemical induced replacement of the weakly bound naphthalene ligand in [Re(η^6-naphthalene)$_2$]$^+$ [**7p**]$^+$ or [Re(η^6-naphthalene)(η^6-benzene)]$^+$ [**6p**]$^+$ by solvents, mono- or multi-dentate ligands. In [Re(η^6-naphthalene)(η^6-benzene)]$^+$ [**6p**]$^+$, the substitution of the naphthalene ligand was achieved with triethyl-phosphite, *tert*-butyl isocyanide and 1,3,5-trimethoxybenzene. The first tri-solvato complex [Re(η^6-benzene)$(ACN)_3$]$^+$ was prepared by the treatment of [**6p**]$^+$ in acetonitrile. The highly unstable [Re(η^6-benzene)$(ACN)_3$]$^+$ react further to the paramagnetic, homoleptic species $[Re(ACN)_6]^{2+}$ ([**44**](PF_6) by prolongation of the reaction time. The oxidation of the rhenium centre (I)→(II) is still not fully understood. Treating [**6p**]$^+$ with dmso gave the stable [Re(η^6-C_6H_6)$(dmso\text{-}S)_3$]$^+$ ([**45**](PF_6)) complex. An interesting structural feature of this compound is the coordination of the dmso ligands via the sulphur atoms. The tri-solvato complexes [Re(η^6-benzene)$(sol)_3$]$^+$ (sol = ACN and dmso) might be new precursors for the synthesis of new piano stool complexes in analogy to the well-established ruthenium chemistry. Further investigation might focus on the substitution with amino acids (e.g. histidine) and proteins to generate novel metal-bioconjugates for a wide range of applications. The paramagnetic, homoleptic

species $[Re(ACN)_6]^{2+}$ is the first Re hexa-solvato complex which may provide access to a new class of rhenium(I/II) compounds. Electrochemistry studies, as well as the investigations of the ligand exchange kinetics of this complex, are ongoing research projects, aiming at the generation of hexa solvato Re(II) complexes as novel precursors. The $[Re(\eta^6\text{-naphthalene})_2]^+$ $[\mathbf{7p}]^+$ showed similar reactivity compare to $[\mathbf{6p}]^+$. In the future this chemistry will be transferred to the lighter homolog technetium, starting with the synthesis of $[^{99(m)}Tc(\eta^6\text{-naphthalene})_2]^+$ and $[^{99(m)}Tc(\eta^6\text{-naphthalene})(\eta^6\text{-benzene})]^+$.

As a conclusion, all these synthesised complexes and in particular the new rhenium precursor, are an important contribution to the fundamental organometallic chemistry of Re- and $^{99(m)}Tc$ and will help to pave the way for new applications of this metals in life sciences.

8 Experimental Part

8.1 General Information

8.1.1 Materials

All reactions were carried out under nitrogen atmosphere on a standard nitrogen/vacuum line unless otherwise stated. The glassware was dried by the use of a heat gun or in an oven at 120 °C at least overnight. Commercially available reagents were purchased reagent-grade and used without further purification. THF was dried over Na/Benzophenone. All chemicals were purchased from Sigma Aldrich (Switzerland), except potassium perrhenate (>99%, Chempur Germany), Lithium trifluoromethanesulfonate (99%, ABCR, Germany), 3-[bis(dimethylamino)methyliumyl]-3H-benzotriazol-1-oxide hexafluorophosphate (≥99%, I^2CNS LLC Switzerland), aniline (99.5%, extra pure, ACROS Organics, Switzerland) *N,N*-dimethyl-formamide (99.8%, extra dry, AcroSeal®, ACROS Organics, Switzerland), hydrochloric acid (32%, Honeywell, Germany), carbon dioxide (>99,9, PanGas, Switzerland), and trifluoroacetic acid (99%, Alfa Aesar, Germany). The chemicals were used without farther purification. Deuterated NMR solvents were obtained from Armar Chemicals (Switzerland).

8.1.2 Characterization

The UV-Vis measurements were carried out on a Perkin Elmer Lambda 35 UV-Vis spectrophotometer between 200 and 900 nm. FT-IR spectra were acquired on a Perkin Elmer Spectrum Two spectrophotometer equipped with a Specac Golden Gate single reflection diamond accessory.

^{1}H-NMR and ^{13}C-NMR spectra were recorded on a BrukerDRX 400 MHz or BrukerDRX 500 MHz spectrometer. ^{1}H and ^{13}C chemical shifts were referenced with the residual solvent resonances relative to TMS. The spectra were fully assigned with the help of various experiments (1D NOE, 1H-COSY, C,H-Correlation and 13C-DEPT).

Electronspray-ionisation mass spectrometry (ESI-MS) was performed on a Bruker esquireTM/LC spectrometer or on a Bruker esquire^{TM}/HCT^{TM} spectrometer. High-resolution mass spectrometry (HR-ESI-MS) was performed on a Bruker maXis QTof high-resolution mass spectrometer (Bruker GmbH, Bremen, Germany).

Preparative HPLC was performed on a Varian ProStar 320 system, using a Dr. Maisch Reprosil C18 100-7 (40 x 250 mm) column. The solvents (HPLC grade) were 0.1% trifluoroacetic acid (solvent A) and acetonitrile (solvent B). The HPLC gradients used are as follow (G1): 0-2 minutes: 40% A (60% B); 2.1-45 minutes: linear gradient from 40% A (60% B) to 0% A (100% B); 45-50 minutes: 100% B. The flow rate was 40 mL/min. Detection was performed at 274 nm; (G2):0-2 minutes: 70% A (30% B); 2.1-

45 minutes: linear gradient from 70% A (30% B) to 35% A (65% B); 45.1-50 minutes: 100% B. The flow rate was 40 mL/min. Detection was performed at 282 nm; (G3): 0-2 minutes: 70% A (30% B); 2.1-45 minutes: linear gradient from 70% A (30% B) to 30% A (70% B); 45.1-55 minutes: 100% B. The flow rate was 40 mL/min. Detection was performed at 274 nm; (G4):0-2 minutes: 75% A (25% B); 2.1-45 minutes: linear gradient from 75% A (25% B) to 35% A (65% B); 45.1-50 minutes: 100% B. The flow rate was 40 mL/min. Detection was performed at 273 nm; (G5):0-2 minutes: 85% A (15% B); 2.1-35 minutes: linear gradient from 85% A (15% B) to 76% A (24% B); 35.1-45 minutes: 100% B. The flow rate was 40 mL/min. Detection was performed at 274 nm; (G6):0-2 minutes: 85% A (15% B); 2.1-45 minutes: linear gradient from 85% A (15% B) to 70% A (30% B); 45.1-50 minutes: 100% B. The flow rate was 40 mL/min. Detection was performed at 274 nm; (G7):0-2 minutes: 65% A (35% B); 2.1-50 minutes: linear gradient from 65% A (35% B) to 50% A (50% B); 50.1-55 minutes: 100% B. The flow rate was 40 mL/min. Detection was performed at 278 nm; (G8):0-2 minutes: 60% A (40% B); 2.1-50 minutes: linear gradient from 60% A (40% B) to 53% A (47% B); 50.1-55 minutes: 100% B. The flow rate was 40 mL/min. Detection was performed at 278 nm; (G9):0-2 minutes: 80% A (20% B); 2.1-45 minutes: linear gradient from 80% A (20% B) to 10% A (90% B); 45.1-50 minutes: 100% B. The flow rate was 40 mL/min. Detection was performed at 274 nm.

X-ray Crystallographic data were collected at 183(2) K or 160(2) K with either Mo Kα radiation (λ = 0.7107 Å) or Cu Kα radiation (λ = 1.54184 Å). Compounds were measured on an Agilent SuperNova, dual source, with an Atlas detector or on an Oxford Diffraction CCD Xcalibur system with a Ruby detector. Suitable crystals were covered with oil (Infineum V8512, formerly known as Paratone N), placed on a nylon loop that is mounted in a CrystalCap Magnetic™ (Hampton Research) and immediately transferred to the diffractometer. Data were corrected for Lorentz and polarisation effects as well as for absorption (numerical). The program suite CrysAlisPro was used for data collection, multi-scan absorption correction and data reduction.[197] Structures were solved with direct methods using SIR97[198] and were refined by full-matrix least-squares methods on F^2 with SHELXL-97.[199] The structures were checked for higher symmetry with help of the program Platon.[200] Supplementary crystallographic data can be obtained free of charge from the Cambridge Crystallographic Data Centre via www.ccdc.cam.ac.uk/structure).

8.2 Synthetic Procedures

8.2.1 [Re(η^6-C_6H_6)$_2$](OTf) ([**1**](OTf)) and ([**1**](PF_6))

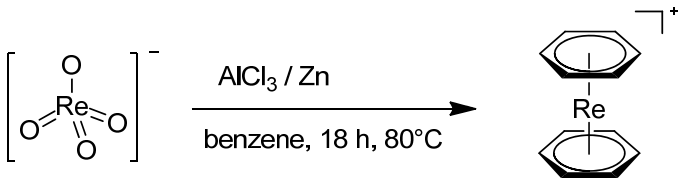

Synthesis: A 1.5 g (5.2 mmol, 1 equiv) portion of $KReO_4$ was suspended in 50 mL benzene. Afterwards, 1.01 g (15.5 mmol, 3 equiv) zinc dust and 8.32 g (62.4 mmol, 12 equiv) anhydrous $AlCl_3$ were added to the suspension. The reaction mixture was stirred for 18 h at 80°C. The solvent was evaporated *in vacuo* and the residue was washed with Et_2O (3 x 60 mL). The solid residue was suspended in 150 ml of H_2O and filtered. 1.22 g (7.8 mmol, .1.5 equiv) lithium triflate (LiOTf) was added to the filtrate. The product was extracted by continuous liquid-liquid extraction (DCM/water) overnight. The organic layer was evaporated which afforded [**1**](OTf) as analytically pure, yellow crystalline powder. Yield: 1.27 g (2.6 mmol, 50%). The corresponding [**1**](PF_6) could be obtained by addition of ammonium hexafluorophosphate (NH_4PF_6) in a yield of 1.51 g (3.21 mmol, 60%).

Analysis: ^{1}H NMR (400 MHz, $(CD_3)_2CO$) δ [ppm]: 6.16 (s, 12H, C*H*$_{arom}$). ^{13}C NMR (100 MHz, $(CD_3)_2CO$) δ [ppm]: 77.65 (*C*H$_{arom}$). ESI-MS: m/z = 343.1 $[M]^+$. IR ν: 3076 (w), 1432 (m), 1256 (s), 1221 (m), 1143 (s), 1027 (s), 1006 (m), 906 (w), 858 (m), 830 (m), 753 (w) cm^{-1}. Anal. Calcd for $C_{13}H_{12}F_3O_3Re_1S$: C 31.77, H 2.46; found: C 31.57, H 2.43. Anal. Calcd for $C_{12}H_{12}F_6PRe$: C 29.57, H 2.48; found: C 29.31, H 2.39.

8.2.2 [Re(η^6-$C_6H_5CH_3$)$_2$](OTf) ([**2**](OTf)) and([**2**](PF_6))

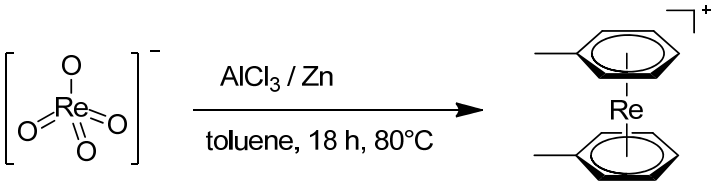

Synthesis: A 0.5 g (1.72 mmol, 1 equiv) portion of $KReO_4$ was suspended in 16 mL toluene. Afterwards, 0.33 g (5.17 mmol, 3 equiv) zinc dust and 2.76 g (20.7 mmol, 12 equiv) anhydrous $AlCl_3$ were added to the suspension. The reaction mixture was stirred for 18 h at 80°C. The solvent was evaporated *in vacuo* and the residue was washed with Et_2O (3 x 60 mL). The solid residue was suspended in 50 ml of H_2O and filtered. 0.40 g (2.58 mmol, 1.5 eq.) lithium triflate (LiOTf) was added

to the filtrate. The product was extracted with dichloromethane (3 x 20 mL). The organic layer was evaporated which afforded [**2**](OTf) as analytically pure, yellow crystalline powder. Single crystals, suitable for X-ray diffraction analysis were obtained by vapour diffusion from Et_2O (antisolvent) into acetone (solvent). Yield: 348 mg (0.69 mmol, 41%). The corresponding [**2**](PF_6) could be obtained by addition of ammonium hexafluorophosphate (NH_4PF_6) in a yield of 0.386 g (0.77 mmol, 45%).

Analysis: ^{1}H NMR (500 MHz, $(CD_3)_2CO$) δ [ppm]: 6.17 (d, $^3J(HH)$ = 5.7 Hz, 4H, *o*-CH_{arom}), 6.05 (t, $^3J(HH)$ = 5.5 Hz, 4H, *m*-CH_{arom}), 6.00 (t, $^3J(HH)$ = 5.3 Hz, 2H, *p*-CH_{arom}), 2.32 (s, 6H, CH_3). ^{13}C NMR (125 MHz, $(CD_3)_2CO$) δ [ppm]: 94.5 (*C*CH_3), 80.1 (*o*-*C*H_{arom}), 77.5 (*p*-*C*H_{arom}), 77.2 (*m*-*C*H_{arom}), 20.7 (*C*H_3). ESI-MS: m/z = 371.1 $[M]^+$. IR ν: 3069 (w), 1526 (w), 1448 (m), 1394 (w), 1256 (s), 1220 (m), 1206 (w), 1158 (s), 1145 (s), 1025 (s), 987 (w), 911 (w), 842 (m), 773 (w), 754 (w) cm^{-1}. HR-ESI-MS $C_{16}H_{20}Re$ $[M]^+$: calculated, 371.0809; found, 371.0805. Anal. calcd. for $C_{14}H_{16}F_6PRe$: C 32.62, H 3.13; found: C 34.66, H 3.01.

^3J

8.2.3 [Re(η^6-*p*-$C_6H_4(CH_3)_2)_2$](OTf) ([**3**](OTf))

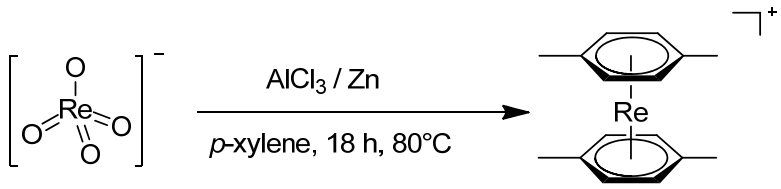

Synthesis: A 0.5 g (1.72 mmol, 1 equiv) portion of $KReO_4$ was suspended in 20 mL *p*-xylene. Afterwards, 0.33 g (5.17 mmol, 3 equiv) zinc dust and 2.76 g (20.7 mmol, 12 equiv) anhydrous $AlCl_3$ were added to the suspension. The reaction mixture was stirred for 18 h at 80°C. The solvent was evaporated *in vacuo* and the residue was washed with Et_2O (3 x 60 mL). The solid residue was suspended in 50 ml of H_2O and filtered. 0.40 g (2.58 mmol, 1.5 eq.) lithium triflate (LiOTf) was added to the filtrate. The product was extracted by continuous liquid-liquid extraction (DCM/water) overnight. The organic layer was evaporated which afforded [**3**](OTf) as analytically pure, yellow crystalline powder. Single crystals, suitable for X-ray diffraction analysis were obtained by vapour diffusion from Et_2O (antisolvent) into acetone (solvent). Yield: 293 mg (0.53 mmol, 31%).

Analysis: ^{1}H NMR (500 MHz, $(CD_3)_2CO$) δ [ppm]: 6.06 (s, 8H, *o*-CH_{arom}), 2.23 (s, 12H, CH_3). ^{13}C NMR (125 MHz, $(CD_3)_2CO$) δ [ppm]: 94.5 (*C*CH_3), 79.5 (*o*-*C*H_{arom}), 19.9 (*C*H_3). ESI-MS: m/z = 399.1 $[M]^+$. IR ν: 3066 (w), 1474 (m), 1394 (m), 1263 (s), 1217 (m), 1146 (s), 1028 (s), 906 (w), 868 (w), 809 (m), 751 (w), 712 (w) cm^{-1}. HR-ESI-MS $C_{16}H_{20}Re$ $[M]^+$: calculated, 399.1123; found, 399.1115.

8.2.4 [Re(η^6-*o*-$C_6H_4(CH_3)_2)_2$](OTf) ([**4**](OTf))

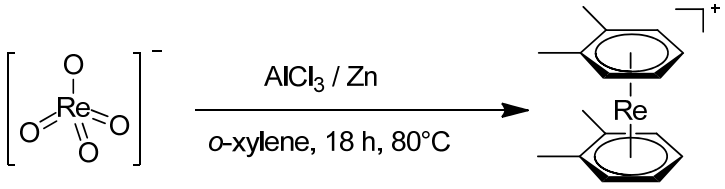

Synthesis: A 0.5 g (1.72 mmol, 1 equiv) portion of $KReO_4$ was suspended in 20 mL *o*-xylene. Afterwards, 0.33 g (5.17 mmol, 3 equiv) zinc dust and 2.76 g (20.7 mmol, 12 equiv) anhydrous $AlCl_3$ were added to the suspension. The reaction mixture was stirred for 18 h at 80°C. The solvent was evaporated *in vacuo* and the residue was washed with Et_2O (3 x 60 mL). The solid residue was suspended in 50 ml of H_2O and filtered. 0.40 g (2.58 mmol, 1.5 eq.) lithium triflate (LiOTf) was added to the filtrate. The product was extracted by continuous liquid-liquid extraction (DCM/water) overnight. The organic layer was evaporated which afforded [**4**](OTf) as analytically pure, yellow crystalline powder. Single crystals, suitable for X-ray diffraction analysis were obtained by vapour diffusion from Et_2O (antisolvent) into acetone (solvent). Yield: 264 mg (0.48 mmol, 28%).

Analysis: ^{1}H NMR (500 MHz, $(CD_3)_2CO$) δ [ppm]: 6.06 (m, 4H, *o*-C*H*$_{arom}$), 5.92 (m, 4H, *m*-C*H*$_{arom}$), 2.29 (s, 12H, C*H*$_3$). ^{13}C NMR (125 MHz, $(CD_3)_2CO$) δ [ppm]: 94.1 (*C*CH_3), 80.4 (*o*-*C*H$_{arom}$), 77.2 (*m*-*C*H$_{arom}$), 18.8 (*C*H_3). ESI-MS: m/z = 399.1 $[M]^+$. IR ν: 3072 (w), 1454 (m), 1391 (w), 1261 (s), 1222 (m), 1148 (s), 1026 (s), 987 (w), 903 (w), 873 (m), 754 (w), 720 (w) cm^{-1}. HR-ESI-MS $C_{16}H_{20}Re$ $[M]^+$: calculated, 399.1123; found, 399.1115.

8.2.5 [Re(η^6-*m*-$C_6H_4(CH_3)_2)_2$](OTf) ([**5**](OTf))

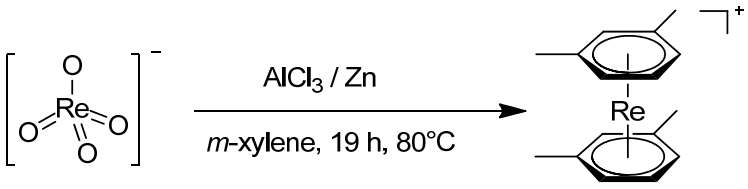

Synthesis: The synthesis was performed by Carla Gotzmann (PhD student, University of Zurich). Potassium perrhenate (504.5 mg, 1.74 mmol, 1 equiv), Zinc powder (345.1 mg, 5.28 mmol, 3 equiv) and Aluminium trichloride (2.30 g, 17.25 mmol, 9.9 equiv) were given to a Schlenk-flask under Nitrogen and 26 mL *m*-xylene were added. The black suspension was heated to 80°C under reflux conditions for 19 h. The reaction was allowed to cool down and the flask was cooled in an ice bath. The reaction mixture was quenched carefully by adding water dropwise. The *m*-xylene solvent phase was separated off with a pipette. The flask with the reaction mixture in water was sonicated carefully to solubilise the black sticky solid. The remaining residue was filtered off and washed very well with

water. The water phase was washed twice with Et_2O and lithium triflate (300 mg, 1.922 mmol, 1.1 equiv) was added to the water phase. Afterwards, the solution was extracted with dichloromethane via liquid-liquid extraction over the weekend. The organic solvent was removed under reduced pressure and the product was further dried *in vacuo*. A yellow solid of [**5**](OTf) (270.3 mg, 0.493 mmol, 29%) was obtained. Single crystals, suitable for X-ray diffraction analysis were obtained by vapour diffusion from Et_2O (antisolvent) into acetone (solvent).

Analysis: ^{1}H NMR (500 MHz, $(CD_3)_2CO$) δ [ppm]: 6.15 (s, 2H, *o*-CH_{arom}), 6.01 (d, ^{3}*J(HH)* = 5.5 Hz, 4H, *o*-CH_{arom}), 5.93 (t, ^{3}*J(HH)* = 5.5 Hz, 2H, *m*-CH_{arom}), 2.25 (s, 12H, CH_3). ^{13}C NMR (125 MHz, $(CD_3)_2CO$) δ [ppm]: 93.2 (*C*CH_3), 82.3 (*o*-*C*H_{arom}), 79.6 (*o*-*C*H_{arom}), 77.0 (*m*-*C*H_{arom}), 20.4 (*C*H_3). ESI-MS: m/z = 399.1 $[M]^+$. IR ν: 3067 (w), 2928 (w), 1526 (w), 1457 (m), 1389 (m), 1261 (s), 1221 (s), 1139 (s), 1065 (w), 1027 (s), 990 (m), 905 (m), 874 (m), 752 (w), 722 (w) cm^{-1}. HR-ESI-MS $C_{16}H_{20}Re$ $[M]^+$: calculated, 399.1117; found, 399.1113.

8.2.6 $[Re(\eta^6\text{-}C_6H_3(CH_3)_3)_2](PF_6)$ ([**6**](PF_6))

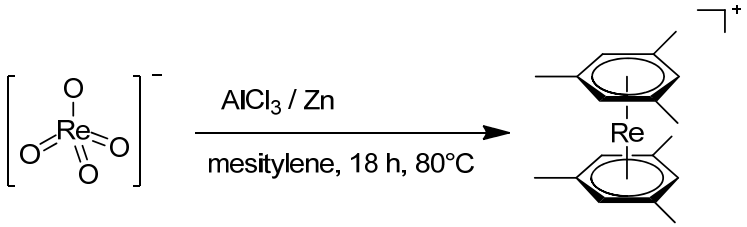

Synthesis: 1.45 g (5 mmol, 1 eq.) of $KReO_4$ was suspended in 40 mL mesitylene. Afterwards, 0.98 g (15 mmol, 3 eq.) zinc dust and 6.68 g (50 mmol, 10 eq.) anhydrous $AlCl_3$ were added to the suspension. The reaction mixture was stirred for 22 h at 80°C. The solvent was evaporated *in vacuo* and the residue was washed with Et_2O (6 x 50 mL). The solid residue was suspended in 50 ml of H_2O and filtered. 1.40 g (7.5 mmol, 1.5 eq.) ammonium hexafluorophosphate (NH_4PF_6) was added to the filtrate. The product was extracted with dichloromethane (6 x 50 mL). The organic layer was evaporated which afforded ([**6**](PF_6)) as analytically pure, yellow crystalline powder. Single crystals, suitable for X-ray diffraction analysis were obtained by vapour diffusion from Et_2O (antisolvent) into acetone (solvent). Yield: 1.57 g (55%).

Analysis: ^{1}H NMR (400 MHz, $(CD_3)_2CO$) δ [ppm]: 5.91 (s, 6H, CH_{arom}), 2.32 (s, 18H, CH_3). ^{13}C NMR (100 MHz, $(CD_3)_2CO$) δ [ppm]: 91.9 (*C*CH_3), 81.3(*C*H_{arom}), 19.9 (*C*H_3). ESI-MS: m/z = 427.1 $[M]^+$. IR ν: 2924 (w), 1535 (w), 1456 (m), 1382 (m), 1302 (w), 1038 (m), 1013 (w), 914 (w), 874 (w), 824 (s), 739 (w) cm^{-1}. Anal. calcd. for $C_{18}H_{24}F_6PRe$: C 37.83, H 4.23; found: C 37.55, H 4.20.

8.2.7 [Re(η^6-$C_6H_4(CH_2)_7CH_3)_2$)](OTf) ([**7**](OTf))

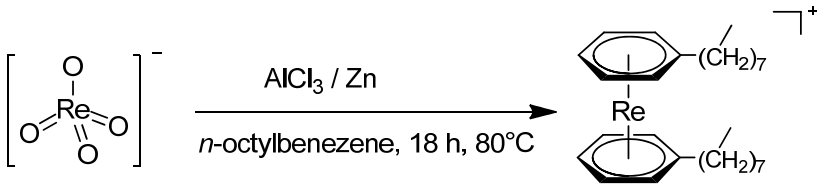

Synthesis: A 0.58 g (2 mmol, 1 equiv) portion of $KReO_4$ was suspended in 16 mL *n*-octylbenzene. Afterwards, 1.177 g (18 mmol, 9 equiv) zinc dust and 2.66 g (20 mmol, 10 equiv) anhydrous $AlCl_3$ were added to the suspension. The reaction mixture was stirred for 20 h at 80°C. Afterwards, the mixture was cooled to room temperature, washed under vigorously stirring with hot heptane (3 x 20 mL) and Et_2O (2 x 50 mL). The residue was dissolved in 50 mL dichloromethane and washed with (2 x 50 mL) water and with 50 mL brine. After drying the organic layer with $MgSO_4$, the solvent was removed *in vacuo*. The crude product was dissolved in 6 mL (0.1 TFA/H_2O/ACN, 1:1) mixture and purified by preparative HPLC (Reprosil 100 C18, 250 mm x 40 mm, 0.1% TFA/CH_3CN, gradient G1). Analytically pure oily yellow [**7**](OTf), [**9**](OTf) and crystalline yellow [**8**](OTf) were extracted from the solutions upon addition of LiOTf. Yields: 379.1 mg (0.52 mmol, 26%) for [**7**](OTf), 57.1 mg (0.09 mmol, 4.7%) for [**8**](OTf) and 22.4 mg (0.03 mmol, 1.3%) for [**9**](OTf). Single crystals, suitable for X-ray diffraction analysis were obtained by slow evaporation of an acetonitrile solution of [**8**](OTf).

Analysis: [Re(η^6-$C_6H_4(CH_2)_7CH_3)_2$)](OTf) ([**7**](OTf)): ^{1}H NMR (500 MHz, CD_3CN) δ [ppm]: 5.91 (d, ^{3}*J(HH)* = 5.5 Hz, 4H, *o*-CH_{arom}), 5.84 (t, ^{3}*J(HH)* = 5.5 Hz, 4H, *m*-CH_{arom}), 5.79 (t, ^{3}*J(HH)* = 5.5 Hz, 2H, *p*-CH_{arom}), 2.26 (t, ^{3}*J(HH)* = 7.3 Hz, 4H, CH_2), 1.51 (quint, ^{3}*J(HH)* = 7.3 Hz, 4H, CH_2), 1.29 (m, 20H, CH_2), 0.88 (t, ^{3}*J(HH)* = 6.5 Hz, 6H, CH_3). ^{13}C NMR (125 MHz, CD_3CN) δ [ppm]: 122.2 (q, *C*F_3), 99.1 (*C*CH_2), 79.3 (*o*-*C*H_{arom}), 77.4 (*p*-*C*H_{arom}), 77.1 (*m*-*C*H_{arom}), 35.6 (*C*H_2), 32.6 (*C*H_2), 32.5 (*C*H_2), 29.9 (*C*H_2), 29.8 (*C*H_2), 29.7 (*C*H_2), 23.4 (*C*H_2), 14.4 (*C*H_3). ESI-MS: m/z = 567.3 $[M]^+$. IR ν: 3070 (w), 2957 (w), 2924 (m), 2854 (w), 1447 (w), 1407 (w), 1260 (s), 1223 (s), 1153 (s), 1029 (s), 906 (w), 861 (w), 753 (w), 722 (w) cm^{-1}. HR-ESI-MS $C_{20}H_{28}Re$ $[M]^+$: calculated, 455.1738; found, 455.1743.

[Re(η^6-$C_6H_5(CH_2)_7CH_3$)(η^6-C_6H_6)](OTf) ([**8**](OTf)): ^{1}H NMR (500 MHz, CD_3CN) δ [ppm]: 6.02 (d, ^{3}*J(HH)* = 5.5 Hz, 2H, *o*-CH_{arom}), 5.91 (t, ^{3}*J(HH)* = 5.5 Hz, 2H, *m*-CH_{arom}), 5.86 (t, ^{3}*J(HH)* = 5.5 Hz, 1H, *p*-CH_{arom}), 5.85 (s, 6H, CH_{arom}), 2.32 (t, ^{3}*J(HH)* = 7.3 Hz, 2H, CH_2), 1.51 (quint, ^{3}*J(HH)* = 7.3 Hz, 2H, CH_2), 1.30 (m, 10H, CH_2), 0.88 (t, ^{3}*J(HH)* = 6.5 Hz, 3H, CH_3). ^{13}C NMR (125 MHz, CD_3CN) δ [ppm]: 122.2 (q, *C*F_3), 99.7 (*C*CH_2), 79.5 (*o*-*C*H_{arom}), 77.5 (*C*H_{arom}), 77.4 (*p*-*C*H_{arom}), 77.1 (*m*-*C*H_{arom}), 35.6 (*C*H_2), 32.5 (*C*H_2), 32.4 (*C*H_2), 29.9 (*C*H_2), 29.8 (*C*H_2), 29.7 (*C*H_2), 23.4 (*C*H_2), 14.7 (*C*H_3). ESI-MS: m/z = 455.2 $[M]^+$. IR ν: 3075 (w), 2957 (w), 2921 (m), 2853 (w), 1449 (w), 1435 (w), 1261 (s), 1223 (s), 1150 (s), 1029 (s), 866 (w), 837 (w), 752 (w), 722 (w) cm^{-1}. HR-ESI-MS $C_{28}H_{44}Re$ $[M]^+$: calculated, 567.2997; found, 567.2994.

[Re(η^6-$C_6H_5(CH_2)_7CH_3$)(η^6-$C_6H_4((CH_2)_7CH_3)_2$)](OTf) ([**9**]OTf)): ^{1}H NMR (500 MHz, CD_3CN) δ [ppm]: 6.00 (s, 1H, CH_{arom}), 5.84 (m, 2H, CH_{arom}), 5.81 (m, 3H, CH_{arom}), 5.76 (m, 2H, CH_{arom}), 5.70 (m, 1H, CH_{arom}), 2.25 (m, 6H, CH_2), 1.51 (m, 6H, CH_2), 1.29 (m, 30H, CH_2), 0.86 (t, ^{3}*J(HH)* = 6.5 Hz, 9H, CH_3). ^{13}C NMR (125 MHz, CD_3CN) δ [ppm]: 122.2 (q, *C*F_3), 98.9 (*C*CH_2), 98.5 (*C*CH_2), 81.6 (*C*H_{arom}), 79.3 (*C*H_{arom}), 79.3 (*C*H_{arom}), 77.5 (*C*H_{arom}), 77.3 (*C*H_{arom}), 76.8 (*C*H_{arom}), 35.6 (*C*H_2), 35.5 (*C*H_2), 32.7 (*C*H_2), 32.6 (*C*H_2), 32.6 (*C*H_2), 32.6 (*C*H_2), 30.0 (*C*H_2), 29.99 (*C*H_2), 29.97 (*C*H_2), 29.91 (*C*H_2), 29.8 (*C*H_2), 23.4 (*C*H_2), 14.4 (*C*H_3). ESI-MS: m/z = 679.4 $[M]^+$. IR ν: 3070 (w), 2953 (w), 2923 (m), 2854 (w), 1465 (w), 1377 (w), 1260 (s), 1223 (s), 1152 (s), 1029 (s), 860 (w), 752 (w), 722 (w) cm^{-1} HR-ESI-MS $C_{36}H_{60}Re$ $[M]^+$: calculated, 679.4246; found, 679.4248.

8.2.8 [Re(η^6-*t*-$C_6H_4C(CH_3)_3)_2$)](OTf) ([**10**](OTf))

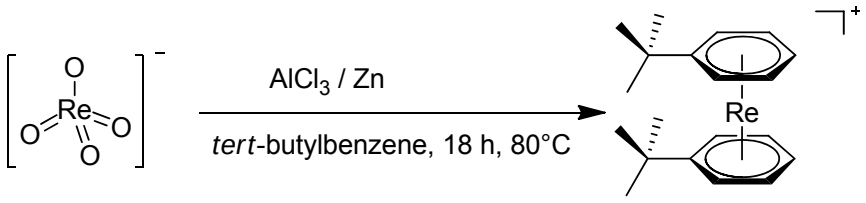

Synthesis: A 0.5 g (1.72 mmol, 1 equiv) portion of $KReO_4$ was suspended in 18 mL *tert*-butylbenzene. Afterwards, 0.33 g (5.17 mmol, 3 equiv.) zinc dust and 2.76 g (20.7 mmol, 12 equiv) anhydrous $AlCl_3$ were added to the suspension. The reaction mixture was stirred for 18 h at 80°C. The solvent was evaporated *in vacuo* and the residue was washed with Et_2O (3 x 60 mL). The crude product was dissolved in 6 mL (0.1 TFA/H_2O/ACN, 1:1) mixture and purified by preparative HPLC (Reprosil 100 C18, 250 mm x 40 mm, 0.1% TFA/CH_3CN, gradient G2). Analytically pure yellow [**10**](OTf), [**11**](OTf) and [**12**](OTf) were extracted from the solutions upon addition of LiOTf. Single crystals, suitable for X-ray diffraction analysis were obtained by slow evaporation of a CH_3CH solution of [**10**](OTf), [**11**](OTf) and [**12**](OTf). Yields: 97.1 mg (0.16 mmol, 9%) for [**10**](OTf), 271.5 mg (0.50 mmol, 29%) for [**11**](OTf) and 30.4 mg (0.04 mmol, 2.6%) for [**12**](OTf).

Analysis: [Re(η^6-*t*-$C_6H_4C(CH_3)_3)_2$)](OTf) ([**10**](OTf)): ^{1}H NMR (500 MHz, CD_3CN) δ [ppm]: 6.10 (d, ^{3}*J(HH)* = 5.8 Hz, 4H, *o*-CH_{arom}), 5.89 (m, 6H, *p*-CH_{arom}, *m*-CH_{arom}), 1.21 (s, 18H, CH_3). ^{13}C NMR (125 MHz, (CD_3CN) δ [ppm]: 122.2 (q, *C*F_3), 109.9 (*C*$C(CH_3)_3$), 76.8 (*p*-*C*H_{arom}), 76.7 (*m*-*C*H_{arom}), 76.0 (*o*-*C*H_{arom}), 35.3 (C*C*$(CH_3)_3$), 30.8 (*C*H_3). ESI-MS: m/z = 455.3 $[M]^+$. IR ν: 3083 (w), 2976 (w), 1471 (w), 1446(w), 1400 (w), 1364 (w), 1260 (s), 1223 (m), 1155 (s), 1136 (s), 1101 (w), 1028 (s), 926 (w), 860 (m), 829 (m), 753 (w) cm^{-1}. HR-ESI-MS $C_{26}H_{28}Re$ $[M]^+$: calculated, 455.1743; found, 455.1737.

[Re(η^6-*t*-$C_6H_5C(CH_3)_3$)(η^6-C_6H_6)](OTf) ([**11**](OTf)): ^{1}H NMR (500 MHz, CD_3CN) δ [ppm]: 6.16 (d, ^{3}*J(HH)* = 5.8 Hz, 2H, *o*-C*H*$_{arom}$), 5.90 (m, 3H, *p*-C*H*$_{arom}$, *m*-C*H*$_{arom}$), 5.89 (s, 6H, C*H*$_{arom}$), 1.22 (s, 9H, C*H*$_3$). ^{13}C NMR (125 MHz, (CD_3CN) δ [ppm]: 122.2 (q, *C*F_3), 110.8 (*C*C(CH$_3$)$_3$), 77.2 (*C*H$_{arom}$), 76.7 (*p*-*C*H$_{arom}$), 76.7 (*m*-*C*H$_{arom}$), 76.5 (*o*-*C*H$_{arom}$), 35.3 (C*C*(CH$_3$)$_3$), 30.8 (*C*H$_3$). ESI-MS: m/z = 399.1 [M]$^+$. IR ν: 3069 (w), 2964 (w), 1465 (w), 1435(m), 1399 (w), 1371 (w), 1257 (s), 1223 (m), 1155 (s), 1145 (s), 1102 (w), 1062 (w), 1028 (s), 863 (m), 829 (m), 755 (w) cm^{-1}. HR-ESI-MS $C_{16}H_{20}Re$ [M]$^+$: calculated, 399.1117; found, 399.1116.

[Re(η^6-*t*-$C_6H_5C(CH_3)_3$)(η^6-*t*-$C_6H_4(C(CH_3)_3)_2$)](OTf) ([**12**](OTf)): ^{1}H NMR (500 MHz, CD_3CN) δ [ppm]: 6.14 (s, 1H, *o*-C*H*$_{arom}$), 6.13 (d, ^{3}*J(HH)* = 5.9 Hz, 2H, *o*-C*H*$_{arom}$), 6.03 (d, ^{3}*J(HH)* = 5.9 Hz, 2H, *o*-C*H*$_{arom}$), 5.96 (t, ^{3}*J(HH)* = 5.3 Hz 1H, *p*-C*H*$_{arom}$), 5.89 (t, ^{3}*J(HH)* = 5.8 Hz, 1H, *m*-C*H*$_{arom}$), 5.85 (t, ^{3}*J(HH)* = 5.8 Hz, 2H, *m*-C*H*$_{arom}$), 1.24 (s, 18H, C*H*$_3$), 1.21 (s, 9H, C*H*$_3$). ^{13}C NMR (125 MHz, (CD_3CN) δ [ppm]: 122.2 (q, *C*F_3), 109.3 (*C*C(CH$_3$)$_3$), 109.1 (*C*C(CH$_3$)$_3$), 77.2 (*p*-*C*H$_{arom}$), 77.1 (*m*-*C*H$_{arom}$), 77.0 (*m*-*C*H$_{arom}$), 75.8 (*o*-*C*H$_{arom}$), 75.3 (*o*-*C*H$_{arom}$), 74.1 (*o*-*C*H$_{arom}$), 35.5 (C*C*(CH$_3$)$_3$), 35.3 (C*C*(CH$_3$)$_3$), 30.9 (*C*H$_3$). ESI-MS: m/z = 511.1 [M]$^+$. IR ν: 3078 (w), 2964 (w), 1466 (w), 1432(w), 1397 (w), 1366 (m), 1260 (s), 1222 (m), 1146 (s), 1028 (s), 869 (m), 830 (m), 754 (w) cm^{-1}. HR-ESI-MS $C_{24}H_{36}Re$ [M]$^+$: calculated, 511.2369; found, 511.2372.

8.2.9 [Re(η^6-$C_{10}H_{12}$)$_2$](OTf) ([**13**](OTf))

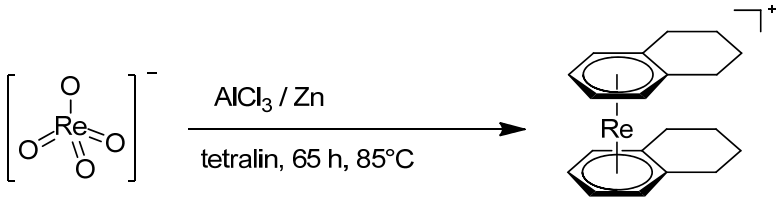

Synthesis: 725 mg (2.5 mmol, 1 equiv) of $KReO_4$ was suspended in 26 mL tetralin. Afterwards, 490 mg (7.5 mmol, 3 equiv) zinc dust and 3.34 g (25 mmol, 10 equiv) anhydrous $AlCl_3$ were added to the suspension. The reaction mixture was stirred for 65 h at 85°C. The solvent was evaporated *in vacuo* and the residue was washed with Et_2O (6 x 50 mL). The solid residue was suspended in 90 ml of H_2O and filtered. 486 mg (3 mmol, 1.2 equiv) lithium triflate (LiOTf) was added to the filtrate. The product was extracted with dichloromethane (6 x 50 mL). The organic layer was evaporated which afforded [**13**](OTf) as analytically pure, yellow crystalline powder. Single crystals, suitable for X-ray diffraction analysis were obtained by vapour diffusion from Et_2O (antisolvent) into acetone (solvent). Yield: 174 mg (0.30 mmol, 12%).

Analysis: ^{1}H NMR (400 MHz, $(CD_3)_2CO$) δ [ppm]: 6.09 (m, 4H, C*H*$_{arom}$), 5.95 (m, 4H, C*H*$_{arom}$), 2.92 (m, 4H, C*H*$_2$), 2.75 (m, 4H, C*H*$_2$), 1.74 (m, 8H, C*H*$_2$). ^{13}C NMR (100 MHz, $(CD_3)_2CO$) δ [ppm]: 96.7 (*C*CH$_{arom}$),

78.7 (CH_{arom}), 78.2 (CH_{arom}), 29.1 (CH_2), 23.0 (CH_2). ESI-MS: m/z = 451.1 $[M]^+$. IR ν: 3070 (w), 2945 (w), 2887 (m), 1449 (m), 1430 (w), 1265 (s), 1223 (s), 1146 (s), 1082 (w), 1027 (s), 906 (w), 862 (w), 753 (w), 714 (w) cm^{-1}. HR-ESI-MS $C_{20}H_{24}Re$ $[M]^+$: calculated, 451.1433; found, 451.1431. Anal. calcd. for $C_{21}H_{24}F_3O_3ReS$: C 42.06, H 4.03; found: C 42.42, H 4.06.

8.2.10 $[Re(\eta^6\text{-}C_{13}H_{10})_2](OTf)$ ([**14**](OTf))

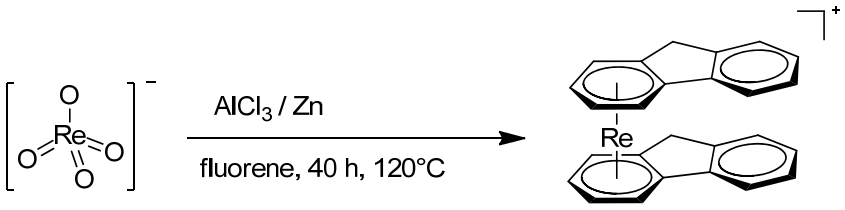

Synthesis: A 0.58 g (2 mmol, 1 equiv) portion of $KReO_4$ was mixed in 4.0 g (78 mmol, 15.6 equiv) fluorene. Afterwards, 0.784 g (12 mmol, 6 equiv) zinc dust and 2.66 g (20 mmol, 10 equiv) anhydrous $AlCl_3$ were added to the suspension. The reaction mixture was stirred for 40 h at 120°C. Afterwards, the mixture was cooled to room temperature, washed under vigorously stirring with 25 ml dibutyl ether and Et_2O (5 x 30 mL). The crude product was suspended in 150 mL deionized water, stirred for 30 minutes, and filtrated through a glass filter. To the filtrate 374 mg (2.4 mmol, 1.2 equiv) lithium trifluoromethanesulfonate was added, followed by extraction with 200 ml dichloromethane. The organic phase was dried with anhydrous magnesium sulfate and concentrated *in vacuo*, yielding 216 mg (16 %) product as a yellow powder. To obtain a second batch the filter cake was suspended again in 150 ml deionized water, followed by 30 minutes of stirring, addition of 374 mg (2.4 mmol, 1.2 equiv) lithium trifluoromethanesulfonate and extraction with 200 ml dichloromethane. After addition of anhydrous magnesium sulfate and concentration *in vacuo,* other 107 mg (8%) of product were obtained. Overall yield of [**14**](OTf): 323 mg (0.48 mmol, 24%). Single crystals, suitable for X-ray diffraction analysis were obtained by vapour diffusion from Et_2O (antisolvent) into acetone (solvent).

Analysis: ^{1}H NMR (500 MHz, CD_3CN) δ [ppm]: *syn*-isomer: 7.30 (m, 2H, CH_{arom}), 7.13 (d, 2H, CH_{arom}), 7.12 (t, 2H, CH_{arom}), 7.04 (d, 2H, CH_{arom}), 6.41 (d, 2H, CH_{arom}), 6.35 (d, 2H, CH_{arom}), 5.96 (d, 2H, CH_{arom}), 5.88 (d, 2H, CH_{arom}), 3.40 (d, 2H, CH_2), 2.45 (d, 2H, CH_2), *anti*-isomer: 7.40 (d, 2H, CH_{arom}), 7.29 (m, 2H, CH_{arom}), 7.25 (m, 2H, CH_{arom}), 6.90 (d, 2H, CH_{arom}), 6.58 (d, 2H, CH_{arom}), 6.45 (d, 2H, CH_{arom}), 5.92 (d, 2H, CH_{arom}), 5.85 (d, 2H, CH_{arom}), 3.19 (d, 2H, CH_2), 1.76 (d, 2H, CH_2). ^{13}C NMR (125 MHz, CD_3CN) δ [ppm]: *syn*-isomer: 143.18 (*C*), 137.35 (*C*), 129.78 (CH_{arom}), 128.30 (CH_{arom}), 126.20 (CH_{arom}), 122.17 (CH_{arom}), 99.14 (*C*), 98.66 (*C*), 76.73 (CH_{arom}), 76.37 (CH_{arom}), 76.30 (CH_{arom}), 71.63 (CH_{arom}), 36.09 (CH_2), *anti*-isomer: 143.44 (*C*), 137.01 (*C*), 129.91 (CH_{arom}), 128.32 (CH_{arom}), 126.49 (CH_{arom}), 122.35 (CH_{arom}), 98.88 (*C*), 98.57 (*C*), 76.13 (CH_{arom}), 75.75 (CH_{arom}), 75.58 (CH_{arom}), 71.99 (CH_{arom}), 35.32 (CH_2), ESI-MS:

m/z =519.1 $[M]^+$. IR ν: 3066 (w), 1613 (w), 1464 (w), 1424 (m), 1255 (s), 1223 (s), 1150 (s), 1029 (s), 990 (w), 949 (w), 906 (w), 854 (w), 757 (m), 716 (m) cm^{-1}. HR-ESI-MS $C_{26}H_{20}Re$ $[M]^+$: calculated, 519.1118; found, 519.1118. Anal. calcd. for $C_{27}H_{20}F_3O_3ReS$: C 48.57, H 3.02; found: C 47.92, H 2.93.

8.2.11 $[Re(\eta^6\text{-}C_{12}H_{10})_2](OTf)$ ([**15**](OTf))

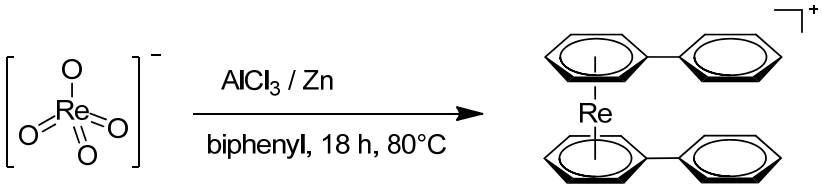

Synthesis: 1.45 g (5 mmol, 1 eq.) of $KReO_4$, 990 mg (15 mmol, 3 eq.) zinc dust and 7.10 g (53 mmol, 11 eq.) anhydrous $AlCl_3$ were mixed in 12.0 g (78 mmol, 15.6 eq.) biphenyl. The reaction mixture was stirred for 22 h at 80°C. Afterwards, the mixture was cooled down to room temperature, washed with heptane (3 x 70 mL) and filtrated. The solid residue was suspended in 140 ml of H_2O and filtered. 780 mg (5 mmol, 1 eq.) lithium triflate (LiOTf) was added to the filtrate. The product was extracted with dichloromethane (3 x 50 mL). The organic phase was evaporated which afforded [**15**](OTf) as analytically pure, yellow crystalline powder. Single crystals, suitable for X-ray diffraction analysis were obtained by vapour diffusion from Et_2O (antisolvent) into acetone (solvent). Yield: 1.235 g (1.9 mmol, 38%).

Analysis: ^{1}H NMR (400 MHz, $(CD_3)_2CO$) δ [ppm]: 7.46 (m, 4H, CH_{arom}), 7.36 (m, 2H, CH_{arom}), 7.29 (m, 4H, CH_{arom}), 6.68 (d, $^3J(HH)$ = 6.05 Hz, 4H, *o*-CH_{arom}), 6.33 (m, $^3J(HH)$ = 5.8 Hz, 4H, *m*-CH_{arom}), 6.18 (m, $^3J(HH)$ = 5.4 Hz, 2H, *p*-CH_{arom}). ^{13}C NMR (100 MHz, $(CD_3)_2CO$) δ [ppm]: 136.7 (*C*H_{arom}), 130.2 (*C*H_{arom}), 129.9 (*C*H_{arom}), 128.8 (*C*H_{arom}), 97.1 (*C*CH_{arom}), 79.2 (*C*H_{arom}), 78.7 (*C*H_{arom}), 78.6 (*C*H_{arom}). ESI-MS: m/z = 495.0 $[M]^+$. IR ν: 3071 (w), 1524 (w), 1497 (w), 1445 (m), 1399 (w), 1272 (s), 1250 (s), 1222 (s), 1143 (s), 1025 (s), 1004 (m), 854 (m), 777 (m), 765 (m), 743 (m), 710 (m) cm^{-1}. HR-ESI-MS $C_{24}H_{20}Re$ $[M]^+$: calculated, 495.1114; found, 495.1116. Anal. calcd. for $C_{25}H_{20}F_3O_3ReS$: C 46.65, H 3.13; found: C 46.68, H 3.09. Anal. calcd. for $C_{24}H_{20}F_3O_3ReS$: C 45.07, H 3.15; found: C 44.67, H 2.82 (with PF_6).

8.2.12 [Re(η^6-$C_{12}H_{10}$)$_2$](OTf) ([**16**](PF_6))

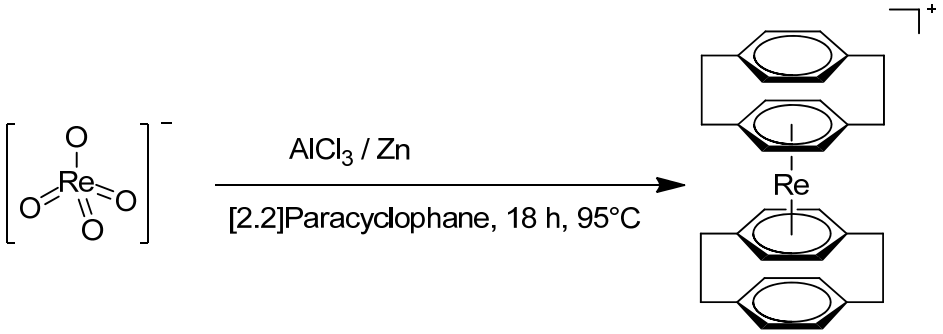

Synthesis: A 0.5 g (1.72 mmol, 1 equiv) portion of $KReO_4$ was suspended in a mixture of mL benzene and 5.0 g [2.2] Paracyclophane. Afterwards, 0.33 g (5.17 mmol, 3 equiv.) zinc dust and 2.76 g (20.7 mmol, 12 equiv) anhydrous $AlCl_3$ were added to the suspension. The reaction mixture was stirred for 18 h at 95°C. Afterwards, the mixture was cooled to room temperature, washed under vigorously stirring with hot heptane (3 x 20 mL) and Et_2O (3 x 60 mL). The mixture was filtrated and the solid residue was suspended in 50 ml of H_2O and filtered again. All aqueous solutions were reduced in volume to less than 8 ml. The crude product was purified by preparative HPLC (Reprosil 100 C18, 250 mm x 40 mm, 0.1% TFA/CH_3CN, gradient G3). The solvent was evaporated and the solid dissolved in water. After the addition of ammonium hexafluorophosphate (424 mg, 2.6 mmol), [**16**](PF_6) precipitated as analytically pure, yellow crystalline powder, which was filtered and dried. Single crystals, suitable for X-ray diffraction analysis were obtained by vapour diffusion of Et_2O into a solution of [**16**](PF_6) in acetone. Yield: 154.2 mg (0.206 mmol, 12%).

Analysis: ^{1}H NMR (400 MHz, $(CD_3)_2CO$) δ [ppm]: 6.83 (s, 8H, CH_{arom}), 4.10 (s, 8H, CH_{arom}), 3.14 (m, 8H, CH_2), 2.58 (m, 8H, CH_2). ^{13}C NMR (100 MHz, $(CD_3)_2CO$) δ [ppm]: 140.8 (C_{arom}), 134.24 (CH_{arom}), 116.9 (C_{arom}), 71.8 (CH_{arom}), 34.8 (CH_2), 32.9 (CH_2). ESI-MS: m/z = 603.3 $[M]^+$. IR ν: 2939 (w), 1498 (w), 1413 (w), 1240 (w), 1065 (w), 829 (s), 720 (w) cm^{-1}. HR-ESI-MS $C_{32}H_{32}Re$ $[M]^+$: calculated, 603.2056; found, 603.2058.

8.2.13 [Re(η^6-$C_6(CH_3)_6$)(η^6-C_6H_6)](OTf) ([**17**](OTf))

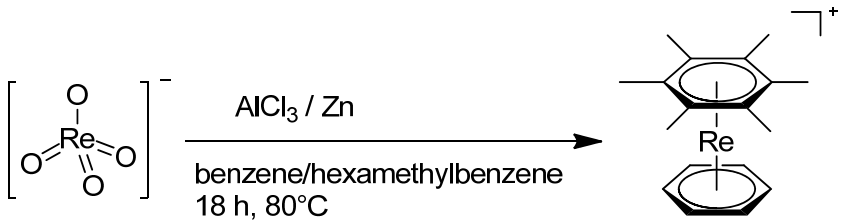

Synthesis: The synthesis, as well as the characterization of compound [17](OTf), were reported in the master thesis of Sara Jordi.[116]

8.2.14 [Re(η^6-$C_{10}H_8$)$_2$](OTf) ([**7p**](OTf))

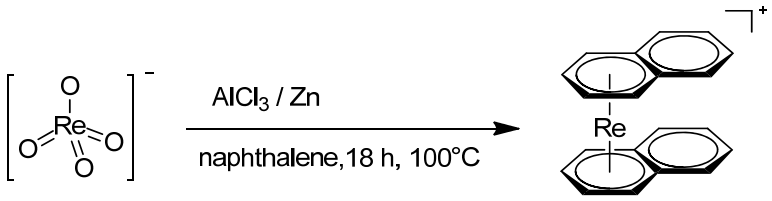

Synthesis: The synthesis as well as the characterization of compound [**7p**](OTf), were reported in literature.[117]

8.2.15 [Re(η^6-$C_{10}H_8$)(η^6-C_6H_6)](OTF) ([**6p**]OTf)

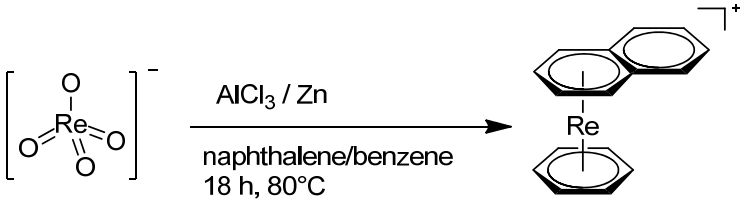

Synthesis: The synthesis, as well as the characterisation of compound [6p](OTf), were reported in literature.[117] The crude product was purified by preparative HPLC (Reprosil 100 C18, 250 mm x 40 mm, 0.1% TFA/CH_3CN, gradient G4). The side-products are purified and characterized. The yields are listed in section 6.1.

Analysis: [Re(η^6-$C_{12}H_{10}$)(η^6-C_6H_6)](PF_6): ^{1}H NMR (500 MHz, $(CD_3)_2CO$) δ [ppm]: 7.65 (m, 2H, CH_{arom}), 7.44 (m, 2H, CH_{arom}), 6.76 (d, 2H, *o*-CH_{arom}), 6.39 (t, 2H, *m*-CH_{arom}), 6.23 (t, 1H, *p*-CH_{arom}), 6.12 (t, 6H, CH_{arom}). ^{13}C NMR (125 MHz, $(CD_3)_2CO$) δ [ppm]: 136.51 (C_{arom}), 129.35 (CH_{arom}), 128.93 (CH_{arom}), 127.90 (CH_{arom}), 95.84 (C_{arom}), 78.03 (CH_{arom}), 77.3 (*o*-CH_{arom}), 76.4 (*p*-CH_{arom}), 76.04 (*m*-CH_{arom}). ESI-MS: m/z = 419.1 $[M]^+$. IR ν: 3098 (w), 2922 (w), 1485 (w), 1435 (m), 1399 (w), 1079 (w), 927 (w), 877 (w), 816 (s), 766 (m), 740 (w) cm^{-1}. HR-ESI-MS $C_{18}H_{16}Re$ $[M]^+$: calculated, 419.0804; found, 419.0797

[Re(η^6-$C_{10}H_{12}$)(η^6-C_6H_6)](PF_6): ^{1}H NMR (500 MHz, CD_3CN) δ [ppm]: 6.03 (t, 2H, CH_{arom}), 5.83 (t, 2H, CH_{arom}), 5.79 (s, 6H, CH_{arom}), 2.89 (m, 2H, CH_2), 2.62 (m, 2H, CH_2), 1.73 (m, 2H, CH_2), 1.68 (m, 2H, CH_2). ^{13}C NMR (125 MHz, CD_3CN) δ [ppm]: 98.55 (*C*-CH_2), 77.81 (CH_{arom}), 77.59 (CH_{arom}), 77.35 (CH_{arom}), 29.30 (CH_2), 22.82 (CH_2). ESI-MS: m/z = 397.0 $[M]^+$. IR ν: 3098 (w), 2960 (w), 1451 (m), 1434 (m), 1053 (w), 909 (w) 816 (s) cm^{-1}. HR-ESI-MS $C_{16}H_{18}Re$ $[M]^+$: calculated, 397.0961; found, 397.0960

[Re(η^6-$C_{10}H_{12}$)(η^6-$C_{10}H_8$)](PF_6): ^{1}H NMR (500 MHz, CD_3CN) δ [ppm]: 7.52 (m, 2H, CH_{arom}), 7.49 (m, 2H, CH_{arom}), 6.74 (dd, 2H, CH_{arom}), 6.02 (dd, 2H, CH_{arom}), 5.70 (dd, 2H, CH_{arom}), 5.30 (dd, 2H, CH_{arom}) 2.61 (m, 2H, CH_2), 1.88 (m, 2H, CH_2), 1.55 (m, 2H, CH_2), 1.42 (m, 2H, CH_2). ^{13}C NMR (125 MHz, CD_3CN) δ

[ppm]: 131.66 (*C*H$_{arom}$), 131.44 (*C*H$_{arom}$), 95.52 (*C*-CH$_2$), 92.55 (*C*-CH$_{arom}$), 79.03 (*C*H$_{arom}$), 76.82(*C*H$_{arom}$), 75.78(*C*H$_{arom}$), 74.30(*C*H$_{arom}$), 28.22 (*C*H$_2$), 22.33 (*C*H$_2$). IR ν: 3062 (w), 2929 (w), 1450 (w), 1432 (w) 1406 (w) 1245 (w) 1051 (w) 1010 (w), 906 (m), 824 (s), 750 (s) cm^{-1}. HR-ESI-MS $C_{20}H_{20}Re$ $[M]^+$: calculated, 447.1117; found, 447.1120

8.3 Supplementary Information: Bis-arene Complexes $[Re(\eta^6\text{-arene})_2]^+$ as Highly Stable Bioorganometallic Scaffolds

Bis-arene Complexes $[Re(\eta^6\text{-arene})_2]^+$ as Highly Stable Bioorganometallic Scaffolds

Giuseppe Meola, Henrik Braband, Paul Schmutz, Michael Benz, Bernhard Spingler, and Roger Alberto

Department of Chemistry, University of Zürich, Winterthurerstrasse 190, CH-8057 Zürich Switzerland

Table of Content

General Information

Materials

Characterization

Synthetic procedures

$[Re(\eta^6\text{-}C_6H_6)_2](OTf)$ ($[1^+]OTf$)

$[Re(\eta^5\text{-}C_6H_6C_4H_9)(\eta^6\text{-}C_6H_6)]$ (2)

$[Re(\eta^5\text{-}C_6H_7)(\eta^6\text{-}C_6H_6)]$ (3)

$[Re(\eta^6\text{-}C_6H_5Br)(\eta^6\text{-}C_6H_6)](PF_6)$ ($[4^+]PF_6$) and $[Re(\eta^6\text{-}C_6H_5Br)_2](PF_6)$ ($[5^+]PF_6$)

$[Re(\eta^6\text{-}C_6H_5COOH)(\eta^6\text{-}C_6H_6)](TFA)$ ($[6^+]TFA$) and $[Re(\eta^6\text{-}C_6H_5COOH)_2](TFA)$ ($[7^+]TFA$)

$[Re(\eta^6\text{-}C_6H_5SCH_2Ph)(\eta^6\text{-}C_6H_6)](PF_6)$ ($[10^+]PF_6$)

$[Re(\eta^6\text{-}C_6H_5NHPh)(\eta^6\text{-}C_6H_6)](PF_6)$ ($[11^+]PF_6$)

$[Re(\eta^6\text{-}C_6H_5SCH_2Ph)_2](PF_6)$ ($[12^+]PF_6$)

$[Re(\eta^6\text{-}C_6H_5NHPh)_2]$ ($[13^+]PF_6$)

$[Re(\eta^6\text{-}C_6H_5CONHCH_2C_6H_5)(\eta^6\text{-}C_6H_6)](PF_6)$ ($[14^+]PF_6$)

$[Re(\eta^6\text{-}C_6H_5CONHCH_2Ph)_2](PF_6)$ ($[15^+]PF_6$)

$[Re(\eta^6\text{-}C_6H_5CONHCH_2CH_2C_8H_{13}O_2)_2](PF_6)$ ($[16^+]PF_6$)

NMR Spectra (^1H, ^{13}C)

^1H NMR $[Re(\eta^6\text{-}C_6H_5Br)(\eta^6\text{-}C_6H_6)](PF_6)$ ($[4^+]PF_6$)

^{13}C NMR $[Re(\eta^6\text{-}C_6H_5Br)(\eta^6\text{-}C_6H_6)](PF_6)$ ($[4^+]PF_6$)

^1H NMR $[Re(\eta^6\text{-}C_6H_5COOH)_2](TFA)$ ($[7^+]TFA$)

^{13}C NMR $[Re(\eta^6\text{-}C_6H_5COOH)_2](TFA)$ ($[7^+]TFA$)

Crystal Data

General Information

Materials

All reactions were carried out under nitrogen atmosphere on a standard nitrogen/vacuum line unless otherwise stated. The glassware was dried by the use of a heat gun or in an oven at 120 °C at least overnight. Commercially available reagents were purchased reagent-grade and used without further purification. THF was dried over Na/Benzophenone. All chemicals were purchased from Sigma Aldrich (Switzerland), except potassium perrhenate (>99%, Chempur Germany), Lithium trifluoromethanesulfonate (99%, ABCR, Germany), 3-[bis(dimethylamino)methyliumyl]-3H-benzotriazol-1-oxide hexafluorophosphate (≥99%, I^2CNS LLC Switzerland), aniline (99.5%, extra pure, ACROS Organics, Switzerland) *N,N*-dimethyl-formamide (99.8%, extra dry, AcroSeal®, ACROS Organics, Switzerland), hydrochloric acid (32%, Honeywell, Germany), carbon dioxide (>99,9, PanGas, Switzerland), and trifluoroacetic acid (99%, Alfa Aesar, Germany). The chemicals were used without farther purification. Deuterated NMR solvents were obtained from Armar Chemicals (Switzerland).

Characterization

The UV-Vis measurements were carried out on a Perkin Elmer Lambda 35 UV-Vis spectrophotometer between 200 and 900 nm. FT-IR spectra were acquired on a Perkin Elmer Spectrum Two spectrophotometer equipped with a Specac Golden Gate single reflection diamond accessory.

^{1}H-NMR and ^{13}C-NMR spectra were recorded on a BrukerDRX 400 MHz or BrukerDRX 500 MHz spectrometer. ^{1}H and ^{13}C chemical shifts were referenced with the residual solvent resonances relative to TMS. The spectra were fully assigned with the help of various experiments (1D NOE, 1H-COSY, C,H-Correlation and 13C-DEPT).

Electronspray-ionisation mass spectrometry (ESI-MS) was performed on a Bruker esquireTM/LC spectrometer or on a Bruker esquire^{TM}/HCT^{TM} spectrometer. High-resolution mass spectrometry (HR-ESI-MS) was performed on a Bruker maXis QTof high-resolution mass spectrometer (Bruker GmbH, Bremen, Germany).

Preparative HPLC was performed on a Varian ProStar 320 system, using a Dr. Maisch Reprosil C18 100-7 (40 x 250 mm) column. The solvents (HPLC grade) were 0.1% trifluoroacetic acid (solvent A) and acetonitrile (solvent B). The HPLC gradients used are as follow (G1): 0-3 minutes: 95% A (5% B); 4-49 minutes: linear gradient from 95% A (5% B) to 82% A (18% B); 49-55 minutes: 100% B. The flow

rate was 45 mL/min. Detection was performed at 260 nm; (G2):0-2 minutes: 85% A (15% B); 2.1-45 minutes: linear gradient from 85% A (15% B) to 70% A (30% B); 45-50 minutes: 100% B. The flow rate was 40 mL/min. Detection was performed at 260 nm; (G3): 0-2 minutes: 80% A (20% B); 2.1-30 minutes: linear gradient from 80% A (20% B) to 70% A (30% B); 30-40 minutes: 100% B. The flow rate was 40 mL/min. Detection was performed at 284 nm; (G4):0-2 minutes: 80% A (20% B); 2.1-35 minutes: linear gradient from 80% A (20% B) to 60% A (40% B); 35-50 minutes: 100% B. The flow rate was 40 mL/min. Detection was performed at 278 nm; (G5):0-2 minutes: 75% A (25% B); 2.1-45 minutes: linear gradient from 75% A (25% B) to 35% A (65% B); 45-50 minutes: 100% B. The flow rate was 40 mL/min. Detection was performed at 282 nm.

Analytical HPLC was performed on a VWR HITACHI Chromaster system, using a Macherey-Nagel Nucleosil C18 100-5 column. HPLC solvents were 0.1% trifluoroacetic acid (solvent A) and methanol (solvent B). Applied HPLC gradient: 0-3 minutes: 100% A; 3.1-9 minutes: 75% A, 25% B; 9.1-20 minutes: linear gradient from 66% A (34% B) to 0% A (100% B); 20-28 minutes: 100% B; 28.1-30: 100% A. The flow rate was 0.5 mL/min. Detection was performed at 250 nm.

Electrochemical measurements were carried out in acetonitrile containing 0.1 M [TBA][PF_6] as a conducting electrolyte. For all Re-Complexes, a Metrohm 757VA Computrace electrochemical analyzer was used with a standard three-electrode setup of glassy carbon working electrode (i.d.= 3 mm), platinum auxiliary electrode and Ag/AgCl reference electrode. All potentials are given vs Ag/AgCl and are referenced with Fc/Fc^+ at 450 mV. Elemental Analysis (EA) measurements were performed on a LecoCHNS-932 elemental analyzer.

UPLC-ESI-MS was performed on a Waters Acquity UPLC System coupled to a Bruker HCT^{TM}, using an Acquity UPLC BEH C18 1.7 µm (2.1 x 50 mm) column. UPLC solvents were formic acid (0.1% in millipore water) (solvent A) and acetonitrile HPLC grade (solvent B). Applied UPLC gradient: 0-0.5 minutes: 95% A, 5% B; 0.51-4.0 minutes: linear gradient from 95% A (5% B) to 0% A (100% B); 4-5 minutes: 100% B. The flow rate was 0.6 ml/min. Detection was performed at 250 nm and 480 nm (DAD).

X-ray Crystallographic data were collected at 183(2) K with either Mo Kα radiation (λ = 0.7107 Å) or Cu Kα radiation (λ = 1.54184 Å). Compound **[15$^+$]PF_6** was measured on an Agilent SuperNova, dual source, with an Atlas detector while compounds **2**, **3**, **[4$^+$]PF_6**, **[5$^+$]PF_6**, **[6$^+$]TFA**, **[7$^+$]TFA**, **[10$^+$]PF_6**, **[11$^+$]PF_6**, **[12$^+$]PF_6**, **[13$^+$]PF_6** and **[14$^+$]PF_6** were measured on an Oxford Diffraction CCD Xcalibur system with a Ruby detector. Suitable crystals were covered with oil (Infineum V8512, formerly known as Paratone N), placed on a nylon loop that is mounted in a CrystalCap Magnetic™ (Hampton Research) and immediately transferred to the diffractometer. Data were corrected for Lorentz and

polarisation effects as well as for absorption (numerical). The program suite CrysAlisPro was used for data collection, multi-scan absorption correction and data reduction.[1] Structures were solved with direct methods using SIR97[2] and were refined by full-matrix least-squares methods on F^2 with SHELXL-97.[3] The structures were checked for higher symmetry with help of the program Platon.[4] Supplementary crystallographic data can be obtained free of charge from the Cambridge Crystallographic Data Centre via www.ccdc.cam.ac.uk/structures (CCDC nr. 1485178-1485189). The high negative electron density near C(6) in compound **2** is most likely caused by a twinning in the b-direction that could not be resolved. Despite the B-alert for compound **3**, a twin refinement for that very compound has already been applied. The high ADP max/min ratio for C(8) in compound **4** originates from the unsubstituted benzene ring that has a tendency to be slightly disordered.

Synthetic procedures

1. $[Re(\eta^6\text{-}C_6H_6)_2](OTf)$ ($[1^+]OTf$):

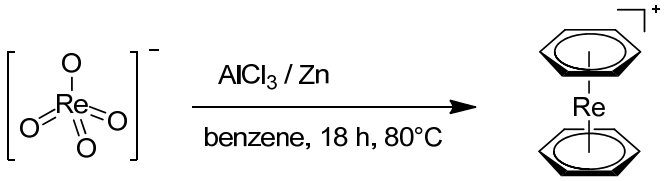

Synthesis: A 1.5 g (5.2 mmol, 1 equiv) portion of $KReO_4$ was suspended in 50 mL benzene. Afterwards 1.01 g (15.5 mmol, 3 equiv) zinc dust and 8.32 g (62.4 mmol, 12 equiv) anhydrous $AlCl_3$ were added to the suspension. The reaction mixture was stirred for 18 h at 80°C. The solvent was evaporated under *vacuo* and the residue was washed with Et_2O (3 x 60 mL). The solid residue was suspended in 150 ml of H_2O and filtered. 1.22 g (7.8 mmol, .1.5 equiv) lithium triflate (LiOTf) was added to the filtrate. The product was extracted by continuous liquid-liquid extraction (DCM/water) over night. The organic phase was evaporated which afforded **$[1^+]OTf$** as analytically pure, yellow crystalline powder. Yield: 1.17 g (50%).

Analysis: ^{1}H NMR (400 MHz, $(CD_3)_2CO$) δ [ppm]: 6.16 (s, 12H, CH_{arom}). ^{13}C NMR (100 MHz, $(CD_3)_2CO$) δ [ppm]: 77.65 (*C*H_{arom}). ESI-MS: m/z = 343.1 $[M]^+$. IR ν: 3076 (w), 1432 (m), 1256 (s), 1221 (m), 1143 (s), 1027 (s), 1006 (m), 906 (w), 858 (m), 830 (m), 753 (w) cm^{-1}. Anal. Calcd for $C_{13}H_{12}F_3O_3Re_1S$: C 31.77, H 2.46; found: C 31.57, H 2.43.

2. [Re(η^5-C$_6$H$_6$C$_4$H$_9$)(η^6-C$_6$H$_6$)] (2):

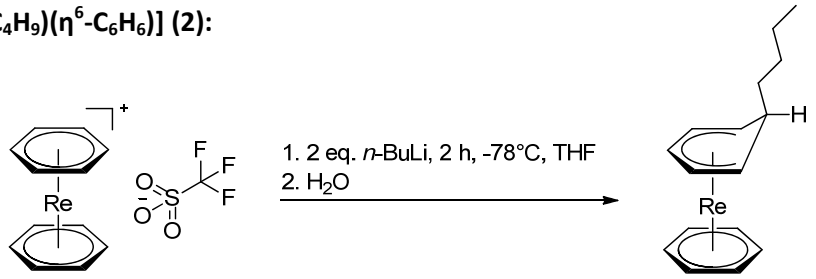

Synthesis: A 80 mg (0.162 mmol) portion of **[1$^+$]OTf** was dissolved in 12 mL of dry THF and cooled to -78°C. Afterwards, 0.21 mL (0.324 mmol, 2 equiv) of *n*-butyllithium (1.6 M hexane solution) was added to the yellow suspension. The reaction mixture was stirred for 2 h at -78°C. During the reaction, the colour of the suspension changed from yellow to orange. The reaction was quenched with 5 mL degassed H_2O. The solvent was evaporated *in vacuo* and the residue extracted with hexane (2 x 2.5mL). The organic phase was evaporated which afforded **2** as analytically pure, orange crystalline powder. Yield: 60 mg (92%). Single crystals, suitable for X-ray diffraction analysis, were obtained by slow evaporation of a solution of **2** in hexane.

Analysis: ^{1}H NMR (500 MHz, C_6D_6) δ [ppm]: 5.84 (t, 1H, *p*-C*H*$_{arom}$), 4.81 (q, 2H, *m*-CH$_{arom}$), 4.64 (s, 6H, C*H*$_{arom}$), 3.54 (quin, 2H, *o*-C*H*$_{arom}$), 2.81 (quin, 1H *ipso*-C*H*), 1.23 (quin, 2H, C*H*$_2$), 1.16 (m, 2H, C*H*$_2$), 0.97 (q, 2H, C*H*$_2$), 0.87 (m, 3H, C*H*$_3$). ^{13}C NMR (125 MHz, C_6D_6) δ [ppm]: 80.02 (*p*-*C*H$_{arom}$), 77.76 (*m*-*C*H$_{arom}$), 67.68 (*C*H$_{arom}$), 45.93 (CH-*C*H$_2$), 43.47 (*C*H), 28.13 (*o*-*C*H$_{arom}$), 26.20 (*C*H$_2$), 22.70 (*C*H$_2$), 14.16 (*C*H$_3$). ESI-MS: m/z = 401.1 [MH]$^+$, IR ν: 3055 (w), 2957 (w), 2953 (m), 2918 (s), 2839 (s), 1465 (s), 1452 (w), 1427 (w), 1379 (m), 1285 (m), 1110 (m), 992 (m), 965 (m), 844 (m), 817 (m), 799 (s), 723 (m) cm^{-1}. Anal. Calcd for $C_{16}H_{21}Re_1$: C 48.10, H 5.30; Found: C 48.15, H 5.17.

3. [Re(η^5-C$_6$H$_7$)(η^6-C$_6$H$_6$)] (3):

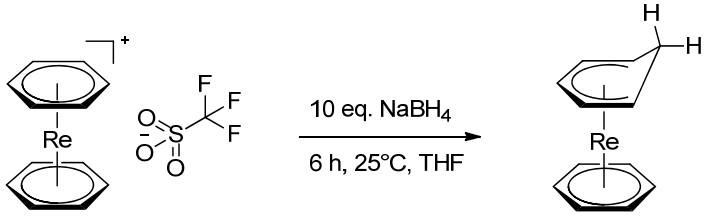

Synthesis: A 80 mg (0.162 mmol) portion of **[1$^+$]OTf** was dissolved in 12 mL of dry THF. A 61.5 mg (1.62 mmol, 10 equiv) portion of $NaBH_4$ was added to the yellow suspension. The reaction was stirred for 6 h at room temperature. The color of the clear solution changed from yellow to orange. The solvent was evaporated in *vacuo* and the residue extracted with hexane (2 x 2.5 mL). Evaporation of the organic phase afforded an analytically pure **3**, as orange crystalline powder. Yield: 29.7 mg (53%). Single crystals, suitable for X-ray diffraction analysis, were obtained by slow evaporation of a hexane solution of **3**.

Analysis: ^{1}H NMR (500 MHz, C_6D_6) δ [ppm]: 5.93 (t, 1H, *p*-C*H*$_{arom}$), 4.88 (t, 2H, *m*-C*H*$_{arom}$), 4.60 (s, 6H, C*H*$_{arom}$), 4.22 (d, 1H, *ipso*-C*H*$_2$), 3.22 (t, 2H, *o*-C*H*$_{arom}$), 2.63 (*q*, 1H, *ipso*-C*H*$_2$). ^{13}C NMR (125 MHz, C_6D_6) δ [ppm]: 80.38 (*p*-*C*H$_{arom}$), 80.34 (*m*-*C*H$_{arom}$), 68.57 (*C*H$_{arom}$), 33.18 (*C*H$_2$), 19.11 (*o*-*C*H$_{arom}$). ESI-MS: m/z = 345.1 $[MH]^+$. IR ν: 3026 (w), 2955 (w), 2757 (m), 2557 (w), 2449 (w), 1472 (w), 1429 (w), 1416 (m), 1379 (m), 1285 (m), 1114 (w), 1049 (m), 996 (m), 977 (m), 965 (s), 921 (m), 882 (s), 812 (s), 789 (m) cm^{-1}. Anal. Calcd for $C_{12}H_{13}Re_1$: C 41.97, H 3.82; Found: C 41.79, H 3.80.

4. [Re(η^6-C_6H_5Br)(η^6-C_6H_6)](PF$_6$) ([4$^+$]PF$_6$) and [Re(η^6-$C_6H_5Br)_2$](PF$_6$) ([5$^+$]PF$_6$):

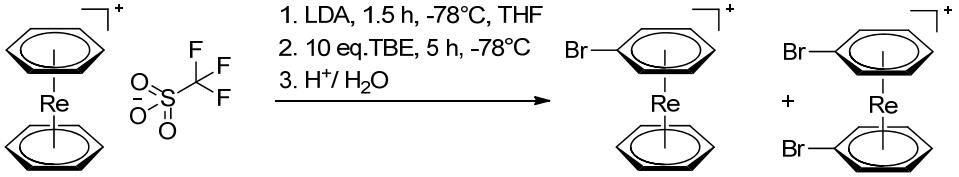

Synthesis: A 300 mg (0.61 mmol) portion of **[1$^+$]OTf** was dissolved in 30 mL of dry THF and cooled to -78°C. A 1.5 mL (1.53 mmol, 2.5 equiv) portion of a 1 M LDA solution (THF/hexane) was added slowly to the yellow suspension. The reaction was stirred for 1.5 h at -78°C, and 0.7 mL (6.1 mmol, 10 equiv) of 1,1,2,2-tetrabromoethane (TBE) was added to the clear orange solution. Stirring was continued for 5 h at -78 °C. The color of the solution changed from orange to yellow. The reaction was quenched with acidified MeOH (MeOH/HCl: 2:1) and the volume of the mixture was reduced under vacuum to 5 mL. The orange solution was extracted with hexane (3 x 2.5 mL) and the remaining solvent was evaporated *in vacuo*. The residue was purified by *preparative HPLC* (Reprosil 100 C18, 250 mm x 40 mm, 0.1% TFA/CH_3CN, gradient G2). Analytically pure yellow **[4$^+$]PF$_6$** and **[5$^+$]PF$_6$** precipitated from the solution upon addition of NH_4PF_6. Single crystals, suitable for X-ray diffraction analysis, were obtained by slow evaporation of a CH_3CN/H_2O (1:1) solution of **[4$^+$]PF$_6$** and **[5$^+$]PF$_6$**. Yields: 167.4 mg (0.26 mmol, 42.6%) for **[5$^+$]PF$_6$** and 62.3 mg (0.11 mmol, 18%) for **[4$^+$]PF$_6$**.

Analysis: [Re(η^6-C_6H_5Br)(η^6-C_6H_6)](PF$_6$) (**[4$^+$]PF$_6$**): ^{1}H NMR (500 MHz, CD_3CN) δ [ppm]: 6.51 (d, 2H, *o*-C*H*$_{arom}$), 6.02 (s, 6H, C*H*$_{arom}$), 6.01 (t, 2H, *m*-C*H*$_{arom}$), 5.87 (t, 1H, *p*-C*H*$_{arom}$). ^{13}C NMR (125 MHz, CD_3CN) δ [ppm]: 84.69 (*C*Br), 81.72 (*o*-*C*H$_{arom}$), 80.98 (*C*H$_{arom}$), 76.94 (*p*-*C*H$_{arom}$), 76.43 (*m*-*C*H$_{arom}$). ESI-MS: m/z = 421.0 $[M]^+$. IR ν: 3097 (m), 1435 (m), 1425 (m), 1426 (m), 1393 (m), 1134 (w), 1050 (m), 930 (w), 811 (s) cm^{-1}. Anal. Calcd for $C_{12}H_{11}Br_1F_6PRe$: C 25.45, H 1.96; Found: C 25.12, H 1.98.

[Re(η^6-$C_6H_5Br)_2$](PF$_6$) (**[5$^+$]PF$_6$**): ^{1}H NMR (500 MHz, CD_3CN) δ [ppm]: 6.55 (d, 4H, *o*-C*H*$_{arom}$), 6.11 (t, 4H, *m*-C*H*$_{arom}$), 5.99 (t, 2H, *p*-C*H*$_{arom}$). ^{13}C NMR (125 MHz, CD_3CN) δ [ppm]: 87.25 (*C*Br), 84.61 (*o*-*C*H$_{arom}$), 79.70 (*p*-*C*H$_{arom}$), 79.49 (*m*-*C*H$_{arom}$). ESI-MS: m/z = 500.9 $[M]^+$. IR ν: 3094 (m), 1468 (w), 1427 (m), 1392

(m), 1278 (w), 1060 (m), 1008 (w), 930 (m), 906 (w), 818 (s) cm^{-1}. Anal. Calcd for $C_{12}H_{10}Br_2F_6PRe$: C 22.34, H 1.56; Found: C 22.30, H 1.68.

5. [Re(η⁶-C_6H_5COOH)(η⁶-C_6H_6)](TFA) ([6⁺]TFA) and [Re(η⁶-$C_6H_5COOH)_2$](TFA) ([7⁺]TFA):

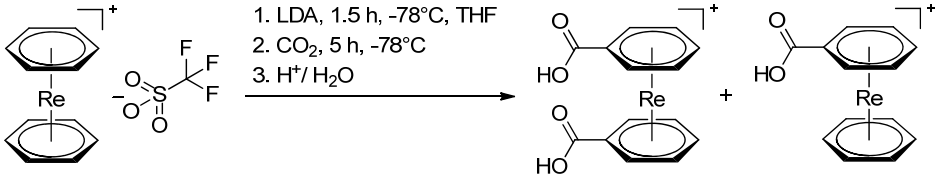

Synthesis: A 300 mg (0.61 mmol) portion of **[1⁺]OTf** was dissolved in 30 mL of dry THF and cooled to -78°C. A 1.5 mL (1.53 mmol, 2.5 equiv) portion of 1 M LDA solution (THF/hexane) was added to the yellow suspension. The reaction was stirred for 1.5 h at -78 °C. Subsequently, CO_2 gas was passed through the clear orange solution for 5 h at -78°C (monitored by UPLC-MS). The color of the solution changed from orange to yellow, and a yellow precipitate was observed. The reaction was quenched by the addition of MeOH/HCl solution and the solvents were evaporated *in vacuo.* The residue was purified by *preparative HPLC* (Reprosil 100 C18, 250 mm x 40 mm, 0.1% TFA/CH_3CN, gradient G1). Yield: 157.7 mg (0.29 mmol, 47.5%) of analytically pure orange **[7⁺]TFA** and 85.2 mg (0.27 mmol, 27%) of analytically pure yellow **[6⁺]TFA**. Crystals, suitable for X-ray diffraction analysis were obtained by slow evaporation of a CH_3CN/H_2O (1:1) solution of **[6⁺]TFA** and **[7⁺]TFA**.

Analysis: [Re(η⁶-C_6H_5COOH)(η⁶-C_6H_6)](TFA) (**[6⁺]TFA**): ^{1}H NMR (500 MHz, CD_3OD) δ [ppm]: 6.70 (d, 2H, *o*-CH_{arom}), 6.26 (t, 2H, *m*-CH_{arom}), 6.20 (t, 1H, *p*-CH_{arom}), 6.13 (s, 6H, CH_{arom}). ^{13}C NMR (125 MHz, CD_3OD) δ [ppm]: 170.54 (*C*OOH), 162.91 (q, *C*OOH, TFA), 118.31 (q, *C*F, TFA), 82.02 (C_{arom}-COOH), 80.06 (C_{arom}), 78.33 (*o*-CH_{arom}), 77.91 (*m*-CH_{arom}), 77.21 (*p*-CH_{arom}). ESI-MS: m/z = 387.1 $[M]^+$. IR ν: 3079 (w), 1705 (s), 1518 (w), 1434 (w), 1395 (m), 1286 (m), 1264 (m), 1169 (s), 1121 (s), 1041 (s), 999 (m), 863 (w), 815 (m),787 (s), 713 (s) cm^{-1}. Anal. Calcd for $C_{15}H_{12}F_3O_4Re$: C 36.07, H 2.42; Found: C 35.74, H 2.28.

[Re(η⁶-$C_6H_5COOH)_2$](TFA) (**[7⁺]TFA**): ^{1}H NMR (500 MHz, CD_3OD) δ [ppm]: 6.70 (d, 4H, *o*-CH_{arom}), 6.30 (t, 4H, *m*-CH_{arom}), 6.24 (t, 2H, *p*-CH_{arom}). ^{13}C NMR (125 MHz, CD_3OD) δ [ppm]: 169.14 (*C*OOH), 162.65 (q, *C*OOH, TFA), 118.24 (q, *C*F, TFA), 81.79 (C_{arom}-COOH), 80.61 (*o*-CH_{arom}), 80.28 (*m*-CH_{arom}), 79.47 (*p*-CH_{arom}). ESI-MS: m/z = 431.1 $[M]^+$. IR ν: 3078 (w), 1732 (s), 1614 (s,) 1527 (w) , 1501 (w), 1401 (m), 1332 (m), 1283 (m), 1263 (m), 1155 (s), 1134 (s), 1114 (s), 1038 (m), 1010 (w), 989 (w), 869 (m), 796 (m), 775 (m), 717 (m) cm^{-1}. Anal. Calcd for $C_{16}H_{12}F_3O_6Re$: C 35.36, H 2.32; Found: C 35.00, H 2.26.

6. [Re(η^6-$C_6H_5SCH_2Ph$)(η$_6$-C_6H_6)](PF$_6$) ([10$^+$]PF$_6$):

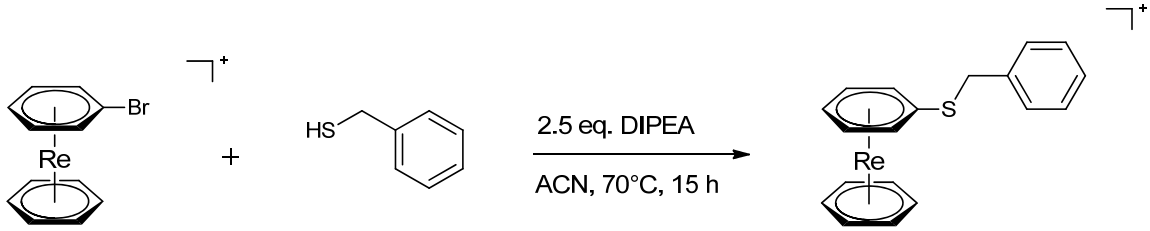

Synthesis: A 30 mg (0.053 mmol) portion of **[10$^+$]PF$_6$** was dissolved in 2 mL acetonitrile. Afterwards, 23 µL (0.13 mmol, 2.5 equiv) of DIPEA and 16 µL (0.13 mmol, 2.5 equiv) of benzyl mercaptan were added to the yellow solution. The reaction mixture was stirred for 15 h at 70°C. The solvent was evaporated in *vacuo* and the residue washed twice with hexane (2 x 2.5 mL) and water (2 x 2 mL). The residue was recrystallized from acetonitrile, yielding crystalline **[10$^+$]PF$_6$** (crystals suitable for X-ray diffraction analysis). Yield: 29 mg (0.048 mmol, 89.9%) of **[10$^+$]PF$_6$**.

Analysis: ^{1}H NMR (400 MHz, CD_3CN) δ [ppm]:7.34-7.30 (m, 5H, C*H*$_{arom}$), 6.13 (d, 2H, *o*-C*H*$_{arom}$), 5.94 (t, 2H, *m*-C*H*$_{arom}$), 5.87 (s, 6H, C*H*$_{arom}$), 5.86 (t, 1H, *p*-C*H*$_{arom}$), 4.11 (s, 2H, C*H*$_2$). ^{13}C NMR (100 MHz, CD_3CN) δ [ppm]: 137.91 (S-CH_2-*C*$_{arom}$), 130.18 (*m*-*CH*$_{arom}$), 129.81 (*o*-*CH*$_{arom}$), 128.73 (*p*-*CH*$_{arom}$), 95.09 (*C*$_{arom}$-S), 81.27 (*o*-*C*H$_{arom}$), 79.47 (*C*$_{arom}$), 77.03 (*m*-*C*H$_{arom}$), 76.88 (*p*-*C*H$_{arom}$), 40.56 (*C*H$_2$). ESI-MS: m/z = 465.1 [M]$^+$. IR ν: 3084 (w), 2921 (w), 1499 (w), 1431 (m), 1391 (w), 1245 (w), 1153 (w), 1074 (w), 925 (w), 825(s), 725 (m) cm^{-1}. HR-ESI-MS $C_{19}H_{18}ReS$ [M]$^+$: calculated, 465.0683; found, 465.0681.

7. [Re(η^6-C_6H_5NHPh)(η^6-C_6H_6)](PF$_6$) ([11$^+$]PF$_6$):

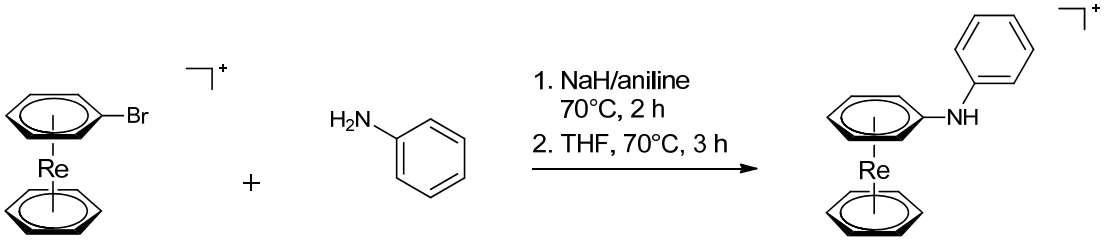

Synthesis: A 12.7 mg (0.530 mmol, 10 equiv) portion of NaH was added to 61 µL of aniline (0.636 mmol, 12 equiv) and the mixture was stirred for 2 h at 70°C. Afterwards, a suspension of **[4$^+$]PF$_6$** (30 mg, 0.053 mmol) in 3 ml THF was added to the mixture. The dark red solution was stirred for 3 h at 70°C. The mixture was cooled to room temperature, quenched with 1 mL water and neutralized with a solution of trifluoroacetic acid (2 mol/L). The solvent was evaporated *in vacuo*. The residue was washed with hexane (2 x 2.5 mL), water (2 x 2 mL) and isolated after *preparative HPLC* (Reprosil 100 C18, 250 mm x 40 mm, 0.1% TFA/CH_3CN, gradient G5). Analytically pure yellow **[11$^+$]PF$_6$** was precipitated from the HPLC eluent by the addition of NH_4PF_6. Single crystals, suitable for X-ray

diffraction analysis were obtained by slow evaporation of an acetonitrile solution of **[11$^+$]PF$_6$**. Yield: 22 mg (0.038 mmol, 71.9%) of **[11$^+$]PF$_6$**.

Analysis: ^{1}H NMR (500 MHz, CD_3CN) δ [ppm]: 7.41 (t, 2H, *m*-C*H*$_{arom}$), 7.18 (t, 1H, *p*-C*H*$_{arom}$), 7.10 (d, 2H, *o*-C*H*$_{arom}$), 6.35 (s, 1H,N*H*), 6.16 (d, 2H, *o*-C*H*$_{arom}$), 5.95 (t, 2H, *m*-C*H*$_{arom}$), 5.71 (t, 1H, *p*-C*H*$_{arom}$), 5.69 (s, 6H, C*H*$_{arom}$). ^{13}C NMR (125 MHz, CD_3CN) δ [ppm]: 140.21 (NH-*C*$_{arom}$), 130.75 (*m*-*CH*$_{arom}$), 125.70 (*p*-*CH*$_{arom}$), 123.12 (*o*-*CH*$_{arom}$), 123.05 (*C*$_{arom}$-NH), 77.72 (*p*-*C*H$_{arom}$), 76.12 (*C*$_{arom}$), 76.86 (*m*-*C*H$_{arom}$), 65.84 (*o*-*C*H$_{arom}$). ESI-MS: m/z = 434.1 [M]$^+$. IR ν: 3428 (m), 1598 (m), 1554, (m) 1528 (s), 1496 (s), 1455 (m), 1431 (m), 1388 (w), 1320 (s), 1254 (w), 1159 (w), 997 (w), 813 (s), 754 (s) cm^{-1}. HR-ESI-MS $C_{18}H_{17}NRe$ [M]$^+$: calculated, 434.0914; found, 434.0913.

8. [Re(η^6-C$_6$H$_5$SCH$_2$Ph)$_2$](PF$_6$) ([12$^+$]PF$_6$):

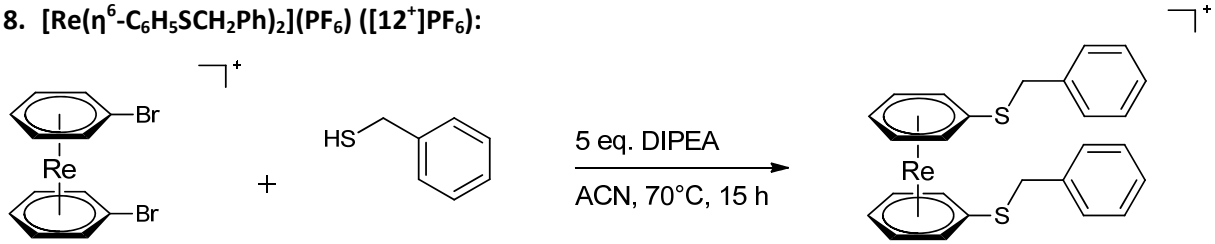

Synthesis: A 30 mg (0.046mmol) portion of **[5$^+$]PF$_6$** was dissolved in 2 mL acetonitrile. After the addition of 40 µL (0.23 mmol, 5 equiv) DIPEA and 27 µL (0.23 mmol, 5 equiv) benzyl mercaptan to the yellow solution, the reaction mixture was stirred for 15 h at 70°C. The solvent was evaporated *in vacuo* and the residue washed with Et_2O (2 x 2.5 mL) and water (2 x 2 mL). The product was recrystallized from acetonitrile, yielding single crystals of **[12$^+$]PF$_6$**, suitable for X-ray diffraction analysis. Yield: 30 mg (0.041 mmol, 88.2%) of **[12$^+$]PF$_6$**.

Analysis: ^{1}H NMR (400 MHz, CD_3CN) δ [ppm]: 7.36-7.28 (m, 10H, C*H*$_{arom}$), 6.04 (d, 4H, *o*-C*H*$_{arom}$), 5.88 (t, 4H, *m*-C*H*$_{arom}$), 5.78 (t, 2H, *p*-C*H*$_{arom}$), 4.13 (s, 4H, C*H*$_2$). ^{13}C NMR (100 MHz, CD_3CN) δ [ppm]: 137.18 (S-CH$_2$-*C*$_{arom}$), 130.14 (*m*-*CH*$_{arom}$), 129.77 (*o*-*CH*$_{arom}$), 128.73 (*p*-*CH*$_{arom}$), 97.15 (*C*$_{arom}$-S), 82.01 (*o*-*C*H$_{arom}$), 78.45 (*m*-*C*H$_{arom}$), 78.24 (*p*-*C*H$_{arom}$), 39.45 (*C*H$_2$). ESI-MS: m/z = 587.1 [M]$^+$. IR ν: 3077 (w), 2922 (w), 1497 (m), 1454 (w), 1424 (m), 1393 (m), 1251 (w), 1144 (w), 1083 (w), 1029 (w), 923 (w), 877(w) 821(s), 778(m), 708 (s) cm^{-1}. HR-ESI-MS $C_{26}H_{24}ReS_2$ [M]$^+$: calculated, 587.0871; found, 587.0871.

9. [Re(η^6-C$_6$H$_5$NHPh)$_2$] ([13$^+$]PF$_6$):

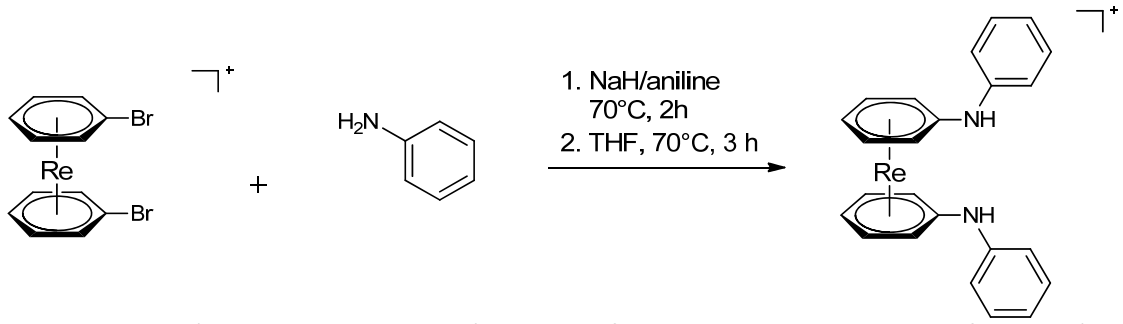

Synthesis: A 17 mg (0.697 mmol, 15 equiv) portion of NaH was added to 75 µL of aniline (0.790 mmol, 17 equiv) and the mixture was stirred for 2 h at 70°C. Afterwards, a suspension of **[5$^+$]PF$_6$** (30 mg, 0.046 mmol) in 3 ml THF was added to the reaction mixture. The dark red solution was stirred for 3 h at 70°C. The mixture was cooled to room temperature, quenched with 1 mL water and neutralized with a solution of trifluoroacetic acid (2 mol/L). The solvent was evaporated in *vacuo*. The residue was washed with hexane (2 x 2.5 mL), water (2 x 2 mL) and the product **[13$^+$]PF$_6$** isolated after purification by *preparative HPLC* (Reprosil 100 C18, 250 mm x 40 mm, 0.1% TFA/CH_3CN, gradient G5) and the addition of NH_4PF_6 to the eluent. Single crystals suitable for X-ray diffraction analysis were obtained by slow evaporation of an acetonitrile solution of **[13$^+$]PF$_6$**. Yield: 21 mg (0.031 mmol, 67.5%) of **[13$^+$]PF$_6$**.

Analysis: ^{1}H NMR (500 MHz, CD_3CN) δ [ppm]:7.33 (t, 2H, *m*-C*H*$_{arom}$), 7.11 (t, 1H, *p*-C*H*$_{arom}$), 7.00 (d, 2H, *o*-C*H*$_{arom}$), 6.27 (s, 1H,N*H*), 5.93 (d, 2H, *o*-C*H*$_{arom}$), 5.72 (t, 2H, *m*-C*H*$_{arom}$), 5.50 (t, 1H, *p*-C*H*$_{arom}$). ^{13}C NMR (125 MHz, CD_3CN) δ [ppm]: 140.50 (NH-*C*$_{arom}$), 130.62 (*m*-*CH*$_{arom}$), 125.22 (*p*-*CH*$_{arom}$), 122.59 (*o*-*CH*$_{arom}$), 118.98 (*C*$_{arom}$-NH), 78.02 (*p*-*C*H$_{arom}$), 73.71 (*m*-*C*H$_{arom}$), 63.51 (*o*-*C*H$_{arom}$). ESI-MS: m/z = 525.1 [M]$^+$. IR ν: 3396 (m, NH), 1599 (m), 1515 (s), 1447 (m), 1384 (w), 1299 (m), 1252 (w), 1146 (w), 992 (w), 820 (s), 749 (s) cm^{-1}. HR-ESI-MS $C_{24}H_{22}N_2Re$ [M]$^+$: calculated, 525.1335; found, 525.1336.

10.[Re(η^6-C$_6$H$_5$CONHCH$_2$Ph)(η^6-C$_6$H$_6$)](PF$_6$) ([14$^+$]PF$_6$):

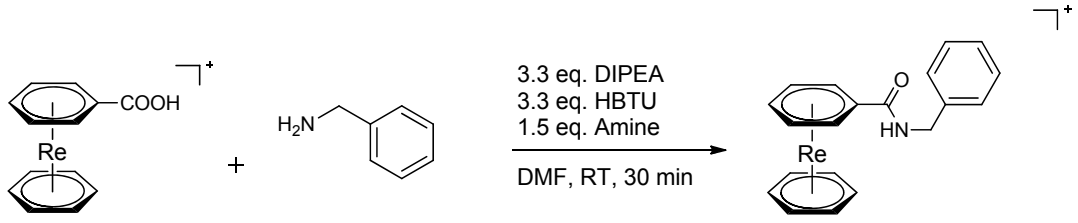

Synthesis: A 30 mg (0.056 mmol) portion of **[6$^+$]PF$_6$** was suspended in 3 mL of dry DMF at room temperature. 32 µL (0.186 mmol, 3.3 equiv) Diisopropylethylamine (DIPEA) was added to the yellow suspension and the reaction mixture was stirred for 2 min, followed by the addition of 70.6 mg (0.186 mmol, 3.3 equiv) of 3-[bis(dimethylamino)methyliumyl]-3H-benzotriazol-1-oxide

hexafluorophosphate (HBTU). After stirring for 5 min, 9 µL (0.084 mmol, 1.5 equiv) benzylamine was added to the yellow solution, which was stirred for further 30 min. After the reaction, the solvent was evaporated *in vacuo.* The residue was washed with hexane (2 x 2.5mL) and purified by *preparative HPLC* (Reprosil 100 C18, 250 mm x 40 mm, 0.1% TFA/CH_3CN, gradient G4). Analytically pure yellow **[14$^+$]PF_6** was precipitated by the addition of NH_4PF_6 to the solution. Single crystals, suitable for X-ray diffraction analysis were obtained by vapour diffusion from Et_2O (antisolvent) into CH_2Cl_2 (solvent). Yield: 27 mg (0.041 mmol, 73%) of **[14$^+$]PF_6**.

Analysis: ^{1}H NMR (500 MHz, CD_3CN) δ [ppm]: 7.41-7.30 (m, 5H, C*H*$_{arom}$), 6.50 (d, 2H, *o*-C*H*$_{arom}$), 6.09 (t, 2H, *m*-C*H*$_{arom}$), 6.21 (t, 1H, *p*-C*H*$_{arom}$), 5.93 (s, 6H, C*H*$_{arom}$), 4.47 (d, 2H, C*H*$_2$). ^{13}C NMR (125 MHz, CD_3CN) δ [ppm]: 166.86 (*C*ONH$_2$), 139.87 (NH-CH$_2$-*C*$_{arom}$), 129.73 (*m*-*CH*$_{arom}$), 128.79 (*o*-*CH*$_{arom}$), 128.50 (*p*-*CH*$_{arom}$), 84.43 (*C*-CO-NH), 80.43 (*C*$_{arom}$), 77.33 (*p*-*C*H$_{arom}$), 77.10 (*o*-*C*H$_{arom}$), 76.89 (*m*-*C*H$_{arom}$), 44.59 (*C*H$_2$). ESI-MS: m/z = 476.1 [M]$^+$. IR ν: 3090 (w), 2922 (w), 1649 (m) 1219 (m), 1539 (m), 1454 (w), 1434 (m), 1300 (w), 1168 (w), 822 (s), 761 (w), 737 (m) cm^{-1}. HR-ESI-MS $C_{20}H_{19}ONRe$ [M]$^+$: calculated, 476.1019; found, 476.1017

11.[Re(η^6-$C_6H_5CONHCH_2Ph)_2$](PF_6) ([15$^+$]PF_6):

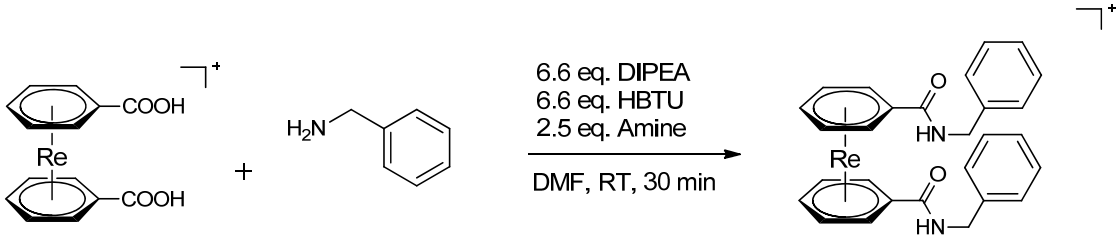

Synthesis: A 30 mg (0.052 mmol) portion of **[7$^+$]PF_6** was suspended in 3 mL of dry DMF at room temperature. After the addition of 64 µL (0.344 mmol, 6.6 equiv) diisopropylethylamine (DIPEA) the yellow suspension was stirred for 2 min. 141 mg (0.344 mmol, 6.6 equiv) 3-[bis(dimethylamino)methyliumyl]-3H-benzotriazol-1-oxide hexafluorophosphate (HBTU) was added and the reaction mixture stirred for 5 min. 15 µL (0.13 mmol, 2.5 eq) benzylamine was added and the yellow solution stirred for further 30 min. Finally, the solvent was evaporated *in vacuo.* The residue was washed with twice with hexane (2 x 2.5mL) and isolated after *preparative HPLC* (Reprosil 100 C18, 250 mm x 40 mm, 0.1% TFA/CH_3CN, gradient G4). Analytically pure yellow **[15$^+$]PF_6** precipitated from the HPLC solution after the addition of NH_4PF_6. Single crystals for X-ray diffraction analysis were obtained by vapour diffusion from Et_2O (antisolvent) into CH_2Cl_2 (solvent). Yield: 31 mg (0.041 mmol, 78.9%) of **[15$^+$]PF_6**.

Analysis: ^{1}H NMR (400 MHz, CD_3CN) δ [ppm]:7.92 (s, 2H, N*H*), 7.39-7.28 (m, 10H, C*H*$_{arom}$), 6.36 (d, 4H, *o*-C*H*$_{arom}$), 6.10 (t, 4H, *m*-C*H*$_{arom}$), 6.02 (t, 2H, *p*-C*H*$_{arom}$), 4.46 (d, 4H, C*H*$_2$). ^{13}C NMR (100 MHz, CD_3CN) δ

[ppm]: 167.44 (*C*ONH$_2$), 139.73 (NH-CH$_2$-*C*$_{arom}$), 129.97 (*m*-*CH*$_{arom}$), 129.12 (*o*-*CH*$_{arom}$), 128.77 (*p*-*CH*$_{arom}$), 88.15 (*C*-CO-NH), 79.98 (*o*-*C*H$_{arom}$), 79.50 (*p*-*C*H$_{arom}$), 79.37 (*m*-*C*H$_{arom}$), 45.06 (*C*H$_2$). ESI-MS: m/z = 587.1 [M]$^+$. IR ν: 3267 (w), 3092 (w), 1645 (m), 1556 (m), 1430 (w), 1296 (m), 1148 (w), 824 (s), 758 (m), 725 (m), 709 (m) cm^{-1}. HR-ESI-MS $C_{28}H_{26}O_2N_2Re$ [M]$^+$: calculated, 609.1543; found, 609.1546.

12. [Re(η^6-C$_6$H$_5$CONHCH$_2$CH$_2$C$_8$H$_{13}$O$_2$)$_2$](PF$_6$) ([16$^+$]PF$_6$):

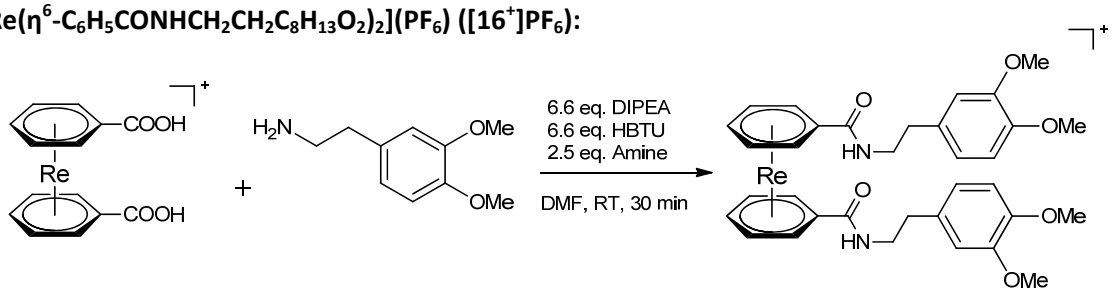

Synthesis: A 30 mg (0.052 mmol) portion of **[7$^+$]PF$_6$** was suspended in 3 mL of dry DMF at room temperature. 64 µL (0.34 mmol, 6.6 equiv) diisopropylethylamine (DIPEA) was added and the yellow suspension was stirred for 2 min. Afterwards, 141 mg (0.34 mmol, 6.6 equiv) of 3-[bis(dimethylamino)methyliumyl]-3H-benzotriazol-1-oxide hexafluorophosphate (HBTU) was added to the solution and the mixture stirred for further 5 min. 22 µL (0.13 mmol) of 3,4-dimethoxyphenethylamine was added to the yellow solution and reaction mixture stirred for 30 min. Finally, the solvent was evaporated in *vacuo.* The residue was washed twice with hexane (2 x 2.5mL) and isolated after *preparative HPLC* (Reprosil 100 C18, 250 mm x 40 mm, 0.1% TFA/CH$_3$CN, gradient G3). Analytically pure yellow **[16$^+$]PF$_6$** precipitated from the HPLC solution after the addition of NH_4PF_6. Yield: 34 mg (0.038 mmol, 72.3%) of **[16$^+$]PF$_6$**.

Analysis: ^{1}H NMR (500 MHz, CD$_3$CN) δ [ppm]: 7.55 (s, 2H, N*H*), 6.87 (d, 4H, *o*-C*H*$_{arom}$), 6.78 (d, 2H, *m*-C*H*$_{arom}$), 6.10 (d, 4H, *o*-C*H*$_{arom}$), 5.98 (t, 4H, *m*-C*H*$_{arom}$), 5.94 (t, 2H, *p*-C*H*$_{arom}$), 3.79 (s, 6H, OC*H*$_3$), 3.76 (s, 6H, OC*H*$_3$), 3.55 (q, 4H, NH-C*H*$_2$), 2.83 (t, 4H,C*H*$_2$-C$_{arom}$). ^{13}C NMR (125 MHz, CD$_3$CN) δ [ppm]: 167.10 (*C*OOH), 150.25 (*m*-*C*$_{arom}$-OCH$_3$), 148.9 (*p*-*C*$_{arom}$-OCH$_3$), 132.84 (CH$_2$-*C*$_{arom}$), 121.94 (*o*-*CH*$_{arom}$), 113.73 (*o*-*CH*$_{arom}$), 112.91 (*m*-*CH*$_{arom}$), 88.61 (*C*-CO-NH), 79.62 (*o*-*C*H$_{arom}$), 79.01 (*p*-*C*H$_{arom}$), 78.75 (*m*-*C*H$_{arom}$), 56.9 (OC*H*$_3$), 42.16 (*C*H$_2$), 35.22 (*C*H$_2$). ESI-MS: m/z = 757.3 [M]$^+$. IR ν: 3056 (w), 1651 (m), 1514 (s), 1441 (m), 1261 (m), 1235 (m), 1149 (m), 1024 (s), 812 (s), 765 (w), 735 (m), 706 (m) cm^{-1}. HR-ESI-MS $C_{34}H_{38}O_6N_2Re$ [M]$^+$: calculated, 757.2284; found, 757.2282.

NMR Spectra

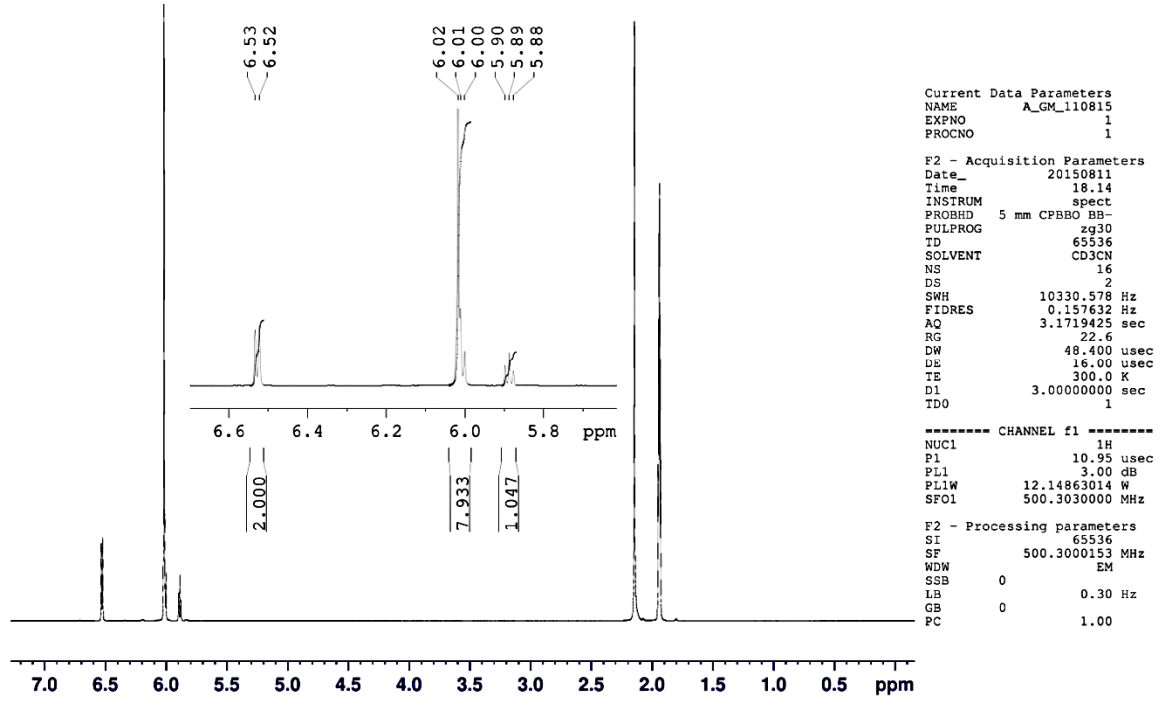

Figure S1: ^{1}H NMR of [Re(η^6-C_6H_5Br)(η^6-C_6H_6)](PF_6) (**[4$^+$]PF_6**)

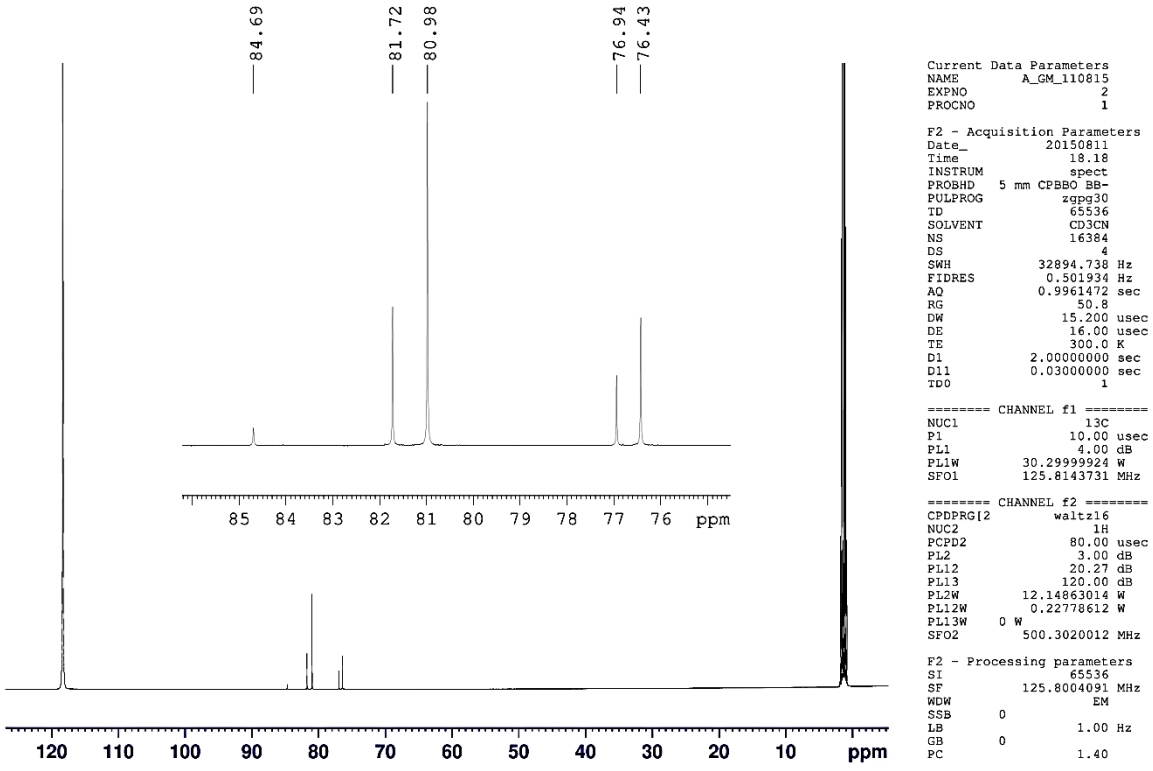

Figure S2: ^{13}C NMR of [Re(η^6-C_6H_5Br)(η^6-C_6H_6)](PF_6) (**[4$^+$]PF_6**)

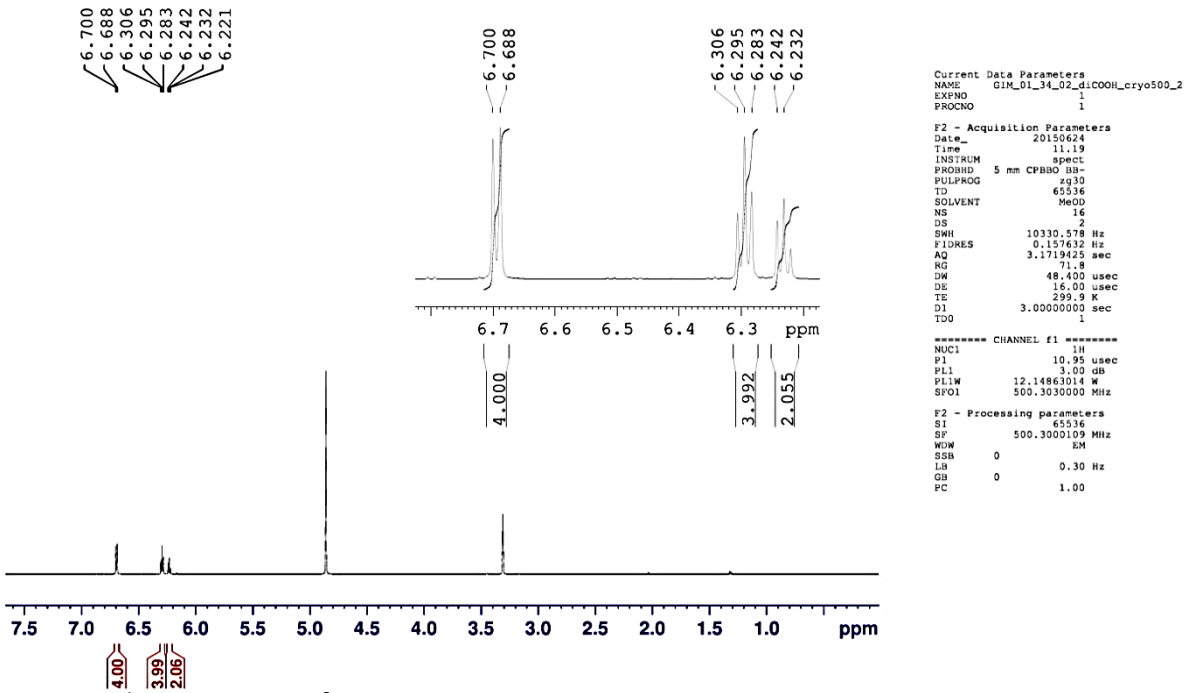

Figure S3: ^{1}H NMR of [Re(η^6-$C_6H_5COOH)_2$](TFA) (**[7$^+$]TFA**)

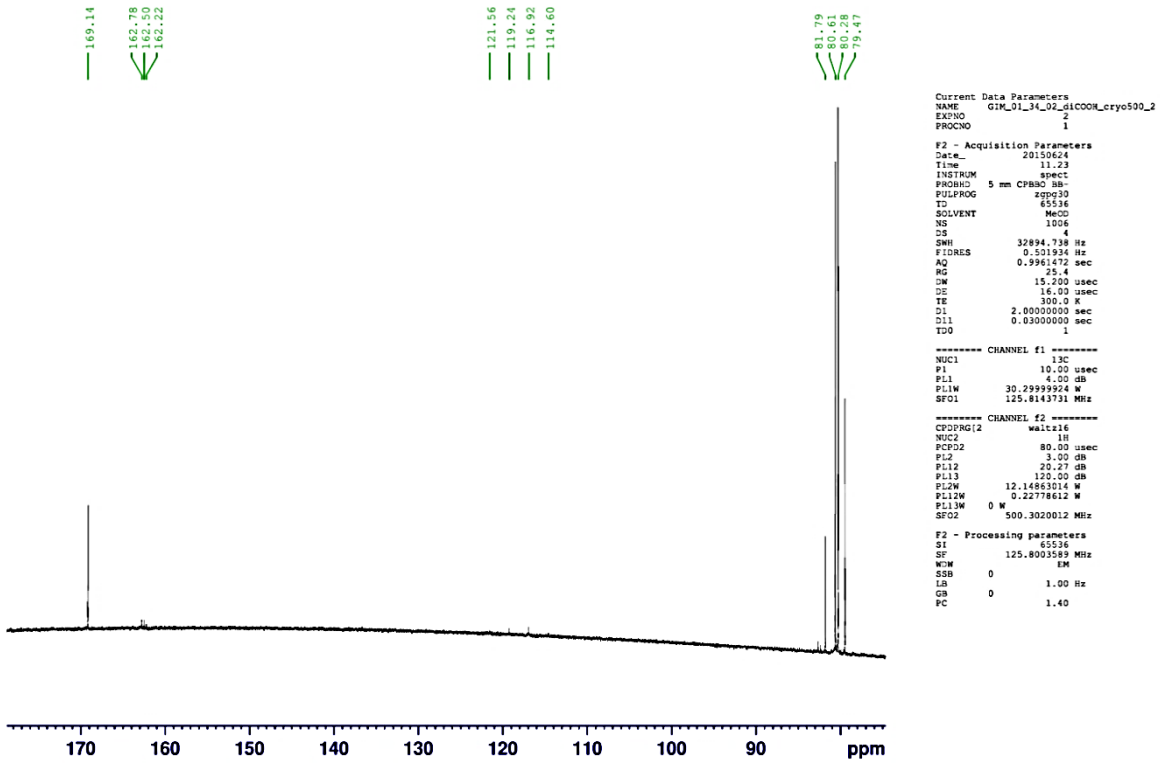

Figure S4: ^{13}C NMR [Re(η^6-$C_6H_5COOH)_2$](TFA) (**[7$^+$]TFA**)

Crystal Data of 2, 3, $[4^+]PF_6$, $[5^+]PF_6$ and $[6^+]TFA$

Table S1. Crystal data and data collection of complexes **2**, **3**, $[4^+]PF_6$, $[5^+]PF_6$ and **[6⁺]TFA**.

	$[Re(\eta^5\text{-}C_6H_6C_4H_9)(\eta^6\text{-}C_6H_6)]$ (**2**)	$[Re(\eta^5\text{-}C_6H_7)(\eta^6\text{-}C_6H_6)]$ (**3**)	$[Re(\eta^6\text{-}C_6H_5Br)(\eta^6\text{-}C_6H_6)](PF_6)$ ($[4^+]PF_6$)	$[Re(\eta^6\text{-}C_6H_5Br)_2](PF_6)$ ($[5^+]PF_6$)	$[Re(\eta^6\text{-}C_6H_5COOH)(\eta^6\text{-}C_6H_6)](TFA)$ (**[6⁺]TFA**)
Empirical formula	$C_{16}H_{21}Re$	$C_{12}H_{13}Re$	$C_{12}H_{11}Br_1F_6PRe$	$C_{12}H_{10}Br_2F_6PRe$	$C_{15}H_{12}F_3O_4Re$
Diffractometer	Xcalibur Ruby	Xcalibur Ruby	Xcalibur Ruby	Xcalibur Ruby	Xcalibur Ruby
Wavelength (Å)	0.7107	0.7107	0.7107	0.7107	0.7107
mol. weight (g/mol)	399.53	343.42	566.29	645.19	499.45
Crystal system	Monoclinic	Monoclinic	Monoclinic	Monoclinic	Monoclinic
Space group	P21/n	P21	P21/n	C2/c	P21/c
a (Å)	8.2264(3)	6.0605(3)	9.1201(4)	8.9058(4)	10.6190(4)
b (Å)	6.2629(2)	12.9391(4)	13.9728(7)	11.9008(5)	9.3147(3)
c (Å)	25.5059(7)	6.1814(3)	11.2214(5)	14.5490(6)	15.3754(6)
α (°)	90	90	90	90	90
β (°)	90.107(3)	106.268(5)	91.496(4)	95.833(4)	108.576(4)
γ (°)	90	90	90	90	90
Volume ($Å^3$)	1314.10(7)	465.32(4)	1429.49(11)	1534.00(11)	1441.60(9)
Z	4	2	4	4	4
Dens.(calc.) (g/cm^3)	2.019	2.451	2.631	2.794	2.301
Abs. coeff. (mm^{-1})	9.222	13.000	11.463	13.289	8.481
F(000)	768	320	1048	1184	944
Crystal size (mm^3)	0.49 x 0.26 x 0.09	0.320 x 0.210 x 0.090	0.23 x 0.06 x 0.04	0.37 x 0.15 x 0.07	0.25 x 0.11 x 0.09
Crystal description	orange block	orange plate	yellow plate	yellow block	yellow block
θ range (°)	2.60 to 32.80	3.149 to 32.885	2.67 to 28.28	2.81 to 30.47	2.80 to 32.86
Index ranges	-12<=h<=11, -9<=k<=9 -38<=l<=38	-8<=h<=8, -19<=k<=19, -9<=l<=9	-12<=h<=6, -17<=k<=18, -14<=l<=14	-12<=h<=12, -16<=k<=16, -20<=l<=20	-16<=h<=16, -13<=k<=13, -22<=l<=22
Refl. collected	21552	12947	8128	10611	17607
Indep. reflections	4580 [R_{int} = 0.0422]	3230 [R_{int} = 0.0328]	3542 [R_{int} = 0.0346]	2345 [R_{int} = 0.0332]	4973 [R_{int} = 0.0338]
Reflections obs.	4189	2715	2967	2194	4370
Criterion for obs.	>2sigma(I)	>2sigma(I)	>2sigma(I)	>2sigma(I)	>2sigma(I)
Completeness to θ	99.9 % to 26.32°	100 % to 25.242°	99.9 % to 26.32°	99.94 % to 26.32°	99.9 % to 30.44°
Absorption corr.	Semi-empirical from equiv.	Analytical	Semi-empirical from equiv.	Semi-empirical from equiv.	Semi-empirical from equiv.
Max. and min. transm.	0.4907 and 0.0931	0.341 and 0.059	0.6571 and 0.1780	0.4564 and 0.0838	0.9949 and 0.6469
Data / restraints / param.	4580 / 0 / 155	3230 / 10 / 136	3542 / 0 / 190	2345 / 0 / 102	4973 / 0 / 209
Goodness-of-fit on F^2	1.103	1.116	1.031	1.066	0.896
Fin. R ind. [I>2sigma(I)]	R1 = 0.0264, wR2 = 0.0554	R1 = 0.0247, wR2 = 0.0582	R1 = 0.0327, wR2 = 0.0649	R1 = 0.0339, wR2 = 0.0906	R1 = 0.0245, wR2 = 0.0529
R indices (all data)	R1 = 0.0310, wR2 = 0.0572	R1 = 0.0298, wR2 = 0.0620	R1 = 0.0435, wR2 = 0.0695	R1 = 0.0367, wR2 = 0.0925	R1 = 0.0306, wR2 = 0.0568
Fin. diff. ρ_{max} ($e^-/Å^{-3}$)	0.735 and -3.160	1.214 and -2.027	1.193 and -1.253	2.286 and -2.594	1.732 and -1.132
CCDC Nr.	1485178	1485179	1485180	1485181	1485182

Crystal Data of [7$^+$]TFA, [10$^+$]PF_6, [11$^+$]PF_6 and [12$^+$]PF_6

Table S2. Crystal data and data collection of complexes **[7$^+$]TFA**, **[10$^+$]PF_6**, **[11$^+$]PF_6** and **[12$^+$]PF_6**.

	[Re(η^6-C_6H_5COOH)$_2$](TFA) (**[7$^+$]TFA**)	[Re(η^6-$C_6H_5SCH_2Ph$)(η^6-C_6H_6)](PF_6) (**[10$^+$]PF_6**)	[Re(η^6-C_6H_5NHPh)(η^6-C_6H_6)](PF_6) (**[11$^+$]PF_6**)	[Re(η^6-$C_6H_5SCH_2Ph$)$_2$](PF_6) (**[12$^+$]PF_6**)
Empirical formula	$C_{16}H_{12}F_3O_6Re$	$C_{19}H_{18}F_6PReS$	$C_{18}H_{17}F_6NPRe$	$C_{26}H_{24}F_6PReS_2$
Diffractometer	Xcalibur Ruby	Xcalibur Ruby	Xcalibur Ruby	Xcalibur Ruby
Wavelength (Å)	0.7107	0.7107	0.7107	0.7107
mol. weight (g/mol)	498.62	609.54	578.50	731.74
Crystal system	Monoclinic	Monoclinic	Orthorhombic	Tetragonal
Space group	P21/m	P21/c	Pbca	P42/ncm
a (Å)	8.0048(3)	10.2707(8)	12.6343(3)	12.5728(4)
b (Å)	11.9770(4)	19.9560(12)	16.2977(4)	12.5728(4)
c (Å)	8.3724(3)	10.1970(7)	17.1886(4)	16.2424(10)
α (°)	90	90	90	90
β (°)	107.984(4)	114.205(9)	90	90
γ (°)	90	90	90	90
Volume (Å^3)	763.47(5)	1906.3(2)	3539.31(15)	2567.52(19)
Z	2	4	8	4
Dens.(calc.) (g/cm^3)	2.364	2.124	2.171	1.893
Abs. coeff. (mm^{-1})	8.027	6.627	7.020	5.016
F(000)	516	1168	2208	1424
Crystal size (mm^3)	0.27 x 0.23 x 0.14	0.24 x 0.17 x 0.06	0.48 x 0.36 x 0.14	0.34 x 0.14 x 0.03
Crystal description	orange block	yellow block	yellow prism	light green plate
θ range (°)	2.56 to 36.31	2.42 to 33.06	2.50 to 32.89	3.24 to 30.51
Index ranges	-13<=h<=13, -19<=k<=19, -12<=l<=13	-15<=h<=15, -29<=k<=30, -13<=l<=15	-18<=h<=19, -21<=k<=24, -25<=l<=24	-10<=h<=17, -17<=k<=17, -18<=l<=23
Refl. collected	13707	15533	26107	13201
Indep. reflections	3836 [R_{int} = 0.0345]	6553 [R_{int} = 0.0364]	6083 [R_{int} = 0.0382]	2086 [R_{int} = 0.0480]
Reflections obs.	3622	5417	5005	1402
Criterion for obs.	>2sigma(I)	>2sigma(I)	>2sigma(I)	>2sigma(I)
Completeness to θ	100.0 % to 36.23°	99.9 % to 26.32°	99.8 % to 30.44°	99.8 % to 26.32°
Absorption corr.	Semi-empirical from equiv.	Semi-empirical from equiv.	Semi-empirical from equiv.	Semi-empirical from equiv.
Max. and min. transm.	0.3995 and 0.2205	0.6919 and 0.2992	0.4398 and 0.1336	0.8641 and 0.5616
Data / restraints / param.	3836 / 0 / 125	6553 / 0 / 253	6083 / 0 / 247	2086 / 0 / 103
Goodness-of-fit on F^2	1.054	1.033	1.087	1.010
Fin. R ind. [I>2sigma(I)]	R1 = 0.0218, wR2 = 0.0498	R1 = 0.0337, wR2 = 0.0795	R1 = 0.0247, wR2 = 0.0561	R1 = 0.0229, wR2 = 0.0497
R indices (all data)	R1 = 0.0237, wR2 = 0.0509	R1 = 0.0438, wR2 = 0.0861	R1 = 0.0347, wR2 = 0.0606	R1 = 0.0419, wR2 = 0.0572
Fin. diff. ρmax (e$^-$/Å^{-3})	1.865 and -1.526	2.210 and -1.441	1.051 and -1.593	1.207 and -0.817
CCDC Nr.	1485183	1485184	1485185	1485186

Crystal Data of $[13^+]PF_6$, $[14^+]PF_6$ and $[15^+]PF_6$

Table S3. Crystal data and data collection of complexes **$[13^+]PF_6$**, **$[14^+]PF_6$** and **$[15^+]PF_6$**.

	$[Re(\eta^6\text{-}C_6H_5NHPh)_2](PF_6)$ (**$[13^+]PF_6$**)	$[Re(\eta^6\text{-}C_6H_5CONHCH_2Ph)(\eta^6\text{-}C_6H_6)](PF_6)\bullet(CH_2Cl_2)$ (**$[14^+]PF_6$**)	$[Re(\eta^6\text{-}C_6H_5CONHCH_2Ph)_2](PF_6)$ (**$[15^+]PF_6$**)
Empirical formula	$C_{24}H_{22}F_6N_2Pre$	$C_{21}H_{21}Cl_2F_6NOPRe$	$C_{28}H_{26}F_6N_2O_2PRe$
Diffractometer	Xcalibur Ruby	Xcalibur Ruby	Agilent SuperNova dual radiation CCD
Wavelength (Å)	0.7107	0.7107	1.54184
mol. weight (g/mol)	669.61	705.46	753.68
Crystal system	Orthorhombic	Monoclinic	Orthorhombic
Space group	Pbca	I2	Pna21
a (Å)	16.950(5)	16.0534(5)	12.91590(13)
b (Å)	14.245(5)	10.0483(3)	11.99680(14)
c (Å)	18.193(5)	14.6158(5)	17.12010(18)
α (°)	90	90	90
β (°)	90	100.718(3)	90
γ (°)	90	90	90
Volume ($Å^3$)	4393(2)	2316.53(11)	2652.75(5)
Z	8	4	4
Dens.(calc.) (g/cm^3)	2.025	2.023	1.887
Abs. coeff. (mm^{-1})	5.673	5.609	10.187
F(000)	2592	1360	1472
Crystal size (mm^3)	0.23 x 0.12 x 0.04	0.54 x 0.35 x 0.29	0.28 x 0.05 x 0.05
Crystal description	yellow plate	yellow block	yellow needle
θ range (°)	2.54 to 32.90	2.47 to 37.84	4.50 to 76.517
Index ranges	-24<=h<=9, -21<=k<=19, -27<=l<=21	-26<=h<=27, -17<=k<=16, -25<=l<=25	-16<=h<=16, -14<=k<=15, -21<=l<=21
Refl. collected	22225	21323	25892
Indep. reflections	7512 [R_{int} = 0.0402]	11740 [R_{int} = 0.0289]	7455 [R_{int} = 0.0367]
Reflections obs.	5528	10885	5060
Criterion for obs.	>2sigma(I)	>2sigma(I)	>2sigma(I)
Completeness to θ	99.9 % to 30.44°	99.9 % to 36.23°	100.0 % to 67.684°
Absorption corr.	Semi-empirical from equiv.	Semi-empirical from equiv.	Gaussian
Max. and min. transm.	0.8049 and 0.4869	0.2931 and 0.1517	0.688 and 0.181
Data / restraints / param.	7512 / 2 / 314	11740 / 1 / 298	5455 / 1 / 361
Goodness-of-fit on F^2	1.037	1.020	1.059
Fin. R ind. [I>2sigma(I)]	R1 = 0.0340, wR2 = 0.0676	R1 = 0.0272, wR2 = 0.0573	R1 = 0.0251, wR2 = 0.0639
R indices (all data)	R1 = 0.0543, wR2 = 0.0774	R1 = 0.0313, wR2 = 0.0595	R1 = 0.0286, wR2 = 0.0676
Fin. diff. ρmax ($e^-/Å^{-3}$)	1.507 and -1.373	0.749 and -1.438	0.943 and -1.227
CCDC Nr.	1485187	1485189	1485188

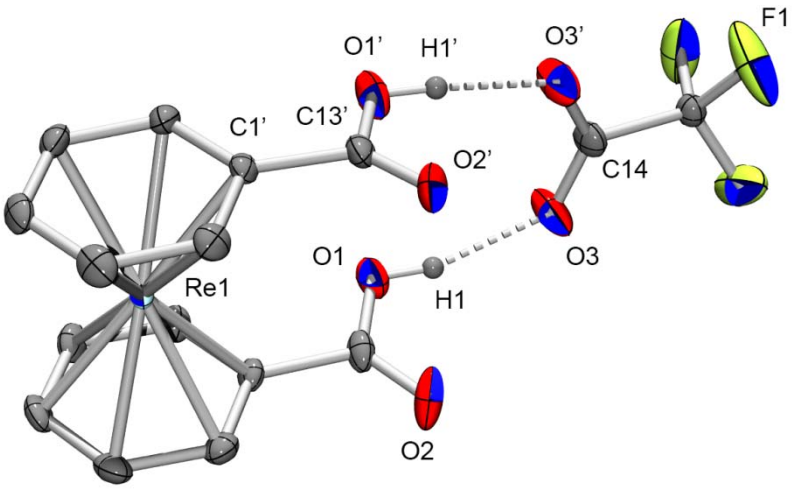

Figure S5: ORTEP representation of [Re(η^6-$C_6H_5COOH)_2$](TFA) [**7**$^+$]PF_6 (right). Hydrogen atoms (except H1 in **7**$^+$) are omitted for clarity, thermal ellipsoids represent 50% probability. Selected Hydrogen bond lengths [Å] for [**7**$^+$]: O1-H1---O3 1.803.

References

(1) *CrysAlis^{Pro} Software system*, Agilent Technologies.

(2) Altomare, A.; Burla, M.C.; Camalli, M.; Cascarano, C.; Giacovazzo, C.; Guagliardi, A.; Moliterni, A.G.G.; Polidori, G.; Spagna, R. SIR97: a new tool for crystal structure determination and refinement. *J. Appl. Cryst*., **1999**, *32*, 115.

(3) Sheldrick, G. M. A short history of SHELX. *Acta. Cryst*., **2008**, *A64*, 112.

(4) Spek, A. L. Single-crystal structure validation with the program PLATON. *J. Appl. Cryst*., **2003**, *36*, 7

8.4 Unpublished Experiment Section: Bis-arene Complexes $[Re(\eta^6\text{-arene})_2]^+$ as Highly Stable Bioorganometallic Scaffolds

8.4.1 $[Re(\eta^6\text{-}C_6H_4COOH_2)(\eta^6\text{-}C_6H_5COOH)]^+$ ([**17**](PF_6))

Synthesis: Product [**17**]$^+$ were isolated from the synthesis of [**6**]$^+$ and [**7**]$^+$. The residue was purified by preparative HPLC (Reprosil 100 C18, 250x40 mm, 0.1% TFA/CH_3CN, gradient see lit.[79]). Analytically pure orange [**17**]$^+$ precipitated from the pure fractions upon addition of NH_4PF_6. Single crystals, suitable for X-ray diffraction analysis were obtained by slow evaporation of a CH_3CN/H_2O (1:1) solution of [**17**](PF_6) Yields: 15.4 mg (0.024 mmol, 4%)

Analysis: ESI-MS: m/z = 475.01 $[M]^+$.

8.4.2 $[Re(\eta^6\text{-}C_6H_5Cl)(\eta^6\text{-}C_6H_6)](PF_6)$ ([**18**](PF_6)) and $[Re(\eta^6\text{-}C_6H_5Cl)_2](PF_6)$ ([**19**](PF_6))

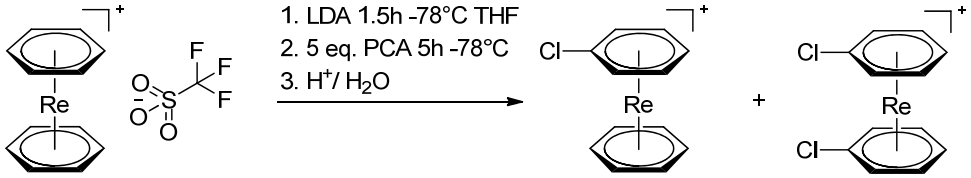

Synthesis: 300 mg (0.61 mmol) of [**1**](OTf) was dissolved in 30 mL dry THF and cooled to -78°C. 1.5 mL (1.53 mmol, 2.5 eq.) of a 1 M LDA in THF/hexane solution was slowly added to the yellow suspension. The reaction was stirred for 1.5 h at -78°C and then 721.9 mg (3.05 mmol, 5 eq.) hexachloroethane (PCA) was added to the clear orange solution. Stirring was continued for 7 h at -78°C and monitored by UPLC-MS. The colour of the solution changed from orange to yellow. The reaction was quenched with MeOH/HCl solution and the volume of mixture reduced under vacuum to 5 mL. The orange solution was extracted with hexane (3 x 2.5 mL) and evaporated in *vacuo*. The residue was purified by *preparative HPLC* (Reprosil 100 C18, 250x40 mm, 0.1% TFA/CH_3CN, gradient G5). The products were precipitated upon addition of NH_4PF_6 to yield analytically pure, yellow [**18**](PF_6), [**19**](PF_6) and [**20**](PF_6) Suitable crystals for X-ray for all compounds were obtained by slow evaporation from CH_3CN/H_2O (1:1). Yields: 151.7 mg (0.28 mmol, 47.6%) for [**19**](PF_6), 52.3 mg (0.09 mmol, 15%) for [**18**](PF_6) and 9.2 mg (0.015 mmol, 2.5%) [**20**](PF_6).

Analysis: $[Re(\eta^6\text{-}C_6H_5Cl)(\eta^6\text{-}C_6H_6)](PF_6)$ ([**18**](PF_6)): ^{1}H NMR (500 MHz, CD_3CN) δ [ppm]: 6.51 (d, 2H, *o*-CH_{arom}), 6.04 (t, 2H, *m*-CH_{arom}), 6.02 (s, 6H, CH_{arom}), 5.83 (t, 1H, *p*-CH_{arom}), ^{13}C NMR (125 MHz, CD_3CN) δ

[ppm]: 100.05 (*C*Cl), 80.77 (*C*H$_{arom}$), 79.74 (*o*-*C*H$_{arom}$), 77.00 (*p*-*C*H$_{arom}$), 75.82 (*m*-*C*H$_{arom}$), ESI-MS: m/z = 377.1 $[M]^+$, IR ν: 3097 (m), 1475 (m), 1430 (m), 1397 (w), 1082 (m), 926 (w), 807 (s) cm^{-1}, HR-ESI-MS $C_{12}H_{11}ClRe$ $[M]^+$: calculated, 377.0101; found, 377.0096.

[Re(η^6-$C_6H_5Cl)_2$](PF_6) ([**19**](PF_6)): ^{1}H NMR (500 MHz, CD_3CN) δ [ppm]: 6.49 (d, 4H, *o*-C*H*$_{arom}$), 6.11 (t, 4H, *m*-C*H*$_{arom}$), 5.90 (t, 2H, *p*-C*H*$_{arom}$), ^{13}C NMR (125 MHz, CD_3CN) δ [ppm]: 101.65 (*C*Cl), 82.25 (*o*-*C*H$_{arom}$), 79.53 (*p*-*C*H$_{arom}$), 78.68 (*m*-*C*H$_{arom}$), ESI-MS: m/z = 411.0 $[M]^+$, IR ν: 3097 (m), 1498 (w), 1428 (m), 1396 (m), 1278 (w), 1088 (m), 1026 (w), 928 (m), 904 (w), 839 (s), 813 (s), 705 (m) cm^{-1}. HR-ESI-MS $C_{12}H_{10}Cl_2Re$ $[M]^+$: calculated, 410.9711; found, 410.9702.

[Re(η^6-$C_6H_4Cl_2$)(η^6-C_6H_5Cl)](PF_6) ([**20**](PF_6)): ^{1}H NMR (500 MHz, CD_3CN) δ [ppm]: 6.71 (dd, 2H, *o*-C*H*$_{arom}$), 6.42 (d, 2H, *o*-C*H*$_{arom}$), 6.19 (t, 2H, *m*-C*H*$_{arom}$), 6.01 (dd, 2H, *m*-C*H*$_{arom}$), 5.95 (t, 1H, *p*-C*H*$_{arom}$). ^{13}C NMR (125 MHz, CD_3CN) δ [ppm]: 103.5 (*C*Cl), 102.59 (*C*Cl), 84.77 (*o*-*C*H$_{arom}$), 81.0 (*p*-*C*H$_{arom}$), 80.9 (*m*-*C*H$_{arom}$), 80.4 (*o*-*C*H$_{arom}$), 78.4 (*m*-*C*H$_{arom}$). ESI-MS: m/z = 444.9 $[M]^+$. IR ν: 3092 (m), 2923 (m), 2851 (w), 1429 (m), 1404 (m), 1383 (m), 1112 (w), 1085 (w), 1029 (w), 821 (s), 737 (m) cm^{-1}. HR-ESI-MS $C_{12}H_9Cl_3Re$ $[M]^+$: calculated, 444.9327; found, 444.9305.

8.4.3 [Re(η^6-$C_6H_4Br_2$)(η^6-C_6H_5Br)](PF_6) ([**21**](PF_6))

Synthesis: Product $[\mathbf{21}]^+$ were isolated from the synthesis of [**4**](PF_6) and [**5**](PF_6)**.** The residue was purified by preparative HPLC (Reprosil 100 C18, 250x40 mm, 0.1% TFA/CH_3CN, gradient see lit.[79]). Analytically pure yellow $[\mathbf{21}]^+$ precipitated from the fractions upon addition of NH_4PF_6. Single crystals, suitable for X-ray diffraction analysis were obtained by slow evaporation of a CH_3CN/H_2O (1:1) solution of [**21**](PF_6). Yields: 12.2 mg (0.016 mmol, 2.7%)

Analysis: ^{1}H NMR (500 MHz, CD_3CN) δ [ppm]: 6.73 (dd, 2H, *o*-C*H*$_{arom}$), 6.42 (d, 2H, *o*-C*H*$_{arom}$), 6.13 (t, 2H, *m*-C*H*$_{arom}$), 6.01 (dd, 2H, *m*-C*H*$_{arom}$), 5.00 (t, 1H, *p*-C*H*$_{arom}$). ^{13}C NMR (125 MHz, CD_3CN) δ [ppm]: 91.90 (*C*Br), 89.45 (*C*Br), 87.21 (*o*-*C*H$_{arom}$), 83.09 (*m*-*C*H$_{arom}$), 81.77 (*o*-*C*H$_{arom}$), 81.28 (*p*-*C*H$_{arom}$), 79.15 (*m*-*C*H$_{arom}$). ESI-MS: m/z = 578.8 $[M]^+$. IR ν: 3086 (w), 1425 (m), 1493 (m), 1212 (w), 1081 (w), 1054 (w), 1017 (w), 814 (s), 702 (m) cm^{-1}. HR-ESI-MS $C_{12}H_9Br_3Re$ $[M]^+$: calculated, 578.7784; found, 578.7776.

8.4.4 [Re(η^6-C_6H_5OMe)(η^6-C_6H_6)](PF_6) ([**22**](PF_6))

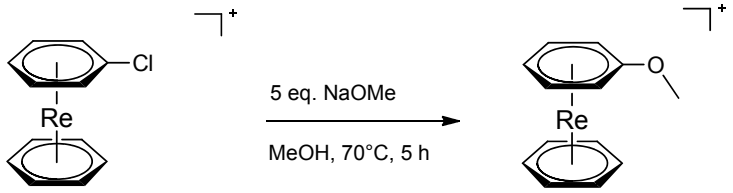

Synthesis: 30 mg (0.057 mmol) [**18**](PF_6) was dissolved in 2 mL methanol. Afterwards, 31 mg (0.287 mmol, 5 eq.) of sodium methoxide were added to the yellow solution. The reaction mixture was stirred for 5 h at 70°C. The solvent was evaporated in *vacuo* and the residue was quenched with 1 mL water. 11.2 mg (0.069 mmol, 1.2 eq.) of NH_4PF_6 were added to the suspension. The product was extracted with CH_2Cl_2 (2 x 2ml) from the aqueous phase. The product was recrystallized from acetonitrile, yielding single crystals of [**22**](PF_6), suitable for X-ray diffraction analysis. Yield: 26.2 mg (0.0501 mmol, 88%) of [**22**](PF_6).

Analysis: ^{1}H NMR (500 MHz, CD_3CN) δ [ppm]: 6.30 (d, 2H, *o*-C*H*$_{arom}$), 5.95 (t, 2H, *m*-C*H*$_{arom}$), 5.83 (s, 6H, C*H*$_{arom}$), 5.68 (t, 1H, *p*-C*H*$_{arom}$), 3.58 (s, 3H, OC*H*$_3$). ^{13}C NMR (125 MHz, CD_3CN) δ [ppm]: 131.76 (*C*$_{arom}$-OCH_3), 77.61 (*p*-*C*H$_{arom}$), 76.84 (*C*$_{arom}$), 74.69 (*m*-*C*H$_{arom}$), 68.23 (*o*-*C*H$_{arom}$), 57.68 (O*C*H$_3$). ESI-MS: m/z = 373.1 $[M]^+$. IR ν: 3106 (w), 2923 (w), 2853 (w), 1518 (m), 1495 (w), 1454 (w), 1434 (m), 1242 (m), 1184 (w), 1051 (w), 1017 (w), 985 (w), 923 (w), 814 (s), 775 (m) cm^{-1}. HR-ESI-MS $C_{13}H_{14}ORe$ $[M]^+$: calculated, 373.0594; found373.0595.

8.4.5 [Re(η^6-C_6H_5-1,3-$C_3H_3N_2$)(η^6-C_6H_6)](PF_6) ([**23**](PF_6))

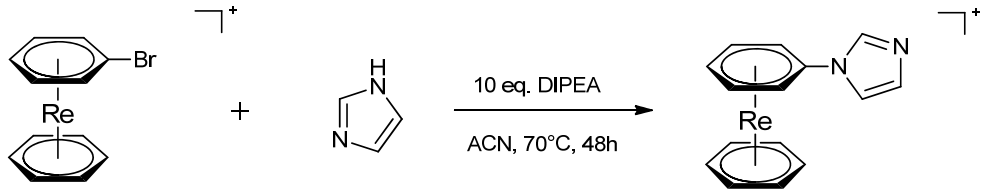

Synthesis: A 5 mg (0.009 mmol) portion of [**4**](PF_6) was dissolved in 2 mL acetonitrile. Afterwards, 15 µL (0.09 mmol, 10 equiv) of DIPEA and 61 mg (0.9 mmol, 100 equiv) of 1*H*-imidazole were added to the yellow solution. The reaction mixture was stirred for 48 h at 70°C. The solvent was evaporated in *vacuo* and the residue washed 3 times with Et_2O (3 x 4 mL). The product was recrystallized from water, yielding single crystals of [**23**](PF_6), suitable for X-ray diffraction analysis. Yield: 4.2 mg (0.008 mmol, 87%) of [**23**]PF_6).

Analysis: ESI-MS: m/z = 409.1 $[M]^+$.

8.4.6 [Re(η^6-$C_6H_5OMe)_2$](PF_6) ([**24**](PF_6))

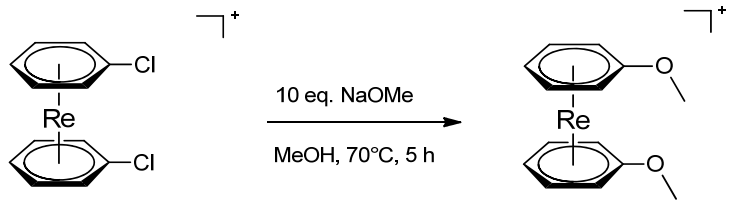

Synthesis: 30 mg (0.054 mmol) [**19**](PF_6) were dissolved in 2 mL methanol. Afterwards, 31 mg (0.529 mmol, 10 eq.) of sodium methoxide were added to the yellow solution. The reaction mixture was 4stirred for 5 h at 70°C. The solvent was evaporated in *vacuo* and the residue was quenched with 1 mL water. 10.5 mg (0.065 mmol, 1.2 eq.) of NH_4PF_6 were added to the suspension. The product was extracted with CH_2Cl_2 (2 x 2ml) from the aqueous phase. The product was recrystallized from acetonitrile, yielding single crystals of [**24**](PF_6), suitable for X-ray diffraction analysis. Yield: 26.9 mg (0.0501 mmol, 91%) of [**24**](PF_6).

Analysis: ^{1}H NMR (500 MHz, CD_3CN) δ [ppm]: 6.19 (d, 4H, *o*-CH_{arom}), 5.84 (t, 4H, *m*-CH_{arom}), 5.60 (t, 2H, *p*-CH_{arom}), 3.59 (s, 6H, OCH_3). ^{13}C NMR (125 MHz, CD_3CN) δ [ppm]: 131.68 (C_{arom}-OCH_3), 77.71 (*p*-CH_{arom}), 73.86 (*m*-CH_{arom}), 66.98 (*o*-CH_{arom}), 57.65 (OCH_3). ESI-MS: m/z = 403.1 $[M]^+$. IR ν: 3108 (w), 2923 (w), 2884 (w), 1508 (m), 1467 (w), 1450 (w), 1437 (m), 1238 (m), 1183 (w), 1055 (w), 1016 (m), 985 (w), 919 (w), 824 (s), 770 (m) cm^{-1}. HR-ESI-MS $C_{14}H_{16}O_2Re$ $[M]^+$: calculated, 403.0702; found, 403.0696.

8.4.7 [Re(η^6-N-((naphthalen-2-yl)-2-(phenylthio)acetamide)$_2$](PF_6) ([**25**](PF_6))

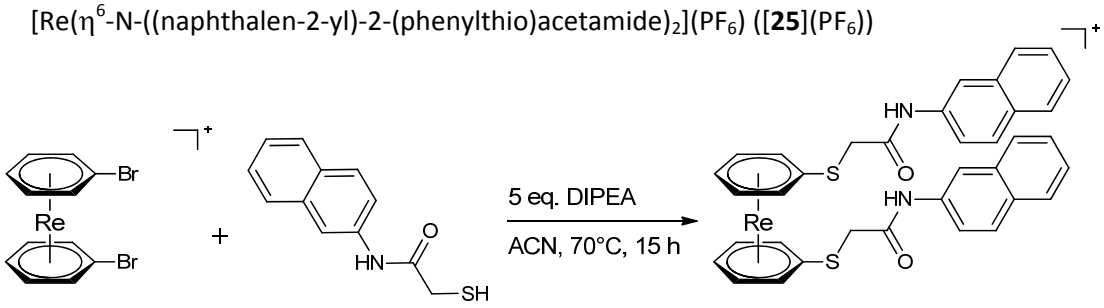

Synthesis: A 30 mg (0.046mmol) portion of [**5**](PF_6) was dissolved in 5 mL acetonitrile. After the addition of 40 µL (0.23 mmol, 5 equiv) DIPEA and 30 mL (0.23 mmol, 5 equiv) N-naphthalen-2-yl-2-sulfanylacetamide to the yellow solution, the reaction mixture was stirred for 15 h at 70°C. The solvent was evaporated *in vacuo* and the residue washed with Et_2O (2 x 4 mL), water (2 x 4 mL) and purified by *preparative HPLC* (Reprosil 100 C18, 250x40 mm, 0.1% TFA/CH_3CN, gradient G3) After addition of NH_4PF_6, the product was recrystallized from acetonitrile, yielding single crystals of [**25**](PF_6), suitable for X-ray diffraction analysis. Yield: 28.2 mg (0.036 mmol, 79%) of [**25**](PF_6).

Analysis: ^{1}H NMR (500 MHz, CD_3CN) δ [ppm]: 8.79 (s, 2H, CON*H*), 8.21 (2, 2H, CH_{arom}), 7.81 (m, 6H, CH_{arom}), 7.52 (d, 2H, CH_{arom}), 7.47 (d, 2H, CH_{arom}), 7.42 (d, 2H, CH_{arom}), 6.37 (2, 4H, o-CH_{arom}), 6.02 (t, 4H, *m*-CH_{arom}), 5.89 (t, 2H, *p*-CH_{arom}), 3.78 (s, 4H, CH_2). ^{13}C NMR (125 MHz, CD_3CN) δ [ppm]: 167.60 (*C*O), 136.90 (C_{arom}), 134.70 (C_{arom}), 131.62 (C_{arom}), 129.70 (CH_{arom}), 128.55 (CH_{arom}), 128.44 (CH_{arom}), 127.764 (CH_{arom}), 126.17 (CH_{arom}), 120.88 (CH_{arom}), 117.21 (CH_{arom}), 97.15 (C_{arom}-S), 82.21 (*o*-CH_{arom}), 78.68 (*m*-CH_{arom}), 78.55 (*p*-CH_{arom}), 40.30 (CH_2). ESI-MS: m/z = 773.1 $[M]^+$. IR ν: 3394 (CO-NH, w), 3301 (CO-NH, w), 3063 (w) 3077 (w), 1669 (m), 1630 (w), 1604 (w), 1584 (w), 1545 (w), 1501 (w), 1470 (w), 1432 (w), 1391 (w), 1304 (w), 1221 (w), 1079 (w), 821 (s), 770 (m) cm^{-1}. HR-ESI-MS $C_{36}H_{30}N_2O_2ReS_2$ $[M]^+$: calculated, 773.1301; found, 773.1292.

8.4.8 [Re(η^6-C_6H_5COEt)(η^6-C_6H_6)](PF_6) ([**26**](PF_6)) and [Re(η^6-$C_6H_5COEt)_2$](PF_6) ([**27**](PF_6))

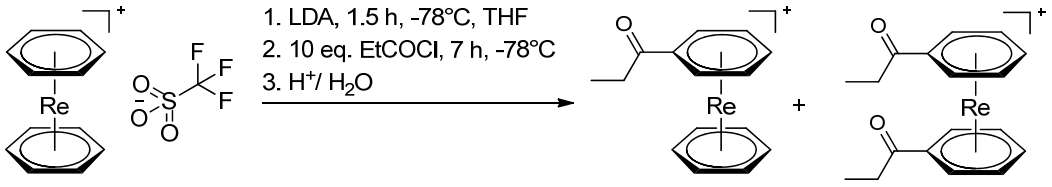

Synthesis: A 100 mg (0.204 mmol) portion of [**1**](OTf) was dissolved in 5 mL of dry THF and cooled to -78°C. A 0.3 mL (0.306 mmol, 1.5 equiv) portion of a 1 M LDA solution (THF/hexane) was added slowly to the yellow suspension. The reaction was stirred for 1.5 h at -78°C, and 70 µL (2.04 mmol, 10 eq.) of propionyl chloride was added to the clear orange solution. Stirring was continued for 7 h at -78 °C. The reaction was quenched with TFA/water (pH=2) and the volume of the mixture was reduced under vacuum to 5 mL. The orange solution was extracted with hexane (3 x 2.5 mL) and the remaining solvent was evaporated *in vacuo*. The residue was purified by *preparative HPLC* (Reprosil 100 C18, 250 mm x 40 mm, 0.1% TFA/CH_3CN, gradient G6). Analytically pure yellow [**26**](PF_6) and [**27**](PF_6) precipitated from the solution upon addition of NH_4PF_6. Single crystals, suitable for X-ray diffraction analysis, were obtained by slow evaporation of a CH_3CN/H_2O (1:1) solution of [**26**](PF_6) and [**27**](PF_6). Yields: 45 mg (0.082 mmol, 41%) for [**26**](PF_6) and 21 mg (0.036 mmol, 17%) for [**26**](PF_6). Yields of dimeric side-products: 12 mg (0.011 mmol, 5.7%) for [**28**]$(PF_6)_2$ and 10 mg (0.010 mmol, 4.5%) for [**29**]$(PF_6)_2$

Analysis: [Re(η^6-C_6H_5COEt)(η^6-C_6H_6)](PF_6) ([**26**](PF_6)): ^{1}H NMR (500 MHz, CD_3CN) δ [ppm]: 6.54 (d, 2H, *o*-CH_{arom}), 6.13 (t, 2H, *m*-CH_{arom}), 6.09 (t, 1H, *p*-CH_{arom}), 6.00 (s, 6H, CH_{arom}), 2.81 (q, 2H, CH_2), 1.11 (t, 3H, CH_3). ^{13}C NMR (125 MHz, CD_3CN) δ [ppm]: 202.7 (*C*OEt), 83.62 (C_{arom}-COEt), 80.29 (C_{arom}), 77.73 (*m*-CH_{arom}), 76.86 (*p*-CH_{arom}), 76.59 (*o*-CH_{arom}), 32.29 (CH_2), 7.80 (CH_3). ESI-MS: m/z = 399.1 $[M]^+$. IR ν:

3096(w), 2984 (w), 2945 (w), 1694 (m, C=O), 1426 (s), 1353 (w), 1211 (m), 1005 (w), 949 (w), 805 (s) cm^{-1}. HR-ESI-MS $C_{15}H_{16}ORe$ $[M]^+$: calculated, 399.0753; found, 399.0754.

$[Re(\eta^6\text{-}C_6H_5COEt)_2](PF_6)$ ([**27**](PF_6)): ^1H NMR (500 MHz, CD_3CN) δ [ppm]: 6.58 (d, 4H, *o*-CH_{arom}), 6.20 (t, 4H, *m*-CH_{arom}), 6.16 (t, 2H, *p*-CH_{arom}), 2.74 (q, 4H, CH_2), 1.11 (t, 6H, CH_3). ^{13}C NMR (125 MHz, CD_3CN) δ [ppm]: 201.84 (*C*OEt), 85.73 (C_{arom}-COEt), 80.20 (*m*-*C*H_{arom}), 79.48 (*p*-*C*H_{arom}), 79.06 (*o*-*C*H_{arom}), 32.66 (*C*H_2), 7.60 (*C*H_3). ESI-MS: m/z = 455.1 $[M]^+$. IR ν: 3094 (m), 2988 (w), 2941 (w), 1699 (s, C=O), 1410 (m), 1349 (w), 1205 (m), 1005 (w), 945 (w), 813 (s) cm^{-1}. HR-ESI-MS $C_{18}H_{20}O_2Re$ $[M]^+$: calculated, 455.1015; found, 455.1012.

$[(\eta^6\text{-}C_6H_6)Re(\eta^6\text{-}C_6H_5C(OH)Et)Re(\eta^6\text{-}C_6H_6)](PF_6)_2$ ([**28**]$(PF_6)_2$): ^1H NMR (500 MHz, CD_3CN) δ [ppm]: 6.38 (d, 2H, CH_{arom}), 6.16 (d, 2H, CH_{arom}), 5.94 (m, 6H, CH_{arom}), 5.86 (s, 12H, CH_{arom}), 3.57 (s, 1H, O*H*), 1.94 (q, 2H, CH_2), 0.81 (t, 3H, CH_3). ^{13}C NMR (125 MHz, CD_3CN) δ [ppm]: 106.12 (C_{arom}-C(OH)Et), 105.88 (C_{arom}-C(OH)Et), 78.68 (*C*H_{arom}), 76.63 (*C*H_{arom}), 76.50 (*C*H_{arom}), 76.44 (*C*-OH), 75.73 (*C*H_{arom}), 75.37 (*C*H_{arom}), 75.36 (*C*H_{arom}), 36.72 (*C*H_2), 8.36 (*C*H_3). ESI-MS: m/z = 377.1 $[M]^{2+}$. IR ν: 3324 (br, w), 3094 (w), 1433 (m), 1425 (m), 1160 (w), 818 (s) cm^{-1}. HR-ESI-MS $C_{27}H_{28}ORe_2$ $[M]^{2+}$: calculated, 377.0622; found, 377.0619.

$[(\eta^6\text{-}C_6H_6)Re(\eta^6\text{-}C_6H_5C(OH)Et)Re(\eta^6\text{-}C_6H_5COEt)](PF_6)_2$ ([**29**]$(PF_6)_2$): ^1H NMR (500 MHz, CD_3CN) δ [ppm]: 6.48 (d, 1H, CH_{arom}), 6.43 (d, 1H, CH_{arom}), 6.38 (d, 1H, CH_{arom}), 6.35 (d, 1H, CH_{arom}), 6.18 (d, 1H, CH_{arom}), 6.15 (d, 1H, CH_{arom}), 6.00 (m, 8H, CH_{arom}), 5.93 (t, 1H, CH_{arom}), 5.88 (s, 6H, CH_{arom}), 3.67 (s, 1H, O*H*), 2.80 (q, 2H, CH_2), 1.90 (q, 2H, CH_2), 1.11 (7, 3H, CH_3), 0.81 (t, 3H, CH_3). ^{13}C NMR (125 MHz, CD_3CN) δ [ppm]: 202.76 (*C*OEt), 108.49 (C_{arom}-C(OH)Et), 105.88 (C_{arom}-C(OH)Et), 84.23 (C_{arom}-COEt), 79.68 (*C*H_{arom}), 79.05 (*C*H_{arom}), 78.89 (*C*H_{arom}), 78.83 (*C*H_{arom}), 78.78 (*C*H_{arom}), 78.60 (*C*H_{arom}), 78.14 (*C*H_{arom}), 78.08 (*C*H_{arom}), 77.90 (*C*H_{arom}), 77.70 (*C*H_{arom}), 77.66 (*C*H_{arom}), 76.59 (*C*H_{arom}), 76.50 (*C*-OH), 76.40 (*C*H_{arom}), 75.72 (*C*H_{arom}), 75.35 (*C*H_{arom}), 75.25 (*C*H_{arom}), 36.65 (*C*H_2), 32.64 (*C*H_2), 8.32 (*C*H_3), 7.86 (*C*H_3). ESI-MS: m/z = 399.1 $[M]^{2+}$. IR ν: 3402 (br, w), 3097 (m), 2943 (w), 1698 (s, C=O), 1436 (w), 1401 (w), 1353 (w), 1210 (w), 1161 (w), 993 (w), 819 (s) cm^{-1}. HR-ESI-MS $C_{30}H_{32}O_2Re_2$ $[M]^{2+}$: calculated, 399.0752; found, 399.0746.

8.4.9 [Re(η^6-1,1,2-triyltribenzene-but-1-ene)(η^6-C_6H_6)](PF_6) ([**30**](PF_6))

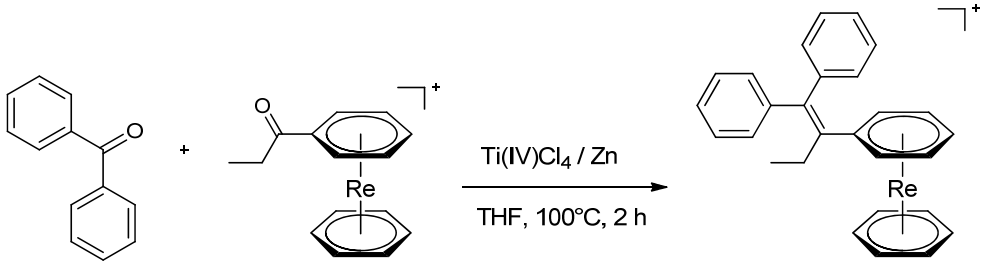

Synthesis: 65 mg zinc dust (0.99 mmol, 24 eq.) was added in 4 mL dry THF. The solution was cooled to 0 °C and subsequently 0.05 mL (0.456 mmol, 11 eq.) $TiCl_4$ was added dropwise. The dark suspension was heated in a microwave device for 1 h at 70 °C. Afterwards, 23 mg (0.04 mmol) of [**26**](PF_6) and 50 mg (0.28 mmol, 6.5 eq.) of benzophenone were suspended in THF (11 mL) and added to the mixture. Further, the grey mixture was heated in a microwave device for 2 h at 100 °C. Reaction control was performed by UPLC-MS. After quenching the reaction for 30 min with 2 mL of water, the solvent (THF) was evaporated in *vacuo*. The remaining aqueous phase was washed with hexane (2 x 4 mL), Et_2O (2 x 4 mL) and three times with 5 mL CH_2Cl_2. The residue was purified by *preparative* HPLC (Reprosil 100 C18, 250 mm x 40 mm, 0.1% TFA/CH_3CN, gradient G7). Analytically pure yellow [**30**](PF_6) precipitated from the solution upon addition of NH_4PF_6. Single crystals, suitable for X-ray diffraction analysis, were obtained by slow evaporation of a CH_2Cl_2 solution of [**30**](PF_6). Yields: 5 mg (0.007 mmol, 18%) for [**30**](PF_6). During the purification via *preparative* HPLC the side-product [Re(η^6-$C_6H_5C(OH)Et$)(η^6-C_6H_6)](PF_6) ([**31**](PF_6)) was isolated. Single crystals, suitable for X-ray diffraction analysis, were obtained by slow evaporation of an acetonitrile solution of [**31**](PF_6). Yields: 12 mg (0.022 mmol, 56%) for [**31**](PF_6).

Analysis: [Re(η^6-1,1,2-triyltribenzene-but-1-ene)(η^6-C_6H_6)](PF_6) ([**30**](PF_6)): ^{1}H NMR (500 MHz, CD_3CN) δ [ppm]: 7.39 (t, 2H, CH_{arom}), 7.32 (t, 1H, CH_{arom}), 7.25 (d, 2H, CH_{arom}), 7.19 (m, 3H, CH_{arom}), 7.01 (m, 2H, CH_{arom}), 5.93 (d, 2H, CH_{arom}), 5.90 (s, 6H, CH_{arom}), 5.76 (m, 3H, CH_{arom}), 2.28 (q, 2H, CH_2), 0.93 (t, 3H, CH_3). ^{13}C NMR (125 MHz, CD_3CN) δ [ppm]: 147.00 (*C*), 143.58 (*C*), 143.36 (*C*), 137.29 (*C*), 131.30 (*C*H_{arom}), 129.80 (*C*H_{arom}), 129.60 (*C*H_{arom}), 129.31 (*C*H_{arom}), 128.42 (*C*H_{arom}), 128.26 (*C*H_{arom}), 103.24 (*C*$_{arom}$), 79.89 (*C*H_{arom}), 78.24 (*C*H_{arom}), 76.61 (*C*H_{arom}), 75.92 (*C*H_{arom}), 30.77 (*C*H_2), 15.29 (*C*H_3). ESI-MS: m/z = 549.1 $[M]^+$. IR ν: 2929 (w), 1489 (w), 1435 (m), 1073 (w), 923 (w), 881 (w), 824 (s), 771 (s), 750 (m), 718 (w), 708 (m) cm^{-1}. HR-ESI-MS $C_{28}H_{26}Re$ $[M]^+$: calculated, 549.1586; found, 549.1587.

Analysis: [Re(η^6-$C_6H_5C(OH)Et$)(η^6-C_6H_6)](PF_6) ([**31**](PF_6)): ^{1}H NMR (500 MHz, CD_3CN) δ [ppm]: 6.19 (d, 2H, *o*-CH_{arom}), 5.95 (t, 2H, *m*-CH_{arom}), 5.92 (t, 1H, *p*-CH_{arom}), 5.89 (s, 6H, CH_{arom}), 4.11 (dd, 1H, C*H*), 1.68 (q, 2H, CH_2), 0.93 (t, 3H, CH_3). ^{13}C NMR (125 MHz, CD_3CN) δ [ppm]: 102.93 (*C*$_{arom}$-C(OH)Et), 77.76 (*C*H_{arom}), 76.72 (*p*-*C*H_{arom}), 76.56 (*m*-*C*H_{arom}), 75.71 (*o*-*C*H_{arom}), 73.71 (*C*(OH)Et), 33.33 (*C*H_2), 10.41

(CH_3). ESI-MS: m/z 401.1 $[M]^+$. IR ν: 3409 (br, w), 3091 (w), 2933 (w), 1434 (w), 1404 (m), 1057 (m), 985 (w), 908 (w), 828 (s), 740 (w) cm^{-1}. HR-ESI-MS $C_{15}H_{18}ORe$ $[M]^+$: calculated, 401.0909; found, 401.0917.

8.4.10 [Re(η^6-4,4'-(2-phenylbut-1-ene-1,1-diyl)diphenol)(η^6-C_6H_6)](PF_6) ([**32**](PF_6))

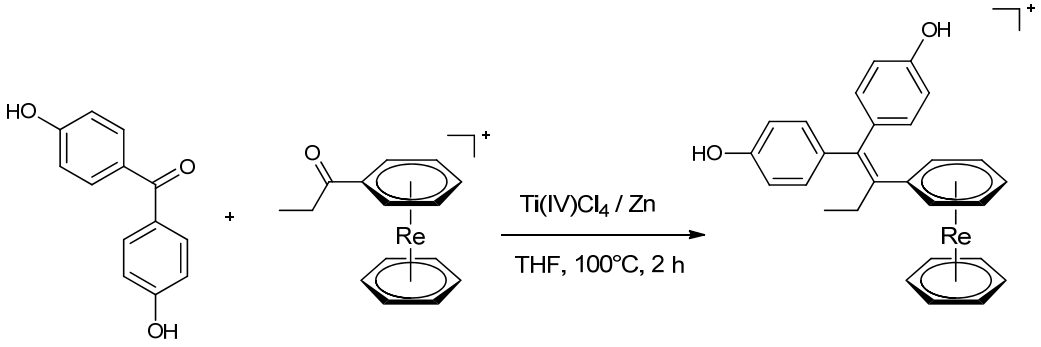

Synthesis: 65 mg zinc dust (0.99 mmol, 24 eq.) was added in 4 mL dry THF. The solution was cooled to 0 °C and subsequently 0.05 mL (0.456 mmol, 11 eq.) $TiCl_4$ was added dropwise. The dark suspension was heated in a microwave device for 1 h at 70 °C. Afterwards, 23 mg (0.04 mmol) of [**26**](PF_6) and 60 mg (0.28 mmol, 6.5 eq.) of 4,4'-dihydroxybenzophenone were suspended in THF (11 mL) and added to the mixture. Further, the grey mixture was heated in a microwave device for 2 h at 100°C. Reaction control was performed by UPLC-MS. After quenching the reaction for 30 min with 2 mL of water, the solvent (THF) was evaporated in *vacuo*. The remaining aqueous phase was washed with hexane (2 x 4 mL), Et_2O (2 x 4 mL) and three times with 5 mL CH_2Cl_2. The residue was purified by was purified by *preparative* HPLC (Reprosil 100 C18, 250 mm x 40 mm, 0.1% TFA/CH_3CN, gradient G8). Analytically pure yellow [**32**](PF_6) precipitated from the solution upon addition of NH_4PF_6. Single crystals, suitable for X-ray diffraction analysis, were obtained by slow evaporation of a CH_2Cl_2 solution of [**32**](PF_6). Yields: 14 mg (0.018 mmol, 46%) for [**32**](PF_6)**.** During the purification via *preparative* HPLC, the side-product Re(η^6-$C_6H_5C(OH)Et$)(η^6-C_6H_6)](PF_6) ([**31**](PF_6)) was isolated. Single crystals, suitable for X-ray diffraction analysis, were obtained by slow evaporation of an acetonitrile solution of [**31**](PF_6). Yields: 7 mg (0.013 mmol, 32%) for [**31**](PF_6)

Analysis: ^{1}H NMR (500 MHz, CD_3CN) δ [ppm]: 7.04 (d, 2H, CH_{arom}), 6.80 (m, 4H, CH_{arom}), 6.60 (d, 2H, CH_{arom}), 5.92 (d, 2H, CH_{arom}), 5.87 (s, 6H, CH_{arom}), 5.79 (t, 2H, CH_{arom}), 5.76 (t, 1H, CH_{arom}), 2.28 (q, 2H, CH_2), 0.91 (t, 3H, CH_3). ^{13}C NMR (125 MHz, CD_3CN) δ [ppm]: 157.22 (C_{arom}-OH), 157.22 (C_{arom}-OH), 146.78 (*C*), 135.52 (*C*), 135.40 (*C*), 135.24 (*C*), 132.96 (*C*H$_{arom}$), 131.31 (*C*H$_{arom}$), 116.06 (*C*H$_{arom}$), 115.82 (*C*H$_{arom}$), 104.13 (C_{arom}), 80.00 (*C*H$_{arom}$), 77.94 (*C*H$_{arom}$), 76.66 (*C*H$_{arom}$), 76.07 (*C*H$_{arom}$), 30.61 (CH_2),

15.19 (*C*H_3). ESI-MS: m/z = 581.1 $[M]^+$. IR ν: 3320 (br, w), 2925 (w), 1668 (w), 1608 (w), 1509 (w), 1424 (m), 1244 (w), 811 (s) cm^{-1}. HR-ESI-MS $C_{28}H_{26}O_2Re$ $[M]^+$: calculated, 581.1484; found, 581.1486.

8.4.11 $[Re(\eta^6\text{-}C_6H_5C(OH)Ph)(\eta^6\text{-}C_6H_6)](PF_6)$ ([**33**](PF_6)) and $[Re(\eta^6\text{-}C_6H_5C(OH)Ph)_2](PF_6)$ ([**34**](PF_6))

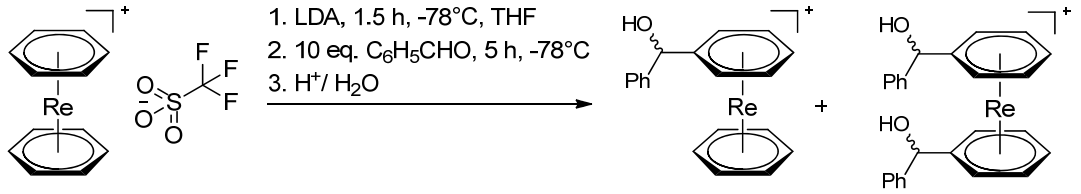

Synthesis: A 50 mg (0.102 mmol) portion of [**1**](OTf) was dissolved in 3 mL of dry THF and cooled to -78°C. A 0.25 mL (0.205 mmol, 2.5 equiv) portion of a 1 M LDA solution (THF/hexane) was added slowly to the yellow suspension. The reaction was stirred for 1.5 h at -78°C, and 102 µL (1.02 mmol, 10 eq.) of benzaldehyde was added to the clear orange solution. Stirring was continued for 5 h at -78 °C. The reaction was quenched with 2M HCl solution (pH=2) and the volume of the mixture was reduced under vacuum to 5 mL. The orange solution was extracted with hexane (3 x 2.5 mL) and the remaining solvent was evaporated under N_2 stream. Single crystals of ([**34**](PF_6), suitable for X-ray diffraction analysis, were obtained from the crude by slow evaporation of the aq. HCl solution. $[\mathbf{33}]^+$ was not isolated because it was formed in trace amount. The product $[\mathbf{34}]^+$ was precipitated after addition of NH_4PF_6 from the aqueous phase. After extraction with dichloromethane (3 x 5 mL), the product was purified by recrystallization from dichloromethane, yielding yellow crystals of [**34**](PF_6), suitable for X-ray diffraction analysis. Yield: 39 mg (0.056 mmol, 55%) of [**34**](PF_6).

Analysis: $[Re(\eta^6\text{-}C_6H_5C(OH)Ph)_2](PF_6)$ ([**34**](PF_6)): ^{1}H NMR (500 MHz, CD_3CN) δ [ppm]: 7.41 (m, 8H, CH_{arom}), 7.32 (t, 2H, CH_{arom}), 6.44 (t, 2H, *o*-CH_{arom}), 6.08 (t, 2H, *o*-CH_{arom}), 5.96 (t, 2H, *m*-CH_{arom}), 5.88 (t, 2H, *m*-CH_{arom}), 5.83 (t, 2H, *p*-CH_{arom}), 5.38 (s, 2H, C*H*), 4.58 (s, 2H, C-O*H*). ^{13}C NMR (125 MHz, CD_3CN) δ [ppm]: 143.87 (C_{arom}), 129.89 (*C*H_{arom}), 129.55 (*C*H_{arom}), 127.34 (*C*H_{arom}), 102.76 (C_{arom}-C(H)OH), 77.76 (*C*H_{arom}), 77.43 (*C*H_{arom}), 77.28 (*C*H_{arom}), 77.22 (*C*H_{arom}), 75.67 (*C*H_{arom}), 74.69 (*C*(H)OH). ESI-MS: m/z = 555.1 $[M]^+$. IR ν: 3320 (br, w, OH), 2920 (w), 1494 (w), 1446 (w), 1406 (w), 1180 (w), 1061 (w), 1024 (w), 924 (w), 827 (s) cm^{-1}. HR-ESI-MS $C_{28}H_{26}Re$ $[M]^+$: calculated, 555.1328; found, 555.1326.

8.4.12 [Re(η^6-$C_6H_5C(OH)(Ph)_2$)(η^6-C_6H_6)](PF_6) ([**35**](PF_6)) and [Re(η^6-$C_6H_5C(OH)(Ph)_2)_2$](PF_6) ([**36**](PF_6))

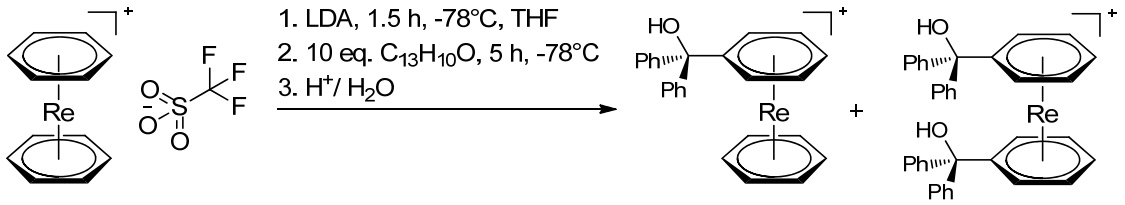

Synthesis: A 50 mg (0.102 mmol) portion of [**1**](OTf) was dissolved in 3 mL of dry THF and cooled to -78°C. A 0.25 mL (0.205 mmol, 2.5 equiv) portion of a 1 M LDA solution (THF/hexane) was added slowly to the yellow suspension. The reaction was stirred for 1.5 h at -78°C, and 189 mg (1.04 mmol, 10 eq.) of benzophenone was added to the clear orange solution. Stirring was continued for 7 h at -78 °C. The reaction was quenched with TFA/water (pH=2) and the volume of the mixture was reduced under vacuum to 5 mL. The orange solution was extracted with hexane (3 x 2.5 mL) and the remaining solvent was evaporated *in vacuo*. The residue was purified by *preparative HPLC* (Reprosil 100 C18, 250 mm x 40 mm, 0.1% TFA/CH_3CN, gradient G9). Analytically pure yellow [**35**](PF_6), [**36**](PF_6) and [**37**](PF_6) precipitated from the solution upon addition of NH_4PF_6. Single crystals, suitable for X-ray diffraction analysis, were obtained by vapour diffusion of cyclohexane into THF solution of [**35**](PF_6). The same approach was used for [**36**](PF_6)and [**37**](PF_6), respectively. Yields: 3.41 mg (0.005 mmol, 5%) for [**35**](PF_6), 34.05 mg (0.04 mmol, 39%) for [**36**](PF_6) and 25.8 mg (0.025 mmol, 24%) for [**37**](PF_6).

Analysis: [Re(η^6-$C_6H_5C(OH)Ph_2$)(η^6-C_6H_6)](PF_6) ([**35**](PF_6)) ^{1}H NMR (500 MHz, $(CD_3)_2CO$) δ [ppm]: 7.36 (m, 10H, CH_{arom}), 6.25 (d, 2H, *o*-CH_{arom}), 6.22 (t, 1H, *p*-CH_{arom}), 6.18 (t, 2H, *m*-CH_{arom}), 6.03 (s, 6H, CH_{arom}). ^{13}C NMR (125 MHz, $(CD_3)_2CO$) δ [ppm]: 146.40 (C_{arom}), 128.86 (CH_{arom}), 128.78 (CH_{arom}), 128.76 (CH_{arom}), 103.89 (C_{arom}-$COPh_2$), 81.15 (*C*-OH), 78.51 (CH_{arom}), 78.32 (*o*-CH_{arom}), 76.58 (*p*-CH_{arom}), 76.02 (*m*-CH_{arom}). ESI-MS: m/z = 525.1 $[M]^+$. IR ν: 2919 (w), 1491 (m), 1445 (m), 1398 (w), 1018 (w), 819 (s), 761 (m) cm^{-1}. HR-ESI-MS $C_{25}H_{22}ORe$ $[M]^+$: calculated, 525.1222; found, 525.1216.

Analysis: [Re(η^6-$C_6H_5C(OH)Ph_2)_2$](PF_6) ([**36**](PF_6)): ^{1}H NMR (500 MHz, $(CD_3)_2CO$) δ [ppm]: 7.33 (m, 20H, CH_{arom}), 6.21 (d, 4H, *o*-CH_{arom}), 6.07 (t, 2H, *p*-CH_{arom}), 5.93 (t, 4H, *m*-CH_{arom}). ^{13}C NMR (125 MHz, $(CD_3)_2CO$) δ [ppm]: 146.05 (C_{arom}), 128.89 (CH_{arom}), 128.80 (CH_{arom}), 128.65 (CH_{arom}), 108.07 (C_{arom}-$COPh_2$), 80.54 (*C*-OH), 79.23 (*o*-CH_{arom}), 77.56 (*p*-CH_{arom}), 77.08 (*m*-CH_{arom}). ESI-MS: m/z = 707.2 $[M]^+$. IR ν: 3328 (w), 3097 (w), 2957 (w), 1493 (m), 1444 (m), 1356 (w), 1148 (w), 1019 (w), 827 (s), 758 (s) cm^{-1}. HR-ESI-MS $C_{38}H_{32}O_2Re$ $[M]^+$: calculated, 707.1954; found, 707.1550.

Analysis: [Re(η^6-C_6H_4(C(OH)Ph_2)$_2$)(η^6-C_6H_5C(OH)Ph_2)](PF_6) ([**37**](PF_6)): ^{1}H NMR (500 MHz, CD_3CN) δ [ppm]: 7.35 (m, 12H, CH_{arom}), 7.26 (m, 6H, CH_{arom}), 7.21 (m, 8H, CH_{arom}), 7.01 (m, 4H, CH_{arom}), 5.91 (d, 2H, *o*-CH_{arom}), 5.87 (s, 4H, *o*-CH_{arom}), 5.78 (t, 1H, *p*-CH_{arom}), 5.60 (t, 2H, *m*-CH_{arom}), 4.97 (s, 1H, O*H*), 4.84 (s, 2H, O*H*). ^{13}C NMR (125 MHz, CD_3CN) δ [ppm]: 145.67 (C_{arom}), 145.37 (C_{arom}), 129.15 (*C*H$_{arom}$), 129.10 (*C*H$_{arom}$), 129.08 (*C*H$_{arom}$), 129.03 (*C*H$_{arom}$), 128.47 (*C*H$_{arom}$), 128.35 (*C*H$_{arom}$), 107.80 (C_{arom}-COPh_2), 106.93 (C_{arom}-COPh_2), 80.79 (*C*-OH), 80.69 (*C*-OH), 80.25 (*o*-*C*H$_{arom}$), 78.54 (*m*-*C*H$_{arom}$), 77.96 (*o*-*C*H$_{arom}$), 77.93 (*p*-*C*H$_{arom}$). ESI-MS: m/z = 889.2 $[M]^+$. IR ν: 3319 (br, w, OH), 2958 (w), 1492 (w), 1425 (m), 1167 (w), 1022 (w), 819 (s), 774 (s) cm^{-1}. HR-ESI-MS $C_{51}H_{42}O_3Re$ $[M]^+$: calculated, 889.2686; found, 889.2676.

8.5 Supplementary Information: A Mixed-Ring Sandwich Complex from Unexpected Ring Contraction in $[M(\eta^6\text{-}C_6H_5Br)(\eta^6\text{-}C_6R_6)]^+$.

A Mixed-Ring Sandwich Complex from Unexpected Ring Contraction in $[M(\eta^6\text{-}C_6H_5Br)(\eta^6\text{-}C_6R_6)]^+$

Giuseppe Meola, Henrik Braband, Daniel Hernández-Valdés, Carla Gotzmann, Thomas Fox, Bernhard Spingler, Roger Alberto*
Department of Chemistry, University of Zurich, Winterthurerstr. 190, CH-8057 Zurich Switzerland.

Table of Content

1. General Information
Materials
Characterization

2. Synthetic procedures
Re-complexes
$[Re(\eta^6\text{-}C_6H_5Br)(\eta^6\text{-}C_6H_6)](PF_6)$ ([**1**]PF_6)
$[Re(\eta^6\text{-}C_6H_5OH)(\eta^6\text{-}C_6H_6)](PF_6)$ ([**2**]PF_6)
$[Re(\eta^5\text{-}C_6H_5O^-)(\eta^6\text{-}C_6H_6)$
$[Re(\eta^5\text{-}C_5H_4CHO)(\eta^6\text{-}C_6H_6)]$ (**3**)
$[Re(\eta^6\text{-}C_6H_5Br)(\eta^6\text{-}C_6(CH_3)_6](PF_6)$ ([**4**]PF_6)
$[Re(\eta^5\text{-}C_5H_4CHO)(\eta^6\text{-}C_6(CH_3)_6)]$ (**5**)

^{99}Tc-complexes
$[^{99}Tc(\eta^6\text{-}C_6H_5Br)(\eta^6\text{-}C_6(CH_3)_6)](PF_6)$
$[^{99}Tc(\eta^6\text{-}C_6H_5O)(\eta^6\text{-}C_6(CH_3)_6]$ (**7**)

^{99m}Tc-procedures
$[^{99m}Tc(\eta^6\text{-}C_6H_5Br)(\eta^6\text{-}C_6(CH_3)_6)]^+$
$[^{99m}Tc(\eta^6\text{-}C_6H_5O)(\eta^6\text{-}C_6(CH_3)_6]$

3. NMR Spectra (^{1}H, ^{2}H, ^{13}C, HSQC, ^{1}H NOE, HMBC)

4. UPLC/ESI-MS Spectra

5. Computational details

6. Crystal Data

7. References

1. General Information

Materials

All Re and ^{99}Tc reactions were carried out under nitrogen atmosphere on a standard nitrogen/vacuum line unless otherwise stated. For the Re reactions, the glassware was dried by the use of a heat gun or in an oven at 120 °C at least overnight. Commercially available reagents were purchased reagent-grade and used without further purification. THF was dried over Na/Benzophenone. All chemicals were purchased from Sigma Aldrich (Switzerland), except hydrochloric acid (32%, Honeywell, Germany), trifluoroacetic acid (99%, Alfa Aesar, Germany), and $(NH_4)[^{99}TcO_4]$ (Oak Ridge). $[^{99m}TcO_4]^-$ was eluted from a ^{99}Mo/^{99m}Tc generator (UltratechneKow FM, Mallinckrodt).

The chemicals were used without farther purification. Deuterated NMR solvents were obtained from Armar Chemicals (Switzerland). $Na[ReO_4]$, and $[Re(\eta^6\text{-}C_6H_5Br)(\eta^6\text{-}C_6H_6)](PF_6)$ ([**1**]PF_6) complex were synthesized according to literature[1-3]

Characterization

^{1}H, ^{13}C, and ^{99}Tc NMR spectra were recorded on a BrukerDRX 400 MHz or BrukerDRX 500 MHz spectrometer. ^{1}H and ^{13}C chemical shifts were referenced with the residual solvent resonances relative to TMS, while ^{99}Tc was referenced relative to the signal of $[^{99}TcO_4]^-$ ($\delta = 0$). The spectra were fully assigned with the help of various experiments (^{1}H, ^{2}H, ^{13}C, HSQC, ^{1}H NOE, HMBC).

Electronspray-ionisation mass spectrometry (ESI-MS) was performed on a Bruker esquireTM/LC spectrometer or on a Bruker esquire^{TM}/HCT^{TM} spectrometer. High-resolution mass spectrometry (HR-ESI-MS) was performed on a Bruker maXis QTof high-resolution mass spectrometer (Bruker GmbH, Bremen, Germany).

Preparative HPLC was performed on a Varian ProStar 320 system, using a Dr. Maisch Reprosil C18 100-7 (40 x 250 mm) column. The solvents (HPLC grade) were 0.1% trifluoroacetic acid (solvent A) and acetonitrile (solvent B). The HPLC gradients used are as follow (G1):0-2 minutes: 73% A (27% B); 2.1-45 minutes: linear gradient from 73% A (27% B) to 65% A (35% B); 45-51 minutes: 100% B. The flow rate was 40 mL/min. Detection was performed at 270 nm. Analytical HPLC was performed on a VWR HITACHI Chromaster system, using a Macherey-Nagel Nucleosil C18 100-5 column. HPLC solvents were 0.1% trifluoroacetic acid (solvent A) and methanol (solvent B). Applied HPLC gradient: 0-3 minutes: 100% A; 3.1-9 minutes: 75% A, 25% B; 9.1-20 minutes: linear gradient from 66% A (34% B) to 0% A (100% B); 20-28 minutes: 100% B; 28.1-30: 100% A. The flow rate was 0.5 mL/min. Detection was performed at 250 nm. HPLC analyses of the ^{99m}Tc complex was performed on a Merck Hitachi LaChrom L 7100 pump coupled to a Merck Hitachi LaChrom L7200 tunable UV detector and a radiodetector. UV/Vis detection was performed at 250 nm. The detection of radioactive ^{99m}Tc complexe was performed with a Berthold LB508 radiodetector equipped with BGO cell. Separations

were achieved on a Macherey-Nagel C18 reversed-phase column (Nucleosil 10 lm, 250 4 mm) using a gradient of MeOH/ 0.1% CF_3COOH as eluent, and a flow rate of 0.5 mL/min. Gradient: t = 0 – 3 min: 0% MeOH; 3 – 3.1 min: 0 – 25% MeOH; 3.1 – 9 min: 25% MeOH; 9 – 9.1 min: 25 – 34% MeOH; 9.1 – 18 min: 34 - 100% MeOH; 18 – 25 min: 100% MeOH, 25 – 25.1 min: 100 - 0% MeOH; 25.1 – 30 min: 0% MeOH. Comparison of the HPLC retention times for the ^{99m}Tc compounds with the corresponding ^{99}Tc compound confirms identity.

Titration was performed on a Mettler Toledo T50 system combined with a DCi 101-SC micro glass pH electrode at 25°C. The ionic strength was kept constant by working in 0.1 mol/L sodium nitrate and the titrant was a sodium hydroxide solution (0.1 mol/L). The concentration of the analyte was 1 mmol/L in a total volume of 5 mL. The initial solution was acidified to a pH of about 3 with the help of diluted HNO_3. The titration curves were fitted with Hyperquad2013.[4]

For technetium content measurements, pure compounds were dissolved in the appropriate solvents. The measurements were carried out with a scintillation cocktail (Packard Ultimate Gold XR) and a liquid scintillation counter (*Hidex 300 SL*).

Electrochemical measurements were carried out in acetonitrile containing 0.1 M TBA[PF_6] as a conducting electrolyte. For all Re-Complexes, a Metrohm 757VA Computrace electrochemical analyzer was used with a standard three-electrode setup of glassy carbon working electrode (i.d. = 3 mm), platinum auxiliary electrode and Ag/AgCl reference electrode. All potentials are given *vs* Ag/AgCl and are referenced with Fc/Fc^+ at 450 mV. Elemental Analysis (EA) measurements were performed on a LecoCHNS-932 elemental analyzer.

UPLC-ESI-MS was performed on a Waters Acquity UPLC System coupled to a Bruker HCT^{TM}, using an Acquity UPLC BEH C18 1.7 µm (2.1 x 50 mm) column. UPLC solvents were formic acid (0.1% in millipore water) (solvent A) and acetonitrile HPLC grade (solvent B). Applied UPLC gradient: 0-0.5 minutes: 95% A, 5% B; 0.51-4.0 minutes: linear gradient from 95% A (5% B) to 0% A (100% B); 4-5 minutes: 100% B. The flow rate was 0.6 ml/min. Detection was performed at 250 nm and 480 nm (DAD).

2. Synthetic procedures

Re-complexes

[Re(η^6-C_6H_5OH)(η^6-C_6H_6)](PF_6) ([2]PF_6)

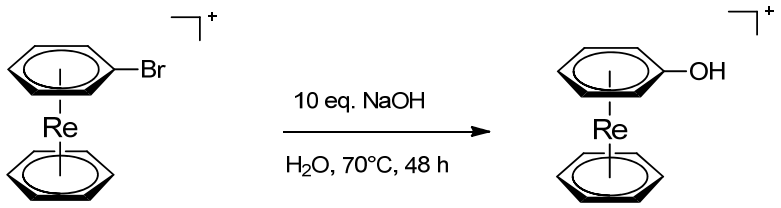

Synthesis: A 30 mg (0.053 mmol) portion of [**1**]PF_6 was suspended in 1.5 mL deionized water. Afterwards, 21.2 mg (0.53 mmol, 10 eq.) of sodium hydroxide were added to the yellow suspension. The reaction mixture was stirred for 48 h at 70°C. The solution was acidified with conc. HCl to pH 2. Subsequently, 13.0 mg (0.08 mmol, 1.5 eq.) of NH_4PF_6 were added to the solution. The product was extracted with CH_2Cl_2 (2 x 2ml) from the aqueous phase. The solvent was evaporated in *vacuo* which lead to analytically pure yellow [**2**]PF_6. Yield: 21.8 mg (0.043 mmol, 81.7%).

Single crystals, suitable for X-ray diffraction analysis were obtained by slow evaporation of an acetonitrile solution of [**2**]OTf.

Note: The reaction also can be performed with [Re(η^6-C_6H_5Cl)(η^6-C_6H_6)](PF_6) as starting material (Condition: 100 eq. NaOH, H_2O, 80°C, 12 h). The [Re(η^6-C_6H_5Cl)(η^6-C_6H_6)](PF_6) complex was synthesized according to literature[2] with hexachloroethane as a reagents agent instead of 1,1,2,2-tetrabromoethene.

Analysis: ^{1}H NMR (500 MHz, CD_3CN) δ [ppm]: 6.28 (d, *J* = 5.69 Hz, 2H, *o*-CH_{arom}), 5.92 (t, *J* = 5.44 Hz, 2H, *m*-CH_{arom}), 5.76 (s, 6H, CH_{arom}), 5.63 (t, *J* = 5.16 Hz, 1H, *p*-CH_{arom}). ^{13}C NMR (125 MHz, CD_3CN) δ [ppm]: 130.16 (C_{arom}-OH), 77.65 (*p*-CH$_{arom}$), 76.62 (C_{arom}), 75.50 (*m*-CH$_{arom}$), 69.68 (*o*-CH$_{arom}$). ESI-MS: m/z = 359.1 $[M]^+$. IR ν: 3511 (w, O-H), 3097 (w), 2927 (w), 1513 (m), 1494 (w), 1432 (m), 1359 (w), 1211 (m), 1148 (w), 1044 (w), 926 (w), 803 (s), 739 (w) cm^{-1}. HR-ESI-MS $C_{12}H_{12}ORe$ $[M]^+$: calculated, 359.0440; found, 359.0442.

Re(η^5-$C_6H_5O^-$)(η^6-C_6H_6):

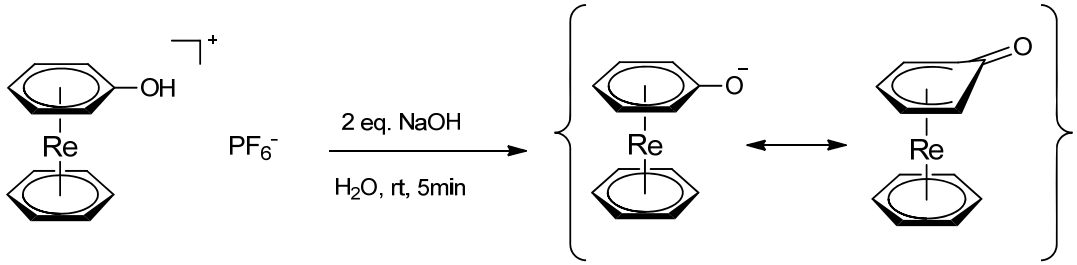

Synthesis: A 20 mg (0.040 mmol) portion of [**2**]PF_6 was dissolved in 1.5 mL deionized water and 80 µL (0.080 mmol, 2 eq.) of a 0.001mol/L sodium hydroxide solution was added. The reaction mixture was stirred for 5 min at r.t. The solvent was evaporated in *vacuo.* The product was extracted with acetonitrile (1 x 2ml) from the solid residual. The solvent was evaporated in *vacuo* which lead to the product Re(η^5-$C_6H_5O^-$)(η^6-C_6H_6) as a micro crystalline yellow powder. Yield: 11.5 mg (0.028 mmol, 71.1%).

Single crystals of Re(η^5-$C_6H_5O^-$)(η^6-C_6H_6) suitable for X-ray diffraction analysis were obtained by slow evaporation of an acetonitrile solution.

Analysis: ^{1}H NMR (500 MHz, CD_3CN) δ [ppm]: 5.65 (dd, *J* = 5.0 Hz, 2H, *m*-CH_{arom}), 5.42 (t, *J* = 5.0 Hz, 1H, *p*-CH_{arom}), 5.39 (d, *J* = 6.2 Hz, 2H, *o*-CH_{arom}), 5.24 (s, 6H, CH_{arom}). ^{13}C NMR (125 MHz, CD_3CN) δ [ppm]: 155.75 (C_{arom}-O^-), 80.30 (*m*-CH_{arom}), 75.24 (*p*-CH_{arom}), 71.24 (*o*-CH_{arom}), 70.41 (CH_{arom}). ESI-MS: m/z = 359.1 $[M+H]^+$. IR ν: 2925 (w), 1514 (s), 1456 (m), 1430 (m), 1317 (m), 1130 (w), 1036 (w), 996 (w), 826 (s), 739 (w) cm^{-1}. HR-ESI-MS $C_{12}H_{11}ORe$ $[M-H]^+$: calculated, 359.0440; found, 359.0440.

Re(η^5-C_5H_4CHO)(η^6-C_6H_6) (3):

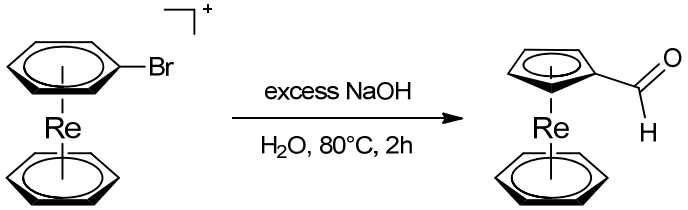

Synthesis: A 30 mg (0.053 mmol) portion of [**1**]PF_6 was suspended in 1.7 mL deionized water. 424 mg (10.6 mmol, 200 eq.) NaOH were added to the suspension. The reaction was performed in a microwave reactor. The reaction mixture was stirred for 2 h at 80°C. The reaction mixture was extracted with Et_2O (3 x 2 mL). After combining the organic phases, the solvent was evaporated in *vacuo* yielding **3** as analytically pure red-orange solid. Single crystals, suitable for X-ray diffraction analysis were obtained by slow evaporation of an acetonitrile solution of **3**. Yield: 14.2 mg (0.040 mmol, 75%).

Analysis: ^{1}H NMR (500 MHz, CD_3CN) δ [ppm]: 9.52 (s, 1H, C*H*O), 5.46 (s, 2H, Cp α-*H*), 5.34 (s, 2H, Cp β-*H*), 4.88 (s, 6H, CH_{arom}). ^{13}C NMR (125 MHz, CD_3CN) δ [ppm]: 189.95 (*C*HO), 86.30 (*C*-CHO), 75.70

(CH_{CP}), 71.07 (CH_{CP}), 64.07 (C_{arom}), ESI-MS: m/z = 359.1 $[M+H]^+$. IR ν: 3088 (w), 2922 (w), 2852 (w), 1647 (s), 1453 (m), 1426 (m), 1413 (m), 1365 (m), 1334 (w), 1249 (m), 1203 (w), 1149 (w), 1125 (w), 1039 (m), 985 (w), 970 (m), 829 (s), 737 (s) cm^{-1}. HR-ESI-MS $C_{12}H_{12}ORe$ $[M+H]^+$: calculated, 359.0440; found, 359.0439.

$[Re(\eta^6\text{-}C_6H_5Br)(\eta^6\text{-}C_6(CH_3)_6](PF_6)$ ([4]PF_6)

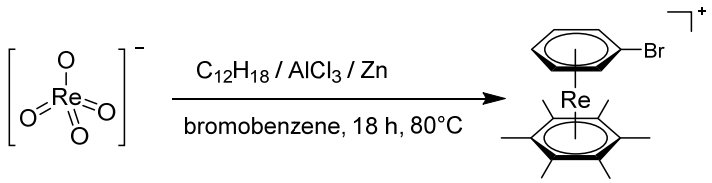

Synthesis: Under N_2-atmosphere a flask was charged with $Na[ReO_4]$ (1.002 g, 3.66 mmol, 1.0 eq.), Zn dust (0.764 g, 11.70 mmol, 3.2 eq.) and hexamethylbenzene (5.877 g, 36.20 mmol, 9.9 eq.). Afterwards, bromobenzene (15 ml) was added. The suspension was stirred for 5 min before $AlCl_3$ (4.873 g, 36.54 mmol, 10.0 eq.) was added followed by another 15 ml of bromobenzene. The mixture was refluxed for 18 h at 80°C. The hot reaction solution was quenched with water and the reaction mixture was filtered to remove the solid. The two phases of the reaction solution were separated, the bromobenzene phase was washed with water (3 x) and the aqueous phase with Et_2O and hexane (3 x). Additionally, to increase the yield, the filtered solid was extracted with CH_2Cl_2 and the organic solution washed with water (3x). All aqueous solutions were combined and reduced in volume to less then 5ml. The crude product was purified by preparative HPLC (Reprosil 100 C18, 250 mm x 40 mm, 0.1% TFA/CH_3CN, gradient G1). The solvent was evaporated and the solid dissolved in water. After the addition of NH_4PF_6 (0.625 g, 3.83 mmol, 1.1 eq.), [**4**]PF_6 precipitated as yellow powder, which was filtered and dried. Yield: 62.4 mg (0.096 mmol, 3%).

Analysis: ^{1}H NMR (500 MHz, $(CD_3)_2CO$) δ [ppm]: 6.10 (d, *J* = 5.4 Hz, 2 H, *o*-CH_{arom}), 5.81 (t, *J* = 5.4 Hz, 2 H, *m*-CH_{arom}), 5.72 (t, *J* = 5.2 Hz, 1 H, *p*-CH_{arom}), 2.45 (s, 18 H, $C_6(CH_3)_6$). ^{13}C NMR (125 MHz, $(CD_3)_2CO$) δ [ppm]: 96.68 (CCH_3), 84.54 (*C*Br), 80.52 (*o*-CH_{arom}), 77.52 (*p*-CH_{arom}), 77.11 (*m*-CH_{arom}), 17.81 (CCH_3). ESI-MS: m/z = 505.1 $[M]^+$. IR ν: 3082 (w), 1789 (m), 1745 (m), 1422 (w), 1390 (m), 1186 (m), 1137 (m), 1069 (w), 1046 (w), 834 (s), 703 (s) cm^{-1}. HR-ESI-MS $C_{18}H_{23}BrRe$ $[M]^+$: calculated, 505.0535; found, 505.0525.

Re(η^5-C_5H_4CHO)(η^6-$C_6(CH_3)_6$) (5):

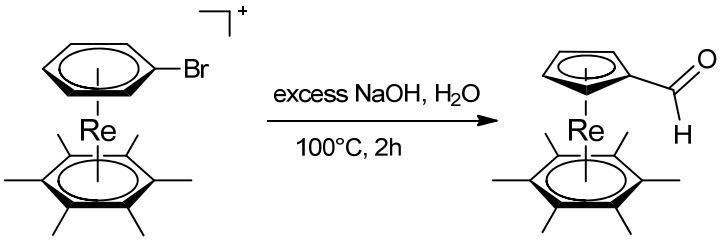

Synthesis: A 15 mg (0.023 mmol) portion of [**4**]PF_6 was suspended in 3.2 mL deionized water. 461.2 mg (11.53 mmol, 500 eq.) of NaOH were added to the suspension. The reaction was heated for to 2 h at 100°C in a microwave reactor. Afterwards, the reaction mixture was extracted with Et_2O (3 x 2 mL). The combined organic phases were evaporated in *vacuo*, to yield analytical pure **5**. Single crystals, suitable for X-ray diffraction analysis were obtained by slow evaporation of an Et_2O solution of **5**. Yield: 4.8 mg (0.011 mmol, 47%).

Analysis: ^{1}H NMR (500 MHz, C_4D_8O) δ [ppm]: 9.26 (s, 1H, C*H*O), 4.85 (s, 2H, Cp α-*H*), 4,77 (s, 2H, Cp β-*H*), 2.18 (s, 18H, CH_3). ^{13}C NMR (125 MHz, C_4D_8O) δ [ppm]: 188.14 (*C*HO), 85.82 (*C*-CHO), 79.86 (*C*-CH_3) 77.58 (*C*H_{CP}), 71.74 (*C*H_{CP}), 19.41 (*C*H_3). ESI-MS: m/z = 443.1 $[M+H]^+$. IR ν: 2918 (s), 2851 (m), 1735 (w), 1660 (m), 1642 (s), 1558 (w), 1443 (m), 1426 (m), 1379 (m), 1355 (m), 1320 (w), 1259 (w), 1232 (m), 1064 (w), 1036 (m), 1014 (m), 982 (w), 905 (m), 826 (m), 739 (s) cm^{-1}. HR-ESI-MS $C_{18}H_{23}ORe$ $[M+H]^+$: calculated, 443.1779; found, 443.1370.

^{99}Tc-complexes

[^{99}Tc(η^6-C_6H_5Br)(η^6-$C_6(CH_3)_6$](PF$_6$) ([6]PF$_6$)

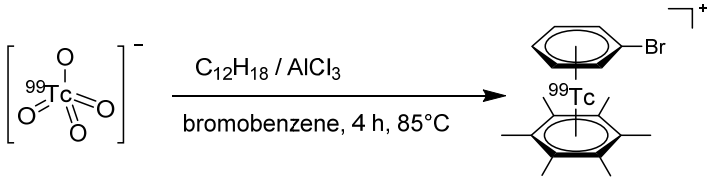

Synthesis: In a 50 mL two-necked flask, K[^{99}TcO_4] (13.2 mg, 0.07 mmol), hexamethylbenzene (80 mg, 0.5 mmol) and $AlCl_3$ (200 mg, 1.50 mmol) were suspended in bromobenzene (4 mL). The solution was stirred at 85 °C for 4 h when H_2O (5 mL) was added to quench the reaction. The solution was filtered and phases were separated. NH_4PF_6 (100 mg, 0.61 mmol) was added to the aq. phase and the colorless precipitate was filtered off. The powder was dried *in vacuo* to afford [**6**]PF_6 as a light yellow powder (30.4 mg, 0.05 mmol, 77%).

It has to be noted: Besides the desired product, significant amounts of a second species are formed under the applied conditions. The byproduct has almost identical chemical, physico-chemical, and structural properties as $[\mathbf{6}]^+$. Therefore, it was not possible to separate the two species. All given

analytical data consider only compound [**6**]$^+$. Studies to identify the nature of the byproduct are currently done in our laboratories.

Analysis: ^{99}Tc-NMR (125 MHz, acetone-d_6): δ [ppm] = -1528.04 ($\Delta\nu_{1/2}$ = 57 Hz). ^{1}H-NMR (500 MHz, acetone-d6): δ [ppm] = 5.75 (*d*, *J* = 5.0, 2 H, *o*-C*H*$_{arom}$), 5.58 (*t*, *J* = 5.0, 2 H, *m*-C*H*$_{arom}$), 5.46 (*t*, *J* = 5.0, 1 H, *p*-C*H*$_{arom}$), 2.39 (*s*, 18 H, CH_3). ^{13}C-NMR (125 MHz, acetone-d_6): δ [ppm] = 85.10 (*br*, 3 C, 2 *o*-*C*H$_{arom}$, 1 Br*C*), 82.07 (*br*, 3 C, 2 *m*-*C*H$_{arom}$, 1 *p*-*C*H$_{arom}$), 17.04 (6 CH_3) ppm. IR ν: 3430 (w), 3083 (w), 2923 (w), 1430 (w), 1391 (m), 1054 (w), 1019 (w), 833 (s), 670 (w), 558 (s), 451 (w), 426 (m) cm^{-1}.

^{99}Tc(η^5-$C_6H_5O^-$)(η^6-$C_6(CH_3)_6$) (7):

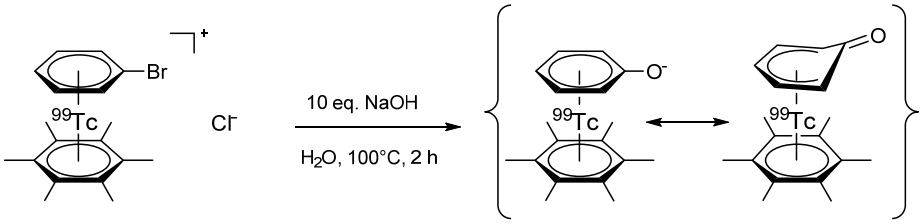

[**6**]PF_6 is insoluble in aqueous media. After anion metathesis in THF with PPh_3Cl_2, the corresponding chloride salt was used (including the unidentified byproduct). 11 mg (0.025 mmol) [**6**]Cl were suspended in 1.5 mL deionized water. 500 mg (12.5 mmol, 500 eq.) of NaOH were added to the solution. The reaction was stirred for 4 h at 100°C. The reaction mixture was extracted with Et_2O (3 x 4 mL). After combination of the organic phase the solvent was evaporated in *vacuo.* Yield: 0.3 mg (0.0008 mmol, 3.2%) of (**7**).

It has to be noted: Since the starting compound is a mixture of compounds with identical chemical properties, this product contains a side product. All given analytical data consider only compound **7**.

Single crystals, suitable for X-ray diffraction analysis were obtained by slow evaporation of an Et_2O solution of **7**.

Analysis: ^{99}Tc-NMR (125 MHz, MeCN-d_6): δ [ppm] = - 1414 ($\Delta\nu_{1/2}$ = 149 Hz)

^{1}H-NMR ((500 MHz, CH_3CN-d_6): δ [ppm] = 4.96 (t, *J* = 5.6 Hz, 2 H, *o*-C*H*$_{arom}$), 4.73 (t, *J* = 5.1 Hz, 2 H, *p*-C*H*$_{arom}$), 4.57 (t, *J* = 5.1 Hz, 2 H, *p*-C*H*$_{arom}$), 2.19 (s, 9 H, $C_6(CH_3)_6$), 2.17 (br, 9 H, $C_6(CH_3)_6$).

IR ν = 3552 (s), 3480 (s), 3416 (s), 3239 (m), 2923 (w), 1639 (s), 1619 (s), 1385 (m), 833 (s), 622 (m), 560 (s), 480 (w) cm^{-1}.

^{99m}Tc-procedures

[^{99m}Tc(η^6-C_6H_5Br)(η^6-$C_6(CH_3)_6$]

Trihexyl(tetradecyl)phosphonium bromide (0.1 mg) dissolved in 0.5 ml methyl tert-butyl ether (MTBE) was added to a capped vial. Under constant rotation of the vial, the solvent was evaporated by a nitrogen stream. The [$^{99m}TcO_4$]$^-$ eluate (1 ml) was added to this vial and stirred for 30 min. The ionic liquid was dissolved in bromobenzene (1 ml) and the solution was added to a vial, charged with $AlCl_3$ (100 mg) and hexamethylbenzene (17 mg) under a nitrogen gas atmosphere. By means of a microwave reactor, the reaction was heated for 45 min at 100°C. Afterwards, 1 ml saline solution was added to the reaction mixture. The vial was vortexed for 20 sec. and centrifuged for 2 min. The aqueous solution was separated with a syringe. The product was formulated by standard SepPak procedure using MeOH as organic solvent (Yield: 62%, 96% radiochemical pure).

^{99m}Tc(η^5-$C_6H_5O^-$)(η^6-$C_6(CH_3)_6$)

The MeOH solution of [^{99m}Tc(η^6-C_6H_5Br)(η^6-$C_6(CH_3)_6$] was dried by heating the vial to 60°C in the heating block with simultaneously purging with nitrogen gas. 3 pellets NaOH were added to the vial followed with 1 ml degassed water. The reaction was heated 60 min at 100°C in the microwave reactor. 1 ml Et_2O was added to the reaction mixture and the vial was vortexed for 30 sec. and centrifuged for 3 min. The aqueous phase was removed and the ether was evaporated. The residue was dissolved in water. Comparison of the HPLC retention time with the ^{99}Tc compound **7** (UV vs. γ-trace) confirmed the nature of ^{99m}Tc(η^5-$C_6H_5O^-$)(η^6-C_6H_6).

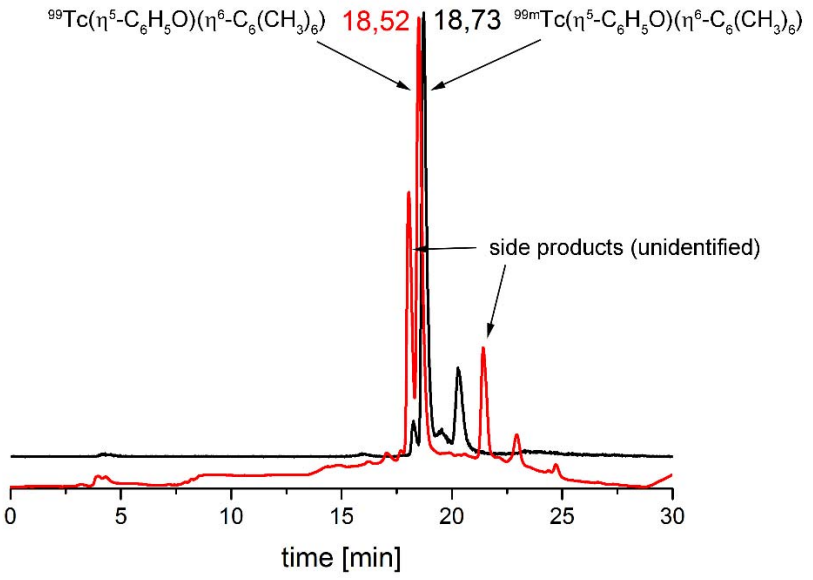

Figure S0: HPLC traces of the coinjection of $^{99m}Tc(\eta^5\text{-}C_6H_5O^-)(\eta^6\text{-}C_6(CH_3)_6)$ (γ-detection, 18.73 min, black line) and $^{99}Tc(\eta^5\text{-}C_6H_5O^-)(\eta^6\text{-}C_6(CH_3)_6)$ (UV-detection, 18.52 min, red line).

3. NMR Spectra and Experiments (^{1}H, ^{2}H, ^{13}C, HSQC, ^{1}H NOE, HMBC)

(^{2}H)-Deuterium Experiment

$Re(\eta^5\text{-}C_5H_{4-n}D_nCDO)(\eta^6\text{-}C_6H_6)$:

Synthesis: The $Re(\eta^5\text{-}C_5H_{4-n}D_nCDO)(\eta^6\text{-}C_6H_6)$ complex was synthesized according to the procedure for the synthesis of **3** with NaOD as base and D_2O as solvent.

Analysis: ^{2}H(D) NMR (76.79 MHz, CH_3CN) δ [ppm]: 9.53 (s, 1D, C*D*O), 5.42 (s, 1.2D, Cp α-*D*), 5.28 (s, 0.2D, β-Cp*D*), 4.81 (s, 0.16D, CH_{arom}). ^{1}H NMR (500 MHz, CH_3CN) δ [ppm]: 9.53 (s, 0.04, C*H*O), 5.42 (s, 0.81H, Cp α-*H*), 5.28 (s, 1.78H, β-Cp*H*), 4.81 (s, 5.6D, CH_{arom}). ESI-MS: m/z = 361.1 $[M+H]^+$ $Re(\eta^5\text{-}C_5H_3D_1CDO)(\eta^6\text{-}C_6H_6)$ and m/z = 362.1 $[M+H]^+$ $Re(\eta^5\text{-}C_5H_4D_2CDO)(\eta^6\text{-}C_6H_6)$ (see figure S22).

$Re(\eta^5\text{-}C_6H_{5-n}D_nO^-)(\eta^6\text{-}C_6H_6)$:

Synthesis:

Methode A: Complex $Re(\eta^5\text{-}C_5H_{4-n}D_nO^-)(\eta^6\text{-}C_6H_6)$ is formed during the synthesis of $Re(\eta^5\text{-}C_5H_{4-n}D_nCDO)(\eta^6\text{-}C_6H_6)$ in minor amounts.

Methode B: $Re(\eta^5\text{-}C_5H_{4-n}D_nO^-)(\eta^6\text{-}C_6H_6)$ was synthesized as major product under these conditions: 10 eq. NaOD, D_2O, 70°C, 48h.

Analysis: ^{1}H NMR (500 MHz, D_2O) δ [ppm] (see figure S1)

$Re(\eta^5\text{-}C_6H_{5-n}D_nOH)(\eta^6\text{-}C_6H_6)$:

Synthesis: Acidification of $Re(\eta^5\text{-}C_6H_{5-n}D_nO^-)(\eta^6\text{-}C_6H_6)$ with conc. HCl.

Analysis: ^{1}H NMR (500 MHz, D_2O) δ [ppm] (see figure S1). ESI-MS: m/z = 360.1 $[M+H]^+$ $Re(\eta^6\text{-}C_6H_4D_1OH)(\eta^6\text{-}C_6H_6)$ and m/z = 361.1 $[M+H]^+$ $Re(\eta^6\text{-}C_6H_3D_2OH)(\eta^6\text{-}C_6H_6)$

^{1}H NMR spectra of deuterated complex

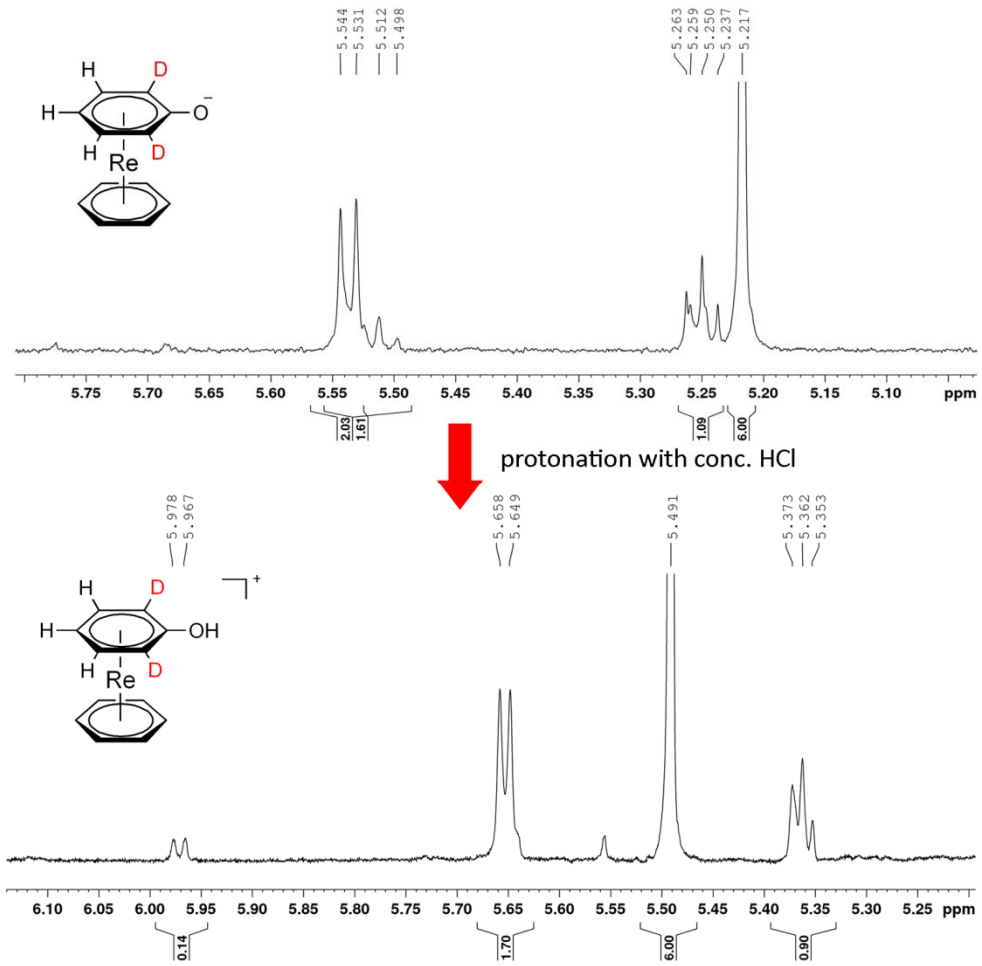

Figure S1: ^{1}H NMR Re(η^5-$C_6H_{5-n}D_nO^-$)(η^6-C_6H_6) (500 MHz, D_2O) (top). ^{1}H NMR of Re(η^6-$C_6H_{5-n}D_nOH$)(η^6-C_6H_6) (500 MHz, D_2O) (bottom).

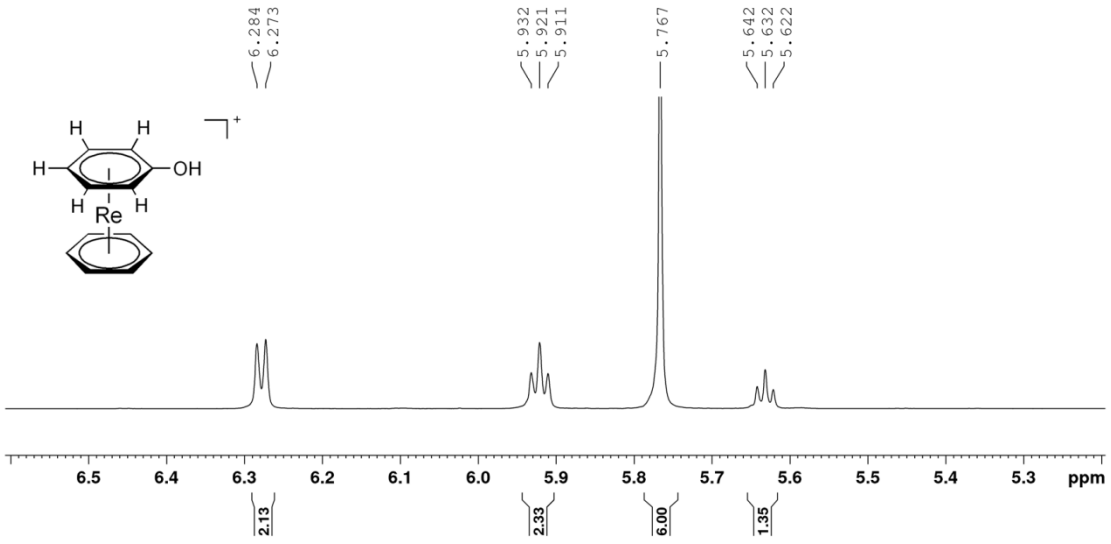

Figure S2: ^{1}H NMR of Re(η^6-C_6H_5OH)(η^6-C_6H_6) [**2**]PF_6 (500 MHz, CD_3CN) (for comparison with S1)

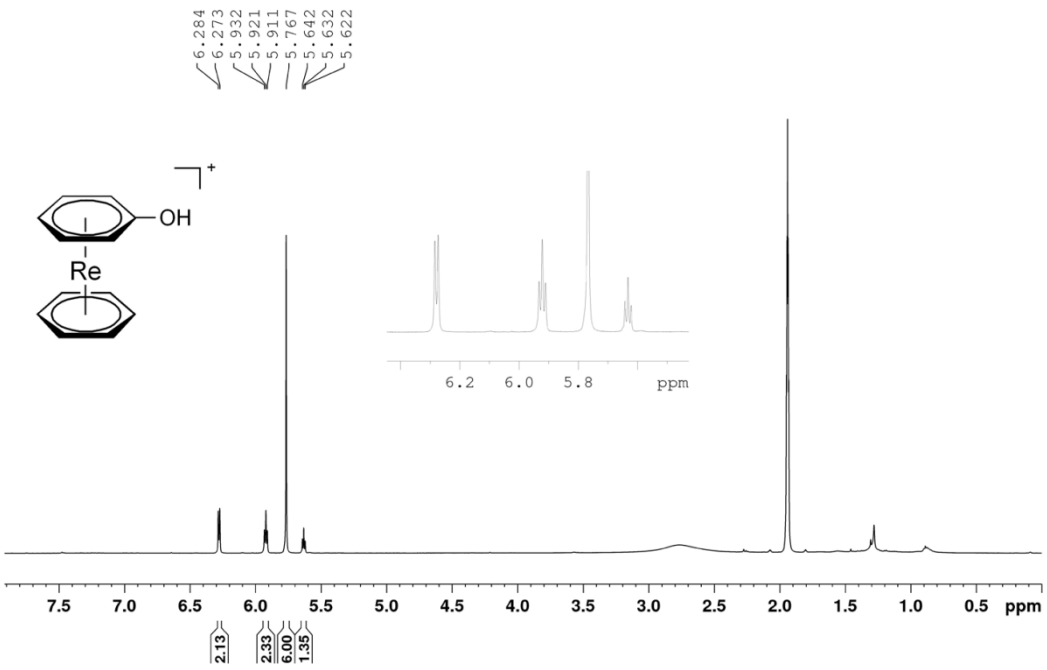

Figure S3: ^{1}H NMR of Re(η^6-C_6H_5OH)(η^6-C_6H_6) [**2**]PF_6 (500 MHz, CD_3CN, full spectrum)

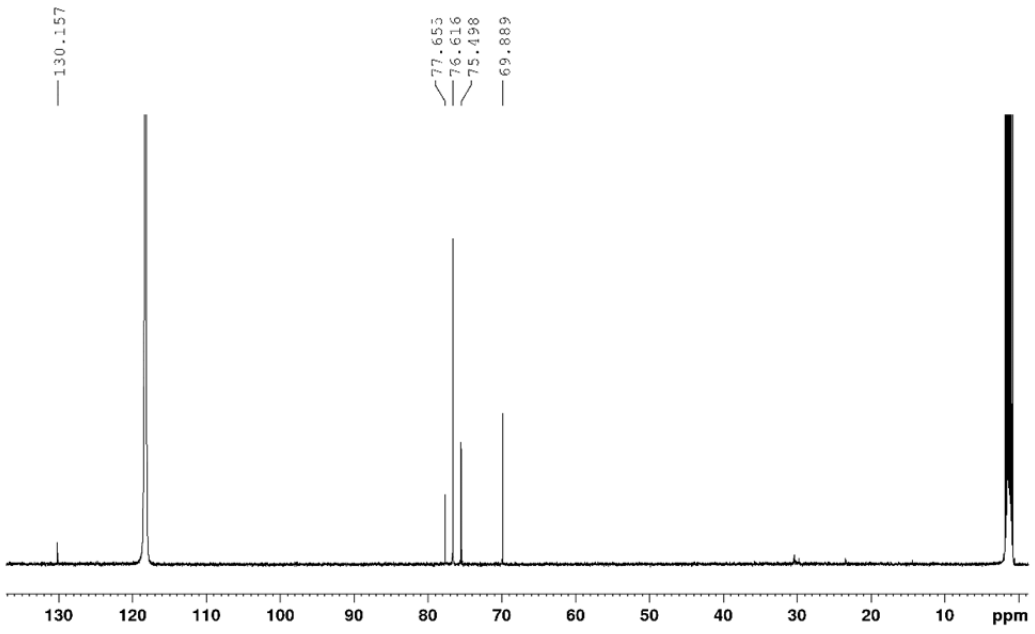

Figure S4: ^{13}C NMR of Re(η^6-C_6H_5OH)(η^6-C_6H_6) [**2**]PF_6 (125 MHz, CD_3CN)

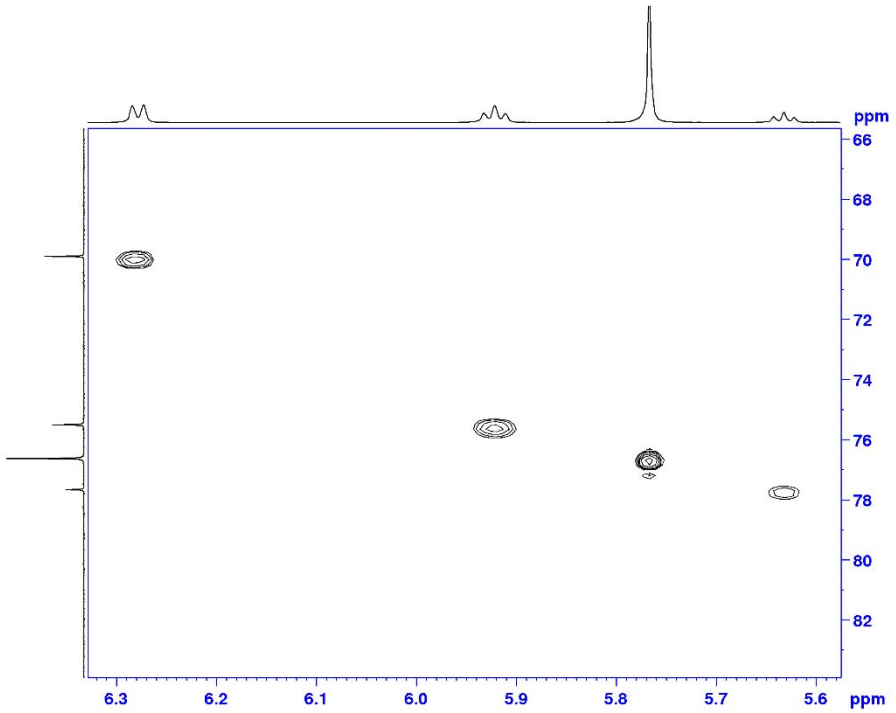

Figure S5: HSQC of Re(η^6-C_6H_5OH)(η^6-C_6H_6) [**2**]PF_6 (500 MHz, CD_3CN)

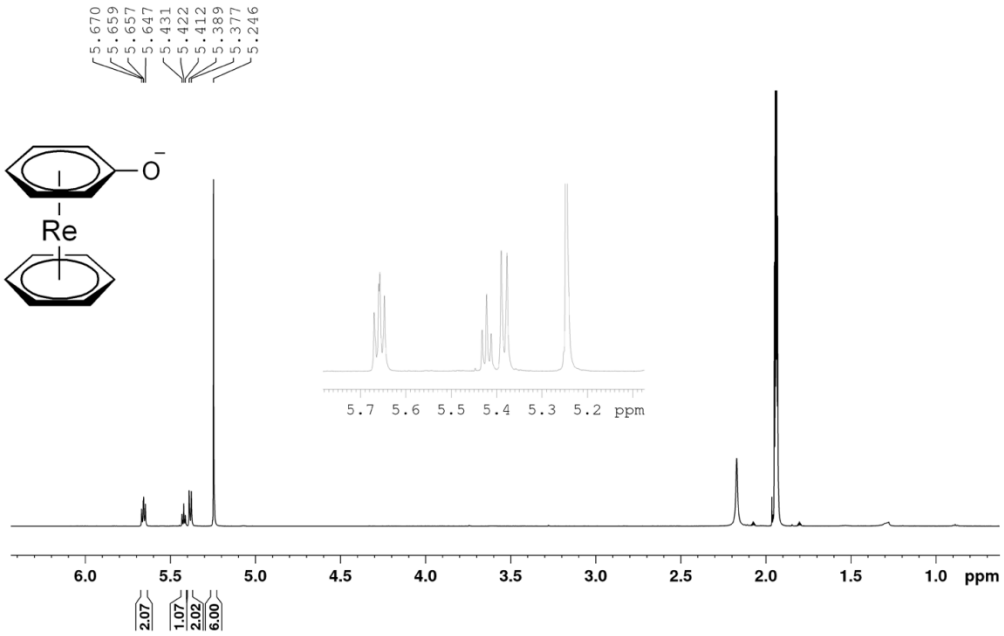

Figure S6: ^{1}H NMR of Re(η^5-$C_6H_5O^-$)(η^6-C_6H_6) (500 MHz, CD_3CN)

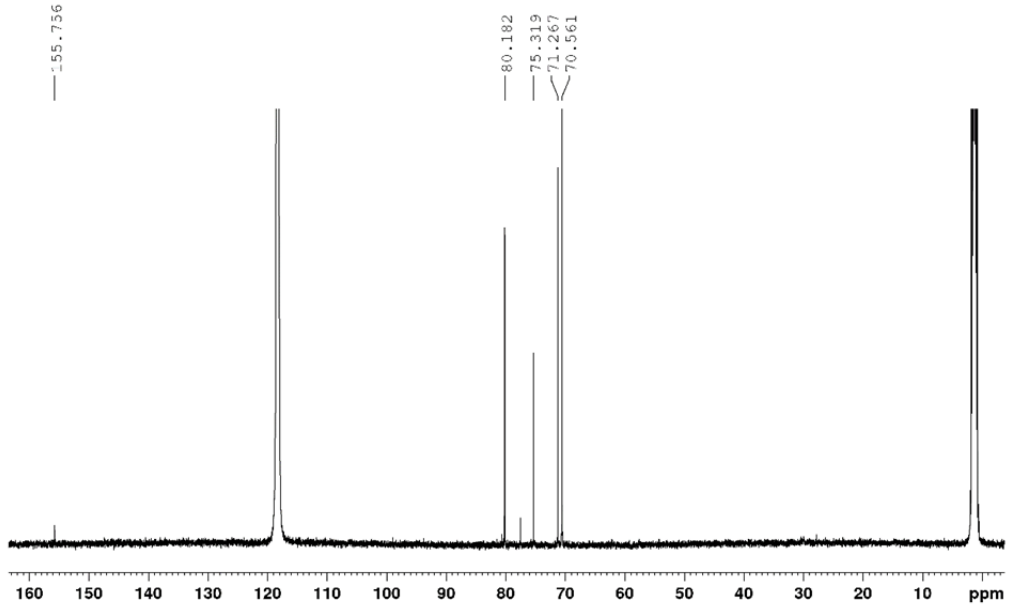

Figure S7: ^{13}C NMR of Re(η^5-$C_6H_5O^-$)(η^6-C_6H_6) (125 MHz, CD_3CN)

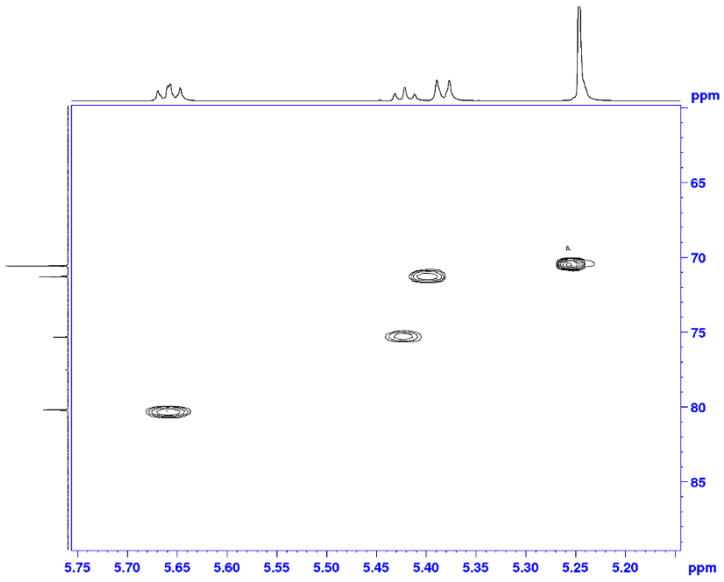

Figure S8: HSQC of Re(η^5-$C_6H_5O^-$)(η^6-C_6H_6) (500 MHz, CD_3CN)

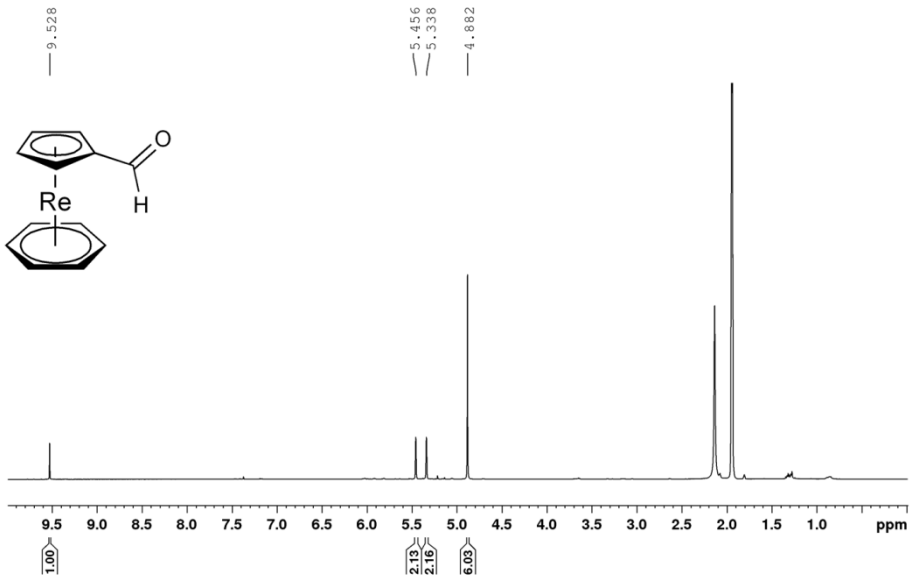

Figure S9: ^{1}H NMR of [Re(η^5-C_5H_4CHO)(η^6-C_6H_6)] (**3**) (500 MHz, CD_3CN)

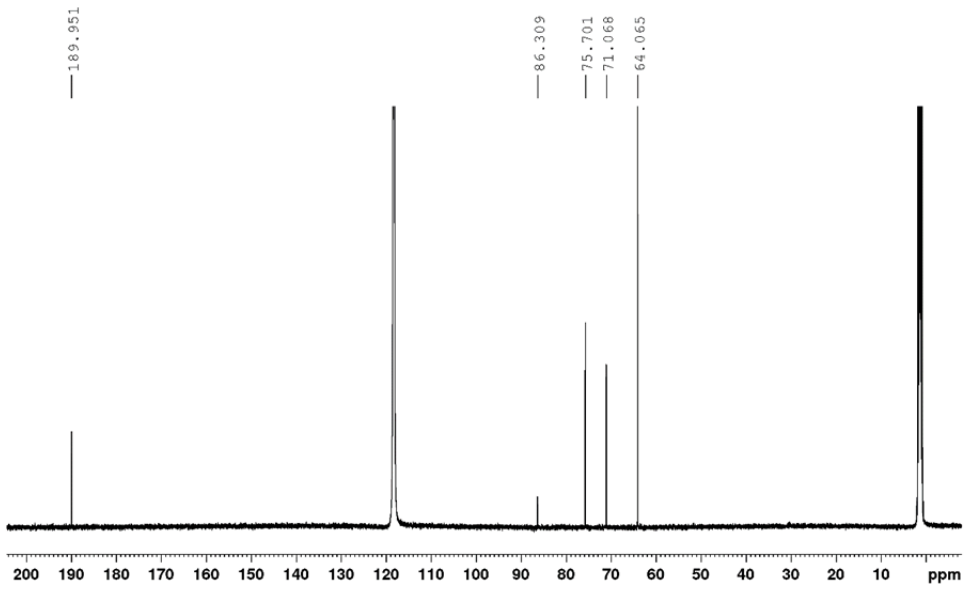

Figure S10: ^{13}C NMR of [Re(η^5-C_5H_4CHO)(η^6-C_6H_6)] (**3**) (125 MHz, CD_3CN)

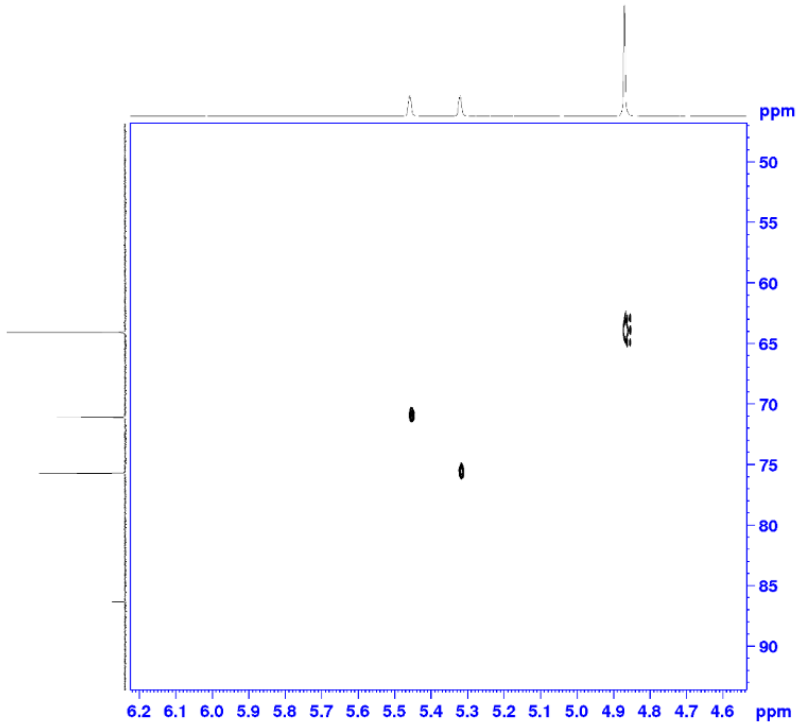

Figure S11: HSQC of [Re(η^5-C_5H_4CHO)(η^6-C_6H_6)] (**3**) (500 MHz, CD_3CN)

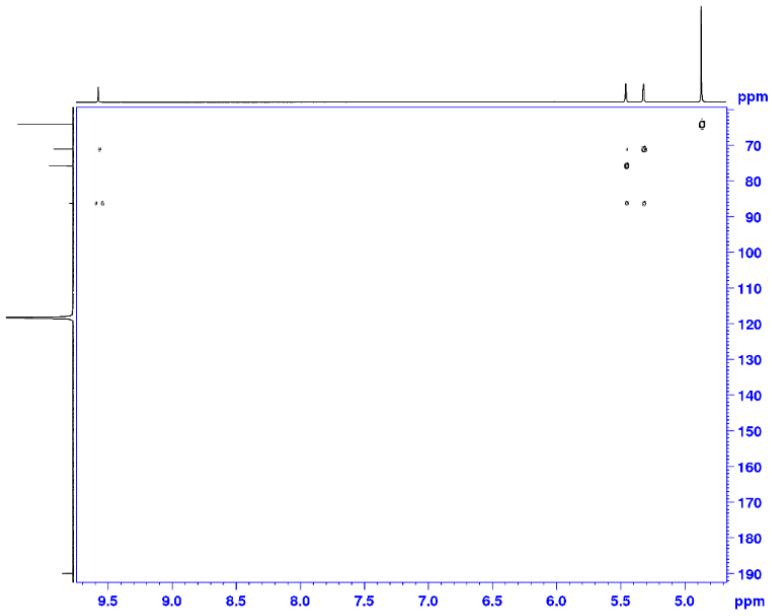

Figure S12: HMBC of [Re(η^5-C_5H_4CHO)(η^6-C_6H_6)] (**3**) (500 MHz, CD_3CN)

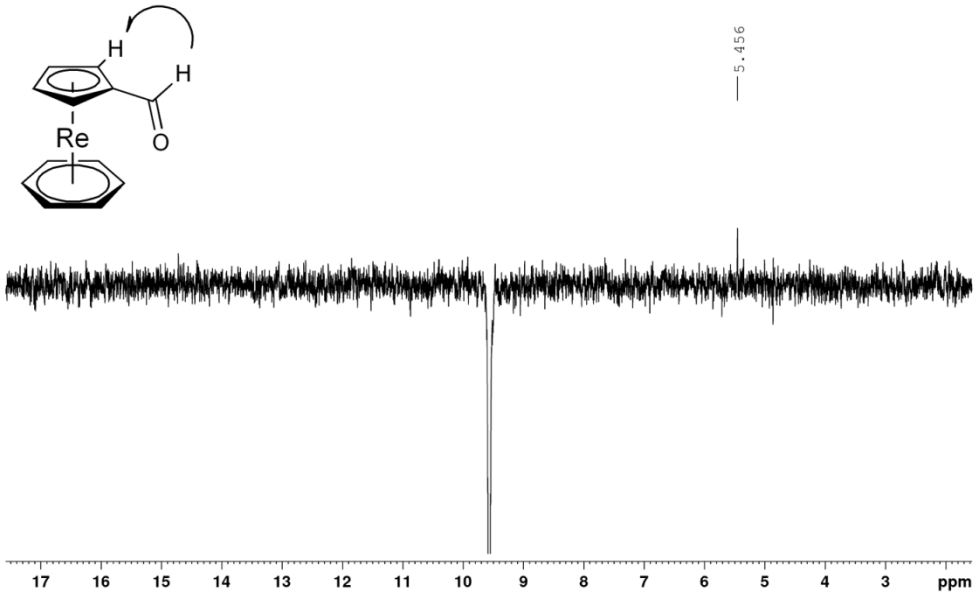

Figure S13: 1D NOE of [Re(η^5-C_5H_4CHO)(η^6-C_6H_6)] (**3**) (500 MHz, CD_3CN)

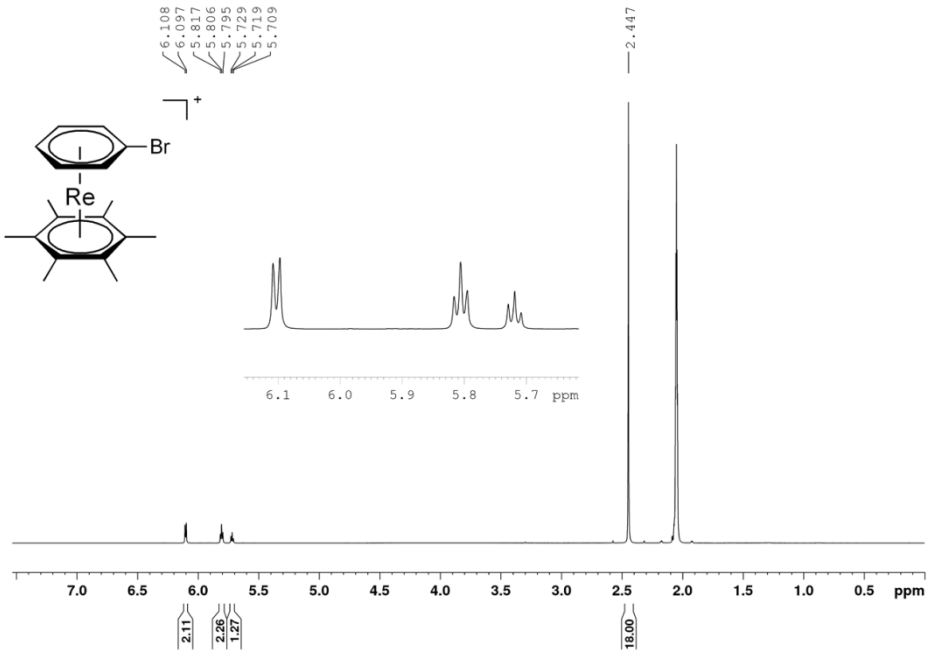

Figure S14: ^{1}H NMR [Re(η^6-C_6H_5Br)(η^6-$C_6(CH_3)_6$]PF_6 [**4**]PF_6 (500 MHz, $(CD_3)_2CO$)

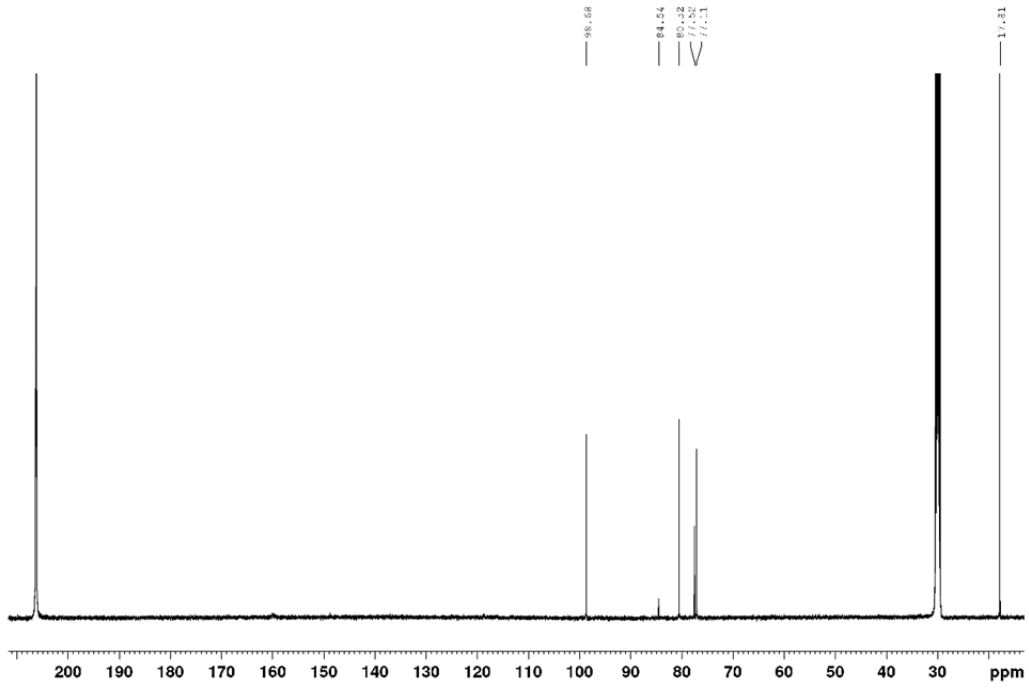

Figure S15: ^{13}C NMR [Re(η^6-C_6H_5Br)(η^6-$C_6(CH_3)_6$]PF_6 [**4**]PF_6 (125 MHz, $(CD_3)_2CO$))

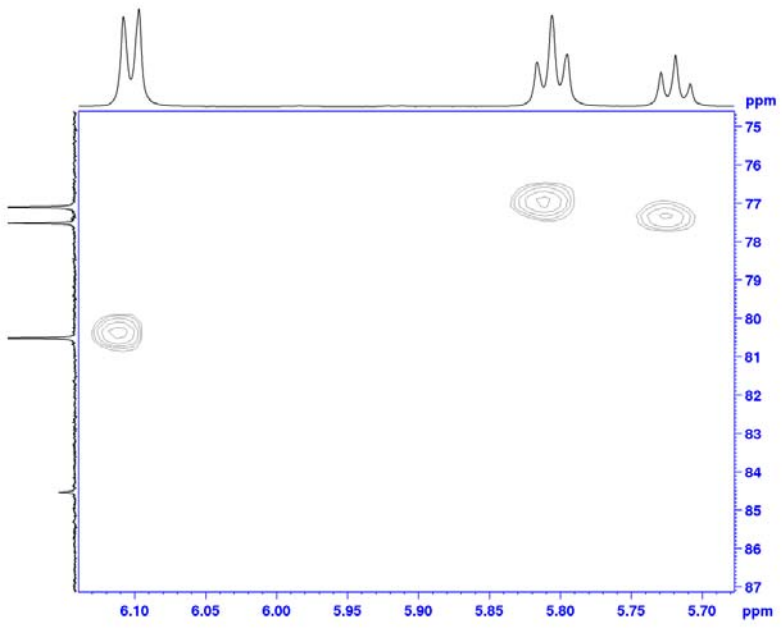

Figure S16: HSQC [Re(η^6-C_6H_5Br)(η^6-$C_6(CH_3)_6$]PF_6 [**4**]PF_6 (500 MHz, $(CD_3)_2CO$))

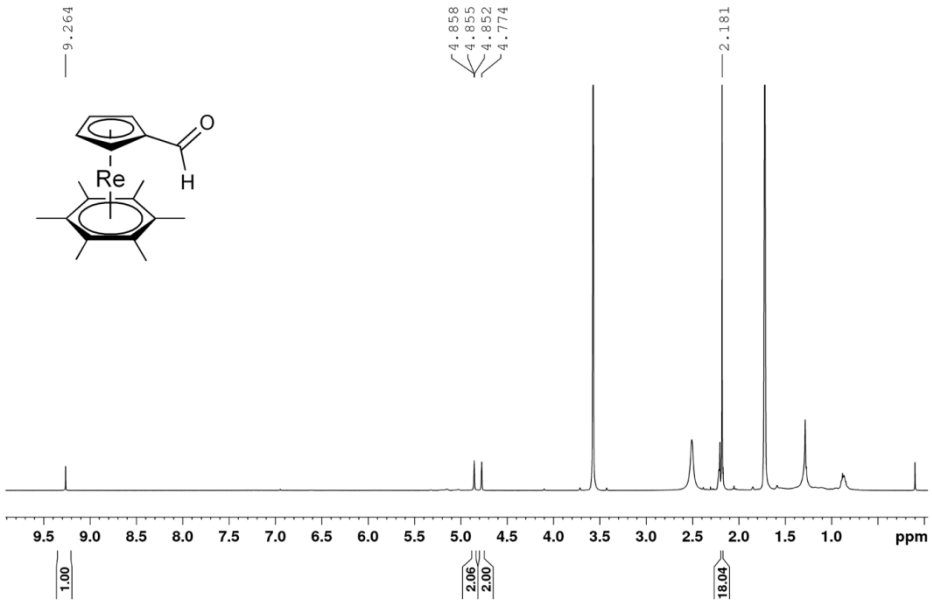

Figure S17: ^{1}H NMR [Re(η^5-C_5H_4CHO)(η^6-$C_6(CH_3)_6$] (**5**) (500 MHz, C_4D_8O)

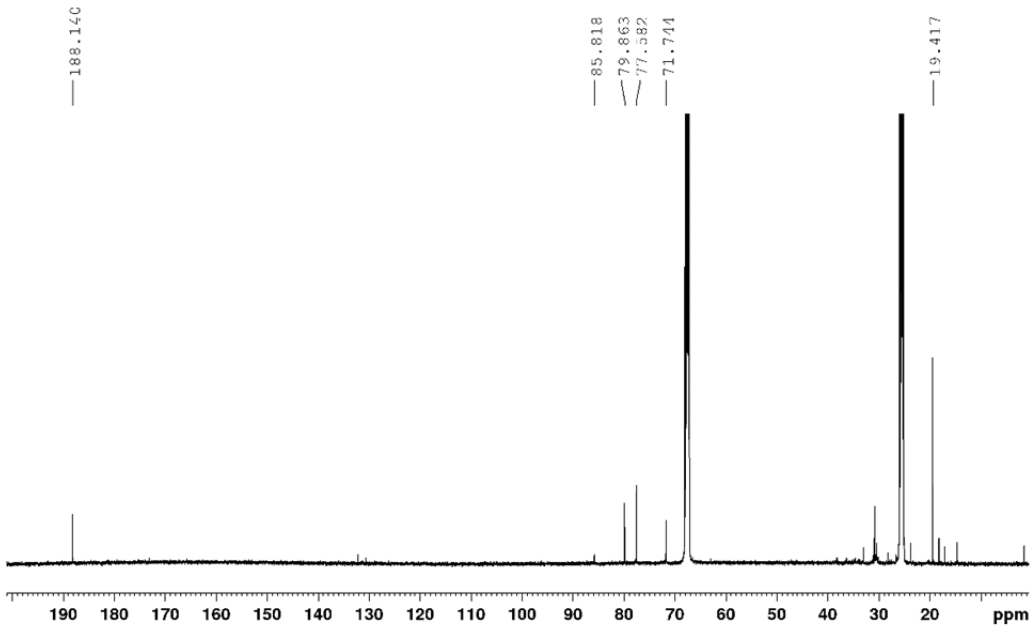

Figure S18: ^{13}C NMR [Re(η^5-C_5H_4CHO)(η^6-$C_6(CH_3)_6$] (**5**) (125 MHz, C_4D_8O))

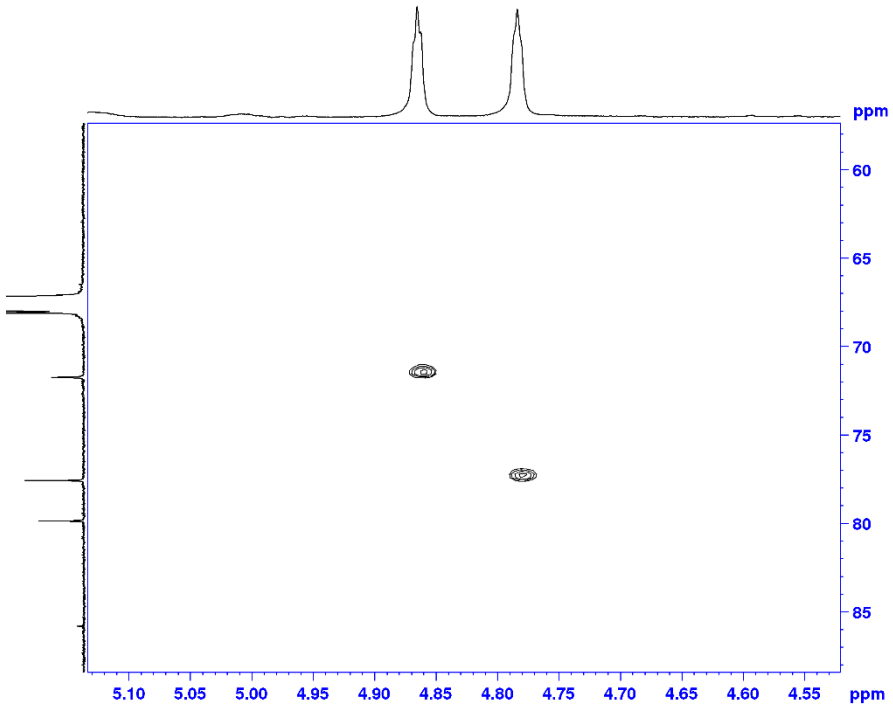

Figure S19: HSQC [Re(η^5-C_5H_4CHO)(η^6-$C_6(CH_3)_6$] (**5**) (500 MHz, C_4D_8O)

4. UPLC-UV Trace UPLC/ESI MS spectra

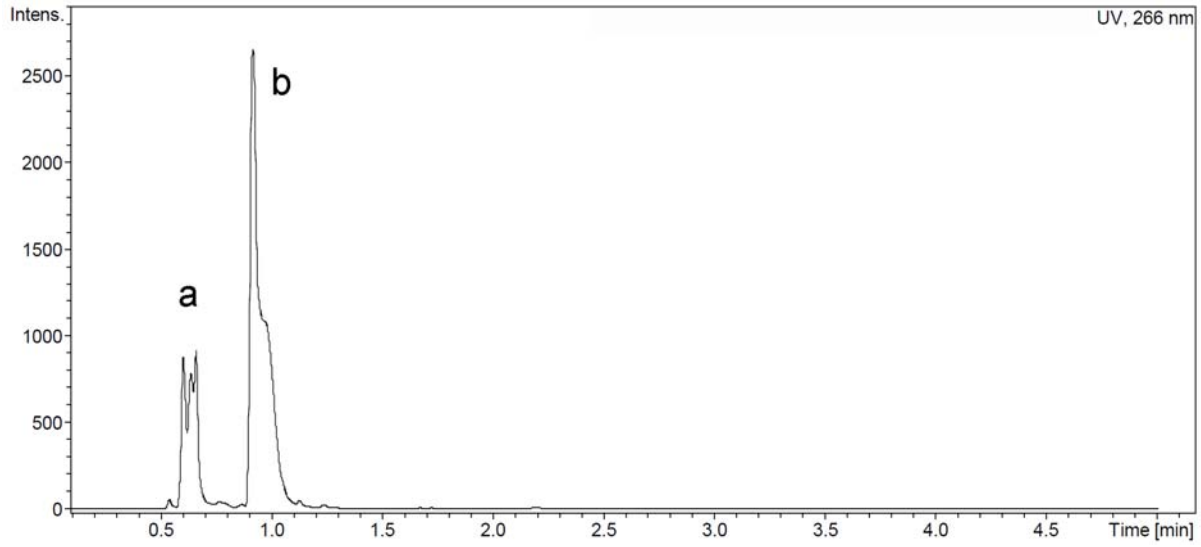

Figure S20: UV trace of the reaction Re(η^6-$C_6H_{5-n}D_nOH$)(η^6-C_6H_6) after 12h. (a) Re(η^6-$C_6H_{5-n}D_nOH$)(η^6-C_6H_6), (b) Re(η^6-$C_6H_{5-n}D_nBr$)(η^6-C_6H_6)

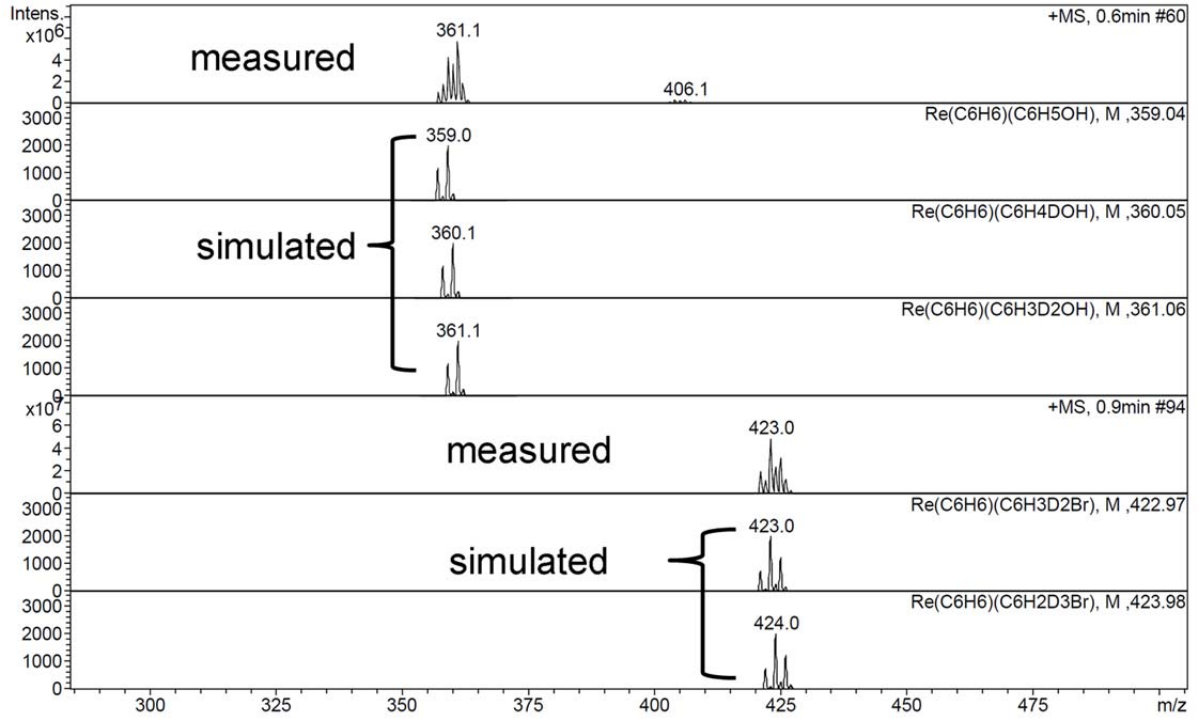

Figure S21: ESI-MS of the reaction Re(η^6-$C_6H_{5-n}D_nOH$)(η^6-C_6H_6) after 12h (synthesis method B).

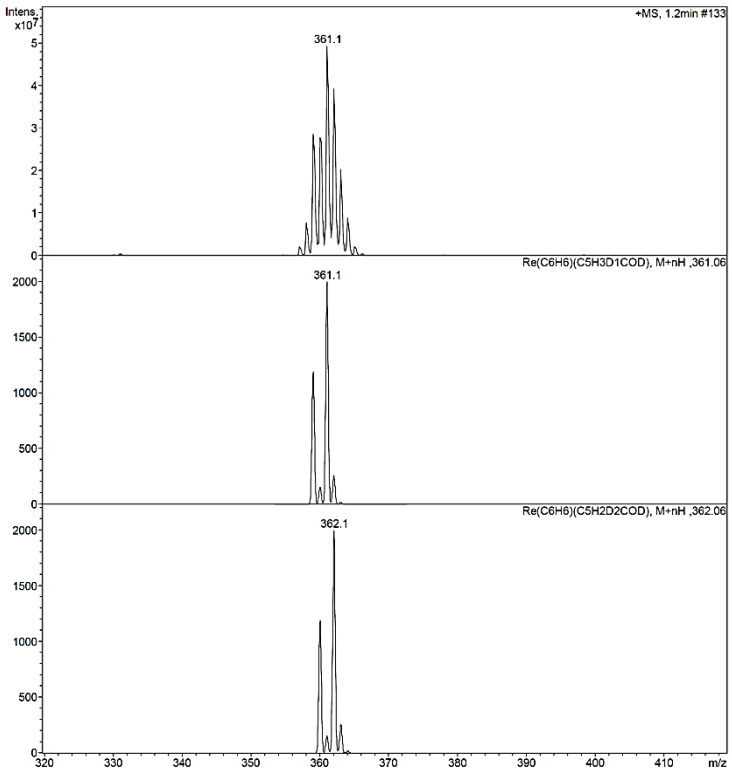

Figure S22: ESI-MS of Re(η^5-$C_5H_{4-n}D_nCDO$)(η^6-C_6H_6)

5. Computational details

All the calculations were performed using the Gaussian 09 program package[9]. The geometries of the complexes **D**, **E**, **2** and **3** were fully optimized using Density Functional Theory (DFT) in the singlet state. The calculations were carried out using M06-L functional[10], the LANL2DZ[11] effective core potential basis set for rhenium, and the 6-31+G(d,p) basis set for C, O, Br and H atoms. The solvent effect was taken into account by the Polarizable Continuum Model[12]. The transition state (**TS**) was located using QST3 method. Vibrational harmonic frequency analysis of all the structures was used to confirm the presence of the transition state and the minima, as well as to establish free energy values. The transition state connecting **D** and **E** was also confirmed following the coordinate of the reaction path.

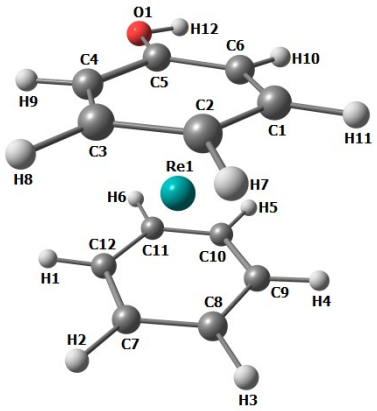

Figure S23: Optimized structure of complex [**2**$^{+}$]

Table S1: Cartesian coordinates complex [**2**$^{+}$]

Atom	X	Y	Z
Re(1)	0.941970	-0.004314	-1.581246
C(1)	0.689526	-2.076899	-2.374271
C(2)	1.483216	-1.350713	-3.298553
C(3)	1.013508	-0.115122	-3.812647
C(4)	-0.268577	0.373532	-3.435032
C(5)	-1.109719	-0.407340	-2.598307
C(6)	-0.594317	-1.588026	-1.996957
C(7)	2.613772	1.427228	-1.136646
C(8)	2.877711	0.171600	-0.521907
C(9)	1.930064	-0.388461	0.384900
C(10)	0.707761	0.285120	0.635989
C(11)	0.413043	1.504097	-0.031134
C(12)	1.378985	2.082411	-0.905927
H(1)	1.140277	2.990513	-1.448163
H(2)	3.314764	1.834367	-1.856610
H(3)	3.790518	-0.365483	-0.753710
H(4)	2.114113	-1.360063	0.829118
H(5)	-0.043485	-0.179570	1.265082
H(6)	-0.551834	1.979199	0.104086
H(7)	2.483595	-1.692673	-3.538449
H(8)	1.645428	0.481939	-4.459940
H(9)	-0.630242	1.327929	-3.800792
H(10)	-1.192086	-2.133420	-1.273249
H(11)	1.070948	-2.984363	-1.920077
O(1)	-2.332811	0.083651	-2.331078
H(12)	-2.783030	-0.469169	-1.678343

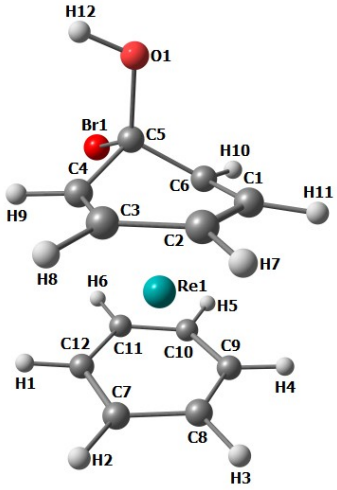

Figure S24: Optimized structure of complex **D**

Table S2: Cartesian coordinates complex **D**

Atom	X	Y	Z
Re(1)	0.113480	0.043750	0.053392
C(1)	-0.349850	-1.964044	-0.762902
C(2)	0.431863	-1.283497	-1.735158
C(3)	0.005162	0.002136	-2.164682
C(4)	-1.221469	0.528972	-1.648652
C(5)	-2.269739	-0.458414	-1.249257
C(6)	-1.562043	-1.357066	-0.295308
C(7)	1.839505	1.444452	0.526561
C(8)	2.063589	0.136690	1.052841
C(9)	1.126818	-0.417663	1.992035
C(10)	-0.066138	0.281087	2.286598
C(11)	-0.373137	1.504112	1.628062
C(12)	0.613888	2.098584	0.770124
H(1)	0.388885	3.029091	0.258214
H(2)	2.545760	1.872497	-0.178165
H(3)	2.974522	-0.401000	0.810379
H(4)	1.302939	-1.396963	2.424667
H(5)	-0.819228	-0.188886	2.912719
H(6)	-1.325247	1.994496	1.796189
H(7)	1.392275	-1.679819	-2.049019
H(8)	0.647896	0.605448	-2.799879
H(9)	-1.516333	1.534110	-1.938593
H(10)	-2.128502	-1.866210	0.479648
H(11)	0.023677	-2.878939	-0.310825
Br(1)	-3.677219	0.609866	-0.147090
O(1)	-2.970869	-1.129302	-2.242506
H(12)	-3.229605	-0.495154	-2.926438

Table S3: Natural population analysis for complex **D**

Atom	Natural charge	Atom	Natural charge	Atom	Natural charge
C(1)	-0.227	C(10)	-0.201	H(7)	0.285
C(2)	-0.241	C(11)	-0.273	H(8)	0.286
C(3)	-0.226	C(12)	-0.230	H(9)	0.281
C(4)	-0.361	H(1)	0.286	H(10)	0.281
C(5)	0.287	H(2)	0.285	H(11)	0.285
C(6)	-0.344	H(3)	0.287	Re(1)	-0.229
C(7)	-0.213	H(4)	0.286	Br(1)	-0.153
C(8)	-0.251	H(5)	0.285	O(1)	-0.752
C(9)	-0.249	H(6)	0.289	H(12)	0.526

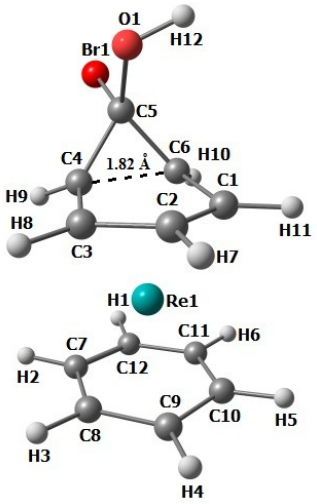

Figure S25: Optimized structure of transition state (**TS**)

Table S4: Cartesian coordinates complex (**TS**)

Atom	X	Y	Z
Re(1)	-0.865754	-0.426712	-3.378326
C(1)	-2.207819	-2.096645	-3.738240
C(2)	-1.027263	-2.329164	-4.509955
C(3)	-0.731913	-1.236467	-5.383555
C(4)	-1.877914	-0.346632	-5.553115
C(5)	-3.198141	-0.970988	-5.760315
C(6)	-3.009452	-1.005233	-4.290080
C(7)	0.299487	1.454498	-3.188756
C(8)	1.167650	0.319877	-3.091554
C(9)	0.922609	-0.686973	-2.118562
C(10)	-0.243532	-0.614406	-1.298889
C(11)	-1.101204	0.528222	-1.368365
C(12)	-0.815404	1.550925	-2.306398
H(1)	-1.519229	2.370054	-2.423826
H(2)	0.466275	2.214199	-3.944329
H(3)	1.989928	0.202989	-3.790712
H(4)	1.539898	-1.579864	-2.093661
H(5)	-0.483293	-1.430047	-0.623932
H(6)	-1.991046	0.592065	-0.751349
H(7)	-0.363168	-3.173081	-4.359928
H(8)	0.158427	-1.154548	-5.994618
H(9)	-1.760521	0.703649	-5.800684
H(10)	-3.675166	-0.409042	-3.673279
H(11)	-2.571930	-2.749587	-2.954112
Br(1)	-4.588597	0.332687	-6.304340
O(1)	-3.237210	-2.120302	-6.498819
H(12)	-3.918225	-2.697390	-6.130947

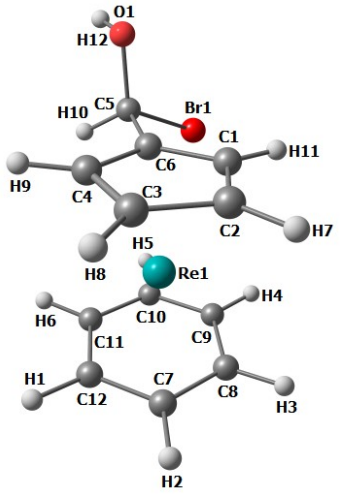

Figure S26: Optimized structure of complex **E**

Table S5: Cartesian coordinates complex **E**

Atom	X	Y	Z
Re(1)	0.170066	0.464633	0.222068
C(1)	-0.158066	-1.646128	-0.425313
C(2)	0.573531	-0.976199	-1.451165
C(3)	-0.232919	0.092299	-1.954776
C(4)	-1.465779	0.094030	-1.234497
C(5)	-2.591715	-1.374634	0.543582
C(6)	-1.416550	-0.975014	-0.270450
C(7)	1.745540	2.020080	0.471364
C(8)	2.086141	0.879475	1.253253
C(9)	1.151714	0.357893	2.197546
C(10)	-0.121739	0.976604	2.352633
C(11)	-0.467394	2.108056	1.559369
C(12)	0.467220	2.628710	0.616435
H(1)	0.183347	3.453256	-0.029322
H(2)	2.430709	2.376865	-0.290603
H(3)	3.034879	0.377566	1.094917
H(4)	1.386020	-0.545744	2.751318
H(5)	-0.861946	0.529393	3.008548
H(6)	-1.462238	2.535515	1.629687
H(7)	1.562535	-1.243703	-1.800425
H(8)	0.036399	0.769197	-2.755490
H(9)	-2.304846	0.760392	-1.392810
H(10)	-3.136027	-0.514588	0.942440
H(11)	0.175976	-2.504421	0.143851
Br(1)	-1.986348	-2.301070	2.268475
O(1)	-3.392063	-2.227972	-0.182016
H(12)	-4.252287	-2.305371	0.251503

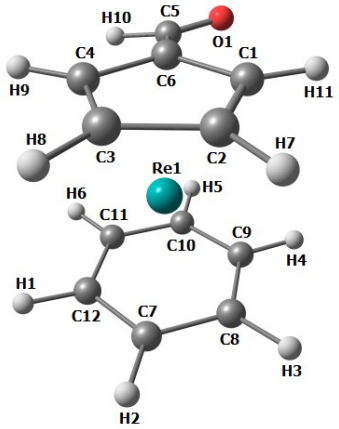

Figure S27: Optimized structure of complex **3**

Table S6: Cartesian coordinates complex **3**

Atom	X	Y	Z
Re(1)	0.105001	0.428632	0.230286
C(1)	-0.197984	-1.662000	-0.460708
C(2)	0.582713	-0.990290	-1.445047
C(3)	-0.188103	0.095211	-1.972101
C(4)	-1.450850	0.110015	-1.313950
C(5)	-2.497458	-1.203934	0.623373
C(6)	-1.471283	-0.991506	-0.380101
C(7)	1.678256	1.981729	0.466746
C(8)	2.034132	0.827525	1.222651
C(9)	1.127290	0.304541	2.194250
C(10)	-0.135881	0.926333	2.385302
C(11)	-0.507181	2.058597	1.602256
C(12)	0.406806	2.591835	0.648119
H(1)	0.109490	3.423184	0.018095
H(2)	2.338510	2.337304	-0.317100
H(3)	2.974471	0.322293	1.030431
H(4)	1.378948	-0.595963	2.743876
H(5)	-0.857569	0.479932	3.062662
H(6)	-1.497652	2.488708	1.704338
H(7)	1.587014	-1.253623	-1.750233
H(8)	0.134947	0.780758	-2.744521
H(9)	-2.269898	0.792212	-1.504723
H(10)	-3.279615	-0.412835	0.642530
H(11)	0.091473	-2.532438	0.112945
O(1)	-2.538168	-2.146570	1.411401

Crystal Data

X-ray Crystallographic data were collected at 183(2) K with either Mo Kα radiation (λ = 0.7107 Å). Compound **7** was measured on a CCD XtaLAB Synergy, dual source, with an Atlas detector while compounds [**2**]OTf, [Re(η^5-$C_6H_5O^-$)(η^6-C_6H_6), **3**, **5**, and **[6]**PF_6 were measured on an Oxford Diffraction CCD Xcalibur system with a Ruby detector. Suitable crystals were covered with oil (Infineum V8512, formerly known as Paratone N), placed on a nylon loop that is mounted in a CrystalCap Magnetic™ (Hampton Research) and immediately transferred to the diffractometer. Data were corrected for Lorentz and polarisation effects as well as for absorption (numerical). The program suite CrysAlisPro was used for data collection, multi-scan absorption correction and data reduction.[5] Structures were solved with direct methods using SIR97[6] and were refined by full-matrix least-squares methods on F^2 with SHELXL-2014.[7] The structures were checked for higher symmetry with help of the program Platon.[8] Supplementary crystallographic data can be obtained free of charge from the Cambridge Crystallographic Data Centre via www.ccdc.cam.ac.uk/structures (CCDC nr. 1520793-1520796, 1529872, 1529873).

Table S7. Crystal data and data collection of complexes [**2**]OTF, [Re(η^5-$C_6H_5O^-$)(η^6-C_6H_6)], **3** and **5**

	[Re(η^6-C_6H_6OH)(η^6-C_6H_6)]OTf ([**2**]OTf)	[Re(η^5-$C_6H_5O^-$)(η^6-C_6H_6)]($Na_{(0.25)}$)($NH_{4\ (0.25)}$)($OH_{(0.25)}$)($PF_{6\ (0.25)}$)	Re(η^5-C_5H_4CHO)(η^6-C_6H_6) (**3**)	Re(η^5-C_5H_4CHO)(η^6-$C_6(CH_3)_6$) (**5**)
Empirical formula	$C_{13}H_{12}F_3O_4ReS$	$C_{48}H_{51}F_6NNa\ O_6PRe_4$	$C_{12}H_{11}ORe$	$C_{18}H_{23}ORe$
Diffractometer	Xcalibur Ruby	Xcalibur Ruby	Xcalibur Ruby	Xcalibur Ruby
Wavelength (Å)	0.7107	0.7107	0.7107	0.7107
mol. weight (g/mol)	507.49	1650.65	357.41	441.56
Crystal system	Monoclinic	Monoclinic	Monoclinic	Monoclinic
Space group	P21/c	C2/c	Ia	P21/c
a (Å)	9.8356(5)	28.120(3)	8.0302(7)	12.4986(6)
b (Å)	10.0518(5)	6.116(5)	10.9282(7)	8.2570(4)
c (Å)	14.6218(8)	26.205(3)	11.4333(12)	15.0774(8)
α (°)	90	90	90	90
β (°)	101.159(5)	92.139(12)	108.358(10)	102.125(5)
γ (°)	90	90	90	90
Volume ($Å^3$)	1314.10(7)	4504(4)	952.27(15)	1521.29(13)
Z	4	4	4	4
Dens.(calc.) (g/cm^3)	2.377	2.434	2.493	1.928
Abs. coeff. (mm^{-1})	8.764	10.838	12.718	7.981
F(000)	960	3096	664	856
Crystal size (mm^3)	0.43 x 0.20 x 0.1	0.150 x 0.110 x 0.080	0.22 x 0.13 x 0.05	0.16 x 0.09 x 0.07
Crystal description	yellow block	yellow block	brown plate	orange block
θ range (°)	2.474 to 32.77	2.900 to 32.886	2.645 to 22.767	2.764 to 28.278
Index ranges	-14<=h<=14, -14<=k<=15 -22<=l<=11	-41<=h<=37, -9<=k<=9, -37<=l<=39	-11<=h<=12, -16<=k<=16, -16<=l<=16	-16<=h<=16, -10<=k<=11, -20<=l<=19
Refl. collected	16646	34053	6007	10971
Indep. reflections	4856 [R_{int} = 0.0504]	7812 [R_{int} = 0.0563]	2868 [R_{int} = 0.0419]	3760 [R_{int} = 0.0592]
Reflections obs.	4266	6735	2717	3066
Criterion for obs.	>2sigma(I)	>2sigma(I)	>2sigma(I)	>2sigma(I)
Completeness to θ	99.9 % to 26.32°	99.0 % to 30.44°	99.9 % to 26.32°	99.9 % to 30.44°
Absorption corr.	Analytical	Semi-empirical from eq..	Analytical	Analytical
Max. and min. transm.	0.501 and 0.100	1.000 and 0.75651	0.580 and 0.192	0.624 and 0.380
Data / restraints / param.	4856 / 0 / 200	7812 / 0 / 313	2868 / 2 / 127	3760 / 0 / 187
Goodness-of-fit on F^2	1.086	1.144	1.073	1.009
Fin. R ind. [I>2sigma(I)]	R1 = 0.0306, wR2 = 0.0695	R1 = 0.0365, wR2 = 0.0734	R1 = 0.0370, wR2 = 0.0857	R1 = 0.0340, wR2 = 0.0692
R indices (all data)	R1 = 0.0359, wR2 = 0.0738	R1 = 0.0463, wR2 = 0.0774	R1 = 0.0403, wR2 = 0.0907	R1 = 0.0448, wR2 = 0.0746
Fin. diff. ρ_{max} ($e^-/Å^{-3}$)	1.621 and -2.205	1.615 and -1.275	2.293 and -2.174	1.774 and -1.097
CCDC Nr.	1520796	1520795	1520793	1520794

Table S8. Crystal data and data collection of complexes [**6**]PF_6 and **7**

	[Tc(η^6-C_6H_5Br)(η^6-$C_6(CH_3)_6$)](PF_6) ([**6**]PF_6)	Tc(η^6-C_6H_5O)(η^6-$C_6(CH_3)_6$) (**7**)
Empirical formula	$C_{18}H_{32}BrF_6PTc$	$C_{18}H_{25}O_2Tc$
Diffractometer	Xcalibur Ruby	XtaLAB Synergy
Wavelength (Å)	0.7107	0.7107
mol. weight (g/mol)	563.25	372.39
Crystal system	Orthorombic	Orthorhombic
Space group	Pnma	Pbca
a (Å)	25.3910(17)	12.7035(2)
b (Å)	11.0770(5)	14.8508(2)
c (Å)	7.0096(4)	16.5406(3)
α (°)	90	90
β (°)	90	90
γ (°)	90	90
Volume ($Å^3$)	1971.49(19)	3120.50(8)
Z	4	8
Dens.(calc.) (g/cm^3)	1.894	1.581
Abs. coeff. (mm^{-1})	2.89	0.93
F(000)	1112	1536
Crystal size (mm^3)	0.30 x 0.19 x 0.13	0.34 × 0.12 × 0.10
Crystal description	yellow stick	yellow stick
θ range (°)	3.0 to 28.9	2.4 to 35.0
Index ranges	-33<=h<=33, -10<=k<=14, -9<=l<=7	-18<=h<=18, -21<=k<=21, -23<=l<=23
Refl. collected	11182	50188
Indep. reflections	2518 [R_{int} = 0.037]	4758 [R_{int} = 0.026]
Reflections obs.	2132	4218
Criterion for obs.	>2sigma(I)	>2sigma(I)
Completeness to θ	98 % to 28.3°	100 % to 30.5°
Absorption corr.	Semi-empirical from eq..	Semi-empirical from eq..
Max. and min. transm.	0.477 and 0.705	0.746 and 0.913
Data / restraints / param.	2518 / 0 / 166	4758 / 1 / 202
Goodness-of-fit on F^2	1.04	1.06
Fin. R ind. [I>2sigma(I)]	R1 = 0.0504, wR2 = 0.1183	R1 = 0.022, wR2 = 0.060
R indices (all data)	R1 = 0.0615, wR2 = 0.1256	R1 = 0.025, wR2 = 0.062
Fin. diff. ρmax ($e^-/Å^{-3}$)	1..29 and -0.98	0.37 and −0.43
CCDC Nr.	1529872	1529873

6. References

[1] Noddack, J.; Noddak, W. *Z. Allgem. Chem.* **1929**, *181*, 1-37.

[2] Brauer, G., Handbuch der Präparativen Anorganische Chemie in drei Bände, 3. Auflage, Ferdinand Enke Verlag, Stuttgart **1981**, 1615, 1632-1633.

[3] Meola, G.; Braband, H.; Schmutz, P.; Benz, M.; Spingler, B.; Alberto, R. *Inorg. Chem.* **2016**, *55*, 11131.

[4] Gans, P.; Sabitini, A.; Vacca, A. *Talanta* **1996**, *43*, 1739-1753

[5] *CrysAlis^{Pro} Software system*, Agilent Technologies.

[6] Altomare, A.; Burla, M.C.; Camalli, M.; Cascarano, C.; Giacovazzo, C.; Guagliardi, A.; Moliterni, A.G.G.; Polidori, G.; Spagna, R. SIR97: a new tool for crystal structure determination and refinement. *J. Appl. Cryst*., **1999**, *32*, 115.

[7] Sheldrick, G. M.; *Acta. Cryst*., **2015**, *C71*, 3-8.

[8] Spek, A. L.; Single-crystal structure validation with the program PLATON. *J. Appl. Cryst*., **2003**, *36*, 7.

8.6 Unpublished Experimental Section: A Mixed-Ring Sandwich Complex from Unexpected Ring Contraction in $[M(\eta^6\text{-}C_6H_5Br)(\eta^6\text{-}C_6R_6)]^+$

8.6.1 $[Re(\eta^6\text{-}C_6H_5OH)(\eta^6\text{-}C_6H_6)](PF_6)$ ([**2**](PF_6))

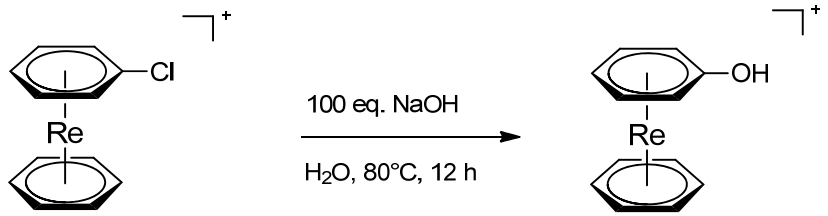

Synthesis: A 30 mg (0.057 mmol) portion of [**18**](PF_6) was suspended in 1.5 mL deion. water. Afterwards, 228 mg (5.7 mmol, 100 eq.) of sodium hydroxide were added to the yellow suspension. The reaction mixture was stirred for 12 h at 60°C. The solution was acidified with conc. HCl to pH 2. Subsequently, 11.2 mg (0.069 mmol, 1.2 eq.) of NH_4PF_6 were added to the solution. The product was extracted with CH_2Cl_2 (2 x 2ml) from aqueous phase. The solvent was evaporated in *vacuo* which afforded an analytically pure yellow [**2**](PF_6). Yield: 25 mg (0.049 mmol, 87%)

Analysis: ^{1}H NMR (500 MHz, CD_3CN) δ [ppm]: 6.28 (d, 2H, *o*-C*H*$_{arom}$), 5.92 (t, 2H, *m*-C*H*$_{arom}$), 5.76 (s, 6H, C*H*$_{arom}$), 5.63 (t, 1H, *p*-C*H*$_{arom}$),^{13}C NMR (125 MHz, CD_3CN) δ [ppm]: 130.16 (*C*$_{arom}$-OH), 77.65 (*p*-*C*H$_{arom}$), 76.62 (*C*$_{arom}$), 75.50 (*m*-*C*H$_{arom}$), 69.68 (*o*-*C*H$_{arom}$). ESI-MS: m/z = 359.1 $[M]^+$. IR ν: 3511 (w, O-H), 3097 (w), 2927 (w), 1513 (m), 1494 (w), 1432 (m), 1359 (w), 1211 (m), 1148 (w), 1044 (w), 926 (w), 803 (s), 739 (w) cm^{-1}. HR-ESI-MS $C_{12}H_{12}ORe$ $[M]^+$: calculated, 359.0440; found, 359.0442.

8.6.2 $[Re(\eta^5\text{-}C_5H_4CHNCH_2C_6H_5)(\eta^6\text{-}C_6H_6)]$ (**38**)

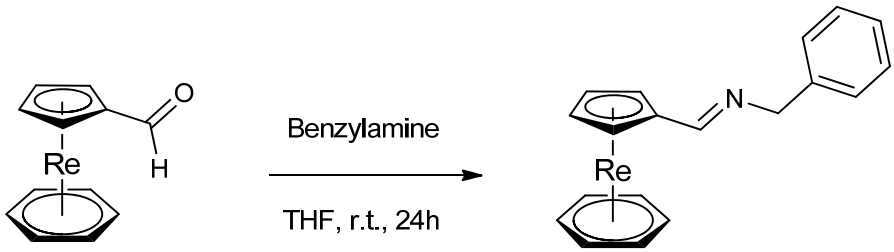

Synthesis: 20 mg (0.056 mmol) **3** was dissolved in 3 mL dry THF. After the addition of 61 µL (0.56 mmol, 10 equiv) benzylamine to the yellow solution, the reaction mixture was stirred for 24 h at room temperature. The remaining solvent was evaporated *in vacuo* and the residue was suspended and washed 3 times with degassed, deion. water (3 x 2 mL, at pH 7) and in cold dry pentan (2 x 1 mL).

The product was recrystallized from THF, yielding single crystals of **38**, suitable for X-ray diffraction analysis. Yield: 23 mg (0.051 mmol, 92%) of **38**

Analysis: ^{1}H NMR (500 MHz, C_4D_8O) δ [ppm]: 8.03 (s, 1H, C*H*=N), 7.24 (m, 2H, CH_{arom}), 7.71 (m, 3H, CH_{arom}), 5.49 (s, 2H, Cp α-*H*), 5.15 (s, 2H, Cp β-*H*), 4.69 (s, 6H, CH_{arom}), 4.49 (s, 2H, CH_2). ^{13}C NMR (125 MHz, C_4D_8O) δ [ppm]: 160.72 (*C*H=N), 141.59 (C_{arom}), 128.53 (*C*H$_{arom}$), 127.27 (*C*H$_{arom}$), 87.88 (*C*-CH), 73.71 (*C*H$_{CP}$), 72.84 (*C*H$_{CP}$), 61.4 (*C*H$_2$) 62.29 (C_{arom}), ESI-MS: m/z = 448.4 $[M-H]^+$. IR ν: 3058 (w), IR ν: 2828 (w), 1636 (s), 1494 (m), 1452 (m), 1419 (m), 1367 (m), 1333 (w), 1245 (m), 1041 (w), 1021 (w), 980 (m), 970 (m), 816 (s), 764 (m), 732 (s) cm^{-1}. HR-ESI-MS $C_{19}H_{18}NRe$ $[M-H]^+$: calculated, 448.1069; found, 448.1060.

8.6.3 [Re(η^5-C_5H_4COH)(η^6-C_6H_6)] (**39**)

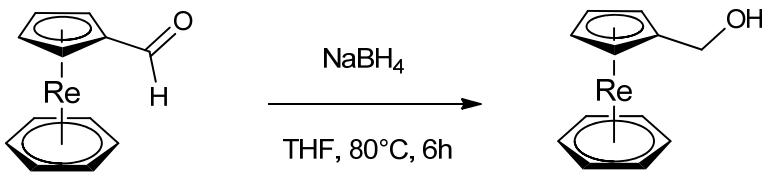

Synthesis: 20 mg (0.056 mmol) **3** was dissolved in 3 mL dry THF. After the addition of 21.2 mg (0.56 mmol, 10 equiv) $NaBH_4$ to the yellow solution, the reaction mixture was stirred for 6 h at 80°C (microwave device). After that, the slightly yellow solution was quenched with 4 mL degassed, deion. water. The remaining THF was evaporated *in vacuo* and the product was extracted 3 times with Et_2O (3 x 2 mL). The product was recrystallized from Et_2O, yielding single crystals of **39**, suitable for X-ray diffraction analysis. Yield: 16.5 mg (0.046 mmol, 82%) of **39**

Analysis: ^{1}H NMR (500 MHz, C_4D_8O) δ [ppm]: 5.15 (s, 2H, Cp α-*H*), 4.97 (s, 2H, Cp β-*H*), 4.66 (s, 6H, CH_{arom}), 3.99 (d, 2H, CH_2) 2.88 (t, 1H, O*H*). ^{13}C NMR (125 MHz, C_4D_8O) δ [ppm]: 96.21 (*C*-CH$_2$), 73.67 (*C*H$_{CP}$), 72.70 (*C*H$_{CP}$), 61.65 (*C*H$_2$) 61.17 (C_{arom}), ESI-MS: m/z = 361.1 $[M-H]^+$. IR ν: 3208 (br, w, OH), 2921 (s), 2852 (s), 1464 (m), 1418 (m), 1375 (m), 1306 (m), 1259 (m), 1235 (m), 1037 (m), 1009 (s), 983 (s), 967 (s), 811 (s), 734 (m) cm^{-1}. HR-ESI-MS $C_{12}H_{13}ORe$ $[M-H]^+$: calculated, 360.0518; found, 360.0519.

8.6.4 $[Re(\eta^5\text{-}C_5H_4CH_2)(\eta^6\text{-}C_6H_6)]^+$ ([**40**](PF$_6$)) and ([**40**](OTF))

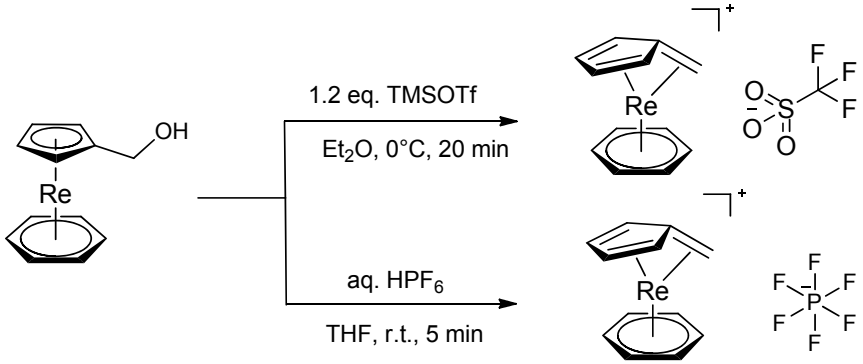

Synthesis of [**40**](PF$_6$): 20 mg (0.055 mmol) **39** was dissolved in 3 mL dry THF. Afterwards, an aqueous solution of HPF_6 (1 mL, 65%) was added dropwise to the yellow solution and further stirred for 20 minutes at room temperature. [**40**]$^+$ was precipitated after the addition of 5 mL deion. water and evaporation of the remaining THF *in vacuo.* After that, the solid yellow product [**40**]$^+$ was washed with water (3 x 3 mL) and dried. Yield: 21.4 mg (0.044 mmol, 81%) of [**40**](PF$_6$)

Synthesis of [**40**](OTF): 20 mg (0.055 mmol) **39** was dissolved in 3 mL dry Et_2O. The solution was cooled with an ice bath to 0°C and a solution of trimethylsilyl trifluoromethanesulfonate (0.2 ml, 10% in Et_2O) was added dropwise. The instantaneously formed precipitate was further stirred for 20 min at room temperature. After decanting of the supernatant, the solid was washed with Et_2O (3 x 3 mL) and dried *in vacuo*. Yield: 23.2 mg (0.047 mmol, 86%) of [**40**](OTF)

Analysis: ^{1}H NMR (500 MHz, CD_3CN) δ [ppm]: 6.01 (m, 2H, C*H*), 5.47 (s, 6H, CH_{arom}), 5.41 (t, 2H, C*H*), 3.95 (s, 2H, CH_2). ^{13}C NMR (125 MHz, CD_3CN) δ [ppm]: 97.19 (*C*=CH_2), 89.82 (*C*H), 83.42 (*C*H), 80.63 (*C*H_{arom}), 52.29 (*C*H_2). ESI-MS: m/z = 343.1 $[M]^+$. IR ν: 3101 (w), 1408 (w), 1244 (s), 1225 (s), 1158 (s), 1028 (s), 908 (w), 838 (m), 762 (w) cm^{-1}(OTf-salt). HR-ESI-MS $C_{12}H_{12}Re$ $[M]^+$: calculated, 343.0491; found, 343.0492.

8.6.5 [Re(η^6-$C_5H_4CH_3$)(η^6-C_6H_6)] (**41**)

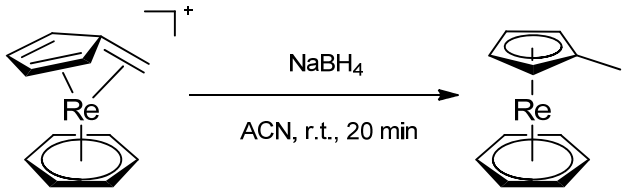

Synthesis: 20 mg (0.041mmol) [**40**](OTF) was dissolved in 2 mL dry actonitrile. After the addition of 15 mg (0.41 mmol, 10 equiv) $NaBH_4$ to the yellow solution, the reaction mixture was stirred for 20 min at room temperature. The acetonitrile was evaporated *in vacuo* and the formed residue was extracted 3 times with Et_2O (3 x 2 mL). Again, the Et_2O was evaporated in vacuo which gaves **41** in analytical pure quality. Futher, **41** was recrystallized from Et_2O, yielding single crystals of **41**, suitable for X-ray diffraction analysis. Yield: 10 mg (0.029 mmol, 71%) of **41**

Analysis: ^{1}H NMR (500 MHz, C_4D_8O) δ [ppm]: 5.07 (s, 2H Cp α-*H*), 4.91 (s, 2H, Cp β-*H*), 4.58 (s, 6H, CH_{arom}), 2.02 (s, 2H, CH_3). ^{13}C NMR (125 MHz, C_4D_8O) δ [ppm]: 89.48 (*C*-CH_3), 75.38 (*C*H_{CP}), 71.77 (*C*H_{CP}), 61.05 (C_{arom}), 16.34 (*C*H_3). ESI-MS: m/z = 345.1 $[M-H]^+$. IR ν: 2921 (s), 2853 (s), 1456 (m), 1417 (m), 1378 (m), 1260 (m), 1224 (m), 1132 (m), 1031 (s), 1009 (s), 987 (m), 967 (m), 810 (s), cm^{-1}. HR-ESI-MS $C_{12}H_{13}Re$ $[M-H]^+$: decomposition.

8.6.6 [Re(η^6-$C_5H_4CH_2S(CH_2)_2OH$)(η^6-C_6H_6)] (**42**)

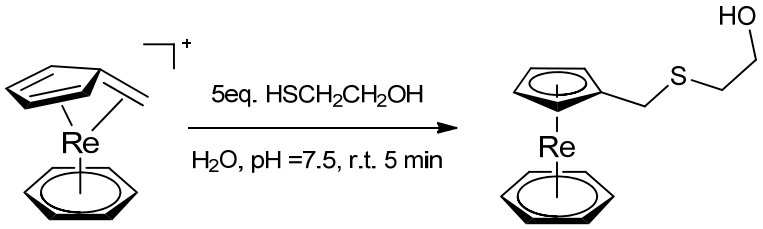

Synthesis: 20 mg (0.041mmol) [**40**](OTF) was dissolved in 3 mL degassed deion. water. The pH of the solution was adjusted with a 2 M Na_2CO_3 solution to pH=7.5. After the addition of 14 µL (0.21 mmol, 5 equiv) 2-Mercaptoethanol to the yellow solution, the reaction mixture was stirred for 20 min at room temperature. Afterwards, the formed white precipitate was washed with degassed deion. water (3 x 3 mL) and dried. The product was recrystallized from Et_2O, yielding single crystals of **42**, suitable for X-ray diffraction analysis. Yield: 15.5 mg (0.037 mmol, 90%) of **42**.

Analysis: ^{1}H NMR (500 MHz, C_4D_8O) δ [ppm]: 5.17 (s, 2H, Cp-*H*), 4.97 (s, 2H, Cp-*H*), 4.64 (s, 6H, CH_{arom}), 3.68 (t, 1H, O*H*), 3.58 (t, 2H, CH_2), 3.39 (s, 2H, CH_2), 2.56 (t, 2H, CH_2) ^{13}C NMR (125 MHz, C_4D_8O) δ [ppm]: 91.29 (*C*-CH_2), 74.49 (*C*H_{CP}), 72.12 (*C*H_{CP}), 62.59 (*C*H_2), 61.58 (C_{arom}), 35.52 (*C*H_2),

34.10 (*C*H_2). ESI-MS: m/z = 420.1 $[M]^+$. IR ν: 3051 (w), 2917 (m), 2849 (m), 1705 (m), 1462 (m), 1418 (m), 1290 (w), 1263 (w), 1241 (w), 1034 (m), 1021 (m), 988 (m), 970 (m), 813 (s) cm^{-1}. HR-ESI-MS $C_{14}H_{17}OReS$ $[M]^+$: decomposition.

8.7 Supplementary Information: Structure and Reactivities of Rhenium and Technetium Bis-Arene Sandwich Complexes $[M(\eta^6\text{-arene})_2]^+$

Structure and Reactivities of Rhenium and Technetium bis-Arene Sandwich Complexes $[M(\eta^6\text{-arene})_2]^+$

Giuseppe Meola, Henrik Braband, Sara Jordi, Thomas Fox, Olivier Blacque, Bernhard Spingler and Roger Alberto

Department of Chemistry, University of Zurich, Winterthurerstr. 190, CH-8057 Zurich Switzerland.

Supplementary Information

Table of Content

1. General Information

1.1 Materials

1.2 Characterization

2. Synthetic procedures

2.1 $[^{99}Tc(\eta^6\text{-hmbz})(\eta^6\text{-}C_6H_5\text{-}NH_3)](PF_6)_2$ ([**1**](PF$_6$)$_2$) and $[^{99}Tc(\eta^6\text{-pmbz})(\eta^6\text{-}C_6H_5\text{-}NH_3)](PF_6)_2$ ([**2**](PF$_6$)$_2$)

2.2 $[^{99}Tc(\eta^6\text{-hmbz})_2](PF_6)$ ([**3a**](PF$_6$)) and $[^{99}Tc(\eta^6\text{-pmbz})(\eta^6\text{-hmbz})](PF_6)$ ([**3b**](PF$_6$))

2.3 $[^{99}Tc(\eta^6\text{-hmbz})(\eta^6\text{-}C_6H_5\text{-Br})](PF_6)$ ([**4**](PF$_6$)) and $[^{99}Tc(\eta^6\text{-pmbz})(\eta^6\text{-}C_6H_5\text{-Br})](PF_6)$ ([**5**](PF$_6$))

2.4 $[^{99}Tc(\eta^6\text{-hmbz})(\eta^6\text{-}C_6H_6)](PF_6)$ and $[^{99}Tc(\eta^6\text{-pmbz})(\eta^6\text{-}C_6H_6)](PF_6)$

2.5 $[Re(\eta^6\text{-}C_6H_6)(\eta^6\text{-napht})](OTF)$ ([**6**](OTf))

2.6 $[Re(\eta^6\text{-napht})_2](OTf)$ ([**7**](OTf))

2.7 $[Re(\eta^6\text{-}C_6H_6)(tep)_3](OTf)$ ([**8**](OTf))

2.8 $[Re(\eta^6\text{-}C_6H_6)(CN\text{-}^tBu)_3](OTf)$ ([**9**](OTf))

2.9 $[Re(\eta^6\text{-}C_6H_6)(HB(pyz)_3)]$ (**10**)

2.10 $[Re(\eta^6\text{-napht})(tep)_3](PF_6)$ ([**11**](PF$_6$))

2.11 $[Re(\eta^6\text{-napht})(triphos)](PF_6)$ ([**12**](PF$_6$))

2.12 $[Re(CN\text{-}^tBu)_6](PF_6)$ ([**13**](PF$_6$))

3. NMR Spectra (^{1}H, ^{2}H, ^{13}C, HSQC, ^{1}H NOE, HMBC)

3.1 [^{99}Tc(η^6-hmbz)(η^6-C_6H_5-NH_3)](PF_6)$_2$ ([**1**](PF_6)$_2$) and [^{99}Tc(η^6-pmbz)(η^6-C_6H_5-NH_3)](PF_6)$_2$ ([**2**](PF_6)$_2$)

3.2 [^{99}Tc(η^6-hmbz)$_2$](PF_6) ([**3a**](PF_6)) and [^{99}Tc(η^6-pmbz)(η^6-hmbz)](PF_6) ([**3b**](PF_6))

3.3 [^{99}Tc(η^6-hmbz)(η^6-C_6H_5-Br)](PF_6) ([**4**](PF_6))

3.4 [^{99}Tc(η^6-pmbz)(η^6-C_6H_5-Br)](PF_6) ([**5**](PF_6))

3.5 [^{99}Tc(η^6-hmbz)((η^6-C_6H_6)](PF_6) and [^{99}Tc(η^6-pmbz)((η^6-C_6H_6)](PF_6)

3.6 [Re(η^6-C_6H_6)(η^6-napht)](OTF) ([**6**](OTf))

3.7 [Re(η^6-napht)$_2$](OTf) ([**7**](OTf))

3.8 [Re(η^6-C_6H_6)(tep)$_3$](OTf) ([**8**](OTf))

3.9 [Re(η^6-C_6H_6)(CN-^{t}Bu)$_3$](OTf) ([**9**](OTf))

3.10 [Re(η^6-napht)(tep)$_3$](PF_6) ([**11**](PF_6))

3.11 [Re(η^6-napht)(triphos)](PF_6) ([**12**](PF_6))

3.12 [Re(CN-^{t}Bu)$_6$](PF_6) ([**13**](PF_6))

4. Crystal Data

5. References

7. General Information

Caution: ^{99}Tc is a weak β^--emitters. All experiments have to be performed in laboratories approved for working with low-level radioactive materials.

7.1 Materials

All Re and ^{99}Tc reactions were carried out under nitrogen atmosphere on standard nitrogen/vacuum lines unless otherwise stated. For the Re reactions, the glassware was dried by the use of a heat gun or in an oven at 120 °C at least overnight. Commercially available reagents were purchased reagent-grade and used without further purification. THF was dried over Na/Benzophenone. All chemicals were purchased from Sigma Aldrich (Switzerland), except hydrochloric acid (32%, Honeywell, Germany), hexamethylbenzene (abcr), trifluoroacetic acid (99%, Alfa Aesar, Germany), and $(NH_4)[^{99}TcO_4]$ (Oak Ridge). The chemicals were used without farther purification. Deuterated NMR solvents were obtained from Armar Chemicals (Switzerland). $Ka[ReO_4]$ was synthesized according to literature.[1,2] The $SiMe_3$ protected aniline ($PhN(SiMe_3)_2$) was prepared, following literature procedure.[3]

7.2 Characterization

^{1}H, ^{13}C, ^{13}C HSQC, ^{29}Si, ^{31}P and ^{99}Tc NMR spectra were recorded on a BrukerDRX 400 MHz or BrukerDRX 500 MHz spectrometer. Chemical shifts of ^{1}H and ^{13}C were referenced with the residual solvent resonances relative to TMS, while ^{99}Tc was referenced relative to the signal of $[^{99}TcO_4]^-$ (δ = 0). Due to a scalar coupling to the ^{99}Tc nucleus (nuclear spin = 9/2), signals of directly bond carbon atoms are very broad, poorly resolved and rarely observed. Therefore, chemical shifts of ^{13}C signals of carbon atoms directly bond to the ^{99}Tc nucleus are not given in the analytical data of the synthetic procedures. Electronspray-ionisation mass spectrometry (ESI-MS) was performed on a Bruker esquireTM/LC spectrometer or on a Bruker esquire^{TM}/HCT^{TM} spectrometer. High-resolution mass spectrometry (HR-ESI-MS) was performed on a Bruker maXis QTof high-resolution mass spectrometer (Bruker GmbH, Bremen, Germany).

Preparative HPLC was performed on a Varian ProStar 320 system, using a Dr. Maisch Reprosil C18 100-7 (40 x 250 mm) column. The solvents (HPLC grade) were 0.1% trifluoroacetic acid (solvent A) and acetonitrile (solvent B). The HPLC gradients used are as follow (G1): 0-2 minutes: 75% A (25% B); 2.1-45 minutes: linear gradient from 75% A (25% B) to 35% A (65% B); 45-51 minutes: 100% B. The flow rate was 40 mL/min. Detection was performed at 273 nm; (G2): 0-2 minutes: 55% A (45% B); 2.1-45 minutes: linear gradient from 55% A (45% B) to 0% A (100% B); 45-50 minutes: 100% B. The flow rate was 40 mL/min. Detection was performed at 300 nm; (G3): 0-2 minutes: 40% A (60% B); 2.1-45 minutes: linear gradient from 40% A (60% B) to 0% A (100% B); 45-50 minutes: 100% B. The flow rate was 40 mL/min. Detection was performed at 300 nm. Analytical HPLC was performed on a

VWR HITACHI Chromaster system, using a Macherey-Nagel Nucleosil C18 100-5 column. HPLC solvents were 0.1% trifluoroacetic acid (solvent A) and methanol (solvent B). Applied HPLC gradient: 0-3 minutes: 100% A; 3.1-9 minutes: 75% A, 25% B; 9.1-20 minutes: linear gradient from 66% A (34% B) to 0% A (100% B); 20-28 minutes: 100% B; 28.1-30: 100% A. The flow rate was 0.5 mL/min. Detection was performed at 250 nm. HPLC analyses of the ^{99}Tc were performed on a Merck Hitachi LaChrom L 7100 pump coupled to a Merck Hitachi LaChrom L7200 tunable UV detector and a radiodetector. UV/Vis detection was performed at 250 nm. The detection of the radioactive ^{99}Tc complexes were performed with a Berthold LB513 radiodetector equipped with YG cell. Separations were achieved on a Macherey-Nagel C18 reversed-phase column (Nucleosil 10 lm, 250 4 mm) using a gradient of MeOH/ 0.1% CF_3COOH as eluent, and a flow rate of 0.5 mL/min. Gradient: t = 0 – 3 min: 0% MeOH; 3 – 3.1 min: 0 – 25% MeOH; 3.1 – 9 min: 25% MeOH; 9 – 9.1 min: 25 – 34% MeOH; 9.1 – 18 min: 34 - 100% MeOH; 18 – 25 min: 100% MeOH, 25 – 25.1 min: 100 - 0% MeOH; 25.1 – 30 min: 0% MeOH. For technetium content measurements, pure compounds were dissolved in the appropriate solvents. The measurements were carried out with a scintillation cocktail (Packard Ultimate Gold XR) and a liquid scintillation counter (*Hidex 300 SL*).

Elemental Analysis (EA) measurements were performed on a LecoCHNS-932 elemental analyzer. UPLC-ESI-MS was performed on a Waters Acquity UPLC System coupled to a Bruker HCT^{TM}, using an Acquity UPLC BEH C18 1.7 µm (2.1 x 50 mm) column. UPLC solvents were formic acid (0.1% in millipore water) (solvent A) and acetonitrile HPLC grade (solvent B). Applied UPLC gradient: 0-0.5 minutes: 95% A, 5% B; 0.51-4.0 minutes: linear gradient from 95% A (5% B) to 0% A (100% B); 4-5 minutes: 100% B. The flow rate was 0.6 ml/min. Detection was performed at 250 nm and 480 nm (DAD). IR-Spectra were recorded on a Perkin-Elmer FT-IR Spectrum Two spectrometer, using KBr pallets (^{99}Tc complexes) or by ATR technique (Re complexes).

8. Synthetic procedures

^{99}Tc-complexes

8.1 [^{99}Tc(η^6-hmbz)(η^6-C_6H_5-NH_3)]$(PF_6)_2$ ([**1**]$(PF_6)_2$) and [^{99}Tc(η^6-pmbz)(η^6-C_6H_5-NH_3)]$(PF_6)_2$ ([**2**]$(PF_6)_2$)

K[$^{99}TcO_4$] (10 mg, 0.05 mmol), hexamethylbenzene (407.7 mg, 2.51 mmol), $AlCl_3$ (206 mg, 1.55 mmol), $PhN(SiMe_3)_2$ (240.7 mg, 1.01 mmol) and Zn-powder (9.5 mg, 0.15 mmol) were added in a 50 mL two-necked flask. The reaction mixture was suspended in cyclohexane (6 mL) and stirred at 80 °C for 4 h. H_2O (7 mL) was added to quench the reaction. The red solution was filtered and phases were separated. HPLC of the aqueous phase showed a mixture of product (61.6%), [$^{99}TcO_4$]$^-$ (27.6%) and [^{99}Tc(Me_6Ph)$_2$]$^+$ (10.8%). For workup, conc. HCl (0.1 mL) was added to the aq. solution and it was stirred at room temperature until ^{29}Si-NMR showed full deprotection of the amine (ca. 23 h). The byproduct [^{99}Tc(η^6-hmbz)$_2$]$^+$ was extracted from the acidic aqueous phase with DCM. NH_4PF_6 (106 mg, 0.65 mmol) was added to the aqueous phase and the formed colorless precipitate was filtered off and dried *in vacuo* to afford [^{99}Tc(η^6-hmbz)(η^6-C_6H_5-NH_3)]$(PF_6)_2$ ([**1**]$(PF_6)_2$) as colorless powder (4.7 mg, 0.007 mmol, 15%).

It has to be mentioned, the powder contains [^{99}Tc(η^6-pmbz)(η^6-C_6H_5-NH_3)]$(PF_6)_2$ ([**2**]$(PF_6)_2$) as second minor specie. Due to extremely similar physical properties all attempts to separate the two species failed. Analytical data are given for the product mixture. Crystal of [**1**]$(PF_6)_2$ suitable for X-ray diffraction analysis were obtained by vapor diffusion of Et_2O into a solution of [**1**](PF_6) in acetone.

^{99}Tc NMR (90 Hz, MeCN-d_3): δ = -1415 ($\Delta\nu_{1/2}$ = 40 Hz), -1461 ppm ($\Delta\nu_{1/2}$ = 30).

^{1}H NMR (500 MHz, acetone-d_6): δ = 5.29 (*t*, *J* = 5.94 Hz, 2 H, NCCHC*H*), 5.09 (*t*, *J* = 5.23 Hz, 1 H, NCCHCHC*H*), 5.05 (*d*, *J* = 5.94 Hz, 2 H, NCC*H*), 2.29 ppm (*s*, 18 H, CH_3).

^{13}C NMR (125 Hz, acetone-d_6): δ = 17.03 ppm (6 CH_3).

IR (KBr): ν = 3495*m*, 3399*s*, 3241*w*, 2923*w*, 1633*m*, 1541*s*, 1458*m*, 1391*m*, 1288*m*, 1147*w*, 1072*m*, 1026*w*, 992*w*, 836*s*, 652*w*, 559*s*, 447*w*, 430*w*, 407*m* cm^{-1}.

^{99}Tc analysis calc. for $C_{18}H_{26}F_{12}NP_2Tc$ (%): 15.33; found: 14.95.

8.2 [^{99}Tc(η^6-hmbz)$_2$](PF$_6$) ([**3a**](PF$_6$)) and [^{99}Tc(η^6-pmbz)(η^6-hmbz)](PF$_6$) ([**3b**](PF$_6$))

In a 50 mL, two-necked flask, K[^{99}TcO$_4$] (10 mg, 0.05 mmol), hexamethylbenzene (160 mg, 0.98 mmol) and AlCl$_3$ (206.3 mg, 1.55 mmol) were dissolved in cyclohexane (6 mL). The solution was stirred at 80 C for 4 h when H$_2$O (6 mL) was added to quench the reaction. The solution was filtered and phases were separated. NH$_4$PF$_6$ (106.2 mg, 0.65 mmol) was added to the aq. phase and the colorless precipitate was filtered off and dried *in vacuo* to afford a colorless powder [^{99}Tc(η^6-hmbz)$_2$](PF$_6$) ([**3a**](PF$_6$)) (20.9 mg, 0.04 mmol, 71%).

It has to be mentioned, the powder contains [^{99}Tc(η^6-pmbz)(η^6-hmbz)](PF$_6$) ([**3b**](PF$_6$)) as by product (ratio 1: 0.7). Due to extremely similar physical properties all attempts to separate the two species failed. Analytical data are given for the product mixture. Crystal of [**3a**](PF$_6$) suitable for X-ray diffraction analysis were obtained by vapor diffusion of Et$_2$O into a solution of [**3a**](PF$_6$) in acetone.

^{99}Tc NMR (90 Hz, CD$_2$Cl$_2$): δ = -1308 ($\Delta\nu_{1/2}$ = 103 Hz), -1346 ppm ($\Delta\nu_{1/2}$ = 83 Hz).

^{1}H NMR (500 MHz, acetone-d$_6$): δ = 5.237 (s, 1H, [^{99}Tc(η^6-hmbz)(η^6-pmbz*H*)]), 2.152 (s, 18 H, [^{99}Tc(η^6-hmbz)(η^6-*pm*bzH)]), 2.083 (s, 6 H, [^{99}Tc(η^6-hmbz)(η^6-*pm*bzH)]), 2.075 (s, 36 H, [^{99}Tc(η^6-*hm*bz)$_2$]), 2.069 (s, 3 H, [^{99}Tc(η^6-hmbz)(η^6-*pm*bzH)]), 2.028 ppm (s, 6 H, [^{99}Tc(η^6-hmbz)(η^6-*pm*bzH)]).

^{13}C NMR (125 MHz, acetone-d$_6$): δ = 18.37 (2 C, [^{99}Tc(η^6-hmbz)(η^6-*pm*bzH)], 16.34 (6 C, [^{99}Tc(η^6-*hm*bz)(η^6-pmbzH)]), 16.16 (12 C, [^{99}Tc(η^6-*hm*bz)$_2$]), 15.34 (1 C, [^{99}Tc(η^6-hmbz)(η^6-*pm*bzH)]), 14.74 ppm (2 C, [^{99}Tc(η^6-hmbz)(η^6-*pm*bzH)]).

IR (KBr): ν = 3416*w* 2920*m*, 1448*m*, 1392*s*, 1294*w*, 1070*m*, 1013*m*, 877*m*, 840*s*, 557*s*, 444*w*, 425*m* cm^{-1}.

^{99}Tc analysis calc. for C$_{24}$H$_{36}$F$_6$PTc (%): 17.40; found: 17.0.

8.3 [^{99}Tc(η^6-hmbz)(η^6-C$_6$H$_5$-Br)](PF$_6$) ([**4**](PF$_6$)) and [^{99}Tc(η^6-pmbz)(η^6-C$_6$H$_5$-Br)](PF$_6$) ([**5**](PF$_6$))

In contrast to the published synthesis of [^{99}Tc(η^6-hmbz)(η^6-C$_6$H$_5$-Br)](PF$_6$) ([**4**](PF$_6$)),[4] this improved procedure allows the separation of simultaneously formed [^{99}Tc(η^6-hmbz)(η^6-C$_6$H$_5$-Br)](PF$_6$) ([**4**](PF$_6$)) and [^{99}Tc(η^6-pmbz)(η^6-C$_6$H$_5$-Br)](PF$_6$) ([**5**](PF$_6$)). In a 50 mL two-necked flask, K[^{99}TcO$_4$] (13.2 mg, 0.07 mmol), hexamethylbenzene (80 mg, 0.5 mmol) and AlCl$_3$ (200 mg, 1.50 mmol) were suspended in bromobenzene (4 mL). The solution was stirred at 80°C for 4 h when H$_2$O (5 mL) was added to quench the reaction. The solution was filtered and phases were separated. NH$_4$PF$_6$ (100 mg, 0.61 mmol) was added to the aq. phases and the pale yellow precipitate was filtered off. Following this procedure, 30.4 mg (0.05 mmol, 77%) of a mixture of [^{99}Tc(η^6-hmbz)(η^6-C$_6$H$_5$-Br)](PF$_6$) ([**4**](PF$_6$)) and [^{99}Tc(η^6-pmbz)(η^6-C$_6$H$_5$-Br)](PF$_6$) ([**5**](PF$_6$)) was isolated.

IR (KBr): ν = 3430*w*, 3083*w*, 2923*w*, 1430*w*, 1391*m*, 1054*w*, 1019*w*, 833*s*, 670*w*, 558*s*, 451*w*, 426*m* cm^{-1}.

^{99}Tc analysis calc. for $C_{18}H_{23}BrF_6PTc$ (%): 17.56; found: 16.54.

For anion metathesis, the solid was dissolved in 20 ml THF and Ph_3PCl_2 (100 mg, 0.3 mmol) dissolved in 1 ml THF was added. The pale yellow precipitate was filtered off and dissolved in 0.5 ml H_2O. The solution was loaded on a C18 syringe column. Separation of the two products $[^{99}Tc(\eta^6\text{-hmbz})(\eta^6\text{-}C_6H_5\text{-Br})]^+$ and $[^{99}Tc(\eta^6\text{-pmbz})(\eta^6\text{-}C_6H_5\text{-Br})]^+$ was achieved by passing through the column ca. 20 ml H_2O and collecting 1 ml fractions. Finally, the column was washed with 2ml MeOH. All fractions were checked by radio HPLC. Fractions which contained the products were checked by ^{99}Tc-NMR. Only fractions, which were pure and showed the same ^{99}Tc signal in the ^{99}Tc-NMR were combined. $[^{99}Tc(\eta^6\text{-pmbz})(\eta^6\text{-}C_6H_5\text{-Br})]^+$ eluted slightly faster from the column as $[^{99}Tc(\eta^6\text{-hmbz})(\eta^6\text{-}C_6H_5\text{-Br})]^+$. Evaporating the solvent under high vacuum leads to the isolation of $[^{99}Tc(\eta^6\text{-hmbz})(\eta^6\text{-}C_6H_5\text{-Br})]Cl$ and $[^{99}Tc(\eta^6\text{-pmbz})(\eta^6\text{-}C_6H_5\text{-Br})]Cl$ as pale yellow powders.

$[^{99}Tc(\eta^6\text{-hmbz})(\eta^6\text{-}C_6H_5\text{-Br})](PF_6)$ ([**4**](PF_6))

^{99}Tc NMR (90 MHz,D_2O): δ = -1563 ppm ($\Delta\nu_{1/2}$ = 54 Hz).

^{1}H NMR (400 MHz, D_2O): δ = 5.585 (*d*, *J* = 5.44 Hz, 2 H, $[^{99}Tc(\eta^6\text{-}C_6\mathit{H}_5Br)(\eta^6\text{-hmbz})]$), 5.241 (*m*, 3 H, $[^{99}Tc(\eta^6\text{-}C_6\mathit{H}_5Br)(\eta^6\text{-hmbz})]$), 2.318 ppm (*s*, 18 H, $[^{99}Tc(\eta^6\text{-}\mathit{hm}bz)]$).

^{13}C NMR (125 MHz, D_2O): δ = 15.9 ppm (6 C, $[^{99}Tc(\eta^6\text{-}\mathit{hm}bz)(\eta^6\text{-}C_6H_5Br)]$).

$[^{99}Tc(\eta^6\text{-pmbz})(\eta^6\text{-}C_6H_5\text{-Br})](PF_6)$ ([**5**](PF_6))

^{99}Tc NMR (112.5 MHz, D_2O): δ = -1603 ppm ($\Delta\nu_{1/2}$ = 41 Hz).

^{1}H NMR (500 MHz, D_2O): δ = 5.90 (s, 1 H, $[^{99}Tc(\eta^6\text{-pmbz}\mathit{H})(\eta^6\text{-}C_6H_5\text{-Br})]$), 5.69 (d, *J* = 5.71 Hz, 2 H, $[^{99}Tc(\eta^6\text{-pmbzH})(\eta^6\text{-}C_6\mathit{H}_5\text{-Br})]$), 5.35 (t, *J* = 5.44 Hz 2 H, $[^{99}Tc(\eta^6\text{-pmbzH})(\eta^6\text{-}C_6\mathit{H}_5\text{-Br})]$), 5.30 (t, 5.37 Hz, 1 H, $[^{99}Tc(\eta^6\text{-pmbzH})(\eta^6\text{-}C_6\mathit{H}_5\text{-Br})]$), 2.31 (s, 3 H, $[^{99}Tc(\eta^6\text{-}\mathit{pm}bzH)(\eta^6\text{-}C_6H_5\text{-Br})]$), 2.25 (s, 6 H, $[^{99}Tc(\eta^6\text{-}\mathit{pm}bzH)(\eta^6\text{-}C_6H_5\text{-Br})]$, 2.21 ppm (s, 6 H, $[^{99}Tc(\eta^6\text{-}\mathit{pm}bzH)(\eta^6\text{-}C_6H_5\text{-Br})]$).

^{13}C NMR (125 MHz, D_2O): δ = 19.25 (br, 2 C, $[^{99}Tc(\eta^6\text{-}\mathit{pm}bzH)(\eta^6\text{-}C_6H_5\text{-Br})]$, 16.36 (br, 1 C, $[^{99}Tc(\eta^6\text{-}\mathit{pm}bzH)(\eta^6\text{-}C_6H_5\text{-Br})]$), 15.75 ppm (br, 2 C, $[^{99}Tc(\eta^6\text{-}\mathit{pm}bzH)(\eta^6\text{-}C_6H_5\text{-Br})]$).

8.4 [^{99}Tc(η^6-hmbz)(η^6-C_6H_6)](PF_6) and [^{99}Tc(η^6-pmbz)(η^6-C_6H_6)](PF_6)

K[^{99}TcO4] (10 mg, 0.05 mmol), hexamethylbenzene (406.3 mg, 2.5 mmol) and AlCl3 (204 mg, 1.5 mmol) were dissolved in benzene (5 mL) in a 50 mL two-necked flask. The solution was stirred at 80°C for 4 h when H_2O (4 mL) was added to quench the reaction. The reaction mixture was filtered, washed with H_2O (2 mL) and phases were separated. NH_4PF_6 (104 mg, 0.64 mmol) was added to the aq. phase and the formed colorless precipitate was filtered off and dried *in vacuo* to afford [^{99}Tc(Me_6Ph)(C_6H_6)](PF_6) as colorless powder (18.7 mg, 0.04 mmol, 79%).
It has to mentioned, the product contains a second minor specie, most likely [^{99}Tc(Me_5HPh)(C_6H_6)](PF_6). Due to extremely similar physical properties all attempts to separate the two species failed. Analytical data are given for the product mixture.

^{99}Tc NMR (112.5 MHz, acetone-d_6): δ = -1546 ($\Delta\nu_{1/2}$ = 49 Hz), -1594 ($\Delta\nu_{1/2}$ = 53 Hz) ppm.
^{1}H NMR (500 MHz, acetone-d_6): δ = 5. 996 (s, 1H, [^{99}Tc(η^6-C_6H_6)(η^6-pmbz*H*)]), 5.483 (s, 6 H, [^{99}Tc(η^6-C_6*H*$_6$)(η^6-pmbzH)]), 5.392 (s, 6 H, [^{99}Tc(η^6-C_6*H*$_6$)(η^6-hmbz)]), 2.418 (s, 18 H, [^{99}Tc(η^6-C_6H_6)(η^6-*hm*bz)]) + (s, 3 H, [^{99}Tc(η^6-C_6H_6)(η^6-*pm*bzH)]), 2.360 (s, 6 H, [^{99}Tc(η^6-C_6H_6)(η^6-*pm*bzH)]), 2.314 ppm (s, 6 H, [^{99}Tc(η^6-C_6H_6)(η^6-*pm*bzH)]).
^{13}C NMR (125 MHz, acetone-d_6): δ = 19.78 (2 C, [^{99}Tc(η^6-C_6H_6)(η^6-*pm*bzH)]), 17.63 (6 C, [^{99}Tc(η^6-C_6H_6)(η^6-*hm*bz)]), 16.95 (1 C, [^{99}Tc(η^6-C_6H_6)(η^6-*hm*bz)]), 16.32 ppm (2 C, [^{99}Tc(η^6-C_6H_6)(η^6-*pm*bzH)]).
IR (KBr): ν = 3435*w*, 3082*w*, 2924*w*, 1855*w*, 1640*w*, 1453*m*, 1386*m*, 1293*w*, 1074*m*, 1026*w*, 974*w*, 838*s*, 558*s*, 451*w, 415m* cm^{-1}.
^{99}Tc analysis calc. for $C_{18}H_{24}F_6PTc$ (%): 20.42; found: 19.54.

Re-complexes

8.5 [Re(η^6-C_6H_6)(η^6-napht)](OTF) ([**6**](OTf))

$KReO_4$ (500 mg, 1.73 mmol), zinc dust (339 mg, 5.18 mmol) and anhydrous $AlCl_3$ (2.3 g, 17.3 mmol) were suspended in a mixture of naphthalene (3.33 g, 25.95 mmol) and benzene (3.45 mL, 38.93 mmol). The reaction mixture was stirred for 18 h at 90°C. Afterwards, the mixture was cooled to room temperature, washed under vigorously stirring with hot heptane (3 x 50 mL) and Et_2O (2 x 50 mL). The mixture was filtrated and the solid residue was suspended in 50 ml of H_2O and filtered again. All aqueous solutions were reduced in volume to less than 8 ml. The crude product was purified by preparative HPLC (Reprosil 100 C18, 250 mm x 40 mm, 0.1% TFA/CH_3CN, gradient G1).

The solvent was evaporated and the solid dissolved in water. After the addition of lithium triflate (404 mg, 2.6 mmol), [**6**](OTf) precipitated as analytically pure, orange crystalline powder, which was filtered and dried. Single crystals, suitable for X-ray diffraction analysis were obtained by vapour diffusion of Et_2O into a solution of [**6**](OTf) in acetone. Yield: 206.1 mg (0.381 mmol, 22%).

^{1}H NMR (400 MHz, acetone-d_6) δ [ppm]: 7.72 (m, 2H, C*H*$_{arom}$), 7.51 (m, 2H, C*H*$_{arom}$), 7.32 (m, 2H, C*H*$_{arom}$), 6.38 (m, 2H, C*H*$_{arom}$) 5.83 (s, 6H, C*H*$_{arom}$).
^{13}C NMR (100 MHz, acetone-d_6) δ [ppm]: 131.90 (2C, *C*H$_{arom}$), 131.43 (2C, *C*H$_{arom}$), 93.28 (2C, *C*-CH$_{arom}$), 80.03 (2C, *C*H$_{arom}$), 77.15 (6C, *C*H$_{arom}$), 75.1 (2C, *C*H$_{arom}$).
ESI-MS: m/z = 393.1 $[M]^+$.
IR ν: 3052*w*, 1454*w*,1413*w*, 1242*s*, 1221*m*, 1143*s*, 1027*s*, 1008*m*, 906*w*, 858*m*, 830*m*, 753*w* cm^{-1}.

8.6 [Re(η^6-napht)$_2$](OTf) ([**7**](OTf))

$KReO_4$ (725 mg, 2.5 mmol), zinc dust (490 mg, 7.5 mmol) and anhydrous $AlCl_3$ (3.34 g, 10 mmol) were suspended in naphthalene (5.0 g, 39 mmol). The reaction mixture was stirred for 18 h at 100°C. The mixture was filtrated and the solid residue was suspended in 50 ml of H_2O and filtered again. Lithium triflate (489 mg, 3 mmol) was added to the filtrate. The product was extracted with dichloromethane (6 x 50 mL). The organic phase was evaporated which afforded [**7**](OTf) as analytically pure, deep red crystalline powder. Single crystals, suitable for X-ray diffraction analysis were obtained by vapour diffusion of Et_2O into a solution of [**7**](OTf) in acetone. Yield: 474.7 mg (0.381 mmol, 32%).

^{1}H NMR (400 MHz, acetone-d_6) δ [ppm]: 7.38 (m, 4H, C*H*$_{arom}$), 6.86 (m, 4H, C*H*$_{arom}$), 6.78 (m, 4H, C*H*$_{arom}$), 6.33 (m, 4H, C*H*$_{arom}$).
^{13}C NMR (100 MHz, acetone-d_6) δ [ppm]: 129.7 (*C*H$_{arom}$), 129.5 (*C*H$_{arom}$), 90.3 (*C*-CH$_{arom}$), 78.0 (*C*H$_{arom}$), 73.3 (*C*H$_{arom}$).
ESI-MS: m/z = 443.0 $[M]^+$.
IR ν: 3059*w*, 1469*w*, 1407*w*, 1371*w*, 1257*s*, 1224*m*, 1139*s*, 1028*s*, 1006*m*, 996*w*, 858*m*, 852*s*, 743*w* cm^{-1}.
Anal. calcd. for $C_{21}H_{16}F_3O_3ReS$: C 42.63, H 2.73; found: C 42.43, H 2.65.

[Re(η^6-C_6H_6)(tep)$_3$](OTf) ([**8**](OTf))

[**6**](OTf) (30 mg, 0.055 mmol) was dissolved in 2 mL acetone. After the addition of triethyl phosphite (188 µL, 1.1 mmol) to the yellow solution, the reaction mixture was stirred for 6 h at 80°C in a microwave reactor. The solvent was evaporated *in vacuo* and the residue washed with Et_2O (4 x 2.5 mL) and water (2 x 2 mL). The product was recrystallized from acetonitrile, yielding colourless single crystals of [**8**](OTf), suitable for X-ray diffraction analysis. Yield: 38 mg (0.041 mmol, 75%) of [**8**](OTf).

^{1}H NMR (500 MHz, MeCN-d_3) δ [ppm]: 5.22 (s, 6H, CH_{arom}), 3.92 (m, 18H, CH_2), 1.23 (t, 27H, CH_3).
^{13}C NMR (125 MHz, MeCN-d_3) δ [ppm]: 84.6 (C_{arom}), 62.3 (CH_2), 16.3 (CH_3).
^{31}P NMR (202 MHz, MeCN-d_3) δ [ppm]: 111.03 (P(OEt)$_3$).
ESI-MS: m/z = 763.2 $[M]^+$.
IR ν: 2983*w*, 2932*w*, 2852*w*, 1436*w*, 1386*w*, 1267*s*, 1224*w*, 1144*m*, 1024*s*, 929*s*, 819*w*, 775*m*, 714*m* cm^{-1}.

8.7 [Re(η^6-C_6H_6)(CN-^{t}Bu)$_3$](OTf) ([**9**](OTf))

[**6**](OTf) (30 mg, 0.055 mmol) was dissolved in 2 mL acetone. After the addition of *tert*-butyl isocyanide (62 µL, 0.55 mmol) to the yellow solution, the reaction mixture was stirred for 9 h at 80°C in a microwave reactor. The solvent was evaporated *in vacuo* and the residue washed with hexane (4 x 2.5 mL) and water (2 x 2 mL). The product was recrystallized from acetonitrile, yielding colourless single crystals of [**9**](OTf), suitable for X-ray diffraction analysis. Yield: 24 mg (0.036 mmol, 65%) of [**9**](OTf).

^{1}H NMR (500 MHz, MeCN-d_3) δ [ppm]: 5.24 (s, 6H, CH_{arom}) 1.48 (s, 27H, CH_3).
^{13}C NMR (125 MHz, MeCN-d_3) δ [ppm]: 139.74 (N*C*), 85.35 (C_{arom}), 58.58 (C(CH$_3$)$_3$), 31.30 (CH_3).
ESI-MS: m/z = 514.2 $[M]^+$.
IR ν: 2978*w*, 2147*s* (NC), 2107*s* (NC), 2059*s* (NC), 1370*w*, 1263*s*, 1199*m*, 1147*s*, 1029*s*, 901*s*, 809*w* cm^{-1}.

8.8 [Re(η^6-C_6H_6)(HB(pyz)$_3$)] (**10**)

[**6**](OTf) (30 mg, 0.055 mmol) was dissolved in 2 mL acetone. After the addition of Potassium tri(1*H*-pyrazol-1-yl)hydroborate (69 mg, 0.275 mmol) to the yellow solution, the reaction mixture was stirred for 6 h at 80°C in a microwave reactor. The solvent was evaporated *in vacuo* and the residue washed with water (4 x 2.5 mL) and extracted with Et_2O (2 x 2 mL). Yellow single crystals of **10**, suitable for X-ray diffraction analysis were obtained by slow evaporation of a Et_2O solution of the ligand/**10** mixture.

8.9 [Re(η^6-napht)(tep)$_3$](PF_6) ([**11**](PF_6))

[**7**](OTf) (40 mg, 0.068 mmol) was dissolved in 4 mL acetone. After the addition of triethyl phosphite (118 µL, 0.68 mmol) to the red solution, the reaction mixture was stirred for 9 h at 100°C in a microwave reactor. The solvent was evaporated *in vacuo* and the residue washed with hexane (2 x 2 mL) and Et_2O (2 x 2.5 mL). The residue was purified by *preparative HPLC* (Reprosil 100 C18, 250x40 mm, 0.1% TFA/CH_3CN, Gradient: G2). Analytically pure yellow [**11**](PF_6) precipitated from the solution upon addition of NH_4PF_6. Single crystals, suitable for X-ray diffraction analysis were obtained by slow evaporation of an acetonitrile solution of [**11**](OTf). Yield: 39 mg (0.041 mmol, 60%) for [**11**](PF_6).

^{1}H NMR (500 MHz, MeCN-d_3) δ [ppm]: 7.53 (m, 2H, C*H*$_{arom}$), 7.45 (m, 2H, C*H*$_{arom}$), 6.08 (s, 2H, C*H*$_{arom}$), 5.33 (t, 2H, C*H*$_{arom}$), 3.78 (t, 18H, C*H*$_2$), 1.15 (t, 27H, C*H*$_3$).
^{13}C NMR (125 MHz, MeCN-d_3) δ [ppm]: 130.83 (*C*H$_{arom}$), 130.21 (*C*H$_{arom}$), 102.7 (*C*$_{arom}$), 84.95 (*C*H$_{arom}$), 80.98 (*C*H$_{arom}$), 62.35 (*C*H$_2$), 16.39 (*C*H$_3$).
^{31}P NMR (202 MHz, MeCN-d_3) δ [ppm]: 108.96 (s, *P*(OEt$_3$)$_3$), -144.62 (sept, *P*F$_6$).
ESI-MS: m/z = 813.2 $[M]^+$.
IR ν: 2982*w*, 2914*w*, 1442*w*, 1386*w*, 1158*w*, 1089*w*, 1020*s*, 939*s*, 833*s*, 772*m*, 710*w* cm^{-1}.

8.10 [Re(η^6-napht)(triphos)](PF_6) ([**12**](PF_6))

[**7**](OTF) (50 mg, 0.084 mmol) was dissolved in 4 mL acetone. After the addition of 1,1,1-tris(diphenylphosphinomethyl)ethane (262 mg, 0.42 mmol) to the red solution, the reaction mixture was stirred for 9 h at 100°C in a microwave reactor. The solvent was evaporated *in vacuo* and the residue washed with hexane (2 x 2 ml) and Et_2O (2 x 2.5 mL). The residue was purified by *preparative HPLC* (Reprosil 100 C18, 250x40 mm, 0.1% TFA/CH_3CN, Gradient: G2). Analytically pure orange-red

[**12**](PF_6) precipitated from the solution upon addition of NH_4PF_6. Single crystals, suitable for X-ray diffraction analysis were obtained by slow evaporation of a dichloromethane solution of [**12**](PF_6). Yield: 52 mg (0.047 mmol, 56%) for [**12**](PF_6).

^{1}H NMR (500 MHz, MeCN-d_3) δ [ppm]: 7.49 (m, 2H, CH_{arom}), 7.36 (m, 2H, CH_{arom}), 7.23 (t, 6H, CH_{arom}), 7.03 (t, 12H, CH_{arom}), 6.63 (s, 12H, CH_{arom}), 6.19 (t, 2H, CH_{arom}), 5.35 (m, 2H, CH_{arom}), 2.36 (d, 6H, CH_2), 1.36 (t, 3H, CH_3).
^{13}C NMR (125 MHz, MeCN-d_3) δ [ppm]: 141.8 (C_{arom}), 133.01 (CH$_{arom}$), 132.8 (CH$_{arom}$), 130.24 (CH$_{arom}$), 129.78 (CH$_{arom}$), 128.87 (CH$_{arom}$), 103.21 (C_{arom}), 83.11 (CH$_{arom}$), 76.22 (CH$_{arom}$), 40.75 (C-CH_3), 39.24 (CH$_3$), 37.86 (CH$_2$).
^{31}P NMR (202 MHz, MeCN-d_3) δ [ppm]: 3.13 (s, P(Ph)$_2$),-144.62 (sept, PF$_6$).
ESI-MS: m/z = 939.2 $[M]^+$.
IR ν: 3059*w*, 2918*w*, 2851*w*, 1611*w*, 1574*w*, 1482*w*, 1433*m*, 1250*w*, 1088*m*, 1001*w*, 828*s*, 733*w* cm^{-1}.

8.11 [Re(CN-^{t}Bu)$_6$](PF_6) ([**13**](PF_6))

[**7**](OTF) (40 mg, 0.068 mmol) was dissolved in 2 mL acetone. After the addition of *tert*-butyl isocyanide (77 µL, 0.68 mmol) to the red solution, the reaction mixture was stirred for 4 h at 100°C in a microwave reactor. The solvent was evaporated *in vacuo* and the residue washed with hexane (2 x 2 ml) and Et_2O (2 x 2.5 mL). The residue was purified by *preparative HPLC* (Reprosil 100 C18, 250x40 mm, 0.1% TFA/CH_3CN, Gradient: G3). Analytically pure colorless [**13**](PF_6) precipitated from the solution upon addition of NH_4PF_6. Single crystals, suitable for X-ray diffraction analysis were obtained by slow evaporation of an acetonitrile solution of [**13**](OTf) Yield: 46 mg (0.056 mmol, 82%) for [**13**](PF_6).

^{1}H NMR (500 MHz, MeCN-d_3) δ [ppm]: 1.44 (s, 54 H, CH_3).
^{13}C NMR (125 MHz, MeCN-d_3) δ [ppm]: 144.3 (NC), 57.65 (C(CH_3)), 31.53 (CH$_3$).
^{31}P NMR (202 MHz, MeCN-d_3) δ [ppm]: -144.62 (sept, PF$_6$).
ESI-MS: m/z = 685.39 $[M]^+$.
IR ν: 2976*w*, 2937*w*, 2039*s* (NC), 1460*w*, 1369*w*, 1232*m*, 1198*m*, 834*s*, 727*w* cm^{-1}.

9. NMR Spectra (^{1}H, ^{2}H, ^{13}C, HSQC, ^{1}H NOE, HMBC)

9.1 [^{99}Tc(η^6-hmbz)(η^6-C_6H_5-NH_3)]$(PF_6)_2$ ([**1**]$(PF_6)_2$) and [^{99}Tc(η^6-pmbz)(η^6-C_6H_5-NH_3)]$(PF_6)_2$ ([**2**]$(PF_6)_2$)

9.1.1 ^{99}Tc NMR

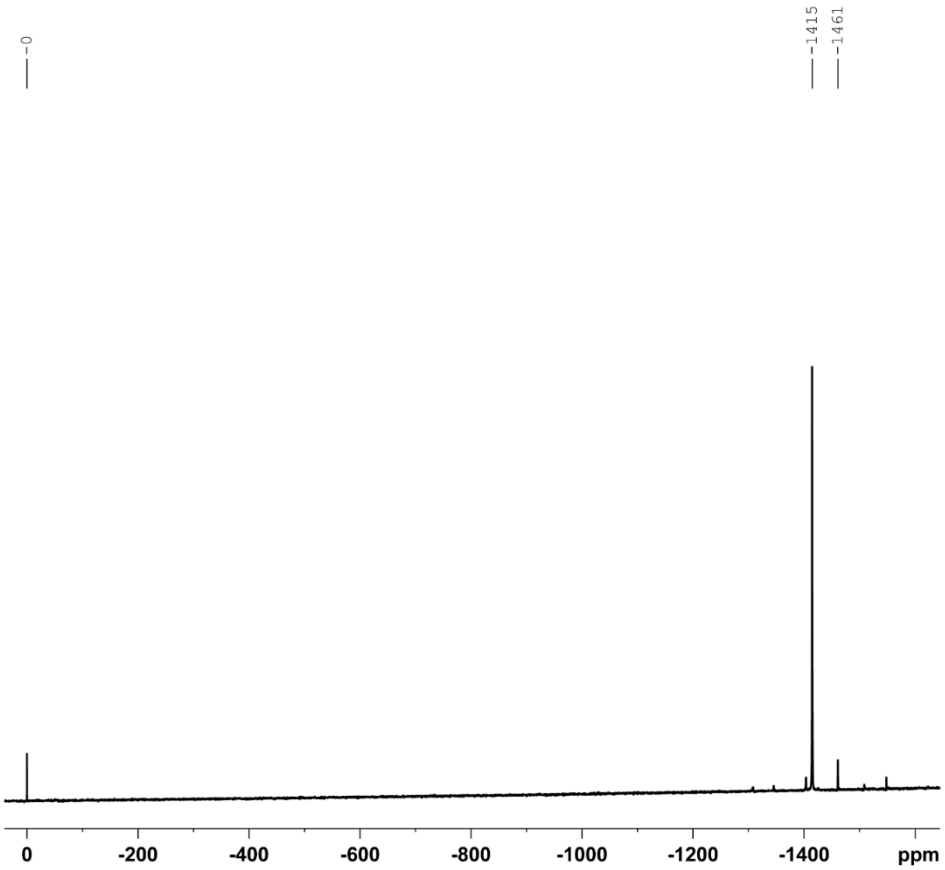

Figure 3.1.1: ^{99}Tc NMR of [^{99}Tc(η^6-hmbz)(η^6-C_6H_5-NH_3)]$(PF_6)_2$ ([**1**]$(PF_6)_2$) and [^{99}Tc(η^6-pmbz)(η^6-C_6H_5-NH_3)]$(PF_6)_2$ ([**2**]$(PF_6)_2$)

9.1.2 ^{1}H NMR

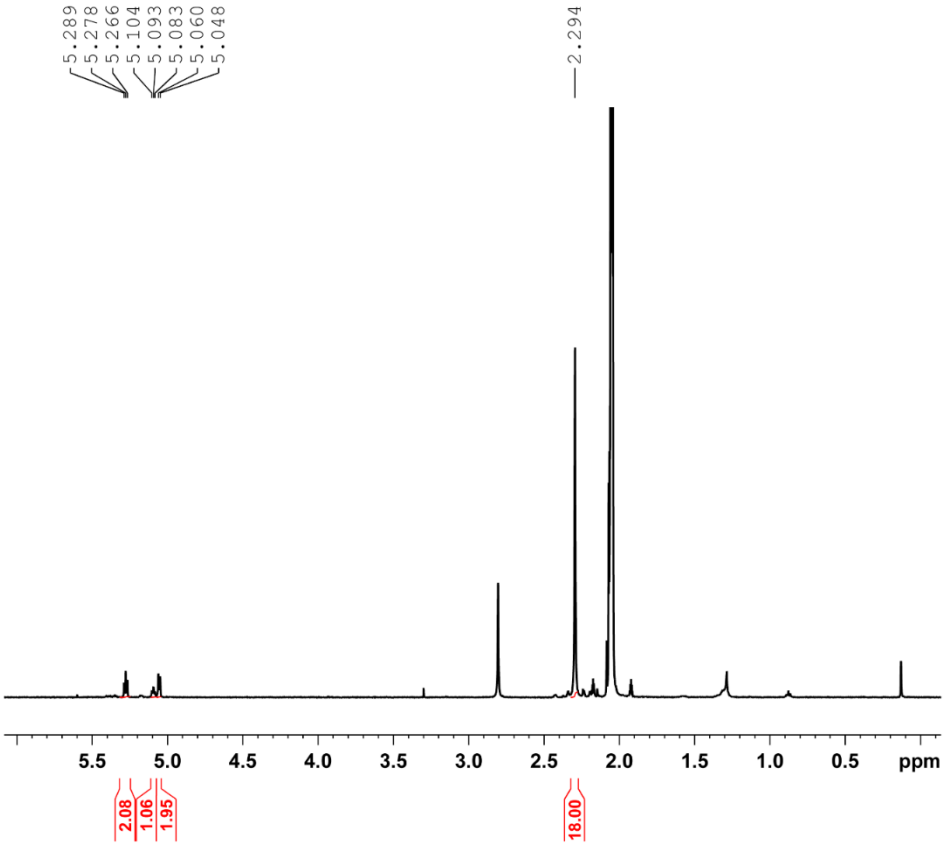

Figure 3.1.2: ^{1}H NMR of [^{99}Tc(η^6-hmbz)(η^6-C_6H_5-NH_3)]$(PF_6)_2$ ([**1**]$(PF_6)_2$) and [^{99}Tc(η^6-pmbz)(η^6-C_6H_5-NH_3)]$(PF_6)_2$ ([**2**]$(PF_6)_2$)

9.1.3 ^{13}C HSQC

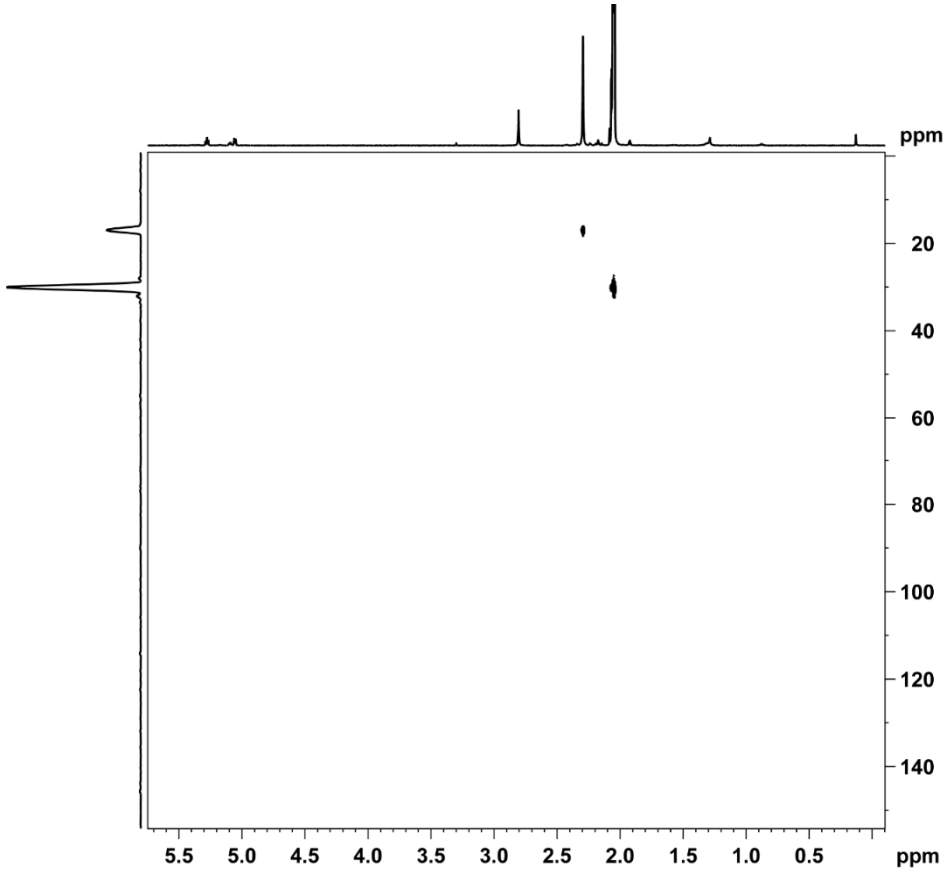

Figure 3.1.3: ^{13}C HSQC of [^{99}Tc(η^6-hmbz)(η^6-C_6H_5-NH_3)]$(PF_6)_2$ ([**1**]$(PF_6)_2$) and [^{99}Tc(η^6-pmbz)(η^6-C_6H_5-NH_3)]$(PF_6)_2$ ([**2**]$(PF_6)_2$)

9.2 [^{99}Tc(η^6-hmbz)$_2$](PF$_6$) ([**3a**](PF$_6$)) and [^{99}Tc(η^6-pmbz)(η^6-hmbz)](PF$_6$) ([**3b**](PF$_6$))

9.2.1 ^{99}Tc NMR

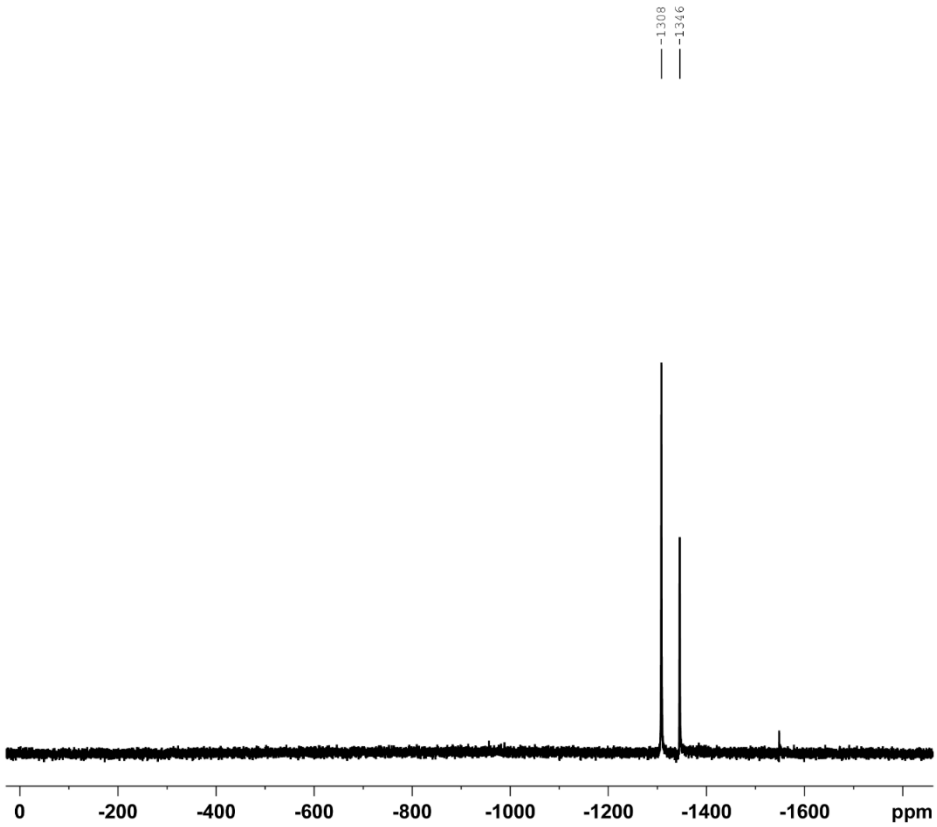

Figure 3.2.1: ^{99}Tc NMR of [^{99}Tc(η^6-hmbz)$_2$](PF$_6$) ([**3a**](PF$_6$)) and [^{99}Tc(η^6-pmbz)(η^6-hmbz)](PF$_6$) ([**3b**](PF$_6$))

9.2.2 ^{1}H NMR

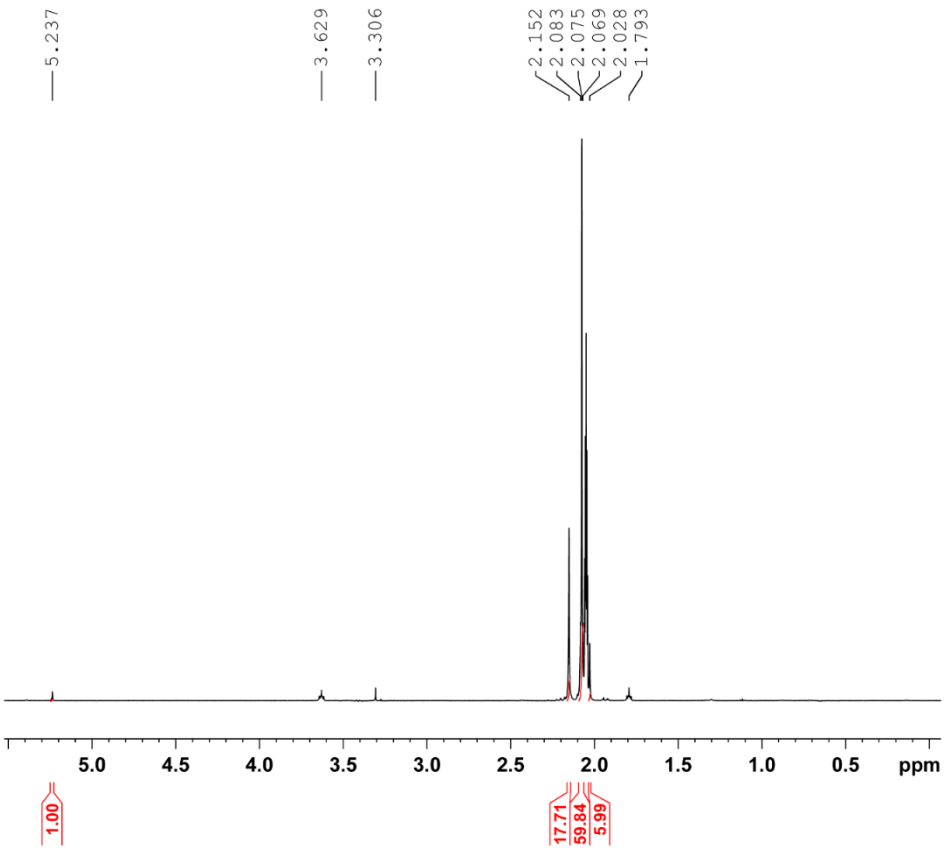

Figure 3.2.2: ^{1}H NMR of [^{99}Tc(η^6-hmbz)$_2$](PF$_6$) ([**3a**](PF$_6$)) and [^{99}Tc(η^6-pmbz)(η^6-hmbz)](PF$_6$) ([**3b**](PF$_6$))

9.2.3 ^{13}C HSQC

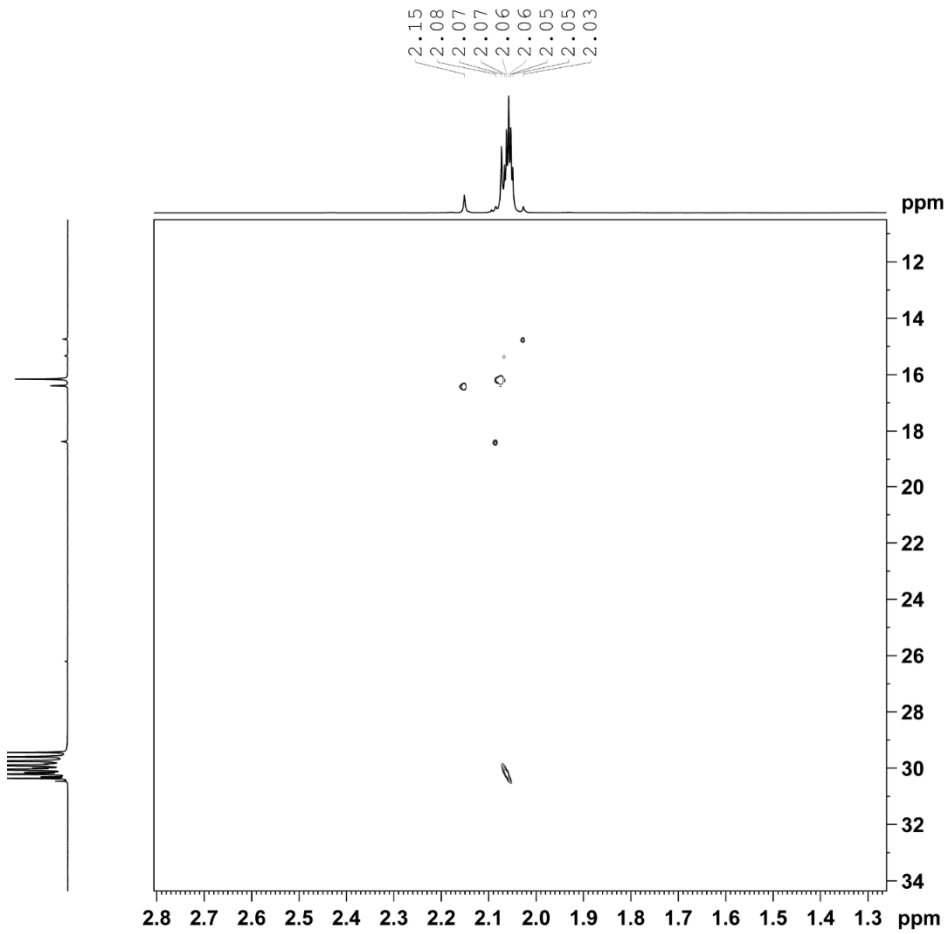

Figure 3.2.3: ^{13}C HSQC of [^{99}Tc(η^6-hmbz)$_2$](PF$_6$) ([**3a**](PF$_6$)) and [^{99}Tc(η^6-pmbz)(η^6-hmbz)](PF$_6$) ([**3b**](PF$_6$))

9.3 [^{99}Tc(η^6-hmbz)(η^6-C_6H_5-Br)](PF_6) ([**4**](PF_6))

9.3.1 ^{99}Tc NMR

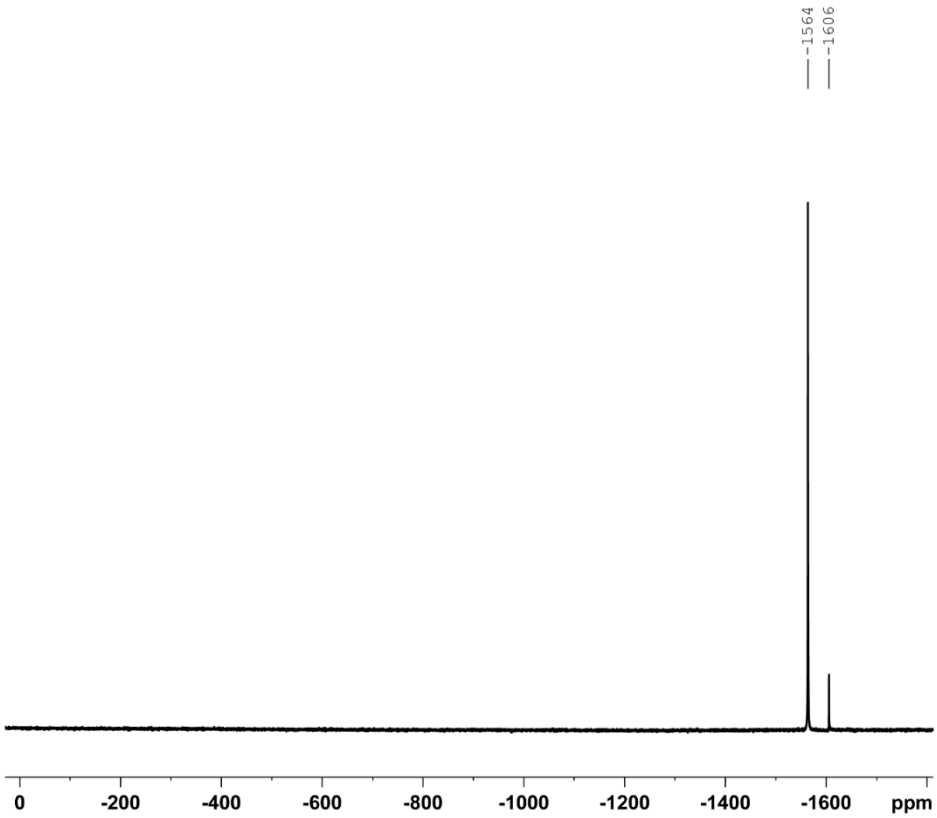

Figure 3.3.1: ^{99}Tc NMR of [^{99}Tc(η^6-hmbz)(η^6-C_6H_5-Br)](PF_6) ([**4**](PF_6))

9.3.2 ^{1}H NMR

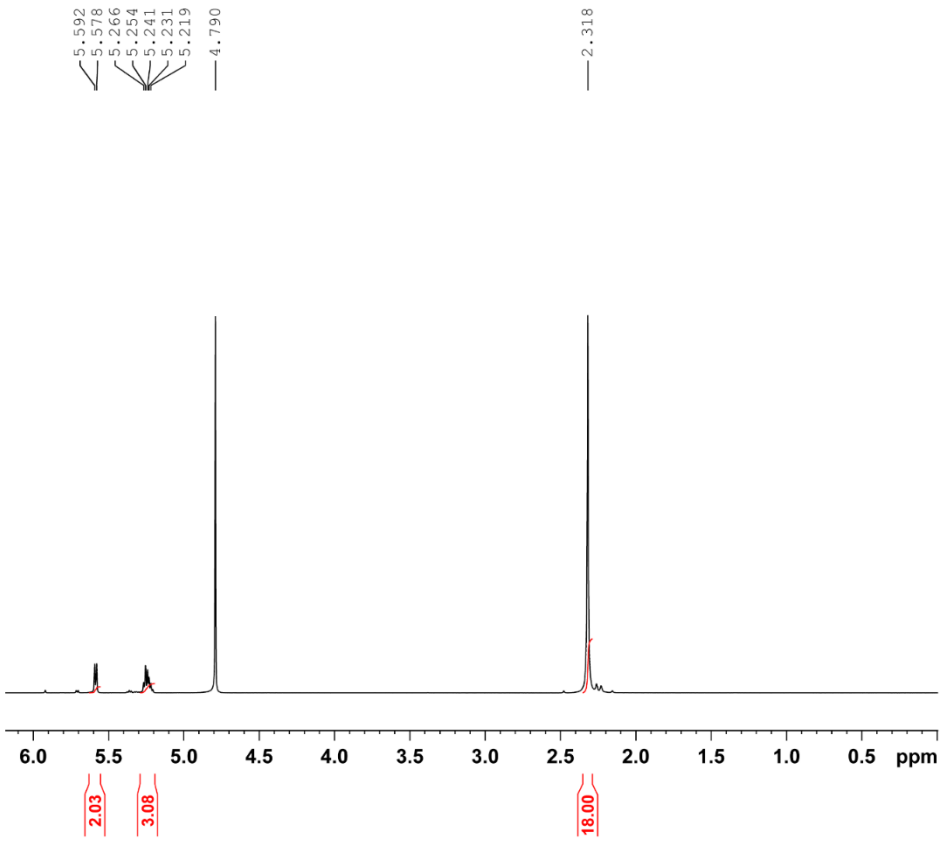

Figure 3.3.2: ^{1}H NMR of [^{99}Tc(η^6-hmbz)(η^6-C_6H_5-Br)](PF_6) ([**4**](PF_6))

9.3.3 ^{13}C HSQC

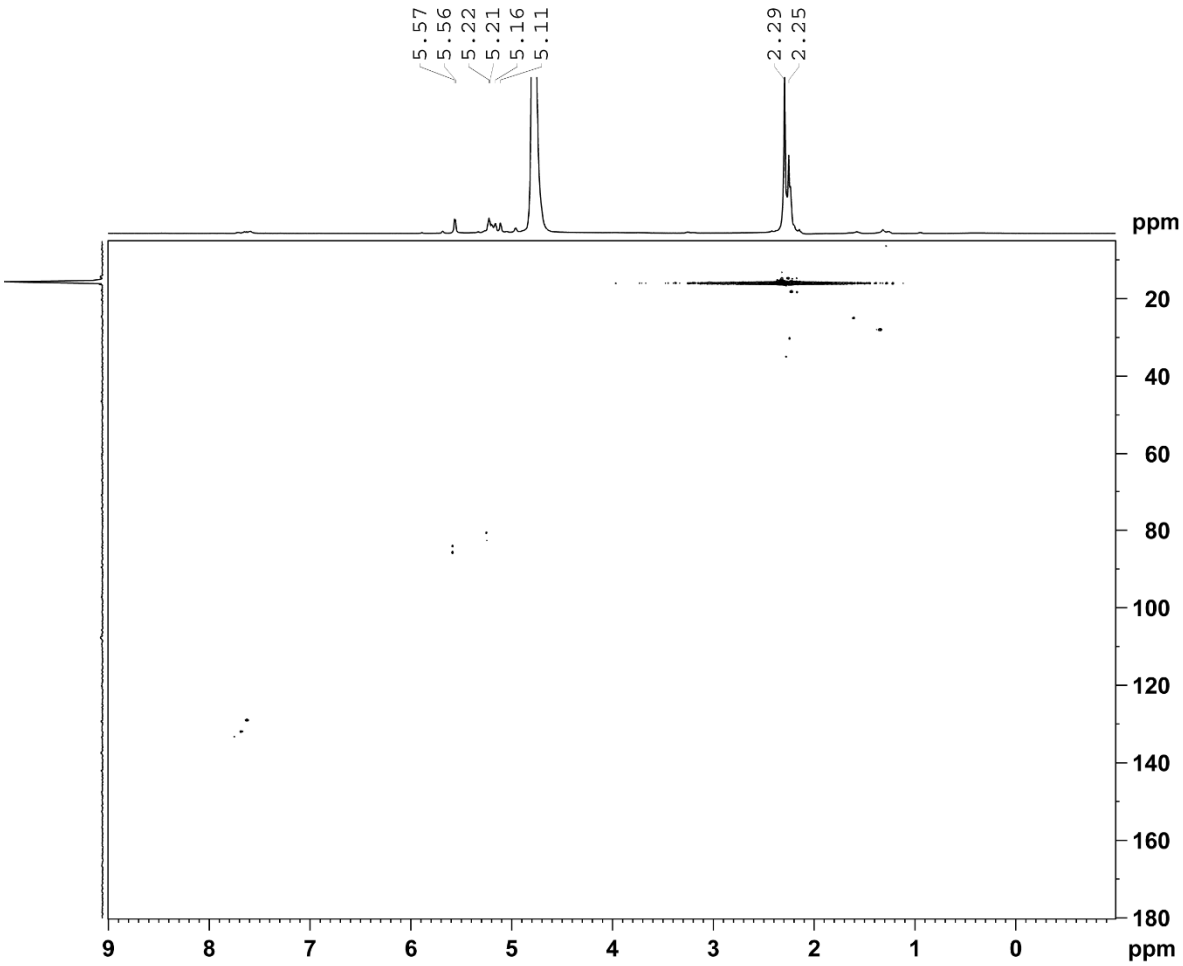

Figure 3.3.3: ^{13}C HSQC of [^{99}Tc(η^6-hmbz)(η^6-C_6H_5-Br)](PF_6) ([**4**](PF_6))

9.4 [^{99}Tc(η^6-pmbz)(η^6-C_6H_5-Br)](PF_6) ([**5**](PF_6))

9.4.1 ^{99}Tc NMR

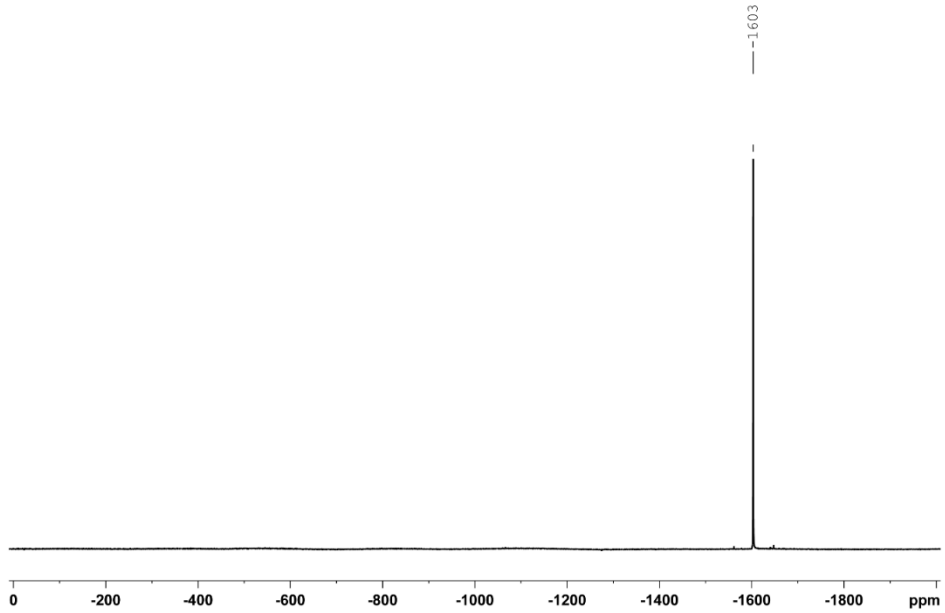

Figure 3.4.1: ^{99}Tc NMR of [^{99}Tc(η^6-pmbz)(η^6-C_6H_5-Br)](PF_6) ([**5**](PF_6))

9.4.2 ^{1}H NMR

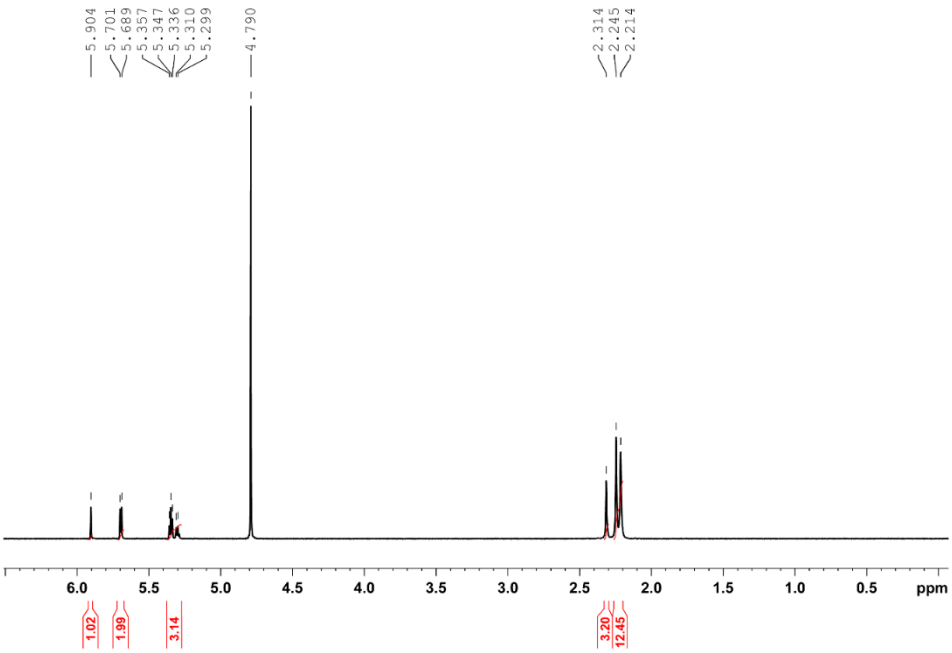

Figure 3.4.2: ^{1}H NMR of [^{99}Tc(η^6-pmbz)(η^6-C_6H_5-Br)](PF_6) ([**5**](PF_6))

9.4.3 ^{13}C HSQC

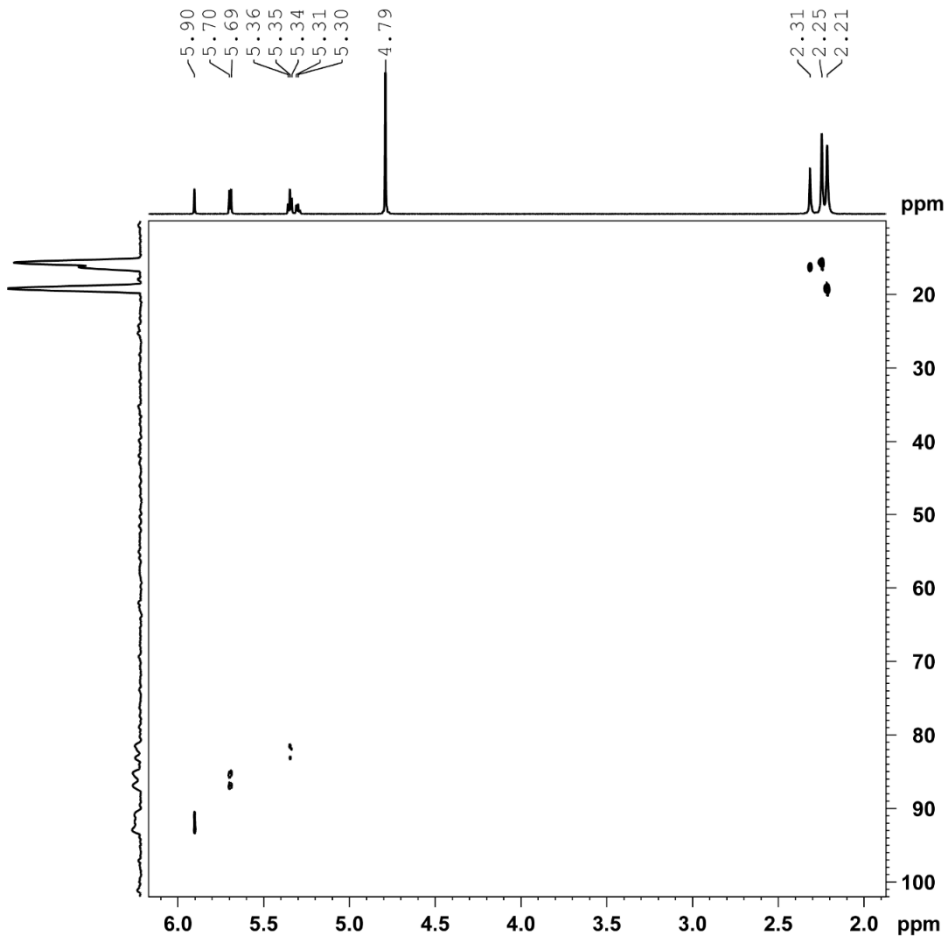

Figure 3.4.3: ^{13}C HSQC of [^{99}Tc(η^6-pmbz)(η^6-C_6H_5-Br)](PF_6) ([**5**](PF_6))

9.5 [^{99}Tc(η^6-hmbz)((η^6-C_6H_6)](PF$_6$) and [^{99}Tc(η^6-pmbz)((η^6-C_6H_6)](PF$_6$)

9.5.1 ^{99}Tc NMR

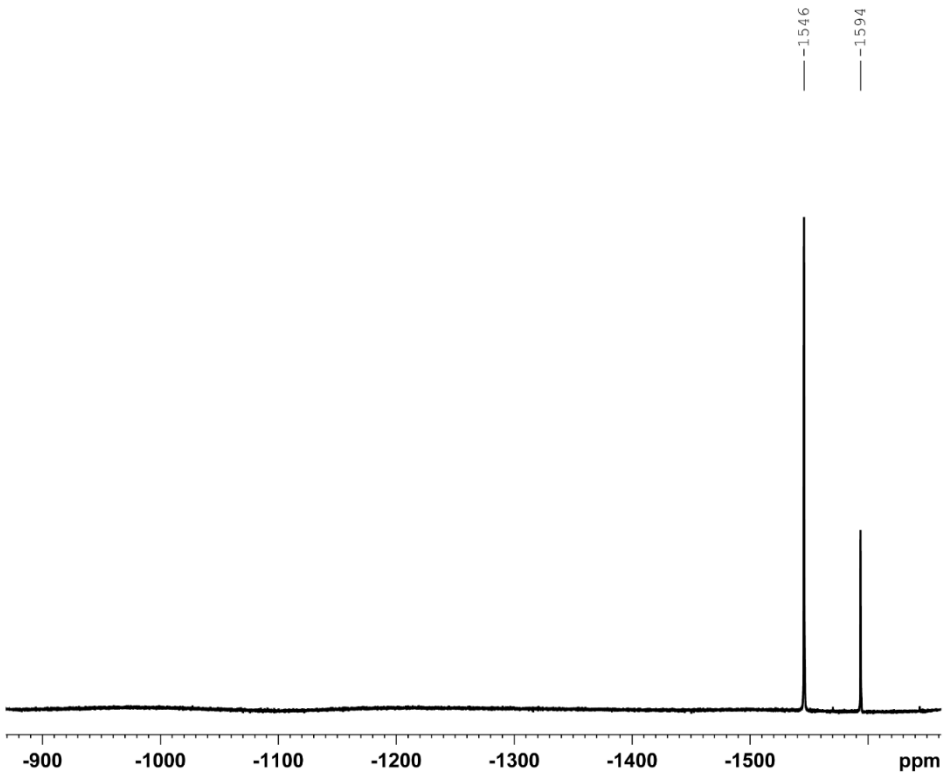

Figure 3.5.1: ^{99}Tc NMR of [^{99}Tc(η^6-hmbz)(η^6-C_6H_6)](PF$_6$) and [^{99}Tc(η^6-pmbz)(η^6-C_6H_6)](PF$_6$)

9.5.2 ^{1}H NMR

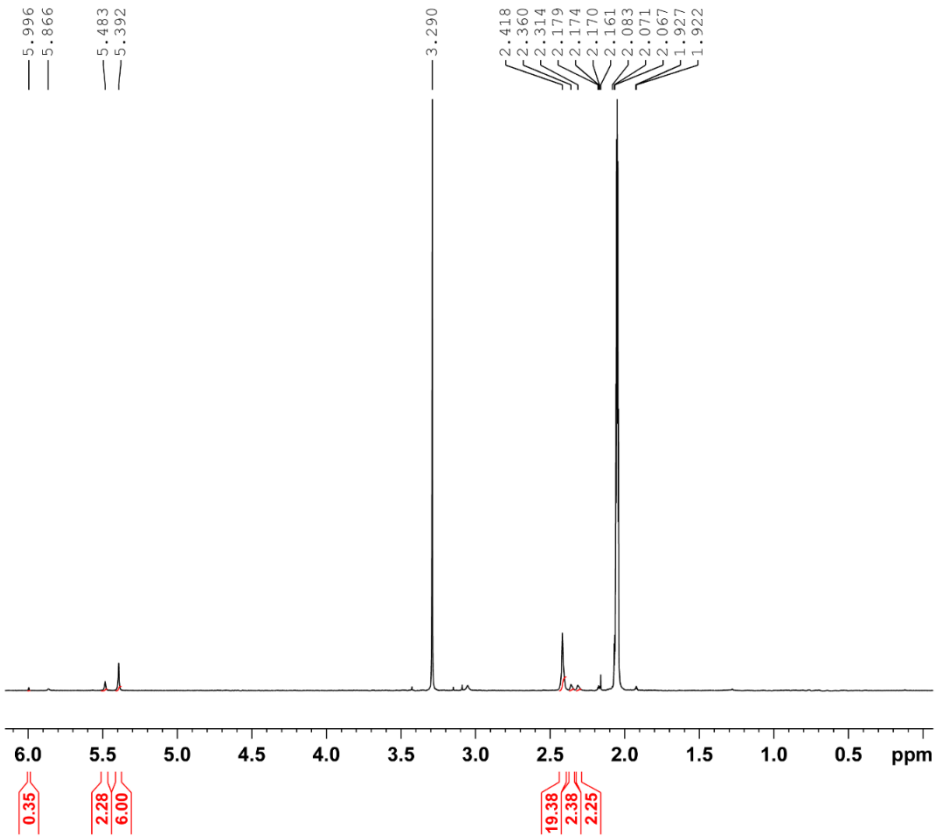

Figure 3.5.2: ^{1}H NMR of [^{99}Tc(η^6-hmbz)(η^6-C_6H_6)](PF_6) and [^{99}Tc(η^6-pmbz)(η^6-C_6H_6)](PF_6)

9.5.3 ^{13}C HSQC

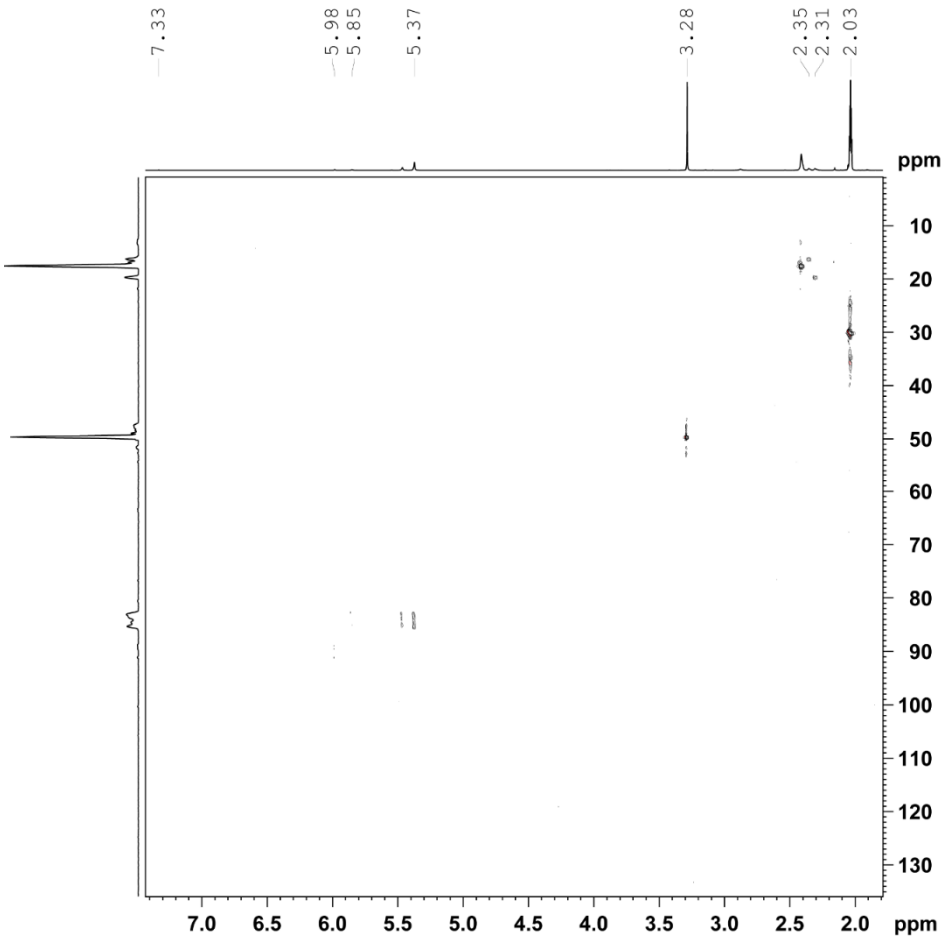

Figure 3.5.3: ^{1}H NMR of [^{99}Tc(η^6-hmbz)(η^6-C_6H_6)](PF_6) and [^{99}Tc(η^6-pmbz)(η^6-C_6H_6)](PF_6)

9.6 [Re(η^6-C_6H_6)(η^6-napht)](OTF) ([**6**](OTf))

9.6.1 ^{1}H NMR

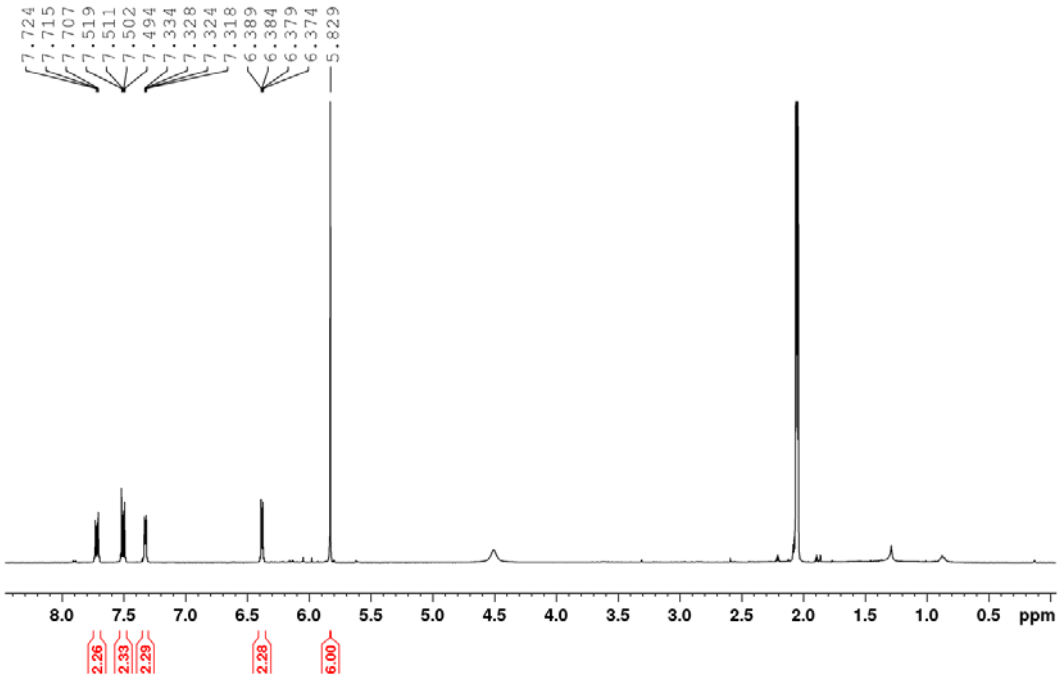

Figure 3.6.1: ^{1}H NMR of [Re(η^6-C_6H_6)(η^6-napht)](OTF) ([**6**](OTf))

9.6.2 ^{13}C NMR

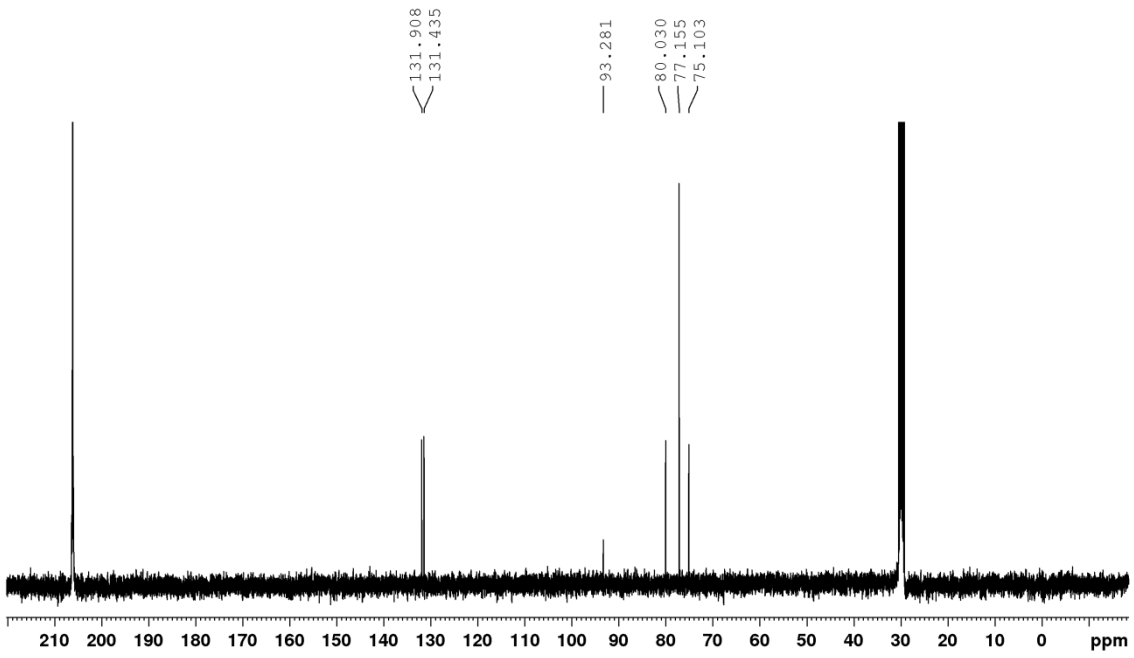

Figure 3.6.2: ^{13}C NMR of [Re(η^6-C_6H_6)(η^6-napht)](OTF) ([**6**](OTf))

9.7 [Re(η^6-napht)$_2$](OTf) ([**7**](OTf))

9.7.1 ^{1}H NMR

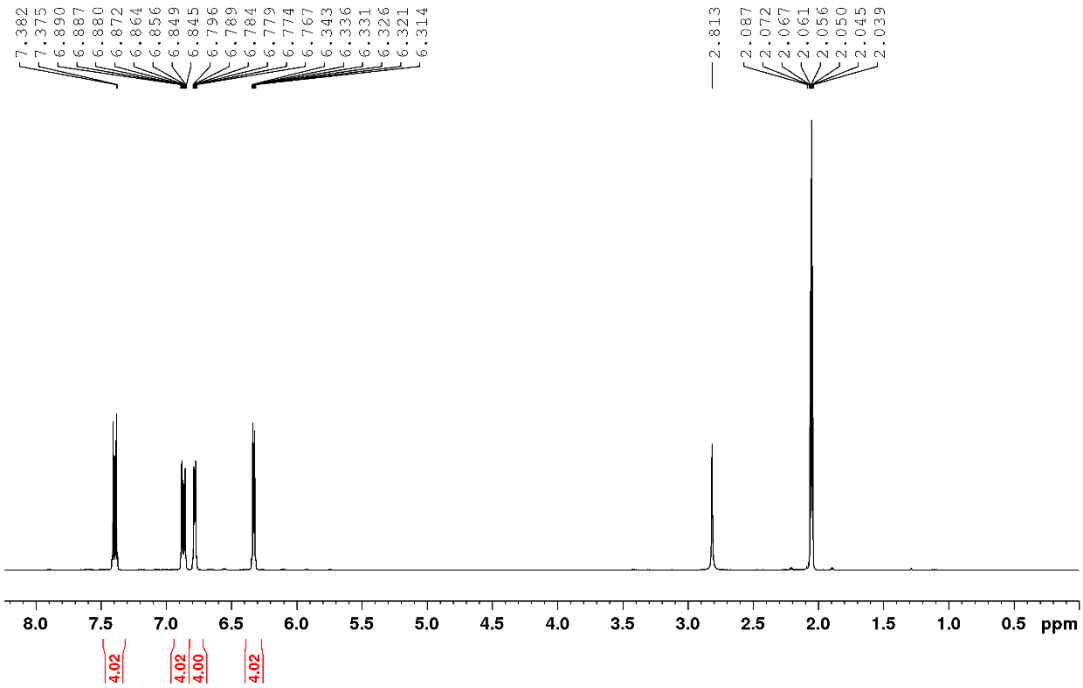

Figure 3.7.1: ^{1}H NMR of [Re(η^6-napht)$_2$](OTf) ([**7**](OTf))

9.7.2 ^{13}C NMR

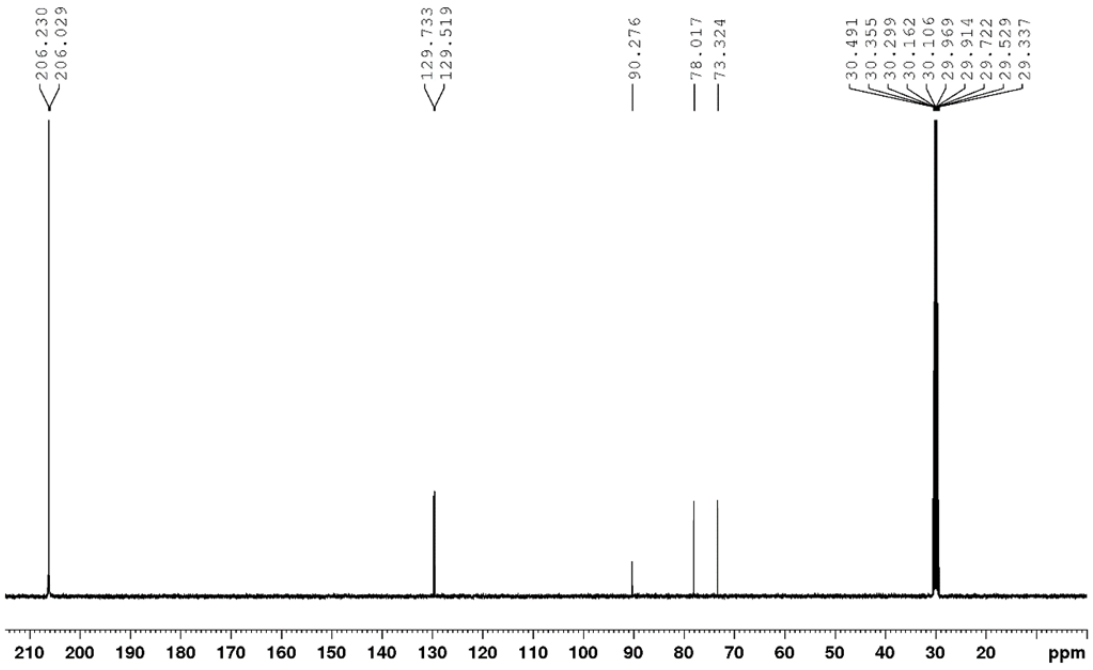

Figure 3.7.2: ^{13}C NMR of [Re(η^6-napht)$_2$](OTf) ([**7**](OTf))

9.8 [Re(η^6-C_6H_6)(tep)$_3$](OTf) ([**8**](OTf))

9.8.1 ^{1}H NMR

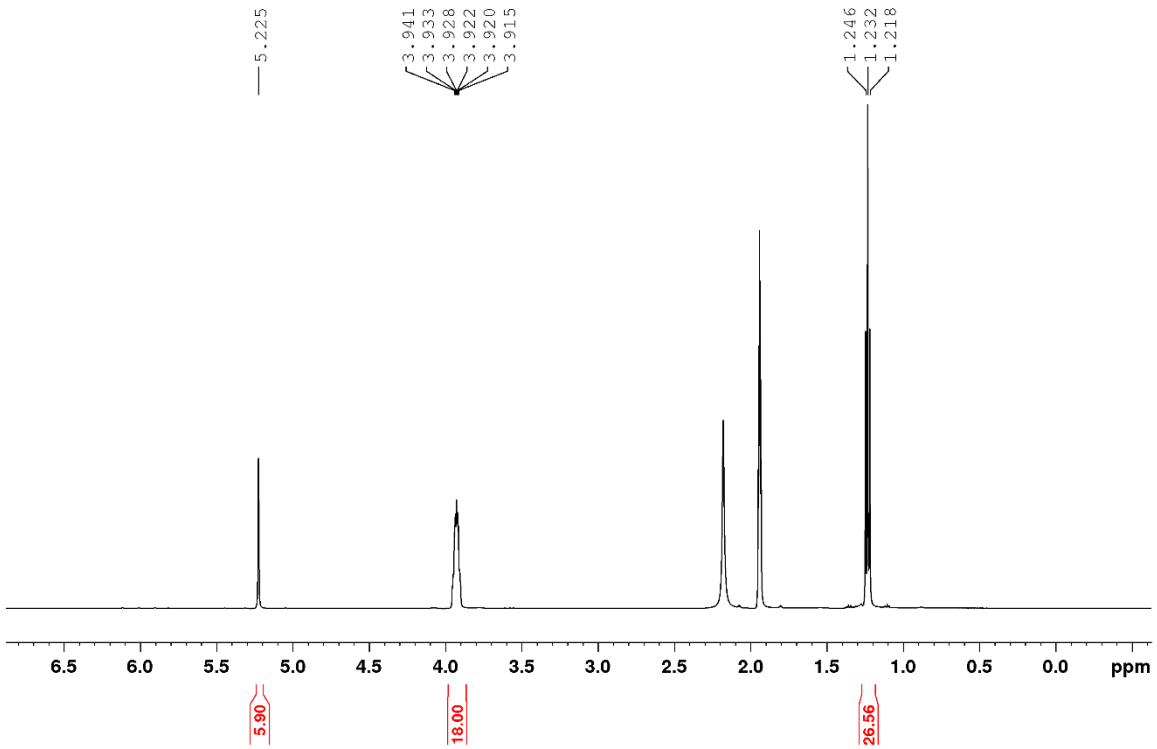

Figure 3.8.1: ^{1}H NMR of [Re(η^6-C_6H_6)(tep)$_3$](OTf) ([**8**](OTf))

9.8.2 ^{13}C NMR

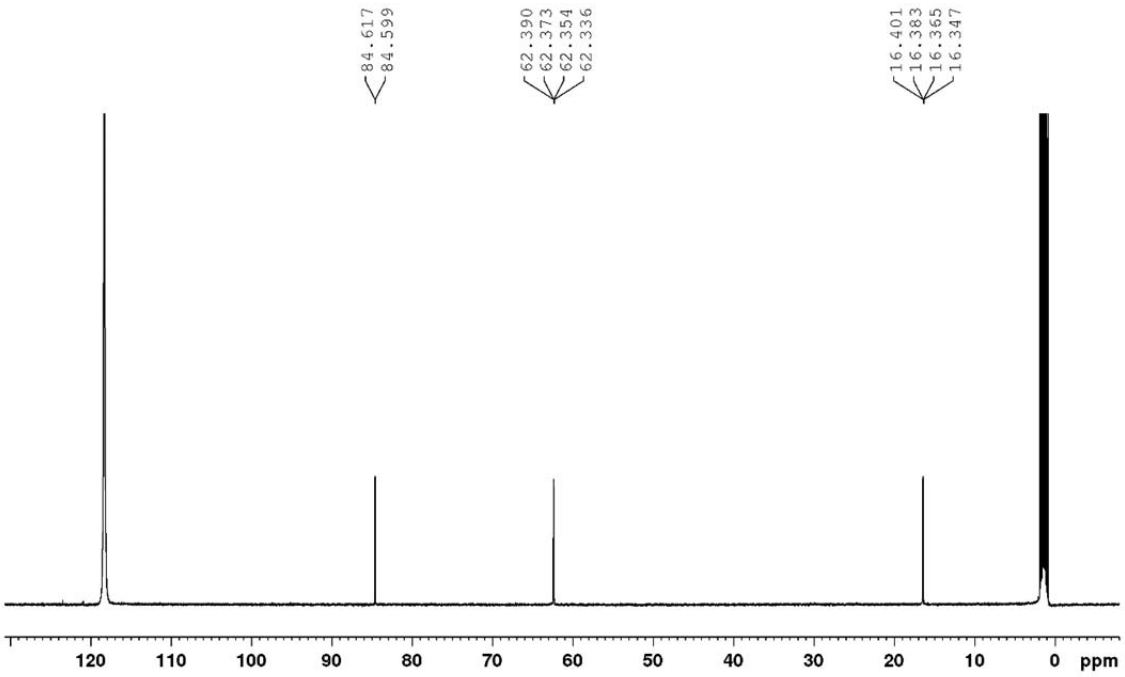

Figure 3.8.2: ^{13}C NMR of [Re(η^6-C_6H_6)(tep)$_3$](OTf) ([**8**](OTf))

9.9 [Re(η^6-C_6H_6)(CN-^{t}Bu)$_3$](OTf) ([**9**](OTf))

9.9.1 ^{1}H NMR

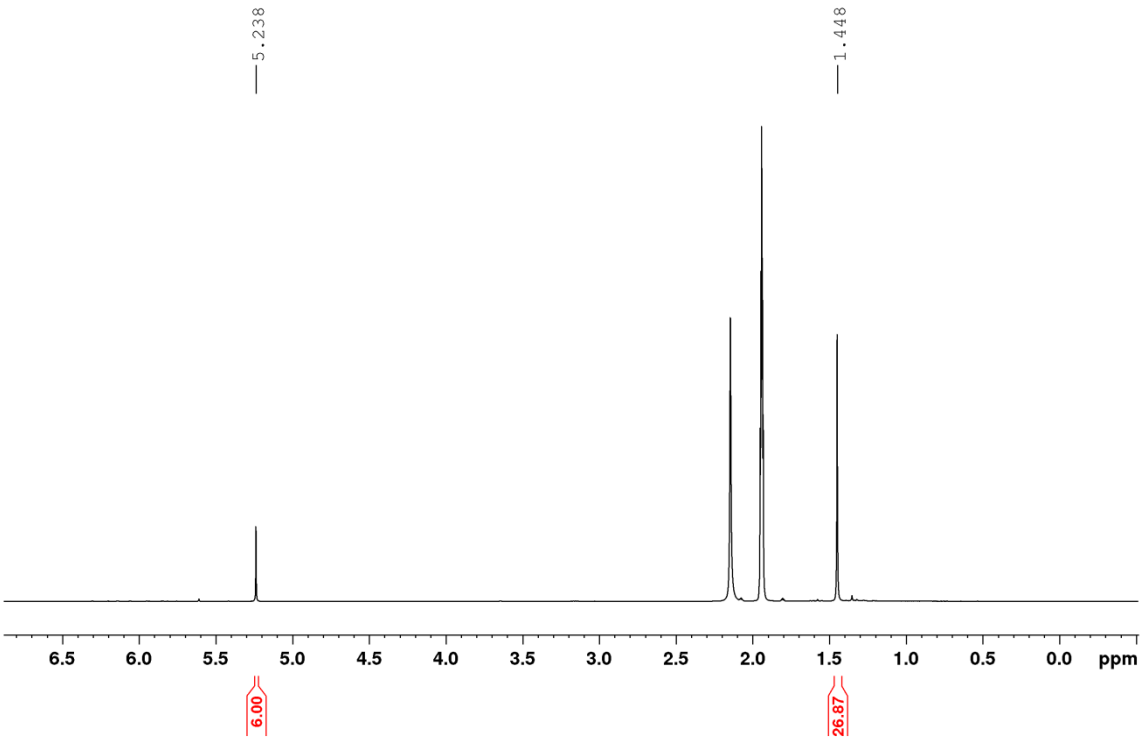

Figure 3.9.1: ^{1}H NMR of [Re(η^6-C_6H_6)(CN-^{t}Bu)$_3$](OTf) ([**9**](OTf))

9.9.2 ^{13}C NMR

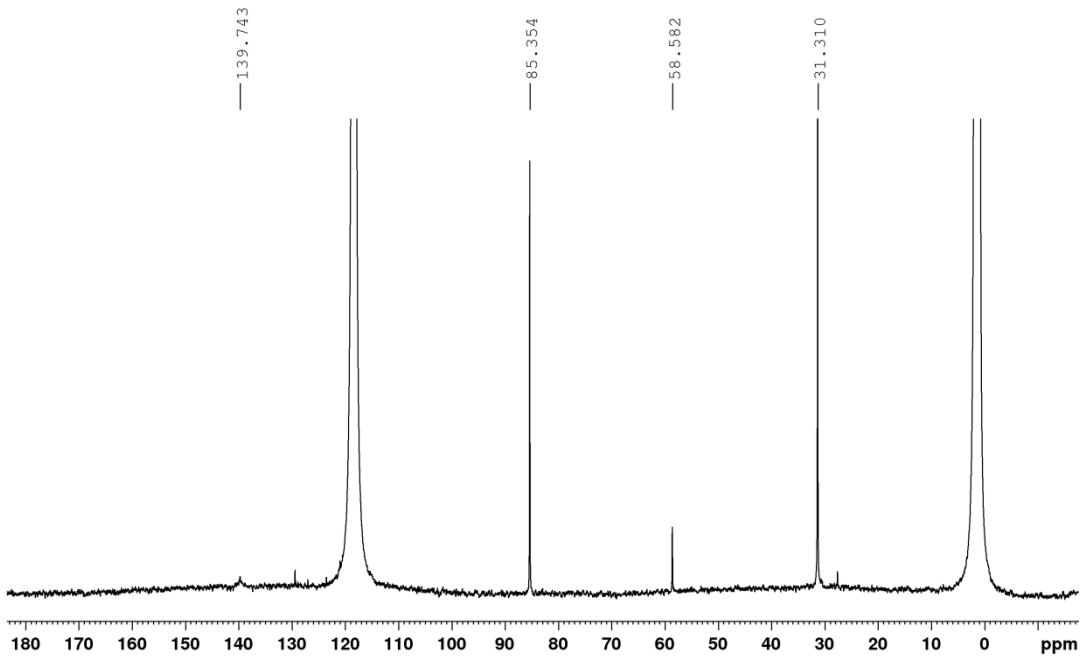

Figure 3.9.2: ^{13}C NMR of [Re(η^6-C_6H_6)(CN-^{t}Bu)$_3$](OTf) ([**9**](OTf))

9.10 [Re(η^6-napht)(tep)$_3$](PF$_6$) ([**11**](PF$_6$))

9.10.1 ^{1}H NMR

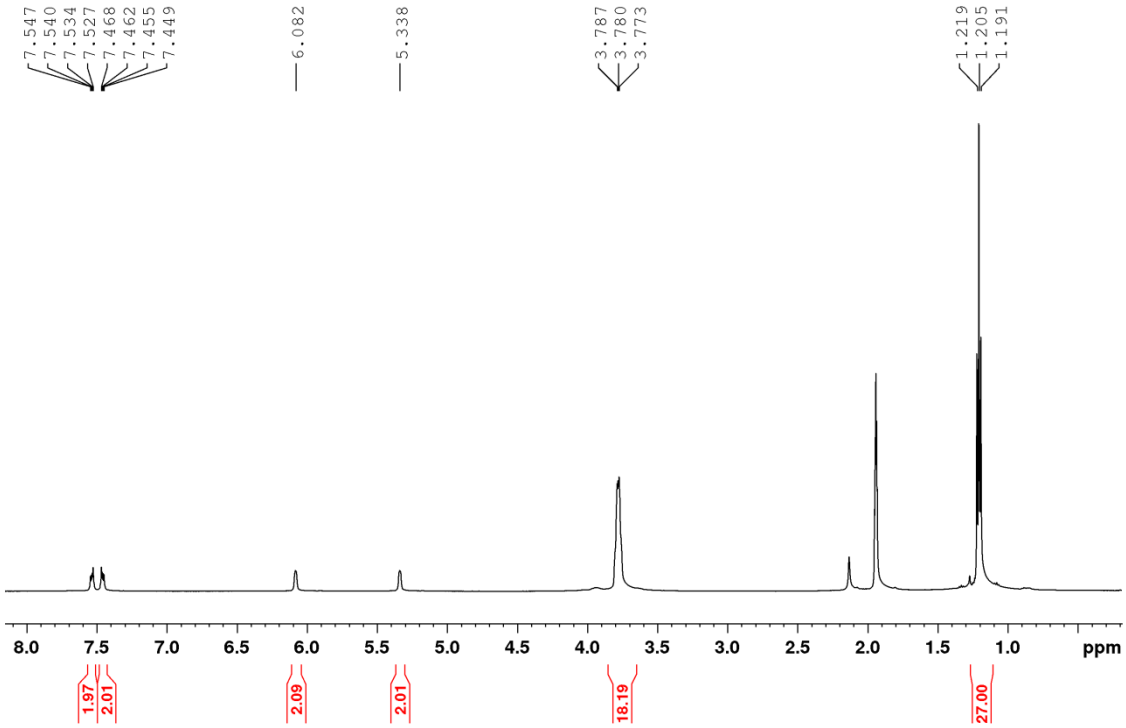

Figure 3.10.1: ^{1}H NMR of [Re(η^6-napht)(tep)$_3$](PF$_6$) ([**11**](PF$_6$))

9.10.2 ^{13}C NMR

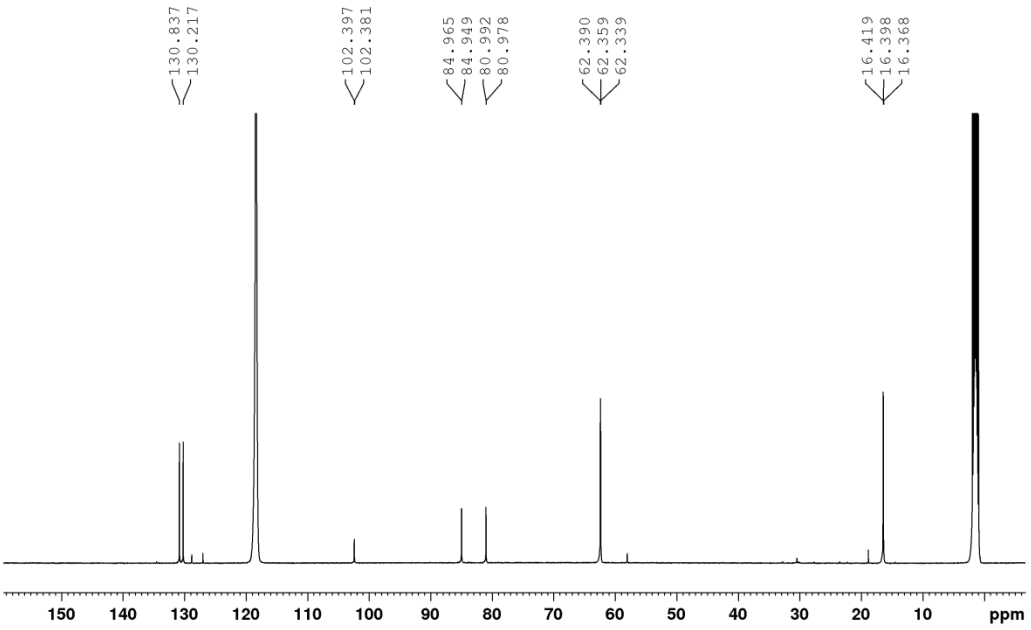

Figure 3.10.2: ^{13}C NMR of [Re(η^6-napht)(tep)$_3$](PF$_6$) ([**11**](PF$_6$))

9.11 [Re(η^6-napht)(triphos)](PF$_6$) ([**12**](PF$_6$))

9.11.1 ^{1}H NMR

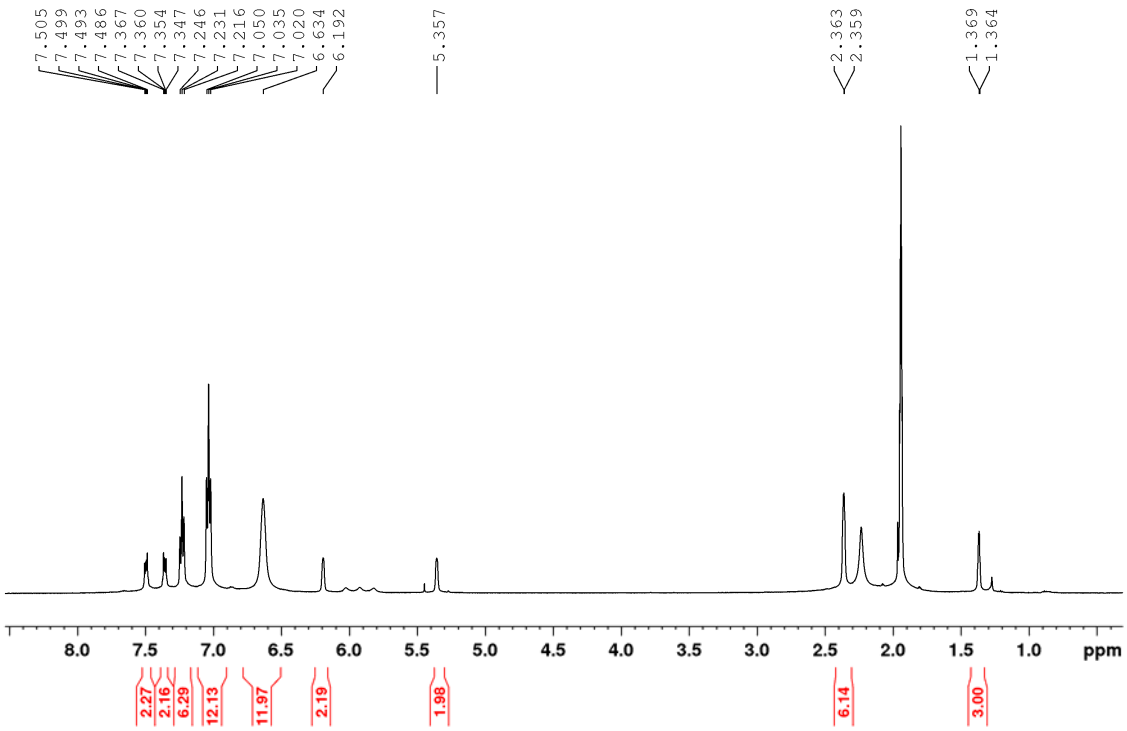

Figure 3.11.1: ^{1}H NMR of [Re(η^6-napht)(triphos)](PF$_6$) ([**12**](PF$_6$))

9.11.2 ^{13}C NMR

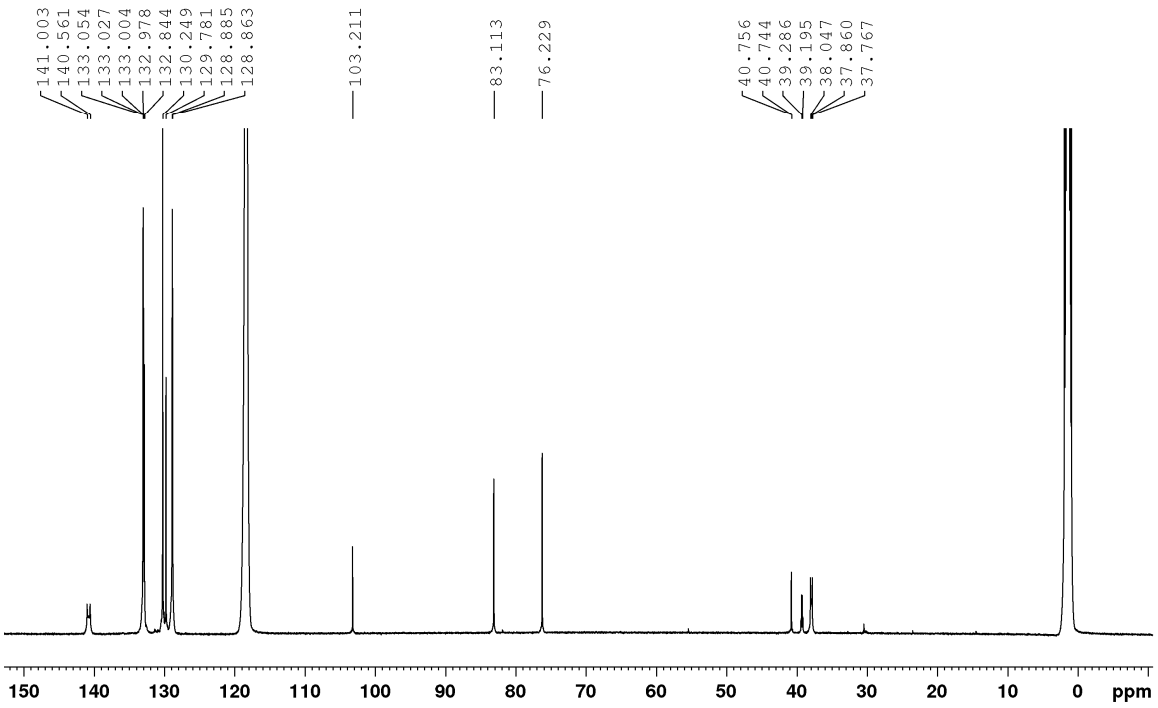

Figure 3.11.2: ^{13}C NMR of [Re(η^6-napht)(triphos)](PF$_6$) ([**12**](PF$_6$))

9.12 $[Re(CN\text{-}^{t}Bu)_6](PF_6)$ ([**13**](PF_6))

9.12.1 ^{1}H NMR

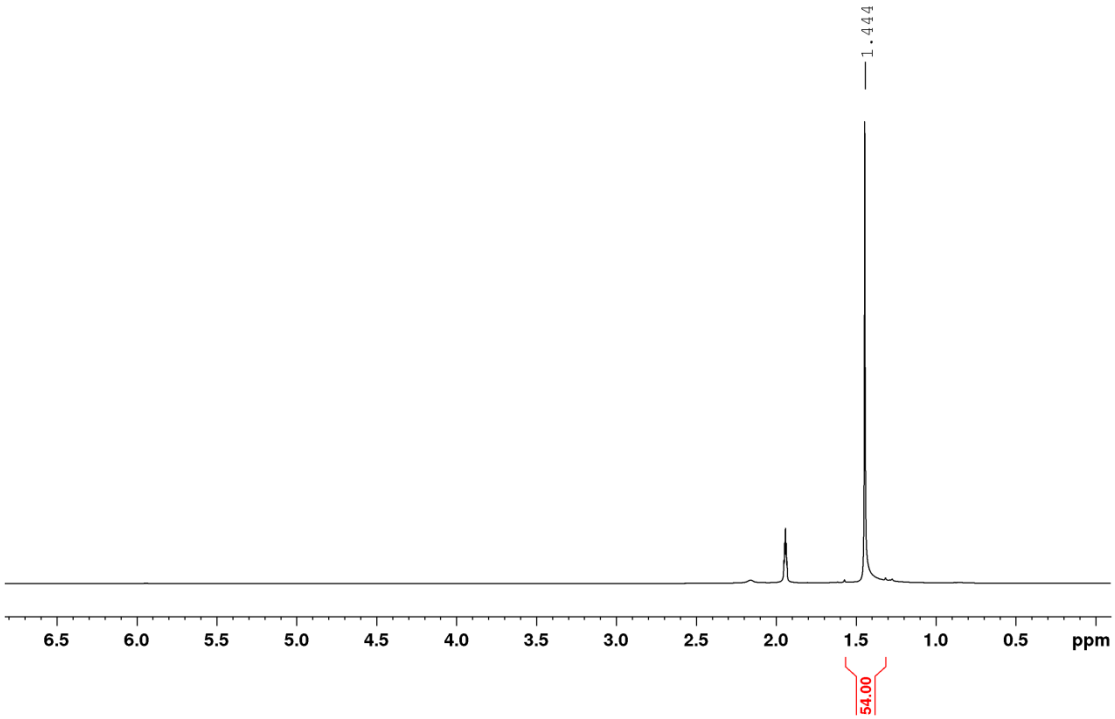

Figure 3.12.1: ^{1}H NMR of $[Re(\eta^{6}\text{-}C_6H_6)(tep)_3](OTf)$ ([**8**](OTf))

9.12.2 ^{13}C NMR

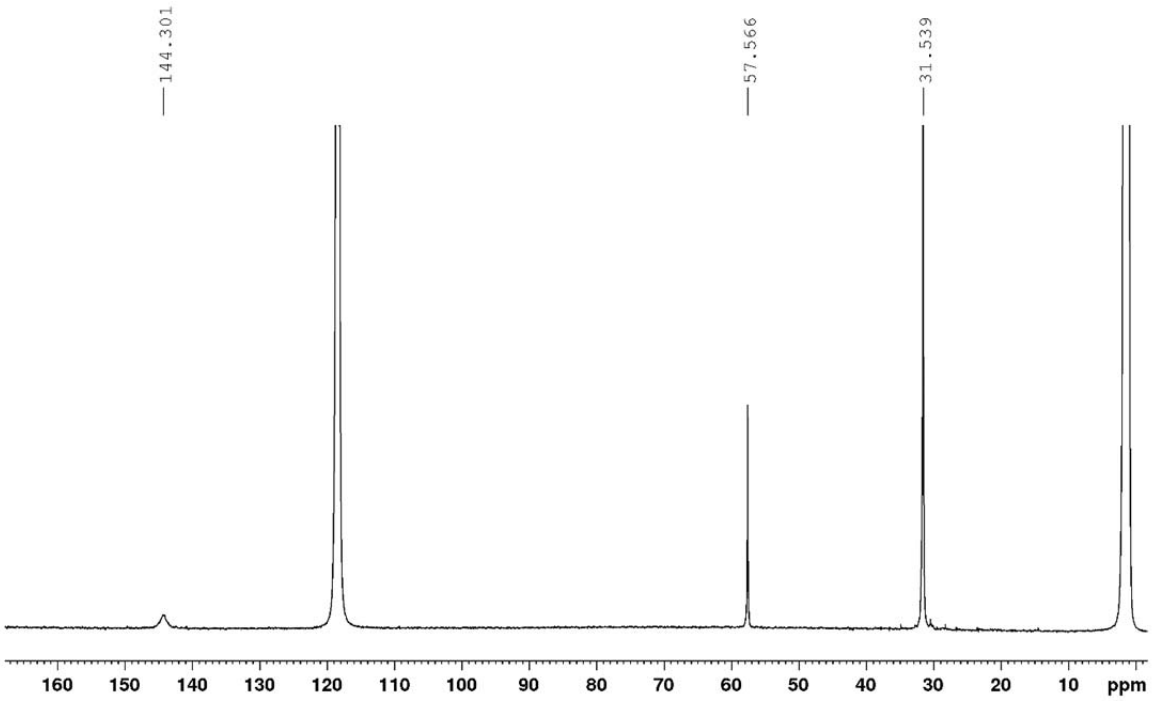

Figure 3.12.2: ^{13}C NMR of [Re(η^6-C_6H_6)(tep)$_3$](OTf) ([**8**](OTf))

4. Crystal Data

Crystallographic data were collected at 183(2) K. Compounds [**1**](PF_6), [**5**]Cl, [**8**](OTf), [**12**](PF_6) were measured on an Rigaku OD XtaLAB Synergy Dualflex diffractometer with a Pilatus 200 K detector with either Mo K_α radiation (λ = 0.7107 Å) or Cu K_α radiation (λ = 1.54184 Å) that were graphite-monochromated. Compounds [**3a**](PF_6), [**6**](OTf), [**9**](OTf), [**10**], [**11**](OTF) and [**13**](OTf) were measured on an Oxford Diffraction CCD Xcalibur system with a Ruby detector with Mo K_α radiation (λ = 0.7107 Å) that was graphite-monochromated. Suitable crystals were covered with oil (Infineum V8512, formerly known as Paratone N), placed on a nylon loop that is mounted in a CrystalCap Magnetic™ (Hampton Research) and immediately transferred to the diffractometer. The program suite CrysAlis^{Pro} was used for data collection, multi-scan absorption correction and data reduction.[5] The structure was solved with direct methods using SIR97[6] and was refined by full-matrix least-squares methods on F^2 with SHELXL-2014.[7] For some structures the GUI ShelXle was used.[8]

The structure of [**1**](PF_6) was refined as a 2-component perfect twin, with a twin ratio of about 70 : 30. The final SHELXL refinements were done on a HKLF5 file containing all component data including overlapped reflections. In the crystal structure of [**9**](OTf), in addition to the $(OTf)^-$ anion, ReO_4^- was found as counter ion (ratio 90 : 10), however, the oxygen atoms of the perrhenate could not be localized. In [**8**](OTf), one single high residual electron density was observed next to the rhenium atom. Maybe this was caused by the needed use of the copper radiation of this 5d-element containing structure.

Supplementary crystallographic data can be obtained free of charge from the Cambridge Crystallographic Data Centre via www.ccdc.cam.ac.uk/structures (CCDC nr. 1554159 - 1554161 and 155438 - 155443).

Crystallographic Tables

Name	[^{99}Tc(η^6-hmbz)(η^6-C_6H_5-NH_2)](PF_6) [1](PF_6)	[^{99}Tc(η^6-hmbz)$_2$](PF_6) [3a](PF_6)	[^{99}Tc(η^6-pmbz)(η^6-C_6H_5-Br)]Cl [5]Cl	[Re(η^6-C_6H_6)(η^6-napht)](OTF) ([6](OTf))
Empirical formula	$C_{18}H_{25}F_6NPTc$	$C_{24}H_{36}F_6PTc$	$C_{17}H_{21}BrTcCl$	$C_{18}H_{14}F_6LiO_6ReS_2$
Diffractometer	XtaLAB Synergy	Xcalibur Ruby	XtaLAB Synergy	Xcalibur Ruby
Wavelength (Å)	0.7107	0.7107	0.7107	0.71073
mol. weight (g/mol)	499.36	568.51	438.70	697.55
Crystal system	Monoclinic	Orthorhombic	Triclinic	Triclinic
Space group	Cc	Pnnm	P-1	P1
a (Å)	8.1171(4)	8.1154(6)	7.0418(4)	9.0801(3)
b (Å)	15.7539(7)	10.4942(6)	9.2033(5)	10.7870(3)
c (Å)	15.0788(7)	13.6880(8)	12.4028(7)	11.5849(3)
α (°)	90	90	87.599(5)	104.912(2)
β (°)	91.370(4)	90	86.191(5)	98.624(2)
γ (°)	90	90	85.980(4)	91.639(2)
Volume (Å^3)	1927.67(16)	1165.73(13)	799.48(8)	1081.41(5)
Z	4	2	2	2
Dens.(calc.) (g/cm^3)	1.717	1.617	1.822	2.142
Abs. coeff. (mm^{-1})	0.89	0.74	3.55	5.897
F(000)	1008	584	436	668
Crystal size (mm^3)	0.21 × 0.07 × 0.04	0.12 × 0.10 × 0.08	0.23 × 0.19 × 0.01	0.360 x 0.210 x 0.070
Crystal description	yellow needle	yellow prism	yellow plate	yellow plate
θ range (°)	2.5–31.0	2.9–31.1	2.8–29.9	2.274-35.022
Index ranges	-10<=h<=10, -19<=k<=19,	-11<=h<=11, -14<=k<=14,	-9<=h<=9, -12<=k<=12,	-14<=h<=14, -17<=k<=17,
	-18<=l<=18	-19<=l<=19	-16<=l<=16	-18<=l<=18
Refl. collected	21006	7912	8837	34421
Indep. reflections	21006	1853	3914	17403 [R(int) = 0.0427]
Reflections obs.	20410	1390	3075	15889
Criterion for obs.	I >2sigma(I)	I >2sigma(I)	I >2sigma(I)	I > 2sigma(I)
Completeness to θ	99% to 25.24°	100% to 30.49°	99% to 28.28°	99.5 % to 33.07°
Absorption corr.	analytical	analytical	analytical	Semi-empirical from equivalents
Max. and min. transm.	0.871, 0.969	0.942 and 0.914	0.495 and 0.986	1.00000 and 0.41615
Data / restraints / param.	21006 / 2 / 250	1853 / 0 / 81	3914 / 0 / 186	17403 / 3 / 613
Goodness-of-fit on F^2	1.06	1.10	1.04	1.021
Fin. R ind. [I>2sigma(I)]	R1 = 0.0498, wR2 = 0.1344	R1 = 0.0355, wR2 = 0.0769	R1 = 0.0428, wR2 = 0.0992	R1 = 0.0372, wR2 = 0.0759
R indices (all data)	R1 = 0.0508, wR2 = 0.1356	R1 = 0.0545, wR2 = 0.0846	R1 = 0.0601, wR2 = 0.1043	R1 = 0.0424, wR2 = 0.0806
Flack parameter	-0.01(5)	-	-	-0.010(4)
Fin. diff. ρ_{max} (e^-/Å^{-3})	0.51 and -0.56	0.43 and -0.47	1.50 and -0.85	1.219 and -1.488
CCDC Nr.	1554160	1554161	1554159	1554400

Name	**[Re(η⁶-C₆H₆)(tep)₃](OTF) ([8](OTf))**	**[Re(η⁶-C₆H₆)(CN-ᵗBu)₃](OTF) ([9](OTf)$_{0.9}$(ReO$_4$)$_{0.1}$)**	**[Re(η⁶-C₆H₆)(HB(pyz)₃)] (10)**	**[Re(η⁶-napht)(tep)₃](OTF) ([11](OTF))**
Empirical formula	$C_{25}H_{50}F_3O_{12}P_3ReS$	$C_{21.9}H_{33}F_{2.7}N_3O_{3.1}Re_{1.1}S_{0.9}$	$C_{15}H_{16}BN_6Re$	$C_{29}H_{53}F_3O_{12}P_3ReS$
Diffractometer	XtaLAB Synergy	Xcalibur Ruby	Xcalibur Ruby	Xcalibur Ruby
Wavelength (Å)	1.54184	0.71073	0.71073	0.71073
mol. weight (g/mol)	910.82	672.89	477.35	961.88
Crystal system	Monoclinic	Triclinic	Monoclinic	Triclinic
Space group	I2/a	P-1	P21/m	P-1
a (Å)	16.22709(11)	9.7977(5)	8.2517(4)	10.4629(3)
b (Å)	15.78790(12)	10.9136(7)	10.2422(6)	12.2103(3)
c (Å)	30.1873(3)	13.8305(6)	8.9263(5)	15.7908(4)
α (°)	90	104.511(5)	90	97.165(2)
β (°)	101.4536(8)	109.525(4)	92.507(5)	102.359(2)
γ (°)	90	93.636(5)	90	94.246(2)
Volume (Å^3)	7579.73(10)	1331.70(12)	753.69(7)	1944.62(8)
Z	8	2	2	2
Dens.(calc.) (g/cm^3)	1.596	1.678	2.103	1.643
Abs. coeff. (mm^{-1})	8.574	5.130	8.069	3.371
F(000)	3672	663	456	972
Crystal size (mm^3)	0.120 x 0.110 x 0.040	0.300 x 0.180 x 0.130	0.120 x 0.050 x 0.040	0.570 x 0.260 x 0.170
Crystal description	colorless block	colorless block	yellow prism	yellow block
θ range (°)	3.173-78.974	2.153-36.318	2.284-32.874	2.483-33.380
Index ranges	-20<=h<=20, -19<=k<=20,	-16<=h<=16, -18<=k<=18,	-11<=h<=12, -15<=k<=15,	-13<=h<=14, -17<=k<=17,
	-30<=l<=38	-23<=l<=23	-13<=l<=13	-23<=l<=23
Refl. collected	41327	55166	9097	42674
Indep. reflections	8073 [R(int) = 0.0472]	12802 [R(int) = 0.0457]	2736 [R(int) = 0.0692]	13377 [R(int) = 0.0423]
Reflections obs.	7249	11886	2473	11837
Criterion for obs.	I > 2sigma(I)	I > 2sigma(I)	I > 2sigma(I)	I > 2sigma(I)
Completeness to θ	100.0 % to 67.684°	99.1 % to 36.23°	100.0 % to 26.32°	99.7 % to 30.44°
Absorption corr.	Gaussian	Semi-empirical from equivalents	Analytical	Semi-empirical from equivalents
Max. and min. transm.	1.000 and 0.458	1.00000 and 0.57410	0.831 and 0.538	1.00000 and 0.38979
Data / restraints / param.	8073 / 87 / 484	12802 / 0 / 316	2736 / 0 / 120	13377 / 0 / 451
Goodness-of-fit on F^2	1.051	1.058	1.051	1.058
Fin. R ind. [I>2sigma(I)]	R1 = 0.0562, wR2 = 0.1724	R1 = 0.0257, wR2 = 0.0662	R1 = 0.0344, wR2 = 0.0691	R1 = 0.0315, wR2 = 0.0715
R indices (all data)	R1 = 0.0598, wR2 = 0.1765	R1 = 0.0287, wR2 = 0.0683	R1 = 0.0398, wR2 = 0.0722	R1 = 0.0401, wR2 = 0.0769
Fin. diff. ρ_{max} (e^-/Å^{-3})	4.771 and -2.578	1.550 and -1.758	2.324 and -2.491	1.617 and -1.161
CCDC Nr.	1554399	1554398	1554397	1554401

Name	**[Re(η^6-napht)(triphos)](PF$_6$) ([12](PF$_6$))**	**[Re(CN-^{t}Bu)$_6$](OTF) ([13](OTf))**
Empirical formula	$C_{52}H_{49}Cl_2F_6P_4Re$	$C_{33}H_{54}F_9Li_2N_6O_{11}ReS_3$
Diffractometer	XtaLAB Synergy	Xcalibur Ruby
Wavelength (Å)	1.54184	0.71073
mol. weight (g/mol)	1168.89	1178.08
Crystal system	Orthorhombic	Triclinic
Space group	P212121	P-1
a (Å)	11.00550(4)	10.191(2)
b (Å)	18.56730(7)	17.740(3)
c (Å)	24.45640(9)	17.909(4)
α (°)	90	117.46(2)
β (°)	90	102.485(19)
γ (°)	90	93.314(16)
Volume (Å^3)	4997.48(3)	2758.0(11)
Z	4	2
Dens.(calc.) (g/cm^3)	1.554	1.419
Abs. coeff. (mm^{-1})	7.435	2.397
F(000)	2336	1184
Crystal size (mm^3)	0.190 x 0.060 x 0.040	0.540 x 0.250 x 0.190
Crystal description	red prism	colorless prism
θ range (°)	2.988-79.687	2.251-30.508
Index ranges	-13<=h<=13, -23<=k<=23,	-14<=h<=11, -25<=k<=25,
	-30<=l<=30	-23<=l<=25
Refl. collected	57867	40102
Indep. reflections	10772 [R(int) = 0.0330]	16824 [R(int) = 0.0387]
Reflections obs.	10651	13188
Criterion for obs.	I > 2sigma(I)	I > 2sigma(I)
Completeness to θ	100.0 % to 67.684°	99.7 % to 30.44°
Absorption corr.	Semi-empirical from equivalents	Semi-empirical from equivalents
Max. and min. transm.	1.00000 and 0.73035	1.00000 and 0.56980
Data / restraints / param.	10772 / 0 / 587	16824 / 0 / 604
Goodness-of-fit on F^2	1.067	1.046
Fin. R ind. [I>2sigma(I)]	R1 = 0.0322, wR2 = 0.0828	R1 = 0.0419, wR2 = 0.1002
R indices (all data)	R1 = 0.0325, wR2 = 0.0830	R1 = 0.0586, wR2 = 0.1114
Flack parameter	-0.021(3)	-
Fin. diff. ρ_{max} (e$^-$/Å^{-3})	1.154 and -0.807	1.332 and -1.682
CCDC Nr.	1554402	1554403

5. References

1. J. Noddack and W. Noddack, *ZAAC* 1929, **181**, 1-37.
2. G. Brauer, *Handbuch der präparativen anorganischen Chemie in drei Bänden, 3. Auflage*, Ferdinand Enke Verlag, Stuttgart, 1981.
3. D. A. Pennington, P. N. Horton, M. B. Hursthouse, M. Bochmann and S. J. Lancaster, *Polyhedron*, 2005, **24**, 151-156.
4. G. Meola, H. Braband, D. Hernández-Valdés, C. Gotzmann, T. Fox, B. Spingler and R. Alberto, *Inorg. Chem.* , 2017, DOI: 10.1021/acs.inorgchem.7b00394.
5. *CrysAlis^{Pro} Software system*; Rigaku Oxford Diffraction, vers. 171.39 Oxford, UK, 2017.
6. Altomare, A.; Burla, M. C.; Camalli, M.; Cascarano, G. L.; Giacovazzo, C.; Guagliardi, A.; Moliterni, A. G. G.; Polidori, G.; Spagna, R. *J. Appl. Cryst.* **1999**, *32*, 115-119.
7. Sheldrick, G. M. *Acta Cryst.* **2015**, *C71*, 3-8.
8. Hübschle, C. B.; Sheldrick, G. M.; Dittrich, B. *J. Appl. Cryst.* **2011**, *44*, 1281-1284.

8.8 Unpublished Experimental Section: Supplementary Information Section: Structure and Reactivities of Rhenium and Technetium bis-Arene Sandwich Complexes [M(η^6-arene)$_2$]$^+$

8.8.1 [Re(η^6-$C_6H_3(OMe_3)_3$)(η^6-C_6H_6)](PF_6) ([**43**](PF_6))

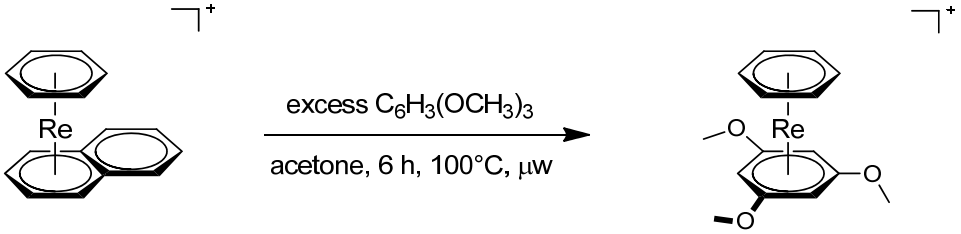

Synthesis: [**6**](PF_6) (20 mg, 0.037 mmol) was dissolved in 2 mL dry acetone. After the addition of 1,3,5-Trimethoxybenzene (622.12 mg, 3.7 mmol, 100 eq.) to the yellow solution, the reaction mixture was stirred for 6 h at 100°C in a microwave reactor. The solvent was evaporated *in vacuo* and the residue washed with Et_2O (5 x 2.5 mL) and water (2 x 2 mL). The product was recrystallized from acetonitrile, yielding yellow crystals of [**43**](PF_6). Single crystals suitable for X-ray diffraction analysis were obtained by slow evaporation from an acetonitrile solution of [**43**](ClO_4). Yield: 11 mg (0.019 mmol, 52%) of [**43**](PF_6).

Analysis: ^{1}H NMR (500 MHz, CD_3CN) δ [ppm]: 6.49 (s, 2H, C*H*$_{arom}$), 5.66 (s, 6H, C*H*$_{arom}$), 3.64 (s, 9H, OC*H*$_3$). ^{13}C NMR (125 MHz, CD_3CN) δ [ppm]: 127.92 (*C*$_{arom}$-OCH_3), 74.82 (*C*H$_{arom}$), 61.69 (*C*H$_{arom}$), 66.98 (*o*-*C*H$_{arom}$), 58.44 (O*C*H$_3$). ESI-MS: m/z = 433.1 [M]$^+$. IR ν: 3078 (w), 1524 (m), 1468 (w), 1407 (w), 1339 (m), 1200 (m), 1156 (m), 1039 (m), 976 (m), 904 (s) cm^{-1}. HR-ESI-MS $C_{15}H_{18}O_3Re$ [M]$^+$: calculated, 433.0808; found, 433.0802.

8.8.2 [Re(ACN)$_6$](PF_6)$_2$ ([**44**](PF_6)$_2$)

Synthesis: [**6p**](PF_6) (20 mg, 0.037 mmol) was dissolved in 2 mL dry acetonitrile. The reaction mixture was stirred for 6 h at 80°C in a microwave reactor. The solvent was evaporated *in vacuo* and the residue washed with dry toluene (4 x 2.5 mL). The product was crystallized from an acetonitrile solution (glovebox) by slow evaporation, yielding red green single crystals of [**44**](PF_6)$_2$, suitable for X-ray diffraction analysis. Yield: 12.0mg (0.017 mmol, 45%) of [**44**](PF_6)$_2$

Analysis: ESI-MS: m/z = 432.1 $[M]^+$. IR ν: 2935 (w), 2264 (w), 1417 (m), 1030 (w), 947 (w), 826 (s) cm^{-1}. HR-ESI-MS $C_{12}H_{18}N_6Re$ $[M]^+$: decomposition.

8.8.3 $[Re(\eta^6\text{-}C_6H_6)(dmso\text{-}S)_3]$ ([**45**](PF_6))

Synthesis: [**6p**](PF_6) (20 mg, 0.037 mmol) was dissolved in 2 mL dry dmso. Afterwards, the reaction mixture was stirred for 1 h at 60°C in a microwave reactor. The solvent was evaporated *in vacuo* and the residue was washed with Et_2O (3 x 3 mL). The product was recrystallized from dmso (glovebox), yielding yellow single crystals of [**45**](PF_6), suitable for X-ray diffraction analysis. Yield: 20.6 mg (0.032 mmol, 86%) of [**45**](PF_6).

Analysis: ^{1}H NMR (500 MHz, CD_3CN) δ [ppm]: 5.36 (s, 6H, CH_{arom}), 3.58 (s, 18H, CH_3). ^{13}C NMR (125 MHz, CD_3CN) δ [ppm]: 82.96 (CH_{arom}), 55.64 (CH_3). ESI-MS: m/z = 499.1 $[M]^+$. IR ν: 3029 (w), 2923 (w), 1427 (w), 1319 (w), 1083 (s), 1072 (s), 1013 (m), 972 (w), 828 (s), 716 (w) cm^{-1}. HR-ESI-MS $C_{12}H_{24}O_3ReS_3$ $[M]^+$: calculated, 499.0439; found, 499.0442.

8.8.4 $[Re(\eta^6\text{-}C_6H_6)(CH_3CN)(bipy)]^+$ ([**46**](PF_6))

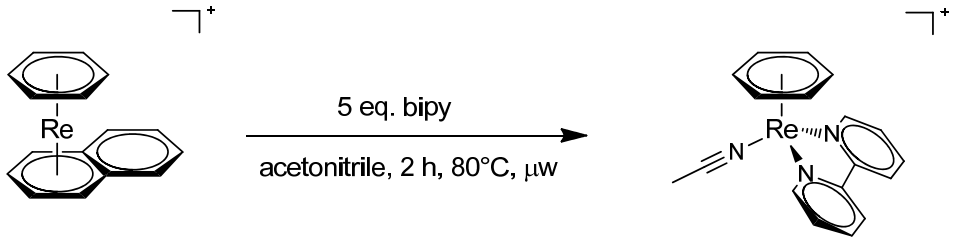

Synthesis: [**6p**](PF_6) (20 mg, 0.037 mmol) was dissolved in 2 mL dry acetonitrile. After the addition of 2,2'-bipyridine (17.3 mg, 0.11 mmol, 3 eq.) to the yellow solution, the reaction mixture was stirred for 2 h at 80°C in a microwave reactor. The solvent was evaporated *in vacuo* and the residue washed with dry toluene (4 x 2.5 mL). The product was recrystallized from an acetonitrile/toluene (1:1, glovebox) solution by slow evaporation, yielding dark violet single crystals of [**46**](PF_6), suitable for X-ray diffraction analysis. Yield: 18.6 mg (0.031 mmol, 83%) of [**46**](PF_6).

Analysis: ^{1}H NMR (500 MHz, CD_3CN) δ [ppm]: 9.61 (d, 2H, C*H*$_{arom}$), 8.62 (d, 2H, C*H*$_{arom}$), 7.92 (t, 2H, C*H*$_{arom}$), 7.53 (t, 2H, C*H*$_{arom}$), 4.70 (s, 6H, C*H*$_{arom}$), 2.40 (s, 3H, C*H*$_3$CN). ^{13}C NMR (125 MHz, CD_3CN) δ [ppm]: 155.78 (*C*$_{arom}$, bipy), 154.45 (*C*H$_{arom}$, bipy), 136.32 (*C*H$_{arom}$, bipy), 126.88 (*C*H$_{arom}$, bipy), 124.10 (CH$_3$*C*N), 123.42 (*C*H$_{arom}$, bipy), 69.79 (*C*H$_{arom}$), 3.50 (*C*H$_3$CN). ESI-MS: m/z = 462.1 $[M]^+$. IR ν: 3078 (w), 2257 (w, C≡N), 1696 (w), 1604 (w), 1462 (m), 1417 (m), 1318 (w), 1255 (m), 1165 (w), 1021 (m), 824 (s), 758 (s), 722 (w) cm^{-1}. HR-ESI-MS $C_{18}H_{17}N_3Re$ $[M]^+$: calculated, 462.0975; found, 462.0974.

8.8.5 $[Re(\eta^6\text{-}C_6H_6)(CH_3CN)(dppe)]^+$ ([**47**](PF$_6$))

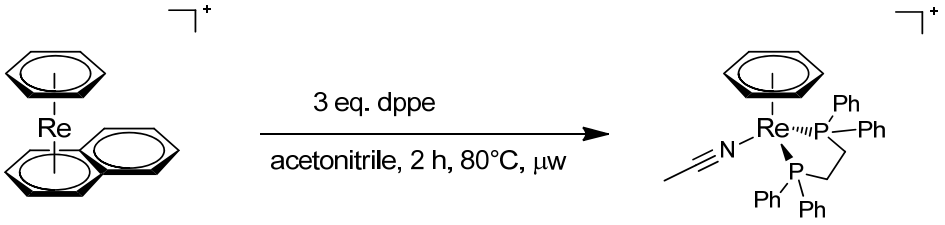

Synthesis: [**6p**](PF$_6$) (20 mg, 0.037 mmol) was dissolved in 2 mL dry acetonitrile. After the addition of 1,2-bis(diphenylphosphino)ethane (44.2 mg, 0.11 mmol, 3 eq.) to the yellow solution, the reaction mixture was stirred for 2 h at 80°C in a microwave reactor. The solvent was evaporated *in vacuo* and the residue washed with dry Et_2O (4 x 2.5 mL). The product was recrystallized from an acetonitrile/toluene (1:1, glovebox) solution by slow evaporation, yielding yellow single crystals of [**47**](PF$_6$), suitable for X-ray diffraction analysis. Yield: 26.7 mg (0.032 mmol, 85%) of [**47**](PF$_6$).

Analysis: ^{1}H NMR (500 MHz, CD_3CN) δ [ppm]: 7.88 (m, 4H, C*H*$_{arom}$), 7.52 (m, 10H, C*H*$_{arom}$), 7.43 (m, 6H, C*H*$_{arom}$), 4.73 (s, 6H, C*H*$_{arom}$), 2.67 (m, 4H, PC*H*$_2$C*H*$_2$P), 1.66 (s, 3H, C*H*$_3$CN). ^{13}C NMR (125 MHz, CD_3CN) δ [ppm]: 139.78 (*C*$_{arom}$), 139.39 (*C*$_{arom}$), 134.05 (d, *C*H$_{arom}$), 131.67 (d, *C*H$_{arom}$), 131.01 (d, *C*H$_{arom}$), 130.30 (dd, *C*H$_{arom}$), 129.73 (d, *C*H$_{arom}$), 129.48 (d, *C*H$_{arom}$), 123.36 (CH$_3$*C*N), 76.52 (*C*H$_{arom}$), 29.21 (P*C*H$_2$*C*H$_2$P), 2.97 (*C*H$_3$CN). ^{31}P NMR (202 MHz, CD_3CN) δ [ppm]: 46.91 (s, (*P*CH$_2$CH$_2$*P*)), -144.26 (sept, *P*F$_6$). ESI-MS: m/z = 704.1 $[M]^+$. IR ν: 3063 (w), 2257 (w, C≡N), 1484 (w), 1434 (m), 1188 (w), 1100 (m), 828 (s), 746 (m) cm^{-1}. HR-ESI-MS $C_{34}H_{33}NP_2Re$ $[M]^+$: calculated, 704.1640; found, 704.1636.

9 References

1. Rosenberg, B.; Van Camp, L.; Krigas, T., *Nature* **1965,** 205, 698.
2. Kelland, L., *Nature Reviews Cancer* **2007,** 7, 573.
3. Oun, R.; Moussa, Y. E.; Wheate, N. J., *Dalton Transactions* **2018,** 47, (19), 6645.
4. de Almeida, A.; Oliveira, B. L.; Correia, J. D. G.; Soveral, G.; Casini, A., *Coordination Chemistry Reviews* **2013,** 257, (19), 2689.
5. Ang, W. H.; Casini, A.; Sava, G.; Dyson, P. J., *Journal of Organometallic Chemistry* **2011,** 696, (5), 989.
6. Thompson, K. H.; Orvig, C., *Science* **2003,** 300, (5621), 936.
7. Gaynor, D.; Griffith, D. M., *Dalton Transactions* **2012,** 41, (43), 13239.
8. Levina, A.; Lay, P. A., *Dalton Transactions* **2011,** 40, (44), 11675.
9. Guo, Z.; Sadler, P. J., *Angewandte Chemie International Edition* **1999,** 38, (11), 1512.
10. Kilpin, K. J.; Dyson, P. J., *Chemical Science* **2013,** 4, (4), 1410.
11. Top, S.; Tang, J.; Vessières, A.; Carrez, D.; Provot, C.; Jaouen, G., *Chemical Communications* **1996**, (8), 955.
12. Nguyen, A.; Vessières, A.; Hillard, E. A.; Top, S.; Pigeon, P.; Jaouen, G., *CHIMIA International Journal for Chemistry* **2007,** 61, (11), 716.
13. Pimlott, S. L.; Sutherland, A., *Chemical Society Reviews* **2011,** 40, (1), 149.
14. Wadas, T. J.; Wong, E. H.; Weisman, G. R.; Anderson, C. J., *Chemical Reviews* **2010,** 110, (5), 2858.
15. Vallabhajosula, S.; Solnes, L.; Vallabhajosula, B., *Seminars in Nuclear Medicine* **2011,** 41, (4), 246.
16. Bartholomä, M. D.; Louie, A. S.; Valliant, J. F.; Zubieta, J., *Chemical Reviews* **2010,** 110, (5), 2903.
17. Velikyan, I., *Medicinal Chemistry* **2011,** 7, (5), 345.
18. Mendes, F.; Paulo, A.; Santos, I., *Dalton Transactions* **2011,** 40, (20), 5377.
19. Morais, G. R.; Paulo, A.; Santos, I., *Organometallics* **2012,** 31, (16), 5693.
20. Palma, E.; Correia, J. D. G.; Campello, M. P. C.; Santos, I., *Molecular BioSystems* **2011,** 7, (11), 2950.
21. Jaouen, G., Top, S. and Vessières, A., Organometallics Targeted to Specific Biological Sites: The Development of New Therapies. In *Bioorganometallics*, 2006.
22. Leonidova, A.; Gasser, G., *ACS Chemical Biology* **2014,** 9, (10), 2180.
23. Viola-Villegas, N.; Rabideau, A. E.; Cesnavicious, J.; Zubieta, J.; Doyle, R. P., *ChemMedChem* **2008,** 3, (9), 1387.
24. Viola-Villegas, N.; Rabideau, A. E.; Bartholomä, M.; Zubieta, J.; Doyle, R. P., *Journal of Medicinal Chemistry* **2009,** 52, (16), 5253.
25. Yan, Y. K.; Cho, S. E.; Shaffer, K. A.; Rowell, J. E.; Barnes, B. J.; Hall, I. H., *Pharmazie* **2000,** 55, (4), 307.
26. Illán-Cabeza, N. A.; García-García, A. R.; Moreno-Carretero, M. N.; Martínez-Martos, J. M.; Ramírez-Expósito, M. J., *Journal of Inorganic Biochemistry* **2005,** 99, (8), 1637.
27. Zhang, J.; Vittal, J. J.; Henderson, W.; Wheaton, J. R.; Hall, I. H.; Hor, T. S. A.; Yan, Y. K., *Journal of Organometallic Chemistry* **2002,** 650, (1), 123.
28. Kermagoret, A.; Morgant, G.; d'Angelo, J.; Tomas, A.; Roussel, P.; Bastian, G.; Collery, P.; Desmaële, D., *Polyhedron* **2011,** 30, (2), 347.
29. Top, S.; Vessières, A.; Pigeon, P.; Rager, M.-N.; Huché, M.; Salomon, E.; Cabestaing, C.; Vaissermann, J.; Jaouen, G., *ChemBioChem* **2004,** 5, (8), 1104.
30. R. Dilworth, J.; J. Parrott, S., *Chemical Society Reviews* **1998,** 27, (1), 43.
31. Jürgens, S.; Herrmann, W. A.; Kühn, F. E., *Journal of Organometallic Chemistry* **2014,** 751, 83.
32. Pampaloni, G., *Coordination Chemistry Reviews* **2010,** 254, (5), 402.
33. Yan, Y. K.; Melchart, M.; Habtemariam, A.; Sadler, P. J., *Chemical Communications* **2005**, (38), 4764.

34. Păunescu, E.; Nowak-Sliwinska, P.; Clavel, C. M.; Scopelliti, R.; Griffioen, A. W.; Dyson, P. J., *ChemMedChem* **2015,** 10, (9), 1539.
35. Morris, R. E.; Aird, R. E.; del Socorro Murdoch, P.; Chen, H.; Cummings, J.; Hughes, N. D.; Parsons, S.; Parkin, A.; Boyd, G.; Jodrell, D. I.; Sadler, P. J., *Journal of Medicinal Chemistry* **2001,** 44, (22), 3616.
36. Aird, R. E.; Cummings, J.; Ritchie, A. A.; Muir, M.; Morris, R. E.; Chen, H.; Sadler, P. J.; Jodrell, D. I., *British Journal Of Cancer* **2002,** 86, 1652.
37. Sergheraert, C.; Brunet, J.-C.; Tartar, A., *Journal of the Chemical Society, Chemical Communications* **1982**, (24), 1417.
38. Sergheraert, C.; Tartar, A., *Journal of Organometallic Chemistry* **1982,** 240, (2), 163.
39. Salmain, M.; Vessières, A.; Varenne, A.; Brossier, P.; Jaouen, G., *Journal of Organometallic Chemistry* **1999,** 589, (1), 92.
40. Patra, M.; Gasser, G.; Wenzel, M.; Merz, K.; Bandow, J. E.; Metzler-Nolte, N., *Organometallics* **2012,** 31, (16), 5760.
41. Rajapakse, C. S. K.; Martínez, A.; Naoulou, B.; Jarzecki, A. A.; Suárez, L.; Deregnaucourt, C.; Sinou, V.; Schrével, J.; Musi, E.; Ambrosini, G.; Schwartz, G. K.; Sánchez-Delgado, R. A., *Inorganic Chemistry* **2009,** 48, (3), 1122.
42. Wolff, J. M.; Sheldrick, W. S., *Journal of Organometallic Chemistry* **1997,** 531, (1), 141.
43. Stodt, R.; Gencaslan, S.; Frodl, A.; Schmidt, C.; Sheldrick, W. S., *Inorganica Chimica Acta* **2003,** 355, 242.
44. Schlüter, A.; Bieber, K.; Sheldrick, W. S., *Inorganica Chimica Acta* **2002,** 340, 35.
45. Wolff, J. M.; Sheldrick, W. S., *Chemische Berichte* **1997,** 130, (7), 981.
46. Stodt, R.; Gencaslan, S.; Müller, Iris M.; Sheldrick, William S., *European Journal of Inorganic Chemistry* **2003,** 2003, (10), 1873.
47. Gray, J. C.; Habtemariam, A.; Winnig, M.; Meyerhof, W.; Sadler, P. J., *JBIC Journal of Biological Inorganic Chemistry* **2008,** 13, (7), 1111.
48. Gray, J. C. Ruthenium and Osmium Bis-Arene Complexes with Biologically-Active Ligands. University of Edinburgh, Edinburgh, 2008.
49. Wilkinson, G.; Rosenblum, M.; Whiting, M. C.; Woodward, R. B., *Journal of the American Chemical Society* **1952,** 74, (8), 2125.
50. Fischer, E. O.; Pfab, W., *Z. Naturforsch.* **1952,** 76, 377.
51. Fischer, E. O.; Hafner, W., *Zeitschrift fur Naturforschung - Section B Journal of Chemical Sciences* **1955,** 10, (12), 665.
52. Trifonova, E. A.; Perekalin, D. S.; Lyssenko, K. A.; Kudinov, A. R., *Journal of Organometallic Chemistry* **2013,** 727, 60.
53. Rybinskaya, M. I.; Kaganovich, V. S.; Kudinov, A. R., *Journal of Organometallic Chemistry* **1982,** 235, (2), 215.
54. Calderazzo, F.; Pampaloni, G., *Journal of Organometallic Chemistry* **1995,** 500, (1-2), 47.
55. Liu, Q.; Lin, Y. H.; Shen, Q., *Acta Crystallographica Section C: Crystal Structure Communications* **1997,** 53, (11), 1579.
56. Štíbr, B.; Bakardjiev, M.; Hájková, Z.; Holub, J.; Padělková, Z.; Růžička, A.; Kennedy, J. D., *Dalton Transactions* **2011,** 40, (22), 5916.
57. Timms, P. L., *Journal of the Chemical Society D: Chemical Communications* **1969**, (18).
58. Timms, P. L., *Journal of Chemical Education* **1972,** 49, (11), 782.
59. Schmidt, E., Klabunde, K. J., Ponce, A. , Smetana, A. and Heroux, D., Metal Vapor Synthesis of Transition Metal Compounds. In *Encyclopedia of Inorganic Chemistry*, 2006.
60. Yoshida, K.; Morimoto, I.; Mitsudo, K.; Tanaka, H., *Tetrahedron* **2008,** 64, (24), 5800.
61. Bennett, M. A.; Matheson, T. W., *Journal of Organometallic Chemistry* **1979,** 175, (1), 87.
62. Muetterties, E. L.; Bleeke, J. R.; Wucherer, E. J.; Albright, T., *Chemical Reviews* **1982,** 82, (5), 499.
63. Osborne, J. H.; Trogler, W. C.; Morand, P. D.; Francis, C. G., *Organometallics* **1987,** 6, (1), 94.
64. Skinner, H. A.; Connor Joseph, A., Metal-Ligand Bond-Energies in Organometallic Compounds. In *Pure and Applied Chemistry*, 1985; Vol. 57, p 79.

65. Schweiger, A.; Günthard, H. H., *Molecular Physics* **1984,** 53, (3), 585.
66. Elschenbroich, C., *Organometallics*. Wiley: 2016.
67. Benz, M.; Braband, H.; Schmutz, P.; Halter, J.; Alberto, R., *Chemical Science* **2015,** 6, (1), 165.
68. Jones, D.; Pratt, L.; Wilkinson, G., *Journal of the Chemical Society (Resumed)* **1962**, (0), 4458.
69. Astruc, D., *Organometallic Chemistry and Catalysis*. Springer Berlin Heidelberg: 2007.
70. Fritz, H. P.; Fischer, E. O., Notizen: Über Aromatenkomplexe Von Metallen Ix. Zum Aromatischen Reaktionsvermögen Von Di-Benzol-Chrom Und Di-Toluol-Chrom. In *Zeitschrift für Naturforschung B*, 1957; Vol. 12, p 67.
71. Fischer, E. O.; Seeholzer, J., *ZAAC - Journal of Inorganic and General Chemistry* **1961,** 312, (5-6), 244.
72. Elschenbroich, C.; Möckel, R., *Angewandte Chemie International Edition in English* **1977,** 16, (12), 870.
73. Kündig, E. P.; Timms, P. L., *Journal of the Chemical Society, Chemical Communications* **1977**, (24), 912.
74. Kündig, E. P.; Timms, P. L., *Journal of the Chemical Society, Dalton Transactions* **1980**, (6), 991.
75. Kaganovich, V. S.; Kudinov, A. R.; Rybinskaya, M. I., *Organomet. Chem. USSR* **1988,** 1.
76. Perekalin, D. S.; Karslyan, E. E.; Petrovskii, P. V.; Borissova, A. O.; Lyssenko, K. A.; Kudinov, A. R., *European Journal of Inorganic Chemistry* **2012,** 2012, (9), 1485.
77. Elschenbroich, C., *Journal of Organometallic Chemistry* **1968,** 14, (1), 157.
78. Elschenbroich, C.; Kühlkamp, P.; Koch, J.; Behrendt, A., *Chemische Berichte* **1996,** 129, (7), 871.
79. Meola, G.; Braband, H.; Schmutz, P.; Benz, M.; Spingler, B.; Alberto, R., *Inorganic Chemistry* **2016,** 55, (21), 11131.
80. Litvak, V. V.; Kun, P. P.; Oleynik, I. I.; Volkov, O. V.; Shteingarts, V. D., *Journal of Organometallic Chemistry* **1986,** 310, (2), 189.
81. Sweigart, D. A., *Journal of the Chemical Society, Chemical Communications* **1980**, (23), 1159.
82. Pierce, D. T.; Geiger, W. E., *Journal of the American Chemical Society* **1992,** 114, (15), 6063.
83. Fischer, E. O.; Schmidt, M. W., *Chemische Berichte* **1967,** 100, (11), 3782.
84. Fischer, E. O.; Wirzmüller, A., *Chemische Berichte* **1957,** 90, (9), 1725.
85. Fischer, E. O.; Schmidt, M. W., *Chemische Berichte* **1966,** 99, (7), 2206.
86. Calderazzo, F.; Poli, R.; Barbati, A.; Zanazzi, P. F., *Journal of the Chemical Society, Dalton Transactions* **1984**, (6), 1059.
87. Rybinskaya, M. I.; Kaganovich, V. S.; Kudinov, A. R., *Bulletin of the Academy of Sciences of the USSR, Division of chemical science* **1984,** 33, (4), 813.
88. Pike, R. D.; Alavosus, T. J.; Camaioni-Neto, C. A.; Williams, J. C.; Sweigart, D. A., *Organometallics* **1989,** 8, (11), 2631.
89. Yau, H. M.; McKay, A. I.; Hesse, H.; Xu, R.; He, M.; Holt, C. E.; Ball, G. E., *Journal of the American Chemical Society* **2016,** 138, (1), 281.
90. Schlom, P. J.; Morken, A. M.; Eyman, D. P.; Baenziger, N. C.; Schauer, S. J., *Organometallics* **1993,** 12, (9), 3461.
91. Green, M. L. H.; O'Hare, D.; Wallis, J. M., *Journal of the Chemical Society, Chemical Communications* **1984**, (4), 233.
92. Green, M. L. H.; O'Hare, D.; Wallis, J. M., *Polyhedron* **1986,** 5, (8), 1363.
93. Baudry, D.; Ephritikhine, M.; Felkin, H., *Journal of Organometallic Chemistry* **1982,** 224, (4), 363.
94. Baudry, D.; Boydell, P.; Ephritikhine, M., *Journal of the Chemical Society, Dalton Transactions* **1986**, (3), 525.
95. Baudry, D.; Cormier, J.-M.; Ephritikhine, M., *Journal of Organometallic Chemistry* **1992,** 427, (3), 349.
96. Green, M. L. H.; O'Hare, D., *Journal of the Chemical Society, Dalton Transactions* **1987**, (2), 403.

97. Green, M. L. H.; O'Hare, D., *Journal of the Chemical Society, Chemical Communications* **1985**, (6), 332.
98. Fischer, E. O.; Wehner, H. W., *Chemische Berichte* **1968,** 101, (2), 454.
99. Baumgärtner, F.; Fischer, E. O.; Zahn, U., *Chemische Berichte* **1961,** 94, (8), 2198.
100. Palm, C.; Fischer, E. O.; Baumgȃrtner, F., *Tetrahedron Letters* **1962,** 3, (6), 253.
101. Wester, D. W.; Coveney, J. R.; Nosco, D. L.; Robbins, M. S.; Dean, R. T., *Journal of Medicinal Chemistry* **1991,** 34, (11), 3284.
102. Herrman, W. A.; Alberto, R.; Bryan, J. C.; Sattelberger, A. P., *Chemische Berichte* **1991,** 124, (5), 1107.
103. Louie, A., *Chemical Reviews* **2010,** 110, (5), 3146.
104. Liu, S., *Chemical Society Reviews* **2004,** 33, (7), 445.
105. Alberto, R., Radiopharmaceuticals. In *Bioorganometallics*, G. Jaouen ed.; 2006.
106. Alberto, R., *Journal of Organometallic Chemistry* **2007,** 692, (6), 1179.
107. Hartinger, C. G.; Metzler-Nolte, N.; Dyson, P. J., *Organometallics* **2012,** 31, (16), 5677.
108. Farrugia, L. J. *Ortep-3 for Windows - a Version of Ortep-Iii with a Graphical User Interface (Gui),*, 1997.
109. Boehm, G.; Wieghardt, K.; Nuber, B.; Weiss, J., *Inorganic Chemistry* **1991,** 30, (18), 3464.
110. Falceto, A.; Casanova, D.; Alemany, P.; Alvarez, S., *Chemistry – A European Journal* **2014,** 20, (45), 14674.
111. Liu, H.; Li, Q.-S.; Xie, Y.; King, R. B.; Schaefer, H. F., *The Journal of Physical Chemistry A* **2011,** 115, (32), 9022.
112. Jonas, K.; Wiskamp, V.; Tsay, Y. H.; Krueger, C., *Journal of the American Chemical Society* **1983,** 105, (16), 5480.
113. Jonas, K.; Koepe, G.; Schieferstein, L.; Mynott, R.; Krüger, C.; Tsay, Y.-H., *Angewandte Chemie* **1983,** 95, (8), 637.
114. Kreiter, C. G.; Georg, A.; Reiß, G. J., *Chemische Berichte* **1997,** 130, (9), 1197.
115. Groom, C. R.; Bruno, I. J.; Lightfoot, M. P.; Ward, S. C., *Acta Crystallographica Section B* **2016,** 72, (2), 171.
116. Jordi, S. Synthesis, Characterisation and Evaluation of a Hypoxia Sensitive $^{99(M)}$Tc-Bisarene Complex. Universitiy of Zurich 2016.
117. Meola, G.; Braband, H.; Jordi, S.; Fox, T.; Blacque, O.; Spingler, B.; Alberto, R., *Dalton Transactions* **2017,** 46, (42), 14631.
118. Elschenbroich, C.; Möckel, R.; Zenneck, U., *Angewandte Chemie* **1978,** 90, (7), 560.
119. Elzinga, J.; Rosenblum, M., *Organometallics* **1983,** 2, (9), 1214.
120. Swann, R. T.; Hanson, A. W.; Boekelheide, V., *Journal of the American Chemical Society* **1986,** 108, (12), 3324.
121. Wolf, H.; Leusser, D.; Jørgensen, M. R. V.; Herbst-Irmer, R.; Chen, Y.-S.; Scheidt, E.-W.; Scherer, W.; Iversen, B. B.; Stalke, D., *Chemistry – A European Journal* **2014,** 20, (23), 7048.
122. Elsegood, M. R. J.; Tocher, D. A., *Polyhedron* **1995,** 14, (20), 3147.
123. Pomije, M. K.; Kurth, C. J.; Ellis, J. E.; Barybin, M. V., *Organometallics* **1997,** 16, (16), 3582.
124. Elschenbroich, C.; Möckel, R.; Massa, W.; Birkhahn, M.; Zenneck, U., *Chemische Berichte* **1982,** 115, (1), 334.
125. Gottlieb, H. E.; Kotlyar, V.; Nudelman, A., *The Journal of Organic Chemistry* **1997,** 62, (21), 7512.
126. Krüger, T.; Vorndran, K.; Linker, T., *Chemistry – A European Journal* **2009,** 15, (44), 12082.
127. Emanuel, R. V.; Randall, E. W., *Journal of the Chemical Society A: Inorganic, Physical, Theoretical* **1969**, (0), 3002.
128. Shen, R.; Chen, T.; Zhao, Y.; Qiu, R.; Zhou, Y.; Yin, S.; Wang, X.; Goto, M.; Han, L.-B., *Journal of the American Chemical Society* **2011,** 133, (42), 17037.
129. Fukuyama, T.; Fujita, Y.; Miyoshi, H.; Ryu, I.; Kao, S.-C.; Wu, Y.-K., *Chemical Communications* **2018,** 54, (44), 5582.
130. Hokamp, T.; Dewanji, A.; Lübbesmeyer, M.; Mück-Lichtenfeld, C.; Würthwein, E.-U.; Studer, A., *Angewandte Chemie International Edition* **2017,** 56, (43), 13275.

131. Newman, S. G.; Gu, L.; Lesniak, C.; Victor, G.; Meschke, F.; Abahmane, L.; Jensen, K. F., *Green Chemistry* **2014,** 16, (1), 176.
132. Barker, G.; Webster, S.; Johnson, D. G.; Curley, R.; Andrews, M.; Young, P. C.; Macgregor, S. A.; Lee, A.-L., *The Journal of Organic Chemistry* **2015,** 80, (20), 9807.
133. Pan, D.; Wang, Y.; Xiao, G., *Beilstein journal of organic chemistry* **2016,** 12, 2443.
134. Fischer, E. O.; Elschenbroich, C., *Chemische Berichte* **1970,** 103, (1), 162.
135. Phillips, L.; Dennis, G. R.; Aroney, M. J., *New Journal of Chemistry* **2000,** 24, (1), 27.
136. Silvon, M. P.; Van Dam, E. M.; Skell, P. S., *Journal of the American Chemical Society* **1974,** 96, (6), 1945.
137. Lord, R. L.; Schauer, C. K.; Schultz, F. A.; Baik, M.-H., *Journal of the American Chemical Society* **2011,** 133, (45), 18234.
138. Satou, T.; Takehara, K.; Hirakida, M.; Sakamoto, Y.; Takemura, H.; Miura, H.; Tomonou, M.; Shinmyozu, T., *Journal of Organometallic Chemistry* **1999,** 577, (1), 58.
139. Yur'eva, L. P.; Nekrasov, L. N.; Peregudova, S. M., *Russian Chemical Reviews* **1993,** 62, (2), 121.
140. Bush, B. F.; Lagowski, J. J., *Journal of Organometallic Chemistry* **1990,** 386, (1), 37.
141. Meola, G.; Braband, H.; Hernández-Valdés, D.; Gotzmann, C.; Fox, T.; Spingler, B.; Alberto, R., *Inorganic Chemistry* **2017,** 56, (11), 6297.
142. Hernández-Valdés, D.; Meola, G.; Braband, H.; Spingler, B.; Alberto, R., *Organometallics* **2018,** 37, (17), 2910.
143. Abd-El-Aziz, A. S.; Bernardin, S., *Coordination Chemistry Reviews* **2000,** 203, (1), 219.
144. Imstepf, S.; Pierroz, V.; Rubbiani, R.; Felber, M.; Fox, T.; Gasser, G.; Alberto, R., *Angewandte Chemie* **2016,** 128, (8), 2842.
145. Sykes, P.; Hopf, H., *Wie Funktionieren Organische Reaktionen?: Reaktionsmechanismen Für Einsteiger*. Wiley-VCH: 2001.
146. Sorrell, T., *Organic Chemistry*. University Science Books: 2006.
147. Brunner, H.; Koch, H., *Chemische Berichte* **1982,** 115, (1), 65.
148. Wilburn, B. E.; Skell, P. S., *Journal of the American Chemical Society* **1982,** 104, (25), 6989.
149. Downton, P. A.; Mailvaganam, B.; Frampton, C. S.; Sayer, B. G.; McGlinchey, M. J., *Journal of the American Chemical Society* **1990,** 112, (1), 27.
150. Loughrey, B. T.; Healy, P. C.; Parsons, P. G.; Williams, M. L., *Inorganic Chemistry* **2008,** 47, (19), 8589.
151. Mandal, S. K.; Sarkar, A., *The Journal of Organic Chemistry* **1998,** 63, (16), 5672.
152. Vessières, A.; Top, S.; Beck, W.; Hillard, E.; Jaouen, G., *Dalton Transactions* **2006**, (4), 529.
153. Lenoir, D., *Synthesis* **1977,** 1977, (08), 553.
154. Leimner, J.; Weyerstahl, P., *Chemische Berichte* **1982,** 115, (12), 3697.
155. Zhao, F.; Zhao, C.; Liu, Z.-Q., *JBIC Journal of Biological Inorganic Chemistry* **2011,** 16, (8), 1169.
156. Nikitin, K.; Ortin, Y.; Müller-Bunz, H.; Plamont, M.-A.; Jaouen, G.; Vessières, A.; McGlinchey, M. J., *Journal of Organometallic Chemistry* **2010,** 695, (4), 595.
157. Togni, A.; Hayashi, T., *Ferrocenes: Homogeneous Catalysis, Organic Synthesis, Materials Science*. VCH Publishers: 1995.
158. Molander, G. A.; Biolatto, B., *The Journal of Organic Chemistry* **2003,** 68, (11), 4302.
159. Ribeiro de Campos, J. D.; Buffon, R., *New Journal of Chemistry* **2003,** 27, (2), 446.
160. Felder, P. Synthesis and Characterisation of Novel Bidentate Ligands Based on Bis(η^6-Benzene)Rhenium(I)$^+$ as a Scaffold for Medicinal and Catalytic Applications. University of Zurich, 2016.
161. Barlow, S.; Cowley, A.; Green, J. C.; Brunker, T. J.; Hascall, T., *Organometallics* **2001,** 20, (25), 5351.
162. Hugo Klahn, A.; Oelckers, B.; Godoy, F.; T. Garland, M.; Vega, A.; N. Perutz, R.; L. Higgitt, C., *Journal of the Chemical Society, Dalton Transactions* **1998**, (18), 3079.
163. Cloke, F. G. N.; Day, J. P.; Green, J. C.; Morley, C. P.; Swain, A. C., *Journal of the Chemical Society, Dalton Transactions* **1991**, (S), 789.
164. Gleiter, R.; Bleiholder, C.; Rominger, F., *Organometallics* **2007,** 26, (20), 4850.

165. Bandy, J. A.; Mtetwa, V. S. B.; Prout, K.; Green, J. C.; Davies, C. E.; Green, M. L. H.; Hazel, N. J.; Izquierdo, A.; Martin-Polo, J. J., *Journal of the Chemical Society, Dalton Transactions* **1985**, (10), 2037.
166. Zou, C.; Wrighton, M. S., *Journal of the American Chemical Society* **1990,** 112, (21), 7578.
167. Rinehart, K. L.; Michejda, C. J.; Kittle, P. A., *Journal of the American Chemical Society* **1959,** 81, (12), 3162.
168. Konietzny, S.; Finze, M.; Reiß, G. J., *Journal of Organometallic Chemistry* **2010,** 695, (18), 2089.
169. Koch, O.; Edelmann, F.; Behrens, U., *Chemische Berichte* **1982,** 115, (4), 1313.
170. Bleiholder, C.; Rominger, F.; Gleiter, R., *Organometallics* **2009,** 28, (4), 1014.
171. Abraham, R. J.; Canton, M.; Reid, M.; Griffiths, L., *Journal of the Chemical Society, Perkin Transactions 2* **2000**, (4), 803.
172. Ceccon, A.; Giacometti, G.; Venzo, A.; Paolucci, D.; Benozzi, D., *Journal of Organometallic Chemistry* **1980,** 185, (2), 231.
173. Godoy, F.; Klahn, A. H.; Lahoz, F. J.; Balana, A. I.; Oelckers, B.; Oro, L. A., *Organometallics* **2003,** 22, (24), 4861.
174. Kölle, V.; Grub, J., *Journal of Organometallic Chemistry* **1985,** 289, (1), 133.
175. Zeng, L.; Gupta, P.; Chen, Y.; Wang, E.; Ji, L.; Chao, H.; Chen, Z.-S., *Chemical Society Reviews* **2017,** 46, (19), 5771.
176. Kilpin, K. J.; Cammack, S. M.; Clavel, C. M.; Dyson, P. J., *Dalton Transactions* **2013,** 42, (6), 2008.
177. Scolaro, C.; Bergamo, A.; Brescacin, L.; Delfino, R.; Cocchietto, M.; Laurenczy, G.; Geldbach, T. J.; Sava, G.; Dyson, P. J., *Journal of Medicinal Chemistry* **2005,** 48, (12), 4161.
178. Perekalin, D. S.; Shvydkiy, N. V.; Nelyubina, Y. V.; Kudinov, A. R., *Mendeleev Communications* **2015,** 25, (1), 29.
179. Battistuzzi, R.; Saladini, M., *Inorganica Chimica Acta* **2000,** 304, (1), 114.
180. Carvalho, M. F. N. N.; Duarte, M. T.; Galvão, A. M.; Pombeiro, A. J. L.; Henderson, R.; Fuess, H.; Svoboda, I., *Journal of Organometallic Chemistry* **1999,** 583, (1), 56.
181. Perekalin, D. S.; Karslyan, E. E.; Trifonova, E. A.; Konovalov, A. I.; Loskutova, N. L.; Nelyubina, Y. V.; Kudinov, A. R., *European Journal of Inorganic Chemistry* **2013,** 2013, (4), 481.
182. Elsegood, M. R. J.; Tocher, D. A., *Journal of Organometallic Chemistry* **1990,** 391, (2), 239.
183. Gould, R. O.; Jones, C. L.; Stephenson, T. A.; Tocher, D. A., *Journal of Organometallic Chemistry* **1984,** 264, (3), 365.
184. Artero, V.; Laurencin, D.; Villanneau, R.; Thouvenot, R.; Herson, P.; Gouzerh, P.; Proust, A., *Inorganic Chemistry* **2005,** 44, (8), 2826.
185. Freedman, D. A.; Magneson, D. J.; Mann, K. R., *Inorganic Chemistry* **1995,** 34, (10), 2617.
186. Lackner, W.; Standfest-Hauser, C. M.; Mereiter, K.; Schmid, R.; Kirchner, K., *Inorganica Chimica Acta* **2004,** 357, (9), 2721.
187. Petersen, N.; Raebiger, J. W.; Miller, J. S., *Journal of Solid State Chemistry* **2001,** 159, (2), 403.
188. Cotton, F. A.; Haefner, S. C.; Sattelberger, A. P., *Journal of the American Chemical Society* **1996,** 118, (23), 5486.
189. Clegg, J. K.; Cremers, J.; Hogben, A. J.; Breiner, B.; Smulders, M. M. J.; Thoburn, J. D.; Nitschke, J. R., *Chemical Science* **2013,** 4, (1), 68.
190. Underwood, C. C.; Stadelman, B. S.; Sleeper, M. L.; Brumaghim, J. L., *Inorganica Chimica Acta* **2013,** 405, 470.
191. Wu, F. J.; Kurtz, D. M., *Journal of the American Chemical Society* **1989,** 111, (17), 6563.
192. Quiros Mendez, N.; Arif, A. M.; Gladysz, J. A., *Organometallics* **1991,** 10, (7), 2199.
193. DuMez, D. D.; Mayer, J. M., *Inorganic Chemistry* **1998,** 37, (3), 445.
194. Abu-Omar, M. M.; Khan, S. I., *Inorganic Chemistry* **1998,** 37, (19), 4979.
195. Casanova, M.; Zangrando, E.; Munini, F.; Iengo, E.; Alessio, E., *Dalton Transactions* **2006**, (42), 5033.
196. Stebler-Röthlisberger, M.; Ludi, A., *Polyhedron* **1986,** 5, (6), 1217.
197. *Crysalis^{pro} Software System*.

198. Altomare, A.; Burla, M. C.; Camalli, M.; Cascarano, G. L.; Giacovazzo, C.; Guagliardi, A.; Moliterni, A. G. G.; Polidori, G.; Spagna, R., *Journal of Applied Crystallography* **1999,** 32, (1), 115.
199. Sheldrick, G., *Acta Crystallographica Section A* **2008,** 64, (1), 112.
200. Spek, A., *Journal of Applied Crystallography* **2003,** 36, (1), 7.

10 Acknowledgement

I would like to sincerely thank Prof. Dr. Roger Alberto for giving me the opportunity to work in his temple of chemistry and his constant support for this thesis. He gave me the freedom to completely follow my own ideas while also being there for advice and great support whenever I needed it, and also for that I am very grateful.

Further, I would like to sincerely thank Dr. Henrik Braband for the interesting discussion and for the daily support he provided during this PhD thesis and also for correcting my thesis. Further, I would like to thank Prof. Dr. David Tilley and Prof. Dr. Gilles Gasser for the helpful discussions and remarks that they provided as members of my PhD committee.

I would like to thank several people for their contribution described in this thesis. I would like to thank Prof. Dr. Enzo Alessio and Dr. Urs Leutenegger for their choice to perform a sabbatical in this topic and for their investigation concerning arene displacement reaction and lithation reactions of the $[Re(\eta^6\text{-benzene})_2$ core. Furthermore, the enthusiastic and diligent work of several Master students is greatly acknowledged. Sara Jordi worked on the synthesis of methylated $[M(\eta^6\text{-arene})_2]^+$ (M = Re, $^{99(m)}$Tc). Patrick Felder worked on the derivatisation of the $[Re(\eta^6\text{-benzene})_2]^+$ moiety with phosphines and pyridines. Furthermore, I would like to thank Nathalie Wyss, Michael Anderegg and Cedric Turtschi for their valuable contribution during a project in the practical course in inorganic chemistry.

A big thanks go to Dr. Paul Schmutz and Michael Benz for introducing me in the synthesis of $[Re(\eta^6\text{-arene})_2]^+$

I would like to thank several people for their help concerning measurements and analyses. The help of Prof Dr. Bernhard Spingler and Dr Olivier Blacque concerning X-ray diffraction analysis of single crystals is greatly appreciated, especially since many of the compounds in this thesis had systematic disorders. Concerning NMR analyses I would like to sincerely thank Dr. Thomas Fox for his great service and his help with NMR analyses in general. I would also like to thank the whole MS-service team for their great service. Furthermore, I would like to thank Heinz Spring for elemental analyses and Hanspeter Stalder and Serkan Sariyildiz for technical support.

I would like to thank Ramona Erni for always being available and helpful with everything that had to be organized.

In particular, I want to thank Robin Güttinger (Züri Boy) and Karla Lineau (Haarla) for your friendship, for all the coffee and beer breaks, for all the time that we spend in the superkondi and muscle pump

as well as the incredible nice time that I enjoyed with you. I would like to thank Giulia Rusconi for all the interesting discussion and laughs shared. Grazie Mille!

Further, I would like to thank Koushik Venkatesan for all the great discussion about science and helpful advice. Of course, a big thank you goes to all the members of the Koushik group for the unforgettable time that we spend together. In particular, I want to thank Tobias von Arx, Dominik Suter, Alexander Szentuki, Lucas Prieto, Marjorie Sonnay and Cristina Mari for all the good time and deep discussion we had.

I would like to thank my lab mates Ngoc An Le and Dr. Wenyu Wu for the enjoyable working atmosphere in our lab.

A big thank you goes to all the past and present of the Alberto group starting from: Michael Felber, Sebastian Imstepf, Stephan Schnidrig, Evelyne Joliat, Johannes Windisch, Cyril Bachmann, Michel Wuillemin, Angelo Frei, Anna Looser, Carla Gotzmann, Daniel Hernandez, Mathias Mosberger, Nico Weder, Robin Bolliger, Peter Müller and Qaisar Nadeem for making my PhD a very unenjoyable time.

I would like to thank the University of Zürich and the Department of Chemistry for a friendly and productive working atmosphere. Furthermore, I would like to thank the CMSZH Graduate School for support and the organisation of all the events.

I would also like to sincerely thank my family and friends for their continuous and unconditional support during my time at the University of Zurich. In particular, I want to give a big thank to my parents and my brother. Last, but certainly not least, I would like to thank my wonderful daughter Sophie for being my sunshine during the past two years.

11 Curriculum Vitae

Personal Information

Name	Giuseppe
Surname	Meola
Date of Birth	17.10.1985
Nationality	Italian
Place of Origin	Italy

Education

University of Zurich, Switzerland

05/2014 - 03/2019 **PhD in Chemistry**
"Synthesis, Derivatization and Characterisation of Rhenium/Technetium Mono- and Bis(η^6-arene) Complexes for the Application in Medicinal chemistry"
Advisor: Prof. Dr. Roger Alberto, Department of Chemistry

03/2011 - 04/2014 **Master of Science in Chemistry**
"Synthesis and characterisation of cubane and heterobimetallic double cubane cluster with the $[M(CO)_3(ER)]^0$ fragment (M = Re, Mn; E = O, S)"
Advisor: Prof. Dr. Roger Alberto, Department of Chemistry

Zurich University of Applied Sciences (ZHAW), Winterthur

10/2004 - 11/2007 **Dipl. Chem. FH**
"Development of Antifreeze-Coatings on the base of Sol-Gel Chemistry
Advisor: Prof. Dr. Martina Hirayama

Gewerbeschule Chur

10/2001 - 11/2004 Technical Berufsmatura

Ems–Chemie AG, Domat/Ems

10/2001 - 11/2004 **Apprenticeship as chemical laboratory assistant**

Work Experience

Zurich University of Applied Sciences (ZHAW), Winterthur

12/2007 - 11/2012 **Scientific assistant**

- Development of latent-reactive hot-melt adhesive composition based on isocyanate-reactive compounds
- Development and characterisation of polymeric coatings with antifreeze or hydrophopic properties

Publications and Patents

First author

Meola G., Braband H., Schmutz P., Benz M., Spingler B., and Alberto R., "*Bis-Arene Complexes [Re(η^6-arene)$_2$]$^+$ as Highly Stable Bioorganometallic Scaffolds"*, *Inorg. Chem.* **2016**, *55* (21), 11131-11139

Meola G., Braband H., Hernández-Valdés D., Gotzmann C., Fox T., Spingler B., and Alberto R., *"A Mixed-Ring Sandwich Complex from Unexpected Ring Contraction in [Re(η^6-C_6H_5Br)(η^6-C_6R_6)](PF$_6$)"*, *Inorg. Chem.* **2017**, *56* (11), 6297-6301

Meola G., Braband H., Jord S., Fox T., Blacque O., Spingler B., and Alberto R., "*Structure and reactivities of rhenium and technetium bis-arene sandwich complexes [M(η^6-arene)$_2$]$^+$"*, *Dalton Trans.*, **2017**, *46*, 14631-14637

Co-author

Alberto R., Meola G., Hernández-Valdés D., (**2019**). "*Technetium and Rhenium Complexes with Aromatic Hydrocarbons as Ligands: An Entry into Biomimetic Imaging".* In T. Hirao and T. Moriuchi (Eds.), *Advances in Bioorganometallic Chemistry* (pp. 215-241). Elsevier

Mokolokolo P. P., Frei A., Tsosane M. S., Kama D. V., Schutte-Smith M., Brink A., Visser H. G; Meola G., Alberto R., Roodt A., *"Nuclearity manipulation in Schiff-base fac-tricarbonyl complexes of Mn(I) and Re(I)"*. *Inorg. Chim. Acta*, **2018**, *471*, 249-256.

Hernández-Valdés D., Blanco-Gonzáleza A., García-Fleitasa A., Rodríguez-Rieraa Z., Meola G., Alberto R., Jáuregui-Hazaa U., *"Insight into the structure and stability of Tc and Re DMSA complexes: a computational study"*, *J. Mol. Graph. Model*., **2016**, *71*, 167-175

Harling S., Meola G., Schaible S., Schulthess A., Brändli C., Meincke O., *"Latent reactive polyurethanes based on toluenediisocyanate-uretdione and polycaprolactones"*, Int J Adhes Adhes., **2013**, *46*, 26-33.

Adrian Schulthess, Hendrik Mathes, Benjamin Grimminger, Olaf Meincke, Steffen Harling, Giuseppe Meola, Stefan Schaible (2013). Latent reaktive Schmelzklebstoffzusammensetzung. Patent: EP 2712879.

Hirayama, Martina; Siegmann, Konstantin; Meola, Giuseppe; Schäfer, Carsten; Dänhardt, Karin (2010). Surface Coatings having Anti-Ice Properties. Patent: WO 2011/082500 A1.

Hirayama, Martina; Siegmann, Konstantin; Meola, Giuseppe (2008). Gefrierpunktserniedrigende Oberflächenbeschichtung. Patent: EP2315769A1